

International Association on the Genesis of Ore Deposits (IAGOD)

Metallogeny of the Pacific Northwest (Russian Far East): Tectonics, Magmatism and Metallogeny of Active Continental Margins

Edited by
A.I. Khanchuk, G.A. Gonevchuk & R. Seltmann



Excursion Guidebook
Published by
Far East Geological Institute
Vladivostok • 2004

A.I. Khanchuk, G.A. Gonevchuk & R. Seltmann (Eds)

Metallogeny of the Pacific Northwest (Russian Far East):

Tectonics, Magmatism and Metallogeny of Active Continental Margins

Guidebook for the Field Excursions in the Far East of Russia: September 1-20, 2004

© INTERNATIONAL ASSOCIATION ON THE GENESIS OF ORE DEPOSITS (IAGOD)

Published by Dalnauka Publishing House, IAGOD Guidebook series 11, Vladivostok, 2004, 176 p., 122 figs., 29 tables.

ISBN 5-8044-0464-4

This guidebook was prepared for the Interim IAGOD Conference on Metallogeny of the Pacific Northwest: Tectonics, Magmatism and Metallogeny of Active Continental Margins, which took place in September of 2004 in Vladivostok, the southernmost port of the Russian Far East. The book describes the geology of a number of important ore districts and deposits in the region. These are the major deposits of fluorine (Voznesenka), boron (Dalnegorsk), tungsten (Vostok-2), platinum (Konder), gold (Pokrovka), and some smaller deposits of tin, lead, zinc, and other metals.

The guidebook also includes a description of South Kamchatka which is an example of young magmatism and modern ore formation. The chapters devoted to the Okhotsk-Kolyma Province address granitoid magmatism of different geodynamic and geochemical types and related ore mineralization.

This book will be of interest to specialists in regional and economic geology, geodynamics, metallogeny, and ore deposits modeling.

Khanchuk, A.I., Gonevchuk, G.A. & Seltmann, R. (Eds) Metallogeny of the Pacific Northwest (Russian Far East): Tectonics, Magmatism and Metallogeny of Active Continental Margins. IAGOD Guidebook series 11, Dalnauka Publishing House, Vladivostok 2004, 176 p.

ISBN 5-8044-0464-4



**INTERNATIONAL ASSOCIATION
ON THE GENESIS OF ORE DEPOSITS**

**RUSSIAN ACADEMY OF SCIENCES
FAR EAST BRANCH
Far East Geological Institute**



**Metallogeny of the Pacific Northwest (Russian Far East):
Tectonics, Magmatism and Metallogeny
of Active Continental Margins**

**INTERIM IAGOD CONFERENCE
1 – 20 September, 2004
Vladivostok, Russia**

EXCURSION GUIDEBOOK

**Edited by
A.I. Khanchuk, G.A. Gonevchuk & R. Seltmann**

**Dalnauka Publishing House
Vladivostok
2004**

CONTENTS

PREFACE

A.I. Khanchuk, G.A. Gonevchuk and R. Seltmann 3

1. GRANITOIDS OF THE OKHOTSK–KOLYMA DIVIDE AND RELATED ORE MINERALIZATION

N.A. Goryachev and M.L. Gelman 5

2. THE KONDER MASSIF OF ULTRAMAFIC AND ALKALINE ROCKS AND RELATED PGM MINERALIZATION

A.M. Lennikov, B.L. Zalishchak and R.A. Oktyabrsky 29

3. THE KOMSOMOLSK ORE DISTRICT

S.M. Rodionov, B.I. Semenyak and V.Yu. Zabrodin 43

4. THE POKROVKA EPITHERMAL GOLD DEPOSIT

V. Khomich and N.G. Vlasov 72

5. THE ARMINSKY ORE DISTRICT

V.I. Gvozdev 87

6. THE DALNEGORSK ORE DISTRICT

G.P. Vasilenko 98

7. SOUTHWEST PRIMORYE (THE VOZNESENKA ORE DISTRICT)

M.D. Ryazantseva 125

8. GEOLOGY, MAGMATISM AND GOLD MINERALIZATION OF SOUTH PRIMORYE (THE ASKOLD STRIKE-SLIP FAULT ZONE, SERGEEVKA TERRANE)

G.R. Sayadyan 137

9. MIOCENE-TO-QUATERNARY CENTER OF VOLCANIC, HYDROTHERMAL AND ORE-FORMING ACTIVITY IN THE SOUTHERN KAMCHATKA

V.M. Okrugin and M.E. Zelensky 147

PREFACE

A.I. Khanchuk¹, G.A. Gonevchuk¹, and R. Seltmann²

¹ Far East Geological Institute, Far East Branch, Russian Academy of Sciences, Vladivostok, Russia

² Natural History Museum, Department of Mineralogy, CERCAMS, London, UK

The Russian Far East occupies a vast territory (about 6.2 mil. km²) stretching from the Arctic Ocean in the north to the Russia/China/Korea boundary in the south. In the east it is bounded by marginal seas of the Pacific Ocean. Known as the Far Eastern Economic Region (FEER), it includes the Sakha Republic (Yakutiya), Primorye, Khabarovsk, Amur, Kamchatka, Magadan, and Sakhalin Territories, Jewish Autonomous Oblast (province), Koryak and Chukotka National Districts (Fig. 1). Approximately it occupies 1/3 of the area of the Russian Federation.

Its location at the junction of the Eurasian and the North American continental and the Pacific Ocean oceanic plates is responsible for the diversity of the geology of the region.

The central structural unit in the territory is the North Asian Craton represented by eastern parts of the Siberia Platform and the Aldan-Stanovoy Shield and the Verkhoyansk Late Paleozoic-Early Mesozoic passive continental margin. To the northeast of the craton is the Verkhoyansk-Kolyma collage of cratonal (Omolon, Okhotsk) and Early Paleozoic continental margin (Prikolyma, Omulevka, and others) terranes. Their neighbors are the Jurassic island arc terranes, accretionary wedge terranes, and turbidite basins. This collage is the product of Early Cretaceous movements, when the Chukotka terrane of the Paleozoic-Early Mesozoic passive continental margin approached the North Asian Craton. The Koryak Highlands terrane of the Jurassic-Cretaceous epi-oceanic island arc and accretionary wedge terranes had formed in the Early Cretaceous epoch as a result of northward subduction of Paleo-Pacific lithospheric plates.

The Mongolo-Okhotsk collage of Mesozoic epi-oceanic terranes, the Pre-Mesozoic collage of different origin terranes of the Amur superterrane, and the Sikhote-Alin collage of Early-Cretaceous epi-oceanic terranes are located south and southeast of the North Asian Craton. A vast area of the Cenozoic collage terranes partially submerged in the ocean and marginal seas is identified east of the Late Cretaceous continent/ocean boundary. Terranes of the Kamchatka

Peninsula, Sakhalin Island, and the Kuril Islands are the fragments of structural elements of the Late Cretaceous-Early Paleogene continent/ocean boundary and Late Cretaceous and Paleogene island arcs. Most of them accreted in the Middle-Late Eocene, only the Kronotsk Peninsula and Kamchatka Cape terranes were accreted in the Neogene.

The diversity of terranes and geodynamic settings has resulted in a diversity of magmatic rocks in the region, mostly in volcano-plutonic belts. To the southeast of the North Asian Craton the Uda Middle Triassic volcano-plutonic arc is located. The Mesozoic-Cenozoic stage of geodynamic evolution in East Asia is characterized by an alternation of subduction and transform (Californian type) settings. These settings are associated with interaction of lithospheric plates, to the southeast of the North Asian Craton and formation of 1) the Okhotsk-Chukotka and East Sikhote-Alin volcano-plutonic belts of the Late Cretaceous active continental margin, 2) a system of Oligocene-Miocene volcanic belts extending from the Chukotka area through West and Central Kamchatka Peninsula to the Kuril Islands, and 3) modern volcanic structures of the Kamchatka Peninsula and the Kuril Islands.

The magmatic rocks of the region which formed at different times and in different geodynamic environments have various chemical characteristics and are accompanied by diverse mineralization.

The territory hosts valuable natural resources: noble, rare and nonferrous metals, precious and decorative stones, chemical and energy raw materials, and construction materials. 2% of Russian oil is produced here, as well as 13% of its coal, a considerable proportion of gold and nonferrous metals, over 50% of its platinum, and all Russia's diamonds. The regional potential of minerals and raw materials is even more impressive, it includes tens of explored deposits, 280 prospected ore occurrences, and about 10,000 ore occurrences worth expert assessment, as well as oil and gas fields. The region is unique in the number of ore-bearing placers with about 30 gold, 126 cassiterite,

tungsten, platinoid, and other metal placer deposits. Mineral resources of the Russian Far East are registered in the State Registrar of the Russian Federation. Their tonnage amounts to: tin – about 2 Mt; tungsten – 0.2 Mt; lead – 1.7 Mt; zinc – 2.4 Mt; copper – 0.8 Mt; silver – 38 kt; gold – 2 kt; fluorite – 18.7 Mt; etc. No-

ble and nonferrous metals, as well as fluorine, boron, and energy resources are the main objects mined within this huge territory. Production of these minerals contributed much to the rapid development of the regional economics, social sphere, science, and culture.

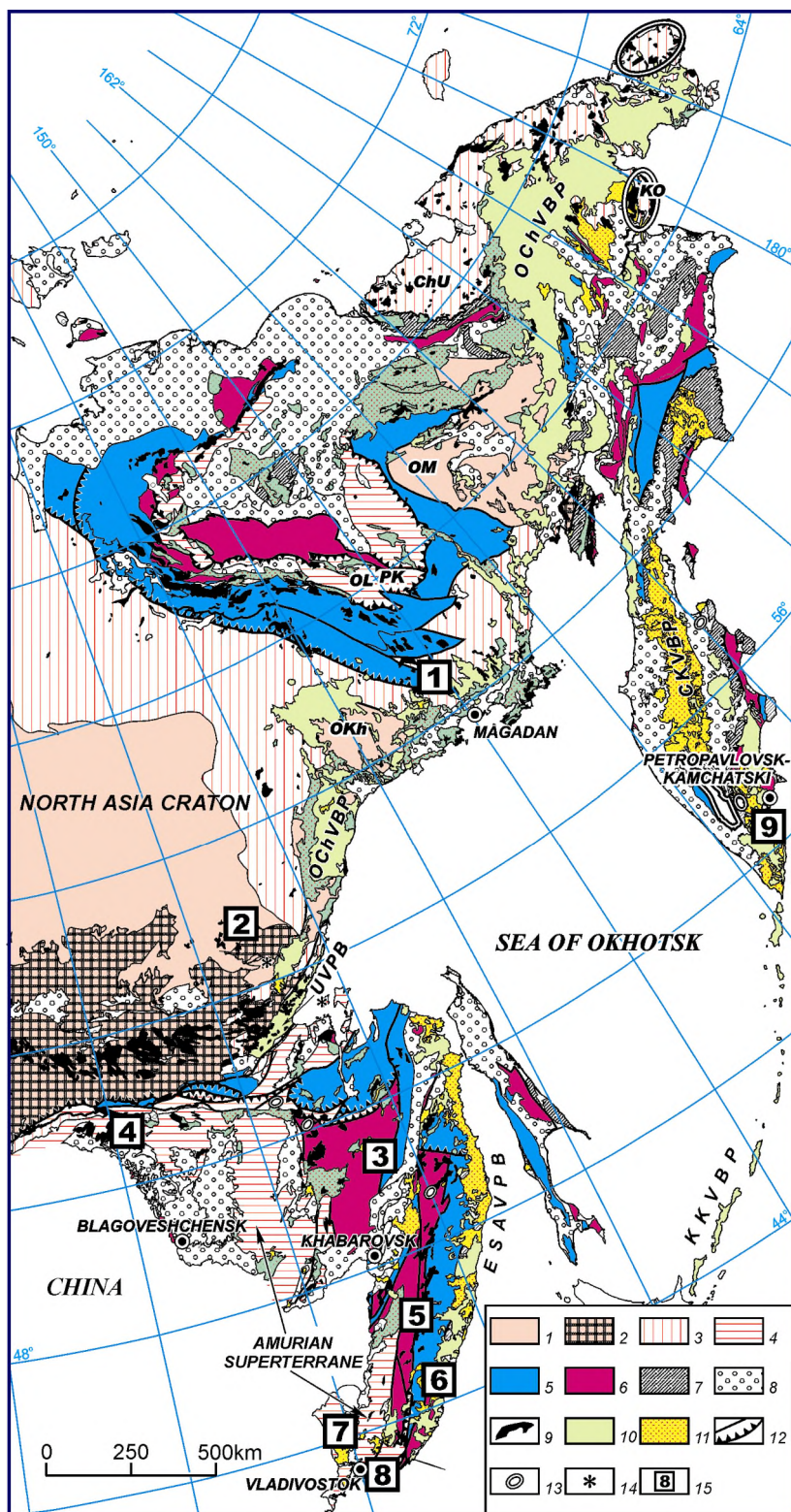


Fig. 1. Generalized map of terranes and overlap assemblages in the Russian Far East.

(1) pre-Cambrian granite-metamorphic complexes; (2) North Asia Craton and Okhotsk and Omolon cratonal terranes; (3) passive continental margins (MZ₁) of the North Asian Craton and the Chukotka terrane; *Terranes*: (4) pre-Mesozoic continental, (5) continental margin turbidite of transform geodynamic setting (MZ-KZ), (6) accretionary-wedge (MZ-KZ), (7) island-arc (MZ-KZ); (8) sedimentary basins (MZ-KZ); (9) syn-strike-slip faulting granitoids (MZ-KZ); *Volcanic-plutonic belts (VPB)*: (10) subduction related, (11) related to transform events (Californian type); (12) faults; (13) complexes of metamorphic core (Cordilleran type); (14) ultramafic zoned plutons; (15) localization of trip objects (a number corresponds to guide charter).

Terranes: OM – Omolon, OKh – Okhotsk, PK – Prikolya, OL – Omulevka, ChU – Chukotka, KO – Koryak. *Volcanic-plutonic belts (VPB)*: ESA – East Sikhote-Alin, KK – Kurils-Kamchatka, Och – Okhotsk-Chukotka, U – Uda, CK – Central Kamchatka



GRANITOIDS OF THE OKHOTSK–KOLYMA DIVIDE AND RELATED ORE MINERALIZATION

N. A. Goryachev and M. L. Gelman

Northeastern Complex Research Institute, Far East Branch, Russian Academy of Sciences, Magadan

INTRODUCTION

Northeastern Asia covers more than two millions square kilometers and is a huge sialic petrographic province. The granitoid magmatism is diverse in age, and the ore mineralization is similarly manifold (Au, Ag, Sn, W, Mo, Co, Cu, U, Hg, and Sb). The total mining production is estimated to date varied about 4 kt Au (mainly recovered from placers), 80 kt Sn, 40 kt W, 2 kt Ag, and 1 kt Co.

REGIONAL GEOLOGY

The Verkhoyansk-Kolyma Folded Belt (Kolyma Geoblock, after L.I. Krasnyi) is situated east of the Siberian Platform. Geology and tectonics of this region were described in many early reviews written in terms of the geosynclinal concept (Springis, 1958; *Geologiya SSSR*, 1970; *Tektonika...*, 1980; *Mesozoiskaya...*, 1983; *Geologicheskoe...*, 1984), whereas later works are based on plate tectonics (Bogdanov and Tilman, 1992; Nokleberg et al., 1994; Shpikerman, 1998; Chekhov, 2000; *Tektonika...*, 2001). The information given hereafter follows a brief summary prepared by Goryachev (1998).

Parfenov (1995) recognizes eight large tectonic blocks in the Mesozoides of northeastern Asia: (1) North Asian Craton including the Siberian Platform and the Verkhoyansk Folded belt (miogeocline); (2) Okhotsk Cratonic Terrane; (3) Kular-Nera Terrane; (4) Kolyma-Omolon Superterrane consisting of the Alazeya-Khetachan composite island-arc terrane, Omulevka River composite terrane of carbonate platform, Munilkan ophiolite terrane, Arga-Tas and Rasokha island-arc and suboceanic terranes, and Omolon cratonic terrane; (5) South Anui Superterrane; (6) Chukotka and (7) Viliga River shelf terranes; (8) Koni-Murgal Terrane (island arc). Particular terranes of the Kolyma-Omolon Superterrane were amalga-

mated in the late Middle Jurassic and the early Late Jurassic. In the southwest, the Kolyma-Omolon Superterrane was unconformably overlain by volcanic and sedimentary rocks of the Late Jurassic Uyandina-Yasachnaya volcanic arc and related In'yali-Debin and Polousnensky forearc and Ikin-Tas backarc basins. Late Jurassic-Neocomian volcanics of the Oloi-Svyatoi Nos arc overlap the superterrane in the north. The Okhotsk, Viliga and Koni-Murgal terranes occupying the southeastern part of the Mesozoides in the northeastern Asia are overlapped by postaccretionary subaerial volcanic and sedimentary rocks deposited in the near-continental portion of the Neocomian Uda-Murgal magmatic arc. Albian and the late Cenomanian Okhotsk–Chukotka marginal volcanic belt (OCVB), more than 3000 km in extent, is a post-accretionary structure of Cretaceous continental margin. The route of the excursion passes across the Verkhoyansk miogeoclinal foldbelt, Viliga River shelf terrane, Koni-Murgal island-arc terrane, and post-accretionary Okhotsk–Chukotka marginal volcanic belt (Fig. 1.1).

The Verkhoyansk Foldbelt is a fragment of the passive margin bordering the Siberian continent (North Asian Craton). The Verkhoyansk Complex of terrigenous rocks is composed of sandy-clayey, silty-clayey, and flyschoid sequences, from Carboniferous to Upper Jurassic in age (*Tektonika...*, 1980).

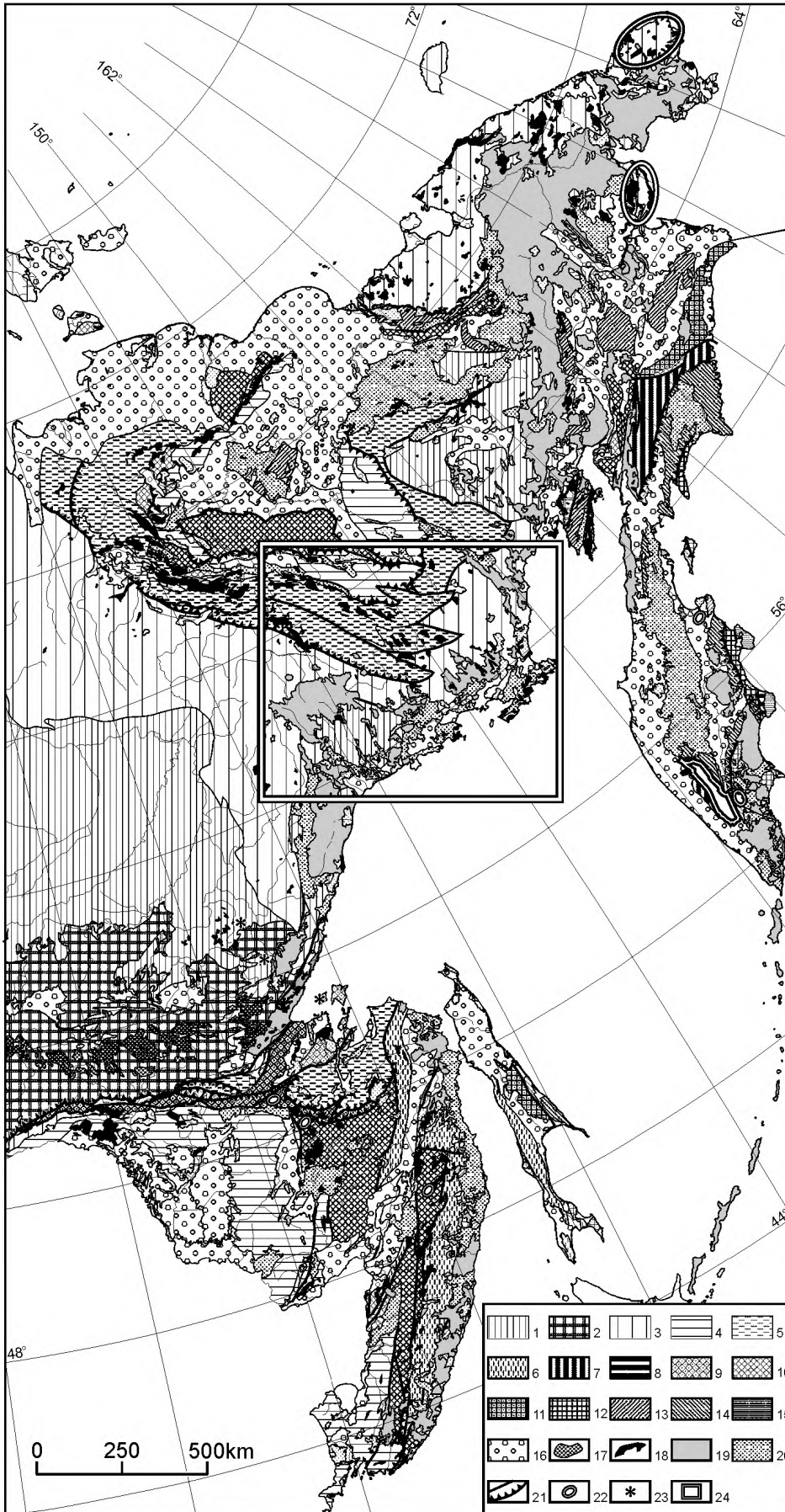


Fig. 1.1. Main Mesozoic-Cenozoic tectonic elements of the Russian Far East, modified after Khanchuk, Ivanov (1999). (1) platform part of North Asia Craton, Okhotsk and Omolon cratone Terranes; (2) Archean and Proterozoic granite-metamorphic assemblages of the Craton and cratone Terranes; (3) Late Paleozoic – Early Mesozoic passive continental margins of the North Asia Craton and Chukcha Terrane; (4) pre-Mesozoic continental terranes; *Turbidite and shale terranes of transform margins of continental lithospheric-plates*: (5) Jurassic, (6) Early Cretaceous, (7) Paleocene-Eocene, (8) Neogene; *Terranes of accretionary prisms of of subduction margins of continental lithospheric-plates*: (9) Paleozoic, (10) Jurassic and Early Cretaceous, (11) Late Cretaceous, (12) Oligocene-Miocene; *Island arc terranes (accretionary prisms and island arcs, undivided)*: (13) Jurassic and Cretaceous, (14) Late Cretaceous, (15) Paleogene; (16) Mesozoic-Cenozoic sedimentary basins; *Strike-slip related of transform margins of lithosperic plates and micro-plates*: (17) Jurassic, (18) Early Cretaceous; (19) Mesozoic-Cenozoic subduction-related volcanic-plutonic belts; (20) Mesozoic-Cenozoic transform continental margin related volcanic-plutonic belts (California type); (21) main faults; (22) metamorphiccore complexes (Cordilleras type); (23) dunite-clinopyroxenite zonal massifs; (24) described territory

The narrow **Kular-Nera Slate Belt** (terrane, after L.M. Parfenov), or the Yana-Kolyma Terrane, after S.A. Byalobzhesky and A.M. Sosunov (1994) and V.I. Shpikerman (1998) is a distal deep-water part of the Verkhoyansk passive margin. Yu.S. Repin and I.V. Polubotko (1996) assumed that Triassic and Jurassic deep-water turbidite shales, siltstones, and sandstones were deposited within the so-called Debin deep-water trough. It is suggested that the Yana-Indigirka minor oceanic basin existed here already by the Middle Paleozoic (Bulgakova, 1991). Triassic and Jurassic sediments fill the present-day In'yali-Debin Synclinorium while Permian rocks are exposed in the Ayan-Yuryakh Anticlinorium. Linear, ridge-shaped, and occasionally overturned folds in a northwestern direction are typical of the In'yali-Debin Synclinorium (Chekhov, 1976). In the Ayan-Yuryakh Anticlinorium, this style of folding is not so obvious. Many researchers suppose that the In'yali-Debin Synclinorium was formed on the broken and thinned margin of the continental plate, probably, as a pull-apart structure.

Occurrences of pyroxene-amphibole gneisses, melanocratic, biotite-rich crystalline schists, and graphite-bearing mafic rocks as xenoliths in Late Mesozoic granitoids confirm the geophysical evidence (Vashchilov, 1963, Mikhailov and Goryachev, 1997) indicating that the Kular-Nera Slate Belt is underlain by a crystalline basement. At the southeastern flank, these structures are conjugated with the Balygychan Uplift and Arman Synclinorium; both structures belong to the Viliga Terrane.

The Kular-Nera Slate Belt (Yano-Kolyma Terrane) accommodates the Main Kolyma Belt of granitoid batholiths, as well as Late Mesozoic dikes and minor intrusions of variable composition including layered gabbroic intrusions and plagioclase peridotite.

The sedimentary rocks underwent greenschist metamorphism localized in the northwestern shear zones; chlorite, sericite, phengite, stilpnomelane, biotite, graphitoids, and ilmenite serve as index minerals (Gelman, 1976, 1977; Gelman et al., 1980; Krutous, 1992). Cordierite-biotite schists were traced in the axial parts of the shear zones. The highest temperature of metamorphism was estimated as 450–700°C (Fedorova, 1991a, b; Shupikov and Nikonov, 1989). Ubiquitous phengite and stilpnomelane indicate that andalusite-sillimanite type of metamorphism developed under a slightly elevated pressure.

The Viliga Terrane (Arman-Viliga Synclinorium) is composed of a thick sequence of marine sedimentary rocks of stratigraphic range from Lower Carboniferous to Upper Jurassic. These rocks were

deformed into linear, largely northeastern folds and dome-shaped structures. Carboniferous and Permian volcanosedimentary rocks contain basaltic lava flows and conglomerate interlayers. Shales and siltstones with limestone and andesite interlayers are prevalent in the Triassic. The Jurassic section consists of shales, siltstones, and sandstones with interlayers of conglomerates, basic and intermediate lavas and tuffs. The contribution of volcanic rocks markedly decreases toward the continent (Korol'kov and Gelman, 1992; Repin and Polubotko, 1996). Jurassic rocks are interpreted as a filling of the backarc basin related to the Koni-Murgal island arc (Nokleberg et al., 1994). The Koni-Murgal Terrane is overlapped by the Uda-Murgal and Okhotsk-Chukotka volcanic belts and intruded by granitoids.

The Koni-Murgal Terrane (andesitic geosyncline after V.F. Belyi) is composed of Paleozoic–Lower Cretaceous volcanosedimentary rocks and lavas belonging to the tholeiitic and calc-alkaline series. The complete section was studied in the Taigonos Block, where it consists of Ordovician–Carboniferous metamorphic schists overlain by Upper Permian, Triassic, Jurassic, Neocomian, and upper Albian sequences. Paleozoic rocks were deposited in an off-shore environment, whereas Triassic–lower Neocomian sediments are related to various marine and near-shore facies. The upper Neocomian sediments accumulated on islands. Volcanic activity fell in the late Triassic and early Jurassic, Middle and Late Jurassic and Late Jurassic–Neocomian. In the Early Cretaceous, the rocks of this terrane were intruded by granitoid plutons and then overlapped by OVCB volcanics in the Late Cretaceous.

The Uda-Murgal volcanic belt (UMVB) extends along margins of the Okhotsk, Viliga, Omolon, and Koni-Murgal terranes. In terms of the geocynclinal concept, the structures of this belt were described as Late Jurassic–Neocomian orogenic basalt-andesite-rhyolite association (*Geologiya SSSR*, 1970; Karchevets, 1975; Belyi, 1977, 1994). In contrast to the marine volcanosedimentary sequences of the Koni-Murgal Terrane, this rock association is composed of subaerial volcanics with an appreciable contribution of silicic rocks (Belyi, 1994). Andesitic breccia and lava unconformably overlie Upper Triassic and Lower Jurassic rocks at the base of the volcanic belt and up-section give way to dacite and high-silicic tuff. Numerous gabbroic, granodiorite, and granite intrusions are associated with volcanics (Umitbaev, 1986). Granodiorite and granite plutons emplaced 140–155 Ma ago in the Viliga Terrane are, probably, also related to the formation of UMVB.

The postaccretionary period in the history of northeastern Asia was characterized by a vigorous outburst of volcanic activity and granitoid magmatism.

The Okhotsk-Chukotka volcanic belt (OCVB) started to evolve along the continental margin (Belyi, 1994). This belt, more than 3000 km in extent, overlapped various Mesozoic terranes (Fig. 1.1). Ancient rift troughs controlled the deposition of a thick (up to 2000 m) sequence consisting of conglomerate, sandstone, and mudstone with sparse flows of andesitic, dacitic, and rhyolitic lavas and pyroclastic rocks. Andesite, basalt, and related tuffs, up to 1000 m in total thickness, lie upsection. Large bodies of overlying ignimbrites fill volcanotectonic depressions. The lower unit (up to 2000 m) of silicic rocks is composed of tuffs with rare ignimbrite and andesitic lava flows. Densely welded quartz latitic, rhyodacitic, and rhyolitic ignimbrites and vitroignimbrites make up the next unit (500–700 m). Lenses of two-pyroxene basaltic andesite and related tuffs, up to 1000 m thick, are distributed throughout the section of silicic rocks. Plagiophyre basalt and basaltic andesite, up to 300 m in thickness, overlie the ignimbrites in the central parts of volcanotectonic structures. They are exposed as lava plateaus west of the Kolyma Highway between the Atka Settlement and Ola River. Omitting some discrepancies in age estimations, the OCVB section can be subdivided into Early Cretaceous basalt-andesite series, Middle Cretaceous dacite-rhyolite and basaltic andesite series, Late Cretaceous rhyolite-trachyrhyolite series, and Late Cretaceous (presumably Paleogene) basalt-trachybasalt and alkali basalt series. The age of the OCVB as a whole is estimated as Albian-Senonian (Belyi, 1994) or Cretaceous-Paleogene (Filatova, 1988).

Volcanotectonic structures, attaining 80–100 km in diameter, are most distinctly contoured in the outer (near-continental) part of the OCVB. Judging from the geophysical evidence, the large bodies of Albian-Cenomanian ignimbrites are localized above the granitic plutons. Subvolcanic and hypabyssal intrusions are concentrated at the margins of volcanic structures.

Early and Late Cretaceous polychronous multiphase plutons are widespread within the OCVB and in its continental framework. The plutons are composed of gabbro (commonly, the older intrusive phases), diorite and tonalite (most abundant rocks), biotite-amphibole granite, and leucogranite (commonly, the younger phases). Sodium prevails over potassium in low-silicic rocks while in granites this proportion

equalizes. Elevated Sr contents are typical. Diorite (tonalite)-granodiorite and granodiorite-granite associations belong to the magnetite series and bear geochemical signatures of the subduction-related I-granites. Small Mo and U deposits are associated with plutons slightly enriched in potassium (Gelman et al., 1997).

Neogene continental sediments reach 500 m and more in thickness even within small basins, e.g., in that crossed by the highway at entrance to Magadan. Coarse-, medium- and fine-grained alluvial and lacustrine loose sediments and locally developed opoka, lignite, and brown coal are typical.

Quaternary sediments attain 100 m in thickness. Late Pleistocene and Holocene alluvium fills the river valleys and make up terraces in the Kolyma River basin and in basins of the Okhotsk Sea slope. Lenses of silicic volcanic ash presumably related to the catastrophic eruption of the Shiveluch volcano in Kamchatka are known within Quaternary sediments near the Stekolny Settlement.

The Main Kolyma plutonic belt is localized in the Kular-Nera Slate Belt close to the boundary with the Kolyma-Omolon Superterrane and extends for more than 1100 km reaching 300 km in width. Diorite (tonalite)-granodiorite, granodiorite-granite, alkali granite, and granite-leucogranite associations are recognized within the plutonic belt (Apeltsyn, 1958; Rudich, 1956; *Geologiya SSSR*, 1970; Zagruzina, 1977; Sobolev, 1989; Shkodzinsky et al., 1992). The general geochronological information is summarized in Table 1.1.

Late Jurassic–Early Cretaceous granitoids belong to the diorite-granodiorite and granite-leucogranite associations. *The diorite-granodiorite association* comprises suites of numerous dikes and small stocks. Dikes of diorite, granodiorite, and granite porphyries reach a few kilometers in extent and few meters (occasionally, tens of meters) in thickness. Dikes are steeply dipping; gently inclined dikes are observed only sporadically. These dikes typically occur in gold ore fields where they cross-cut barren quartz veins and predate the gold-quartz mineralization (Svetly, Yugler, Utinsky deposits, etc.). The intrusive stocks vary in composition from diorite to amphibole-biotite granite. Dikes near contacts of stocks were reported to be metamorphosed and cut by aplitic veins. The observed transition of plutons into dikes suites and separate extended dikes via offsets is accompanied by a shift in composition and development of porphyritic texture.

The isotopic age (in Ma) of granitoid associations, after Kotlyar et al. (2001), Newberry et al. (2000), and Goryachev (1998)

Rock association	Rb-Sr	Ar-Ar	K-Ar
Granite-leucogranite	169-143; 113-77	148.3-137.5; 79.9-77.5	155-125; 107-90
Diorite-granodiorite	158-141	146.5-140.4	153-140
Granodiorite-granite	136-113	110-99	134-105
Alkali granite	63	76	90-77

The amount of dark-colored minerals in the older melanocratic rocks varies from 25 to 45 vol %; pyroxene and amphibole are predominant. Gabbrodiorite contains high-Mg orthopyroxene and clinopyroxene. In diorite and quartz diorite, pyroxene (augite) is associated with Fe-Mg-hornblende [$f = \text{FeO}/(\text{FeO} + \text{MgO}) = 0.48$]. Pyroxene contains up to 0.62 wt % Cr_2O_3 . The high-Ti biotites (2.4–5.2 wt % TiO_2) are subdivided into magnesian ($f = 0.37$ –0.48) and high-Fe ($f = 0.52$ –0.74) and high-Al varieties. The first variety is probably older and the second is younger. The quantity of plagioclase (An_{45-85}) attains 60 vol %. Quartz and orthoclase are almost ubiquitous. Hypersthene ($f = 0.48$ –0.54) and hornblende ($f = 0.57$) in association with biotite ($f = 0.62$ –0.77) are common in the younger biotite-amphibole granodiorite, granite, and granite porphyry. Garnet, apatite, allanite, ilmenite, pyrite, pyrrhotite, arsenopyrite, chalcopyrite, and other sulfides were identified as accessory minerals. Inclusions of low-Ti magnetite (0.23 wt % TiO_2 in diorite and 1.06–2.34 wt % TiO_2 in granodiorite) and Cr-spinel were detected in ilmenite (Gamyranin et al., 1991). Apatite contains <0.2 wt % Mn and 0.2–0.9 wt % Cl. Pyrope-almandine garnet is enriched in the grossular end member (1.3–20.5 mol % Py, 58.9–79.8 mol % Alm, 14.5–21.5 mol % Gros, 0.2–1.9 wt % Andr, and 2.5–5.3 wt % Spes).

Thus, the above described plutonic rocks may be classified as ilmenite-series I-type granitoids of the calc-alkaline series with a slight prevalence of sodium over potassium. Data points of intrusive rocks belonging to this series are localized at the boundary between the hypersthene and pigeonite, or calc-alkaline and tholeiitic series on AFM diagram. On the discriminant diagram proposed by Pearce et al. (1984), they fall into the field of volcanic arcs (Fig. 1.2). The absence of Eu minimum is typical. Dikes underwent carbonatization, albitization, chloritization, and epidotization to much greater extent than stocks. The gold-quartz mineralization is related to these intrusions.

Dikes and stocks intrude Upper Jurassic sedimentary rocks and cross-cut the folds which are metamorphosed at contacts with Early Cretaceous granodiorite-granite plutons. Numerous K-Ar age determinations vary from 165 to 140 Ma (Kotlyar et al., 2001). The Rb-Sr isochron yielding 147 Ma and the primary Sr isotope ratio of 0.7071 was obtained for the Salgyntar pluton (Kotlyar et al., 2001). The Rb-Sr isochron for the Krasivy pluton yielded 145 Ma and $\text{Sr}_i = 0.711$ (Goryachev, 1998). The Rb-Sr isochron age of the Dubach-Beicha pluton is 152 Ma with $\text{Sr}_i = 0.706$ (Palymaskaya, 1991). The Pb-Pb age of the Burgagyn pluton is 149 Ma (Moll-Stalcup et al., 1995). This estimate is close to the K-Ar biotite age of 152 Ma (Goryachev, 1998) and Ar-Ar age of 152 Ma (Newberry et al., 2000).

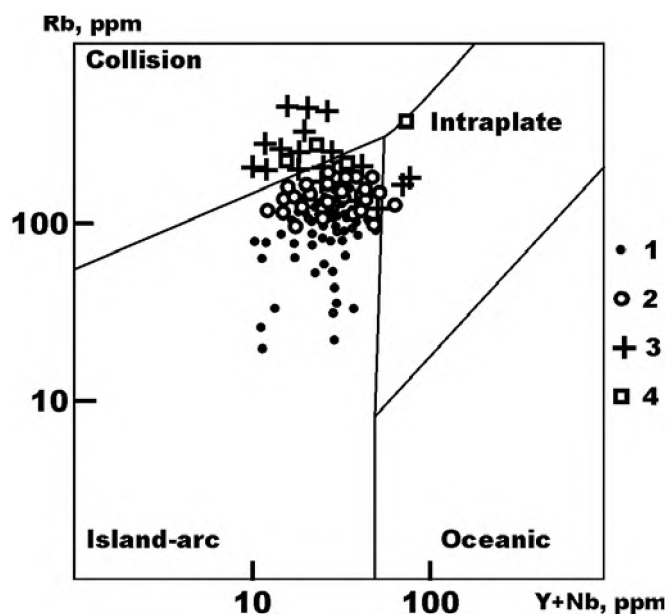


Fig. 1.2. Compositions of granitic rocks from the Yana-Kolyma belt plotted on the discriminant Rb-(Y+Nb) diagram (Pearce et al., 1984).

Rock associations: (1) diorite-granodiorite, (2) granodiorite-granite, (3) granite-leucogranite, (4) Late Cretaceous Li-F granite

The *granite-leucogranite association* comprises large homogeneous batholith-like plutons, up to 7,000 km² in area, localized in the axial part of the Yana-Kolyma Collision Zone and composed of biotite and two-mica granites with accessory ilmenite, cordierite, garnet, less abundant sillimanite and andalusite. Almost all plutons are located in anticlines. Most of the plutons are conformable with respect to folding, and their contacts are commonly traced parallel to the bedding of the country rocks. The plutons can be classified into three groups by their dimensions and morphology: (1) large (hundreds and thousands of square kilometers in area) sheetlike intrusions, concordant to the country rocks, e.g., Chibagalakh, Ch'yorgo, southern Greater Annachag pluton; (2) medium-sized (hundreds km²), approximately equant plutons (Bol'shie Porogi, Okhazha, Canyon), and (3) small (tens of km²) plutons, approximately equant or irregular in plan (Myakit, Deryas-Yurega, etc.).

In all groups, the rocks of the main facies and the younger dikes are virtually indistinguishable in composition. The selvages of plutons of the first group are occupied by melanocratic diorite and granodiorite (up to 10–15% of area). Xenoliths of high-Al gneisses, crystalline schists, and amphibolites are typical (Trunilina, 1992; Shkodzinsky et al., 1992).

Disseminated tin mineralization is associated with pervasive greisenization (Kotlyar, 1958; Flerov et al., 1979). The near-contact granitic injections into hornfels and xenoliths of metamorphic rocks are noticed in plutons of the second group. Leucocratic two-mica selvages, greisen zones, and blanket-shaped lodes with tin and less abundant tungsten mineralization are typical of plutons related to the third group (Myakit and Chuguluk plutons). Plutons of the three groups can be regarded as a vertical series with a sequentially shallower depth of emplacement.

The main facies is composed of medium- and coarse-grained biotite (5–10%) granites. Some plutons contain high-Ti biotite (3–4 wt % TiO₂) with $f = \text{FeO}/(\text{FeO} + \text{MgO}) = 0.71\text{--}0.77$; in other plutons, biotite is low-Ti (<3 wt % TiO₂) and with $f = 0.91\text{--}0.95$ (Sobolev, 1989; Trunilina, 1992; Shkodzinsky et al., 1992). The average f value of biotite increases in granitic rocks of the second and especially third groups. Quartz grains attain 1–5 mm in diameter and occupy no less than 25–30 vol %. Potassium feldspar (up to 40 vol %) prevails over plagioclase. Both microcline and orthoclase are noticed. Perthite and myrmekite are typical. The content of zoned plagioclase (An₃₀₋₃₅ in core and An₂₀₋₃₀ in marginal zones) commonly reaches 15–25 vol %. Ilmenite with up to 7 wt % MnO, garnet, andalusite, cordierite (0.23% Na₂O,

19.14% FeO, 1.03% MnO, 0.98% MgO, 31.7% Al₂O₃, 47.46% SiO₂), tourmaline, apatite, titanite, and sparse sulfides are identified as accessory minerals. Granitic texture is typical; myrmekites are abundant in granites of the first group. Late dikes and sills are composed of aplite-like inequigranular and pegmatoid granites, often with andalusite and tourmaline. Aplites and rare pegmatites are hosted in granites of the first and second groups. Garnet and tourmaline are common in pegmatites; iron-bearing gahnite (Zn,Fe)Al₂O₄ – a zinc spinel (ZnAl₂O₄) – was noticed (Goryachev and Kolesnichenko, 1990).

The silica content in rocks of the main facies varies from 69–72 to 75–77 wt %. Granites are commonly oversaturated with alumina; potassium slightly prevails over sodium. High Rb and low Sr contents are typical. Relationships between normative quartz, albite, and orthoclase contents are close to the ternary minimum at a water pressure of 1–2 kbar. The mineral and chemical compositions of the granite-leucogranite association reliably fit the S-type granites. The Rb versus (Y+Nb) relationships correspond to collision granites (Figs. 1.2, 1.3).

Rocks of the granite-leucogranite association were emplaced into Oxfordian and Kimmeridgian volcanics of the Uyandina-Yasachnaya Volcanic Belt and into Upper Jurassic terrigenous sediments of the In'yali-Debin Synclinorium. The granites are, in turn, cut by Early Cretaceous plutons and granite porphyry dikes. Granites of the abyssal group that intrude Callovian country rocks have the oldest Rb-Sr age of 169–162 Ma while the mesabyssal and hypabyssal granites are characterized by younger Rb-Sr ages of 154–151 Ma. The Ar-Ar method yields 145–135 Ma for all groups (Goryachev, 1998; Newberry et al., 2000). The recent K-Ar and Rb-Sr determinations suggest an older (up to Middle Jurassic) age of this association (Shpikerman, 2000; Kotlyar et al., 2001). However, it should be kept in mind that the overestimated Rb-Sr age of S-granites is a common and well-known phenomenon (Chappel and White, 1992).

Plutons of diorite-granodiorite and granite-leucogranite associations are spatially separated and contacts between them were not observed. It cannot be ruled out that they are coeval and related to the same collision event.

The Early Cretaceous granitoids are classified as *granodiorite-granite association*. They complete the collision cycle and are widespread in the Kular-Nera Slate Belt. The relatively small plutons, up to 300 km² in area, are composed of granodiorite passing into adamellite and of granite (Basugun, Stolovy, and

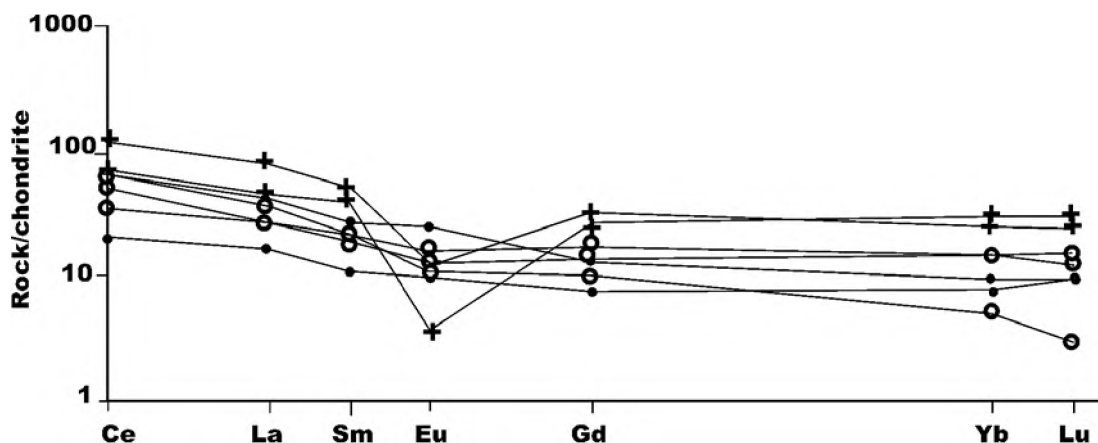


Fig. 1.3. The chondrite-normalized REE patterns for granitic rocks of the Yana-Kolyma belt. See Fig. 1.2 for legend

northern part of the Greater Annachag plutons). Diorite and quartz diorite intrusions are rare. Dark-colored minerals (biotite with $f = 0.60$ – 0.71 and hornblende with $f = 0.57$) occupy 6–13% of rock volume. The f value of coexisting biotite and amphibole increases up to 0.72–0.77 and 0.76–0.79, respectively in marginal and apical portions of plutons. Ilmenite, allanite, apatite, garnet, zircon, and sulfides (arsenopyrite, loellingite, etc.) are noticed as accessory minerals (Gamyagin et al., 1991; Goryachev, 1998). The rocks are typically oversaturated with alumina and enriched in potassium in comparison with similar rocks of the Late Jurassic–Early Cretaceous diorite-granodiorite association.

Granitic rocks of this association intrude Early Cretaceous volcanics in the Taryn volcanic structure, older granite-leucogranite association (Greater Annachag pluton) and diorite of the older diorite-granodiorite association (Basugun pluton). The Rb-Sr isochron age yields 128 ± 2.1 Ma and $Sr_i = 0.7141$ for the Basugun pluton. The K-Ar age of 127 Ma was reported for the northern Greater Annachag pluton. The biotite-amphibole granodiorite and granite plutons in the OCVB framework intrude volcanics of the Uda-Murgal arc and their fragments were found as xenoliths in Middle Cretaceous volcanic and subvolcanic rocks (*Mesozoiskaya...*, 1983). Granitic rocks are relatively rich in amphibole; sodium prevails over potassium in the main phases while the final silicic derivatives are potassic; magnetite is noticed (Sobolev, 1989). The age of granitic rocks was estimated as 140–110 Ma (Kotlyar et al., 2001).

Late Cretaceous granitoids are divided into granite-leucogranite and alkali granite associations. *The granite-leucogranite association* is widespread in Mesozoids. In the OCVB, granites and leucogranites are closely associated with Late Cretaceous rhyolites.

The exposed area of the biotite-bearing and two-mica leucogranite plutons reaches 300–500 km². The leucogranite is high-K and enriched in Rb. Accessory fayalite is typical; magnetite, allanite, fluorite, and tourmaline are noticed (Sobolev, 1989). Tin deposits are associated with leucogranites.

The alkali granite association largely consists of silicic plutonic rocks with biotite, aegirine, riebeckite, and arfvedsonite exposed as small (<100 km²) plutons. Monzodiorite is present as an older intrusive phase. The content of dark-colored minerals amounts to 3–8 vol %. Magnetite, rutile, and zircon are the most abundant accessory minerals; xenotime, fergusonite, and other REE-bearing minerals are also common. The total sum of alkali metal oxides attains 9–12 wt % with prevalence of Na₂O; elevated Zr, Y, and Nb contents are typical and indicate the presence of A-type granites (Goryachev and Khanchuk, 2002).

REGIONAL METALLOGENY

Specific metallogenic patterns of the Yana-Kolyma Fold System are determined by accretionary and postaccretionary metallogenic belts (Shpikerman and Goryachev, 1996; Nokleberg et al., 1997; Goryachev, 2002). The gold mineralization was formed at an accretionary stage including the deposits associated with Late Jurassic–Early Cretaceous diorite-granodiorite plutons and Early Cretaceous granodiorite-granite plutons. Economic tin and tungsten deposits are related to Late Jurassic and Early Cretaceous granite-leucogranite plutons dated as 145–130 Ma. Thus, the W-Sn-Au metallogeny is characteristic of the accretionary stage. Postaccretionary metallogeny is expressed in the formation of Au-Ag (Shkol'noe), Au-Sb (Sur'myanoe, Krokhalinoe, Bortovoe), and sparse Hg (Kuz'michanskoe) prospects pre-

sumably related to the Middle Cretaceous diorite (tonalite)-granodiorite association. Tin mineralization (Butugychag, Oboronoe), tungsten mineralization (Gusinoe), and uranium ore are related to Late Cretaceous granites. The youngest Au-Ag deposits (Karamken, Ushelnoe) and Ag-Sb deposits (Utro) are associated with Late Cretaceous rhyolite subvolcanic intrusions localized in the OCVB.

GEOLOGICAL HISTORY OF MESOZOIDES

The pre-accretionary (pre-Late Mesozoic) history of the Mesozoides in northeastern Asia is regarded as a sequence of rifting events (Goryachev, 1998; Shpikerman, 1998). The acceleration of the Kula Plate motion in the Late Mesozoic, opening the Canadian Basin, and change in kinematics of the North American Plate (Zonenshain and Natapov, 1987) gave rise to the formation of the Uyandina-Yasachnaya, Svyatoi Nos-Oloi, and other island arcs. The subsequent collision events resulted in a complete structural rearrangement. Oceanic and suboceanic basins were closed giving way to the formation of the Yana-Kolyma Collision Zone, folding, emplacement of granitic plutons, and related ore formation. The southeastern periphery of this zone was a region with interference of tectonic and magmatic processes induced by collision and subduction at the northeastern and southeastern continental margins, respectively (Goryachev, 2002). When spreading in the Canadian Basin ceased and the Kula Plate went on the move, the Okhotsk-Chukotka volcanic belt started to develop along a new continental margin.

SUBJECTS OF EXCURSION

The studied profile includes the southeastern Yana-Kolyma Folded Belt crossing the Ayan-Yuryakh Anticlinorium, In'yali-Debin Synclinorium, and structures of the Viliga Terrane. This is one of the most interesting areas of Late Mesozoic granitoid magmatism in northeastern Asia to get familiar with granitoids of various ages, compositions, and depth facies occurring in the Yana-Kolyma Fold System and with granitic rocks of the Okhotsk-Chukotka volcanic belt associated with volcanics.

The Magadan gabbro-granite batholith is exposed in cliffs of the Sea of Okhotsk coast in the vicinity of Magadan and on nearby islands. The area of outcrops on land extends in a latitudinal direction and covers 750 km². The batholith roof is broken into blocks, mainly as a result of neotectonic displace-

ments. The highest point of exposed granitoids lies at 935 m above sealevel. According to drilling results, the roof subsides elsewhere down to 200 m below sealevel. Plutonic rocks intrude Late Jurassic basic and silicic volcanics; the latter are developed only locally.

The Magadan batholith was built up in the course of a multistage emplacement sequence (Andreeva et al., 1999). Oldest is the Nyuklya Cape bimodal gabbro-granite series (138 Ma) followed by the Ola gabbrodiorite-granite series which is more sodic. The Magadan gabbrodiorite-granite potassic-sodic multiplex series (105 Ma) is the most widespread and completes the Early Cretaceous intrusive megarhythm. Late Cretaceous megarhythm begins with emplacement of the Svetly gabbro-granite series of sodic rocks (homologue of the older Nyuklya Cape series) and ends with emplacement of the Dukcha diorite-granodiorite sodic multiplex series (96 Ma). The rocks of all series have a low initial ⁸⁷Sr/⁸⁶Sr ratio of 0.7025–0.7045.

Small gabbro bodies crop out at Kamenny Venets and Nyuklya capes and are the oldest plutonic rocks in the batholith. Gabbro is a layered and characterized by spheroidal parting in central parts of the intrusive bodies. The dark brown, almost black color and coarse-grained (5–10 mm) texture in the central parts of intrusions pass to a lighter greenish gray color and fine-grained texture in marginal zones. Gabbroic and less abundant ophitic textures are typical. Anorthosite interlayers are noticed. The mineral composition is as follows (vol %): labradorite-bytownite (55–76), amphibole (15–23), diallage (5–18), hypersthene (0.5–11), and olivine (0.5–5.0); biotite, quartz, and K–Na-feldspar occur in insignificant amounts; titanite, apatite, zircon, spinel, garnet, and magnetite are accessory minerals. The high-Al chemical composition of gabbro is typical. Younger gabbroic rocks are devoid of olivine and gradually pass into gabbrodiorite and diorite that commonly surround granitoids or occur as large xenoliths therein.

Tonalite grading into granodiorite occupies 590 km² of the total batholith area. This is a light gray medium-grained rock having hypidiomorphic and monzonitic textures. The mineral composition (vol %) includes zoned plagioclase, An₂₈₋₄₀ (50), transitional microcline (12), quartz (25), and dark-colored minerals including amphibole, biotite, and less abundant augite (13). The microcline content in the small bodies drops to 4 vol %.

Pinkish gray, bright pink, and light gray coarse- and medium-grained biotite and amphibole-biotite

granites grade into porphyritic varieties and granite porphyry near contacts. Magnetite, titanite, apatite, zircon, and allanite are accessory minerals.

Subalkali and alkali granites were traced along the northern boundary of the batholith. The subalkali fine-grained, micropegmatitic or panidiomorphic granites consist of transitional microcline-perthite (60 vol %), quartz (37%), biotite (1%), and sparse grains of amphibole, titanomagnetite, and epidote (2 vol % in total). Amphibole, ore minerals, biotite, and epidote fill the interstitial space between quartz and feldspars and develop along fractures therein. The Rb-Sr age of granites is 117 Ma; $Sr_i = 0.7032$ (Andreva et al., 1999).

Small Mo deposits (Usinskoe, Osennee) and U prospects are associated with granitoids (Gelman et al., 1997).

The Sphinx granitic pluton and large-volume ignimbrites The Arman Depression – a typical volcanotectonic structure of the OCVB – is situated in the interfluvium of the Arman and Khasyn rivers, between 80 and 120 km west of the Kolyma Highland. A dome-shaped uplift of the basement, about 20 km in diameter, serves as the eastern framework of the depression. The dome core is composed of Jurassic marine sediments and Middle Cretaceous continental sandstone and conglomerate. These rocks host the Sphinx granitic pluton, about 2 km in diameter near its apex (Fig. 1.4). The pluton is composed of medium-grained amphibole-biotite granite and granodiorite with accessory apatite, zircon, allanite, and magnetite. Concentric conic and radial offsets surround the main body of pluton. The plutonic dome is rimmed by ignimbrite flows inclined outward. Immediately near the Sphinx pluton, the flows dip at angles of 55–60°; at a distance of 1.5–2.0 km the slope decreases to 25°. The uppermost ignimbrite flow lies approximately horizontally. The granitic pluton widens with depth underlying the entire ignimbrite field. Discrete outcrops of granites are observed in stream channels. The total area occupied by granitoids covers 165 km².

Numerous sills, dikes, and laccoliths of granite and granodiorite porphyries, felsite, and rhyolite reside on the limbs of the dome-shaped structure. The thickness of minor intrusions varies from 1–2 m to a few hundred meters. They are arranged either concentrically with respect to the granitic pluton or are cross-cutting (radial). The porphyry intrusive sheets, 100 m and more in thickness, were also emplaced into the main pluton. Structural and temporal relationships testify to the genetic links between granites, porphyry intrusions, and ignimbrites:

(1) Granite, granite porphyry, and intrusive rhyolites intrude Middle Cretaceous sandstones and conglomerates.

(2) All intrusive rocks and ignimbrites are, in turn, cut by dikes of Late Cretaceous hypersthene andesite and dacite.

(3) Fragments of medium-grained granite, up to 30 cm in size, were found in the uppermost ignimbrite flow unconformably overlying the older rocks. Granite fragments (up to 25 cm in size) and granitic rubble are also contained in the dike of hypersthene dacite that cuts the granite porphyry 10 m from the northern contact of the pluton.

(4) The lower (outward inclined) ignimbrite units contain homeogenic granitic inclusions similar to the granites from the Sphinx pluton.

(5) The core of the pluton is composed of medium-grained granite with plagioclase phenocrysts, up to 4 mm in size. The grain size diminishes toward the contacts and within offsets. Near the pluton roof, the grain size in the groundmass decreases to 0.1 mm. The rock texture becomes micropegmatitic. Plagioclase phenocrysts are reduced to 2–3 mm in dimensions, and large quartz grains appear. Granitic fragments in the ignimbrites and the hypersthene dacite dike match the granite from the pluton core, but are slightly enriched in K–Na feldspar. The degree of groundmass crystallinity and amount of plagioclase phenocrysts decreases from the sole to the roof of the sills. The granite porphyry groundmass is felsitic, micropegmatitic, micropoikilitic, and hypidiomorphic. No correlation between degree of crystallinity and dimensions of intrusive bodies was established. Intrusive rhyolite contains sporadic and small plagioclase phenocrysts.

Alunite-dickite altered rocks, Au-Ag deposits and prospects (Karamken, Ushchel'noe, Finish, etc.), and mercury occurrences are known from the Arman Depression (Speranskaya, 1963; Yeregin, 1974; Umitbaev, 1986).

The Karamken Au-Ag deposit (Ocherki..., 1994) is situated at the headwaters of the Khasyn River at the eastern margin of the Arman volcanotectonic structure. Orebodies are localized in a half-ring caldera filled with Middle Cretaceous silicic volcanics and rimmed by older volcanosedimentary and intermediate volcanic rocks. A composite sill of andesite, dacite, and rhyolite plunges toward the caldera center at angles 30–40° being controlled by arcuate faults. Two Middle Cretaceous sills, a western sill of plagiogranite porphyry and an eastern sill of granodiorite porphyry adjoin the composite sill in the north.

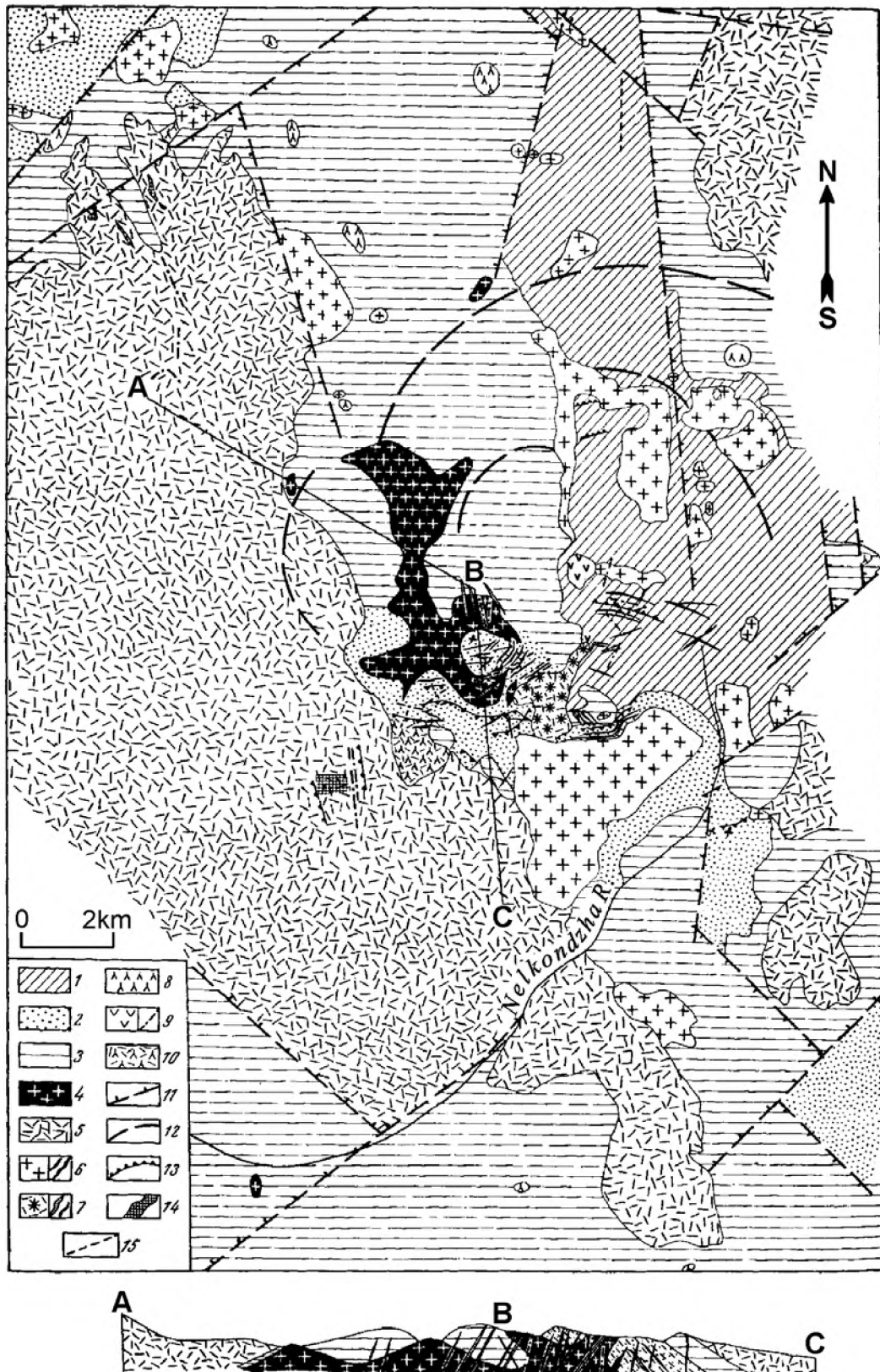


Fig. 1.4. Schematic geological map of the Arman volcanic structure and section along line A-B-C, after Speranskaya (1963). (1) Middle Jurassic terrigenous rocks; (2) Cenomanian-Turonian (2) sandstone, conglomerate, and (3) andesite; *Late Cretaceous igneous rocks*: (4) granitoids; (5) ignimbrite; (6) granite and granodiorite porphyries, (7) intrusive rhyolite and felsite, (8) hypersthene andesite, (9) intrusive hypersthene andesite, (10) hypersthene dacite; (11) normal faults; (12) ring faults; (13) strike and dip symbols; (14) altered volcanic rocks; (15) Paleogene basaltic dikes

The zonal fields of argillic and propylitic alteration were contoured within the ore field (Yeremin, 1974). Orebodies as adularia-quartz, carbonate-quartz, and quartz filling veins and as less abundant systems of nearly meridional thin veins steeply dip to the northeast. The veins are 0.6–3.0 m thick and extend for 500–600 m. The content of ore minerals is low (<1% of gangue material), but they are extremely diverse in composition: more than 60 minerals were found at the deposit (Ocherki..., 1994). Tiny disseminations of ore minerals dispersed in the gangue mass are often segregated as linear belts parallel to the vein selvages. Pyrite, sphalerite, chalcopyrite, canfieldite, freibergite, tennantite, naumannite, electrum, and native silver are the most abundant ore minerals. Quartz, adularia, and calcite dominate as gangue materials. An elevated Sn content is typical of the ore owing to the presence of canfieldite. Stannite occurs at deeper levels, and cassiterite appears below 400–500 m where the Sn grade reaches 3%. The fineness of gold varies from 650 to 570. Auriferous silver and native silver with up to 3.5% Au are noted. The Au-bearing phases

contain up to 2.2 wt % Se, 0.2 wt % Hg, and 1.6 wt % Cu. Selenium is also commonly detected in Ag-bearing polybasite (3.1 wt % Se) and canfieldite (5–11 wt % Se). The Se content abruptly drops with depth. The Au:Ag ratio in ore is 1:3 and occasionally falls to 1:100. The deposit is exhausted; 34 t of gold was mined out.

The Ushel'noe (Gorge) prospect is similar to the Karamken deposit but is smaller in dimensions.

The West Butugychag granitic pluton is situated at the interfluvium of Ten'ka and Detrin rivers, right tributaries of the Kolyma River (Fig. 1.5). Upper Permian clastic country rocks are transformed into hornfels. The pluton, equant in plan, occupies an area of ~35 km² and is accompanied by numerous thin off-sets. The northern, western, and southern contacts dip at angles of <30° while the eastern contact is steeper (up to 50°). Roof pendants are retained in the central part of pluton. The depth of erosion is estimated as 800 m. Coarse-grained porphyritic granite of the main intrusive phase passes into medium- and fine-grained varieties near the contact. Supplementary intrusions

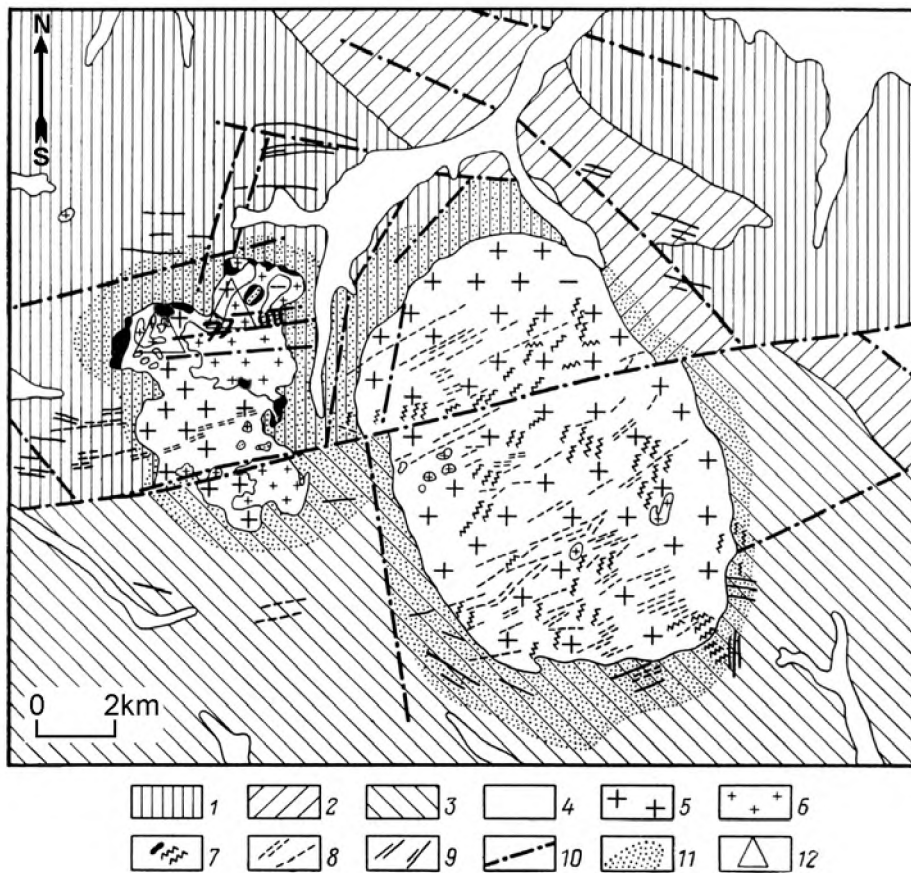


Fig. 1.5. Schematic geological map of the Butugychag ore field, after. Mikhailov.
Permian sedimentary rocks: (1) sandy-clayey, (2) sandy, (3) clayey; (4) loose sediments; (5) coarse- and medium-grained granites; (6) granite porphyry; (7) aplite dikes and stocks; (8) postgranitic dikes (granite porphyry, diorite porphyry, spessartite, diabase, and dolerite); (9) pregranitic dikes; (10) faults; (11) aureole of contact metamorphism; (12) tin deposit

are composed of aplites, fine-grained granites, and pegmatites. The granite of the main intrusive phase consists (vol %) of plagioclase An₁₅₋₄₅ (29–32), microcline (33), dark gray to black quartz (34–35), biotite (1–3) and accessory fluorite, ilmenite, allanite, zircon, titanite, garnet, and cassiterite (0.1–0.2). Potassic alteration along with subsequent albitization and greisenization are extensively developed. The cassiterite-quartz mineralization, fluorite and molybdenite occurrences are related to this granitic pluton.

The Butugychag Sn deposit is localized in the western part of the pluton (*Geologiya...*, 1986). The ore-bearing veins reach a few hundred meters in extent. Numerous offsets and bulges, up to 0.4 m thick, alternate with thread-like pinches. Towards their end the veins branch out into bundles of thin veinlets. Orebodies are linear stockwork zones of short, en echelon arranged veinlets (Fig. 1.6). The stockworks lie beneath the roof of pluton and occasionally adjoin it. Some veinlets penetrate the hornfels aureole. The vertical range of ore mineralization is measured in hundreds of meters.

Axial parts of veins and veinlets are composed of comb quartz, often in association with fluorite, muscovite, siderophyllite, calcite, and a small amount of sulfides; selvages consist of orthoclase. Cassiterite is closely associated with orthoclase overgrowths and replaces the feldspar crystals. The granitic wallrock is commonly greisenized. Cassiterite of the second generation and wolframite are related to the muscovite that replaces the feldspar. Sulfides make up the late mineral assemblage and together with carbonates occur at deeper levels than cassiterite.

The Ulakhan granitoid pluton is situated at the divide between the Ten'ka, Nel'koba, and Chalbyha rivers. The pluton extends for 20 km in a northwestern

direction reaching 9 km in width. The exposed area is about 80 km². Granitic rocks intrude the Upper Permian clastic sequence as two intrusive phases: older granodiorite and younger leucogranite.

Granodiorite is a medium-grained rock with plagioclase and less abundant amphibole phenocrysts, up to 1 cm in size. The rock consists (vol %) of microcline and orthoclase, the former being predominant (16), zoned oligoclase–andesine (46), quartz (31), biotite (6), amphibole (1), and accessory allanite, magnetite, apatite, and zircon.

The fine-grained leucogranite forms numerous dikes, up to 1 m thick, and three small stocks (0.12–1.3 km²) in the central part of pluton. The mineral composition is as follows (vol %): potassium feldspar (32), oligoclase (29), quartz (37), biotite (2), rare amphibole grains, and accessory allanite and zircon.

The postmagmatic alteration is insignificant: feldspars are slightly sericitized and biotite is partly replaced by chlorite.

The Igumenov Au deposit is one of the largest vein deposits in the Russian Northeast. More than 11 t of gold were mined out in 1946–1956. Remaining reserves are estimated as 5.5 t. The deposit, which is situated in the Ten'ka River basin and localized in the Ayan-Yuryakh Anticlinorium, was studied in detail by Firsov (1958). The host Upper Permian shales form an extended anticline of northwestern direction, a few kilometers in width, with dip angles of 5–20° on its limbs. The anticline plunges to the northwest at angles of 15–18°. The ore is metamorphosed in contact aureole of the Ulakhan pluton.

The gold-quartz veins fill steeply dipping longitudinal fissures in the fold crest (Fig. 1.7). The veins extend as sheetlike bodies, 0.5–0.8 m thick with bulges (up to 3.5 m) and pinches (~0.1 m), for 600–2000 m and dip at angles of 50–85° to the northeast.

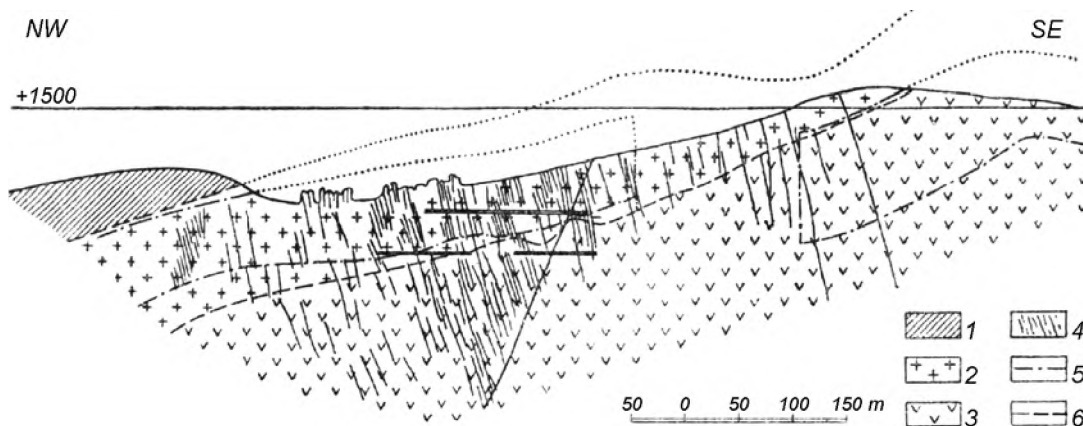


Fig. 1.6. Geological section across the Butugychag deposit, after Volodin. (1) hornfels; (2) medium-grained porphyritic biotite granite; (3) fine-grained porphyritic biotite granite; (4) veins; (5) ore zone contour; (6) intrusive contacts

The whole system of conjugated veins is traced for 4 km. The veins are broken by postmineral faults of three directions. The oldest faults existed before the vein filling but subsequently were rejuvenated as postmineral strike-slip faults. Younger low-angle reverse and strike-slip faults have a total slip as far as 100 m in a southwestern direction. The latest steeply dipping transverse normal and strike-slip faults displace the veins for less than 50 m. Cross-cutting relationships between gold-bearing veins and younger leucogranite dikes were observed in underground workings.

The low-sulfide (1–3% of sulfides) ore consists of arsenopyrite-quartz and gold-base metal mineral assemblages. Superimposed gold-bearing veins with molybdenite, pyrrhotite, loellingite, arsenopyrite, gold, and bismuth sulfotellurides are genetically related to the leucogranite. The latest carbonate-quartz-

stannite-base metal and adularia-quartz veins are probably related to the subvolcanic intrusions of spherulitic rhyolite (Firsov, 1958; Tyukova, 1989; Goryachev, 1998).

The Au grade increases in the upper levels with distance from the Ulakhan pluton. The average grade is 12–13 g/t Au. Local pockets and ore shoots complicate the general distribution of gold.

The Burgagyn granitoid stock is situated on the right bank of Ten'ka River in the southern Ayan-Yuryakh Anticlinorium and intrudes Upper Permian sedimentary rocks. The stock occupies about 5 km² and is elongated in the nearly N-S direction. Two intrusive phases are recognized: the older diorite and quartz diorite and the younger granodiorite and granite accompanied by dikes of aplite and aplite-like granite. The latitudinal dike suite of granite porphyry, diorite porphyry, and basalt cut the plutonic rocks

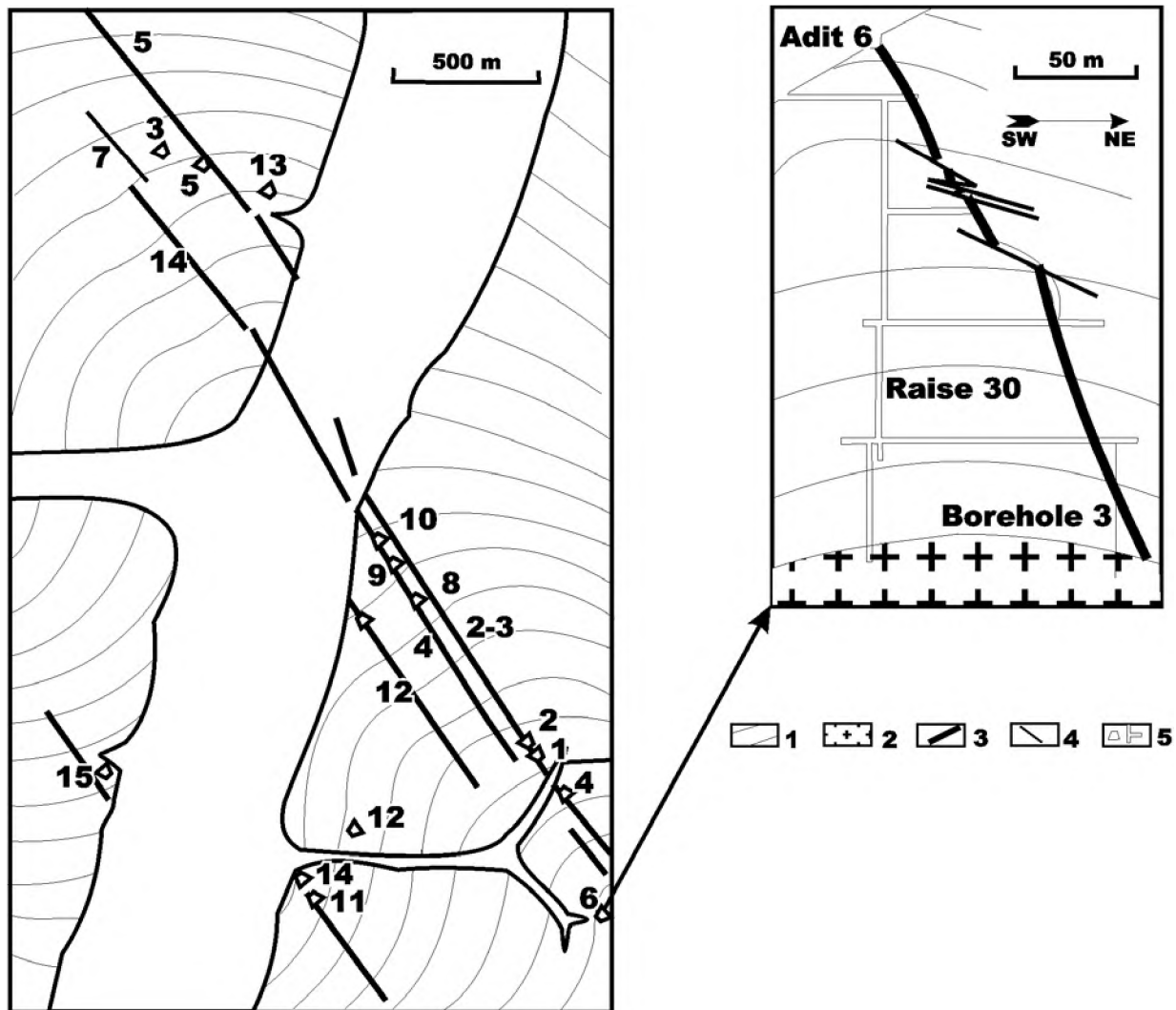


Fig. 1.7. Schematic geological map and section of the Igumenov deposit, after Firsov (1958).

(1) Permian sedimentary rocks transformed into hornfels; (2) granite; (3) gold-quartz veins; (4) faults; (6) workings

belonging to both phases. Dark-colored minerals in intermediate rocks of the first phase are composed of common hornblende, high-Ti (4.1 wt % TiO₂) biotite with $f = 0.74$, hypersthene ($f = 0.48-0.53$), and clinopyroxene ($f = 0.49$). The assemblage of hornblende and lower-Ti (2.8–3.6 wt % TiO₂) biotite with $f = 0.76-0.77$ is typical of granodiorite belonging to the second phase. Feldspars are composed of zonal plagioclase (An₆₈₋₂₅) and orthoclase (Shevchenko, 1996). Ilmenite (2.6–3.7 wt % MnO), being prevalent among accessory minerals, contains pyrophanite (in granodiorite) and magnetite (in diorite) inclusions. Apatite (0.1% MnO, 2.05% F, 0.71% Cl, and 0.5% REE) is observed in all rocks. Garnet (10% Py, 16% Gros, and 67% Alm) was identified in granodiorite along with

zircon and rare corundum grains. Pyrrhotite, pyrite, chalcopyrite, Co-bearing (up to 3.8 wt % Co) loellinite, and high-As arsenopyrite occur as ore minerals. Greisen zones and stockworks of quartz veins with gold mineralization are related to the granitoids.

The Burgagyn stock corresponds to diorite–granodiorite association in mineral and chemical compositions. The K-Ar, Ar-Ar, U-Pb, and Rb-Sr estimates yield an age of 146–152 Ma (Newberry et al., 2000; Goryachev, 1998).

The Shkol'noe Au deposit of a peculiar gold-silver-quartz type is localized in the Burgagyn stock (Fig. 1.8). The nearly latitudinal lenticular quartz veins, up to 1 m thick, are arranged *en-echelon* down dip forming a common vein zone. Particular veins

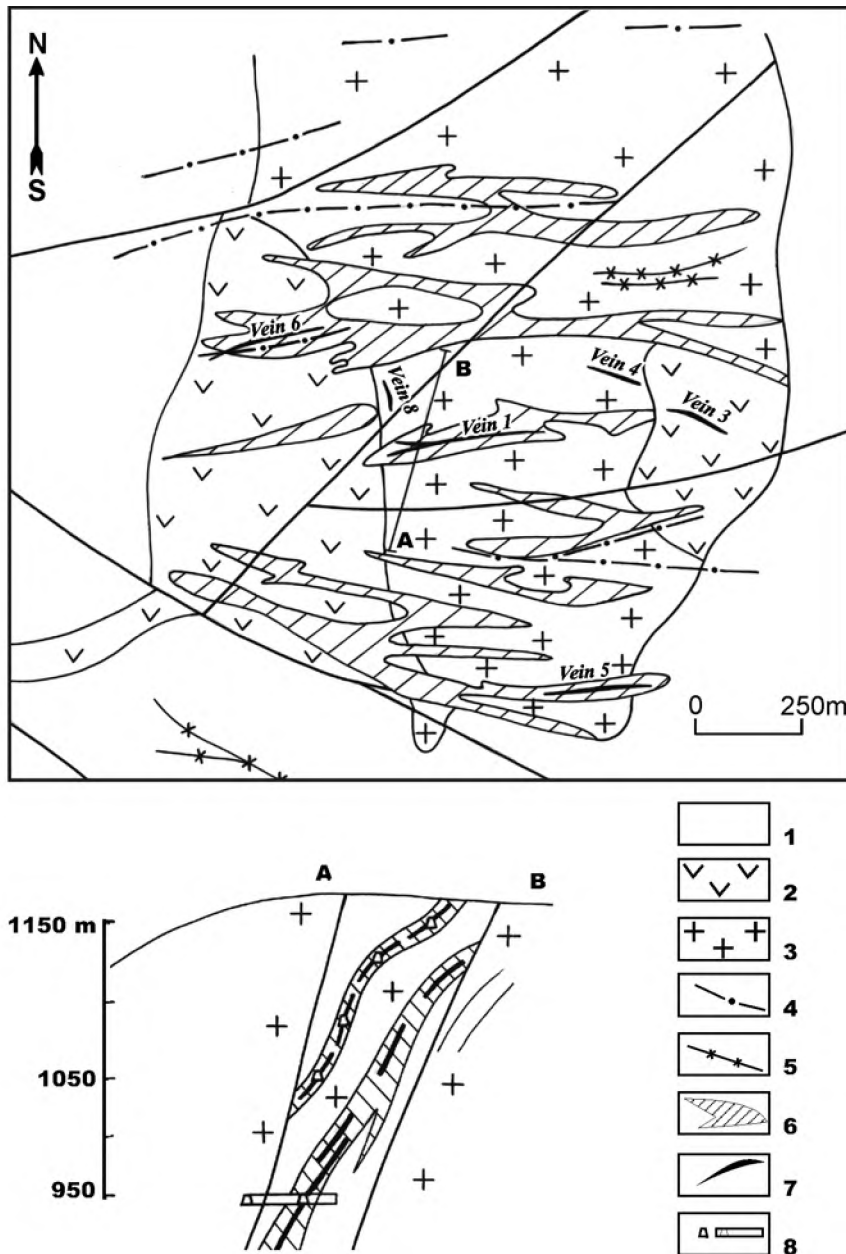


Fig. 1.8. Schematic geological map of the Shkol'noe deposit, after Goryachev et al. (1994). (1) Permian sedimentary rocks; (2) diorite; (3) granodiorite and granite; (4) diorite porphyry, (5) granite porphyry; (6) zone of metasomatic alteration; (7) gold-silver-quartz veins; (8) workings (shown only on the section)

extend for a few hundred meters along strike and down dip.

The veins are composed of fine-grained, often drusy or rodlike milky white quartz with fine disseminations and sporadic pockets of freibergite (16–25 wt % Ag) and native gold. Pyrite, sphalerite, galena, arsenopyrite, jamesonite, boulangerite, and pyrargyrite are less abundant. Ore minerals (1–3 vol %) form elongated segregations in quartz. The Au/Ag ratio in ore is close to unity. The fineness of gold (730–880) varies with depth in a wavelike manner (Goryachev, 1992). The variety with a low fineness (up to 600) is developed only locally. The ore is high-grade, especially at the upper levels, where the grade reaches 50 g/t. At a depth of a few hundred meters the grade diminishes. The host granitoids are affected by phyllic and argillic alteration and often contain fine pyrite and arsenopyrite disseminations.

The gold-silver-quartz veins cross-cut not only granitic rocks but also postgranitic dikes having an age of about 100 Ma (Alshevsky and Lyuskin, 1990; Newberry et al., 2000). The K-Ar age of phyllic and argillic altered rocks is 124 Ma.

A gold-quartz vein with arsenopyrite, loellingite, bismuth tellurides, sulfotellurides, and maldonite was found on the western flank of deposit. The cross-cutting dike of basaltic andesite is dated as 119 Ma. Stibnite-quartz veins are localized in the zone where the Southern Fault transects the hornfels.

Granitoids of the Omchak ore district. This district includes the well-known Natalka gold deposit and is related to the Ten'ka metallogenic zone of the Yana-Kolyma belt (Fig. 1.9). The zone extends for 150 km in a northwestern direction toward the Kulu River. This direction controls numerous shear zones and zones of greenschist metamorphism in Upper Permian clastic rocks, as well as basic and acid dikes. Small plutons are localized in the framework of this metallogenic zone. The Necha granitoid pluton occupies an area of ~230 km² and consists of two domes divided by a screen of Permian sedimentary rocks. The pluton is composed of amphibole-biotite porphyritic granite and granodiorite that are cut by lenticular leucogranite bodies. Cretaceous volcanics are retained as a roof pendant. The granitic rocks were likely emplaced into the core of an ancient volcano.

The inset map demonstrates the localization of plutons in the central Ayan-Yuryakh Anticlinorium: (1-3) Permian rocks, (4) Triassic rocks, (5) volcanic rocks of the Okhotsk-Chukotka belt, (6) granitic plutons, (7) main gold deposits.

The Vanin stock between the Letchik and Vanin creeks, right tributaries of the Omchak River, belongs to the subvolcanic facies. The main body of the stock is composed of quartz diorite and granodiorite while younger andesite, dacite, and rhyolite occur in its western portion. In the south, the stock is surrounded by explosion breccia consisting of large fragments of diorite, dacite, rhyolite, andesitic and dacitic tuffs, siltstone, and quartz veins cemented by a rhyolitic matrix. A similar breccia exposed two kilometers away contains only siltstone fragments. The breccia is severely pyritized close to the Vanin stock and cut by veins of chalcedony-like quartz with fine pyrite and arsenopyrite disseminations.

Small intrusive bodies composed of rocks varying in composition from gabbrodiorite and monzodiorite to quartz diorite, granodiorite, and quartz syenite are also known within the Omchak ore cluster. Dikes of lamprophyres (spessartite), diorite and granodiorite porphyries, and rhyolite concentrate in ore fields. Lamprophyres and diorite porphyry are the oldest. Most dikes are oriented concordant to the strike of sedimentary rocks; some dikes are related to fault zones. Dikes vary in thickness from 1–2 to 6–8 m; particular dikes are 15–20 m thick. The rocks of minor intrusion make up a continuous series from 50 to 77.5 wt % SiO₂. The enrichment in potassium is typical; potassium feldspar is contained in intermediate rocks in appreciable amounts, up to their transition to monzonite and syenite.

The Natalka Au deposit was discovered in 1942 and then became a subject of studies for many researchers. The consolidated description of this deposit is given by Goncharov et al. (2002). The Main and Northwestern faults bound a wedge-shaped tectonic block that hosts the ore mineralization. This block is composed of Permian clastic rocks, more than 2.5 km in total thickness (Pionersky, Atkan, and Omchak formations listed from older to younger). These rocks form the Natalka Syncline extending for 4.5 km in a northwestern direction having a width of 2.5 km.

Longitudinal and oblique tectonic sutures that complicate the southwestern limb of the Natalka Syncline control the ore zones. In cross section they look like a bundle converging downward. Sulfide disseminations, linear stockworks, and veins are combined in the ore zones. The linear stockworks are composed of longitudinal and diagonal systems of veinlets that pass along strike and down dip into short veins, up to 10–20 cm in thickness. The stockworks are accompanied by sporadic or continuous silicification. Vein material amounts to <5% of the total ore mass (Yeremin and Osipov, 1974); the rest is sulfide disseminations.

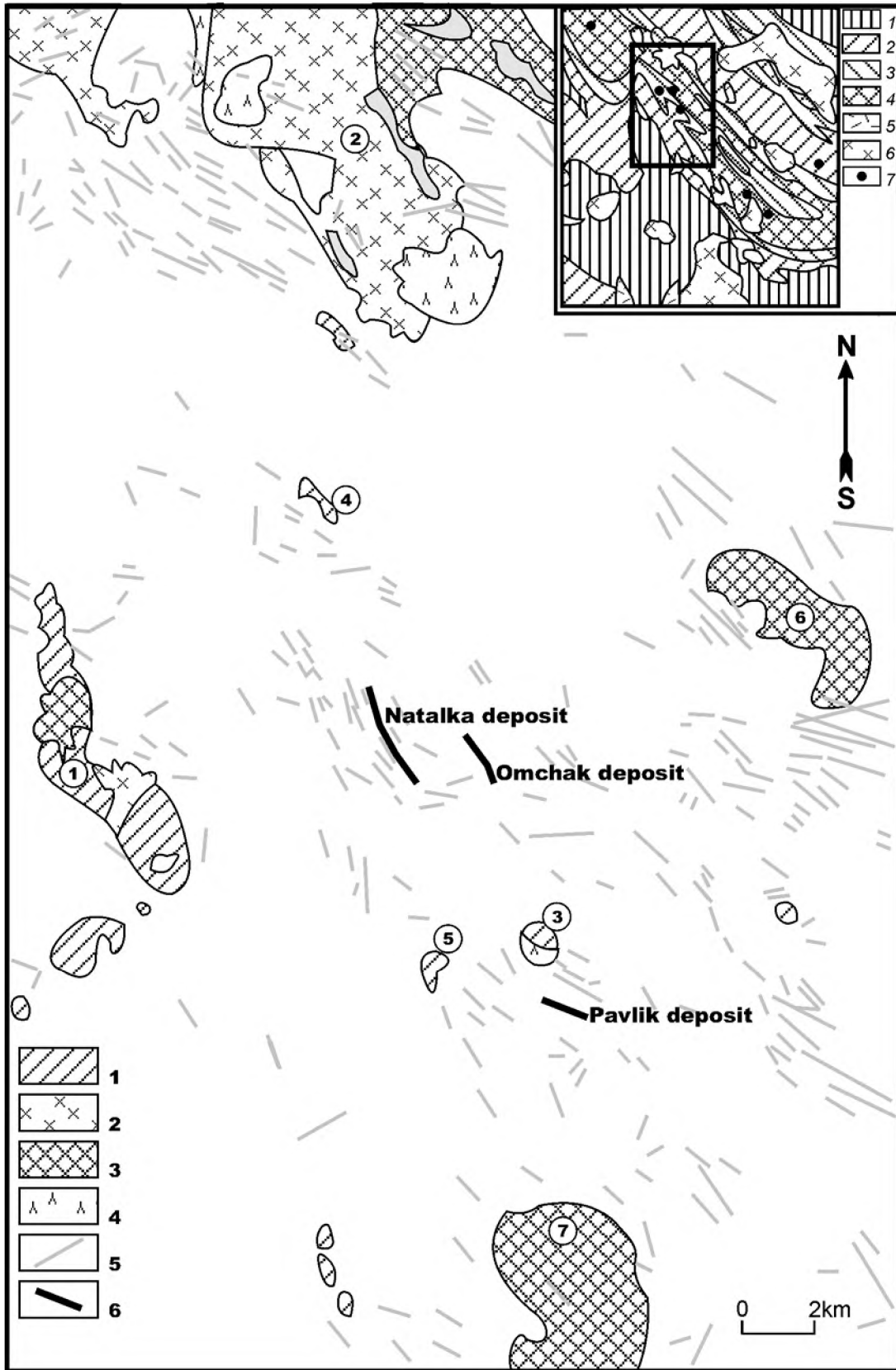


Fig. 1.9. Granitic plutons in the Omchak ore cluster.

(1) gabbro and diorite; (2) granodiorite; (3) granite; (4) Lower Cretaceous volcanics; (5) dikes; (6) gold deposits.

Plutons (numerals on map): (1) Intrigan-Peresykino, (2) Nechin, (3) Vanin paleovolcano, (4) Butuz, (5) Vilka, (6) Mirazh, (7) Tengkechan

Gold is distributed unevenly in the ore zone concentrating in elongated ore shoots, concordant and discordant with respect to the host rocks. Diamicrites of the Atkan Formation are most favorable for localization of the ore. Submicroscopic gold occurs in arsenopyrite and pyrite in quantities of tens and hundreds ppm. Quartz veins and veinlets contain gold clots, wires, sheets, spongy, dendritic grains, and crystals, up to 2–3 mm in size. Pyrrhotite, albite, adularia, ankerite, dolomite, calcite, less abundant scheelite, and rare ‘fahlore’ (2.0–12.7% Ag), bournonite, boulangerite, and stibnite are associated with gold.

At the Pavlik deposit, similar to the Nataika deposit and situated near the Vanin stock, the orebodies are cut by a dike of explosion rhyolite breccia. This indicates that the ore mineralization is not younger than Early Cretaceous as supported by K-Ar age of premineral dikes (155–130 Ma) and postmineral dikes (115–55 Ma). The Ar-Ar age of metasomatic rocks yields 135 Ma (Firsov, 1985; Newberry et al., 2000).

The Trubny granitic pluton is situated in the middle reaches of the Debin River, a left tributary of the Kolyma River. The pluton, about 35 km² in area, extends for 15 km in a northwestern direction and is 1–4 km wide. The low-angle contacts have tortuous contours. Granites intrude the syncline core composed of Middle Jurassic sandstone, siltstone, and shale. The hornfels aureole attains 2 km in width. The Trubny pluton consists of biotite and two-mica granites with alkali feldspar and quartz phenocrysts. The average mineral composition is as follows (vol %): albite-oligoclase (25–30), alkali feldspar (30–35), quartz (30–40), biotite (2–10), muscovite (<1); cordierite, apatite, zircon, and ilmenite are accessory minerals; acicular tourmaline is noticed. Final injections of granite porphyry, aplite-like granite, and aplite completed emplacement of the pluton.

The Greater Annachag granitic batholith occupies the mountain range on the right bank of the Debin River and extends to the Kolyma River. The Mount Aborigin (2589 m) is one of the highest peaks in the Chersky Mountain System. The batholith, 1360 km² in area, consists of two morphologically separate southern and northern portions of different ages (Fig. 1.10). The southern portion is composed of the older two-mica granite with accessory garnet, cordierite, and other high-alumina minerals. Two intrusive domes occur in anticlines made up of Upper Triassic and Lower Jurassic sequences. As with the folds, the intrusive domes are elongated in the northwestern direction and are divided by a roof pendant of

hornfels. The orientation of feldspar megacrysts, small flattened hornfels xenoliths, melanocratic and leucocratic schlieren, and lenticular quartz segregations stresses a ridge-shaped morphology of the southern dome with steep lateral contacts.

About 80% of the southern intrusive body is occupied by coarse-grained porphyritic two-mica granite of the main intrusive phase and by inequigranular two-mica granites of supplementary intrusions. The

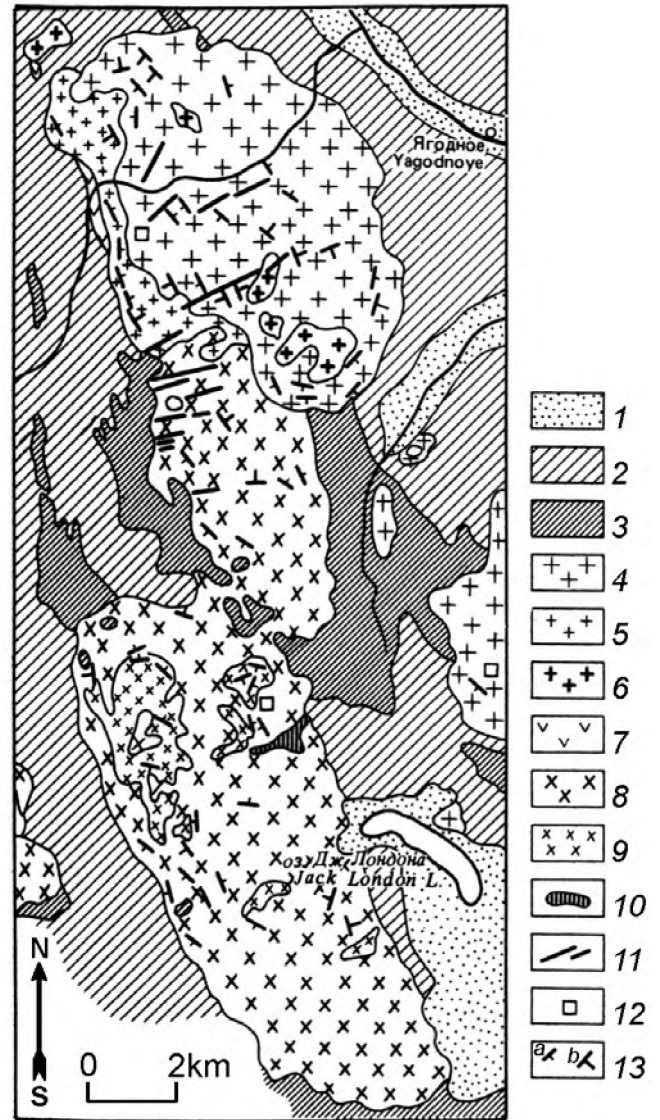


Fig. 1.10. Schematic geological map of the Greater Annachag granitoid pluton.

- (1) Quaternary sediments; (2) Jurassic and (3) Triassic sandstones, siltstones, and shales; *igneous rocks*: (4) coarse-grained biotite granite, (5) granodiorite, monzonite, granodiorite porphyry, (6) quartz syenite, (7) quartz monzonite, (8) coarse-grained two-mica cordierite- and garnet-bearing granite; (9) inequigranular granite; (10) subvolcanic dacite; (11) trachyandesite, basalt, and subalkali rhyolite dikes; *primary banding of granite*: (12) horizontal; (13) inclined: (a) steeply and (b) gently dipping

inequigranular granite forms a large body in the core of the southern ridge-shaped dome. The morphology of this body is interpreted as an overturned drop with numerous offsets.

The mineral composition of the main intrusive phase is as follows (vol %): zoned plagioclase, An₅₄₋₁₀ (32 ± 2), microcline (25 ± 2), quartz (34 ± 2), biotite with $f = 0.77$ (5 ± 1), muscovite (3 ± 0.5), and cordierite (~1). Garnet, andalusite, spinel, ilmenite, apatite, zircon, monazite, xenotime, rutile, as well as anatase, scheelite, pyrite, pyrrhotite, chalcopyrite, and arsenopyrite are accessory minerals. Muscovite largely replaces biotite. Plagioclase aggregates, occasionally with biotite and quartz, 1.5–2.5 cm in diameter, are incorporated into the medium-grained biotite-quartz-microcline groundmass. Garnet and cordierite are enclosed in plagioclase crystals. Cordierite is often idiomorphic relative to plagioclase while garnet is severely corroded. The near-contact zones, 10–50 m wide, are composed of distinctly porphyritic rocks containing plagioclase, quartz, biotite, microcline, cordierite, and garnet phenocrysts.

The texture of the inequigranular granite is variable. The mineral composition is close to that of the main intrusive phase (vol %): plagioclase (30 ± 3), microcline (29 ± 3), quartz (34 ± 3), biotite (4 ± 1), and muscovite (2 ± 1); however, plagioclase is more sodic.

The northern portion of the Greater Annachag batholith is composed of younger granite with a slightly elevated alkalinity. In general, this is an asymmetric dome elongated in a northwestern direction and related to the same N-S fault that controls the localization of the southern domes. The eastern and northern contacts gently (15–20°) plunge beneath sedimentary rocks. According to the geophysical evidence, the batholith is connected in the southeast with the Uaza-Ina pluton. The western contact dips outward at angles of 50–80° while the southern contact plunges at angles 50–60° beneath the southern granites. A quartz monzonite dike impregnated with sulfides is traced for 7 km along the western margin of the batholith having a thickness of about 300 m. This dike is cut off by the contact of the granite. Acid metavolcanics, which were found as roof pendants, and quartz monzonite dike are regarded as relics of a volcanic structure that was intruded by granites. A small subvolcanic dacitic body that intrudes the southern granite is probably related to the same stage of volcanic activity. Thus, the younger granites in the north of the batholith reveal close relations to volcanics.

The coarse-grained biotite granite occupies approximately 70% of the area of the northern portion of the batholith and passes into a fine-grained variety in the apical part. In the west, the granite gives way to granodiorite and granodiorite porphyry, quartz syenite, and monzodiorite. Supplementary intrusions of leucogranite and granite porphyry occur. Granites are cut by dikes of trachyandesite, rhyolite, and basalt extending in the northeastern direction. The mineral composition of the main intrusive phase is as follows (vol %): plagioclase, An₁₀₋₃₀ with cores of andesine-labradorite (30 ± 2), orthoclase-perthite (32 ± 4), quartz (35 ± 3), biotite (3.0 ± 0.5); zircon and allanite are accessory minerals. Small miarolitic cavities filled with carbonate and chlorite, pegmatite lenses with tourmaline, muscovite, pyrite, arsenopyrite, and less abundant gadolinite and Bi minerals are observed in the granite. The structure of the Greater Annachag batholith is shown in Fig. 1.10.

The Odinokii granitoid stock is situated on the left bank of Debin River. The stock is an ellipse (7×3 km) in plan with a long northwestern axis extending conformably with Middle Jurassic country shales and siltstones. The stock is composed of a medium-grained granite. In the northwest and southeast, quartz diorite occurs near the contact. The light gray granite is composed of plagioclase, An₃₀₋₅₇ (36 vol %), K-Na-feldspar (21%), quartz (32%), biotite (9%), and hornblende (2%). Veins of fine-grained biotite granite, aplite, granite porphyry and lamproites cut the granite. A quartz vein with arsenopyrite, Bi minerals, and native gold was found in the central part of the stock.

The granitic batholith of Bol'shie Porogi (Big Rapids) crops out as a mountain chain transected by the Kolyma River valley. The batholith covers an area of 600 km² as an ellipse elongated in the meridional direction. The northern and eastern contacts dip steeply (70–80°) outward; the southern and western contacts are inclined at angles of 30–50°. The batholith is composed of monotonous porphyritic biotite granite: plagioclase, An₂₅ (52 vol %), microcline (27%), quartz (34%), and biotite (8%). The hypidiomorphic texture is coarse-to-medium-grained, occasionally fine-grained. Tabular megacrysts of potassium feldspar, about 2 cm in size, are typical. Myrmekite is extensively developed, and potassic alteration is noticed. Rounded xenoliths of granitized rocks are observed. Adamellite rims are traced along the contacts. Biotite is characterized by $f = 0.63-0.66$ and contains 2.5–3.5 wt % TiO₂. The chemical composition of granite from the central and near-contact (numerals in parentheses) facies is as follows (wt %, av-

erage of 6 samples): 71.52 (69.85) SiO₂, 0.46 (0.46) TiO₂, 14.57 (15.35) Al₂O₃, 0.54 (0.78) Fe₂O₃, 1.85 (2.84) FeO, 0.05 (0.06) MnO, 0.68 (1.12) MgO, 2.14 (2.72) CaO, 3.35 (3.26) Na₂O, and 4.34 (3.51) K₂O.

The Stolovy granitic pluton is situated at the divide between Orotukan and Utinay rivers, right tributaries of the Kolyma River. The pluton, 32 km² in area (7.3×4.5–5.0 km), is composed of uniform pinkish gray medium-grained, slightly porphyritic granite having the following mineral composition (vol %): plagioclase, An₂₅₋₅₀ (36), K–Na-feldspar (27), quartz (26), biotite (11), hornblende (3), apatite, zircon, allanite, titanite, and ilmenite as accessory minerals (1). Xenoliths of country rocks were observed near the contacts. The near-contact zone is enriched in dikes of fine-grained granites, aplites, pegmatites, and quartz veins. Gold occurrences are associated with this granite.

The Utinskoe Au deposit (Ocherki..., 1994; Goryachev, 1998) is localized a few kilometers north of the Stolovy granitic pluton. Orebodies are contoured as mineralized dikes of intermediate and acid compositions cut by variously oriented quartz, quartz-albite, and quartz-albite-calcite composition veinlets locally impregnated with arsenopyrite, pyrite, sphalerite, boulangerite, jamesonite, and native gold. Particular

dikes were traced for 10–12 km with mineralized segments, up to 5 km long (Fig. 1.11). The thickness of dikes varies from 0.1 to 20 m.

Dike no. 7 was explored to a depth of 600 m. This dike extends along a tectonic zone, 1–10 m thick, as a sheet of diorite porphyry, 0.5–3.5 m in thickness, accompanied by parallel offsets. Pinches and boudinage are typical. Acicular phenocrysts of dark-colored minerals concentrate near the dike contacts and are oriented parallel to the curved contacts. The diorite porphyry is sericitized, albitized, chloritized, carbonated and contains arsenopyrite and pyrite. Segments with the highest veinlet density are enriched in gold. Gold concentrates in extended ore shoots with a grade of 50–300 g/t. The fineness of gold varies from 650 to 980 throughout the deposit and from 880 to 980 in dike no. 7. Pyrrhotite-arsenopyrite-albite-ankerite-quartz, gold-chalcopyrite-sphalerite-galena, gold-tetrahedrite-jamesonite-boulangerite, and antimonite-chlorite-calcite mineral assemblages are recognized (Gamyanin et al., 1991). The ore contains 93–95% of quartz, 3–4% of carbonates, 1–2% of albite, and about 1–3% of sulfides. Lateral and vertical mineral zoning with a prevalence of sulfosalts at the upper levels is typical. Dikes on the right bank of the Kolyma River belong to the diorite-granodiorite association (158–145 Ma). The mineralized dikes are metamorphosed at

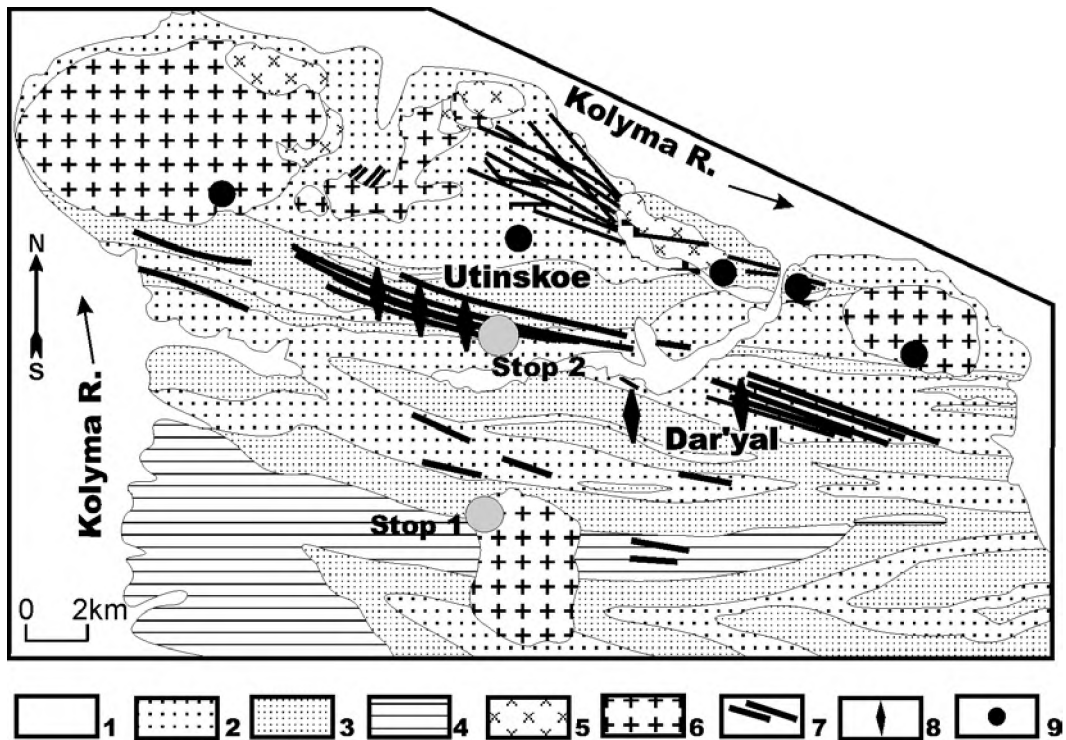


Fig. 1.11. Schematic geological map of the Basugun'insky ore-magmatic cluster, after Goryachev (1998). (1) alluvial sediments; (2) Middle Jurassic, (3) Lower Jurassic, and (4) Upper Triassic sandy and clayey rocks; plutons belonging to (5) diorite-granite and (6) granodiorite-granite associations; (7) dikes of diorite-granodiorite association; (8) gold-quartz deposits; (9) gold-rare-metall-quartz deposits

5 Ma). The mineralized dikes are metamorphosed at contacts with intrusions of the granodiorite-granite association (125–115 Ma) (Gamyandin et al., 1991).

The Gusiny granitoid pluton, 41 km² in area, is situated in the lower reaches of the Gerba River. The pluton intrudes Upper Triassic and Jurassic rocks and is overlain by Late Cretaceous volcanics. The uneven intrusive contacts are accompanied by numerous offsets. The pluton was emplaced during two intrusive phases. The first phase is composed of monzonite, quartz monzonite, monzodiorite, and quartz monzodiorite. These inequigranular and occasionally porphyritic rocks occupy more than 80% of the pluton area. The rocks contain rounded melanocratic inclusions, especially abundant near the contact. The second phase consists of granodiorite passing into tonalite and granite that occur near the contacts and in the northwestern portion of the pluton porphyritic varieties are noticed. Granodiorite contains xenoliths of plutonic rocks belonging to the first phase. The porphyritic granodiorite consists of potassium feldspar

(24 vol %), plagioclase, An₃₅ (41%), quartz (28%), biotite (7%), hornblende (<1%), and ilmenite.

The Butarny granitic pluton, 4.5 km² in area, is situated at the headwaters of Nechayanny Creek. The medium-grained biotite granite grades into porphyritic rocks near the contacts. Aplite dikes are traced. The clastic country rocks with limestone interlayers are Triassic and Jurassic in age. The clastic rocks are transformed into hornfels, and carbonate rocks are replaced by skarn. In the southeast, the granite is overlapped by basaltic andesite and andesite of the Ola Formation and cut by diorite porphyry and dolerite dikes. Granite affected by phyllic alteration was reported from borehole cores.

The Butarny Au deposit is localized in the western part of a granitic pluton bearing the same name. The ore mineralization concentrates in zones of quartz veins and veinlets, 1–3 m thick and up to 1 km long. These zones were traced by boreholes to a depth of 100 m. Orebodies are arranged *en-echelon* in shear zones between two steeply dipping faults of north-

Table 1.2

Average chemical composition (wt %) of granitic rocks from some plutons (main intrusive phases), after Kotlyar et al. (2001)

Oxide	West Butugychag (32)	Gusiny (1)	Butarny (2)	Ulakhan (13)	Burgagyn (15)	Trubny (3)	North Greater Annachag (5)	South Greater Annachag (10)	Odinokii(9)	Big Rapids (8)	Stolovy (12)	Sphinx (5)
SiO ₂	75.44	65.48	68.48	69.43	68.37	70.38	71.75	72.25	69.34	71.33	66.77	73.19
TiO ₂	0.12	0.65	0.42	0.33	0.33	0.42	0.23	0.21	0.29	0.46	0.46	0.21
Al ₂ O ₃	13.22	15.3	15.49	15.69	15.57	15.28	14.76	14.90	15.36	14.58	15.98	14.28
Fe ₂ O ₃	0.89	2.19	0.88	0.64		1.00	0.58	0.49	0.82	0.52	1.22	0.63
FeO	1.11	2.19	2.70	2.31	4.21	2.32	1.27	1.11	2.63	1.88	3.41	1.52
MnO	0.04	0.03	0.44	0.06	0.05	0.05	0.03	0.03	0.03	0.05	0.04	
MgO	0.13	1.67	0.88	0.85	0.81	0.82	0.46	0.52	1.05	0.74	1.27	0.39
CaO	1.01	4.20	2.08	3.17	3.01	1.44	1.42	1.54	2.69	2.15	2.82	1.29
Na ₂ O	3.05	2.45	3.78	3.64	3.69	3.05	3.82	3.41	3.19	3.37	3.36	3.88
K ₂ O	4.55	4.44	4.1	3.36	3.27	4.20	4.59	4.53	3.80	4.47	4.04	3.73
P ₂ O ₅	0.02			0.12	0.15	0.26	0.13	0.20	0.07	0.13	0.15	
LOI	0.50	1.16		0.36	0.58	0.95	0.67	0.59	0.90	0.49	0.62	
Total	100.08	101.77		99.96	100.04	100.17	99.71	99.78	100.17	100.17	100.14	
Rb	370 (4)			86 (31)		170 (3)	210 (9)	140 (16)	135 (8)	145 (7)	134 (6)	
Sr	40			290		104	110	83	126	130	133	
Ba	120			730		470	186	260	645	550	910	
Y												
Nb												
Zr												
Cl	<50			260		<50	90	67	115	<50	114	
Sr ₀							0.7085	0.7082			0.7086	

eastern direction and in auxiliary shear and tensile fractures. The native gold is fine-grained and largely confined to arsenopyrite along with native bismuth and bismuthine. Gold grains hosted in quartz are detected only sporadically. Quartz and arsenopyrite underwent cataclasis. Thin zones of phyllic and argillic alteration with disseminated arsenopyrite rim the vein and veinlet systems. Late veinlets of comb zoned quartz with fine-crystalline arsenopyrite and acicular stibnite are localized on the northern flank of the deposit. It is suggested that the gold mineralization of the first stage was formed in the Early Cretaceous (granite is dated as 136–138 Ma) while the late stibnite-arsenopyrite mineralization is related to the evolution of the Okhotsk-Chukotka volcanic-plutonic belt.

EXCURSION POINTS

Stop 1. *The Magadan batholith*

Subalkali and alkali granites were traced along the northern boundary of the batholith. In particular, a pink leucocratic subalkali granite of the northern batholith margin crops out at the cliffs of the Uptar River bank (45 km of the main highway). The fine-grained, micropegmatitic or panidiomorphic subalkali granite consists of the transitional microcline-perthite (60 vol %), quartz (37%), biotite (1%), and sparse amphibole, titanomagnetite, and epidote grains (2 vol % in total). Amphibole, opaque mineral, biotite, and epidote fill the interstitial space between quartz and feldspars and develop along fractures therein. The Rb-Sr age of granite is 117 Ma; $Sr_1 = 0.7032$ (Andreeva et al., 1999).

Stop 2. *The Sphinx granitic pluton*

The granites exposed in the Agan and Sphinx river valleys will be examined. The dome core is composed of Jurassic marine sediments and Middle Cretaceous continental sandstone and conglomerate. These rocks host the Sphinx granitic pluton, about 2 km in diameter near its apical portion. The pluton is composed of medium-grained amphibole-biotite granite and granodiorite with accessory apatite, zircon, allanite, and magnetite. Concentric conic and radial offsets surround the main body of pluton. The plutonic dome is rimmed by ignimbrite flows inclined outward. Immediately near the Sphinx pluton, the flows dip at angles of 55–60°; at a distance of 1.5–2.0 km, the slope decreases to 25°. The uppermost ignimbrite unit lies approximately horizontally.

Stop 3. *The Karamken gold and silver deposit*

The epithermal gold and silver deposit has been mined out by the time being. It will be examined at the surface of the Main ore zone. Fragments of ore-bodies and host volcanic rocks will be seen in surface workings.

Stop 4. *The West Butugychag leucogranitic pluton*

The western portion of the pluton near its contact is exposed along the Butugychag Creek, where various textural types of granites, aplite dikes, and cassiterite-quartz veins crop out. The coarse-grained porphyritic granite of the main intrusive phase passes into the medium- and fine-grained varieties near the contact. The supplementary intrusions are composed of aplite, fine-grained granite, and pegmatite. The granite of the main intrusive phase consists (vol %) of plagioclase An_{15-45} (29–32), microcline (33), dark gray to black quartz (34–35), biotite (1–3) and accessory fluorite, ilmenite, allanite, zircon, titanite, garnet, and cassiterite (0.1–0.2). The potassic alteration is extensively developed along with subsequent albitization and greisenization. The cassiterite-quartz mineralization, fluorite, and molybdenite occurrences are related to this granitic pluton.

Stop 5. *The Butugychag tin deposit*

The cassiterite druses on granitic walls of ore veins, quartz-K-feldspar-fluorite veins and veinlets in granites, sulfide veinlets, and greisen zones will be demonstrated in workings within ore zones mined out by the present time. Besides the geological observations, participants in the excursion will have an opportunity to see remains of the prisoner camp once well-known in the Dalstroi territory; prisoners were mining tin and uranium ore.

Stop 6. *The Igumenov gold deposit*

Various types of gold-quartz veins affected by contact metamorphism induced by the Ulakhan granitic pluton, as well as the postmineral granite itself will be demonstrated in the adit dumps. Quartz veins contain gold, pyrrhotite, bismuth minerals and are cut by zeolite veinlets.

Stop 7. *The Shkol'noe silver-gold deposit*

Gabbrodiorite, diorite, granodiorite, granite, and aplite of the Burgagyn pluton will be examined together with high-grade gold-silver-quartz veins of the Shkol'noe deposit. Postmineral diorite porphyry and basalt dikes are available for observation.

Stop 8. *Dikes at the Natalka gold deposit*

The strongly deformed granite porphyry and diorite porphyry dikes will be demonstrated within the mylonite zone crossed by the Omchak River. A granite porphyry dike with antimonite-gold mineralization

may also be observed at the placer site. The gold-quartz vein zone with visible gold is localized 100 m apart.

Stop 9. *The Trubny granitic pluton*

Granite with cordierite crystals, up to 1 cm in size, will be seen near the bridge across the Debin River.

Stop 10. *The North Greater Annachag granitic pluton*

The distinctly porphyritic granite and tourmaline-bearing pegmatites crop out along the way to the Dzhelgalu Settlement.

Stop 11. *The Odinskii granitic pluton*

Biotite and amphibole-biotite Au-bearing granites are exposed as a block field.

Stop 12. *The Bol'shie Porogi (Big Rapids) granitic pluton*

The contact zone of the pluton will be examined in a quarry at the outskirts of the Sinigor'e town. Coarse- and medium-grained, slightly porphyritic high-alumina granite cut by aplite dikes and sporadic quartz veins are exposed in the quarry.

Stop 13. *The Stolovy granitic pluton*

The block field of granitic rocks occurs at the Utinsky Pass. The biotite granite and granodiorite belong to the main Au-bearing intrusive complex of the region.

Stop 14. *The Utinskoe gold deposit*

Dike of porphyritic rock and so-called dike-type gold-quartz deposit are exposed in the trench. This deposit type differs in many respects from the Au-bearing dikes known in Australia and the United States.

Stop 15. *The Gusiny granodioritic pluton*

Granodiorite with numerous mafic inclusions at 20 km of the Omsukchan highway demonstrates an effect of magma mingling.

Stop 16. *The Butarny granitic pluton and related gold deposit*

Granitic rocks and gold-quartz veins will be shown in borehole cores. Ore zones, hydrothermally altered and unaltered granites of the ancient Uda-Murgal arc may be seen in trenches.

REFERENCES

Al'shevsky, A.V. and Lyuskin, A.D., Setting of low-sulfide plutogenic ore mineralization in the Yana-Kolyma Belt in the light of geochronological data, Abstracts of papers, *Izotopnoe datirovanie rudnykh formatsii* (Isotopic dating of ore deposits), Kiev, 1990, pp. 171–174.*

Andreeva, N.V., Ponomareva, A.P., Kruk, N.N., et al., *Magadanskii batolit: stroenie, sostav i usloviya formirovaniya* (The Magadan batholith: structure, composition, and formation conditions), Magadan: Northeast Complex Research Institute, Far East Division, Russian Academy of Sciences, 1999, 264 p.*

Apeltsyn, F.R., *Otlichitelnye cherty petrografii i petrokhimii raznovozrastnykh formatsii malykh intruzii Glavnogo zolotonosnogo poyasa Severo-Vostoka SSSR* (Distinctive petrographic and petrochemical features of minor intrusions of different age in the Main gold-bearing belt in the Northeast of the USSR), Magadan, 1957, 116 p.*

Belyi, V.F., *Stratigrafiya i struktury Okhotsko-Chukotskogo vulkanogennogo poyasa* (Stratigraphy and Structures of the Okhotsk-Chukotka volcanic belt), Moscow: Nedra, 1977, 171 p.*

Belyi, V.F., *Geologiya Okhotsko-Chukotskogo vulkanogenogo poyasa* (Geology of the Okhotsk-Chukotka volcanic belt), Magadan: Northeast Complex Research Institute, Far East Division, Russian Academy of Sciences, 1994, 76 p.*

Bogdanov, N.A. and Tilman, S.M., *Tektonika i geodinamika Severo-Vostoka Azii* (Tectonics and geodynamics of the northeastern Asia), Tectonic map of the northeastern Asia at a scale of 1 : 5,000,000, Explanatory Notes, Moscow: Institute of Lithosphere, Russian Academy of Sciences, 1992, 54 p.*

Bulgakova, M.D., *Rannii-srednii paleozoi Severo-Vostoka SSSR (sedimentologicheskii analiz)* (Early and Middle Paleozoic in the Northeast of the USSR: sedimentological analysis), Yakutsk: Yakutian Scientific Center, Siberian Division, Academy of Sciences of the USSR, 1991, 104 p.*

Chappell, B.W. and White, A.J.R., I- and S-type granites in the Lachlan Fold Belt, *Trans. Roy. Soc. Edinburgh: Earth Sci.*, 1992, vol. 83, pp. 1–26.

Chekhov, A.D., Tectonics of the In'yali-Debin Synclinorium, in: *Skladchatye sistemy Dalnego Vostoka* (Fold systems of the Far East), Vladivostok: Far East Scientific Center, Academy of Sciences of the USSR, 1976, pp. 3–64.*

Chekhov, A.D., *Tektonicheskaya evolyutsiya Severo-Vostoka Azii* (Tectonic evolution of the northeastern Asia), Moscow: Nauchnyi Mir, 2000, 204 p.*

Fedorova, S.S., Behavior of major components in metamorphic rocks of the Derbeke-Nelgekhe ore zone, in: *Regionalnaya geologiya i poleznye iskopaemye Yakutii* (Regional geology and mineral resources of Yakutia), Yakutsk: Yakutsk State University, 1991, pp. 125–132.*

Fedorova, S. S., Methods of study of zonal metamorphism of the Verkhoyansk terrigenous complex during geological mapping at a scale of 1 : 50,000, in: *Magmaticheskie kompleksy rudnykh raionov Severo-Vostoka SSSR i ikh krupnomasshtabnoe geologicheskoe kartirovanie* (Igneous rock complexes in ore districts of the Northeast of the USSR and their large-scale geological mapping), Magadan: Northeast Complex Research Institute, Far East Division, Russian Academy of Sciences, 1991, pp. 106–117.*

Filatova, N.I., *Periokeanicheskie vulkanogennye poyasa* (Perioceanic volcanic belts), Moscow: Nauka, 1988, 262 p.

Firsov, L.V., *Struktura, mineralogiya i orudnenie Igumenovskogo zolotorudnogo mestorozhdeniya* (Structure, mineralogy, and ore mineralization of the Igumenovsky gold deposit), Magadan, 1958, 72 p.*

Firsov, L.V., *Zoloto-kvartsevaya formatsiya Yano-Kolymskogo poyasa* (Gold-quartz deposits of the Yana-Kolyma belt), Novosibirsk: Nauka, 1985, 217 p.*

Flerov, B.L., Trunilina, V.A., and Yakovlev, Ya.V., *Olovyanno-volframovoe orudnenie i magmatizm Vostochnoi*

* In Russian.

- Yakutii* (Tin-tungsten ore mineralization and magmatism of the eastern Yakutia), Moscow: Nauka, 1979, 275 p.*
- Gamyagin, G.N., Goryachev, N.A., Alpatov, V.V., et al., Basugun'insky ore-magmatic cluster, in: *Rudno-magmaticheskie sistemy Vostoka SSSR* (Ore-magmatic systems in the eastern USSR), Yakutsk: Yakutian Scientific Center, Siberian Division, Academy of Sciences of the USSR, 1991, pp. 81–94.*
- Gelman, M.L., Role of regional metamorphism in the gold mineralization of the Northeast of the USSR, *Dokl. Akad. Nauk SSSR*, 1976, vol. 230, no. 6, pp. 1406–1409.*
- Gelman, M.L., The Upper Yana-Chukotka fold region, in: *Metamorficheskie komplekсы Azii* (Metamorphic complexes of Asia), Novosibirsk: Nauka, 1977, pp. 246–253.*
- Gelman, M.L., Andreeva, N.V., and Goryachev, N.A., *Magadanskii gabbro-granitnyi batolit i mestorozhdeniya molibdena v ego potodakh* (The Magadan gabbro-granite batholith and related molybdenum deposits), Magadan: Northeast Complex Research Institute, Far East Division, Russian Academy of Sciences, 1997, 73 p.*
- Gelman, M.L., Berezner, O.S., Krutous, M.P., et al., Mapping of shallow-seated metamorphic complexes in ore districts of the Northeast of the USSR, in: *Metodika kartirovaniya metamorficheskikh kompleksov* (Methods of mapping of metamorphic complexes), Novosibirsk: Nauka, 1980, pp. 136–149.*
- Geologicheskoe stroenie SSSR i zakonmernosti razmeshcheniya poleznykh iskopaemykh* (Geology of the USSR and systematic patterns in localization of mineral resources), vol. 8. The eastern USSR, Leningrad: Nedra, 1984, 560 p.*
- Geologiya olovorudnykh mestorozhdenii SSSR* (Geology of tin deposits in the USSR), Lugov, S.F., Ed., vol. 2, Moscow: Nedra, 1986, 429 p.*
- Geologiya SSSR* (Geology of the USSR), vol. 30. The northeastern USSR, Book 2, Moscow: Nedra, 1970, 536 p.*
- Goncharov, V.I., Voroshin, S.V., and Sidorov, V.A., *Natalkinskoe zolotorudnoe mestorozhdenie* (The Natalka gold deposit), Magadan: Northeast Complex Research Institute, Far East Division, Russian Academy of Sciences, 2002, 250 p.*
- Goryachev, N.A., *Zhilnyi kvarts zolotorudnykh mestorozhdenii Yano-Kolymskogo poyasa* (Veined quartz at gold deposits in the Yana-Kolyma Belt), Magadan: Northeast Complex Research Institute, Far East Division, Russian Academy of Sciences, 1992, 136 p.*
- Goryachev, N.A., *Geologiya mezozoiskikh zolotokvartsevnykh zhilnykh poyasov Severo-Vostoka Azii* (Geology of Mesozoic gold-quartz vein belts in the northeastern Asia), Magadan: Northeast Complex Research Institute, Far East Division, Russian Academy of Sciences, 1998, 210 p.*
- Goryachev, N.A., Late Jurassic – Early Cretaceous ore lode deposits and magmatic assemblage of northeastern Asia continental margin, *Proc. the 2nd Intern. Symp. Geosciences in NE Asia and the 9th China-Korea Joint Symp. of Geology on Crustal Evolution in NE Asia*, Sun, G., Cao, L., and Hu, K., Eds., Changchun, China, 2002, pp. 77–78.
- Goryachev, N.A. and Kolesnichenko, P.P., Granite and greisen of the Myakit intrusion as a case of local ore-magmatic system, in: *Rudno-magmaticheskie sistemy Severo-Vostoka SSSR* (Ore-magmatic systems of the Northeast of the USSR), Khabarovsk: Khabarovsk Polytechnical Institute, 1990, pp. 41–53.*
- Goryachev, N.A. and Khanchuk, A.I., The origin of Late Cretaceous alkaline granitoids and basalts in the Upper Kolyma River area (the slab window tectonic model), in: *Deep-seated magmatism, magmatic sources and the problem of the plumes*. Proc. Intern. Workshop, Vladivostok: Dalnauka, 2002, pp. 261–274.
- Kalinin, A.I., Kanishchev, V.K., Orlov, A.G., and Gash-told, V.V., Structure of the Natalka ore field, *Kolyma*, 1992, no. 10–11, pp. 10–14.*
- Karchevets, V.P., Stratigraphy of volcanic rocks in the southwestern Okhota-Kolyma divide, Abstracts of Papers, *Mezozoi Severo-Vostoka SSSR* (Mesozoic in the Northeast of the USSR), Magadan, 1975, pp. 92–94.*
- Khanchuk, A.I. and Ivanov, V.V., Geodynamics of the Russian East and gold mineralization in Mesozoic-Cenozoic, in: *Geodinamica i metallogeniya* (Geodynamics and metallogeny), Vladivostok, Dal'nauka, 1999, pp. 7–29.*
- Korolkov, V.G. and Gelman, M.L., *Geological map of the USSR at a scale of 1 : 1,000,000, Sheet P-56 (O-56), Seimchan. Explanatory Notes*, St. Petersburg: All-Russia Geological Research Institute, 1992, 100 p.*
- Kotlyar, S.G., Granitization in the Khayargastakh batholith, in: *Materialy po geologii i poleznykh iskopaemykh Severo-Vostoka SSSR* (Geology and mineral resources of the Northeast of the USSR), vol. 12, Magadan, 1958, pp. 109–117.*
- Kotlyar, I.N., Zhulanova, I.L., Rusakova, T.I., and Gagieva, A.M., *Izotopnye sistemy magmaticeskikh i metamorficheskikh kompleksov Severo-Vostoka Rossii* (Isotopic systems of magmatic and metamorphic complexes in the Northeast of Russia), Magadan: Northeast Complex Research Institute, Far East Division, Russian Academy of Sciences, 2001, 319 p.*
- Krutous, M.P., The low-temperature metamorphism of host rocks and methods of its study in gold-bearing districts of the Northeast of the USSR during geological mapping at a scale of 1 : 50,000, in: *Metamorficheskie komplekсы Severo-Vostoka SSSR, ikh rudonosnost i geologicheskoe kartirovanie* (Metamorphic complexes in the Northeast of the USSR, their ore potential and geological mapping), Magadan: Northeast Complex Research Institute, Far East Division, Russian Academy of Sciences, 1992, pp. 124–143.*
- Mezozoiskaya tektonika i magmatizm Vostochnoi Azii* (Mesozoic tectonics and magmatism of the eastern Asia), Moscow: Nauka, 1983, 232 p.*
- Mikhailov, B.K. and Goryachev, N.A., Interpretation of geophysical fields in Mesozoic of the northeastern Asia and setting of gold-quartz mineralization, Abstracts of Papers, *Zolotoe orudnenie i granitoidnyi magmatizm Severnoi Patsifiki* (Gold mineralization and granitoid magmatism in the northern Pacific), Magadan: Northeast Complex Research Institute, Far East Division, Russian Academy of Sciences, 1997, pp. 48–49.*
- Natapov, L.M., Geology and geodynamic evolution of the northeastern Asia, *DSc (Geol.-Mineral.) Thesis*, Moscow, 1990.
- Natapov, L.M. and Surmilova, E.P., *Geological map of the USSR at a scale of 1 : 1,000,000, Sheet Q-54, -55, Khonuu, Explanatory Notes*, Leningrad: All-Union Geological Research Institute, 1986, 120 p.*
- Newberry, P.J., Layer, P.W., Gans, P.B., et al., Preliminary analysis of chronology of Mesozoic magmatism, tectonics, and ore mineralization in the Northeast of Russia: evidence from ⁴⁰Ar/³⁹Ar datings and trace element geochemistry of igneous and mineralized rocks, in: *Zolotoe orudnenie i granitoidnyi magmatizm Severnoi Patsifiki* (Gold mineralization and granitoid magmatism of the northern Pacific), vol. 1. Geology, geochronology, and geochemistry, Magadan: Northeast Complex Research Institute, Far East Division, Russian Academy of Sciences, 2000, pp. 181–205.*
- Nokleberg, W.J., Parfenov, L.M., Monger, J.W.H., et al. Circum-North Pacific tectonostratigraphic terrane map, *USGS Open-File Report 94-714*, 1994. 221 p.

- Nokleberg, W.J. et al., Mineral deposits and metallogenic belts, Russian Far East, Mainland Alaska, and Canadian Cordillera, *USGS Open-File Report 97-161*, 1997.
- Ocherki metallogenii i geologii rudnykh mestorozhdenii Severo-Vostoka Rossii* (Studies of metallogeny and geology of ore deposits in the Northeast of Russia), Sidorov, A.A. and Goryachev, N.A., Eds., Magadan: Northeast Complex Research Institute, Far East Division, Russian Academy of Sciences, 1994, 107 p.*
- Palymenskaya, Z.A., Intrusive rock associations in the southeastern Yana-Kolyma Fold Region and their relationships with ore mineralization, in: *Magmaticheskie komplekсы rudnykh raionov Severo-Vostoka SSSR i ikh krupnomasshtabnoe geologicheskoe kartirovanie* (Igneous rock complexes in ore districts of the Northeast of the USSR and their large-scale geological mapping), Magadan: Northeast Complex Research Institute, Far East Division, Russian Academy of Sciences, 1991, pp. 59–72.*
- Repin, Yu.S. and Polubotko, I.V., *Nizhnyaya i srednyaya yura Severo-Vostoka Rossii* (Lower and Middle Jurassic in the Northeast of Russia), Magadan: Northeast Scientific Center, Far East Division, Russian Academy of Sciences, 1996, 47 p.*
- Rudich, K.N., *Materialy po geologii i poleznym iskopaemyam Severo-Vostoka SSSR* (Geology and mineral resources of the Northeast of the USSR), vol. 10, Magadan, 1956.*
- Shevchenko, V.M., *Intruzivnye komplekсы verkhov'ev reki Kolyma i Primagadan'ya* (Intrusive complexes of the Kolyma River headwater and Magadan region), Magadan: Northeast Scientific Center, Far East Scientific Center, Russian Academy of Sciences, 1996, 95 p.*
- Shkodzinsky, V.S., Nedosekin, Yu.D., and Surin, A.A., *Petrologiya pozdnemezozoiskikh magmaticheskikh porod Vostochnoi Yakutii* (Petrology of Late Mesozoic igneous rocks of the eastern Yakutia), Novosibirsk: Nauka, 1992, 238 p.*
- Shpikerman, V.I., *Domelovaya minerageniya Severo-Vostoka Azii* (Pre-Cretaceous minerageny of the northeastern Asia), Magadan: Northeast Complex Research Institute, Far East Division, Russian Academy of Sciences, 1998, 333 p.*
- Shpikerman, V.I. and Goryachev, N.A., Plate-tectonic metallogeny of accretionary fold systems, in: *Metallogeniya skladchatykh sistem s positsii tektoniki plit* (Metallogeny of fold systems in terms of plate tectonics), Yekaterinburg, Uralian Division, Russian Academy of Sciences, 1996, pp. 64–78.*
- Shupikov, V.A. and Nikonov, V.N., The zonal metamorphism and its influence on the composition and formation conditions of ore deposits in the Indigirka part of the Main belt in the Northeast SSSR, in: *Geologiya i poleznye iskopaemye tsentralnoi chasti Glavnogo metallogenicheskogo poyasa Severo-Vostoka SSSR* (Geology and mineral resources of the central Main metallogenic belt in the Northeast of the USSR), Yakutsk: Yakutian Branch, Academy of Sciences of the USSR, 1989, pp. 54–65.*
- Sobolev, A.P., *Mezozoiskie granitoidy Severo-Vostoka SSSR i problemy ikh rudonosnosti* (Mesozoic granitoids in the Northeast of the USSR and problems of their ore potential), Moscow: Nauka, 1989, 249 p.
- Speranskaya, I.M., Okhotsk Igimbrite Province, *Bull. Volc.*, vol. XXX, 1967, pp. 99–111.
- Springis, K.Ya., *Tektonika Verkhoyano-Kolymskoi skladchatoi oblasti* (Tectonics of the Verkhoyansk-Kolyma Fold Region), Riga: Izd-vo AN LatvSSR, 1958, 337 p.*
- Tektonika, geodinamika i metallogeniya respubliki Sakha (Yakutia)* (Tectonics, geodynamics, and metallogeny of the Sakha Republic, Yakutia), Parfenov, L.M., Ed., Moscow: Knizhny Mir, 2001, 587 p.*
- Trunilina, V.A., *Geologiya i rudonosnost pozdnemezozoiskikh magmaticheskikh obrazovaniy severo-vostoka Yakutii* (Geology and ore potential of Late Mesozoic igneous rocks in the northeastern Yakutia), Novosibirsk: Nauka, 1992, 257 p.*
- Tyukova, E.E., *Mineralogo-geneticheskie osobennosti mestorozhdenii Pionerskogo rudnogo uzla* (Mineralogy and genesis of deposits in the Pionersky ore cluster), Magadan: Northeast Complex Research Institute, Far East Division, Academy of Sciences of the USSR, Pts. 1 and 2, 1989.
- Umitbaev, R.B., *Okhotsko-Chaunskaya metallogenicheskaya provintsiya* (Okhota–Chauna metallogenic province), Moscow: Nauka, 1986, 286 p.*
- Vashchilov, Yu.Ya., Deep faults in the southern Yana-Kolyma Fold Zone and Okhota–Chauna volcanic belt and their role in formation of granitic intrusions and structures: evidence from geophysical data, *Sov. Geol.*, 1963, no. 4, pp. 54–72.*
- Vashchilov, Yu.Ya., Morphology and tectonic setting of some igneous rock bodies in the extreme Northeast of the USSR: evidence from geophysical data, *Byull. Mosk. O-va Ispyt. Prir., Otd. Geol.*, 1968, no. 5, pp. 94–100.*
- Yeremin, R.A., *Gidrotermalniy metamorfizm i orudnenie Armanskoi vulkanostruktury* (Hydrothermal metamorphism and ore mineralization of the Arman volcanic structure), Novosibirsk: Nauka, 1974, 106 p.*
- Yeremin, R.A. and Osipov, A.P., Genesis of the Nataalka gold deposit, *Kolyma*, 1974, no. 6, pp. 41–43.*
- Zagruzina, I.A., Late Mesozoic granitoids at the eastern coast of the Chauna Bay, western Chukotka, in: *Pozdnemezozoiskie granitoidy Chukotki* (Late Mesozoic granitoids of Chukotka), Magadan: Northeast Complex Research Institute, Siberian Division, Academy of Sciences of the USSR, 1965, pp. 4–140.*
- Zonenshain, L.P. and Natapov, L.M., The tectonic history of the Arctic Region, in: *Aktualnye problemy tektoniki okeanov i kontinentov* (Topical problems of oceanic and continental tectonics), Moscow: Nauka, 1987, pp. 31–57.*

THE KONDER MASSIF OF ULTRAMAFIC AND ALKALINE ROCKS AND RELATED PGM MINERALIZATION

A. M. Lennikov, B. L. Zalishchak and R. A. Oktyabrsky

Far East Geological Institute (FEGI), Far East Branch, Russian Academy of Sciences, Vladivostok

INTRODUCTION

The Konder massif of ultramafic and alkaline rocks is a unique creation of nature. This geologic structure, almost perfectly circular in plan, resembles an ancient meteoritic crater (Fig. 2.1). The massif is situated in the northern Khabarovsk Territory, 250 km west of the Ayan Settlement in the middle reaches of the Maya River. The boundary ring range, about 7 km in diameter, towers for about 1000 m above sealevel. The elevation of the highest southeastern arc reaches approximately 1400 m. The circular Konder basin was formed at the centre of a dome-shaped intrusion as a result of nonuniform erosion. The chromite-bearing dunite that occupies the largest inner zone of the massif was eroded most readily. Clinopyroxenite, gabbroclinopyroxenite, gabbroids, monzonitoids, and granophyre granite that surround the dunite core are more resistant against weathering. These rocks are, in turn, encircled by durable sandstone and siltstone transformed into hornfels.

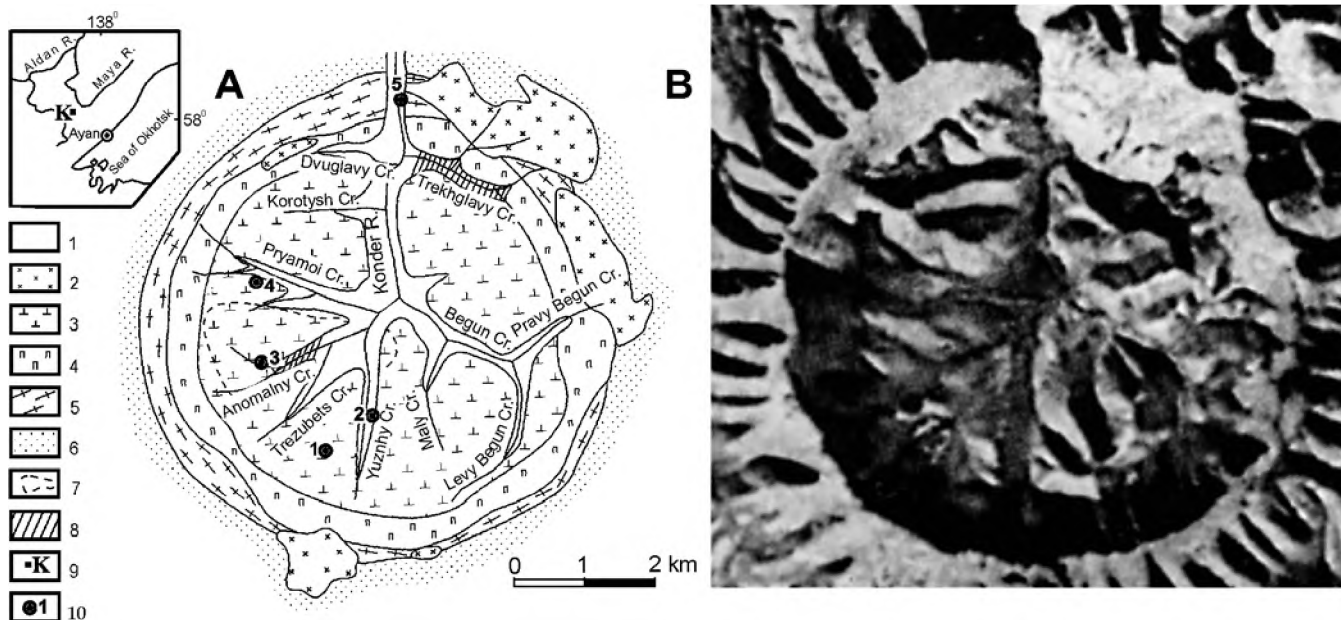


Fig. 2.1. The Konder massif.

A: Schematic geological map. Simplified after Yemel'yanenko et al. (1987), Nekrasov et al. (1994), and Sushkin (1995):

(1) alluvial PGM-bearing sediments; (2) granodiorite, monzonite, and diorite; (3) dunite; (4) olivine and magnetite clinopyroxenites and melanogabbro; (5) massive and (6) gneissose hornfels after Riphean carbonate and terrigenous rocks; (7) field of phlogopite-magnetite clinopyroxenite dikes in dunite; (8) alluvial sediments enriched in gold; (9) Konder PGM deposit; (10) stops of excursion routes. (K) Konder massif on inset map.

B: satellite photograph. The scale for the map and photograph is equal

HISTORY OF GEOLOGICAL INVESTIGATIONS

The Konder massif was found by geologist Kulesh (1937). Subsequently, it was investigated by Shklyayev (1942) and then by Arkhangel'skaya and Katz (1955). The first large-scale geological map was prepared by Mil'to, Yel'yanov and others as a result of mapping that was carried out in 1956–1957 by the expedition of the All-Union Aerogeological Trust (Andreev, 1987). Thematic geological studies were performed in 1960–1966 and yielded the first information on the platinum group metals (PGM) placers (Rozhkov et al., 1962) and petrography of the Konder rocks (Andreev, 1987). A new stage of geological exploration began since 1982, when the expedition of the Far East Regional Geological Survey (Khabarovsk) started its activity aimed at the estimation of platinum group element (PGM) potential of the Konder massif. Further, the PGM mineralization, geology, petrography, and mineralogy of the massif were studied by a team of geologists-scientists Moscow, Leningrad, Magadan, Irkutsk, Novosibirsk, Khabarovsk, and Vladivostok (Nekrasov et al., 1994; Sushkin, 1995).

GENERAL GEOLOGY

Besides the Konder central-type massif with dunite core, a few other concentrically zoned platiniferous massifs of ultramafic and alkaline rocks are known in the central Aldan Shield (Inagli) and in its southeastern part (Chad and Sybakh). All these massifs were formed at a depth of 1–2 km (Bogomolov, 1964; Yel'yanov and Moralev, 1972) and are eroded to some or other extent giving rise to variable proportions of specific rocks exposed at the present day surface (Nekrasov et al., 1994). The Sybakh and Inagli massifs are the least eroded, whereas the Konder and especially Chad massifs were eroded to a greater depth.

Contact aureole of the Konder massif

At the present-day denudation level, the Konder massif intrudes Riphean sandstone and siltstone, a base of horizontally lying sedimentary cover overlapping Archean crystalline basement. The thickness of the Riphean sequence is about 450 m (Bogomolov, 1964). The dome-shaped structure, which resulted from the emplacement of the Konder intrusion, consists of an outer zone with centrifugal dipping at angles 30–45° (occasionally, up to 80°) and an inner

zone with centripetal dipping at angles from 40–50 to 80° (Yemel'yanenko et al., 1989; Marakushev et al., 1990). The outer and inner zones are divided by a ring fault (Fig. 2.1). The outer zone, more than 500 m in width (Bogomolov, 1964), is composed of unevenly metamorphosed sandstone and siltstone. Cordierite-biotite hornfels with magnetite, schorl-dravite tourmaline, and andalusite are most abundant [$f = \text{FeO}/(\text{FeO} + \text{MgO}) = 0.46\text{--}0.60$ for cordierite and $0.68\text{--}0.73$ for biotite]. The inner zone of the contact aureole, about 100 m wide, is composed of fine-grained, garnet-biotite, garnet-cordierite-biotite, biotite, biotite-cordierite, and cordierite-biotite-muscovite gneisses ($f = 0.96$ for garnet with about 33% of spessartine end member and >0.60 for biotite). Magnetite, ilmenite with high Fe_2O_3 , gahnite (Zn-spinel), schorl-dravite tourmaline, sillimanite, and andalusite are contained in the gneisses. Relict blocks of massive hornfels (Lennikov et al., 1991; Oktyabrsky et al., 1992) indicate that gneisses of the inner zone were formed as a result of hornfels reworking under impact of the Konder intrusion. The gneissose hornfels locally alternate with carbonate units. The largest of these units, which rims the Konder massif in the north and northwest, consists of dolomite and brucite marbles (brucite replaces periclase), forsterite-brucite calciphyre, monticellite, monticellite-melilite, grossular-fassaite, vesuvianite, and wollastonite skarn with clintonite (brittle mica), scapolite, clinohumite, Al-spinel, Ti-magnesioferrite, qandilite (Ti–Mg-spinel), geikielite, perovskite, and pyrrhotite (Nekrasov et al., 1994; Oktyabrsky et al., 1992).

According to the thermometric data (Nekrasov et al., 1994), the highest temperature during formation of the contact aureole reached 700–900°C. The high temperature and oxidizing environment ($f_{\text{O}_2} = 10^{-11}\text{--}10^{-8}$ bar) made formation of gahnite and qandilite possible.

Gahnite occurs in metapelites of the northern inner zone. The mineral is represented by a Fe-rich variety [$f_{\text{total}} = \text{FeO}/(\text{FeO} + \text{MgO}) = 0.66\text{--}0.82$] with a moderate ZnO content (22.76–31.78 wt %) typical of high-temperature metapelites (Oktyabrsky et al., 1992). Qandilite was found in calciphyre and brucite marble of the northern inner zone. The mineral contains up to 27.34 wt % TiO_2 and is similar in composition to the Ti–Mg spinel previously found in Greenland and Iraq (Oktyabrsky et al., 1992).

Age of the Konder massif

No reliable evidence for the age of the Konder massif and its counterparts (Inagli, Chad, Sybakh) is available until now. As was suggested from the pio-

neering investigations, these massifs are coeval with the Neoproterozoic Inagli carbonatite-bearing complex consistent with K-Ar dates in a range of 500–650 Ma. However, numerous subsequent K-Ar datings of the Konder rocks did not confirm the oldest estimate of 650 Ma obtained for the coarse-flake phlogopite from magnetite clinopyroxenite intruding dunite in the southwestern sector of the Konder pluton. All determinations carried out at the same time and at the same Laboratory of Geochronology, Far East Geological Institute for biotite from the Arbarastakh alkaline ultramafic massif yielded 550–650 Ma, i.e., were close to the estimates reported before. Thus, the extreme instability of K–Ar isotope system and its uselessness for assessment of true age of the Konder rocks is evident, and this statement can be spread over Sm-Nd, Rb-Sr and Re-Os results (Kostoyanov, 1998; Pushkarev et al., 2001).

Geologic relationships also remain equivocal for a long time. A part of the Konder igneous rocks including biotite pyroxenite, monzonite, diorite, and granodiorite was presumably referred to Mesozoic reactivation. However, chromite grains completely identical to the low-Al high-Fe₂O₃ chromite from Konder ultramafics were found in the Middle Riphean terrigenous rocks occurring in the immediate vicinity of the Konder massif and affected by contact metamorphism (Shnai and Kuranova, 1981). The host hornfels revealed some evidence for accessory PGM (Yemel'yanenko et al., 1989).

Thus, the lower age limit, at least, for chromite-bearing dunite is not younger than Middle Riphean. It looks likely that ultramafic rocks were formed at the Early–Middle Riphean boundary 1.20–1.35 Ga ago. However, this inference is in conflict with the single Rb–Sr age determination of 1.6 Ga obtained for the granophyre granite that intrudes the magnetite-free clinopyroxenite in the western Konder massif (Yemel'yanenko, 1989). It cannot be ruled out that this granite is a product of contact anatexis of Archean crystalline basement heated by Konder ultramafics, so that the Rb–Sr age is overestimated.

GEOLOGICAL SETTING AND PETROGRAPHY OF ROCKS

The circular core of the Konder massif, about 6 km in diameter, is composed of dunite and rimmed with arcuate and ring bodies of clinopyroxenite (Andreev, 1987). Near the contact, dunite grades into clinopyroxene-bearing pseudo-olivinite. The latter is absent only in the eastern part of core, where the cli-

nopyroxenite framework widens for 600 m; elsewhere, it does not exceed 200 m. Olivine clinopyroxenite largely occurs close to the dunite core and gives way to magnetite-bearing and olivine-free clinopyroxenite in the outermost zone. Both varieties of fine- and medium-grained clinopyroxenites make up thin (<1 m) dikes in dunite, largely in the near-contact zone of the core. The coarse-grained phlogopite-bearing magnetite clinopyroxenite occurs as dikes, up to 40 m thick, in the southwestern sector of the dunite core. Inclusions and schlieren of thick-platy high-Fe olivinite are known from the olivine clinopyroxenite at a distance of 180 m from dunite.

Dunite

Dunite of the Konder massif is a massive, fine-to-medium-grained inequigranular rock with olivine grains varying in size from fractions to tens of millimeters. Olivine crystals, up to 5–7 cm in length, can be seen in sporadic bodies of pegmatoid dunite. The fine-grained dunite occurs in the marginal part of the core except in its eastern sector where coarse-grained pegmatoid dunite occupies the divide between the Trekhglavy (Three-headed) and Pravy Begun (Right Runner) creeks (Fig. 2.1). The main body is composed of medium-grained dunite locally grading into a coarse-grained variety. According to drilling results, the coarse-grained dunite becomes predominant at a depth more than approximately 200 m. The segregation of coarse-grained and pegmatoid dunitites is effected through a gradual increase in the number of large (3–30 mm) olivine grains merging into schlieren. The pegmatoid dunite also occurs as dike-shaped bodies, 30–50 m thick and 100–150 m long. However, in this case, this rock also reveals a gradual transition to the host inequigranular dunite as takes place in schlieren. The pegmatoid "dikes" and schlieren are commonly localized in the center of the dunite core within a zone about 1.5 km in diameter. They are especially abundant (up to 20–80% area) at relatively high hypsometric levels in association with rounded schlieren (up to 30 cm in diameter) of pegmatoid olivine clinopyroxenite.

Relatively large (up to 5–6 mm) olivine grains are commonly twinned and often contain inclusions of Cr-diopside, high-Cr (up to 2.25 wt % Cr₂O₃) phlogopite, chromite, and Cr-magnetite forming symplektitic, tabular, and most abundant octahedral in-growths. Tetraferriphlogopite and richterite are confined to fractures within olivine grains. Serpentinization of olivine develops insignificantly, mostly along faults, in zones of pegmatoid dunite, and close to the

dikes and veins of apatite-phlogopite clinopyroxenite and nepheline syenite. The drilling results indicate that the rate of serpentinization decreases with depth and this process completely wanes at a depth of 400–450 m from the surface (Yemel'yanenko, 1989).

Olivine from fine- and medium-grained dunite corresponds to $Fo_{93.1-87.9}$ in composition (Nekrasov et al., 1994). Olivine in clinopyroxene-bearing dunite from the marginal zone of the core is somewhat richer in FeO ($Fo_{87.6-86.8}$). The pegmatoid dunite in the central part of the core and olivinite inclusions in olivine clinopyroxenite contain $Fo_{85.3-84.9}$ and $Fo_{84.0-81.6}$, respectively. Schlieren of pegmatoid olivine clinopyroxenite hosted in dunite contain $Fo_{87.3}$, whereas the olivine composition in clinopyroxenite surrounding the dunite core and forming dikes therein attains Fo_{70} . The high-Mg olivine ($Fo_{92.2-89.3}$) is typical of pseudo-olivinite, an inequigranular fine-grained dunite, slightly magnetic owing to the presence of the liquidus magnetic high- Fe_2O_3 chromite and the solidus Cr-magnetite (Oktyabrsky et al., 1992). The highest-Mg olivine ($Fo_{93.1-92.9}$) was found in fine-medium-grained dunite from the southern part of core at the water divide between Yuzny (South) and Trezubets (Trident) creeks.

Large olivine grains reveal a zonal distribution of CaO varying from 0.42 wt % in the grain core to 0.38 wt % in the marginal zone. Small olivine grains contain 0.11–0.30 wt % CaO. In particular cases, small grains are richer in CaO than the large grains of the same sample, e.g., 0.17 wt % against 0.06 wt % in a large grain. The highest CaO content (up to 0.5–0.7 wt %) was detected in high-Mg olivine ($Fa_{92.2-91.9}$) with small inclusions of Cr-magnetite (6–7 wt % Cr_2O_3); the rock occurs in the southeastern sector of the dunite core. The central zone enriched in pegmatoid and coarse-grained dunite is distinguished by a generally low CaO content in olivine (0.09–0.18%). Elsewhere in the dunite core including its marginal zone, the CaO content in olivine is higher (0.2–0.4 wt %).

In general, the CaO content in olivine from dunite does not correlate with Mg-number. At the same time, the positive correlation is evident for the case of olivine clinopyroxenite where the CaO content in $Fo_{87.5}$ drops down to 0.15 wt % and lower (Nekrasov et al., 1994).

The enrichment of olivine in CaO is a general specific feature of meimechite and dunite from shallow-seated ultramafic massifs of the northern Siberian Platform. The CaO content is above 0.2 wt % everywhere including the high-Mg olivine from the Bor-

Uryakh massif. Olivine from platiniferous dunite in the Urals is also similar to the Konder counterpart in CaO content, although mostly this olivine contains no more than 0.3 wt % CaO and the lowest value is close to the maximum content in olivine from Alpine-type ultramafics.

Like olivine from ultramafic rocks of the Maimecha-Kotui province, olivine from the Konder massif contains TiO_2 (0.01–0.07 wt %) and Cr_2O_3 (0.01–0.10 wt %), whereas both oxides are completely lacking in olivine from Alpine-type ultramafics (Velinsky and Bannikov, 1986). Despite a widely scattering Cr_2O_3 content in olivine from the Konder dunite, a negative correlation with Mg-number of olivine is evident consistent with data reported by Sobolev et al. (1989). This tendency also remains in olivine clinopyroxenite from the framework of dunite core and is especially clear in olivine from the olivine clinopyroxenite dikes cutting dunite, probably as a result of fast high-temperature crystallization under reducing conditions. Olivine from the Konder dunite is similar in Cr_2O_3 content to analogues from Bor-Uryakh and Guli massifs, but has a lower Cr content than olivine from meimechite (0.04–0.08 wt %).

NiO and MnO concentrations in Konder olivines demonstrate a reverse mutual correlation within the entire Fo range. The correlation between MnO (NiO) and Fo is negative (positive) as commonly established for primary magmatic olivine in other ultramafic rocks.

The thermodynamic computation of equilibrium parameters of the gas phase contained in olivine yielded 1375 and 1180°C for liquidus and solidus, respectively at $f_{O_2} = 10^{-9}$ – 10^{-10} MPa (Nikol'sky et al., 1988). This estimate bears some information on the temperature of olivine crystallization and is consistent with results of the calculations carried out by Kuznetsova (FEGI, Far East Division, RAS) using the method proposed by Reverdatto and Sal'ko (1967). According to this calculation (see Nekrasov et al., 1994), the ultramafic melt that provided a maximum temperature of contact metamorphism at about 900°C (Bogomolov, 1964; Lennikov et al., 1991) was initially heated up to 1380°C.

The Cr-spinel, abundant in dunite and olivine clinopyroxenite from the central Konder massif, is largely composed of subferri- and subaluminumferri-chromite, both accessory and ore-forming. The accessory Cr-spinel occurs as disseminated octahedral and less frequent flattened and rounded equant grains, from 0.01 to 2–3 mm in size. Rounded and lenticular schlieren, veinlike bodies, and pockets (up to $0.7 \times 1.5 \text{ m}^2$

in size) of densely impregnated ore Cr-spinel are distributed throughout the massif revealing no systematic patterns in spatial localization. The morphology of Cr-spinel grains is the same, but they are larger in dimensions varying from 1 to 5–7 mm in diameter. Three generations of the accessory Cr-spinel are recognized (Oktyabrsky et al., 1992). The first generation (chromite I) is represented by the largest octahedral crystals (0.3–3.0 mm) occurring in interstitial space between olivine grains or as inclusions in these grains. The second generation (chromite II) comprises irregular and equant (with hints on facing) small (0.02–0.40 mm) grains within large olivine individuals; dendritic (~0.1 mm) segregations in olivine are also notable. The third generation (chromite III) is exhibited by small (0.1–0.3 mm) faced and less abundant anhedral Cr-spinels dispersed between the smallest olivine grains.

The Cr-spinel is associated with $Fo_{92.9-87.9}$ in dunite and $Fo_{87.6-87.3}$ in olivine clinopyroxenite of the central facies. The chemical composition of Cr-spinel covers a range from a sporadic high-Cr (61.7–63.7 wt % Cr_2O_3) variety via the main mass of ferrichromite to the Cr-bearing magnomagnetite. The Cr_2O_3 content in Cr-spinel from dunite varies from 55.0 to 19.6 wt %; in magnomagnetite from olivinite and in the magnetic fraction of densely impregnated Cr-spinel, the respective ranges are 7.6–8.6 and 10–12 wt %. A difference in FeO and Fe_2O_3 contents is also significant. The ferric component prevails only in chromite III. The MgO content varies to a lesser extent from 3 to 11 wt %. The ore chromite is distinguished by the highest MgO content.

Cr-spinel from dunite and olivine clinopyroxenite of the central facies contains an appreciable quantity of titanium. The lowest Ti content is typical of ore Cr-spinel and chromite I (0.4–0.8 wt % and up to 1.55 wt % TiO_2 , respectively). The accessory Cr-spinels from pegmatoid and coarse-grained dunite and from olivine clinopyroxenite of the central facies are somewhat richer in TiO_2 (1.07–1.95 wt %). The TiO_2 range in Cr-bearing magnetite is narrower but higher in level (1.80–2.12 wt %). Two magnetic fractions from schlieren (3–5 cm) of densely impregnated chromite in dunite are close in composition to the above mineral but are richer in Cr_2O_3 (10–12 wt %) and TiO_2 (5.15–5.29 wt %).

Cr-spinels from Konder are moderate- and low-Al. The highest Al_2O_3 content (5.9–7.9 wt %) was detected in the ore Cr-spinel and accessory spinel of the first generation (chromite I) in dunite. The Al_2O_3 content in chromite II from the pegmatoid olivine cli-

nopyroxenite and chromite III from the fine-grained rocks drops to 5.2–3.3 wt % and from 4.6–2.4 to 0.8 wt %, respectively. The alumina content in Cr-bearing magnetite from olivinite (1.8–2.5 wt %) and densely impregnated chromite schlieren in dunite (1.97–2.49 wt %) varies in approximately the same way. All Cr-spinels from the near-contact inequigranular fine-grained magnetic dunite are depleted in alumina. The perfectly faced and large (0.6 mm) crystals of the liquidus chromite with $f_{total} = FeO/(FeO + MgO) = 0.85$ contain here only 4.42 wt % Al_2O_3 , i.e., 1.5–2.0 times less than in the ore Cr-spinel and liquidus chromite I. The solidus chromite III is composed of Cr-magnetite.

The f_{total} value of 0.63–0.76 is typical of chromite I from dunite and olivine clinopyroxenite, 0.72–0.80, of chromite II, and 0.80–0.89, of chromite III, whereas in ore Cr-spinel it equals 0.59–0.70.

Cr-spinels in pseudo-olivinite of marginal part of the Konder massif consisting of inequigranular low-magnetic fine-grained dunite (see above) are composed of the liquidus ferrichromite (chromite I) with $f_{total} = 0.83–0.85$ and the solidus Cr-magnetite (chromite III) with $f_{total} = 0.92$. According to our data, the true olivinite contains small (0.2 mm) inclusions of the liquidus Cr-bearing (7.6–8.6 wt % Cr_2O_3) magnetite incorporated into high-Mg olivine (Fo_{92}).

Cr-spinel crystals from the Konder massif reveal diffusion zoning with transition from ferrichromite in grain cores to Cr-magnetite at margins. This zoning was established in large crystals of the liquidus chromite I from pegmatoid dunite with cores containing 50.55 wt % Cr_2O_3 and in small (0.1 mm) grains of the solidus chromite III from medium- and fine-grained inequigranular dunites. The liquidus chromite II as inclusions in olivine is devoid of zoning. A much wider range of zoning can be expected for densely impregnated fine-grained Cr-spinel. The nonmagnetic fraction consists of high- Fe_2O_3 chromite with 49.65 wt % Cr_2O_3 and 0.73 wt % TiO_2 while the magnetic fraction is composed of Cr-bearing titanomagnetite similar in composition to accessory counterparts from peridotite of the Guli pluton and olivinite of the Bor-Uryakh massif (Vasil'ev, 1981). The considerable increase in TiO_2 content is probably caused by enrichment of residual melt in titanium. On the contrary, magnetite resulting from serpentinization is enriched in Cr_2O_3 (4.06 wt %) but contains only 0.17 wt % TiO_2 . This mineral occurs as wormlike inclusions in Cr-spinel and as thin rims around Cr-spinel grains.

The composition of particular zones and the general trend of Cr-spinel zoning commonly coincide

with compositional variation during magmatic crystallization. For example, the transition from the liquidus Cr-spinel to its solidus descendant in fine- and medium-grained inequigranular dunite is accompanied by a significant increase in the magnetite end member from 13–16 to 33–59 vol % and by a decrease in chromite end member from 41–51 to 22–28 vol %. The Cr/(Cr + Al) value remains rather constant along with insignificant depletion in spinel end member as a result of the concordant decrease in Al and Cr content against a wide variation in Fe/(Fe + Mg) ratio (0.55–0.95). A marked increase in Cr/(Cr + Al) took place only during formation of the solidus chromite III and, occasionally, chromite II in pegmatoid and coarse-grained dunite due to faster depletion in Al relative to Cr, probably as a result of increase in alkalinity.

The transition from large-size liquidus chromite I to small-size liquidus chromite II incorporated into olivine was accompanied by a more pronounced depletion in spinel component. The opposite tendency was established for crystallization of near-contact dunite and in the contact zone of coarse-grained dunite and pegmatoid olivine clinopyroxenite of the central facies. In this case, chromite I is more oxidized and depleted in Cr₂O₃ (33.37 wt %) than chromite II with 40.99 wt % Cr₂O₃ against the approximately equal MgO contents (5.03 and 5.36 wt %), which abruptly drop to 2.93 wt % in chromite III.

It was also established that the FeO/(FeO + MgO) value increases coherently both in the liquidus and solidus Cr-spinels in pegmatoid dunite approaching the contact of the massif and in the near-contact inequigranular magnetic fine-grained dunite as compared with dunite from the center of massif. Thus, if the crystallization of the initial fine- and medium-grained dunite started with high Fe₂O₃ chromite, then low-Al high-Fe₂O₃ chromite was formed on the liquidus of pegmatoid and near-contact varieties and Cr-bearing magnetite was a liquidus phase of olivinite. It can also be stated that the FeO/(FeO + MgO) ratio in the liquidus chromite I gradually increased from 0.65 to 0.75 and the degree of oxidation measured by Fe₂O₃/(Fe₂O₃ + FeO) varied from 0.35 to 0.42 outward from the center of massif and with decreasing depth of erosion. The FeO/(FeO + MgO) ratio of the ore Cr-spinel also slightly increases from 0.63 to 0.70 in this direction. The similar continuous range from the high-Cr chromite to the Cr-bearing magnetite is clearly expressed in dunite and peridotite intrusions of the Maimecha-Kotui region (Vasil'ev, 1981). Cr-spinel from these rocks also reveals zoning up to the formation of the outer titanomagnetite rims.

Thus, the compositional variation of the Konder Cr-spinels is controlled by sequential crystallization of evolving magmatic melt and by the reaction of this melt with solid phases and the subsequent diffusion exchange of components under subsolidus conditions. The general trend of this variation is provided by isomorphic replacements of Cr, Mg, and Al by Fe²⁺, Fe³⁺ and Ti. In other words, the quantity of magnetite component increases at the expense of chromite and spinel components from the liquidus chromite I to the solidus chromite III.

The chemical evolution of Cr-spinels clearly indicates that the ultramafic rocks of the Konder massif belong to the complexes of elevated alkalinity.

The formation of the dunite core was completed by crystallization of native metals (Si-bearing and pure α -iron, tin, copper, and antimony) along with rare grains, polymineral veinlets and lenses of pentlandite, pyrrhotite, chalcopyrite, pyrite, and arsenopyrite (PGM are not detected).

Clinopyroxenite of the outer ring

The dunite core of the Konder massif is surrounded by a continuous ring of olivine, olivine-bearing, and magnetite clinopyroxenites (up to kosvite¹), gabbropyroxenite and magnetite gabbro. The study of the internal structure and composition of this framework along five complete cross sections revealed an inverse relationship between the volume occupied by magnetite-bearing pyroxenite and gabbro, on the one hand, and the ring width, on the other. The narrowest (about 160 m) southern segment of the ring at the divide of the Yuzhny (South) and Begun (Runner) creeks (figure) is almost entirely composed of magnetite clinopyroxenite and about 30% of magnetite gabbro. In a wider (~250 m) northwestern segment at the headwater of the Dvuglavy (Double-headed) Creek, the ore clinopyroxenite occupies about 80% of the ring, gabbro is lacking, and barren clinopyroxenite occurs in a subordinate amount. In three other sections in the western part of the ring, 350 m wide, at the headwater of Pryamoi (Straight) Creek, in the southeastern segment, 370 m wide, at the divide between Levy Begun and Pravy Begun (Left Runner and Right Runner) creeks, and in the widest (550–600 m) eastern part at the headwater of the Pravy Begun Creek only 50, 5, and 10–20% of ore clinopyroxenite, respectively, and 30, 10, and 5% of gabbroic rocks are present.

¹ Kosvite is a magnetite-rich clinopyroxenite. The term was proposed by L. Duparc in the early XX century after the Mount of Kosvinsky Kamen in the Urals.

The contact between dunite and clinopyroxenite extends along the ring faults and is expressed in topography as local depressions crossing the radial ranges. The rocks in the contact zone are commonly disintegrated into rubble with sporadic relatively large fragments. This makes difficult to interpret the contact, and views on its nature remain controversial. Yemel'yanov et al. (1989) described it as a ring of green olivine-diopside metasomatically altered rocks, 0.2–50 m thick, while Orlova (1991) observed an alternation of clinopyroxenite and pseudo-olivinite, 8–10 m thick, with formation of a transitional wehrlite.

Clinopyroxenite dikes

The southwestern part of the dunite core within an area of 4 km² is intruded by a swarm of clinopyroxenite dikes and veinlets varying from 1–3 cm to 30–40 m in thickness and from few meters to 200–300 m in length. The dikes and veinlets are commonly zonal and complicated with numerous offsets, bulges, and pinches. They are often branching, change their dip angles and strike azimuths, and, in general, form a stockwork. The thickest dikes tend to dip toward the center of the massif at angles of 40–60°. This indicates that their localization is controlled by fractures that arose during emplacement of a large deep-seated clinopyroxenite body as supported by geophysical data and drilling results. The borehole drilled in the central Konder massif down to a deep of 811 m (Yemel'yanenko et al., 1989) has shown that clinopyroxenite veins, veinlets, and dikes merge at a depth of 300–780 m into a common body with a distinct layering (Orlova, 1991). At the surface, the clinopyroxenite veins are separated from country dunite by chilled contacts. The thick (10–40 m) dikes contain angular dunite xenoliths and blocks, up to 1.0–1.5 m in diameter.

The fine- and medium-grained clinopyroxenites with magnetite (10–20 vol %) and apatite (5–10 vol %) are generally predominant. The very fine-grained variety is less abundant. The clinopyroxenite is inequigranular, hypidiomorphic, locally sideronitic and can be compared with kosvite. Elongated phenocrysts of light greenish Cr-free clinopyroxene reach 2–6 mm in size. Equant and oblong olivine grains (F_{076.4}), 0.1–0.5 mm in size, sporadically occur in the medium-grained ore clinopyroxenite. Titanomagnetite, which is associated with apatite in fine- and medium-grained clinopyroxenites, contains 4.7–5.8 wt % TiO₂ and occasionally is intergrown with smaller (0.05–0.30 mm) grains of oxidized ilmenite (5.9–8.8 wt % Fe₂O₃ and 3.7–3.8 wt % MgO), rounded pyrrhotite grains (0.05–0.20 mm), and chalcopyrite.

The coarse-grained clinopyroxenite with pyroxene crystals, up to 5–7 cm in size, has lost the porphyritic texture and is transformed into a pegmatoid rock. The clinopyroxene in this rock is also free of Cr but is somewhat less magnesian (mg-number is 0.76–0.80) and contains more rough sheets of ore mineral resembling a sagenitic pattern. Phlogopite, amphibole, and magnetite-apatite varieties of clinopyroxenite are recognized. Brown vesuvianite crystals (1×2 mm) and more abundant anhedral titanite grains (1–2 mm) were found in the coarse-grained clinopyroxenite at the divide between the Yuzhny and Trezubets creeks.

Alkaline rocks

The veins of alkaline rocks mainly localized in the marginal part of the Konder massif and partly within its exocontact zone are the youngest intrusions.

In addition to the syenite proper, varieties transitional to alkali and nepheline syenite and monzonite are known from Konder. The two-feldspar (zonal andesine-oligoclase albite + K-Na-feldspar) and alkali feldspar (albite, K-Na-feldspar) varieties with clinopyroxene, common hornblende, and biotite are recognized. Alkali Fe-Mg-silicates are absent. Garnet-clinopyroxene, corundum-biotite, clinopyroxene-biotite, aegerine-augite, and leucocratic syenites are distinguished. The total alkalinity, the contribution of sodium and iron sequentially increases in this series while the saturation with alumina falls down.

The garnet-clinopyroxene two-feldspar syenite contains melanite, aegirine-augite, andesine (An₄₀), and Na-rich alkali feldspar. The corundum-biotite syenite has a trachytoid texture and consists of zoned plagioclase (An₅₋₂₀₋₄₀), perthitic Na-rich alkali feldspar, biotite, corundum (10–20%), a small amount of magnetite, titanite, rutile, albite, and zeolite. Veins composed of this rock are accompanied by contact metasomatic zones in the host diorite. Aegirine-augite syenite contains zoned albite-oligoclase, Na-rich alkali feldspar, albite, a sporadic quartz, zoned aegirine-augite, biotite, zoned hastingsite, titanite, apatite, and titanomagnetite. Albite and albite-oligoclase, perthitic Na-rich alkali feldspar, biotite, clinopyroxene with 7.8% of aegirine end member, magnetite, titanite, and apatite occur in leucocratic syenite. The alkali syenite and related pegmatites, locally with a trachytoid texture is a feldspathic rock grading to nepheline-bearing varieties. In addition to the Na-rich alkali feldspar and albite, this rock contains aegirine, arfvedsonite, lamprophyllite, ramsayite, murmanite, eudialyte, biotite, titanite, zircon, magnetite, ilmenite, apatite, huttonite, anatase, scheelite, as well as hydrothermal minerals (natrolite, sodalite, analcime, mordenite, epidote, chlorite, prehnite, catapleiite, zirfesite) and supergene

minerals (vermiculite, sungulite, cerussite, clay minerals). Tonsbergite consisting of Na-rich alkali feldspar, albite, aegirine, and arfvedsonite grades into alkali syenite proper and lujavrite. Albite syenite contains albite, aegirine, magnesioarfvedsonite, lamprophyllite, eudialyte, apatite, and insignificant admixture of nepheline, cancrinite, zeolite, and hydromica. Ijolite and related alkaline ultrabasic rocks with nepheline (10–80%) are divided into the arfvedsonite-aegirine and hastingsite-aegirine-augite varieties. Lujavrite and related pegmatites are composed of nepheline, Na-rich alkali feldspar, albite, and aegirine. They are characterized by a banded structure, gradual transition to pegmatite, alkali syenite, and ijolite deviating toward foyaite and mariupolite. The minor minerals include arfvedsonite, biotite, lamprophyllite, eudialyte together with replacing catapleiite and zirfessite, apatite, ramsayite, murmanite, pectolite, loparite, thorite, huttonite, zircon, titanite, ilmenite, the autometasomatic cancrinite, albite, analcime, sodalite (including hackmanite), natrolite, and late hydrothermal zeolites and hydromica. The pectolite and cancrinite (nepheline-free) lujavrites occur as separate bodies. Mariupolite consisting of nepheline, albite, and aegirine grades into alkali syenite and lujavrite. Miaskite stands out by its extremely complex mineral composition. This is a melanite-biotite-aegirine-augite-hastingsite rock occasionally containing epileucite and approximately equal amounts of nepheline, Na-rich alkali feldspar, zonal albite-oligoclase, and albite. Titanite, apatite, titanomagnetite and locally developed cancrinite and pectolite are permanent minor minerals. Melanite and hastingsite are typically replaced by biotite while hastingsite, by arfvedsonite, aegirine, and titanite; melanite is replaced by andradite and titanite. Zeolites, muscovite, and alteration products after nepheline were formed at the hydrothermal stage. The biotite miaskite is composed of nepheline, Na-rich alkali feldspar, albite-oligoclase and albite in approximately equal amounts with 5–10 vol % of biotite and with magnetite. The zonal aegirine-augite, aegirine, and hastingsite-arfvedsonite occur sporadically. Corundum, apatite, fluorite, melanite, albite, cancrinite, muscovite, and hydrothermal spreustein, liberenite, zeolites, green-blue mica, chlorite, muscovite, epidote, calcite, and hydromica are common. Coronas consisting of biotite replaced by radiate aegirine are typical. The hydrothermally altered syenite is a mixture of clay minerals, zeolites, gibbsite, albite, and relics of aegirine-augite, biotite, and fluor-hydroxyl-apatite. The hedenbergite-aegirine and albite-magnesioarfvedsonite alkali granites occur also.

Pneumatolytic and hydrothermal veins and veinlets cut the Konder massif occupying from 2–5 to 60–70% of the exposed local areas. Veins and veinlets

are controlled by a network of orthogonal, oblique, and tortuous fractures. Veinlets consist of minerals inherited from host rocks and newly formed diopside, augite, aegirine, anthophyllite-gedrite, tremolite-actinolite, kaersutite, hastingsite-arfvedsonite, richterite and related asbestos varieties, biotite, titanomagnetite, apatite, titanite, plagioclase, Na-rich alkali feldspar, nepheline, zeolites (natrolite, thomsonite, mordenite, etc.), pectolite, humite, perovskite, sulfides, PGM, gold, carbonates, serpentine, and sodalite.

Intrusive rocks in the exocontact aureole

Dikes, veins, and small plugs composed of monzodiorite with rounded and angular xenoliths of the pyroxenites and gabbro, as well as with fragments carried up from crystalline basement and sedimentary cover are known from the exocontact aureole together with minor intrusions of granitic rocks, diorite porphyry, andesite, dacite, spessartite, and shonkinitic picrite. All of these rocks, except granitoids, were referred by Yemel'yanenko et al. (1989) to the early phase of the Mesozoic Aldan Complex (along with gabbro and clinopyroxenite dikes) while Orlova (1991) correlates them with the Jurassic-Cretaceous Ket-Kap Complex.

MINERALOGY OF PGM PLACER DEPOSIT

According to the results of prospectors' mining (Sushkin, 1996), the major portion of the Konder platinum heavy concentrate consists of irregular, lump-shaped, angular, and perfectly faced grains of variable dimensions up to nuggets (12% of the total mined platinum including 4% that fall on the nuggets more than 10 g in weight). Nuggets of about 1 kg are seldom found. More than ten such nuggets were found during the washing seasons 1984–1994 including 4 nuggets, each of more than 1.5 kg in weight, and a unique 3.5-kg nugget. Euhedral platinum crystals are mainly cubic in habit. Particular hexahedral crystals dominate in small-size fractions. The amount of various twins and intergrowths of two–three individuals, up to 17 mm in dimension, increases among coarser grains. Gold films, 0.05–1.0 mm thick, surround many small platinum grains. In some cases, these films are coupled with crystalline gold. The gold films are without any doubt endogenic, because they consist of closely intergrown tiny crystals of Cu-bearing gold, Au- and Te-bearing sulfide, and some Pd and Pt compounds. The films on crystal edges ground during transport provides additional morphological evidence for their relatively high-temperature origin (Sushkin, 1995). However, the micrometer-thick gold films of high fineness on rounded platinum nuggets most likely are low-temperature (Nekrasov et al., 1994).

Native gold, silver, lead, tin, copper, nickel, iron, antimony, and bismuth occur along with platinum both in bedrock and stream placers (Emel'yanenko et al., 1989). In the areas, where small gold nuggets (1–10 g) have been found, the bulk native gold in the Konder placer does not exceed 3–5% of platinum heavy concentrate. Native silver, occasionally as nuggets, from 3–5 to 200 g in weight, is extremely sporadic in the placer (Sushkin, 1995).

More than 50 PGM, Au- and Ag-bearing minerals including new and rare species were identified in loose sediments over 20 years of study of noble-metal mineralization. Many of these minerals were also detected in bedrock. The specific mineral assemblages are related to one of two principal sources: (1) chromite-bearing dunite in the massif core and adjacent clinopyroxenite and (2) veins of phlogopite-magnetite clinopyroxenite that intrude dunite and spatially associated sulfide lenses in the southwestern part of massif. Isoferroplatinum (Pt_3Fe) as the main PGM is very heterogeneous as concerns saturation with iron and other PGM. Two varieties of this mineral were identified in the chromite-bearing dunite: (1) early, high-temperature variety in association with chromite and olivine and (2) late variety that fills the interstitial space in lenses and veins of massive chromite (Nekrasov et al., 1994). The early isoferroplatinum is relatively rich in other PGM and characterized by a variable Fe content (7.5–11.5 wt %) that decreases with depth (Fig. 2.2). Inclusions of Os, Ir, Ru, and Pt minerals are typical. In contrast, the late Pt-Fe alloys are free of such inclusions and are depleted in other PGM, except Pt, retaining the same Fe content. Platinum from dikes of phlogopite-magnetite clinopyroxene typically occurs as cubic crystals locally coated with a film of Cu-bearing gold. The composition is close to isoferroplatinum from source (1) but the iron content is higher (9.5–11.5 wt % Fe). Clinopyroxene, amphibole, phlogopite, magnetite, and apatite inclusions are often incorporated into the ore mineral.

Other PGM occur in extremely low quantities as small (commonly, no larger than few tens of micrometers) globular and tabular inclusions within isoferroplatinum and as outer rims around these grains. Their own segregations are extremely sporadic. Nevertheless, these microinclusions turned out to be very diverse and attracted the main interest of mineralogists.

Native osmium is the most abundant end member of the Os-Ir-Ru-Pt solid solution occurring as inclusions in the high-temperature isoferroplatinum hosted in dunite and massive chromite; native Pt, Ir, and Ru are observed only as rare inclusions, 10–170 μm in size. Inclusions of the native Ru were found only the third time over the world, and this finding is the purest one (Nekrasov et al., 1994).

We also established for the first time a contrasting Pt and Ir distribution in an inclusion of native Os incorporated into isoferroplatinum enriched or depleted in these metals. In the first case, the tabular, globular, and worm-shaped Os inclusions are markedly enriched in Pt and Ir (up to 6 and 17% wt, respectively). Moreover, the largest Os grains reveal a zonal distribution of Ir with its maximum in the center. The second variety of the native Os is represented by relatively coarse-crystalline aggregates (50×350 μm) containing no more than 2 wt % Pt and Ir. The interstitial space is filled with pure isoferroplatinum.

The transitional compounds of the Os-Ir-Ru-Pt system are no less specific (Fig. 2.3). In addition to the predominant iridosmine and platinosmiridium, the rutheniridosmine with a wide range of Ru contents (40–65 at. %) has been detected. Osmiruthenium, platiniridosmine, osmiplatinum, and osmiridium are extremely rare. The almost binary RuOs and more complex PtIrRuOs were found for the first time in addition to alloys native ruthenium (Nekrasov et al., 1994).

Marginal zones of isoferroplatinum grains from massive chromitite are characterized by diverse PGM, first of all, as concerns PGM sulfides and sulfoarsenides, laurite-erlichmanite disulfides and irarsite-hollingworthite sulfoarsenides are most abundant. Their composition is rather stable with predominance of end members and limited development of transitional compounds. Zoned grains are fairly common. The outer zones of Os-laurite and Ru-erlichmanite are mostly enriched in Ru, whereas the margins of irarsite

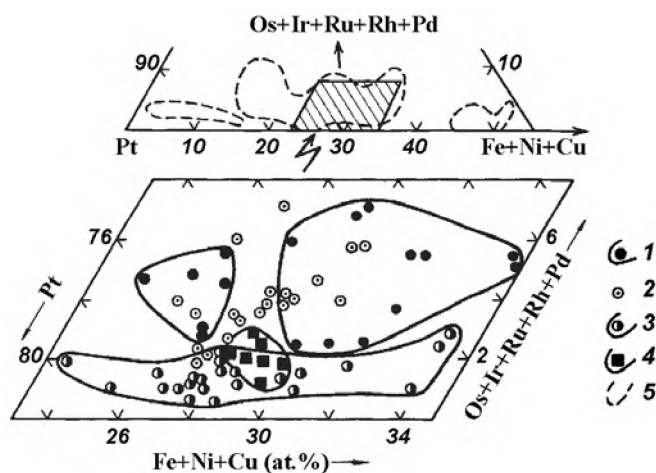


Fig. 2.2. Composition of native accessory isoferroplatinum from chromite-bearing dunite of the Konder massif.

1-3: Parts of the dunite core of the Konder massif: (1) highest eroded, (2) others; (3) massive chromite veins and schlieren in dunite; (4) magnetite pyroxenite forming dikes in dunite; (5) field contours for native Pt-Fe solid solutions from chromite-bearing dunite of ultramafic formations (after Zhemovskiy et al., 1985)

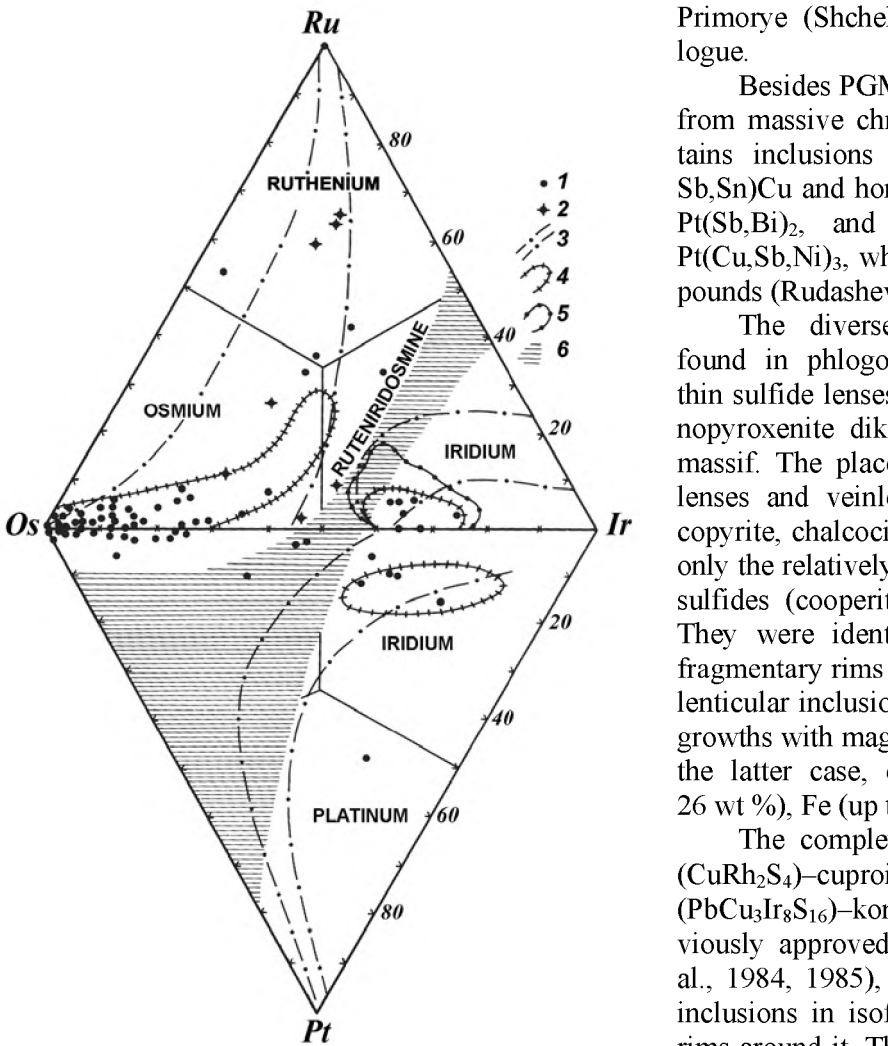


Fig. 2.3. Diagram of representative composition of Os-Ir-Ru-Pt system, at. % (after Harris and Cabri, 1991). of the Konder massif.

(1) after Nekrasov et al. (1994); (2) after Mochalov (1994); (3) fields of solid solution compositions of PGM from alpine-type ultrabasic rocks (after Dmitrenko et al., 1985); (4) the same from massifs of an alkali-ultrabasic formation (after Rudashevsky, 1989); (5) the same from the Konder massif (after Mochalov, 1994); (6) miscibility gaps (after Harris and Cabri, 1991)

and hollingworthite are commonly enriched in Ir and their cores in Rh.

PGM arsenides are commonly represented by sperrylite as small (50–250 μm) inclusions in the outer zones of the relatively pure isoferroplatinum. Separate hexagonal crystals, up to 1.5 mm in size, were also noticed. Rare small inclusions of Pt sesquiarsenide were also found in the same isoferroplatinum grain (wt %: 51.62 Pt, 1.08 Rh, 10.57 Ir, 0.28 Os, 0.16 Cu; 2.20 S; 33.14 As; total 99.05). The formula of this possible new mineral is $(Pt, Ir, Rh)_2(As, S)_3$. The phase $(Pt, Rh)_2(As, S)_3$ from the Au-Pt placer in the southern

Primorye (Shcheka et al., 1991) is its closest analogue.

Besides PGM listed above, pure isoferroplatinum from massive chromitite segregations in dunite contains inclusions of Sn-Sb tulameenite $(Pt, Pd)_2(Fe, Sb, Sn)Cu$ and hongshiite $(Pt, Pd)(Cu, Sn, Sb)$, geversite $Pt(Sb, Bi)_2$, and unnamed $(Pd, Pt, Cu)_3(Bi, Sb)$ and $Pt(Cu, Sb, Ni)_3$, which, probably, are new natural compounds (Rudashevsky et al., 1992).

The diverse noble-metal mineralization was found in phlogopite-magnetite clinopyroxenite and thin sulfide lenses localized in dunite close to the clinopyroxenite dikes in the southwestern part of the massif. The placers derived from erosion of sulfide lenses and veinlets composed of pentlandite, chalcocopyrite, chalcocite, bornite, and cubanite contain not only the relatively pure platinum but also PGM monosulfides (cooperite and more complex compounds). They were identified in many platinum grains as fragmentary rims (up to 10 μm and more), equant and lenticular inclusions along grain boundaries and intergrowths with magnetite, pentlandite, and pyrrhotite. In the latter case, cooperite is enriched in Ir (up to 26 wt %), Fe (up to 20 wt %), and Ni (up to 18 wt %).

The complex malanite $(CuPt_2S_4)$ –cuprorhodsite $(CuRh_2S_4)$ –cuproiridsite $(CuIr_2S_4)$ and inaglyite $(PbCu_3Ir_8S_{16})$ –konderite $(PbCu_3Rh_8S_{16})$ sulfides, previously approved as new minerals (Rudashevsky et al., 1984, 1985), occur as equant and veinlet-shaped inclusions in isoferroplatinum and as thin corrosion rims around it. These minerals were also identified in sulfide lenses and veinlets hosted in dunite feeding into the placer. Most of analyzed complex sulfides were identified as malanite, occasionally with elevated Rh and Ir contents (up to 13.6 and 26.6 wt %, respectively). The rest of the minerals are composed of cuproiridsite (up to 49 wt % Ir), its new extremely Rh-rich variety (up to 17.8 wt % Rh), Ir-cuprorhodsite (25.5 wt % Ir), and a new Pt-rich variety of this mineral with 30.3 wt % Pt. Inaglyite, saturated to the limit with Rh (11.05–12.56 wt %), is prevalent among the studied Cu–Pb-bearing sulfides. One mineral identified as konderite has a much lower Ir content (20,12 wt %) than in the compound formerly described as a new mineral (Rudashevsky et al., 1984, 1992). Two sulfide specimens enriched in Pt may be a new platinum analogue of inaglyite and konderite: $Cu_{3.13-3.33}Pb_{0.78-0.89}Ir_{1.99-2.06}Rh_{1.87-1.91}Pt_{3.17-3.29}S_{16}$ (Fig. 2.4).

In the gold-bearing part of the Konder placer localized in the field of the same phlogopite-magnetite clinopyroxenite, a predominantly pure platinum of cubic habit is associated with replacing tetraferro-

platinum, tulameenite, and hongshiite. The tetraferroplatinum is distinguished by a constant composition with insignificant admixture of Cu (up to 3 wt %) and Ni (up to 1.5 wt %). Tulameenite with an approximately constant Pt content reveals a wide variation of Fe (8.5–13.0 wt %) and Cu (8.8–12.8 wt %). Rare tulameenite grains associated with bornite demonstrate a nonuniform Ni (up to 3.5 wt %) and Ir (up to 2.5 wt %) distribution with enrichment of grain margins in these elements. Hongshiite was established to be most variable in composition. Both end members and transitional compounds of a hypothetical Pt(Cu, Fe)–Pd(Cu, Fe) series were detected in the same reaction rims surrounding the isoferroplatinum. Separate globular hongshiite grains with a concentric zoned structure vary in composition from a complex solid solution (Pt,Pd)(Cu,Fe) to PdCu, a new Pd analogue of hongshiite.

In the same placer, we found a Sn-bearing variety of hongshiite (wt %: 69.3 Pt, 12.8 Pd, 9.7 Cu, 7.2 Sn, total 99.0) more saturated with Sn than the previously described variety (Rudashevsky et al., 1992) and a complex Au-bearing sulfide (wt %: 52.47 Pd, 11.53 Au, 4.94 Ag, 15.64 Bi, 8.46 Pb, 0.69 Ni, 7.34 S, total 101.07) with a generalized formula $(\text{Pd,Au,Ag,Ni})_{10}(\text{Bi,Pb})_2\text{S}_4$. This mineral occurs as a discontinuous rim around inhomogeneous hongshite grains. According to experimental studies in the Au–Ag–S and Au–Bi–S systems (Nekrasov et al., 1994), it could be formed only at a relatively low temperature (200–350°C) and extremely high activity of the sulfide sulfur ($f_{\text{S}_2} \sim 10^{-2}$ – 10^{-3} Pa). We detected one more new mineral within this rim—a palladium germanide corresponding to the formula Pd_2Ge (wt %: 75.62 Pd, 1.12 Ag, 23.89 Ge, total 100.63).

Despite the considerable variation in all components, the integer ratios of Pd or (Pd + Pt + Ag) to (As + Bi + Sb) in most complex Pd and Pt arsenides is close to 3:1, i.e., similar to the guanginite (Fleischer, 1987). Most antimonidobismutharsenides belong to this group except two antimonidoarsenides, two bismutharsenides, and two bismuthtellurarsenides. One of the former fits an isomertierite formula $(\text{Pd}_{9.66}\text{Pt}_{1.34})_{11}(\text{Sb}_{2.18}\text{As}_{1.73}\text{Te}_{0.05})_{3.96}$. Judging from cation/anion ratio varying from 7/2 to 9/2, other bismutharsenides are close to arsenopalladinite. Most of the complex Pd and Pt arsenides occur as small isolated inclusions in isoferroplatinum, in Pd analogue of hongshite, and in the Pd- and Cu-bearing gold, where they are commonly associated with sobolevskite and other Pd-bismuthides and antimonid-bismuthides of PGM occasionally occurring as aggregates, up to

90 μm in size. The association with sperrylite is not so abundant.

Palladium bismuthides, antimonidobismuthides, and antimonides of the sobolevskite-sudburyite series are relatively rare. Small (10–25 μm) sobolevskite inclusions close in stoichiometry to PdBi mainly occur in Cu-bearing gold and are rare in isoferroplatinum. Many bismuthide grains are zonal: their margins are enriched in Pd up to Pd_3Bi . The latter mineral was also found as individual inclusions within the Cu-bearing gold along with rare froodite (Pd_2Bi) grains. Several small (up to 25 μm) sudburyite (PdSb) grains were found as intergrowths with sobolevskite and $\text{Pd}_3(\text{Bi,Sb})$ phase incorporated into gold together with crystals of native antimony, $5 \times (2-3)$ mm² in size.

Insizwaite (PtBi_2) and palladium bismuthoplumbide are limited in abundance. The latter was found in Cu-bearing gold as inclusions, 5–15 μm in size. The chemical composition of this presumably new compound (wt %: 57.72 Pd, 34.71 Pb, 7.02 Bi, 1.2 Pt, total 100.45) corresponds to the formula $(\text{Pd}_{7.91}\text{Pt}_{0.09})(\text{Pb}_{2.47}\text{Bi}_{0.50})_{2.97}$. Rare inclusions within the Cu-bearing gold are composed of zvyagintsevite $(\text{Pd,PtAu})_3(\text{Sn,Pb})$.

Minerals of the sobolevskite (PdBi)–kotulskite (PdTe) series are also not abundant. Owing to complete isomorphism between Te and Bi, inclusions consisting of two or three phases of significantly different transitional compositions are detected within one host mineral (Cu-bearing gold or platinum). A Bi-free phase with a high Sb content (wt %: 42.42 Pd, 0.57 Ag; 15.64 Sb, 38.81 Te, total 98.31), may be a new

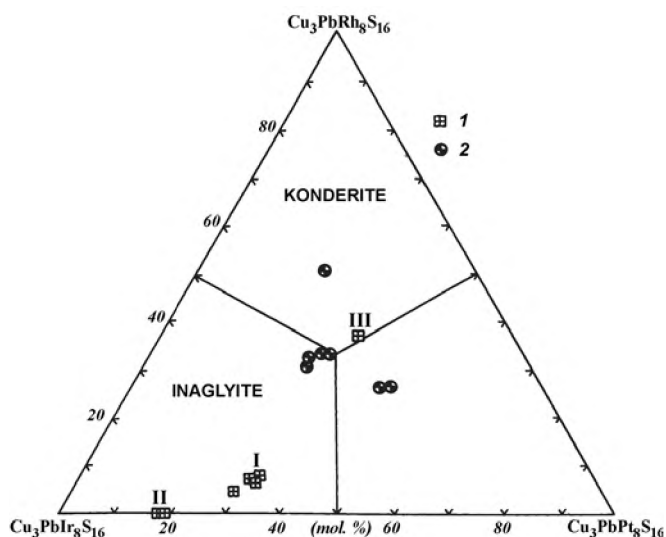


Fig. 2.4. Compositions of Cu-Pb-bearing complex sulfides of PGM.

(1) inaglyite (I, II) and konderite (III) from the Inagli (I), Nizhni Tagil (II), and Konder (III) massifs (after Rudashevsky et al., 1984a,b); (2) inaglyite, konderite, and what may be a new platinum analogue

mineral $\text{Pd}(\text{Sb}_{0.31}\text{Te}_{0.75})_{1.06}$ belonging to the kotulskite (PdTe)-sudburyite (PdSb) series.

We also found Bi-Te-palladinite, which is more abundant than minerals of the sobolevskite-kotulskite series and occurs as small (10–15 μm) inclusions within bornite and gold of a low fineness. This mineral is characterized by a fine zoning within a range of 2–3 wt % Pd and 0.5–1.5 wt % of other elements. Particular individuals of Bi-Te-palladinite were broken down with formation of two–three phases. One of them commonly is Pd oxide, and the rest of them were identified as Bi_3Te and native bismuth. The Bi_3Te compound makes up its own foliaceous segregations, up to 0.5 mm in size. In aggregates with gold of high fineness, the Bi_3Te phase postdated the former and cemented the gold grains. Graphically intergrown gold and native bismuth were also observed. Out of the gold grains, the latter grades to a Bi monocrystal and $\text{Au}-(\text{BiPb})_3\text{Te}$ aggregate.

The platinum and palladium stannides mostly form small (15–60 μm) inclusions within cupriferous gold, tulameenite, and isoferroplatinum. They can be subdivided into three groups by chemical composition. The first group is characterized by a complete absence of Cu and insignificant (up to 1 wt %) Sb admixture. The Pt + Pd sum amounts to 82 wt %, and the Sn content, to ~17 wt %. In general, the composition can be recalculated into the rustenburgite formula $(\text{Pt,Pd})_3\text{Sn}$. The second group comprises the multi-component high-Cu (up to 14 wt % Cu) alloys of the Pt-Pd-Sn-Cu-Fe system; Ni (up to 0.4 wt %) and Bi (up to 1.3 wt %) occur as admixtures. The substantial variation of Sn content (9.0–16.5 wt %) along with relatively constant Pt + Pd sum (68–72 wt %) and permanent presence of Fe (up to 5.8 wt %) is typical of the compounds belonging to this group. These phases are associated with sobolevskite and Pd-Cu-gold. The high-Pd solid solution of hongshiite type can be referred to the third group.

The PGM formation is completed with oxide and hydroxide compounds. Most of them were formed at a low temperature, but some species are suggested to be rather high-temperature products of interaction between the postmagmatic solutions and the early magmatic PGM. Oxides and hydroxides commonly replace tulameenite and hongshiite inclusions hosted in isoferroplatinum. Besides Pt, they contain Fe and Cu. Pd, Os, Rh, and Ir oxides and hydroxides are much less abundant in placers. Thin palladium hydroxide film coats the Pd-hongshiite, whereas Ir, Os, and Rh hydroxides partly replace irarsite-hollingworthite, complex monosulfides and other PGM (Nekrasov et al., 1994).

The gold mineralization in the Konder massif is extremely diverse. As follows from numerous micro-

probe results, not only native and Ag-bearing gold but also Cu-, Cu-Pd-, and Cu-Pt varieties (Nekrasov et al., 1994; Nekrasov et al., 2001), exceptionally rare in nature (Novgorodova, 1983, 1984), are present herein.

The gold minerals were formed later than the cubic platinum crystals and, probably, somewhat later than PGM sulfides and sulfoarsenides but contemporaneously with various Pd-bearing compounds including Pt-Pd-hongshiite, complex sulfides, arsenides, antimonides, bismuthides, tellurides, stannides, plumbides, and palladium germanide.

The compounds of gold and other metals can be divided into three broad groups (Fig. 2.5), which are distinguished by proportions of Au, Cu, Ag, Pd, and Pt (Nekrasov et al., 2001).

The first group of solid solutions comprises compounds based on Au and Cu and belonging to the Au-Cu, Au-Cu-(Pd,Pt), and Au-Cu-Ag systems. They form fine tabular and spindle-shaped inclusions in Ag-bearing gold of high fineness or serve as host minerals containing inclusions of the Ag-bearing gold. In addition, both types of Cu-bearing and native gold intergrowths occur as zoned rims around the platinum crystals and occasionally around other minerals. The Cu-bearing gold from Konder reveals a bimodal copper distribution that demonstrates a high abundance of "cuproauride" Au_3Cu , which is lacking in other natural assemblages (Murzin et al., 1987; Novgorodova, 1983; Sazonov et al., 1994), and tetraauricupride (AuCu) with a whole range of Cu contents from 6.89 to 24.99 wt %. The Cu content of 44.27 wt % corresponding to auricupride (Cu_3Au) was detected only in one sample. Auricupride in association with tetraauricupride is more typical of some other occurrences of Cu-bearing gold in the absence of Au_3Cu (Novgorodova, 1983). Some phases of Cu-bearing gold contain Ag (0.33–5.39 wt %) that replaces Cu when its content in gold is no lower than 14 wt %. The Pt and Pd admixtures (0.22–11.79 wt % and 0.18–10.27 wt %, respectively) were established in a broader range of compositions within the Au-Cu series (8–25 wt % Cu). Pt and Pd are present in various proportions, either separately or together. The elevated Pt content is inherent only in AuCu , i.e., in compositions enriched in Cu. The Cu-free Pd-bearing gold (wt %: 94.32 Au, 2.58 Pd) was detected at margins of a complex grain of Pd-Cu-bearing gold with zvyagintsevite $(\text{Pd,Pt,Au})_3(\text{Sn,Pb})$ inclusions.

The second broad group of natural Au compounds comprises its solid solutions with Ag (1.71–62.73 wt %). This is mainly a low-Cu (0.58–3.13 wt %) native gold of moderate and high fineness. The Au-Ag solid solutions richer in Ag, i.e., close to electrum and auroan silver in composition, also occur in heterogeneous grains.

The third broad group of the three-component compounds with 3–5 wt % Cu and 5–9 wt % Ag can be regarded as another group of gold phases. If concentration of this pair of elements in gold is still higher, then the three-component alloy becomes unstable below 370–410°C (experimental results reported by Nekrasov et al., 1991) and breaks down into Au-Cu-(Ag) and Au-Ag-(Cu) phases. The phase proportions in representative intergrowths with exsolution textures and the distribution of data points on the Ag-Cu-Au diagram show that the initial composition of Au-Ag-Cu alloys that underwent exsolution during postcrystallization cooling was as follows (at. %): from 51–55 to 72–75 Au, from 5–8 to 20–22 Ag, and from 12–14 to 32–35 Cu.

In addition to the close intergrowths of Cu- and Ag-bearing gold in heterogeneous grains and the gold powder on platinum grains, gold of high fineness occurs as films coating platinum nuggets in the Konder placer. Individual gold grains with a high fineness (up to 990) at margins and a lower fineness (750–820) in the core are sporadically found. The gold of the high fineness was likely formed within the placer as a result of different Ag and Au solubility in groundwater (Nekrasov et al., 1994). Gold grains with a high fineness in core and low fineness (including electrum) at margins are probably related to acid rocks from outer zones of the Konder massif.

EXCURSION POINTS

Stop 1: Study of rocks in the southwestern sector along the divide between the Yuzny and Trezubets

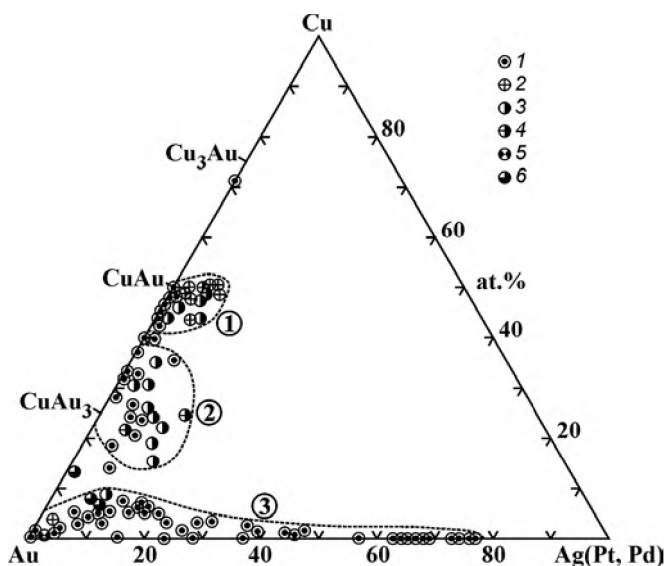


Fig. 2.5. Au-Cu-Ag(Pt, Pd) diagram for copper and silver gold solid solutions from the Konder massif.

Solid solutions: (1) Au-Cu, Au-Cu-Ag, and Au-Ag; (2) Au-Cu-Pt; (3) Au-Cu-Pd; (4) Au-Cu-Pt-Pd; (5) Au-Cu-Pt with Ag; (6) Au-Cu-Pd with Ag. See text for other explanations

creeks (bulldozer cuttings, trenches, natural outcrops) up to the monzonite and granodiorite block field. The chromite-bearing dunite with sporadic dikes of phlogopite-magnetite clinopyroxenite, arfvedsonite granite, and fragmentary spots of aegirine syenite are available to observe.

Stop 2: Study of the largest chromitite vein of the Konder massif in the vicinity of the Mount Os'minog (Devilfish).

Stops 3 and 4: Routes along the Pryamoi (Straight) Creek and Anomal'ny (Anomalous) Creek where the chromite-bearing dunite is cut by dikes of magnetite-phlogopite clinopyroxenite with Ti-vesuvianite and titanite and dikes of alkaline rocks (syenite, ijolite, etc.) with local pegmatoid segregations of arfvedsonite, lamprophyllite, and ramsayite. At the end of outcrop, the dunite gives way to the ring of olivine clinopyroxenite that is cut by the dikes similar to those in dunite. Further outward, the magnetite clinopyroxenite free of olivine, gabbropyrroxenite, and gabbro can be observed in trenches and prospect holes in the marginal part of the massif.

Stop 5: Study of the contact zone in the gorge of Konder River. Massive and gneissose hornfels after sandstone and siltstone containing gahnite (Zn-spinel), monticellite-perovskite calciphyre, and apopericase brucite marble with rare silicate-qandilite interlayers can be observed.

Stop 6: Route along the Trekhglavy (Three-headed) Creek across the chromite-bearing dunite, ring of olivine and magnetite clinopyroxenite, gabbropyrroxenite, vesuvianite and wollastonite skarn.

REFERENCES

Andreev, G.V., *Konderskii massiv ultraosnovnykh i shchelochnykh porod* (The Konder massif of ultramafic and alkaline rocks), Novosibirsk: Nauka, 1987, 76 p.*

Bogomolov, M.A., Nature of crystalline schists and carbonate rocks near the Konder massif, in: *Petrografiya metamorficheskikh i izverzhennykh porod Aldanskogo shchita* (Petrography of metamorphic and igneous rocks of the Aldan Shield), Moscow: Nauka, 1964, pp. 32–56.*

Dmitrenko, G.G., Mochalov, A.G., Palandzhyan, S.A., and Goryacheva, E.M., *Himicheskie sostavy porodoobrazuyushchih i akcessornykh mineralov alpinotipnykh ultramafitov Koryakskogo nagor'ya* (Chemical compositions of rock-forming and accessory minerals of alpine-type ultramafics of Koryak Plateau.) Ch.2. *Mineraly platinovykh elementov. Preprint. Magadan: CVKNII DVNC AN SSSR* (Pt. 2. Minerals of platinum elements (preprint), Magadan: USSR Acad. Sci., Far East Centre, North-Eastern Complex Research Inst.), 1985, 61 p.*

Fleischer, M., *Glossary of mineral species*, Tucson: Mineralogical Record Inc., 1987.

Harris, D.C. and Cabri, L.J., Nomenclature of platinum-group-element alloys: review and revision, *Can. Mineral.*, 1991, vol. 29, pp. 231–237.

* In Russian.

- Ivanov, O.K. and Rudashevsky N.S., Compositions of olivine and Cr-spinel from dunite in the Platinum Belt, the Urals, in: *Mineraly mestorozhdenii Urala* (Minerals from the Uralian deposits), Sverdlovsk: Uralian Scientific Centre, Academy of Sciences of the USSR, 1987, pp. 16–35.*
- Kostoyanov, A.I., The Re-Os model age of platinum minerals, *Geol. Rudn. Mestorozhd.*, 1998, no. 6, pp. 545–550.*
- Lennikov, A.M., Oktyabrsky, R.A., Sapin, V.I., et al., New data on rocks in metamorphic framework of the Konder massif, *Dokl. Akad. Nauk SSSR*, 1991, vol. 319, no. 5, pp. 1187–1191.*
- Marakushev, A.A., Yemel'yanenko, E.P., Nekrasov, I.Ya., et al., Formation of concentrically zoned structure of the Konder alkaline ultramafic massif, *Dokl. Akad. Nauk SSSR*, 1990, vol. 311, no. 1, pp. 167–170.*
- Mochalov, A.G., *Mineralogiya platinoïdov iz dunitov// Geologiya, petrologiya i rudonosnost Konderskogo massiva*. (Mineralogy of platinum-group elements from dunites, in: Geology, petrology, and ore mineralization of the Konder massif), Moscow: Nauka, 1994, pp. 92–106.*
- Murzin, V.V., Kudryavtsev, V.I., Berzon, R.O., and Sustavov, S.G., The Cu-bearing ore in rodingite zones, *Geol. Rudn. Mestorozhd.*, 1987, no. 5, pp. 96–99.
- Nekrasov, I.Ya., *Geokhimiya, mineralogiya i genesis zolotorudnykh mestorozhdenii* (Geochemistry, mineralogy, and genesis of gold deposits), Moscow: Nauka, 1991, 302 p.*
- Nekrasov, I.Ya., Lennikov, A.M., Oktyabrsky, et al., *Petrologiya i platinonosnost kol'tsevykh shchelochno-ultraosnovnykh kompleksov* (Petrology and platinum potential of ring alkaline-ultramafic complexes), Moscow: Nauka, 1994, 381 p.*
- Nekrasov, I.Ya., Ivanov, V.V., Lennikov, A.M., et al., Rare natural polycrystalline alloys based on gold and copper from a platinum placer in the Konder alkaline-ultrabasic massif, southeastern Aldan shield, Russia, *Geol. of Ore Deposits*, 2001, vol. 43, no. 5, pp. 406–417 (translated from *Geologia Rudnykh Mestorozhdenii*, 2001, vol. 43, no. 5, 452–464).
- Nikol'sky, N.S., Lennikov, A.M., Oktyabrsky, R.A., and Kononova, N.P., Thermodynamic parameters of gas phase equilibrium in olivine from the Konder massif, in: *Problemy magmatizma, metamorfizma i orudneniya Dal'nego Vostoka* (Problems of magmatism, metamorphism, and ore mineralization in the Far East), Yuzhno-Sakhalinsk: Far East Division, Academy of Sciences of the USSR, 1988, pp. 103–105.*
- Novgorodova, M.I., *Samorodnye metally v gidrotermal'nykh rudakh* (Native metals in hydrothermal ores), Moscow: Nauka, 1983, 287 p.*
- Novgorodova, M.I., Crystal chemistry of native metals and natural intermetallic compounds, in: *Itogi nauki i tekhniki VINITI* (Achievements of Science and Engineering, Ser. Crystal Chemistry), 1994, vol. 29.*
- Oktyabrsky, R.A., Lennikov, A.M., Zalishchak, B.L., et al., Cr-spinels from the Konder massif, *Izv. Ross. Akad. Nauk, Ser. Geol.*, 1992, no. 8, pp. 76–90.*
- Oktyabrsky, R.A., Lennikov, A.M., Shcheka, S.A., et al., Rare spinels from contact aureole of the Konder massif, *Miner. Zhurn.*, 1992, vol. 14, no. 2, pp. 38–47.*
- Oktyabrsky, R.A., Shcheka, S.A., Lennikov, A.M., and Afanasyeva, T.B., The first occurrence of qandilite in Russia, *Miner. Mag.*, 1992, vol. 56, no. 2, pp. 385–389.
- Orlova M.P. Geological structure and genesis of the Konder ultramafic massif, *Tikhookean Geol.*, 1991, vol. 1, pp. 80–88.*
- Pushkarev, Yu.D., Kostoyanov, A.I., Orlova M.P., et al. Sm-Nd, Rb-Sr, K-Ar, and Re-Os isotopic constraints on the origin of PGM mineralization in the Konder massif, Khabarovsk region, Russia, in: *Mineral deposits at the beginning of the 21st century*, Piestrzynski et al., eds., Lisse: Swets and Zeitlinger Publ., 2001.
- Reverdatto, V.V. and Sal'ko, A.K., Magmatic temperature of the Bor-Uryakh massif, *Geol. Geofiz.*, 1967, no. 5, pp. 119–122.*
- Rozhkov, I.S., Kitsul, V.I., Razin, L.V., and Borishanskaya, S.S., *Platina Aldanskogo shchita* (Platinum of the Aldan Shield), Moscow: Izd. Akad. Nauk SSSR, 1962, 280 p.*
- Rudashevsky, N.S., Evolution of chemical composition of osmium, ruthenium, and iridium hexagonal solid solutions in different ultramafites formations, *Geologiya i Geofizika*, 1989, no. 10, pp. 68–74.*
- Rudashevsky, N.S., Burakov, V.E., Malich K.N., and Khaetsky, V.V., Accessory PGM in chromitite of the Konder alkaline ultramafic massif, *Miner. Zhurn.*, 1992, vol. 14, no. 15, 1992, pp. 12–32.*
- Rudashevsky, N.S., Men'shikov, Yu.P., Mochalov A.G., et al., Cuprorhodsite CuRh_2S_4 and cuproiridsite CuIr_2S_4 as new natural PGM thiospinels, *Zap. Vsesoyuzn. Mineral. Obshch.*, 1985, pt. 114, no. 2, pp. 187–195.*
- Rudashevsky, N.S., Men'shikov, Yu.P., Begizov, V.D., et al., Inaglyite $\text{Cu}_3\text{Pb}(\text{Ir},\text{Pt})_8\text{S}_{16}$ as a new mineral, *Zap. Vsesoyuzn. Mineral. Obshch.*, 1984a, pt. 113, no. 6, pp. 712–717.*
- Rudashevsky, N.S., Mochalov A.G., Trubkin, N.V., et al., Konderite $\text{Cu}_3\text{Pb}(\text{Rh},\text{Pt},\text{Ir})_8\text{S}_{16}$ as a new mineral, *Zap. Vsesoyuzn. Mineral. Obshch.*, 1984b, pt. 113, no. 6, pp. 703–711.*
- Sazonov, A.M., Romanovsky, A.E., Grinev, O.M., et al., The noble-metal mineralization of the Guli intrusion, Siberian Platform, *Geol. Geofiz.*, 1994, no. 9, pp. 51–65.*
- Shnai, G.K. and Kuranova, V.N., New evidence for age of dunite in composite massifs of ultramafic-alkaline composition, *Dokl. Akad. Nauk SSSR*, 1981, vol. 261, no. 4, pp. 950–952.*
- Shcheka, S.A., Vrzhosek, A.A., Sapin, V.I., and Kiryukhina N.I., Transformation of PGM from the Primorye placers, *Miner. Zhurn.*, 1991, vol. 13, no. 1, pp. 31–40.*
- Sobolev, A.V., Kamenetsky, V.S., and Kononkova, N.N., New petrological and geochemical data on ultramafic volcanics from the Valagin Range, the eastern Kamchatka, *Geokhimiya*, 1989, no. 12, pp. 1694–1709.*
- Sushkin, L.B., Specific features of native elements at the Konder deposit, *Tikhookean Geol.*, 1995, vol. 14, no. 5, pp. 97–102.*
- Vasil'ev, Yu.R., Accessory Cr-spinels as an indicator on formation conditions of ultramafic igneous rocks, in: *Voprosy geneticheskoi petrologii* (Problems of genetic petrology), Novosibirsk: Nauka, 1981, pp. 61–85.*
- Velinsky, V.V. and Bannikov O.L., *Oliviny al'pinotipnykh giperbazitov* (Olivines of Alpine-type ultramafic rocks), Novosibirsk: Nauka, 1986, 104 p.*
- Yel'yanov, A.A. and Moralev, V.M., Massifs of ultramafic and alkaline rocks: depth of formation and erosion level, *Geol. Rudn. Mestorozhd.*, 1972, no. 5, pp. 32–40.*
- Yemel'yanenko, E.P., Maslovsky, A.N., Zalishchak, B.L., et al., Localization of ore mineralization in the Konder alkaline ultramafic massif, in: *Geologicheskie usloviya lokalizatsii endogenogo orudneniya* (Geologic conditions of localization of endogenic ore mineralization), Vladivostok: Far East Division, Academy of Sciences of the USSR, 1989, pp. 100–113.*
- Zhernovskiy, I.V., Mochalov, A.G., and Rudashevsky, N.S., Phase heterogeneity of isoferroplatinum rich in iron, *Dokl. Akad. Nauk SSSR*, 1985, vol. 283, no. 1, pp. 196–200.*



THE KOMSOMOLSK ORE DISTRICT

S.M. Rodionov¹, B.I. Semenyak², V.Yu. Zabrodin³

¹*Institute of Tectonics and Geophysics, Far East Branch, Russian Academy of Sciences, Khabarovsk*

²*Far East Geological Institute, Far East Branch, Russian Academy of Sciences, Vladivostok*

³*State Geological Exploration Enterprise, Khabarovsk*

INTRODUCTION

The Komsomolsk ore district is a part of the Eastern Asia Tin Belt, which stretches from Indonesia in the south to the Chukotka Peninsula at the north (Fig. 3.1). The northern part of the Eastern Asia Tin Belt located within the Far East of Russia (Figs. 3.1, 3.2), which is one of the largest tin regions in the world. About 43,000 tonnes of tin in concentrate were produced in the Russian Far East from 1991 to 1995.

The geodynamic settings of the tin areas of the Russian Far East are determined by their location at intersections of different tectonic-stratigraphic units of the following types (Fig. 3.3): (1) Cratonal and (or) metamorphosed continental margin terranes composed of Paleozoic and older metamorphic rocks; (2) Accretionary wedge or subduction zone terranes composed predominantly of Paleozoic and early Mesozoic cherty-volcanic-terrigenous rocks; (3) Turbidite basin terranes composed predominantly of continental slope terrigenous Mesozoic rocks with local tectonic lenses and inclusions of deep-water oceanic calcareous, sandy-argillaceous, and cherty-volcanic rocks of Paleozoic and early Mesozoic age; and (4) Overlapping and connected assemblages of calc-alkaline volcanic-plutonic belts of predominantly late Mesozoic and early Tertiary age (Rodionov, 2000_{1,2}).

Such geodynamic settings are illustrated by relating the tin deposits to the corresponding structural elements (Fig. 3.4) and to composition features of tin magmatic complexes (Fig. 3.5).

GEODYNAMIC SETTING OF THE KOMSOMOLSK ORE DISTRICT

The area is composed of the following tectonic-stratigraphic terranes (Nokleberg et al., 2003), which are shown on the map (Fig. 3.6) by corresponding symbols and are arranged alphabetically below by map symbols.

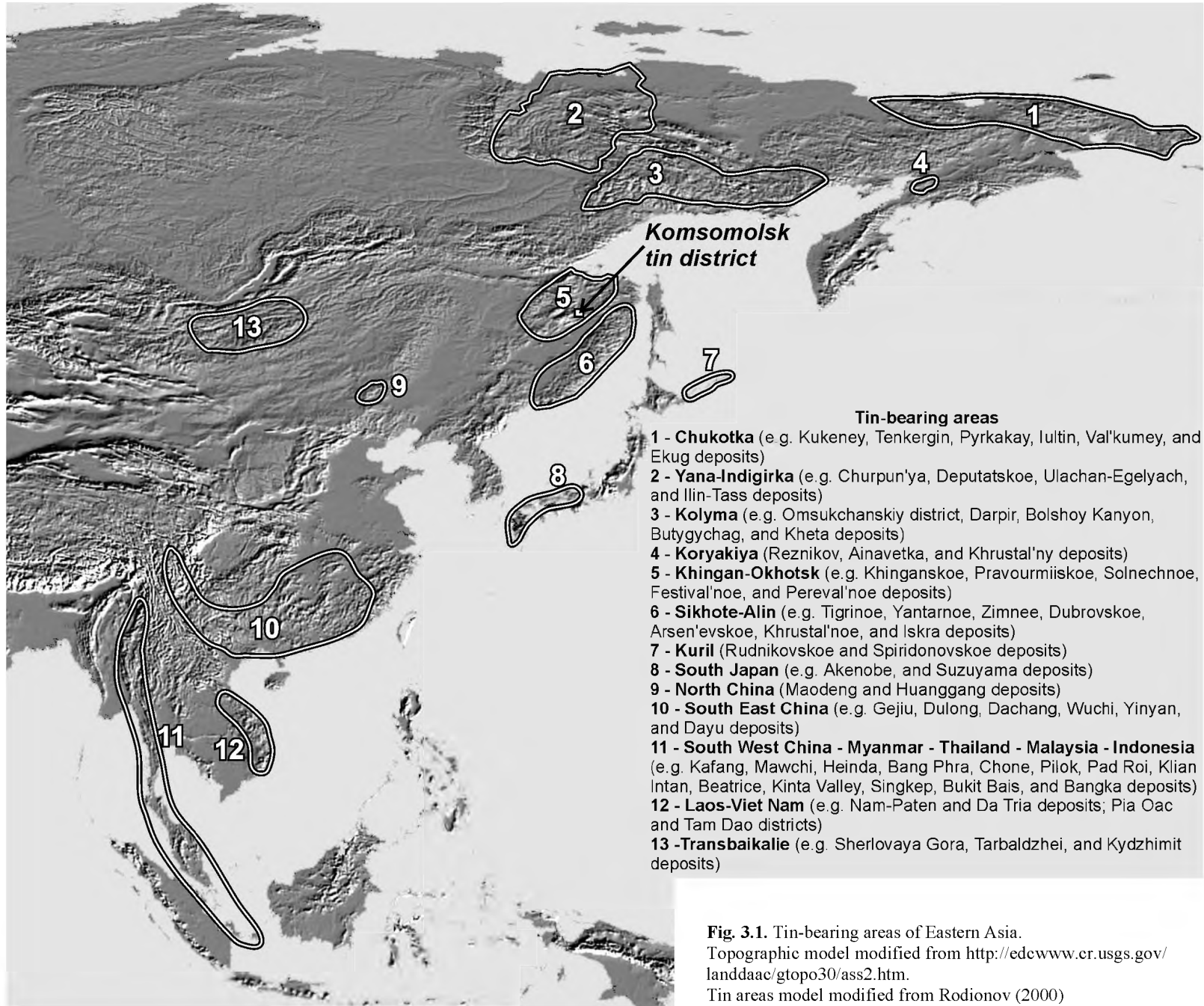
The Komsomolsk ore district lies within the Badzhal accretionary wedge terrane (unit BD), which occupies an area between the Bureya metamorphic (cratonal) terrane (unit BU) to the west and the Zhuravlevsk-Amur River continental margin turbidite terrane (unit ZRA) to the east. The ore district is located near the boundary of Badzhal terrane and Zhuravlevsk-Amur River terrane. The junction area is overlapped by magmatic assemblages of the Cretaceous

Khingan-Okhotsk volcanic-plutonic belt (unit *ko* – volcanic part and unit *kog* – plutonic part) and the Neogene-Quaternary Central Asian plateau basalt belt (unit *ca*).

Zhuravlevsk-Amur river turbidite terrane

The composition and structure of the Zhuravlevsk-Amur River terrane (see Fig. 3.6) can be observed in continuous outcrops along the right bank of the Amur River opposite Komsomolsk-on-Amur City (Kirillova et al., 2002) (Fig. 3.7). This outcrop is composed of the following rock types:

1). *Aleuopelites (mudstone) containing a horizon of mixtites*. Matrix and fragments of aleuopelites (mudstone) can be differentiated sometimes only by thin bedding and colour. Massive (up to 1 m in size) gray sandstones, gray limestone nodules (0.4 m), cal-



S.M. RODIONOV, B.I. SEMENYAK, V.YU. ZABRODIN

Fig. 3.1. Tin-bearing areas of Eastern Asia. Topographic model modified from <http://edcwww.cr.usgs.gov/landdaac/gtopo30/ass2.htm>. Tin areas model modified from Rodionov (2000)

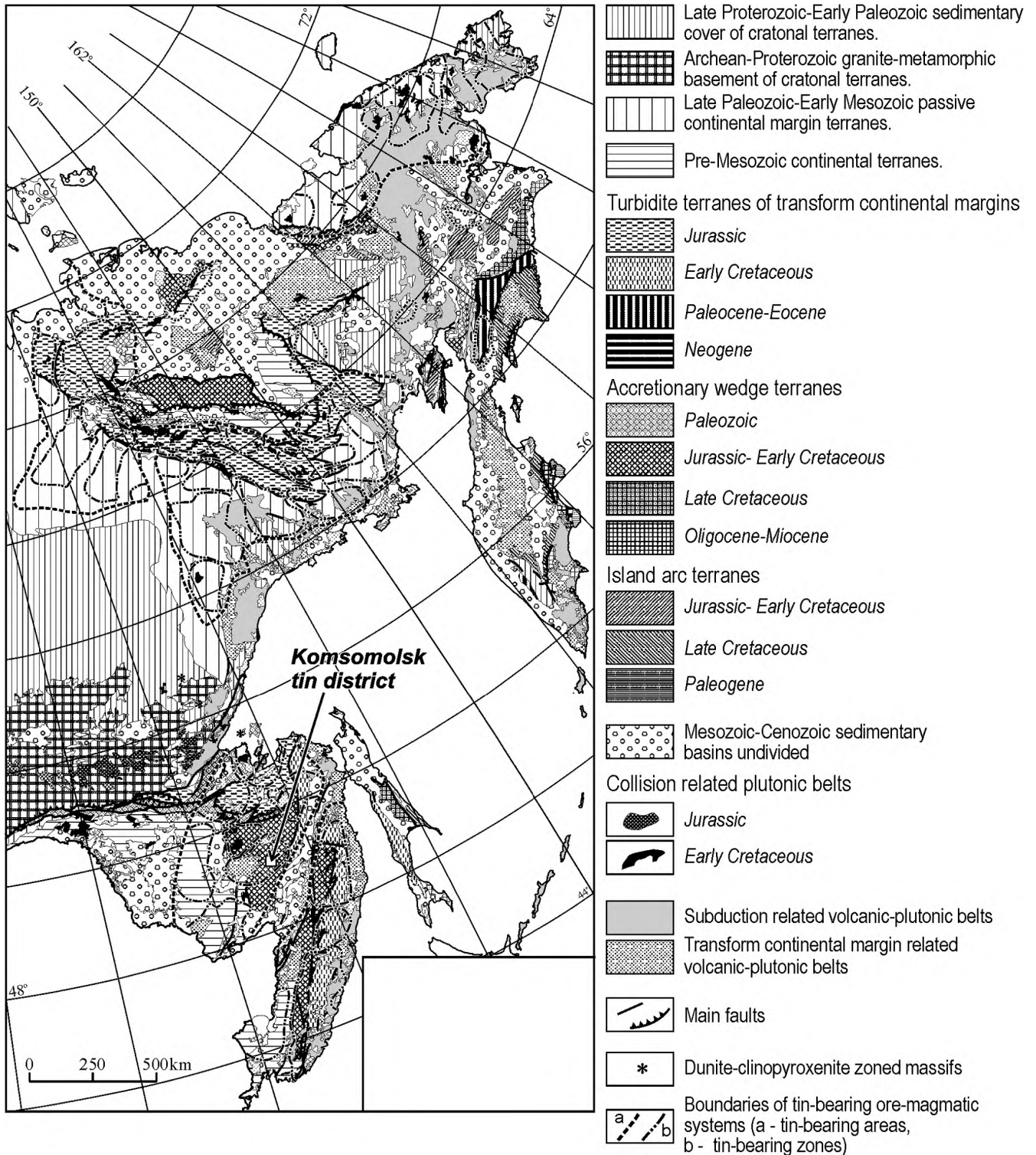


Fig. 3.2. Main Mesozoic-Cenozoic tectonic elements and tin-bearing areas of Far East Russia. Tectonic map modified from "Circum-North Pacific Tectonic-Stratigraphic Terrane Map", 1:5000000 Scale (Nokleberg et al., 1998; Khanchuk, Ivanov, 1999); Tin-bearing areas from "Tin metallogeny map of Magadan Oblast", 1:1500000 Scale (Rodionov et al., 1992, unpublished) and "Tin metallogeny map of Far East Russia", 1:1500000 Scale (Rodionov et al., 1990, unpublished)

careous sandstones, and thin lenses of green acid tuffs are rare.

2). Black aleuropelites (mudstone) with sparse bands of compact dark gray siliceous aleuropelites

(mudstone) with a thickness of 2-5 cm. Blocks of sandstones, lenses and fragments of limestones are extremely rare. The rocks are highly schistose, deformed into narrow folds and cut by faults. Radiolari-

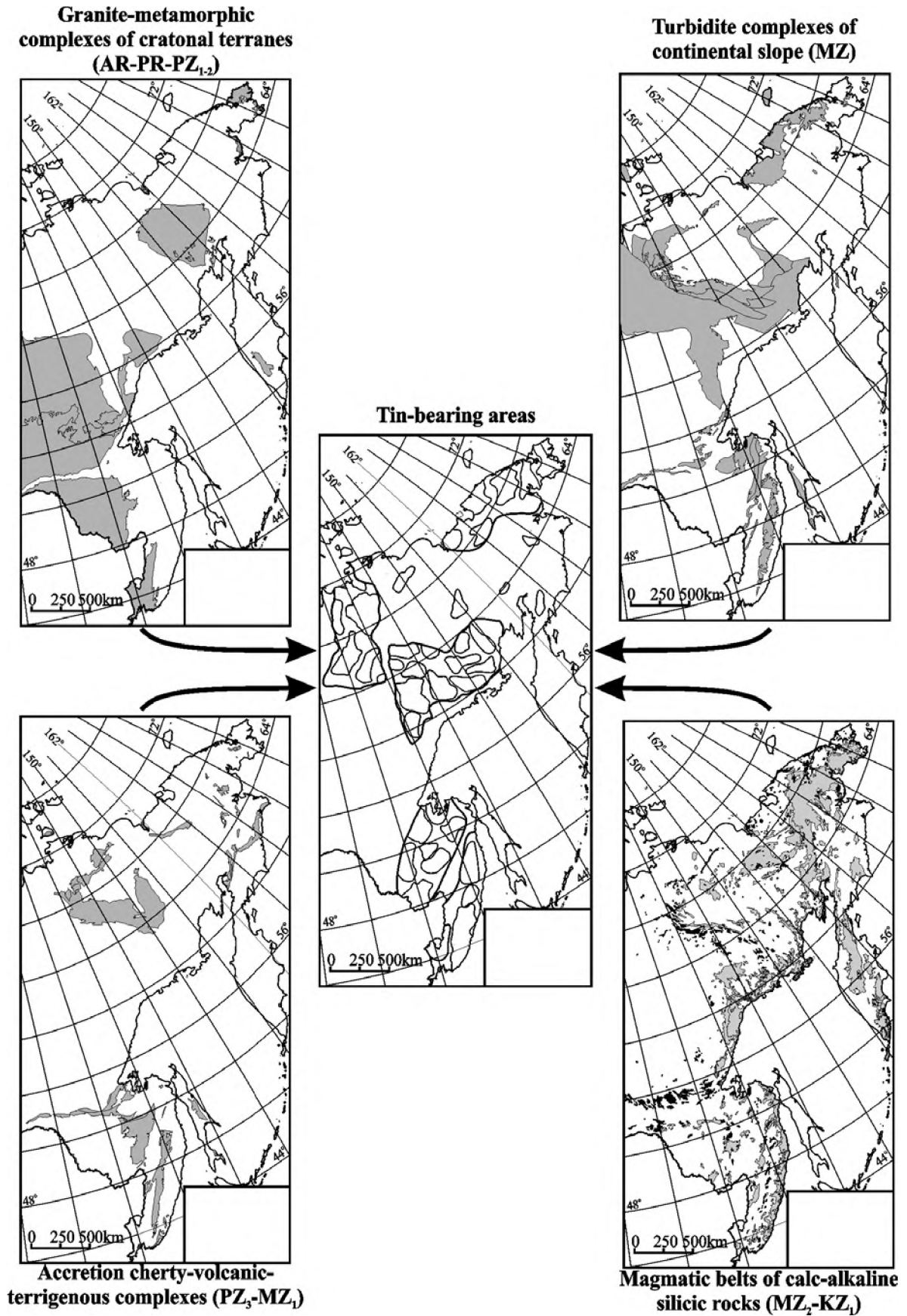


Fig. 3.3. Combination of genetically different rock complexes favorable for localization of tin-bearing areas in Far East Russia

ans of Early-Late Tithonian – Latest Tithonian age were extracted from the nodular siliceous mudstone of this unit.

3). *Gray fine sandstones with packets of thin-bedded turbidites up to 0.2 m thick.* Over about a 50 m distance, the degree of rock schistosity gradually increases. Rocks are metamorphosed; the shales are marked by lenticular texture. Besides sandstone lenses, lenticular limestones, blocks of gray cherts were detected.

4). Irregular alternation of gray fine sandstones containing mudstone beds, and beds composed of two- and three-component turbidites (J₃V-K₁V). The thickness of isolated components varies from 5 to 20 cm. Fine-grained sandstones are indurated and silicified. Thin lenticular light green tuff interbeds are sporadically distributed. Silification might be related to volcanic activity. Often patterns of flow burrows are seen. Non-plutonic sandy dykes about 7 cm thick occur in the mudstones containing bioturbation traces and phosphatic concretions. Dark siliceous mudstone yields radiolarians of the latest Tithonian age.

5). Black siltstones, mudstones with rare marly concretions, sparse laminite beds (1-3 mm thick), and gray siliceous mudstone beds with a thickness of 1-2 cm. Contacts are usually parallel and sometimes wavy. Black siltstones or silty sandstones with vertical and horizontal burrows, trace fossils, plant debris, and sulphides are predominant in the outcrops. An increased bituminosity has been discovered in these siltstones. Siltstone (3-5 cm) and sandstone (5-7 cm) beds alternation is observed very rarely. The fauna of Anopaea and buchiids is found more frequently and that of ammonites occurs in minor amount. Among the buchiids Valanginian species are predominant, those of the Berriasian are infrequent, as also are Volgian species.

6). *Gray greenish-gray indurated well-sorted sandstones with rare thin-bedded sandstone and siltstone beds.* Abundance of black plant debris along the bedding planes provides formation of lamination in the sandstones. At the base of the sandstone beds one can see uneven contacts, channel cuts, roiling and sliding textures. Common are cross bedding, ripples, and hummocky cross stratification. These are features of a shallow water environment within the activity of storm waves. A rich buchiid fauna has been found here: *Buchia volgensis* Lah., *B. uncitoides* Pavl., *B. cf. sibirica* Sok., *A. cf. keyserlingi* Lah., *A. ex gr. lahuseni* Pavl., ammonite *Sarasinella cf. hyatti* Stanton, *Inoceramus aff. ovatus* Stanton., along with indefinable plant remains.

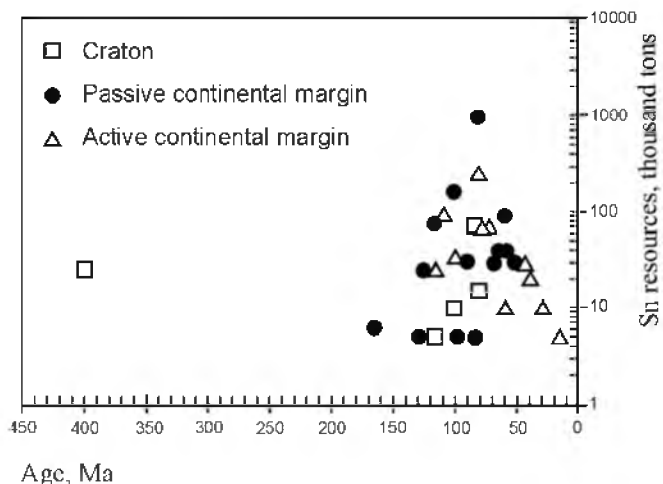


Fig. 3.4. Geodynamic setting of Sn resources. Each point corresponds to one tin district

7). *Alternation of thick-, medium-, and thin-bedded turbidites is observed over a distance of approximately 1 km.* At the base of the thick-bedded turbidites coarse-grained sandstones and gravelstones with eroded boundaries at the base are sometimes distinguished. *The rock is folded to anticline.* The northern limb of the anticline is composed of mostly medium-bedded turbidites containing sandstone beds 8-15 cm in thickness, and aleuopelites, 5-12 cm thick, composing packets (10-50 m thick) alternated with thin-bedded turbidites 8-30 m in thickness (sandstone beds are 1-2 cm and aleuopelite – 2-3 cm thick) and isolated thick-bedded turbidites (0.5-2.5 m thick). Beds of gray fine sandstones about 20 m thick are

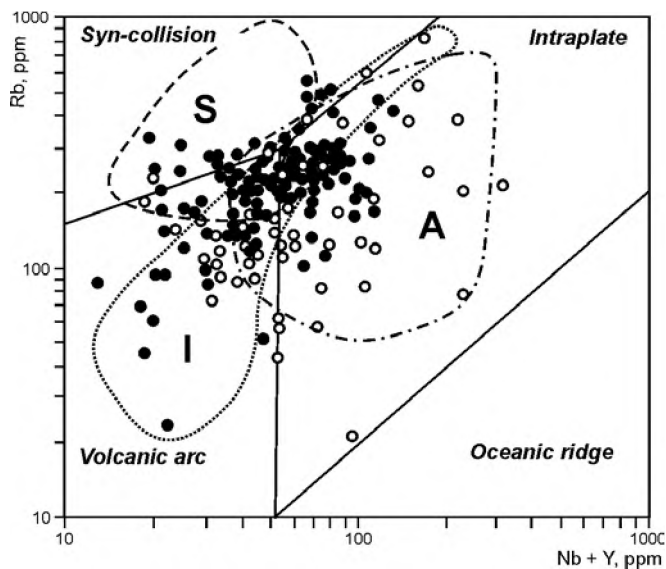


Fig. 3.5. Tin magmatic complexes of North East (white circles) and South East (black circles) Russia in magmatic rock classifications after Pearce et al. (1984), Chappel and White (1974, 2001), and Whalen et al. (1987). Using data from Gonevchuk (2002)

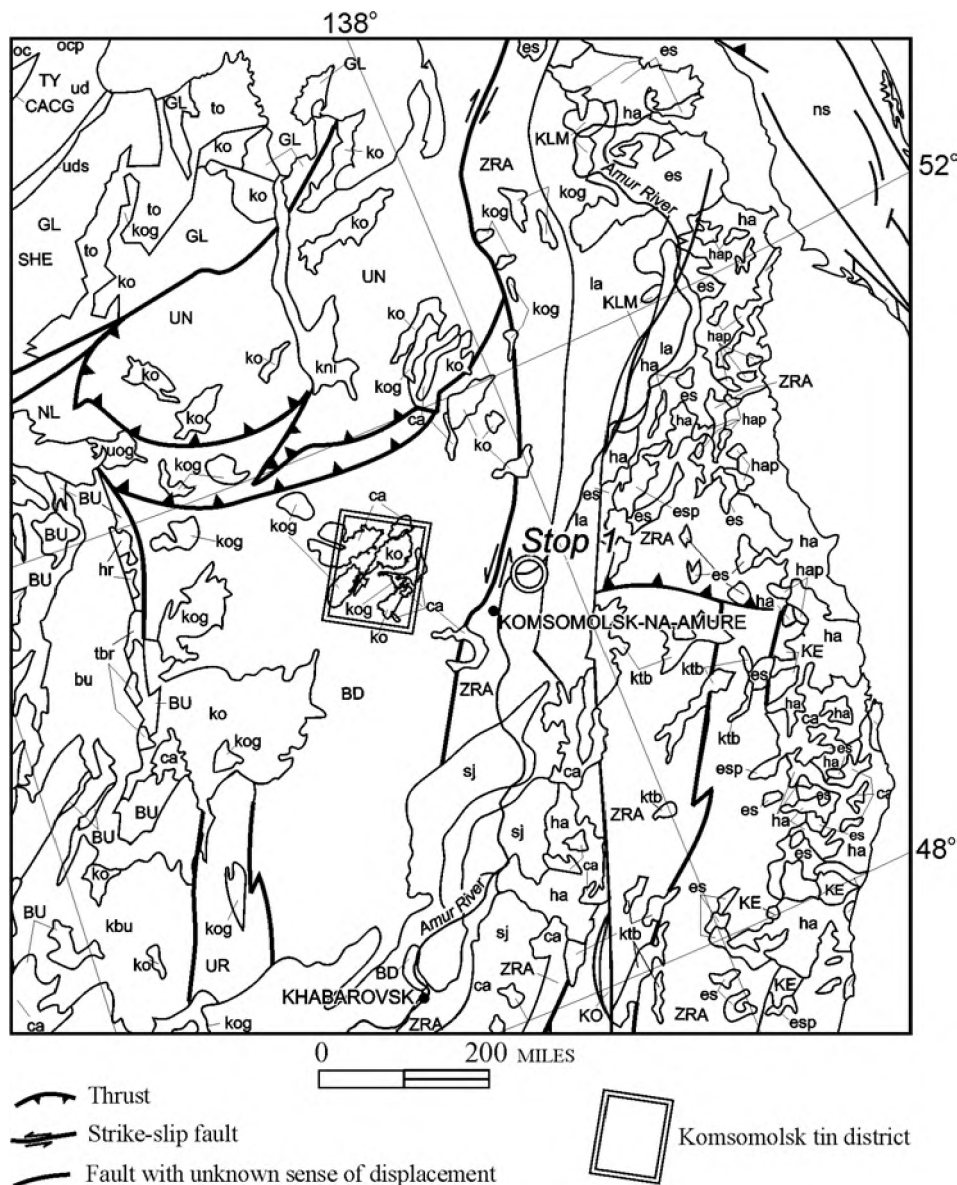


Fig. 3.6. Regional position of the Komsomolsk tin district (modified from "Preliminary Northeast Asia geodynamic map (1:5000000 Scale)". Compiled by Nokleberg et al. (2003).

Tectonic-stratigraphic terranes: BD – Badzhal terrane (Accretionary wedge, type B) (Permian through Jurassic); BU – Bureya terrane (Metamorphic) (Neoproterozoic and older through Triassic); CACG – Chogar terrane (Granulite-orthogneiss) (Archean); GL – Galam terrane (Accretionary wedge, type B) (Cambrian through Early Carboniferous); KE – Kema terrane (Island arc) (late Early Cretaceous); KLM – Kiselyovka-Manoma terrane (Accretionary wedge, type B) (Jurassic and Early Cretaceous); KO – Khor terrane (Island arc) (Early Paleozoic?); NL – Nilan terrane (Accretionary wedge, type B) (Devonian through Permian); SHE – Shevli terrane (Passive continental margin) (Early Cambrian through Late Devonian); TY – Tynda terrane (Tonalite-trondhjemite-gneiss) (Archean and Paleoproterozoic); UN – Ulban terrane (Continental margin turbidite) (Late Triassic through Middle Jurassic); UR – Urmi terrane (Passive continental margin) (Archean through Middle Triassic); ZRA – Zhuravlevsk-Amur River terrane (Continental margin turbidite) (Late Jurassic and Early Cretaceous). *Overlap assemblages: magmatic belts:* ca – Central Asian plateau basalt belt (Neogene and Quaternary); es – Volcanic part of East Sikhote-Alin volcanic-plutonic belt (Late Cretaceous through Miocene); esp – Plutonic part of East Sikhote-Alin volcanic-plutonic belt (Late Cretaceous through Miocene); ha – Volcanic part of Hasan-Amurian volcanic-plutonic belt (Paleocene to early Miocene); hap – Plutonic part of Hasan-Amurian volcanic-plutonic belt (Paleocene to early Miocene); hr – Kharinsk granitic assemblage (Triassic); kbu – Khanka-Bureya granitic belt (Ordovician and Silurian); ko – Volcanic part of Khingan-Okhotsk volcanic-plutonic belt (Cretaceous); kog – Plutonic part of Khingan-Okhotsk volcanic-plutonic belt (Cretaceous); ktb – Khungari-Tatibi granitic belt (Mid-Cretaceous); oc – Volcanic part of Okhotsk-Chukotka volcanic-plutonic belt (late Early Cretaceous and Late Cretaceous); ocp – Plutonic part of Okhotsk-Chukotka volcanic-plutonic belt (late Early Cretaceous and Late Cretaceous); tbr – Tyrma-Bureinsk granitic assemblage (Permian); ud – Uda volcanic-plutonic belt (Late Jurassic and Early Cretaceous); uo – Volcanic part of Umlekam-Ogodzhin volcanic-plutonic belt (Cretaceous); uog – Plutonic part of Umlekam-Ogodzhin volcanic-plutonic belt (Cretaceous). *Sedimentary basins:* bu – Bureya sedimentary basin (Early Jurassic to Early Cretaceous); kni – Konino-Nimelen sedimentary basin (Neogene and Quaternary); to – Torom sedimentary basin (Late Triassic through Early Cretaceous); uds – Uda sedimentary basin (Late Jurassic and Cretaceous); sj – Middle Amur sedimentary basin (Mesozoic and Cenozoic).

See remaining explanation in the text

found only occasionally. The sequence coarsens upwards. Sometimes about 90% of fragments in the conglomerates consist of flattened fragments of black mudstones. Fragments of sandstones, cherts and well-rounded quartz occur infrequently. The thickness of proximal turbidite beds attains 10-20 m. They are commonly composed of conglomerates (0.5-1.5 m), gravelstones (0.5-0.7 m), and coarse to medium sandstones (2-3 m). Medium-bedded turbidite beds with thickness varying from 5 to 40 m are occasionally found.

Badzhal accretionary wedge terrane

Badzhal accretionary wedge terrane consists of a wide spectrum of Paleozoic and Mesozoic rocks (Zabrodin, 2003₁, 2003₂). Mesozoic rocks are the most widespread. They host tin deposits within the Komsomolsk ore district (Fig. 3.8). The rocks of the Badzhal terrane are shown on Fig. 3.8 by a single symbol due to their very complicated structure. The description of the rocks is arranged below by age.

Upper Triassic (Norian) sediments are widespread in the western part of the district. A generalised sequence of the deposit is as follows (from bottom to top):

- 200 meters bench of fine-grained and medium-grained sandstone with thin (0.3-1.2 m) interlayers of mudstone and thick (30-40 m) interlayers of tuff-cherty rock. Conglomerate and sedimentary breccias present in the basement.
- 600 meters bench of polymictic sandstone, calcareous sandstone with rare interlayers (up to 50 m) of mixtite with clayey matrix. Sometimes the bench contains turbidite.
- 450 meters bench of mixtite with clayey and sandy matrix.
- 300 meters bench of sandstone intercalated with mixtite.
- 300 meters bench of tuff-cherty rock with interlayers of cherty rock (up to 40 m), calcareous sandstone (up to 20 m), lenses of sedimentary breccias and mixtite.
- The total thickness of Late Triassic deposit is up to 1900 meters.

Upper Triassic (Rhaetian) – Lower Jurassic (Hettangian) sediments are known only as an allochthon. They consist of grey and red jasper, greenish and greyish tuff-chert and clayey-cherty rock with mudstone interlayers. Basalt layers and limestone lenses occur in the lower part of the allochthon. The thickness of the allochthon is about 400 m. Age of the sequence was determined by conodont remnants and radiolarians.

Two suites represent the middle Jurassic. Lowest of them, the so-called Khurlinskaya suite, predominantly consists of heteroclastic mixtite composed olistostrome horizons or separated layers and lenses. Sandy turbidites are present as well. Cherty rock is very rare. Total thickness of the Khurbinskaya suite is estimated as 1800-1900 m. Radiolarian age of the suite is distinguished as Toarcian. The Ulbinskaya suite has the same composition but turbidite prevails over mixtite. Turbidites are represented by rhythmically intercalated sandstone and mudstone of gradational texture. Upper part of the suite contains lens-like bodies of chert and tuff-chert rocks included in basalt. Total thickness of the suite is assumed as 1500 meters. Radiolarian age of the suite is Bathian-Callovian.

Late Jurassic sediments of the district are also subdivided into two suites. The Silinskaya suite consists predominantly of sandstone with small amount of psephte and mixtite. Tuff-chert rock, chert, clayey shale, and basalt are very rare. The total thickness of the suite is about 1400 meters. The rock contains remnants of *Astarte cf. cordata* Traut., *Oxytoma (Oxytoma) expansa* (Phill.), *Lithacoceras (?)* sp., *Buchia* sp., and *Partschiceras* sp. Based on this and radiolarians the age of the suite is distinguished as Oxfordian-Kimmeridgian. The Padalinskaya suite forms at isolated sites. It consists of turbidite and mixtite with a clayey matrix. The presence of carbonized plants and rare thin coal interlayers indicates a shallow water environment of deposition. Based on the presence of *Buchia russiensis* Pavl., *B. cf. fischeriana* (Orb.), *B. cf. terebtatuloides* (Lah.), *Partschiceras schetuchaense* Chud., *Carpolithes cinctus* Heer., and *Cinguloturris* sp. cf. *C. carpatica* (Dum.), *Atchaeodyctiomitra* sp. cf. *A. carpatica* (Loz.) the age of the suite is Volgian. The thickness of the suite is about 1500 m.

The Lower Cretaceous Gorinskaya suite is the youngest sedimentary suite of the host rocks of the ore district. The suite consists of sandstone and mudstone with lenses and interlayers of conglomerate and gritstone. The visible thickness of the suite is about 500 meters. The age of the rock is determined as Berriasian based on the assemblage of *Hsuuum ex gr. maxswell* Pess., *Xitus cf. spicularis* Al., *Pseudoencyrtis* sp.

Komsomolsk fragment of the Khingan-Okhotsk volcano-plutonic belt

The Khingan-Okhotsk volcanic-plutonic belt includes several magmatic zones, such as (from southwest to north-east) Khingan-Olono, Badzhal, Dusse-Alin, Yam-Alin, Komsomolsk, Selitkan, and so on,

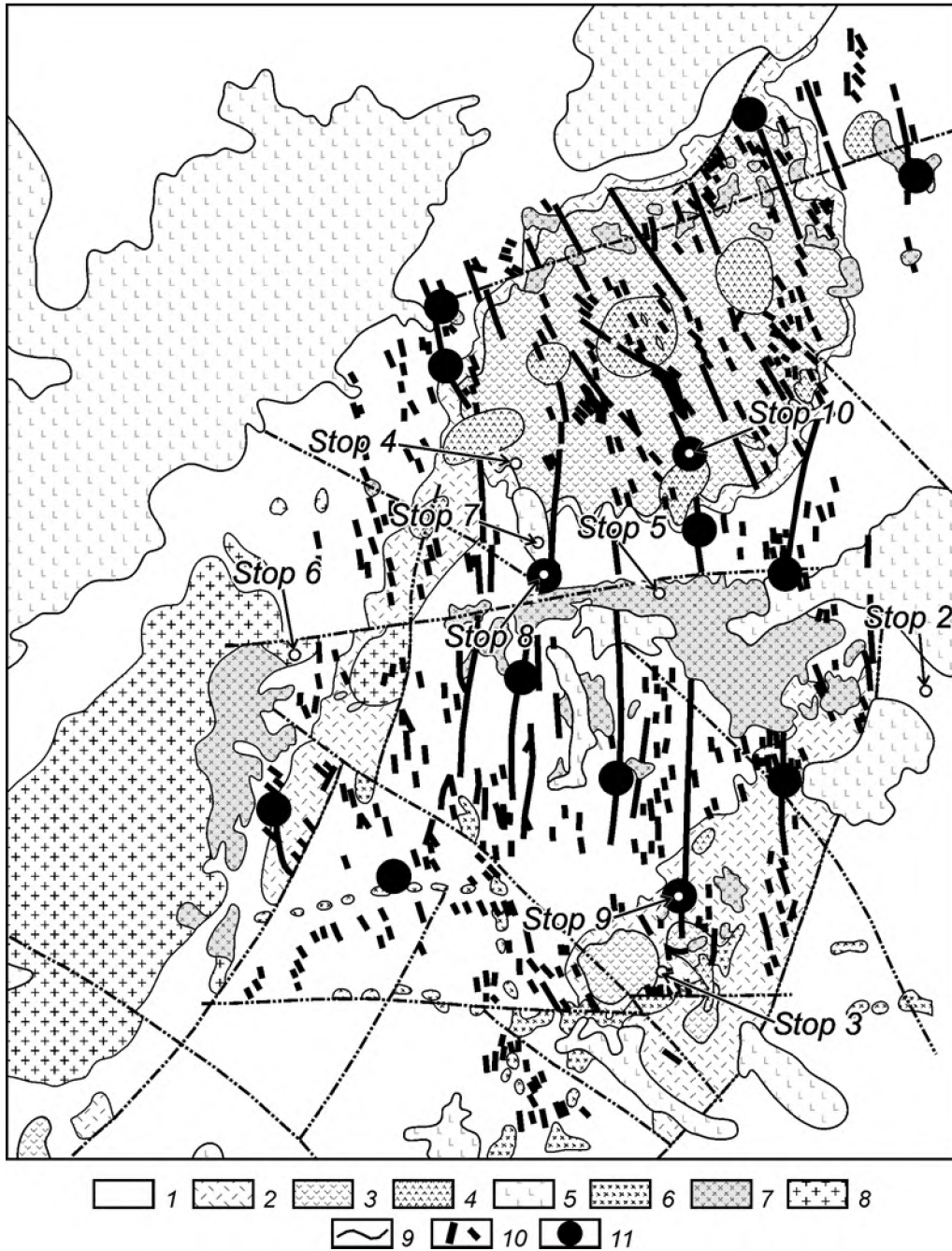


Fig. 3.8. Geologic scheme of Komsomolsk tin district, after Ognyanov (1986).
 1 – turbidite (J_3-K_1), 2 – rhyolite flow (K_{1-2}), 3 – andesite flow (K_{1-2}), 4 – subvolcanic andesite (K_2), 5 – basalt (N-Q), 6 – diorite-granodiorite (Puril complex) (K_{1-2}), 7 – monzonite (Silinka complex) (K_{1-2}), 8 – granite (Chalba complex) (K_2), 9 – faults, 10 – ore-bearing structure, 11 – Sn deposits

forming an extensive magmatic area of general NNE trend (see Fig. 3.6). Included in this area magmatic zones overlap several terranes of different composition and nature. The inhomogenous basement of the Khingian-Okhotsk volcanic-plutonic belt is reflected in the composition of its volcanic and plutonic rocks. All the considered zones were formed during the same geological time and at the beginning of intensive development of subaerial

volcanic rocks in the Early Albian. All of these zones are characterized by approximately the same set of volcanic formations of andesitic and rhyolitic composition and slightly differ only by the occasional absence of plutonic formations of granodiorite-granite or diorite-granodiorite composition. In spite of slight differences in the composition of the rocks, their petrochemical features are close. All magmatic zones locate within a single large complicated dome uplift,

which is accompanied by a sharp increase of lithosphere thickness and a deep zone of low density (Reynlib, Romanovskiy, 1975; Lishnevskiy, 1965; Pacific..., 1991).

The belt of volcanic-plutonic assemblages is divided into two types – andesite-granodiorite and rhyolite-granite (Bolotnikov, Kravchenko, 1976; Volcanic ..., 1984; The geology of tin ... , 1986). The age of the magmatic rocks of the belt as a whole, covers the interval 135-55Ma (Krivovichev et al., 1996; Krymskiy et al., 1997; Lebedev et al., 1997; Ishihara et al., 1997; Gonevchuk et al., 1998, 2000; Rodionov, 2000₂, 2001_{1,2,3}; Sato et al., 2002). The age of magmatic zones decreases from SW to NE. The characteristics of the final phases of volcanic-plutonic assemblages of the belt, represented by granite, are relatively elevated general alkalinity with high K/Na (Gonevchuk et al., 2000), the presence of accessory topaz, monazite, zircon, and ilmenite, elevated F, Li, and Rb contents (Brusnicyn et al., 1993), high feldspar contents, and lower contents of plagioclase. The granites are of I-S type, REE trends demonstrate distinct negative Eu anomaly (Fig. 3.9). The Rb/(Nb+Y) ratio characterizes them as intra-plate granites (see Fig. 3.5).

The geodynamic nature of the Khingan-Okhotsk belt still remains the subject of debate. Faure and Natal'in (1992) and Natal'in (1993) suggested that the Khingan-Okhotsk volcano-plutonic belt formed in an active continental margin, which was accompanied by the coeval formation of an Early Cretaceous accretionary complex including the Amur complex. On the other hand, Faure and Natal'in (1992) indicated that the magmatic activity in this belt began in the Barre-

mian and lasted throughout the entire Late Cretaceous, although direct chronological data were not presented. The age discordance between the magmatic arc and the accretionary complex may be resolved on the basis of new radiometric age data for the tin deposits and surrounding igneous rocks within the Khingan-Okhotsk volcano-plutonic belt, which suggest a relatively short period of magmatism in the Middle Cretaceous.

Later it was suggested that the Khingan-Okhotsk belt developed in pre-Cenonian time in environment of active continental margin of Andian type, which was changed to a collision environment in post-Cenonian time (Rodionov, Natal'in, 1988). Nokleberg et al., (1998) suggested that the Khingan-Okhotsk magmatic arc formed as a result of an oblique subduction of paleo-Pacific plate under continental margin in the Early Cretaceous. Sato et al., (2002), considering the correlation of the initial period of magmatic processes of the Khingan-Okhotsk belt and a period of accretion of the Kiselevka-Manoma terrane (Albian-Cenomanian), confirmed the model of belt formation as a result of oblique subduction, suggesting that the subducted part of the plate presented itself as a back-arc basin similar to the modern Andaman basin in the Sunda arc.

When interpreting the geodynamic nature of the Khingan-Okhotsk belt it is important also to take into account that all tin ore districts with large tin deposits are normally situated above the zone of maximum gradient of lithosphere thickness. Furthermore, the Badzhal district is located above a large regional asthenosphere uplift, which may be interpreted as a "slab-window" (Karsakov et al., 2000; Romanovskiy et al., 2001).

Many details of the formation processes of the Khingan-Okhotsk belt can be satisfactorily explained using a reconstructed Mesozoic-Cenozoic transform continental margin (Khanchuk et al., 1997; Khanchuk, Ivanov, 1999_{1,2}; Khanchuk, 2001). In general the situation may be described as a transition from oblique subduction to mutual lateral sliding of the plates. As a result of such sliding in earlier subducted parts of the lithosphere plate the breakups appear ("slab-window"), through which asthenospheric mantle penetrates. The mechanism of transform continental margin development and origin of "slab-window" is studied using the example of the western margin of North America (Benz et al., 1992), as well as described in other regions (Parfenov et al., 1998; Tychkov, Vladimirov, 1997; Khanchuk et al., 1997; Khanchuk, Ivanov, 1999_{1,2}; Khanchuk, 2001).

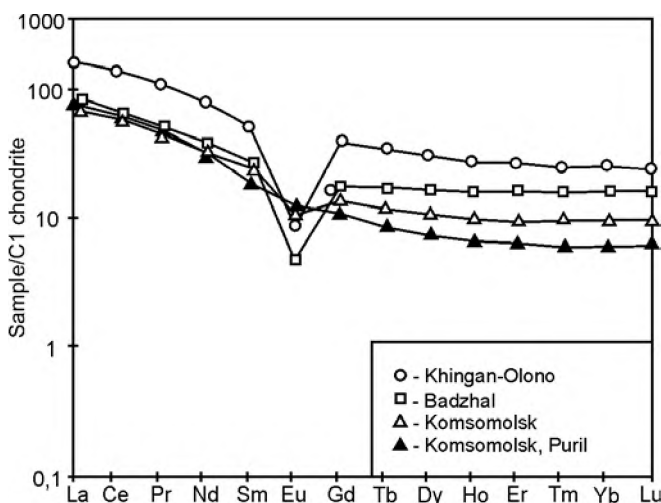


Fig. 3.9. Chondrite-normalized REE patterns of the intrusive rock of Khingan-Okhotsk belt, after Gonevchuk et al. (2000)

The Kholdami sedimentary-volcanogenic suite

The lowest section of the volcanogenic-sedimentary part of the Khingan-Okhotsk volcanic-plutonic belt is represented by the Kholdomi suite (K_{1-2} hl). Volcanogenic-sedimentary and volcanogenic rocks of felsic composition composed two graben-like depressions (Western and Eastern) and the peripheral part of Amut trough (see Fig. 3.8). They overlap Jurassic and Lower Cretaceous sedimentary rock with sharp angular unconformity.

The Kholdomi suite has a rhythmical structure. A Western graben-like depression includes four rhythms and an Eastern graben-like depression includes five rhythms. Each rhythm consists of two horizons. The structure of the Kholdomi suite in the southern part of Eastern graben-like depression within the Kurmidzha paleocaldera will be investigated. The deposit of the lower horizon of the first rhythm is composed of conglomerate with interlayers of tuff-sandstone and lenses (up to 10 m thick) of rhyolite tuff. Visible thickness of the horizon is about 500 m. The upper horizon consists of vitrocrystalloclastic tuffs of rhyolite and rhyodacite with a conglomerate interlayer at the bottom. Total thickness of the first rhythm is about 600 m. The lower horizon of the second rhythm consists of conglomerate with rare thin (tens of centimeters) lenses of tuff-sandstone and tuff-mudstone. The thickness of the horizon varies from 20 to 100 m decreasing to the south. The upper horizon consists of psammitic tuff of rhyolite and rhyodacite with crystals, rocks and glass fragments. It includes thin (3-5 m) single lenses of conglomerate and tuff-sandstone and thickness is about 70-90 m. The total thickness of the second rhythm is up to 180 m.

The deposits of the third rhythm are exposed along the Kurmidzha Creek stream. The section structure (from bottom to the top) is as follows.

Conglomerate with rare interlayers of gritstone (0.7 m), tuff-sandstone, and tuff-mudstone (0.2-0.5 m)	145 m
Psammitic crystal-vitric tuff of rhyodacite	25 m
Conglomerate	35 m
Vitric tuff of rhyolite	15 m
Conglomerate	35 m
Psammitic vitric tuff of rhyolite	15 m
Conglomerate with rare lenses of tuff-conglomerate	15 m
Total thickness	280 m

The same structure of the horizon was intersected by drill-holes around the Geophysical ore zone of the Festival'noe tin deposit.

The fourth rhythm is well exposed along the left tributary of the Kurmidzha Creek. The section of the lower horizon is as follows.

Conglomerate with several interlayers of gritstone	62 m
Conglomerate with several interlayers of sandstone	91 m
Sandstone with interlayers of gritstone	3 m
Black tuff-siltstone with gritstone interlayer	3 m
Total thickness of the horizon	160 m

The section of the upper horizon of the fourth rhythm is as follows.

Psammitic crystal-vitric tuff of dacite and dacite-andesite	90 m
Tuff-conglomerate	80 m
Psammitic crystal-vitric tuff dacite-andesite	20 m
Total thickness of the horizon	190 m

The fifth rhythm is predominantly of monotonous conglomerate, which contains lens-like interlayers of fine-grained sandstone and rare dacite lenses in the upper part of the section. The thickness of the rhythm is up to 350 meters.

The thickness of the separated rhythms within graben-like depression varies from zero to hundreds of meters. The total thickness of the suite varies respectively from 30 to 1800 meters.

Pyroclastic deposits of the Kholdomi suite correspond chemically to rhyolite (first and second rhythms), rhyodacite (third rhythm), and dacite (fourth and fifth rhythms). Tuffs of the fourth rhythm differ from other similar rocks by relatively low content of SiO_2 (67.49% as against 72.26-74.32%) and relatively high content of CaO. Rhyolite and rhyodacite tuffs of the first and third rhythms are characterized by relatively low alkalinity ($Na_2O \geq K_2O$).

The age of the suite is based on numerous faunal determinations. The lower part of the suite is characterized by *Coniopteris* sp., *Phoenicopsis* sp., *Podozamites* ex gr. *lanceolatus* L. et H., *Pitiophyllum* cf. *angustifolium* Nath., *Cephalotaxopsis heterophylla* Holl., *Sequoia* типа *S. fastigiata* (Sternb.) Heer, *Ginkgo* sp. indet., *Platanus* sp., *Dicotyledones* sp. For medium and upper parts the following forms are more typical: *Ginkgo* sp., *Cephalotaxopsis heterophylla* Holl., *C. mycrophylla laxa* Holl., *Sequoia ambigua* Heer., *S. fastigiata* (Sternb.) Heer., *S. concinna* Heer., *S. minuta* Sveshn., *Platanus* sp., *Pterosperrmites* sp., *Carpolithes* sp., *Protophyllum* cf. *praestans* Lesq., *P. cf. beconteanum* Lesq. Based on this the age of the Kholdomi suite is Late Albian – Cenomanian.

Numerous subvolcanic and extrusive stock-like and dike-like bodies of rhyolite, rhyodacite, dacite, explosive breccia, and granite porphyry are assumed to be comagmatic with the effusives of Kholdomi suite. The largest subvolcanic body (about 5 square km) is on the watershed of the Silinka and Gerbi Rivers. It is the so-called "Intrusive of Myao-Chan Ridge". The body has an ellipse-like shape on the surface. It is funnel-shaped in cross section. The outer part of the body consists of rhyolite with coarse phenocrysts and a weakly crystallized matrix. The crystals of dark-coloured minerals and feldspar are oriented parallel to the contact of the body. The inner part of the body consists of granite porphyry with a well-crystallized matrix. The central part is composed of rhyolite clastic lava. The thickness of the volcanic flow is greatest in the vicinity of the subvolcanic body and gradually decreases away from it.

Small bed-like bodies of subvolcanic rhyolite are known in the Eastern graben-like depression. Besides

that, rare dike-like subvolcanic rhyolitic bodies occur in the northern flanks of the Western and Eastern depressions.

Representative chemical compositions of Kholdami volcanic rocks are shown in table 3.1. Results of isotope age dating are shown in table 3.2.

The Amut volcanogenic suite

The Late-Cretaceous Amut volcanogenic suite is composed predominantly of effusive rocks of intermediate and felsic composition. The suite is widespread within the Amut trough and locally in other places. The relation of Amut and Kholdomi suites is not determined till now. The unconformable superposition of andesite of the Amut suite over pyroclastic rock of the fourth rhythm of Kholdomi suite was observed in the southern part of the Amut trough (Figs. 3.10, 3.11). In other places the Amut volcanics unconformably overlie Jurassic sedimentary rocks.

Table 3.1

Representative chemical compositions of volcanogenic rocks of the Komsomolsk ore district, after Gonevchuk (2002)

Component	1	2	3	4	5	6	7
SiO ₂	72.81	71.82	74.23	68.05	58.49	59.80	74.06
TiO ₂	0.30	0.27	0.17	0.43	0.82	0.72	0.20
Al ₂ O ₃	14.40	14.10	13.40	14.45	16.53	15.60	13.50
Fe ₂ O ₃	0.51	0.52	1.01	0.68	1.60	1.09	0.72
FeO	1.41	2.14	1.03	2.65	5.55	5.82	1.31
MnO	0.03	0.05	0.02	0.07	0.15	0.14	0.04
MgO	0.59	0.67	0.40	0.93	3.71	4.0	0.71
CaO	2.16	2.05	1.18	2.59	6.86	5.61	1.57
Na ₂ O	3.89	3.81	1.95	2.62	1.94	2.11	1.46
K ₂ O	2.30	3.33	4.13	4.00	1.75	2.23	4.95
Rb	89	130	116	45	24	66	140
Sr	253	200	213	232	291	300	176
Ba	428	650	nd	nd	1241	487	nd
Zr	142	136	nd	nd	230	133	nd
Ni	8	7	6	6	8	9	8
Co	3	3	6	3	8	10	3
Cr	25	20	22	20	55	63	18
V	26	26	30	39	90	130	34
Cu	51	21	26	20	37	54	19
Sn	14	12	7	7	7	10	10
Pb	43	37	40	41	23	20	29
Zn	29	28	45	48	35	41	50
B	212	119	76	107	31	35	125
n	20	28	18	52	17	32	20

Note: 1-4 – volcanogenic rocks of Kholdami suite: rhyolite tuff of first (1), second (2), third (3), and fourth (4) rhythms; 5-6 – volcanogenic rocks of Amut suite: andesite of lower (5) and upper (7) part of the section; 7 – rhyolite of the medium part of the section.

Isotope age dating of volcanogenic rock of the Komsomolsk ore district

Part of the suite	Rock	Age, Ma	Method	References
First and second rhythms of Kholdami suite	Rhyolite and tuff rhyolite	125-130	K-Ar	Bondarenko, 1977
Third and fourth rhythms of Kholdami suite	Rhyolite and tuff rhyolite	100±4	K-Ar	Rub et al., 1964
First and second rhythms of Kholdami suite	Rhyolite tuff	86±12	Rb-Sr; $I_{Sr}=0.70499$	Gonevchuk, 2002
Fourth rhythm of Kholdami suite	Rhyolite-dacite, rhyolite, tuff rhyolite	111±23	Rb-Sr; $I_{Sr}=0.70829$	-"-
First and third horizons of Amut suite	Andesite porphyry	90-100	K-Ar	Bondarenko, 1977
Second horizon of Amut suite	Rhyolite tuff	86-96	K-Ar	-"-
Amut suite as a whole	Andesite, rhyolite	102±6	Rb-Sr; $I_{Sr}=0.70749$	Gonevchuk, 2002

The lower part of the suite in the vicinity of the Pereval'noe tin deposit is characterized by the following section:

- Psammitic-psephitic tuff of andesite with single andesite lenses 40-90 m
- Andesite 10-35 m
- Psephitic tuff of andesite 20-100 m
- Complicate interbedding of andesite and psephitic tuff of andesite 100-150 m
- Psammitic-psephitic tuff of andesite with single andesite lenses 40-110 m
- Andesite 40-90 m
- Psephitic and agglomeratic andesite tuff with rare andesite lenses 30-130 m
- Total thickness of the section varies from 370 to 450 meters.

Andesite tuff in the vicinity of the Pereval'noe tin deposit is shown in Fig. 3.12. In other places the structure of the lower horizon of the suite varies. But the common feature is the predominance of lava in the

western flank of the trough and an increase in pyroclastic deposits to the east.

A consistent layer of crystal-vitric rhyodacite tuff forms the medium part of the suite. Average thickness of the layer is about 10-30 m, sometimes – up to 80 meters. In places the layer has a lamellar structure due to the presence of several thin (10-50 cm) interlayers of rhyodacite aleuritic tuff.

The upper part of the suite has a very complicated structure, which varies from place to place. Andesite lava prevails in the central part of the trough. It is predominantly of pyroxene andesite composition with hornblende-pyroxene in the lower part and with numerous lenses and interlayers of psephitic and psammitic tuff or ash tuff along the whole section. Ash tuff usually contains numerous carbonized plant remnants. In places it contains well preserved imprints of Late Cretaceous flora. The layer of psephitic and agglomeratic andesite tuff is at the top of the section here. The presence of andesite-basalt at the bottom

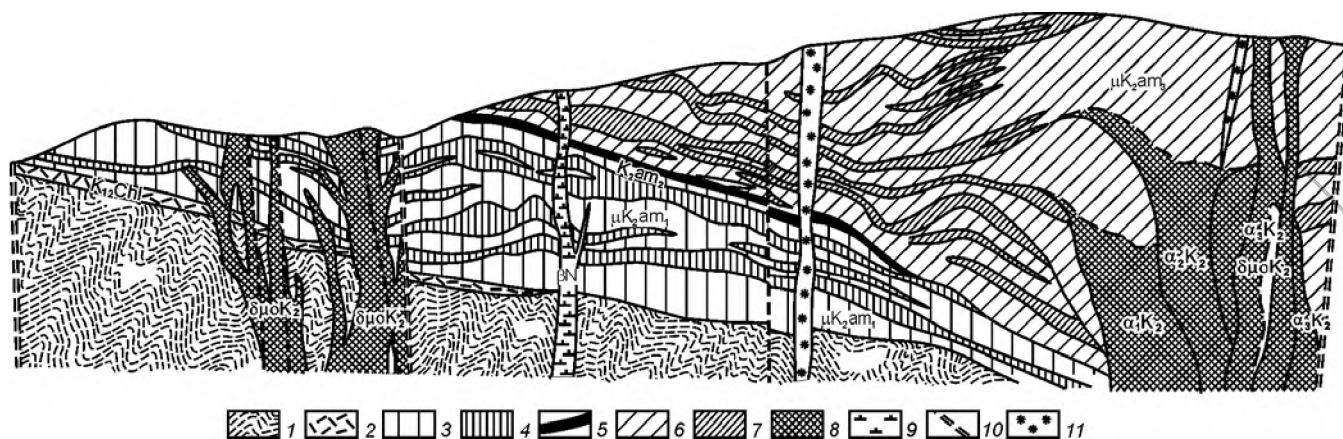


Fig. 3.10. Schematic cross-section of the southern flank of the Amut trough, after Geology... (1971).

1 – Jurassic – Early Cretaceous sedimentary sequence, 2 – Kholdami suite, rhyolite tuff, 3-7 – Amut suite: 3 – psammitic-psephitic andesite tuff, 4 – andesite lava, 5 – vitrocrystalloclastic rhyodacite tuff, 6 – andesite lava of predominantly pyroxene andesite composition, 7 – psammitic tuff and ash tuff, 8 – subvolcanic intrusives, 9 – Cenozoic olivine basalt, 10 – faults, 11 – mineralised fracture zones



Fig. 3.11. Unconformable superposition of andesite of the Amut suite over pyroclastic rock of the fourth rhythm of the Kholdomi suite

and amygdaloidal andesite at the top of the section is feature of the section.

Pyroclastic deposits prevail in the upper part of the suite in the western part of the Amut trough. The section is subdivided here into four horizons. The lower horizon (about 330 m) consists predominantly of pyroxene-hornblende andesite including a layer (70 m) of psemmitic-psephitic andesite tuff. The second horizon (420 m) has a more complicated structure. It is characterized by the predominance of pyroclastic deposits (300 m) over lava (120 m). It is a rough interstratification of predominantly psephitic tuff and ash tuff of andesite with andesite or dacite-andesite lavas, which form 8 flows. The thickness of an individual layer varies from 1 to 40 meters. The third horizon (230 m) consists of andesite lava layers (100 and 40 m) and a layer of andesite ash tuff. The fourth horizon is composed of andesite lava-breccias (100 m) and psammitic andesite tuff (20 m). The total thickness of the section is about 1100 meters.

In the northeast part of the trough the suite section includes two horizons. The lower horizon (80-150 m) consists of pyroxene-hornblende andesite. The upper horizon (about 150m) is composed of psephitic and psammitic andesite tuff including a thin lava horizon

of complicated structure. The total thickness of the suite is up to 2100 meters.

Vegetation remnants from the tuff are represented by *Cephalotaxopsis heterophylla* Holl., *C. microphylla laxa* Holl., *Cladophlebis cf. arctica* (Heer) Krysht., *Sphenolepsis sternbergiana* (Dunk.) Schenk., *Torreya gracillima* Holl., *Sequoia ambigua* Heer., *S. fastigiata* (Sternb.) Heer, *Platanus embicola* Vachr., *Phyllites* sp., and so on. Based on this the age of the Amut suite is Cenomanian-Turonian.

Subvolcanic dacite, dacite-andesite, trachyandesite, diorite, diorite porphyry, and their breccias are genetically related to the effusives of the Amut suite. A subvolcanic neck (400×250 m) in the vicinity of the Solnechnoe tin deposit is composed of dacite-andesite explosive breccias. The root zone of a complicated strato-volcano was discovered in the vicinity of the Pereval'noe tin deposit. The zone consists of several small necks (from 0.005 to 0.25 km² each) composed of dacite-andesite and quartz diorite porphyry. Several large subvolcanic bodies are known in the central part of Amut trough (see Fig. 3.8).

Representative chemical compositions of Amut volcanic rocks are shown in table 3.1. Results of radiometric age dating are shown in table 3.2.



Fig. 3.12. Andesite tuff of Amut suite. Open-pit of Pereval'noe tin deposit

Intrusive rocks

In the Komsomolsk ore district igneous rocks form an association known as the Myao-Chan magmatic series (Izokh et al., 1967), which includes three magmatic complexes (I) Puril granodiorite-granite (115-110 Ma), (II) Silinka granodiorite-monzonite (85-94 Ma) and (III) Chalba granitic complex (90 Ma). The first of those is not related to tin mineralization.

Silinka intrusive massif

According to the results of the investigation of igneous rocks of the Komsomolsk district, the granitoids of the Silinka complex were recognised as the most promising tin-bearing igneous complex. The Silinka tin-bearing complex is composed of a suite of intrusive rocks ranging from gabbro to leucogranite, with a predominance of quartz diorite and melanocratic granodiorite. They were formed in a time interval from 100 to 85 Ma (K-Ar and Rb-Sr dating). The main intrusive body of the complex – the so-called Silinka massive is located in the central part of the Komsomolsk ore district (see Fig. 3.8).

The complex includes three phases. Gabbro, gabbro-diorite, and diorite porphyry of the first phase occur locally in the northern part of Silinka massif, where small bodies and xenoliths in diorite of the sec-

ond phase of the complex also occur. Separate small stocks and dikes also occur in marginal parts of the Kurmidzha paleocaldera, as well as in the northeastern margin of the Amut trough, where they intersect the Kholdami suite, subvolcanic rocks of the Amut suite, and Jurassic sediments. The bodies have an irregular form in plan with an area from 0.15 to 0.4 km². In the northeastern part of the Silinka massif gabbros intrude Jurassic sediments and, in turn, are intersected by diorite, quartz diorite, granodiorite, and dikes of fine-grained granite of the later phases of the complex. SiO₂ contents of 52.52-55.78 vol. % suggest a diorite composition. However, plagioclase (up to anorthite in the grain center) and abundance of pyroxene defines them as leucocratic gabbro. The presence of potassium feldspar, reflects unusually high contents of potassium (at the average 1.55%) for normal gabbro, indicating that these rocks belong to the monzonite group. In contrast to the diorite of the second phase the rocks are characterized by a more sharply expressed prevalence of Na₂O over K₂O.

Quartz diorite, diorite, diorite-porphyry, and quartz diorite porphyry of the second phase form several magmatic areas in different parts of the ore district. The most intensive development of these rocks occurs in central part of the district to form the large Silinka massif. The participants of the excursion will



Fig. 3.13. Silinka massive on the right side of Silinka River valley



Fig. 3.15. Macrostructure of Silinka granitoids

have a possibility to investigate the rocks of Silinka massive in the open pit on the right side of the Silinka River valley.

The large Silinka massif (Figs. 3.13, 3.14, 3.15) forms about 65% by volume of the intrusive rocks of the Silinka complex. It is discordant to its folded Jurassic-Lower Cretaceous sedimentary host. It is thought that the massif marks the zone of the Silinskiy deep-seated fault. The contacts of the massif are close to vertical or steeply dipping to the centre. The exocontact part and roof of the massif is complicated by



Fig. 3.14. Outcrop of granodiorite of the Silinka intrusive complex

multiple branches of vein-like apophysis and stock-like bodies. The massif has a very complicated structure, since it is made up of several phases of igneous rock. The main part of the massif is composed of diorite and quartz diorite of the second phase related to each other by a gradual transition. In the most widespread quartz diorite the amount of plagioclase varies from 50 to 60 vol.%, potassium feldspar – from 5 to 10 vol.%, quartz – from 10 to 17 vol.%, hornblende – from 10 to 30 vol.%, pyroxene – from 0 to 20 vol.%. In diorite the contents of the quartz and potassium feldspar do not exceed 5 vol.%, but hornblende content is low. Such differences in composition characterize diorite porphyry and quartz diorite porphyry (the latter differs from the first by the presence of plagioclase and dark colored minerals of 0.5-3.5 mm size, which amounts to 25-30%, seldom up to 40% among the porphyry separations). For all rocks is most typical zonality of plagioclase, which in one and the same crystal has an inverse nature. Under direct zonality the composition of plagioclase changes from An90 in the center to An28-47 in marginal parts. The borders between zones within one event are clear, in other – gradual. In spite of specified signs of monzonite type of the rocks, from petrochemical point of view these rocks, as well as their subvolcanic and effusive analogues, belong to normal calc-alkaline series. With increasing contents of silica from 54.31 to 63.28% their amount of alkalis grows as well (from 3.98 to 6.79%), and K/Na normally increases from 0.87 in diorite to 1.02 in quartz diorite.

Granodiorite, granite, granodiorite porphyry, granite porphyry, monzogranite, and aplite present the third phase of the complex. The granites occur as small intrusive bodies in the eastern part of the Chalba intrusion and form dikes in granodiorite and quartz

diorite (see Fig. 3.8). They have also been revealed at depths of 600-650 m in a borehole and in the shaft in one of the deposits of the central part of the district (Gonevchuk et al., 1984). Their mineral composition is typical of granitoids of the monzonite series. Plagioclase enriched in anorthite (of 38 to 60mol % An, in relic zones up to 75mol % An) is present in association with potassium feldspar (orthoclase), orthopyroxene (more rarely clinopyroxene) and biotite. Biotite is enriched in MgO (up to 14 wt %), TiO₂ (up to 5 wt %), Ni, Co, Cr, and V, which are typical elements of basaltic melts. Hornblende is also present in the Silinka granitoids. The amount of these minerals varies in rocks of different composition. For example, the amount of dark-colored minerals in granodiorite may be 40 vol % while in leucogranite it is less than 5 vol %; plagioclase content in granodiorite is up to 40 vol % of rock but does not exceed 10 vol % in leucogranite.

Tourmaline (schorl) is present as a rock-forming mineral with a high Fe/Fe+Mg ratio (more than 80%) in the leucogranites of the Silinka complex. Tourmaline is present as an accessory in all rocks of the Silinka complex; also, there is a high boron content in the igneous rocks. In addition to tourmaline, ilmenite (titanomagnetite), apatite, allanite (containing nearly 30 wt.% of REE), sphene, zircon, and garnet (almandine -85 mol.%, pyrope nearly 6 mol.%, spessartine nearly 10 mol.%) are also present. According to the chemical composition, the Silinka granitoids belong to the calc-alkaline series of the "transitional" I-S-type. Except for aplites, the rocks of the Silinka complex are characterized by a low alkalinity, as a consequence of low Na₂O content and normal K₂O content. Representative chemical compositions of intrusive rocks of Silinka complex are shown in table 3.3.

The evolution of tin content from early phases of the complex to late phases is characterized by a gradual increase from 4 ppm (gabbro) to 14 ppm (granodiorite), with a decrease to 12 ppm in granite and 8 ppm in aplite. Low Sn contents in rock-forming minerals (2 ppm in pyroxene, 35 ppm in amphibole, and 20 ppm in biotite) show that it may have been accumulated in the residual magmatic chamber. Boron may have accumulated together with Sn, as the B content increases from 21 ppm in gabbro to 54 ppm in granites. Direct correlation between Sn and F also occurs.

Based on radiometric data (K-Ar method), the age of the complex varies from 114 to 80 Ma (Rub et al., 1962; Izokh et al., 1967; Ishihara et al., 1997; Sato

et al., 2000, 2002; Gonevchuk, 2002). A single Rb-Sr date corresponds to this interval and constitutes 98±19 Ma ($I_{Sr} = 0.70755$) for diorite-granodiorite and 85 Ma ($I_{Sr} = 0.7076$) for granite from deep horizons of Solnechnoe tin deposit (table 3.4). Rb/Sr, Rb/(Nb+Y) ratios as well $I_{Sr} = 0.707550 \pm 0.0005$ shows that the granites may have been derived from an andesite melt contaminated by felsic sialic material. Chondrite-normalized REE patterns show that the granites might have formed as a result of metasediment melting. The relation of TiO₂ and Sn in the rocks is very close to the same relation in sandy-clayey deposits, which is evidence in favour of suggestions about the origin of these rocks being the result of melting of terrigenous sedimentary rocks in a low-crust environment. From the relation of K and Rb these rocks correspond to the area of mixing of crust and mantle materials.

Chalba intrusive massif

Granites of the Chalba complex occur as a large pluton (100 km²) in the western part of the Komsomolsk ore district (see Fig. 3.8) and are similar to granites of the Silinka complex in their mineral and chemical composition. It is suggested that they were formed as a result of advanced melting of the metamorphic Mesozoic substrate under the impact of a mantle diapir. In addition, a large pluton is inferred to be hidden at depth beneath the district. It is suggested that Chalba massive has a laccolith-like shape extending in a northeastern direction in accordance with the strike of the deep-seated Chalba fault.

The massif intrudes Upper Triassic – Jurassic sedimentary rocks causing formation of a hornfels aureole from 2 to 5 km wide. In places it is overlain by Miocene trachybasalt. The contacts of the massif dip sharply under the host sediment. The western contact of the massif is steep and eastern one is comparatively gentle.

The different phases of the rock are asymmetrically distributed inward of the massive. So, coarse-grained biotite granite and leucocratic granite band by width of 2 km is tracked along the west rectilinear contact. To the east these granites gradually are replaced by medium-grained porphyritic hornblende-biotite granite with fine-grained matrix and even granite porphyry, containing xenoliths of hornfels and diorite-like rock. The phenocrysts sometimes find weaken in general horizontal orientation or are bent under 5°. This orientation often corresponds to well expressed system of gentle fissures, quite often conditioning hammock jointing of the granite.

Representative chemical compositions of intrusive rocks of the Silinka complex, after Gonevchuk (2002)

Parameter	1	2	3	4	5	6	7	8
SiO ₂	53.97	59.58	64.49	70.19	74.85	75.27	75.29	70.72
TiO ₂	1.01	0.74	0.60	0.41	0.22	0.15	0.10	0.37
Al ₂ O ₃	16.19	15.72	14.91	13.94	13.04	12.66	12.72	13.76
Fe ₂ O ₃	1.55	1.08	1.08	0.50	0.36	0.44	1.02	0.86
FeO	7.69	6.14	4.52	3.03	1.33	1.07	0.79	1.92
MnO	0.19	0.14	0.11	0.08	0.05	0.02	0.02	0.07
MgO	5.71	3.94	2.92	1.46	0.48	0.60	0.24	1.46
CaO	8.57	6.51	4.88	2.70	1.08	1.06	0.83	2.02
Na ₂ O	6.90	2.43	2.44	2.59	2.47	2.49	2.15	2.64
K ₂ O	1.06	2.23	2.79	4.08	5.35	5.29	5.56	5.06
F	0.03	0.08	0.07	0.08	0.20	0.04	0.04	0.10
Li	nd	20	30	41	25	20	nd	55
Rb	74	102	148	178	161	189	136	190
Sr	253	388	236	201	134	142	161	191
Ba	256	448	658	687	155	170	430	540
Zr	106	141	153	144	131	95	70	170
Nb	nd	11	11	22	15	10	12	12
Y	nd	24	22	40	20	25	13	22
Ni	8	18	19	16	14	11	13	18
Co	13	10	13	7	3	2	3	7
Cr	139	62	72	78	34	32	37	70
V	287	116	101	96	31	32	20	99
Cu	24	39	47	30	89	30	35	35
Sn	4	11	14	11	12	7	8	9
Pb	12	25	30	35	52	56	21	36
Zn	25	62	57	42	32	37	27	53
B	21	39	36	51	38	52	700	101
n	24	24	24	19	12	12	5	8

Note: 1 – gabbro and quartz gabbro, 2 – diorite and quartz diorite, 3 – granodiorite, 4 – monzogranite, 5 – fine-grained biotite granite, 6 – aplite, 7 – tourmaline granite, 8 – granite from deep horizons of the Solnechnoe tin deposit.

The Chalba granites pertain to rocks of normal calc-alkaline series. Silica content in hornblende-biotite granite varies from 69 to 73 wt.%, but in coarse-grained biotite varieties and in leucogranite – from 74 to 76.8 wt.%. Total alkalinity changes from 6.3 to 8.5 wt.% with prevalence of K₂O on Na₂O (K₂O/Na₂O = 1.2-1.5, seldom – to 2.0). Herewith in contrast with granitoids of the previous phase the content of Na₂O with growing of silica content remains constant then concentrations of K₂O increase from 3.76 to 6.15 wt.%. Chalba granites are characterized also by high total Fe content (2.35-2.44 wt.%) and weakly oversaturated by Al₂O₃ in relation to the sum of the alkalis and calcium. Representative

chemical compositions of intrusive rocks of Chalba complex are shown in the table 3.5. Radiometric age data of Chalba intrusive rocks are shown in the table 3.6.

Central Asian plateau basalt belt

The youngest volcanic rock is presented in the ore district by Miocene and Quaternary plateau basalt (see Fig. 3.8). Outcrops of Miocene basalt are accessible in the vicinity of the Solnechnoe tin deposit.

Miocene plateau basalt is represented by the Kizinskaya suite, which consists of trachybasalt, trachydolerite, tuff of trachybasalt, clay, sandy loam, and lignite. The suite is preserved from erosion on the

Table 3.4

Radiometric age data for Silinka intrusive complex

Massif	Rock, mineral	Method	Age, Ma	Reference
Verkhne-Silinka	Granite, biotite	K-Ar	81-84 (±3)	Gonevchuk, 2002
Silinka	Quartz gabbro		113	Izokh et al., 1967
	Diorite		98±6	Gonevchuk, 2002
	Granodiorite		95-96±5	Izokh et al., 1967; Rub et al., 1962
Deep horizons of Solnechnoe tin deposit	Granite		81-85 (±5)	Gonevchuk, 2002
	K-feldspar		86.2±1.8	Ishihara et al., 1997
Silinka	Diorite, granodiorite (whole rock)	Rb-Sr	98±18 I _{Sr} =0.70755	Gonevchuk, 2002
Chalba	Granodiorite, pyroxene granite (whole rock)		97±25 I _{Sr} =0.70552	Gonevchuk, 2002
Deep horizons of Solnechnoe tin deposit	Granite (whole rock)		85 I _{Sr} =0.7076	Gonevchuk, 2002

watersheds only. In the vicinity of the Solnechnoe tin deposit it has the following section.

Trachybasalt massive or porous	2 m
Trachydolerite with bunches of halloysite and zeolite	1 m
Porous trachybasalt with zeolite bunches and halloysite inclusions	4.8 m
Trachydolerite	0.8 m
Porous trachybasalt with zeolite bunches	1.7 m
Trachydolerite with rare bunches of zeolite	2.5 m
Porous trachybasalt with zeolite	6.2 m
Trachydolerite with rare bunches of zeolite	2.7 m
Porous trachybasalt with numerous zeolite bunches	12 m
Trachydolerite with bunches of halloysite and zeolite	41.4 m
Porous trachybasalt with zeolite bunches and calcite crystals in the caverns	8.6 m
Trachydolerite with zeolite bunches	6.9 m
Dark-grey sandy clay with fragments of trachybasalt, andesite, and sandstone	6.6 m
Trachybasalt massive or porous with zeolite bunches, halloysite veinlets, and tuff interlayers	23.6 m
Dark-grey clay with woody lignite	4 m
Sandy clay with fragments of trachybasalt, quartz-tourmaline rock, sandstone	11.5 m
Different colored clay with lignite lenses	13 m
Clay and sand with sandstone fragments	1 m
Porous trachybasalt	5 m
Grey and orange clay with woody lignite	4 m
Sandy clay with fragments of trachybasalt and ore quartz	7 m
Porous trachybasalt with zeolite and halloysite bunches	21 m
Dark-brown clay with woody lignite	1 m
Tuff of trachybasalt	3.3 m
Porous trachybasalt	4 m
Grey clay	2.2 m
Total thickness of the suite is over	200 m

The Miocene age of the rock is based on the spore-pollen complex from the clay. The K-Ar age of one sample (laboratory of Kyoto University, Japan) is 14.8 Ma (pers. comm.).

Table 3.5

Representative chemical compositions of Chalba intrusive rocks, after Gonevchuk (2002)

Parameter	Coarse-grained biotite granite (n=22)	Fine-grained leucocratic granite (n=12)
SiO ₂	72.17	75.64
TiO ₂	0.37	0.11
Al ₂ O ₃	13.52	12.54
Fe ₂ O ₃	0.62	0.87
FeO	1.73	1.57
MnO	0.03	0.03
MgO	0.96	0.33
CaO	1.66	0.93
Na ₂ O	2.95	2.89
K ₂ O	4.76	4.85
F	0.12	0.06
Li	55	80
Rb	205	235
Sr	150	57
Ba	414	154
Zr	183	63
Nb	27	16
Y	40	13
Ni	7	10
Co	3	2
Cr	18	32
V	29	13
Cu	21	44
Sn	13	9
Pb	77	35
Zn	55	60
B	27	32

Table 3.6

Radiometric age data of Chalba intrusive rocks

Rock, mineral	Method	Age, Ma	Reference
Coarse-grained granite, whole rock	K-Ar	76-86	Gonevchuk, 2002
Fine-grained granite, whole rock		75±5	
Coarse-grained granite, biotite		90.1 ±2.0	
do.		90.2±2	
do.		89.9±2.0	
do.		90.0±2.0	
do.		101±5.0	
do.		103±5.0	
do.		88±4.0	
do.		93±5.0	
do.		85±5.0	
Pyroxene granite, biotite		94.3±2.1	Gonevchuk, 2002
do.		94.2±2.1	
do.		114±5.0	
do.		107±5.0	
Fine-grained pyroxene granite, biotite		86±1.9	
do.		86.4±1.9	
Schlieren pegmatite with tourmaline		80	Ishihara et al., 1997
Granite, muscovite		83.9±1.7	
do.		82.9±2.1	
do.	85.1±1.8		
do.	85.5±2.2	Gonevchuk, 2002	
Coarse-grained granite, whole rock	77±7; I _{Sr} =0.7063		
Fine-grained leucocratic granite, whole rock	72±15; I _{Sr} =0.70795		
Granodiorite, pyroxene granite	97±25; I _{Sr} =0.70552		

TIN DEPOSITS OF THE KOMSOMOLSK ORE DISTRICT

In the Russian literature, the Komsomolsk ore district is considered to be a type locality of tin mineralization of the cassiterite-silicate-sulfide type. More than 185,000 tonnes of tin were mined in the district from 1959. The description of the deposits below is based on (Radkevich et al., 1967, 1971; Metallogeny..., 1988; Dubrovskiy et al., 1979; Gonevchuk et al., 2000, Korostelev et al, 2001). Mineralization of the deposits is represented by quartz-tourmaline metasomatite bodies of 1 to 3 km in extent. Their thickness is about 30 m and their vertical extent reaches a few

hundreds of metres. At the Solnechnoe deposit – one of the largest in this district, the orebodies are traced until they pinch out in the granite hidden at a depth; the vertical extent of mineralization reaches 700–800 m. The position of these orebodies is controlled by N-S faults and also by northwestern tectonic fractures (see Fig. 3.8). There are also bodies of mineralized tectonic and explosive breccias that are localized at the intersection of N-S and W-E faults.

The mineral composition of ore at the deposits of the Komsomolsk district is similar except for some insignificant features. More than 50 hypogenic minerals are known from the district. Main minerals are quartz, tourmaline, cassiterite, wolframite, arsenopyrite, chalcopyrite, galena, and sphalerite. They form five mineral assemblages in the following succession: (1) quartz-tourmaline, (2) quartz-cassiterite with wolframite, scheelite, arsenopyrite, (3) quartz-pyrrhotite-ihalcopyrite, (4) quartz-carbonate-galena-sphalerite, and (5) quartz-pyrite-calcite with fluorite. In the western part of the ore district, small quartz-feldspar veins and linear greisen bodies (quartz, muscovite and tourmaline) with low cassiterite and molybdenite occur in the exo- and endocontacts of granitic bodies. The same mineralization is present in the exo- and endocontacts of granitic bodies discovered at a depth of about 1 km at the Solnechnoe deposit indicating the relationship of tin mineralization to the granites. The REE mineralization in the western part of the Komsomolsk ore district is considered to be related to the Chalba granites.

In the southern and especially southeastern parts of the ore district the tin mineralization is less abundant or absent at all. There are usually occurrences of molybdenum, copper, and gold. This mineralization type has been poorly studied. Northern and northeastern parts of the district are characterized by mercury mineralization.

Solnechnoe tin deposit

The Solnechnoe deposit is situated in the western part of the district where Jurassic – Lower Cretaceous sedimentary rocks are intruded by granitoids of the Silinka complex (Silinka massif). The deposit was mined by open-pit and underground working from the early 1960 to the early 1990. Today the mine is not operating. Open-pit and underground working were not maintained so of it is now full water (Fig. 3.16).

The deposit is represented by the Glavnaya ore zone located in the Solnechnaya N-S tectonic structure. From the north towards the south the zone is divided into a number of intervals, – i.e. the Northeast-



Fig. 3.16. Morning in the dead open-pit of the Solnechnoe tin deposit

ern, Northern, Central, Silinsky, Southern, and Dal'niy. The ore zone, as well as the fault hosting it, forms curves with N-S and northeastern trends, and is accompanied by northwestern apophyses.

The Glavnaya zone is basically composed of quartz tourmalinite, rimmed by a cover of quartz-sericite metasomatite. The ore zone structure is shown in Figs. 3.17, 3.18. Only in a few sites is tourmalinite subordinate to younger quartz veins with cassiterite,

wolframite, and sulfide. The orientation of the quartz veins and veinlets almost always coincides with the orientation of the whole zone. The evidence shows that in the initial stage, quartz metasomatically developed on tourmalinite, and then crystallized in open voids as a combed variety. Younger quartz-sulfide veins and veinlets have been traced along the whole extension of the zone along the strike and down dip. Brecciated ore is common (Fig. 3.19). The upper horizons of the zone are less enriched in sulfide compared with deeper horizons where sulfide frequently plays a significant role. The youngest sulphides – galena, stannite, boulangerite, and jamesonite occur in veinlets.

The Glavnaya zone was formed during five successive stages of mineralization: quartz-tourmaline, quartz-cassiterite with wolframite, scheelite, tourmaline-II, quartz-sulfide, quartz-carbonate-sulfide, and quartz-calcite (locally). The zone was formed (at the interval explored) under temperatures of 425-70°C. Average temperatures of successive associations form almost a continuous row, which is suggestive of continuous mineral formation. At upper horizons of the ore zone, at about 300 m interval, there a lower temperature of mineral formation of the quartz-cassiterite

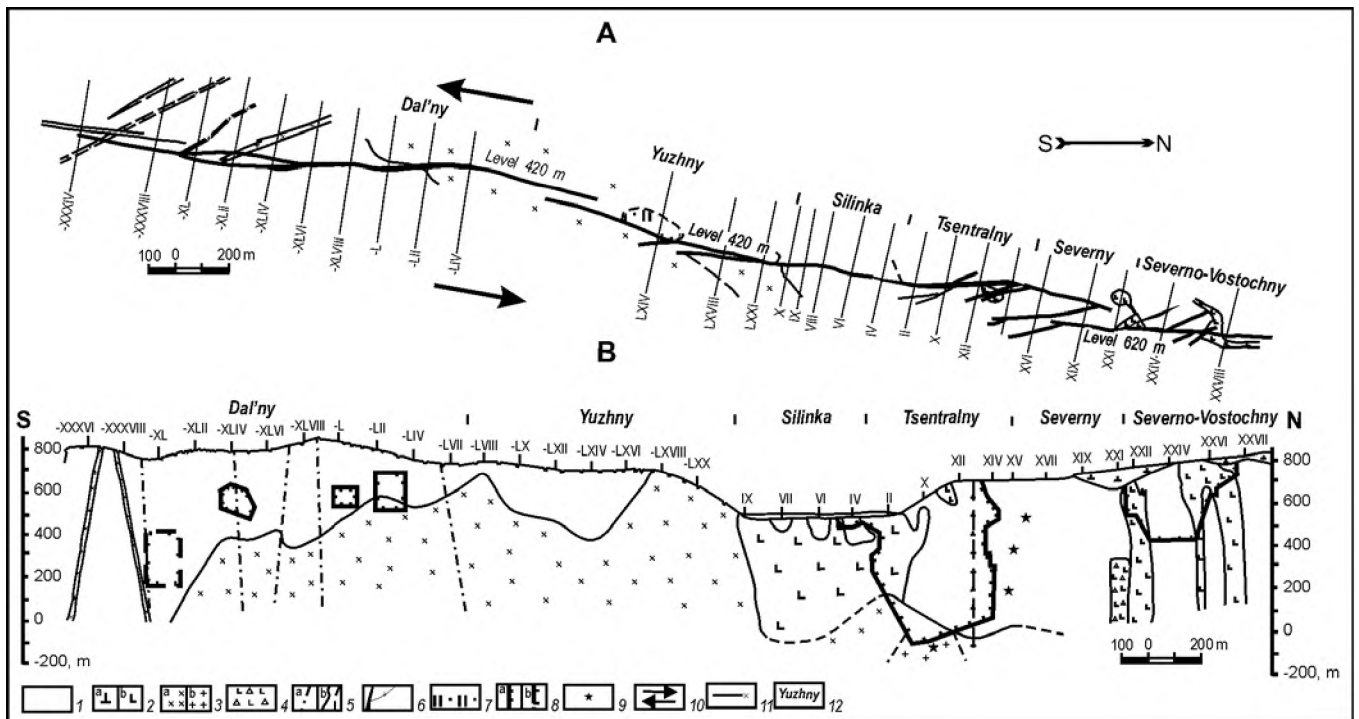


Fig. 3.17. Plan (A) and vertical plane projection (B) of the Glavnaya zone of the Solnechnoe deposit, after Korostelev et al. (2001).

(1) terrigenous rocks (sandstone, siltstone); (2) basalt (a) and quartz diorite porphyrite; (3) granodiorite (a) and granite (b); (4) eruptive breccia; (5) faults (a), geological contacts (b): established (firm line) and assumed (dotted line); (6) quartz-tourmaline metasomatite zones; (7) quartz metasomatite; (8) industrial ore body contours: established (a) and assumed (b); (9) molybdenite; (10) block movement direction along the Solnechny fault; (11) survey traverse and its number; (12) Glavnaya zone intervals

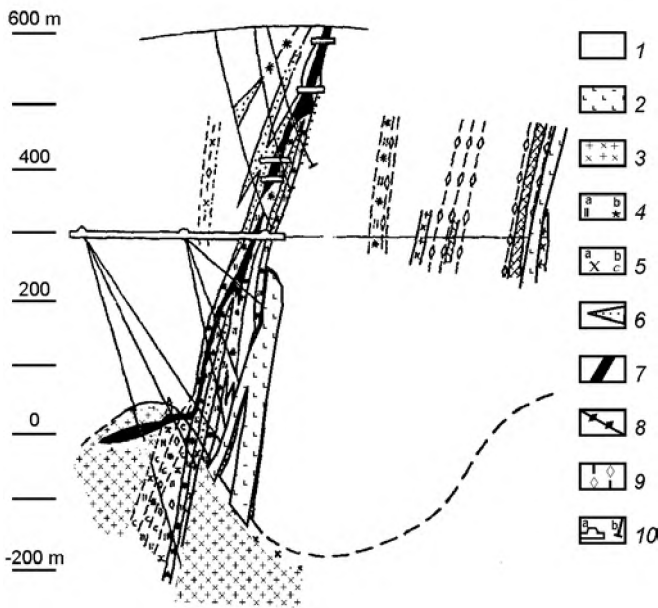


Fig. 3.18. Vertical cross-section of the Glavnaya zone of the Solnechnoe deposit, after Korostelev et al. (2001). (1) Jurassic terrigenous-sedimentary rocks; (2) diorite porphyry (quartz diorite) of the Silinka complex; (3) granite and granodiorite; *metasomatites*: (4) quartz-tourmaline (a – quartz, b – tourmaline), (5) quartz-chlorite-muscovite (a – chlorite, b – muscovite); (6) quartzite; (7) sections saturated by quartz with cassiterite; *minerals observed visually in a borehole core within granitoids*: (8) cassiterite, (9) molybdenite; (10) underground openings (a) and boreholes (b)



Fig. 3.19. Brecciated tin ore of the Solnechnoe tin deposit

association with 400-425 to 350-375°C at 15°C gradient at 100 m. Horizontal temperature zoning has been observed relative to a granitoid massif on the southern flank of the deposit. Approaching that massif, the temperature of the ore-bearing quartz within the zone increases by 20-25°C. A conclusion about a considerable extension of the ore bodies at depth, based on the evidence of mineralogical and thermobarogeochemical rock studies was confirmed by finding ore bodies and mineralization of new types at deeper horizons of the deposit.

In the Central interval of the deposit, the ore mineralization has been traced down to an unexposed granite stock, and in the stock itself, it is represented by steeply dipping and gently sloping greisen-like formations with tin, molybdenum, and bismuth. Molybdenum mineralization occurs linear to the eastern lying contact of the Glavnaya zone among hornfelsed sedimentary rocks. It occurs in a thick veinlet zone trending north-westward which is cut by the Glavnaya tin-bearing zone. The largest veins are accompanied by a series of thin veinlets, and they have a quartz-tourmaline and quartz-feldspar composition. Among veined minerals there are biotite, apatite, carbonate, and fluorite. Molybdenite is associated with bismuthinite, native bismuth, and bismuth telluride. Together with arsenopyrite, in molybdenite-bearing veins and veinlets cobalt-bearing löllingite occurs (Korostelev et al., 2001).

Festival'noe tin deposit

The Festival'noe tin deposit is confined to the southern part of the ore district, on the southern flank of the Pereval'nenskaya structure. Host rocks in the lower horizons are represented by Middle Jurassic sand-siltstone deposits of the Ul'binskaya suite and coarse-grained Lower Cretaceous sedimentary rocks, and in the upper horizons – by alternating tuffs of rhyolite and tuffaceous-sedimentary rocks of the Upper Cretaceous Kholdami suite (Figs. 3.20, 3.21). Tin ore mineralization is concentrated in several ore zones. The Yagodnaya, Vodorazdel'naya, and Geofizicheskaya zones located in the main structure, and also numerous zones in the branching structures such as – the Zapadnaya, Pologaya, Slepaya, etc. are ore-bearing. Ore mineralization has been traced over a distance of 3.5 km up to 700 m and more. Using in vertical extent the example of the Festival'noe deposit it is possible to trace the role of the interblock movement along the main ore-bearing structure in the morphology of ore bodies and the distribution of mineralization. The size of such movement here is determined

from the shift of the uneven base of volcanic strata along the entire strike of the ore zone. The zone sharply changes its thickness and mineralization becomes distributed in the fissures where the size of a shift component sharply decreases (for example, at the fold curves).

The deposit is characterized by a typical set of ore mineral associations. The surface of the discordant boundary between volcanic and sedimentary rocks plays a very important role in the distribution of the mineral associations. Below this surface, a tourmaline and quartz-cassiterite ore with wolframite and scheelite associations prevails. Above this surface, a pyrrhotite-chalcopyrite association plays a very important role. Stannite, which is frequently substituted by cassiterite of the second generation, is widespread in it. The morphology of the ore bodies occurring in volcanic rocks depends on the character of the section of the latter ones. Usually, at the intersection of tuff horizons there form pinches, and in the horizons of conglomerate, on the contrary, there are observed swells of ore bodies (Fig. 3.22). At deeper horizons in accordance with the structural zoning, tourmalinization occurs along a series of convergent joints and embraces the sites between the joints, acquiring a voluminous nature (Figs. 3.23, 3.24). Sericite (muscovite) is added to the leading minerals in the deeper levels of the deposit. The mineral composition of the older metasomatites suggests they are peculiar tourmaline greisens. Vein-like bodies of tourmalinite are usually accompanied by a wall of altered rocks. Quartz and sericite (near tourmalinite), chlorite, carbonate, and epidote (at a distance from tourmalinite) are most common in that external facies. From spatial and age relationships of the minerals of the deposit there are revealed five stages of an ore process; 1 – quartz-tourmaline; 2 – quartz-cassiterite; 3 – quartz-sulfide (pyritic); 4 – sulfide-carbonate (polymetallic) and 5 – quartz-calcitic.

The Festival'noe deposit has a peculiar zoning of mineralization, and with this feature it is compared with the classical Cornwall deposits. From the upper horizons of ore bodies to the lower ones there are four zones: lead-zinc, tin-copper, copper-tungsten-tin, tungsten-tin. Unavailability of data on the uppermost (eroded) and the deepest (below the level studied) horizons does not permit observation of ore zoning throughout the section. Based on the data available, the appearance of tin-molybdenum-bismuth mineralization of greisen type can be suggested at depth.

The ore zones of the deposit (in a relatively small vertical interval) formed under temperatures of 450-

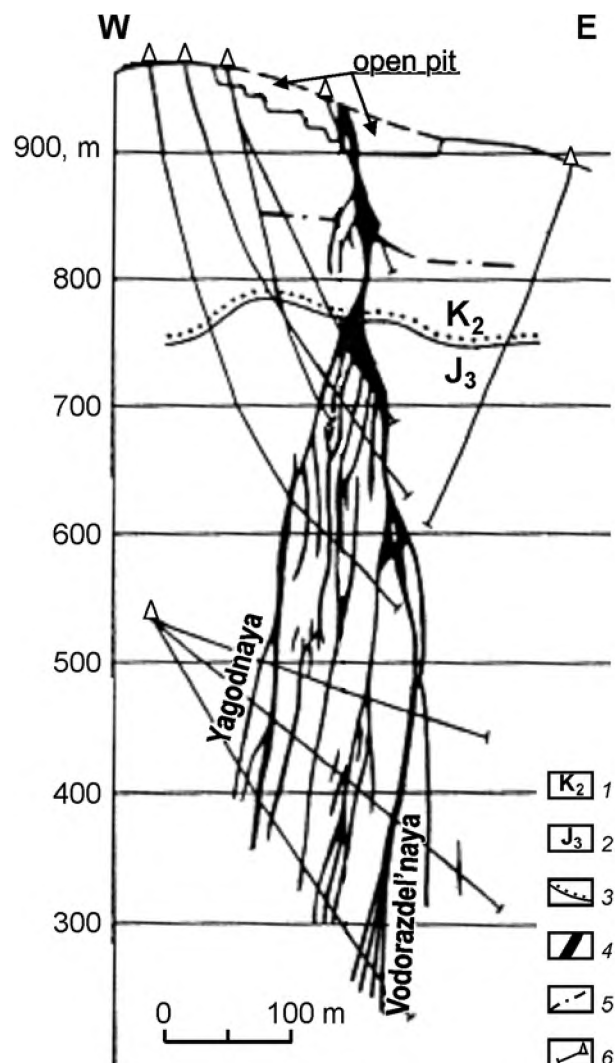


Fig. 3.20. Cross-section of a central part of the Festival'noe tin deposit, after Van-Van-E et al. (1992).

(1) Late Cretaceous tuff-sandstone, tuff-conglomerate, and tuff-siltstone of the Kholdami Suite; (2) Late Jurassic differently-grained sandstones with siltstone interbeds of the Silinka Suite; (3) stratigraphic unconformity boundary; (4) ore zones and bodies; (5) fault; (6) boreholes

100°C. In that temperature interval quartz-tourmaline and quartz-cassiterite parageneses are most high-temperature (450-300°C); chalcopyrite-pyrrhotite and galena-sphalerite with temperatures of 350-250 and 300-200°C are intermediate; quartz-carbonate with pyrite and fluorite association is the lowest in the temperature – 250-100°C. Wide ranges of optimal temperatures are typical of all basic minerals, the consequence of which is the presence in ore of repeated generations, distant from each other in an enriched paragenetical sequence. Coincident temperatures of successive associations predetermine a close coexistence in the upper horizons of late generations of cassiterite with sulfide.

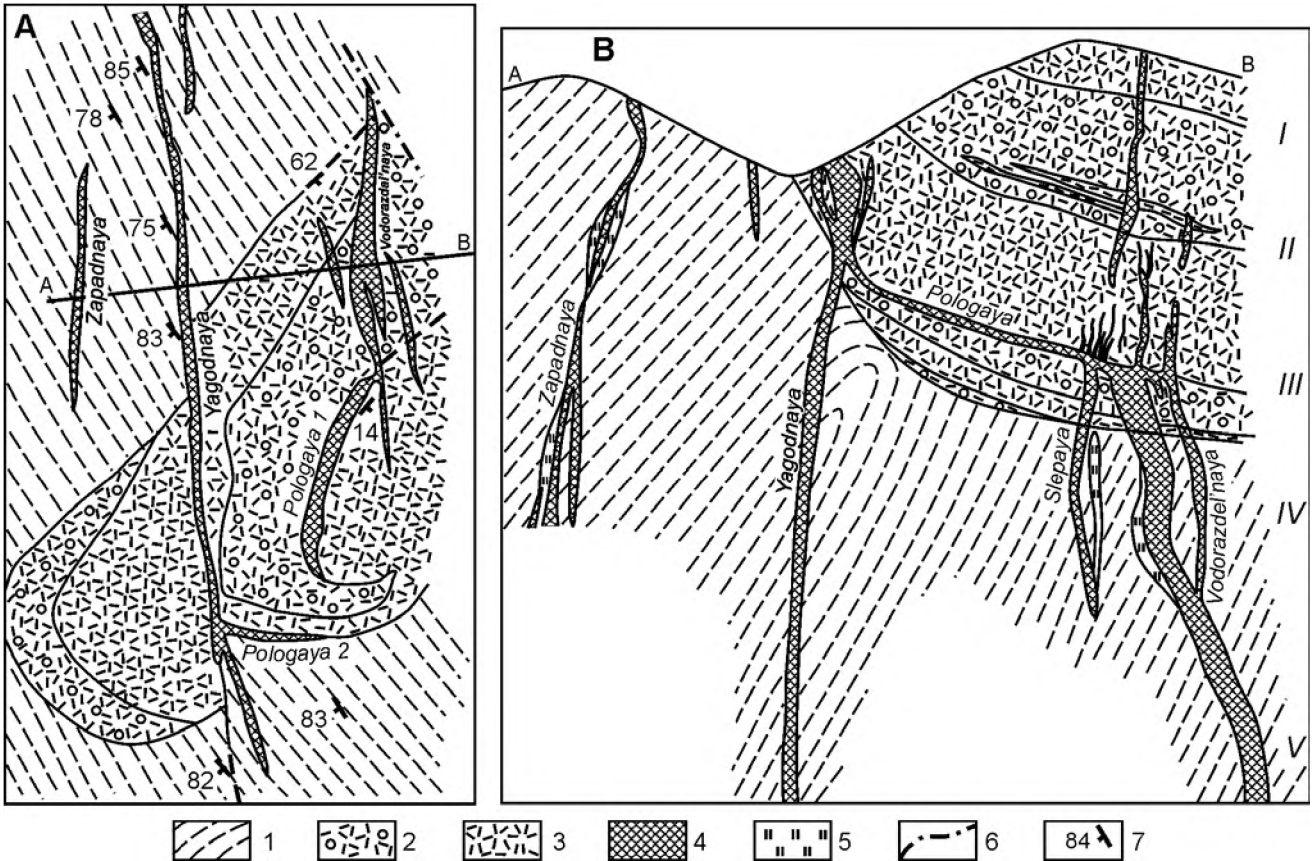


Fig. 3.21. Geologic plan of the III survey levels in a northern part of the Festival'noe tin deposit (A) and cross-section (B) along the A-B line, after Dubrovskiy et al. (1979).
 1 – Late Jurassic sandstone, 2 – Cretaceous tuff conglomerate, 3 – Cretaceous rhyolite tuff, 4 – ore zones (quartz-tourmaline metasomatite with ore mineralization), 5 – quartz-sericite alteration, 6 – faults, 7 – dip directions of structural elements. I-V – survey levels

Concerning the temperature zoning, its complicated nature should be noted. In the structure of the temperature field of the deposit there simultaneously exists vertical and horizontal zoning, which results in combined (voluminous) zoning. For the main ore zones varying bends of geoisotherms have been established:

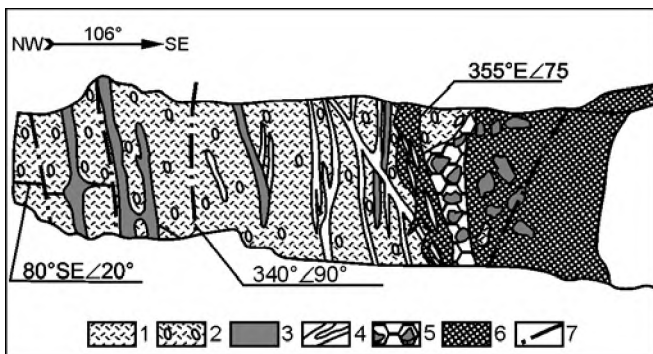


Fig. 3.22. Morphology of Yagodnaya zone hosting by volcanogenic rock (underground working), after Dubrovskiy et al., (1979).
 1 – rhyolite tuff, 2 – tuff conglomerate, 3 – tourmaline alteration, 4 – quartz vein, 5 – quartz-tourmaline breccias, 6 – quartz-chalcopyrite vein, 7 – faults

in the Yagodnaya zone it is clearly expressed northward, and in the Geofizicheskaya zone – less visible

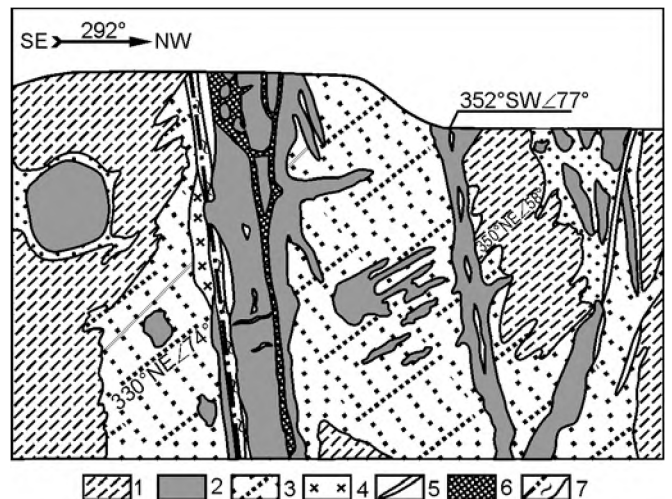


Fig. 3.23. Morphology of Vodorazdel'naya zone in sedimentary rock (underground working), after Dubrovskiy et al. (1979).
 1 – sandstone, 2 – tourmaline alteration, 3 – sericite alteration, 4 – chlorite alteration, 5 – quartz-cassiterite vein, 6 – sulfide vein, 7 – faults

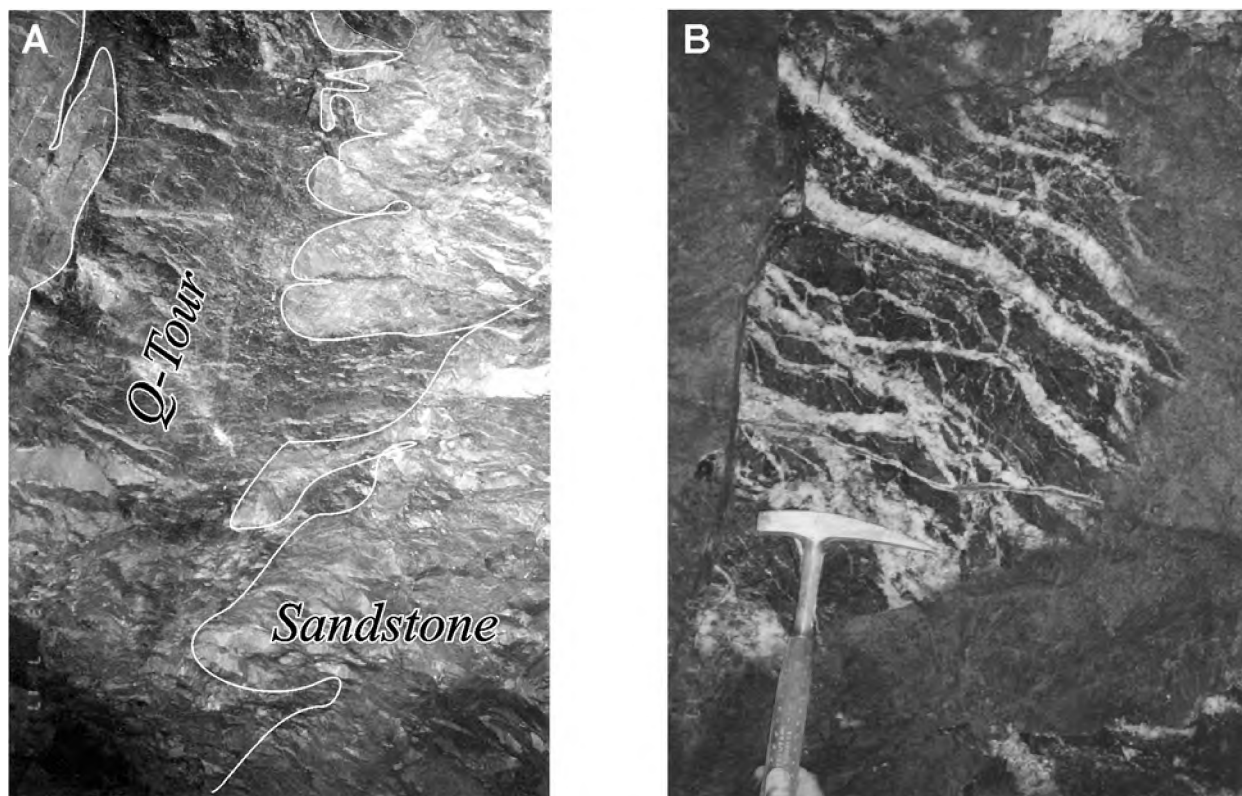


Fig. 3.24. Morphology (A) and internal structure (B) of quartz-tourmaline zone at deep level of the Festival'noe tin deposit

southward. With depth, there occurs an increasing flattening of isotherms. A summarized temperature gradient for the deposit is about 15°C on 100 m.

Compositionally complicated concentrated (mainly because of sodic chloride) hydrothermal solutions which have the features of aggregate transformation at the deepest (isolated facts) and the highest horizons participated in ore formation. The reasons for manifestation of pneumatolytic solutions on vertically opposite "ends" of a deposit are doubtless various. In deeper horizons this fact can testify to a deep pneumatolytic mineralization of, for example, greisen type, in the upper horizons – about ore formation in a sub-surface environment which caused a considerable pressure range.

Peraval'noe tin deposit

The Pereval'noe deposit is located in the northern half of the N-S Pereval'nensky fault of sinistral fault type (Figs. 3.25, 3.26). Mineralization has been traced with gaps along distance of 5 km occurring in the Severnaya, Silinskaya, Yuzhnaya, and Maiskaya imbricate zones, and have total vertical amplitude over 600 m. The intrusive formations of the Silinsky complex (diorite, granodiorite) are host rocks for the Silinskaya zone along a considerable distance. The Yuzhnaya and Maiskaya zones occur in alternating



Fig. 3.25. Open pit of the Pereval'noe tin deposit

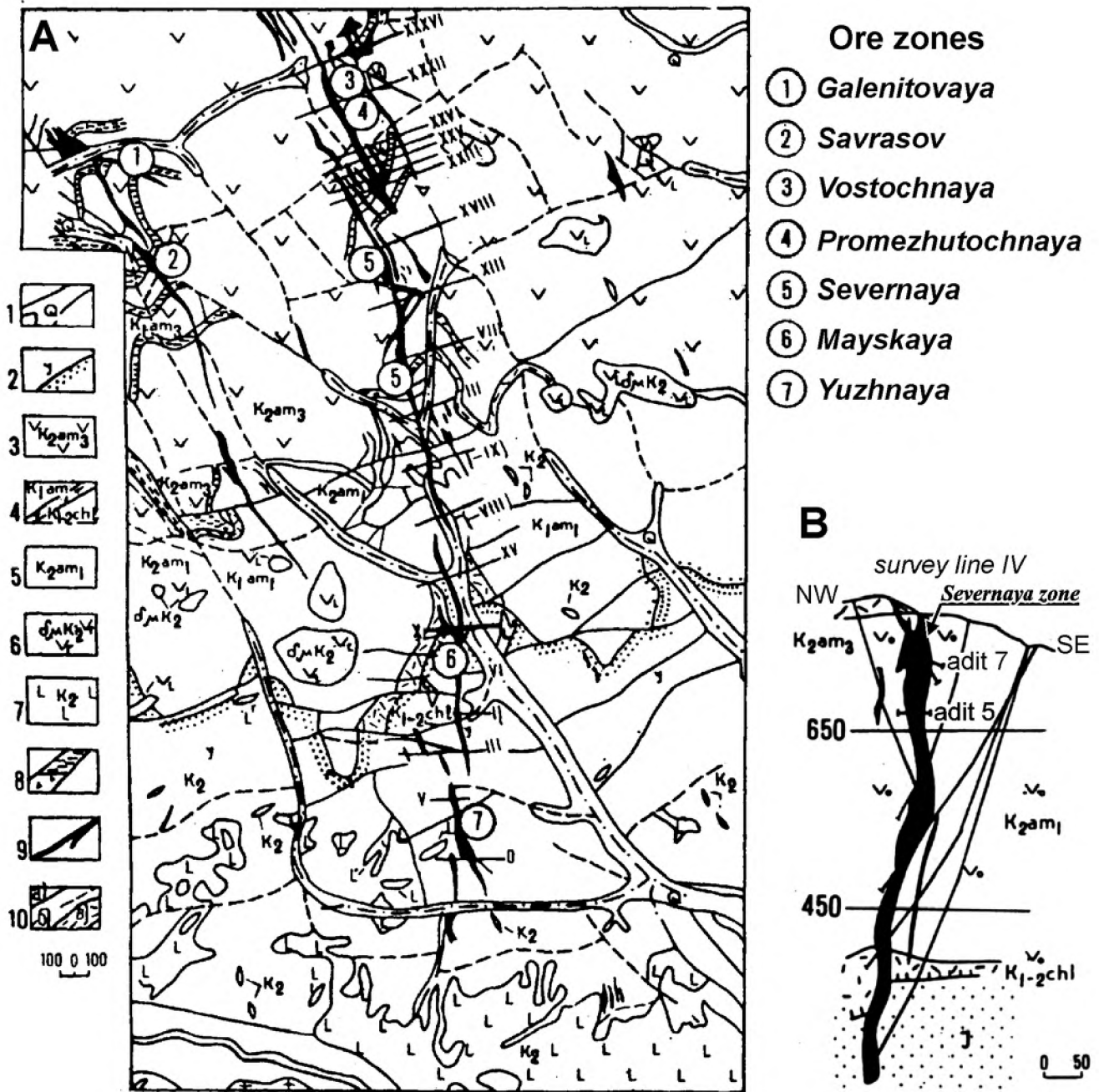


Fig. 3.26. Schematic geological map (A) and cross-section along the survey line IV (B) of the Pereval'noe deposit, from Van-Van-E et al. (1992).

(1) alluvial sediments; (2) differently-grained sandstones with siltstone interbeds of the Silinka Suite; (3) porphyry of a lava unit of the Amut Suite; (4) quartz porphyry tuff marker layers of the Kholdami and Amut Suites; (5) porphyry tuff of a pyroclastic unit of the Amut Suite; (6) extrusive and subvolcanic andesitic dacite, and diorite porphyry; (7) less silicic granitoids; (8) brecciation and higher-fissuring zones; (9) mineralized crush zones; (10) faults and crush zones: (a) established, (b) supposed, (c) schistosity zones

sandstones and siltstones of the Upper Jurassic Silinskaya suite, and Severnaya zone – in the Late Cretaceous andesitic volcanic rocks of the Amut suite. The latter is characterized by a very weak level of erosion; – it is unexposed over a considerable distance.

The Silinskaya, Yuzhnaya, and Mayskaya zones are composed of quartz-tourmaline metasomatite, forming vein-like bodies sometimes with gaps, apophyses, sites with altered strike and dip. Cassiterite and wolframite occur primarily metasomatically with tourmaline (except the Silinskaya zone where part of

the cassiterite is deposited in younger quartz veins). In the Maiskaya and Yuzhnaya zones the leading position is occupied by quartz-sulfide (arsenopyrite-chalcopyrite-pyrrhotite) and quartz-carbonate-sulfide (galena-sphalerite) mineral associations superimposed as thick veins and veinlet zones on older tourmalinite with cassiterite and wolframite.

In the Severnaya zone, a quartz-tourmaline core is rimmed by a thick cover of propylite occurring in andesites and up to several hundred meters above it. The quartz-cassiterite association forms a veined core occurring in the center of the zone, and cuts tourmalinite and the propylitic cover above it. At the uppermost level, mineralization is in veinlets. Above-ore propylitic cover is strongly enriched in lead and zinc making up the main minerals of quartz-carbonate-sulfide (galena-sphalerite) association here.

The structural peculiarity of the Pereval'noe deposit is the development of a system of apophyses between neighboring zones on the sites of their imbricated joint or splitting into variously-oriented components. Morphologically those apophyses can be regarded as stockworks.

Some peculiar parageneses occur. Thus, in the upper parts of the Severnaya zone, quartz-cassiterite veinlets and veins have higher contents of chlorite, and on its lying walls – feldspar separations. Within the Maiskaya zone, in rich stibnite and boulangerite quartz-carbonate veinlets there occurs late arsenopyrite, and in the Yuzhnaya zone – a superimposed system of intermittent veinlets with stibnite and boulangerite. The mineral associations combined within the zones are frequently connected by gradual transitions. On the whole, however, a succession of deposited mineral associations corresponding to the stages of an ore process has been distinctly revealed: 1 – quartz-tourmaline with facies of sericite metasomatite and propylite; 2 – quartz-cassiterite-wolframite with quartz-cassiterite-feldspar facies; 3 – quartz-arsenopyrite-pyrrhotite-chalcopyrite; 4 – quartz-carbonate-galena-sphalerite with stannite, boulangerite, stibnite and late arsenopyrite; 5 – quartz-calcite with pyrite.

EXCURSION POINTS

Stop 1. The Zhuravlevsk-Amur River terrane. The right bank of the Amur River opposite Komsomolsk-on-Amur City (Figs. 3.6 and 3.7).

Stop 2. Upper Triassic (Norian) sediment rocks of the Badzhal terrane. The left side of the Pravaya Silinka River valley (Fig. 3.8).

Stop 3. The Jurassic and Lower Cretaceous Kholdami sedimentary-volcanogenic suite. Around the Geophysical ore zone of the Festival'noe tin deposit (Fig. 3.8).

Stop 4. The Late Cretaceous Amut volcanogenic suite. The Amut River valley (Figs. 3.8, 3.10, 3.11, and 3.12).

Stop 5. The Silinka intrusive massif. The right side of the Levaya Silinka River valley (Figs. 3.8, 3.13, 3.14, and 3.15).

Stop 6. Granites of the Chalba complex. The left bank of the Chalba River (Fig. 3.8).

Stop 7. The Miocene and Quaternary plateaubasalt of the Kizinskaya suite. The North-Eastern open-pit of the Solnechnoe tin deposit (Fig. 3.8).

Stop 8. The Solnechnoe Tin Deposit. The left side of the Levaya Silinka River valley (Figs. 3.8, 3.16, 3.17, 3.18, 3.19, and 3.20).

Stop 9. The Festival'noe Tin Deposit. The right side of the Kholdami River valley (Figs. 3.8, 3.21, 3.22, 3.23, and 3.24).

Stop 10. The Pereval'noe Tin Deposit. The right side of the Pravaya Khurmuli River valley (Figs. 3.8, 3.25, and 3.26).

REFERENCES

- Benz N.M., Zandt C., Oppenheimer D.H. Lithospheric structure of Northern California from teleseismic images of the upper mantle // *Journal of Geophysical Research*. 1992. V.97. №B4. P.4791-4807.
- Bolotnikov A.F., Kravchenko N.S., 1976. Petrogenesis of Late-Mesozoic volcanic-plutonic assemblages of Around-Amur area. *In: Volcanic and volcanic-plutonic complexes of Eastern Asia*. Vladivostok: FESC, pp. 24-35 (*in Russian*).
- Bondarenko E.L. Radiological age of volcano-plutonic associations and ores of the Badzhal zone// *Regularities of development of endogenous mineralization in the Far East*. Vladivostok, 1979. P. 101-150. (*in Russian*).
- Brusnitsin A.I., Panova A.I., Smolensky V.V. Findings of Li-F type granites in the Upper Urmiisky node// *Izvestiya VUZov, Geology and Exploration*, 1993, N 6, p. 150-157. (*in Russian*).
- Chappell B., White A. Two contrasting types of granites. – *Pacific Geol.*, 1974. V.8, N2., pp. 173-174.
- Dubrovsky V.N., Malinovsky E.P., Rodionov S.M. Structure and zoning of tin deposits of the Komsomolsk district. Moscow: Nauka, 1979, 136 p. (*in Russian*).
- Faur M., Natal'in B.A. The geodynamic evolution of the eastern Eurasian margin in Mesozoic time. *Tectonophysics*, 208, 992.p.397-411.
- Gonevchuk V.G., 2002. Tin-bearing systems of the Far East: magmatism and ore genesis. Vladivostok: Dal'nauka. 298p (*in Russian*).
- Gonevchuk V.G., Kokorin A.M., Korostelev P.G., Radkevich E.A., Semenyak B.I., 1984. Tin-ore formations of South Far East. – *Tikhookeanskaya (Pacific) Geology*, N6, pp. 72-81 (*in Russian*).

- Gonevchuk V.G., Seltmann R., Gonevchuk G.A. Tin mineralization and granites of the main ore districts of Central Amur region, Russian Far East // Ore-bearing granites of Russia and adjacent countries. Moscow, IMGRE, 2000, p. 113-126.
- Gonevchuk V.G., Semenyak B.I., Ishikhara S., Gonevchuk G.A., Korostelev P.G. Age of tin-bearing greisens of Priamurye and some problems of genesis of tin mineralization (Russia): Geologiya Rudnykh Mestorozhdenii. 1998. V. 40, N 4, p. 326-335. (*in Russian*).
- Ishikhara S., Gonevchuk V.G., Gonevchuk G.A. Korostelev P.G., Sayadyan G.R., Semenyak B.I., Ratkin V.V., 1997. Mineralization age of granitoid-related ore deposits in the Southeastern-Russian Far East. – Resource Geology, v.47, №5, p.255-261.
- Izokh E.P., Kolmak L.M., Nagovskaya G.I., Russ V.V. Late Mesozoic intrusions of the Central Sikhote-Alin and related ores. Moscow: Gosgeoltechizdat, 1957, 247 p. (*in Russian*).
- Karsakov L.P., Malyshev Yu.F., Bepalov V.Ya., Gagaev V.N., Rodionov S.M., Romanovsky N.P., Troyan V.B., Gu Feng, Duang Zhuiyan, Chzhao Chuntszing, Lu Tszasun. Abyssal structure and gold and tin metallogeny of the South Far East of Russia and North-East China (comparative analysis)// Geological Survey and mineral-raw material base of Russia on the threshold of the XXI age. All-Russia Meeting of geologists and scientific-practical conference. Abstracts. Sankt-Peterburg, VSEGEL, 2000, CD-ROM. (*in Russian*).
- Khanchuk A.I. Pre-Neogene tectonics of the Sea-of-Japan region: A view from Russian side // Earth Science (Chikyū Kagaku), 2001, vol.55, p.275-291.
- Khanchuk A.I., Golozubov V.V., Martynov Yu.A., Simanenko V.P. Early Cretaceous and Paleogene transform continental margins (Californian type) of the Far East of Russia//Tectonics of Asia: program and abstracts of the XXX Tectonic Meeting. Moscow: GIN, 1997, p. 240-243. (*in Russian*).
- Khanchuk A.I., Ivanov V.V. Geodynamics of East Russia in Meso-Cenozoic and gold mineralization. In: Geodynamics and metallogeny. Vladivostok, Dal'nauka, 1999, p. 7-30. (*in Russian*).
- Kirillova, G.L., Natal'in, B.A., Zhabrev, S.V., Sakai, T., Ishida, K., Ishida, N., Ohta, T., Kozai, T., (2002). Upper Jurassic-Cretaceous deposits of East Asian continental margin along Amur River. Field excursion guidebook. The 30-th Anniversary of IGCP. Khabarovsk: ITIG FEB RAS. 72 p.
- Korostelev P.G., Gonevchuk V.G., Semenyak B.I., Suchkov V.I., Kokorin A.M., Gonevchuk G.A., Gorelikova N.V., Kokorina D.K., 2001. Solnechnoe deposit (Komsomolsk district, Khabarovsk territory) as the sample object of the cassiterite-silicate formation. In: Ore deposits of continental margins. Issue 2, volume 1, pp. 131-155 (*in Russian*).
- Krivovichev V.G., Brusnitsyn A.I., Zaytsev A.N., 1996. Isotopic age and geochemical peculiarities of granite of Verkhneurmi massif (Around-Amur Area, Far East). – Geochemistry; №2, pp. 106-111 (*in Russian*).
- Krymskiy R.Sh., Gavrilenko V.V., Belyatskiy B.K., Smolenskiy V.V., Levskiy L.I., 1997. Age and genesis of W-Sn mineralization of Verkhneurmi ore field (Around-Amur Area) by Sm-Nd and Rb-Sr data – Petrology, №5, pp. 552-560 (*in Russian*).
- Lebedev V.A., Ivanenko V.V., Karpenko M.I. Geochronology of volcano-plutonic complex of the Upper Urmiisky ore field (Khabarovsk Krai, Russia): data of K-Ar, ³⁹Ar-⁴⁰Ar, and Rb-Sr isotope methods//Geologiya rudnykh mestorozhdenii, 1997, V. 39, N 4, p. 362-371.
- Lishnevskiy E.P., 1965. About active role of intrusions in mountain building process. – Geotectonics, №3, pp. 77-84 (*in Russian*).
- Metallogeny of the main tin-ore districts of the South Far East.* Vladivostok: Publishing House of the Far East Scientific Center, USSR Acad. Sci., 1988, 164 p. (*in Russian*).
- Natal'in B.A., 1993. History and modes of Mesozoic accretion in Southeastern Russia. – The Island Arc. V. 2, N. 1, pp.15-34.
- Nokleberg W.J., Ariunbileg S., Badarch G., Berzin N. A., Bulgatov A. N., Chimed N., Deikunenko A.V., Dejidmaa G., Diggle M.F., Distanov E.G., Dorjgotov D., Gerel O., Gordienko I.V., Gotovsuren A., Duk-Hwan Hwang, Khanchuk A.I., Koch R.D., Miller R.J., Obolenskiy A.A., Masatsugu Ogasawara, Demberel Orolmaa, Oxman V.S., Parfenov L.M., Popeko L.I., Prokopiev A.V., Rodionov S.M., Smelov A.P., Sotnikov V.I., Sadahisa Sudo, Timofeev V.F., Tret'yakov F.F., Vernikovskiy V.A., Mao Ye, Zadgenizov A.P., 2003. Preliminary Publications Book 2 from Project on Mineral Resources, Metallogenesis, and Tectonics of Northeast Asia. USGS Open-File Report 03-203 <http://geopubs.wr.usgs.gov/open-file/of03-203>
- Nokleberg W.J., Parfenov L.M., Monger J.W.H., Norton I.O., Khanchuk A.I., Stone D.B., Scholl D.W., Kazuya Fujita. Phanerozoic tectonic evolution of the Circum-North Pacific. USGS Open-file report 98-754, 1998, 125 p.
- Ognyanov N.V. Geology of tin-ore districts and deposits of Khingan-Okhotsk tin-bearing region. In: The geology of tin deposits of Soviet Union. 1986. Vol. 2, b.1. M.: Nedra. Pp.340-399 (*in Russian*).
- Pacific outlying of Asia. Magmatism* / A.D. Scheglov, ed., 1991. M.: Nauka, 264 p (*in Russian*).
- Parfenov L.M., Nokleberg U. J., Khanchuk A.I. Principles of compilation and main subdivisions of the legend for the geodynamic map of the North and Central Asia, South Russian Far East, Korea, and Japan// Tikhookeanskaya Geologiya, 1998, N 3, p. 3-13.
- Pearce J.A., Harris N.B.W., Tindle A.G. Trace element discrimination diagrams for the tectonic interpretation of granitic rocks. – Journ. Petrology, 1981. V. 76, pp. 956-983.
- Radkevich E.A. (editor). Geology, mineralogy, and geochemistry of the Komsomolsk district: Moscow: Nauka, 1971, 335 p. (*in Russian*).
- Radkevich E.A., Asmanov V.Y., Bakulin Yu.I., Gagaev V.N., Zitinev N.N., Kvyatkovskiy E.M., Kokorin A.M., Kokorina D.K., Korostelev P.G., Kushev V.B., Mikhailov M.A., Onikhimovskiy V.V., Seleznev P.N., Stepanova M.V. Geology, mineralogy and geochemistry of the Komsomolsk district. Moscow : Nauka, 1971. 335 p. (*in Russian*).
- Radkevich E.A., Korostelev P.G., Kokorin A.M., Ryabov V.K., Stepanova M.V., Kokorina D.K., Golovkov G.S., Bakulin Yu.I., Kushev V.B., Seleznev P.N., Klemin V.P., Radkevich R.O. Mineralized zones of the Komsomolsk district. Moscow : Nauka, 1967. (*in Russian*).
- Reynlib E.L., Romanovskiy N.P., 1975. Investigation of ore-bearing dome-like magmatic structures by geophysical data. In: Geology of Far East. Vladivostok, FESC, pp.110-115 (*in Russian*).
- Rodionov S.M., 2000₁. General features of tin provinces of Russian Far East. // CD-Rom: 31st International Geological Congress, Rio-de-Janeiro, Brazil, August 6-17. Abstract Volume.
- Rodionov S.M. 2000₂. Tin metallogeny of the Russian Far East. // Ore-bearing granites of Russia and adjacent countries. Moscow, IMGRE, c. 234-262.
- Rodionov S.M. Petrogeochemical evolution of tin-bearing ore-magmatic systems of East Russia// Tectonics, abyssal structure, and geodynamics of East Asia. III Kosygin'skie readings (January 23-25, 2001, Khabarovsk). Khabarovsk, ITiG of the

- Far Eastern Branch, Russian Acad., Sci., 2001₃, p. 225-238. (*in Russian*).
- Rodionov S.M. Specific features of evolution of the tin-bearing magmatic complexes// Mesozoic and Cenozoic magmatic and metamorphic formations of the Far East. Materials of the 5th Far East regional petrographic meeting. Khabarovsk, October 30 – November 2. – Khabarovsk, 2001₁, p. 87-89. (*in Russian*).
- Rodionov S.M. Tectonic and petrogeochemical evolution of tin-bearing ore-magmatic systems in folded belts of the Far East of Russia// Tectonics of Neogaea: general and regional aspects: Materials of the XXXIV Tectonic Meeting (January 30 – February 3, 2001). Moscow: GEOS, 2001₂, V. 2, p. 148-150. (*in Russian*).
- Rodionov S.M., Natal'in B.A. Geodynamic regimes of occurrence of porphyry type deposits// Mineralization of porphyry type in the Far East. Vladivostok, Publishing House of the Far East Scientific Center of the Siberian Branch, USSR Acad. Sci., 1988, p. 46-64. (*in Russian*).
- Romanovsky N.P., Gu Feng, Malyshev Yu.F., Rodionov S.M., Karsakov L.P., Chzhao Chuntszing, Duan Zhuiyan. Abyssal structure and metallogeny of gold of the South Far East of Russia and North-East China: Problems of geology and metallogeny of North-East Asia on the boundary of the thousand years. Materials of the XI session of the North-East Branch of VMO "Regional scientific-practical conference dedicated to 100 years from birthday of Yu.A. Bilibin" (Magadan, May 16-18, 2001): Magadan, SVKNII, 2001, V. 1, p. 73-75. (*in Russian*).
- Rub M.G., Features of substance composition and genesis of ore-bearing volcano-plutonic complexes, Moscow: Nauka, 1970. 363 p (*in Russian*).
- Rub M.G., Onikhimovsky V.V., Bakulin Y.I. Glavatskaya V.N., Koshman P.N., Makeev B.V., Rastuntsev A.P., Seleznev P.N., Terentenko N.A., Yanonis V.V., 1964. Granitoids of Myao-Chan district and related post-magmatic formations. Moscow: Proceedings of IGEM, USSR Acad. Sci., N 62. 171 p. (*in Russian*).
- Sato K., Nedachi M., Rodionov S.M. et al. Granitoids and related mineralization in Sikhote-Alin, Far East Russia. // The Society of Resource Geology, May 17-19, Tokyo, 2000, p. 121 (Abstracts with Programs).
- Sato K., Vrublevsky A.A., Rodionov S.M., Romanovsky N.P., Nedachi M. Mid-Cretaceous episodic magmatism and tin mineralization in Khingan-Okhotsk volcano-plutonic belt, Far East Russia // Resource Geology, 2002. vol.52, №1, p.1-14.
- The geology of tin deposits of Soviet Union*. 1986. / S. F Lugov, ed. Vol. 1-2. M.: Nedra, 332 p (*in Russian*).
- Tychkov S.A., Vladimirov A.G. Model of moving-apart of subducted oceanic lithosphere in the zone of the Indo-Eurasian collision// Doklady RAS, 1997, V. 354, N 2, p. 238-241. (*in Russian*).
- Van-Van-E A.P., Orlova T.A., Peltsman I.S. Atlas of multifactor models Far East tin deposits. Khabarovsk: FEIMRM. 1992. 167 p.
- Volcanic belts of Eastern Asia*. Geology and Metallogeny. / A.D.Scheglov, ed., 1984. M.: Nauka, 504 p (*in Russian*).
- Whalen J.B., Curce K.L., Chappell B.M. A-type granites: geochemical characteristics, discrimination and petrogenesis. – Contr. to Miner. Petrol. 1987. V. 95, N 4. Pp. 407-419.
- Zabrodin V.Yu., Grigoriev V.B., Kremenetskaya N.A. 2003₁. State geological map of Russian Federation Scale 1:200,000. Second Edition. Komsomolsk Series. Sheet M-53-XI. S-Petersburg: VSEGEI, (in press) (*in Russian*).
- Zabrodin V.Yu., Grigoriev V.B., Kremenetskaya N.A. 2003₂. State geological map of Russian Federation Scale 1:200,000. Second Edition. Komsomolsk Series. Sheet M-53-XVII. S-Petersburg: VSEGEI, (in press) (*in Russian*).



THE POKROVKA EPITHERMAL GOLD DEPOSIT

V. G. Khomich¹ and N. G. Vlasov²

¹*Far East Geological Institute (FEGI), Far East Branch, Russian Academy of Sciences, Vladivostok*

²*Pokrovka Mine Joint-Stock Company, Blagoveshchensk*

INTRODUCTION

The Pokrovka gold-silver deposit is situated in the Magdagachi district, Amur region, 12 km north of Tygda station on the Transbaikal Railway (Fig. 4.1), 450 km from Blagoveshchensk and 1730 km from Vladivostok.

Mining of gold in the district started in 1910–1914 when the first placers were found. In the Sergeevsky Creek valley, where the Pokrovka deposit is localized, placer gold was mined since 1936, mainly from pits and shafts, down to 16 m deep. Au-bearing quartz bodies were crossed by some workings in bedrock, but they did not attract the attention of prospectors. In 1974, V.D. Mel'nikov – Head of the Amur Laboratory for Geology of Gold, FEGI – sampled an old dump and recommended prospecting for near-surface gold mineralization in the Sergeevsky Creek valley. The subsequent geological mapping at a scale of 1:50,000 combined with geophysical, geochemical, and geological exploration resulted in the discovery of the Pokrovka deposit.

The flat country and waterlogged place of the Pokrovka ore field were crucial reasons to choose a borehole spacing pattern of initially 40×40 m with increased resolution of the grid to 20×20 m. Approximately 1300 boreholes, about 135 km in total length, have been drilled out in order to contour the stockwork-type orebodies and to measure resources contained therein. Geophysical exploration included aerogamma, electrical, magnetic, and mercury gas surveying, gravity measurements, logging, etc.

The Pokrovka deposit is the largest of the explored and mined gold fields in the Amur region. The identified gold reserves amount to 1.4 million oz with a grade of 4.1 g/t Au in ore suitable for open-pit mining. Undiscovered resources are estimated as 300 thou. oz Au ; the ore in stock contains 250 thou. oz Au.

GEOLOGICAL SETTING OF THE POKROVKA ORE FIELD

The Pokrovka ore field is localized in the western Umlekan-Ogodzha volcanic-plutonic belt that was active in the Jurassic and Cretaceous along the boundary between the Bureya microcontinent and Mongolo-Okhotsk thrust-fold system (Fig. 4.2). The Gonzha inlier of Precambrian rocks is a northern fragment of the Bureya microcontinent. This inlier is composed of gneisses belonging to the Upper Archean (?) Gonzha Group (isotopic age was estimated as 2160 ± 100 Ma) and Paleoproterozoic greenstone sequences. The

Gonzha Group is composed of amphibole, pyroxene-amphibole-biotite, and kyanite-biotite gneisses with amphibolite and quartzite interlayers, 4.5–5.0 km in total thickness, and associated ultramafics. Paleoproterozoic intrusive sheets of gneissic quartz diorite, granodiorite, and granite were intruded into the above rocks. The Paleoproterozoic Chalovaya Group, up to 2000 m thick, consists of chlorite and actinolite-epidote schists, metadiabases, and phyllites with embedded ultramafic bodies. Late Mesozoic intrusions and volcanics are abundant in the inlier framework. They make up a discontinuous chain of ring, dome, and linear structures accompanied by meso- and epi-

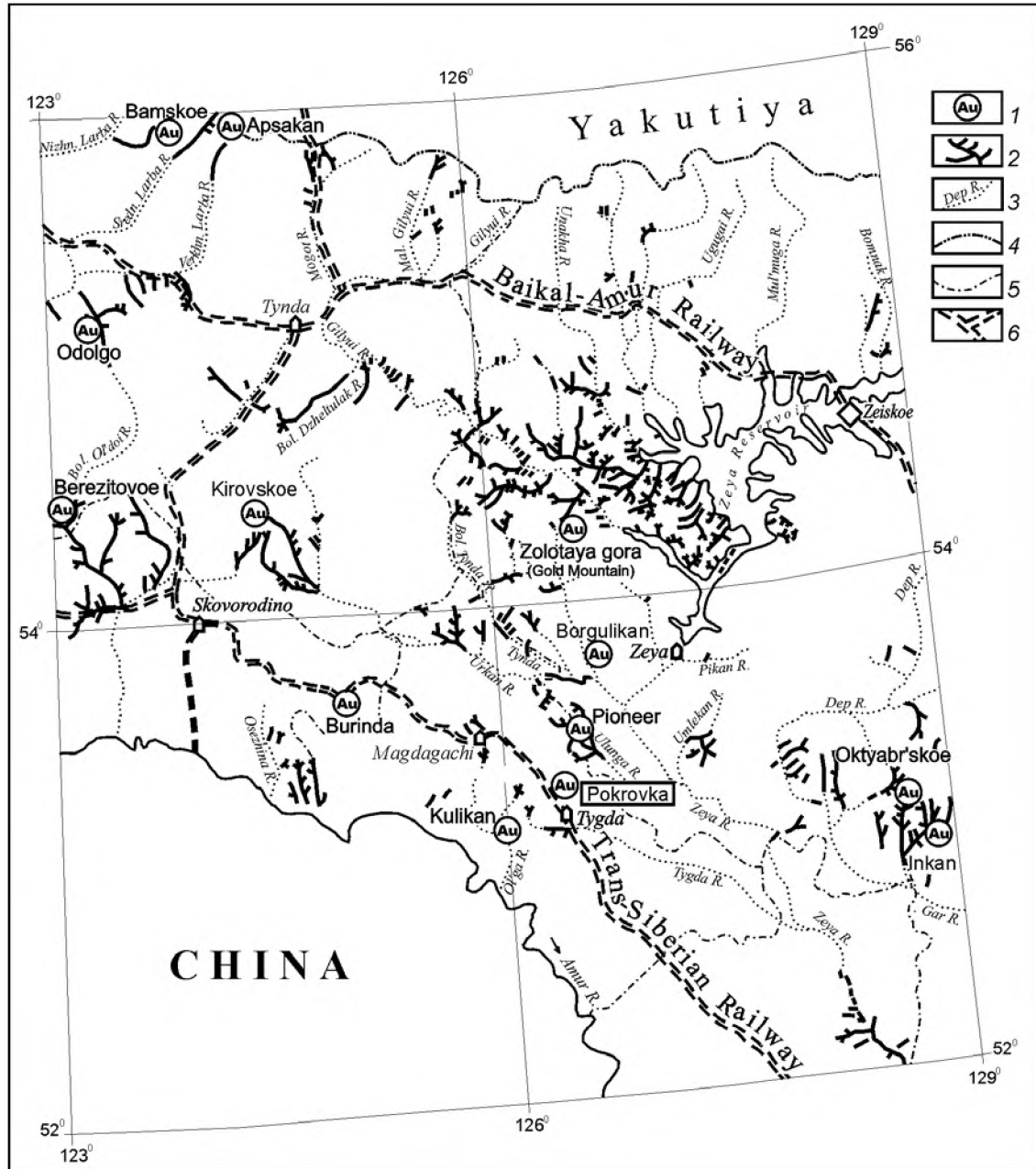


Fig. 4.1. Index map.

(1) gold deposits; (2) large gold placers; (3) rivers; (4) administrative territorial borders; (5) large settlements; (6) railways

thermal Au, Au-Ag, and Au-Mo porphyry mineralization (Fig. 4.2).

Four igneous rock associations: Late Jurassic (plutonic), Early Cretaceous (volcanic-plutonic), Early and Late Cretaceous (volcanic) are recognized in the Umlekan Zone (*Geologicheskaya karta...*, 1991). The plutonic association is, in turn, subdivided into the Upper Amur Complex of granite and granodiorite and Magdagachi Complex of subalkali granite and granosyenite. We refer both to the Late Jurassic–Early Cretaceous. The volcanic-plutonic association includes the Taldan Formation of intermediate volcanics

and the Burinda Complex of gabbro, monzodiorite, and granite. The Early Cretaceous volcanic association is composed of stratified andesite, dacite, and more silicic volcanics of the Kerak Sequence and comagmatic subvolcanic intrusions, which are predominant. The Late Cretaceous volcanic association consists of the bimodal (trachybasalt-trachyrhyolite) Gal'kino Formation and a complex of subvolcanic intrusions bearing the same name.

The Ulunga volcanotectonic depression is situated in the center of the Umlekan Zone, and the Pokrovka ore field is localized in its western marginal

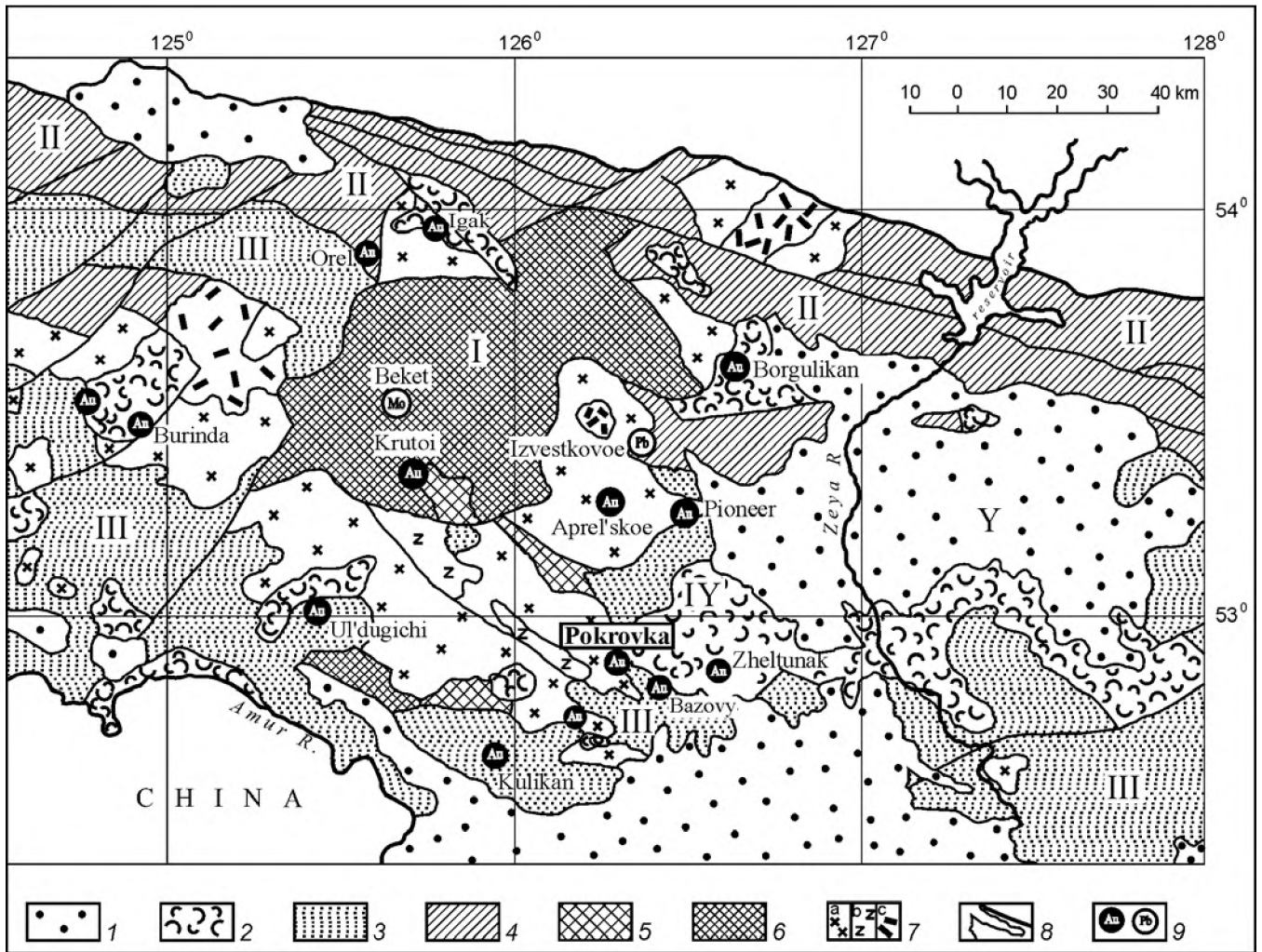


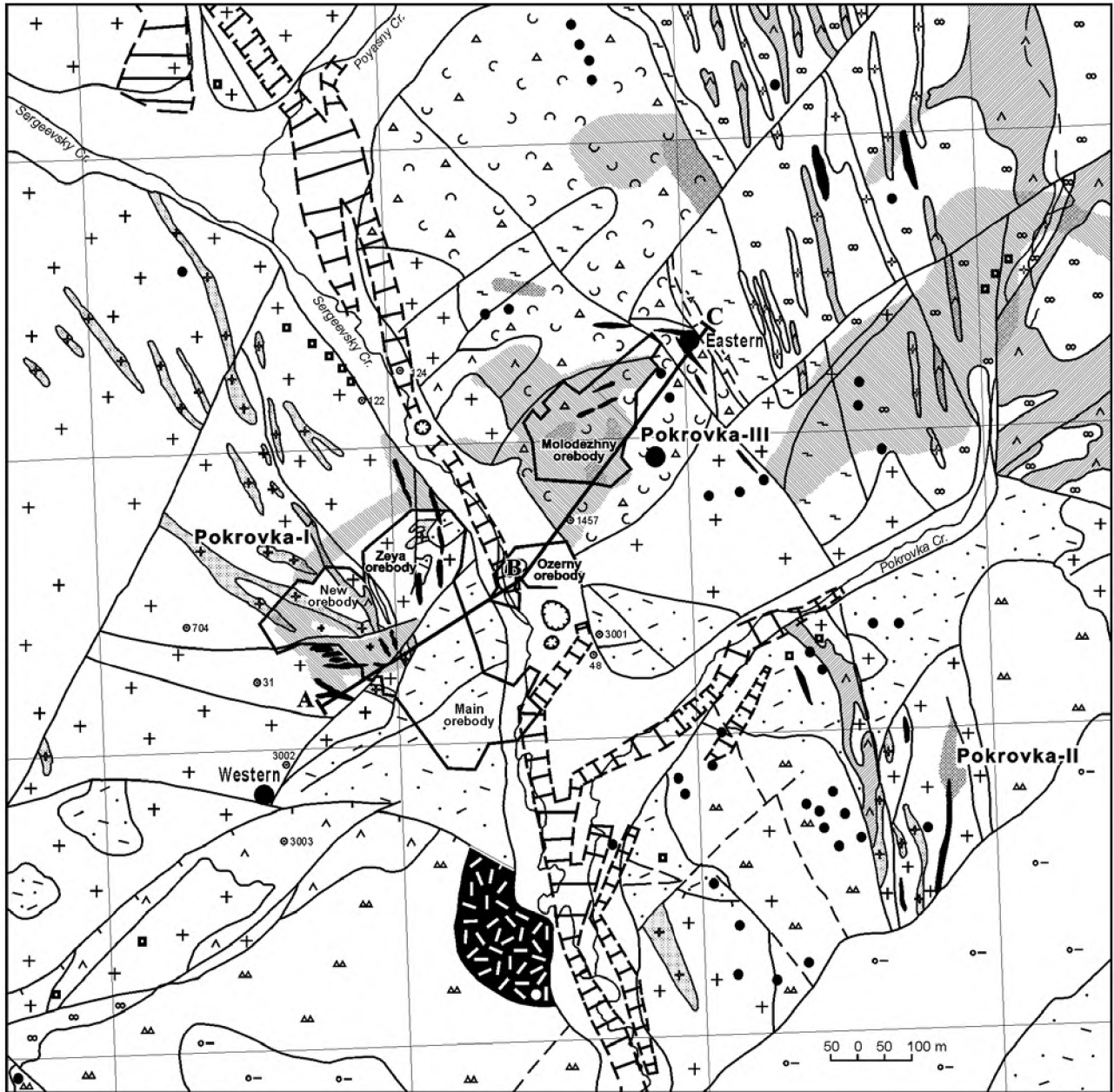
Fig. 4.2. Geological and metallogenic scheme of the Gonzha district, after Khomich (2001). Stratified sequences: (1) Neogene and Quaternary sediments, (2) Cretaceous volcanics, (3) Jurassic terrigenous rocks; (4) Paleozoic metasedimentary and metavolcanic rocks; (5) Lower Paleozoic and Neoproterozoic metamorphic rocks; (6) Paleoproterozoic and Archean (?) metamorphic rocks; (7) Late Mesozoic intrusions: (a) Late Jurassic–Early Cretaceous diorite-granodiorite-granite complex, (b) Late Jurassic–Early Cretaceous granosyenite porphyry, (c) Late Cretaceous granite porphyry; (8) major faults; (9) ore deposits (Au, etc.). Major tectonic units: (I) Gonzha inlier of Precambrian rocks; (II) Mongolo-Okhotsk thrust-fold system; framework of the Gonzha inlier: (III) Osezhina terrigenous trough, (IV) Umlekan volcanic-plutonic zone (Ulunga volcanotectonic depression), (V) Amur-Zeya depression

part. The walls and basement of the depression are composed of Middle and Upper Jurassic siltstone-sandstone sequence that fills the Osezhina Foredeep. These rocks are deformed in linear, brachyform, and box folds with dip angles of 40–50° on limbs. Large folds extend for 4–10 km with a width of 1–5 km. Late Jurassic–Early Cretaceous meso- and hypabyssal granitoid plutons of the Upper Amur and Magdagachi complexes are exposed in the walls of the depression.

According to the geophysical data, the Ol'ga, Sergeevsky, Arbi, and other granitoid plutons are interpreted as interformational intrusive sheets, 1.0–1.5 km thick, separating Precambrian basement of the Gonzha Inlier from Jurassic sedimentary cover.

The Pokrovka ore field is situated at the Sergeevsky pluton margin. More precisely, the ore field is localized at the junction of the Sergeevsky local intrusive dome with the superimposed Ulunga volcanotectonic depression. Other gold deposits and prospects of the region occupy a similar position in marginal parts of local intrusive domes conjugated with younger volcanotectonic depressions (Fig. 4.2). The characteristic geologic features of the Pokrovka ore field include (from smaller to larger): vent of paleovolcano and related subvolcanic intrusions and dikes; marginal part of the interformational (?) granitoid pluton; junction zone of this pluton and superimposed volcanic depression; Late Mesozoic intrusive

THE POKROVKA EPITHERMAL GOLD DEPOSIT



Geological cross section along line ABC

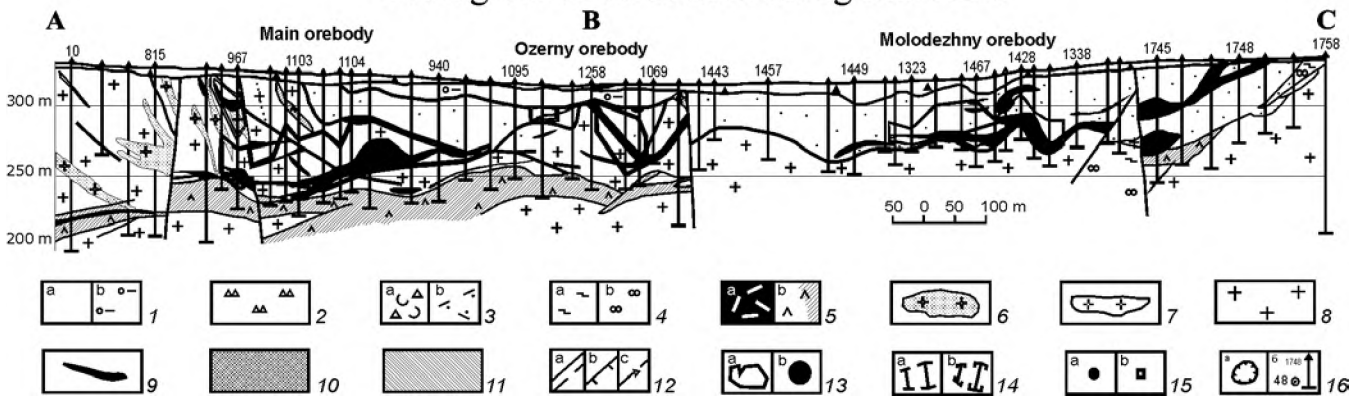


Fig. 4.3. Geologic map of the Pokrovka deposit and cross section, after Vasil'ev et al. (2000) and Khomich (1986, 2001).
 (1) Neogene and Quaternary sediments: (a) alluvial sand, pebbles, loam, clay, and rubble; (b) inequigranular sand and kaolinite-

framework, and dome-shaped inlier of Precambrian basement. The above-listed structural elements are typical of many gold ore fields in the Transbaikal region and Far East.

GEOLOGY OF THE POKROVKA DEPOSIT

Upper Jurassic siltstones and sandstones are unconformably overlain by a Cretaceous volcanosedimentary sequence. Late Jurassic–Early Cretaceous granitoids of the Upper Amur Complex, thick dikes of megaphyric granites of the Magdagachi Complex, younger dikes and larger subvolcanic intrusions of intermediate and acid compositions belonging to the Burinda and Kerak complexes occur at the deposit (Fig. 4.3).

The local Pokrovka paleovolcanic edifice rests upon the southeastern margin of the Sergeevsky granitoid pluton. Geophysical data indicate that the thickness of the pluton does not exceed 1.0–1.2 km. Lava flows and pyroclastic units, vent facies, extrusions, subvolcanic, cryptovolcanic, and hydrothermally altered rocks are recognized within the volcanic edifice. The total thickness of the volcanic pile is estimated from geophysical exploration and drilling results at no greater than 300–400 m (Fig. 4.4).

Three structural stages are recognized at the deposit. The upper stage consists of poorly cemented and virtually undeformed Paleogene and Neogene clastic sediments. The middle stage is composed of sedimentary and volcanic rocks of the Pokrovka and Kerak sequences (Fig. 4.4). This stage is separated from the overlying platform cover and underlying basement by structural and stratigraphic unconformities and zones of weathering. The lower stage, i.e., a basement (socle) of the paleovolcanic edifice is made up of Jurassic terrigenous rocks and granitoids of the Sergeevsky pluton.

Paleogene and Neogene sediments are postmineral. They contain not only fragments of underlying rocks and ore-bearing quartz, but also clastic gold.

Rocks of the Pokrovka Sequence with clasts and large blocks of ore-bearing chalcedony-like quartz are regarded as a special unit of the volcanic stage (Khomich, 2001). Volcanic rocks of the middle structural stage were affected by hydrothermal metasomatic alteration and underwent supergene weathering. Terrigenous and igneous rocks of the lower structural stage also experienced multifold metasomatic alteration.

Faults in the ore field are subdivided into pre-syn-, and postvolcanic and classified as pre-, syn-, and postmineral with respect to the ore formation. Normal, upthrow, and thrust faults are distinguished. The prevolcanic, steeply and gently dipping faults, diverse in orientation, often control the localization of dikes (granite porphyry with phenocrysts of variable size, spessartite, diorite porphyry, and dacite). The position of faults is predetermined in many respects by primary inhomogeneity of the Sergeevsky pluton, especially in its apical portion, where granite porphyry dikes with small phenocrysts occur. The lower limit of the dike belt coincides with a boundary between slightly porphyritic and equigranular granitoids. Synvolcanic fault zones are filled with dikes and subvolcanic intrusions comagmatic to the Burinda and Kera volcanics. Slip along these faults varies from few centimeters to few meters. The extended steeply dipping fault planes are accompanied by gouge and zones of clastic deformation, up to 5–10 m thick, as well as by slickensides and trails.

Postvolcanic faults are clearly expressed in the topography. They are interpreted from aerial photographs by linear and curvilinear streams, asymmetric valleys, escarpments, sinks, and are mapped by displacements of geologic boundaries. Gently dipping faults are commonly traced at the base of volcanic units and at contacts of sheetlike dacite and diorite porphyry subvolcanic intrusions. A number of gently dipping shear zones extend within the so-called Main dacite sill separating the slightly porphyritic and equigranular granitoids; similar shear zones are observed along the hanging and lying walls of the Main sill. As a

montmorillonite clay; (2) Upper Cretaceous (?) sedimentary breccia (fanglomerate), coarse, poorly cemented conglobreccia with rubblestone lenses; (3) Lower Cretaceous lavas and tuffs: (a) lithic tuff of dacitic composition, (b) andesitic, dacitic, and rhyodacitic lavas and lava breccias; (4) Jurassic terrigenous rocks (pre-volcanic basement): (a) mudstone, (b) polymictic sandstone; *large subvolcanic intrusions and dikes*: (5) dacite and granodiorite porphyry (a) in lateral vent of paleovolcano and (b) elsewhere, (6) granite porphyry with medium-sized and small phenocrysts, (7) megaphyric granite porphyry; (8) Late Jurassic–Early Cretaceous biotite granodiorite and granite of the Sergeevsky pluton (Upper Amur Complex); *veins and metasomatically altered rocks*: (9) quartz veins and vein zones, (10) zone of silicification and quartz veinlets, (11) talus with blocks of silicified rocks; (12) faults and fault zones: (a) steeply dipping including those overlapped by younger rocks, (b) gently dipping (thrust faults), (c) zones of brecciation, shearing, and mylonitization; (13) Au-bearing areas (a) and (b) gold occurrences; (14) placers suitable for mining (a) and (b) areas of most intense feeding of placers from bedrock and transitional sources; (15) location of samples from talus with high Au content (0.5 g/t and more) (a) and (b) samples with visible gold in heavy concentrates; (16) abandoned prospectors' pits and shaft sinks (a) and (b) some boreholes shown on the map and cross section and their numbers

rule, these zones are spatially related to aphyric dacite and to a phyrlic variety with small phenocrysts. However, they are also known at the contacts of the coarse-crystalline dacite with country granitoids. Most of the faults are premineral. Brecciation of veins and metasomatic bodies, cross-cutting quartz, quartz-car-

bonate, carbonate veins and veinlets composed of pre-, syn- and postore mineral assemblages are indications of synmineral displacements. Gaps in Au-bearing veins, fragments of quartz, carbonate, and quartz-sulfide veins embedded into the shear zones, and displacements of contacts, interlayers, and postmineral Late

System	Series	Sequence	Member	Unit	Thickness, m	LITHOLOGY	
C r e t a c e o u s	U p p e r	Sequence B (Pokrovka)	B - II	c		> 80	Yellow-brown and brown arkose sandstone, rubblestone, gritstone, fine-pebble conglomerate, and poorly cemented fine-clastic breccia
				b		> 80	Earthy gray, unsorted sandy, rubbish, and block (mainly granitic) deposits with interlayers of fine-grained bituminous sandstone
				a		> 80	Cherry-red, brick-red, and dirty greenish brown fanglomerates consisting of blocks and angular fragments composed of the Sergeevsky granitoids, granite porphyry, andesite, spessartite, and varicolored chalcedony-like quartz. Sandy and rubbish aggregate contains gold clasts. Cement is made up of limonitized clayey material. Interlayers of inequigranular sandstone, rubblestone, and gritstone are noticed
			B - I	c		> 60	Dark gray and brown-black lignites with conglobreccia, gritstone, and sandstone interlayers
				b		> 60	Gray, greenish gray, medium- and coarse-clastic conglobreccias consisting of angular clasts and blocks (up to 30 cm and more in size) of sandstone, siltstone, mudstone, granitoids, volcanosedimentary rocks, andesite dikes, diorite, granodiorite, granite porphyry dikes, and quartz veins; gritstone and sandstone interlayers are embedded into the conglobreccia
				a		> 60	Gray and dirty gray fine- and medium grained rubbish sandstones with carbonaceous interlayers and fine-clastic conglobreccia
				A - IV	b		> 50
	a		> 50		Brownish gray, ashy, light gray, and greenish gray massive (locally with flow banding) aphyric dacite and dacite porphyry with small plagioclase and biotite phenocrysts		
	A - III	b			80	Dark gray, ashy, and gray psammitic and psephitic lithic tuffs intercalating with inequigranular tuffaceous sandstone, gritstone, lithic and crystal tuffs. These rocks are replaced in the lateral direction by lava flows (aphyric and phyrlic andesites and dacite); size of phenocrysts increases toward the vent	
		a		80	Gray, dirty gray lithic tuffs of dacitic composition with light-colored fragments of volcanic rocks and granitoids (3-5, occasionally up to 10 cm in diameter), interlayers of psammitic tuff and tuffaceous sandstone. The clastic rocks are replaced in the lateral direction by crystal and lithic tuffs, flows of aphyric and phyrlic dacites colored in greenish gray, brownish-greenish gray, and brown tints		
	L o w e r	Sequence A (Kerak)	A - II	b		90	Intercalation of fine-grained massive and bedded tuffaceous sandstones, tuffites, psammitic and ash tuffs of brown, brownish gray, gray, dark gray, and black colors with lithic and crystal tuffs; amount of the latter increases toward the center of depression. Black rocks are enriched in coaly detritus
				a		90	Dirty greenish gray lithic tuffs and ignimbrites with fiamme composed of dark green volcanic glass (up to 10-15 mm across) and fragments of dacitic and granitic rocks, up to 3-5 cm in size. Thin (up to 0.5 m) interlayers of tuffaceous sandstone, bedded psammitic tuff, separate flows of brownish gray, dark dirty green, and dark ashy phyrlic dacites with small phenocrysts and aphyric dacites are observed. Dacites are massive, vaguely banded, and fractured
			A - I	b		30	Gray, dirty gray, greenish gray, and dark gray fine- and medium-grained massive and bedded tuffaceous sandstones, tuffites, psammitic lithic tuff with interlayers of psephitic tuff and tuffaceous gritstone
				a		30	Greenish gray, greenish ashy, medium and coarse tuffaceous breccias, tuffaceous conglomerates, and psephitic lithic tuff

Fig. 4.4. Stratigraphic column of the Pokrovka paleovolcanic depression, after Khomich (2001)

Cretaceous (?) sediments serve as additional evidence for postmineral movements.

The paleovolcanic edifice is a pivotal element in the structure of the Pokrovka ore field. Remnants of the paleovolcano, which are retained until now, include (1) funnel-shaped lateral vent, up to 600 m in diameter, filled with megaphyric dacite and granodiorite porphyry (Fig. 4.3), (2) related extrusions, (3) lava flows and pyroclastic units, (4) thin volcanic veneer at depression margins, as well as (5) dikes of aphyric dacite and diverse porphyries that cut the granitoid pluton and its framework (Fig. 4.5).

METASOMATIC ALTERATION AND MINERAL COMPOSITION OF ORE

The main ore-bearing areas (I–III) of the Pokrovka ore field are hosted in Late Jurassic–Early Cretaceous granitoids and Lower Cretaceous dacitic lava and pyroclastic rocks near the vent of the paleovolcano (Fig. 4.3). Almost all ore-bearing lodes in areas I and II reside in a granitoid sheet sandwiched between the roof of the Main dacite sill (below) and the sole of the volcanic pile (above). In area I, the mineralized

zones occur close to the sill roof while in area II they are localized at a greater distance. The ore zone in area III is hosted in metasomatically altered dacitic pyroclastic rocks.

Hydrothermal metasomatic alteration markedly modified the appearance of rocks at the base of paleovolcanic edifice and in the Lower Cretaceous section composed of dacitic and less silicic lavas and tuffs. Various facies of propylitic and argillic alteration, feldspathization, carbonatization, silicification, and sulfide mineralization are established in granitoids and volcanic rocks (Fig. 4.6). Weathering and rock disintegration under supergene conditions enhanced the hypogene argillic alteration within the uppermost interval of 40–50 m. No unaltered rocks were found in the ore-bearing areas.

The Pokrovka deposit differs from other epithermal Au–Ag deposits in the east of Russia in the extensive development of the hydromica-kaolinite zone of weathering, up to 30–50 m thick and with 50–55% of clay minerals. Gossans enriched by 20–25% in Au and containing free gold of a high fineness (850–900), sulfide impregnations, and gypsum-bearing units occur within the zone of weathering.

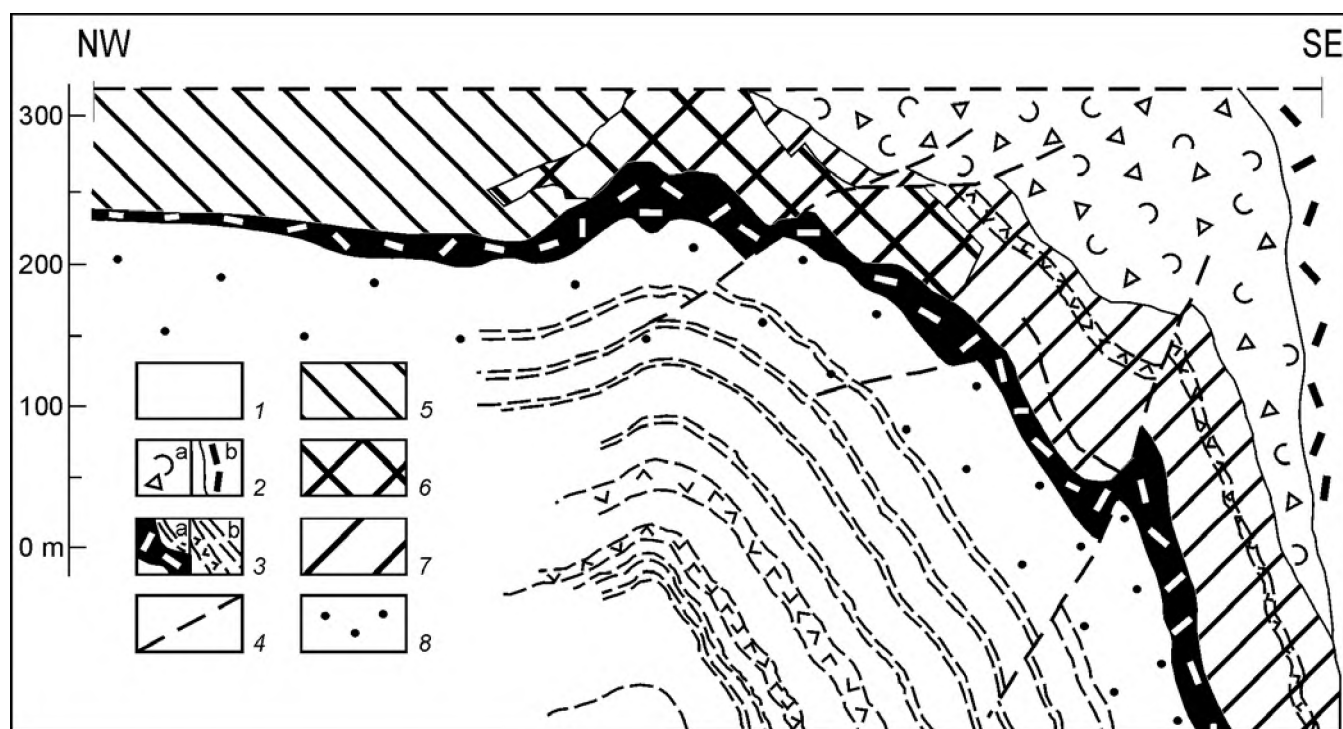


Fig. 4.5. A generalized section across central part of the Pokrovka ore-magmatic system.

(1) Late Jurassic–Early Cretaceous granitoids of the Sergeevsky pluton; (2) Lower Cretaceous volcanics: (a) near-vent facies of the Pokrovka paleovolcano, (b) ethmolith of quartz diorite porphyry and dacite–granodiorite porphyry filling the vent; (3) subvolcanic intrusions of andesitic and dacitic compositions: (a) Main sill of dacite–granodiorite porphyry that controls the lower boundary of gold mineralization and its offsets, (b) sill-like intrusions of andesite, spessartite, microdiorite, and diorite porphyry, variable in thickness; (4) faults; areas of Au–Ag mineralization: (5) subeconomic, (6) economic, (7) poorly explored; (8) subore zone of feldspathized granitoids

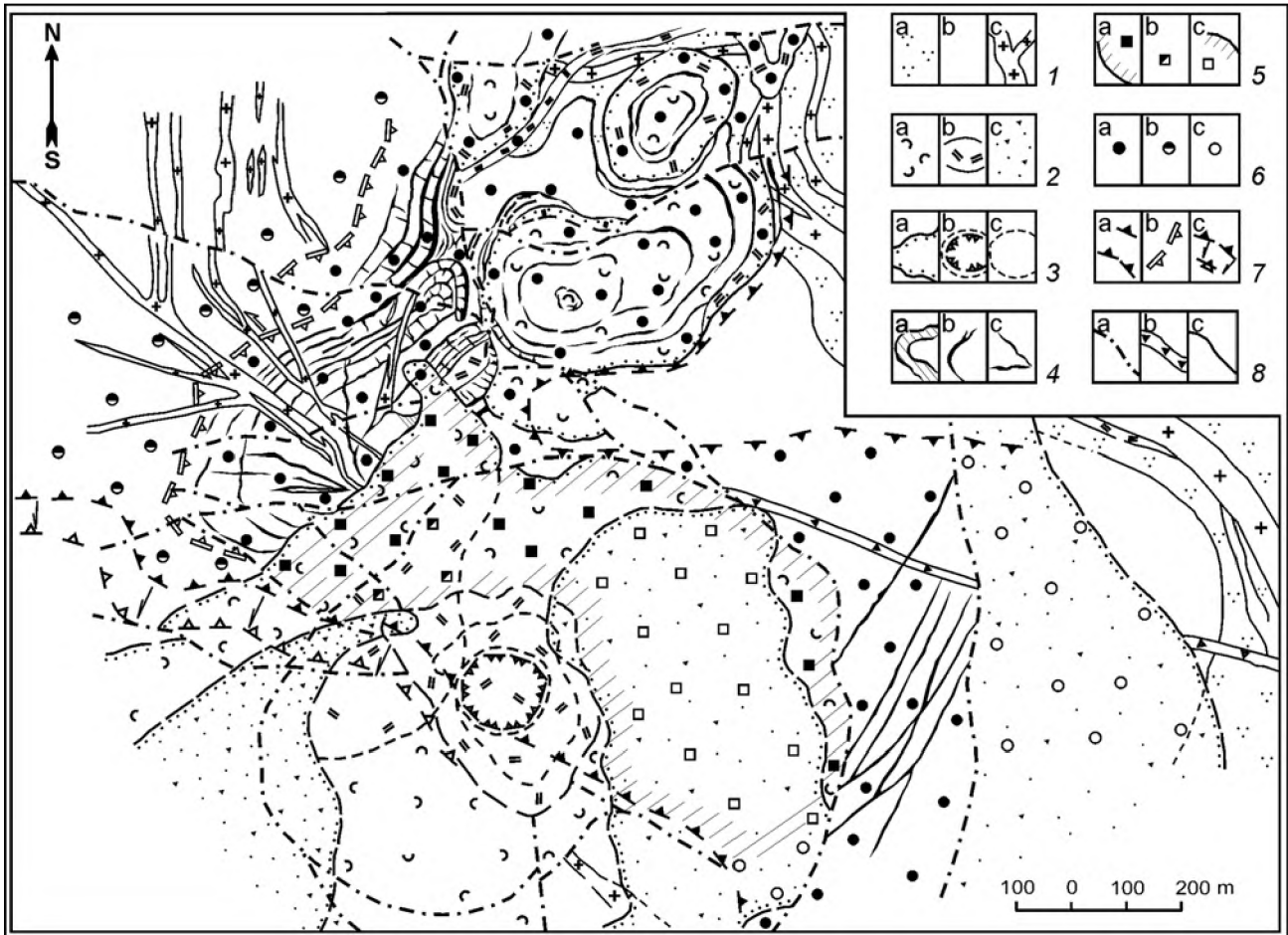


Fig. 4.6. Schematic map of hydrothermal alteration at the Pokrovka deposit, after Khomich et al. (1978).

(1) basement of the paleovolcanic edifice: (a) terrigenous rocks (mudstone, siltstone, sandstone), (b) granodiorite and granite, rocks hosting the ore mineralization, (c) granite porphyry dikes; (2) subvolcanic intrusions, extrusions, volcanic and sedimentary rocks: (a) stratified volcanic rocks of dacitic composition, unspecified; (b) ethmolith, sills of dacite or granodiorite porphyry, and related lava flows; (c) sedimentary breccia, conglobreccia, rubblestone with fragments of ore-bearing quartz; (3) geological boundaries: (a) contour of stratified volcanic rocks, (b) volcanic vent projected on the present-day surface, (c) facies boundaries in subvolcanic intrusions and extrusive bodies; (4) veins and metasomatic rocks: (a) zones of metasomatic silicification, (b) large gently dipping quartz veins, (c) steeply dipping veins and veinlet zones; (5) zone of sulfide mineralization: (a) beneath young loose sediments, (b) beneath the lava tongue extending from dacite–granodiorite porphyry extrusion, (c) buried beneath postmineral sedimentary rocks; (6) zone of argillic alteration and silicification: (a) beneath young loose sediments, (b) partly buried beneath insignificantly altered rocks, (c) buried beneath postmineral sedimentary rocks; (7) contours: (a) zone of intense feldspathization, argillic alteration, and silicification, (b) hidden part of this zone, (c) zone of slight alteration in the southwestern ore field (arrows indicate the direction of alteration zone plunging); (8) major faults (a), steeply dipping linear bodies of explosion breccia (b), boundaries of geological bodies (c)

The pre- and synmineral metasomatic alterations are separated by tectonic displacements and formation of polymict and monomict explosion breccias. Fragments in breccia are composed of granitoid rocks, mudstone, and shale carried up from the lower structural stage. The aggregate and cement consists of finely ground, partly bituminous black material with pyrite, marcasite, and melnikovite-pyrite disseminations. Linear bodies of the explosion breccia are often juxtaposed with late quartz veins and vein suites. The postmineral breccia contains fragments of quartz veins cemented with quartz-hydromica material.

Ore formation was accompanied by development of contrasting primary geochemical haloes of Hg, Ag, Sb, As, Au, Zn, Pb, Cu, W, Mo, Sn, and Bi (elements are listed in order they occupy in zoning). The contour line of 0.3 m/g Au depicts a continuous ore zone with particular economic orebodies suitable for mining. They have no distinct geologic boundaries and are selected only from sampling as spots of disseminated, stringer-disseminated, veinlet, and vein Au–Ag mineralization hosted in silicified and argillized rocks.

The mineral composition of the ore is rather simple (Novikov, 1983). Quartz (50–95%), carbonates

(2–5%), hydromica (up to 5–12%), adularia (up to 3–5%), kaolinite (as much as 7%), sericite, and chlorite are major gangue minerals. The quantity of ore minerals varies from 0.5 to 3.5% (no more than 1%, on the average). Pyrite, marcasite, and arsenopyrite are most abundant; chalcopyrite, sphalerite, galena, pyrrhotite, hematite, magnetite, freibergite, argentite, molybdenite, stibnite, and cinnabar are less frequent; proustite, pyrargyrite, polybasite, native gold, silver, and copper are much less abundant. Pyrite is slightly auriferous; As, Cu, and Pb are detected as impurities. Magnetite, sphalerite, galena, as well as grains of chalcopyrite, bornite, enargite, aikinite, and tennantite, up to 0.1 μm in size, were detected in the early quartz-galena-sphalerite and quartz-carbonate-polysulfide assemblages. Sphalerite with chalcopyrite emulsion prevails over galena that contains rounded freibergite grains, up to 50 μm in diameter. According to the spectroscopy results, sphalerite contains Ag, Cd (>0.1%), Sb (up to 0.1%), Cu (up to 0.03%), Mn (0.001%), Bi (0.003%) while Ag (up to 0.3%), Bi, and Sb (up to 0.1%) were detected in galena. Native gold is finely dispersed, mainly as grains, 0.005–0.1 mm (occasionally up to 0.15 mm) in size. The fineness of gold is low (625–735, largely 680–690 units). Spongy, mossy, flaky, rounded, and tear-shaped gold grains are

typical. The rounded and tear-shaped gold grains are more abundant at depth than other morphological varieties. Larger (up to 0.35 mm) gold segregations with fineness of 650–675 occur in association with silver sulfosalts. The fineness of gold from the late quartz-carbonate veinlets increases by 40–50%. Trace elements in gold include Fe (0.009–0.051%), Sb (90.002–0.005%), Mn (0.0003–0.0004%), Cu (0.0006%), Cr (0.0007%), Pb (0.005%), and Hg (0.001%). Silver as a concomitant component (Au/Ag = 1:1–2:3) concentrates in sulfides, sulfosalts, and gold. Pt (0.25–1.0 g/t), Os (0.031–0.05 g/t), and Pd (0.044–0.071 g/t) were detected in group samples containing 5.0 g/t Au and 2.5–11.0 g/t Ag; Ir, Rh, and Ru were noticed in a few samples (Stepanov and Moiseenko, 1993; Stepanov, 2000).

OREBODY MORPHOLOGY

Several veins of various thickness and orientation are localized in each area as elements of gently dipping vein and metasomatic zones, occasionally reaching 40–60 m in thickness. In area I, the largest ore-bearing zone extends close to the hanging wall of the Main dacite sill (Fig. 4.7). Veins, attaining 4–5 m and more in thickness, are known from the Main,

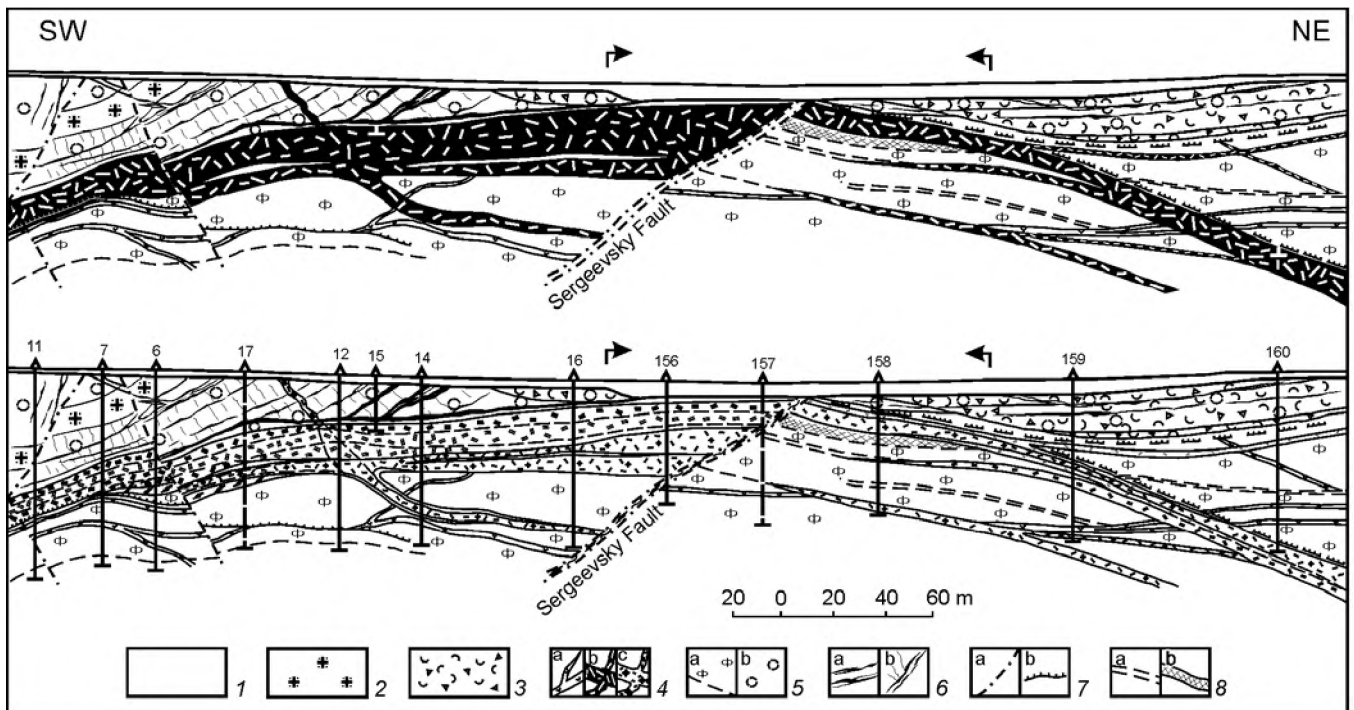


Fig. 4.7. Zoning of hydrothermal alteration in the central part of the deposit (cross section). (1) granitoids of the Sergeevsky pluton, unspecified; (2) granite porphyry dikes with small phenocrysts; (3) volcanic rocks of dacitic and rhyodacitic composition; (4) sill-like bodies: (a) andesite and microdiorite, (b) dacite and granodiorite porphyry on the upper section, (c) the same on the lower section; (5) zones of metasomatic alteration: (a) feldspathization, (b) argillic alteration and silicification; (6) ore-bearing quartz bodies and veinlet zones: (a) gently and (b) steeply dipping, (7) zones of (a) fracturing and (b) brecciation. Arrows show the place where the roof of the Main dacite sill is contiguous to the bottom of volcanics

Zeya, and Ozerny orebodies (Fig. 4.3) where they are surrounded by suites of nearly parallel, closely spaced, and en echelon arranged small lenticular auxiliary veins, veinlets, and spots of metasomatic silicification. The orebodies extend for hundreds of meters along the strike. Veins hosted in transverse and longitudinal steeply dipping fault zones are localized at a greater distance from the Main sill and make up divergent swarms with counter dipping.

CHARACTERISTICS OF INJECTION BODIES CONTROLLING THE ORE LOCALIZATION

The Pokrovka deposit is situated in the marginal part of the Sergeevsky granitoid pluton and near the vent of a younger paleovolcano. This geological setting played an important role in the spatial distribution and morphology of the vein-metasomatic orebodies.

The marginal part of the pluton was initially inhomogeneous: from the bottom to the top of 300–400-m interval, the porphyritic biotite granite gives way to slightly porphyritic and then to equigranular massive granite and granodiorite occasionally passing into quartz diorite. The rock structure changes in the same

direction from massive to vaguely and distinctly banded. In the near-contact zone, dark-colored minerals and feldspars reveal a planar orientation. The steepest banding (70–80°) is observed at the contact with Jurassic sedimentary rocks and gradually becomes more gentle (50–40°) toward the pluton interior, 500–800 m apart from the outer contact. The banding orientation and character of the gravity field confirm the dome-shaped morphology of the Sergeevsky pluton roof in the Pokrovka area. In the eastern part of the ore field, roof pendants composed of Jurassic mudstone and siltstone, 5–40 m thick, occur beneath the volcanics (Fig. 4.3). The internal heterogeneity of the granitoid pluton is emphasized by the distribution of basic and intermediate dikes at a greater depth in comparison with dacitic subvolcanic intrusions. Granite porphyry dikes with small phenocrysts are localized still higher. Signs of heterogeneity and banding were observed not only in the Sergeevsky pluton, but also in large sill-like bodies of dacite–granodiorite porphyry and in granite porphyry.

All explored Au-bearing hydrothermal metasomatic orebodies in the central part of deposit are localized above the Main dacite sill. Its morphology indicates that a hidden dome exists in this area (Fig. 4.8).

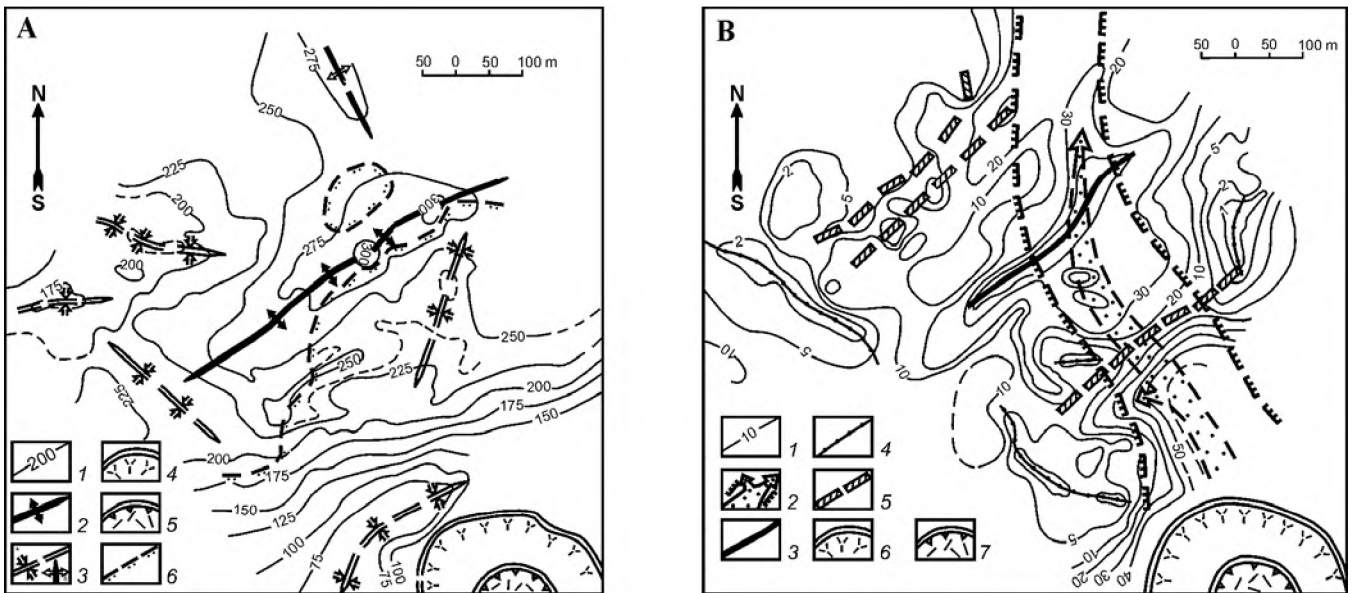


Fig. 4.8. (A) Contour lines of the Main sill roof; (B) Isopachs of the Main dacite–granodiorite porphyry sill controlling the lower boundary of the Au–Ag mineralization.

Map A. (1) contour lines of the sill roof (contour interval is 25 m); (2) axis of the hidden dome; (3) axes of local (a) negative and (b) positive structures on the dome limbs; (4) zone of abrupt twisting of sill near the vent; (5) projection of paleovolcanic vent (stem of feeder); (6) contour of Lower Cretaceous volcanic rocks.

Map B. (1) isopachs (contour intervals are 1, 2, 5, and 10 m); (2) inferred position of magma conduit and its offsets during emplacement of dacitic melt; (3) axis of sill bulge in the core of hidden dome; (4) axes of sill pinches; (5) gradient zones (intervals of local complication of sill morphology); (6) zone of abrupt twisting of sill near the vent; (7) projection of paleovolcanic vent (stem of feeder)

The Main sill reveals a complex internal structure. Thicker segments of the sill contain flat granitoid lenses, up to 5 m thick, extending for tens and occasionally for hundreds of meters. Several rhythms are recognized in these segments; each of them is characterized by grading upsection of granodiorite porphyry with large and medium-sized phenocrysts into dacite with small phenocrysts and eventually into aphyric dacite. The thickest (40–45 m and more) bulge consists of three rhythms. In segments where the sill thickness decreases down to 20 m, only two rhythms are observed. In segments, less than 10 m thick, only dacite with small phenocrysts and aphyric varieties occur. Some rhythms exhibit a symmetric zoning. The central zone is composed of granodiorite and granite porphyries with large (~5 mm) quartz, feldspar, and biotite phenocrysts and the outer zones consist of aphyric dacite, sporadically with fine flow banding. Nearly conformable low-angle zones of boudinage, shearing, and mylonitization are traced along boundaries between aphyric and aphyric dacites and between dacite and granitoid lenses incorporated into the Main sill. The lateral displacement along these zones is estimated as far as 40–50 m.

At the northwestern, northern, and southeastern flanks of the Main sill, where its thickness markedly decreases, it is overlain by nearly concordant bodies of explosion hydrothermal breccia. Thin segments of the sill (1 m and less) commonly reveal a linear orientation (Figs. 4.8A and 4.8B). The general decrease in the thickness of Main sill and its offsets away from the feeding conduit is occasionally distorted, e.g., near some large faults the sill is split into several nearly parallel offsets separated by wedge-shaped granitoid screens. The rhythmic structure of the thickest portion of the Main sill serves as evidence for multifold injections of melt along gently dipping channels. The multifold injections increased the total thickness of the Main sill and accentuated a hidden dome (Fig. 4.8A).

LOCALIZATION OF GOLD AND SILVER MINERALIZATION

The lenticular (with bulges and pinches) mineralized granitoid sheet in area I is localized between the sole of the volcanic pile and the roof of the Main dacite sill (Fig. 4.9). Economic ore bodies and zones extend for a distance of 400–600 m to the northwest and southwest of a line marking the thinnest granitoid sheet. No economic orebodies were penetrated by boreholes southeast of this line. In the pay zone, the

thickness of the lenticular granitoid sheet varies from 5 to 150 m. In segments more than 150 m thick, the number of Au-bearing orebodies is drastically reduced. Thus, the economic mineralization is concentrated within an area with rather definite geologic boundaries. The lower boundary coincides with the roof of the Main dacite sill, and is traced along the base of the volcanic pile. The eastern and southeastern boundaries are controlled by the shortest distance between the sill roof and the base of volcanics. The southern and southwestern boundaries of economic ore mineralization remain vague. We refer these boundaries to the line marking the greatest thickness of the granitoid lens (Fig. 4.9). The western, northwestern, and northern boundaries of the economic portion of the deposit are traced as gradient zones characterized by variable thickness and morphology of the Main sill with synforms at dome limbs and the thinnest segments of the sill (1 m and less, see Fig. 4.10).

It should be noted that the morphology of Au-bearing orebodies markedly changes where the thickness of the mineralized granitoid sheet attains a minimum. Gently dipping orebodies are prevalent here. Where the granitoid sheet pinches out and the roof of the Main sill is contiguous to the base of volcanics, the bodies of stringer-disseminated ore become concordant to the stratification of the volcanic sequence and are controlled by inter- and intraformational crush belts, especially typical of area III (Fig. 4.11).

The economic portion of the vein and metasomatic zone in area II is also hosted in granitoids and spatially related to the dacite extrusion or subvolcanic intrusion, similar to the Main sill from area I in many respects. However, because the thickness of granitoid sheet here exceeds 150 m, the ore mineralization is dispersed throughout a large body of host rocks and therefore is low-grade.

In conclusion, we once again would like to draw attention to the ore-controlling role of dacite and granodiorite porphyry subvolcanic bodies and the implication for interpretation of the ore field structure. The Main sill controls not only the lower boundary of ore mineralization. Up to 85% of identified resources at the Pokrovka deposit are localized within the dome above the Main sill. The economic ore mineralization is localized above bulges of subvolcanic intrusions and is limited in extent by gradient zones of variable thickness. The gold mineralization is virtually lacking close to the thinnest segments of the Main sill or where the sill completely pinches out (Fig. 4.10).

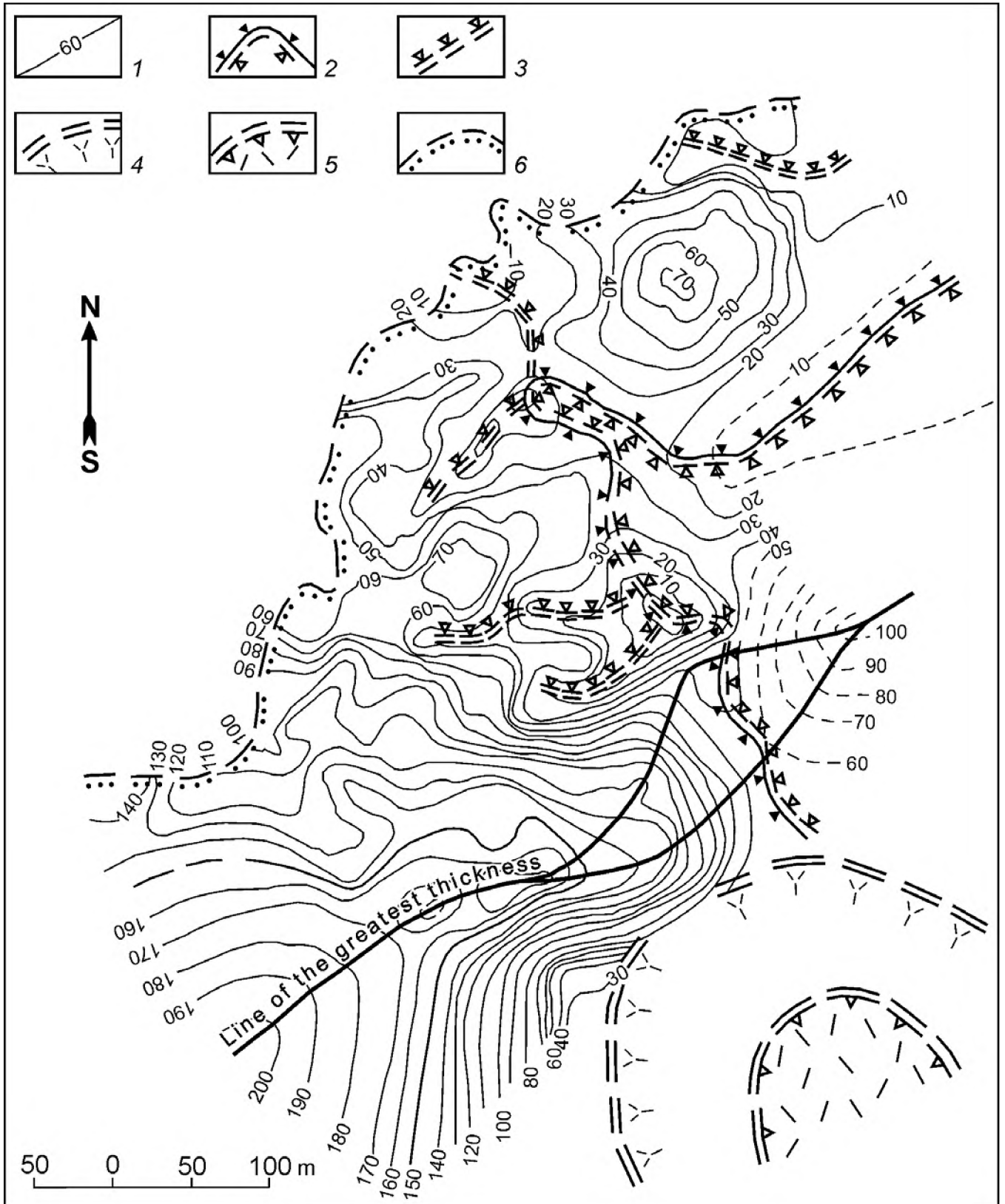


Fig. 4.9. Isopachs of Sergeevsky granitoid sheet, a host of the ore mineralization (Pokrovka-I area).
 (1) isopachs (contour interval is 10 m); (2) zone (line) of the shortest distance between the Main sill roof and the sole of volcanic pile; (3) local segments the shortest distance between the Main sill roof and the lower boundary of volcanic pile (local "biclines" of special type); (4) zone of abrupt twisting of the Main sill; (5) projection of paleovolcanic vent (stem of feeder); (6) present-day limits of volcanics filling the local depression

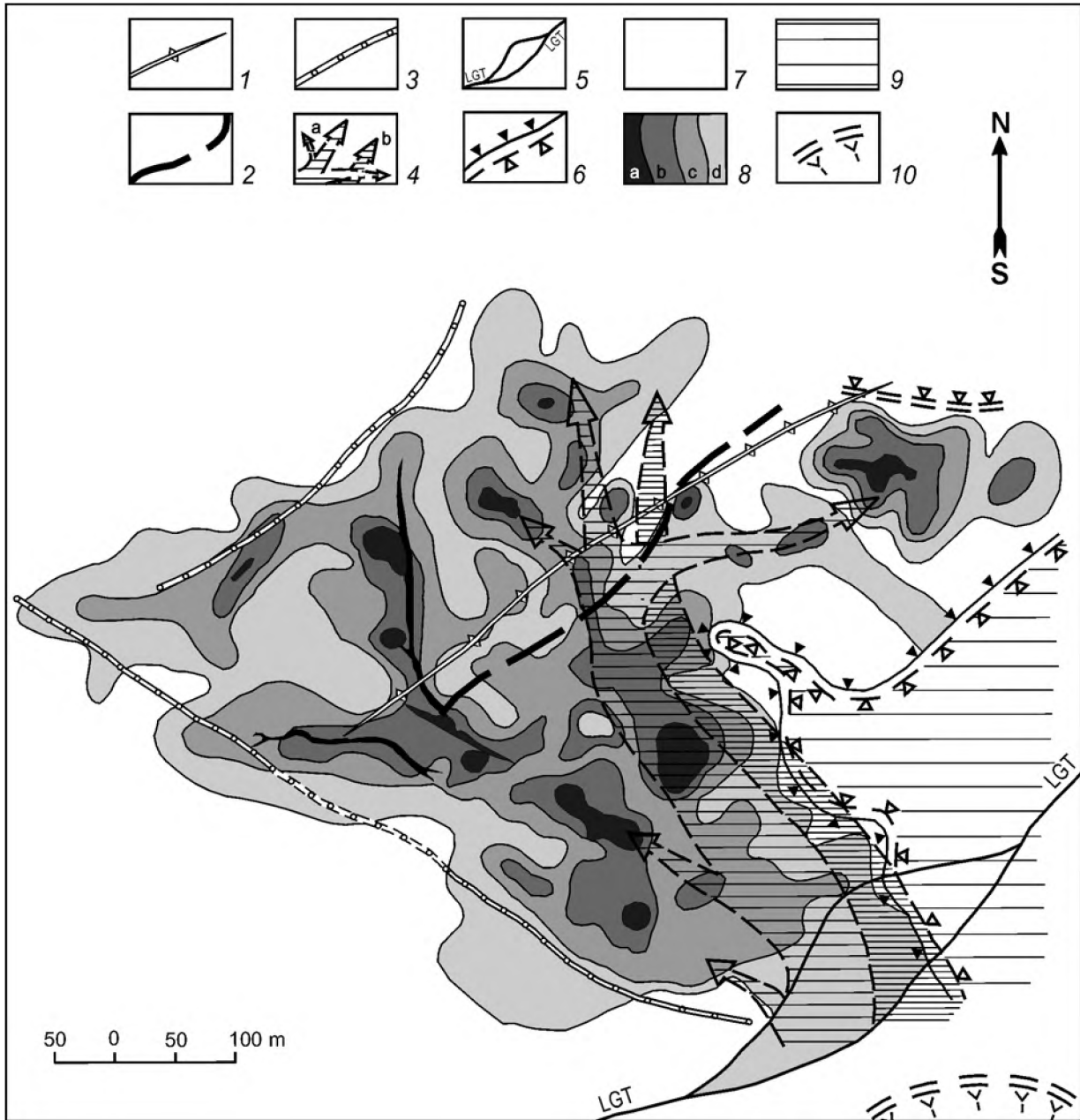


Fig. 4.10. Generalized plan of injection structures and gold mineralization at the Pokrovka deposit, after Khomich (1990, 2001). Axes of major injection structures: (1) hidden dome, (2) bulge of the Main sill in the dome core, (3) pinches of the Main dacite–granodiorite porphyry sill; (4) inferred conduits of melts and fluids; (a) conduit that fed the Main sill, (b) conduit for ore-forming postmagmatic hydrothermal solutions in the Pokrovka-I area; (5) line of greatest thickness (LGT) in granitoid lense that hosts ore mineralization; (6) line (zone) of the shortest distance between the Main sill roof and lower boundary of volcanic pile (see Fig. 4.9); (7) granitoids of the Sergeevsky pluton; (8) ore zone at Pokrovka deposit projected on the horizontal plane; contour lines of productivity: (a) very high, (b) high, (c) medium, (d) low; (9) part of lenticular sheet of the Sergeevsky granitoids (beyond the line of shortest distance between the Main sill roof and the lower boundary of volcanic pile) devoid of economic Au mineralization; (10) zone of abrupt twisting of Main sill near the vent

MINING OF THE DEPOSIT

Since 1994, the Pokrovka Mine Joint-Stock Company (Chairman of Board of Directors P.A. Maslovsky, Director General S.E. Yermolenko, Chief Engineer V.N. Alekseev, and Chief Geologist N.G.

Vlasov) is the owner of the license for mining activity at the Pokrovka gold deposit, prospecting and geological exploration in the vicinity of this deposit (Fig. 4.12). The pilot open-pit mining started in 1995. All-year-round recovery of gold from oxidized ore was initiated in 1999 using heap leaching with cyanide-

THE POKROVKA EPITHERMAL GOLD DEPOSIT

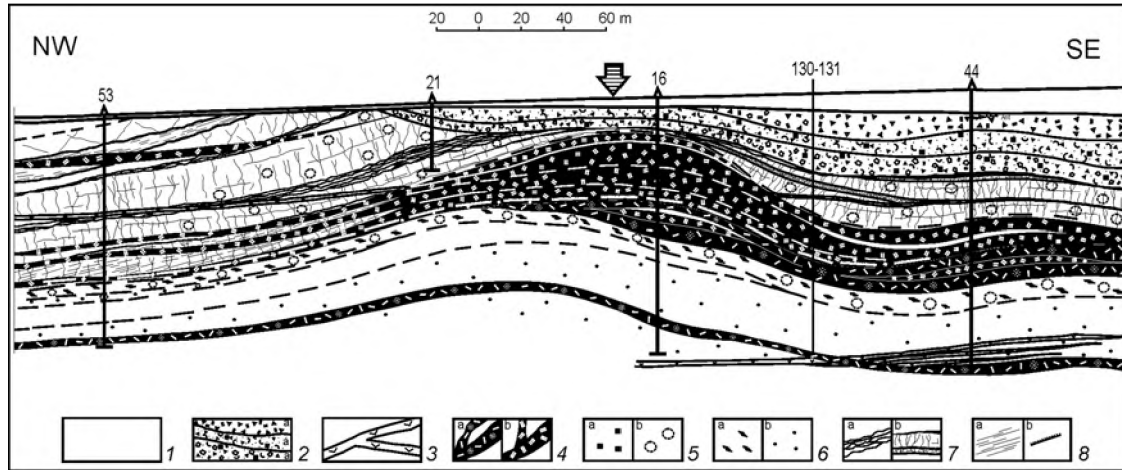


Fig. 4.11. Section showing the difference in the rate of ore mineralization on slopes of the hidden dome on opposite sides of the zone with the shortest distance between the Main sill roof and the bottom of the volcanic pile.
 (1) granitoids of the Sergeevsky pluton; (2) volcanic rocks; (3) andesite and microdiorite dikes; (4) dacite and granodiorite porphyry sills including the Main sill that controls the lower boundary of gold mineralization and its offsets: (a) granodiorite and dacite porphyries; (b) dacite porphyry with small phenocrysts and aphyric dacite; metasomatic alteration: (5) supraore zone of (a) sulfide mineralization, (b) ore-bearing zone of argillic alteration, including replacement by hydromica, and silicification; (6) subore zone of (a) carbonatization and (b) feldspathization of granitoids; (7) ore-bearing veins and zones: (a) closely spaced gently dipping quartz veins (vein zone), (b) systems of steeply dipping ladder veins between the gently dipping quartz bodies; (8) faults of various morphology: (a) fracture zones, (b) low-angle fault planes. The zone of the shortest distance between the Main sill roof and the sole of volcanic pile is shown by arrow

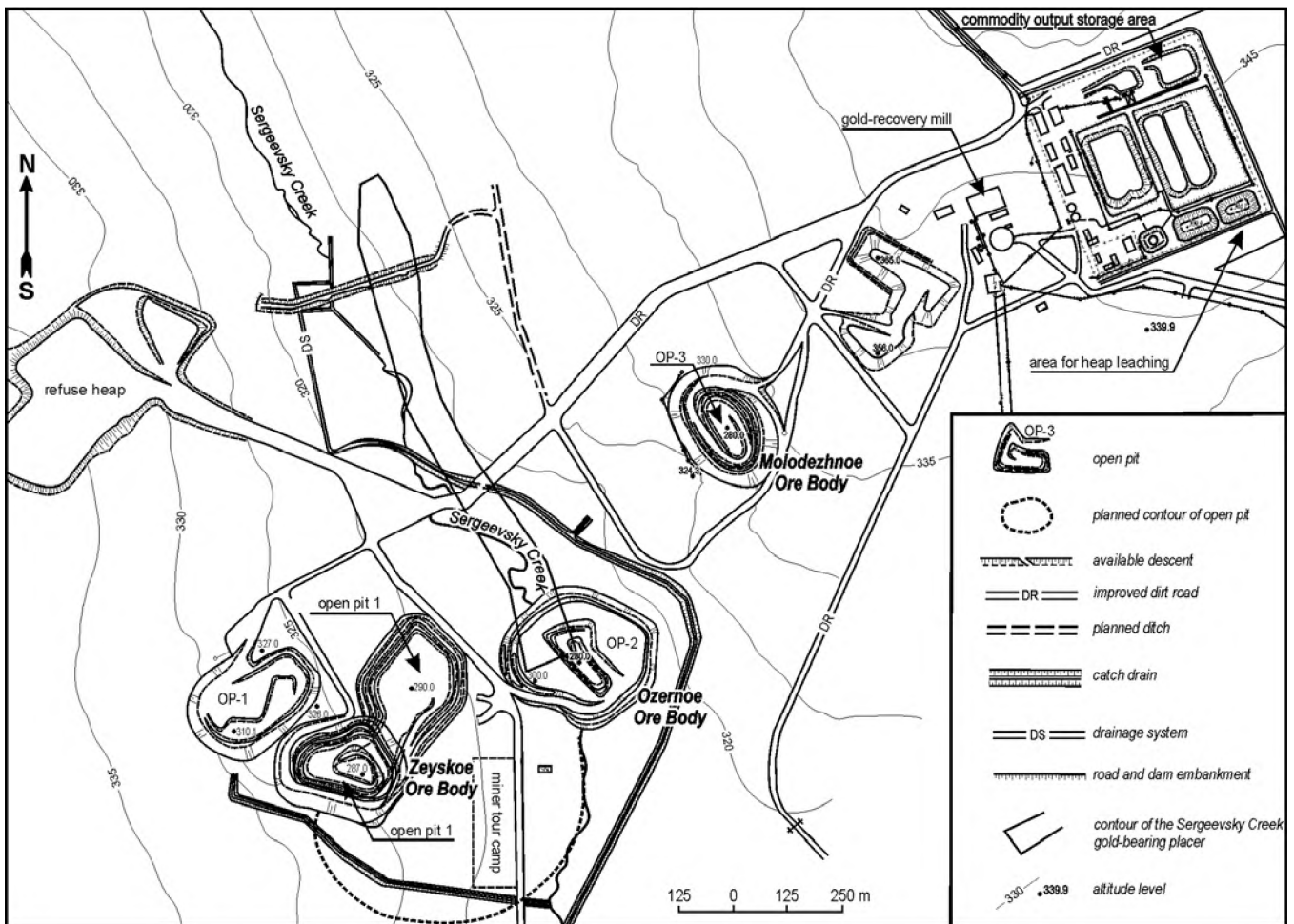


Fig. 4.12. Sketch of the Pokrovka Mine Joint-Stock Company engineering structure within the Pokrovka deposit

bearing solutions and their subsequent processing on a Meril Crowe hydrometallurgical plant. 482 and 693 kt ore were processed and 1600 kg and 2551.5 kg Au were recovered in 2000 and 2001, respectively. The hydrometallurgical plant (HMP) was put into operation in 2002. The ore taken from the open pit is transported to HMW with dump trucks of high capacity.

REFERENCES

- Dementienko, A.I. and Vlasov, N.G., *Pokrovskoe zolotorudnoe mestorozhdenie* (The Pokrovka gold deposit), Booklet for excursion, International Scientific Conference: Genesis of ore deposits and methods of noble metal mining, Blagoveshchensk: Amur Complex Research Institute, 2000, 13 p.*
- Geologicheskaya karta Khabarovskogo kraia i Amurskoi oblasti, masshtab 1 : 500 000. Ob'yasnitel'naya zapiska* (Geological map of the Khabarovsk and Amur regions at a scale of 1:500,000. Explanatory notes), Khabarovsk: PGO Dal'geologiya, 1991, 51 p.*
- Khomich, V.G., Geology and localization of ore mineralization in a local volcanotectonic structure of the Upper Amur region, in: *Struktury rudnykh polei i mestorozhdenii vulkanicheskikh poyasov* (Structures of ore fields and deposits in volcanic belts), Vladivostok: Far East Scientific Center, Academy of Sciences of the USSR, 1986, pp. 118–136.*
- Khomich, V.G., Control of hypabyssal ore mineralization by injection structures, *Dokl. Akad. Nauk SSSR*, 1990, vol. 315, no. 3, pp. 694–699.*
- Khomich, V.G., The Pokrovka gold deposit (geology and ore localization), in: *Rudnye mestorozhdeniya kontinental'nykh okrain* (Ore deposits at continental margins), vol. 2, no. 2, Vladivostok: Dal'nauka, 2001, pp. 284–321.*
- Khomich, V.G., Vanenko, V.N., Sorokin, V.P., et al., Hydrothermal metasomatic altered rocks and explosion breccia at the Pokrovka gold deposit, in *Novye dannye o mineral'no-syr'evykh resursakh tsentral'noi chasti zony BAM* (New data on mineral resources of the central Amur-Baikal Railway Zone), Blagoveshchensk: Far East Scientific Center, Academy of Sciences of the USSR, 1978, pp. 119–128.*
- Novikov, V.P., Mineral composition of ore from a near-surface gold deposit in the Amur region, in: *Mineral'nye tipy rudnykh mestorozhdenii v vulkanogennykh poyasakh i zonakh aktivizatsii Severo-Vostoka Azii* (Mineral types of ore deposits in volcanic belts and reactivation zones of the northeastern Asia), Vladivostok: Far East Scientific Center, Academy of Sciences of the USSR, 1983, pp. 170–175.*
- Stepanov, V.A., *Geologiya zolota, serebra i rtuti* (Geology of gold, silver, and mercury), Pt. 2, Vladivostok: Dal'nauka, 2000, 160 p.*
- Stepanov, V.A. and Moiseenko, V.G., *Geokhimiya zolota, serebra i rtuti* (Geochemistry of gold, silver, and mercury), Pt. 2, Vladivostok: Dal'nauka, 1993, 228 p.*
- Vasil'ev, I.A., Kapanin, V.P., Kovtonyuk, G.P., et al., *Mineral'no-syr'evaya baza Amurskoi oblasti na rubezhe vekov* (Mineral potential of the Amur region from XX to XXI century), Blagoveshchensk, 2000, 168 p.

* In Russian.



THE ARMINSKY ORE DISTRICT

V. I. Gvozdev

Far East Geological Institute (FEGI), Far East Branch, Russian Academy of Sciences, Vladivostok

HISTORY OF DEVELOPMENT

Intensive geological exploration of the Arminsky ore district in northern Primorye (see Preface) started in the early 1950s (*Olovorudnye...*, 1986). Several Sn-W and W deposits including Tigrinoe, Zabytoe, Rudnoe, Zimnee, etc. were discovered here in the 1950s as a result of geological mapping and prospecting at a scale of 1:50,000. The large Vostok-2 skarn tungsten deposit was discovered in 1961. The exploration of this deposit was completed by 1965; identified resources were estimated as more than 100 kt WO_3 . The first stage of the integrated mining and concentrating works was started in 1966. The open pit and concentrating mill were put into operation in 1977. The second stage of the integrated works was put into operation in 1984 and provided annual mining and processing of 350 kt of ore with 1.65% WO_3 , 0.65% Cu, and 3% P (Khanchuk et al., 1995).

The Joint Stock Company Primorsky Ore-concentrating Group of Mines, which was set up in 1993 (<http://www/fegi.ru/primorye/mining/gok2.htm>), currently produces scheelite and copper concentrates. The upper portion of the deposit (900-720 m levels) was mined in an open-pit from 1969-1987. The depth interval between 720 and 560 m was mined out from adits. The underground mining of the lower levels (560-360 m) continues from a shaft. The tungsten concentrate is exported to Japan, United States, Australia, and other countries.

The exploration of the Zabytoe and Tigrinoe deposits was carried out in the 1980-1990s.

GENERAL GEOLOGY OF THE ORE DISTRICT

The Arminsky ore district (AOD) is situated in the northern Primorye within the Central Sikhote-Alin Fold belt (see Preface). According to modern interpretation (Khanchuk et al., 1995), AOD covers fragments of the Samarka and Zhuravlevka terranes (Fig. 5.1).

The Samarka Terrane consists of turbidite and chaotic (olistostrome) sequences, several thousand meters thick, with genetically heterogeneous and diachronous inclusions, largely of paleoceanic origin (Devonian ophiolites, Upper Paleozoic and Triassic cherts, limestones, and basalts) embedded therein. Middle Jurassic (Calloviaan)-Early Cretaceous radiolarians were found in the turbidites and the mudstone matrix of mixtites. The normally stratified flysch members without olistostromes occur in the upper part of the Samarka Terrane section, about 1500 m in total thickness (Fig. 5.2).

The Zhuravlevka Terrane is a turbidite basin localized at the transform continental margin and composed of Lower Cretaceous terrigenous rocks, more than 10,000 m thick. Siltstone and mudstone with olistostrome units (exotic blocks of limestone, interlayers of intraplate high-Ti picrites and basalts) are predominant in the lower (Berriasian-Valanginian) part of the section. The upper (Hauterivian-Albian) part largely consists of sandstones with numerous units of two- and three-component flysch (Fig. 5.2). All rocks were deformed into NE folds in the late Albian. The Central Sikhote-Alin and Tigrinaya River faults serve as terrane boundaries.

Plutonic rocks in the northwestern Arminsky ore district, which will be visited during the excursion, are related to the Dalnensky, or Tatibi intrusive complex of Albian-Cenomanian age (Ivanova, 1975; Stepanov, 1977; Levashev et al., 1991; Khanchuk et al., 1995; Khetchikov et al., 1996, 1997; Rub et al., 1982;

Krymsky et al., 1997, 1998). Plutons were emplaced into the country rocks of the Samarka and Zhuravlevka terranes close to the Central Sikhote-Alin Fault. The Dalnensky Complex comprises a series of mainly hypabyssal intrusions: (1) amphibole-biotite monzodiorite, granodiorite, and adamellite (Dalnensky pluton and marginal facies of the Biserny pluton dated as 128 ± 16 Ma), (2) amphibole-biotite and biotite granites of the Central stock at the Vostok-2 deposit, 111 ± 9 Ma, and (3) biotite-bearing leucogranite making up the main intrusive phase of the Biserny pluton, 98 ± 15 Ma. Sodic-potassic and potassic granitic rocks contain garnet as a typical mineral. Their geochemical and mineralogical signatures fit I-granites of ilmenite series, or granites of transitional I-S type. The initial $^{87}\text{Sr}/^{86}\text{Sr}$ ratios were estimated as 0.7047-0.7048 in

rocks of the Dalnensky and Biserny pluton and as 0.70675 in the Central stock at the Vostok-2 deposit (Khetchikov et al., 1996, 1997).

Ore mineralization. The Arminsky ore district is among the well-known tungsten ore districts in Primorye and Russia. Various genetic and mineral types of ore deposits are known (Fig. 5.1). The Vostok-2 skarn scheelite-sulfide deposit, Tigrinoe and Zabytoe tungsten-bearing greisen and quartz-cassiterite deposits, Zimnee and Taehznoe cassiterite-sulfide deposits should be mentioned. High-temperature skarn (W) and greisen (W-Sn) deposits localized near the Central Sikhote-Alin Fault give way to the lower-temperature hydrothermal vein deposits containing tin-base-metal and Au-Ag ores towards the Coastal volcanic belt in the east.

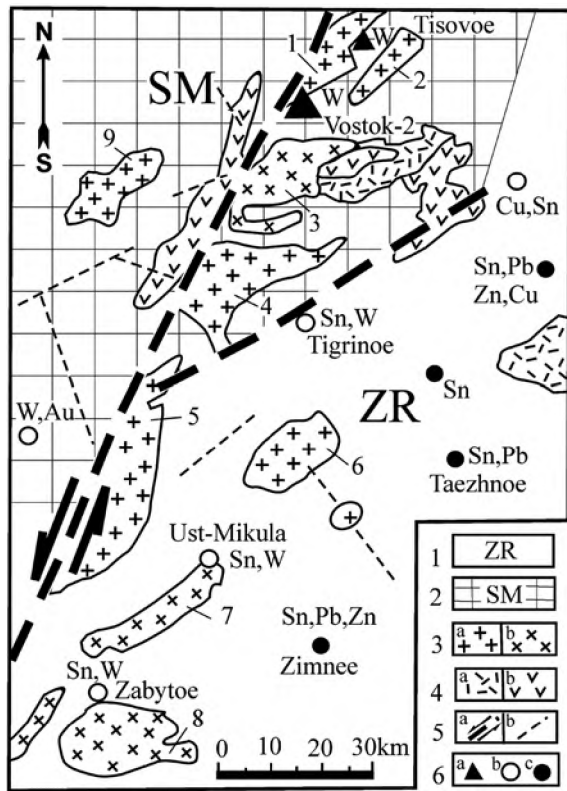


Fig. 5.1. Geological scheme of the Arminsky ore district. (1) Triassic-Jurassic turbidite-olistostrome sequence of the Zhuravlevka Terrane (Zr); (2) Upper Permian sedimentary rocks of the Samarka Terrane (Sm); (3) Cretaceous plutonic rocks: (a) diorite, monzodiorite, granodiorite and (b) granite; (4) Cretaceous volcanic rocks: (a) acid, (b) intermediate; (5) faults (a) major, (b) auxiliary; (6) ore deposits: (a) scheelite-bearing skarn, (b) quartz veins and greisen with wolframite and cassiterite, (c) quartz-cassiterite-sulfide veins and metasomatic bodies. Major faults (letters in figure): (C) Central Sikhote-Alin; (T) Tigriny. Granitic plutons: (1) Biserny, (2) Kayalinsky, (3) Dalnensky, (4) Izluchensky; (5) Dalne-Arminsky, (6) Arminsky, (7) Ust-Arminsky, (8) Priiskovy, (9) Mombiasansky

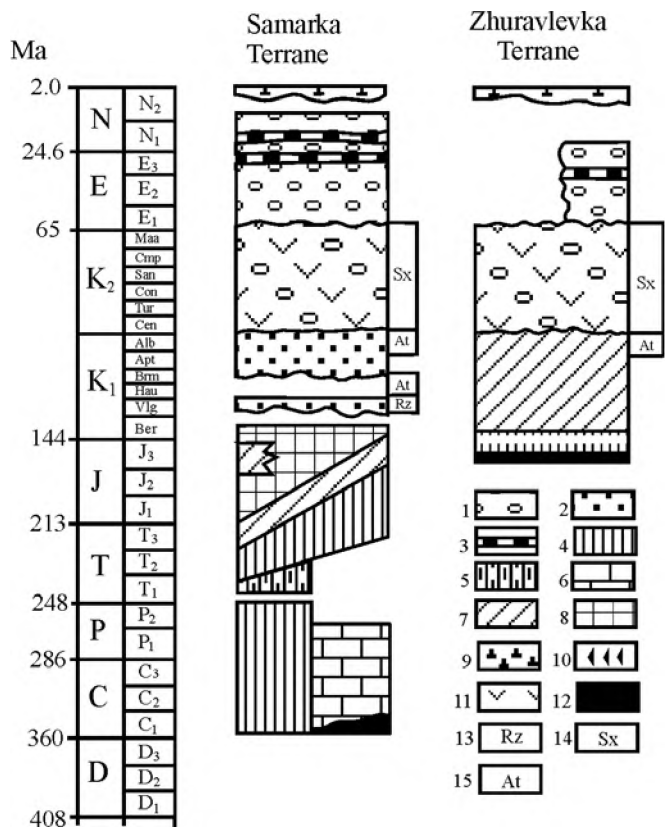


Fig. 5.2. Tectonostratigraphy of the Samarka and Zhuravlevka terranes, after Khanchuk et al. (1995).

Sedimentary rocks: (1) continental, (2) near-shore marine, (3) coal-bearing, (4) bedded chert, (5) cherty-clayey, (6) carbonate rocks of guyots and seamounts, (7) turbidites of continental slope and rise; (8) subduction-related melange. *Volcanic rocks:* (9) intraplate basaltic series, (10) intraplate bimodal series, (11) island-arc subduction-related series, (12) oceanic basalts. *Plutonic rocks:* (13) alkali gabbroids and ultramafics of intraplate series, (14) subduction-related diorite-granite series, (15) anatectic collision granites

THE VOSTOK-2 DEPOSIT

Geology. The Vostok-2 deposit is situated in the Central Sikhote-Alin Foldbelt. The deposit is localized in the northern Samarka Terrane not far from the Central Fault in the southern framework of the Biserny pluton (Fig. 5.3). The country sedimentary rocks are largely composed of sandstones, cherty slates, siltstones, and limestones transformed into quartz-biotite hornfels (often with amphibole and

feldspars) and marbles. The latter are subsequently replaced by skarn at contacts with the Biserny pluton and Central stock.

Plutonic rocks. As was mentioned above, three sequentially emplaced groups of plutonic rocks are recognized. The older group (~128 Ma) is composed of biotite-amphibole (occasionally, pyroxene-bearing) diorite, monzodiorite, and granodiorite mainly known from the Dalnensky pluton. The biotite and amphibole-bearing granodiorite of the Central stock belongs

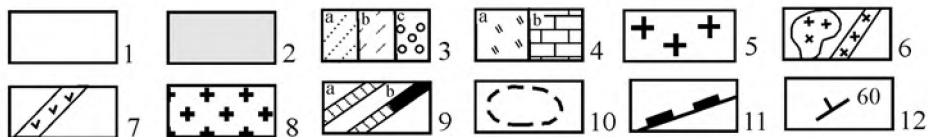
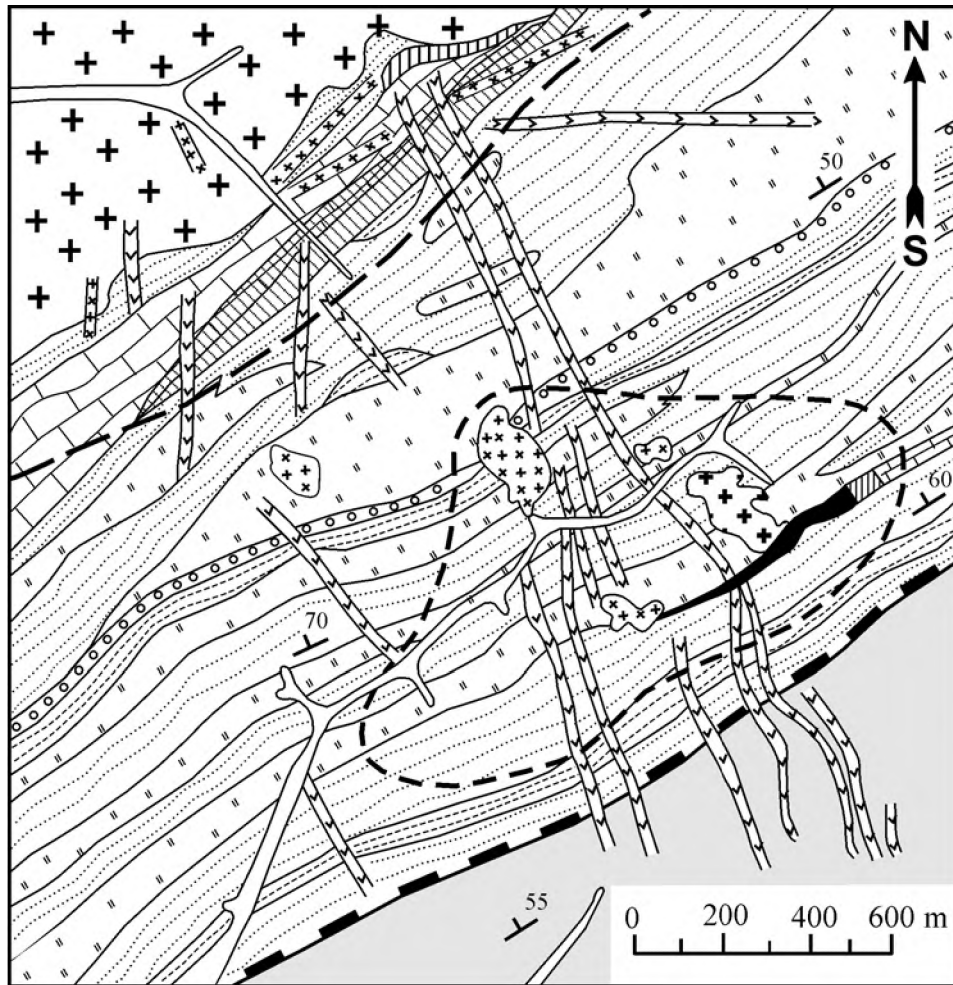


Fig. 5.3. Geological map of the Vostok-2 deposit. Simplified after Ivakin, Levshuk, and Gaaz (1965), Stepanov (1977), and Khanchuk (2000).

(1) Quaternary sediments; (2) cherty and clayey sequence with Upper Jurassic matrix, after Khanchuk (2000); (3) Dalninsky carbonate-cherty-sandstone sequence with Middle and Upper Jurassic matrix: (a) sandstone, (b) siltstone, (c) conglomerate and (4) paleoceanic inclusions: (a) Middle Triassic-Lower Jurassic bedded chert, (b) Carboniferous (?) limestone. Late Cretaceous (5) granites of the Biserny pluton, (6) stocks and dikes of granite porphyry, pegmatite, aplite, and quartz porphyry; (7) diorite porphyry and diabase dikes; (8) Early Cretaceous plagiogranite and granodiorite of the Central stock; (9) skarn: (a) barren, (b) ore-bearing; (10) boundary of contact metamorphic aureole (hornfels, marble, quartzite) and hydrothermally altered rocks (phyllitic, etc.); (11) boundary between the upper and lower part of accretionary prism, after Khanchuk (2000); (12) strike and dip symbols

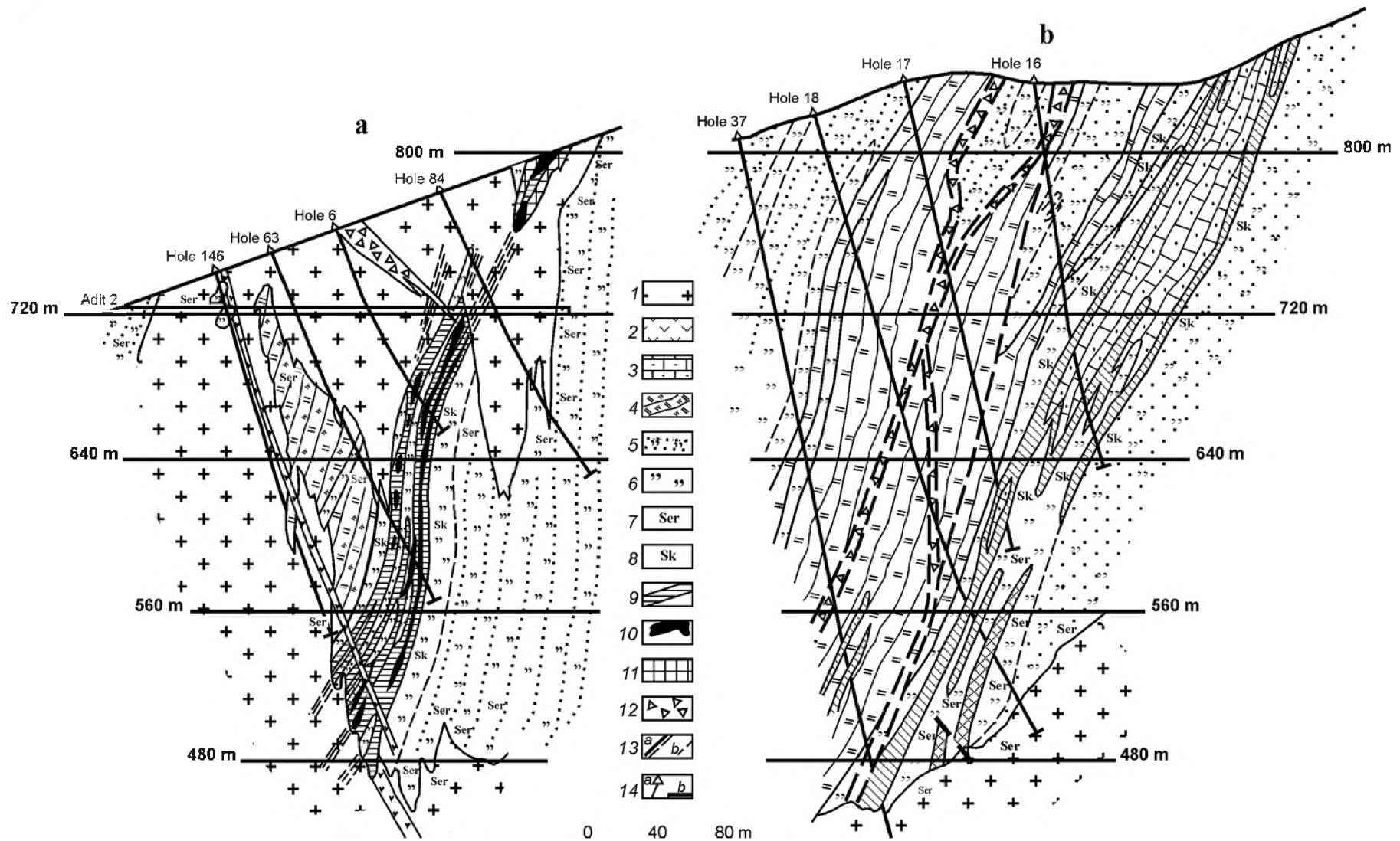


Fig. 5.4. Geological sections across (a) central and (b) northeastern parts of the Vostok-2 deposit. Modified after Ivakin et al. (1965) and Stepanov (1977).

(1) plagiogranite and granodiorite of the Central stock; (2) diabase and diorite porphyry dikes; (3) marmorized limestone and marble; (4) recrystallized cherty rocks (secondary quartzite); (5) sandstone partly transformed into hornfels; (6) biotite hornfels; (7) quartz-sericite altered rocks; (8) skarnified rocks; (9) skarn with scheelite and sulfide impregnations; (10) scheelite-bearing massive sulfide ore; (11) quartz-scheelite ore with apatite; (12) hydrothermal breccia; (13) faults (a) and facies boundary (b); (14) boreholes (a), adits (b)

to the next group (~111 Ma). Porphyritic biotite-bearing leucogranite of the younger group (~98 Ma) forms the Biserny pluton.

Ore mineralization. Orebodies are hosted in skarn that replaces marble, and to a lesser extent, hornfels. The scheelite-sulfide mineralization is superimposed on skarn (Fig. 5.4). A marble layer extending in a northeastern direction and dipping to the northwest at angles 60-70° controls the orebody morphology. The deposit was formed during four stages: (1) contact metamorphism, (2) skarn formation, (3) ore deposition, and (4) postmineral stage.

In the first stage, the country terrigenous rocks (siltstone, shale, and sandstone) were transformed into hornfels at the contact with granitoid plutons; limestone was recrystallized into marble. Dark gray and gray marbles occur in the outer zone of the contact aureole, while white marble appears closer to the contact.

Skarn zones were formed at contacts between marble and aluminosilicate rocks (granites and hornfels). Judging from their morphology (veinlets, layers, lenses) and mineral composition, the skarn lodes are

of infiltration and bimetasomatic origin. Early barren and late ore-bearing skarn varieties are distinguished. The former is abundant at the Tisovoe prospect in the framework of the Biserny granitoid pluton (Fig. 5.5a). Wollastonite and garnet (grossular) are major minerals; tungsten and sulfide mineralization is lacking. The ore-bearing skarn is localized at the Vostok-2 deposit in the contact zone of Central stock (Fig. 5.5b). Pyroxene is the major mineral while garnet and wollastonite are of subordinate importance (Stepanov, 1977).

Orebodies with economic tungsten mineralization were formed in the third stage as metasomatic layers, lenses, and pockets hosted in skarn, as well as in greisen and quartz veins superimposed thereon. Scheelite is the major ore mineral. Pyrrhotite and chalcopyrite dominate among sulfides; arsenopyrite, sphalerite, and bismuth minerals are less abundant.

Postmineral quartz-carbonate and carbonate veinlets, occasionally with pyrite are products of hydrothermal activity at the final postmineral stage.

Mineralogy. More than 50 hypogene minerals are known from the deposit. Pyroxene, plagioclase, amphi-

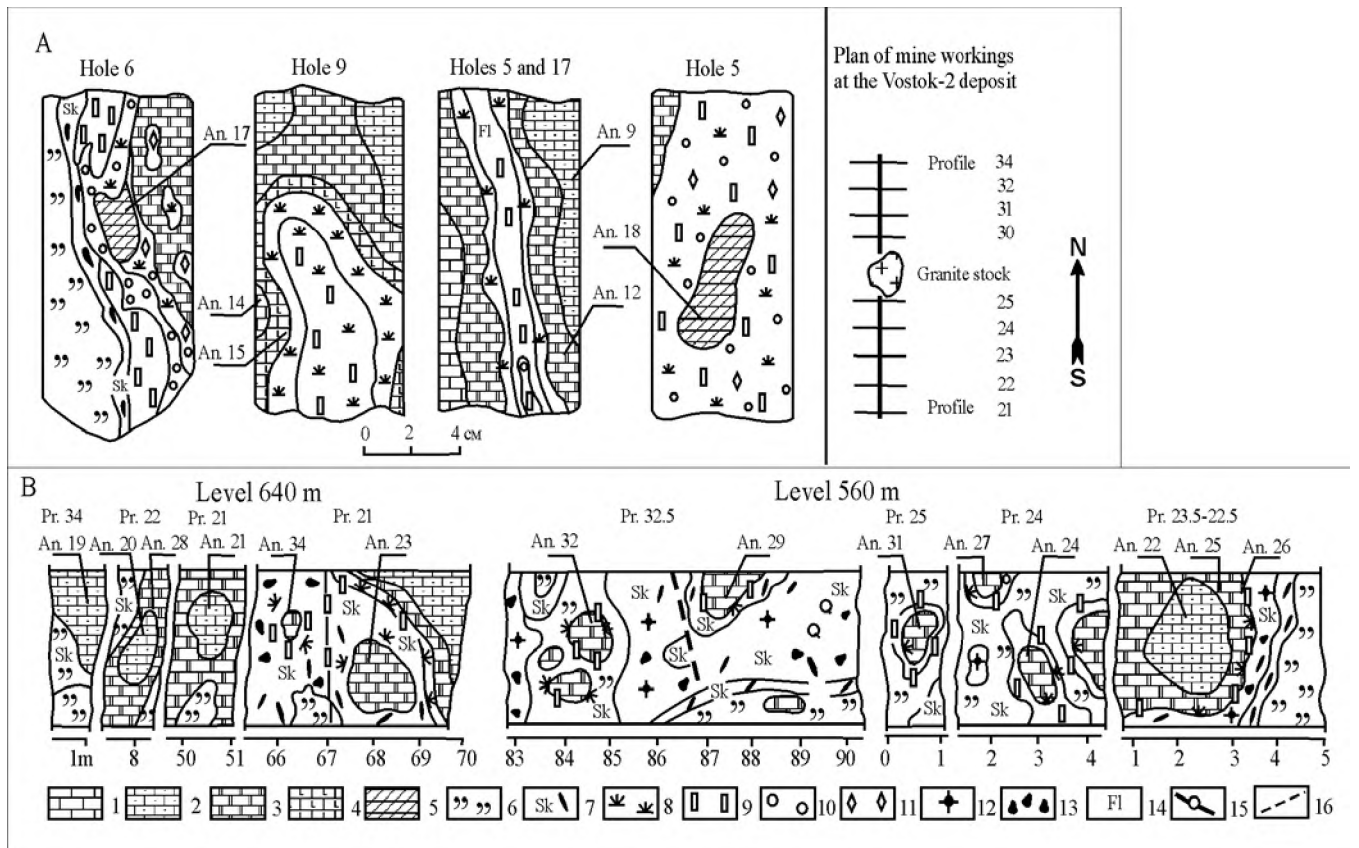


Fig. 5.5. Fragments of skarn and ore zones (A) in boreholes at the Tisovoe prospect and (B) in mine workings at the Vostok-2 deposit, after Gvozdev et al. (2000).

(1) limestone; (2) dark gray and gray marbles; (3) light gray and white marbles; (4) blue marble; (5) redeposited calcite; (6) hornfels; (7) skarnified hornfels; (8) wollastonite and wollastonite skarn; (9) pyroxene and pyroxene skarn; (10) garnet; (11) vesuvianite; (12) scheelite and quartz-scheelite ores; (13) sulfides and sulfide ore; (14) fluorite; (15) quartz-calcite ore; (16) faults. Analysis numbers correspond to Table 5.1

bole, mica, and quartz are most abundant as gangue minerals; calcite, wollastonite, garnet, axinite, and vesuvianite are less abundant. Pyrrhotite, chalcopyrite, and scheelite are the major ore minerals. Arsenopyrite, sphalerite, pyrite, marcasite, galena, and stannite are of secondary importance. Minerals of Bi, Sb, Pb, Te, Au (native bismuth, bismuthinite, cosalite, kobellite, hedleyite, joseite, native gold etc.) are also noticed.

Pyroxene corresponds to the ferrosalite-hedenbergite series and contains up to 3.38 wt % MnO; garnet is composed of grossular. Amphibole is represented by actinolite and less abundant cummingtonite. Plagioclase fits andesine and labradorite in composition; more calcic plagioclase is known from feldspathic metasomatic rocks. Biotite is predominant in hornfels, muscovite in greisen. Scheelite contains up to 30 ppm Nb, 300 ppm Sr, and 45-60 ppm MoO₃. The total REE sum in scheelite attains 720 ppm, Y amounts to 170 ppm. Sphalerite contains about 14 wt % FeO, up to 0.38 wt % MnO, 1.82 wt % Cd and 15 ppm In (Ivanov, 1974, Stepanov, 1977).

Formation conditions. According to thermobarogeochemical studies, the skarn bodies were

formed under the effect of alkaline solutions (pH 9-11) heated to 500-520°C. The quartz-scheelite ore was deposited from slightly acid and neutral solutions (pH 6-7) at 420-350°C. Minerals of the sulfide stage precipitated from alkaline solutions (pH >10) under reducing conditions and at a temperature of <350°C (Stepanov, 1977).

The cryometric study of fluid inclusions in quartz from granitic stock and ore confirmed the presence of Mg, Ca, and Na salts. Potassium salts are typical of inclusions in the ore-bearing quartz; CO₂ was detected in all types of inclusions (Khetchikov et al., 1991).

The oxygen isotopic composition in quartz from igneous rocks and ore is characterized by δ¹⁸O varying from 11.0 to 13.4 ‰. The oxygen and carbon isotopic compositions in carbonate-bearing rocks are shown in Table 5.1 and δ³⁴S of sulfide minerals, in Fig. 5.6.

THE TIGRINOE DEPOSIT

Geology. The Tigrinoe Sn-W deposit is situated near the southeastern margin of the Izluchinsky

Table 5.1

δ¹⁸O and δ¹³C of carbonate rocks from the Vostok-2 deposit

Analysis	δ ¹⁸ O, ‰	δ ¹³ C, ‰	Note
<i>Tisovoe prospect</i>			
9	23.4	3.3	Dark and light gray marble, 5 cm apart from the skarn zone
12	21.3	2.4	White medium-grained marble
14	20.7	1.1	Blue marble close to the zone of the early wollastonite skarn
15	18.4	0.3	Blue marble at the contact with skarn
17	16.6	-2.6	White calcite in the early pyroxene-garnet-vesuvianite-wollastonite skarn
18	13.5	-2.9	White redeposited calcite in the pyroxene skarn
<i>Vostok-2 deposit</i>			
19	22.6	3.2	Dark gray marble at the flank of deposit
20	20.8	2.9	Gray marble from central part of a large block in the skarnified zone
21	20.7	2.9	The same
22	23.6	2.9	The same
23	22.3	2.3	Light gray and white marbles between the gray marble and skarn zone
24	24.8	2.3	The same
25	25.0	2.3	The same
26	23.6	2.5	The same
27	23.2	2.3	The same
28	24.8	2.2	The same
29	22.2	2.2	The same
31	18.8	1.9	The same
32	16.5	0.3	The same, 0.5 cm from the skarn zone
34	14.3	-0.5	The same

Note: δ¹⁸O and δ¹³C are calculated relative to SMOW and PDB standards, respectively. The accuracy of δ¹⁸O and δ¹³C measurements is ± 0.2‰. Location of analyses is shown in Fig. 5.5.

granitoid pluton of Late Cretaceous age (Fig. 5.7). The Jurassic and Cretaceous country rocks are related to the volcanosedimentary sequence of the Zhuravlevka Terrane (Khanchuk et al., 1995) and largely composed of siltstone with shale, sandstone, and conglomerate interlayers (Rodionov et al., 1984).

Plutonic rocks. The ore-bearing rare-metal Li-F granite makes up the Lesser and Greater stocks

(Figs. 5.7 and 5.8) and a suite of dikes. Their K-Ar and Rb-Sr ages were estimated as 67-90 Ma (Rub et al., 1986, 1991, 1998; Gonevchuk et al., 1987, 1991, 1998; Ishihara et al., 1997; Thomson et al., 1996).

The granite porphyry of the Greater stock, its offsets, and several dikes is regarded as the early intrusive phase. Quartz phenocrysts with granophyre rims, as well as alkali feldspar and plagioclase (An₁₀₋₁₈)

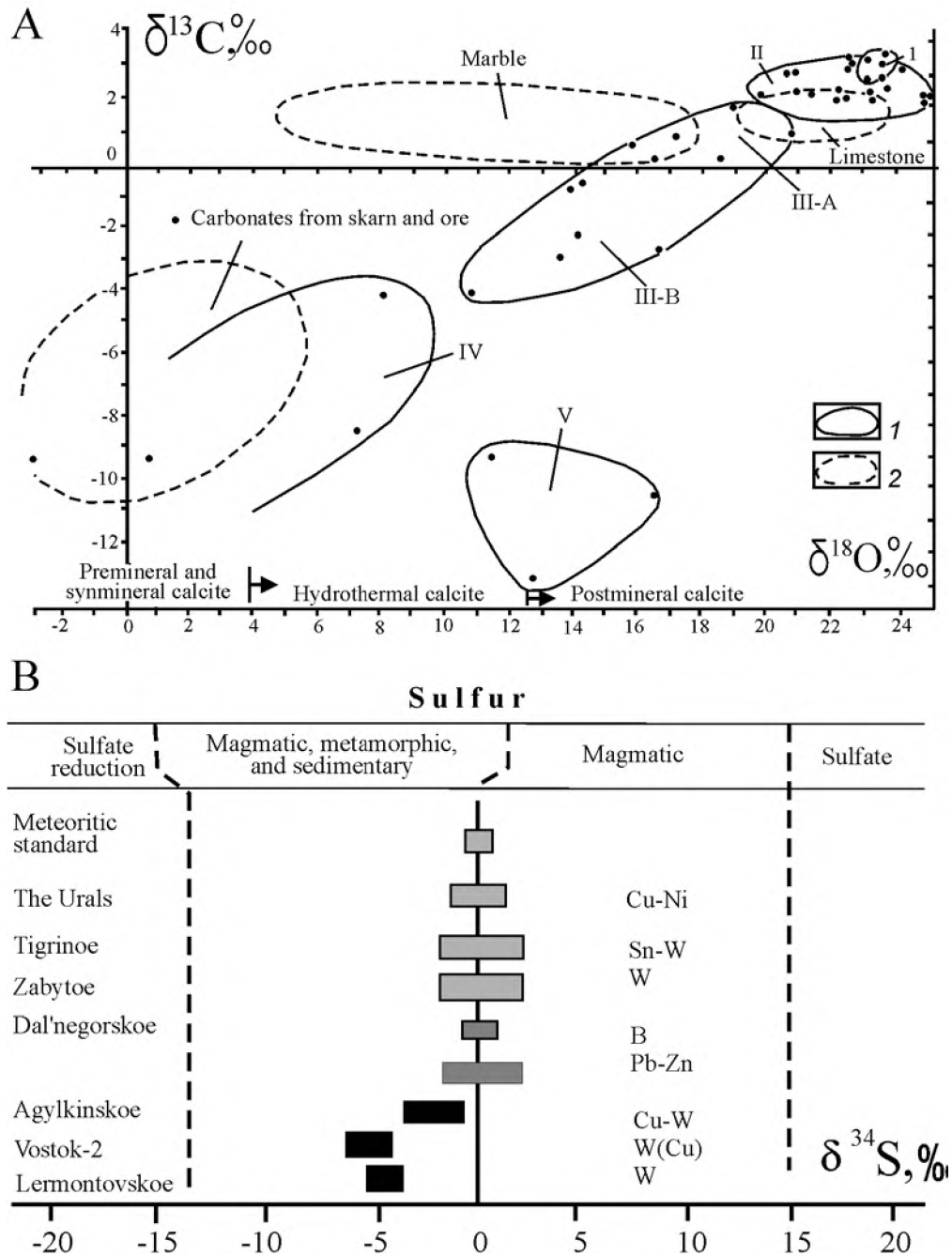


Fig. 5.6. (A) Carbon and oxygen isotopic compositions of carbonate rocks and (B) sulfur isotopic composition of sulfides from the Vostok-2 deposit, after Gvozdev et al. (2000, 2001).

(1) fields of $\delta^{18}O$ and $\delta^{13}C$ of rocks from the Vostok-2 deposit: (I) limestone, (II) contact aureole; (III-A) marble at the contact with skarn; (III-B) redeposited carbonates in skarn zones; (IV) calcite from synmineral veinlets; (V) calcite from postmineral veinlets; (2) fields of $\delta^{18}O$ and $\delta^{13}C$ of rocks from the borosilicate and base-metal deposits of the Dalnegorsk district

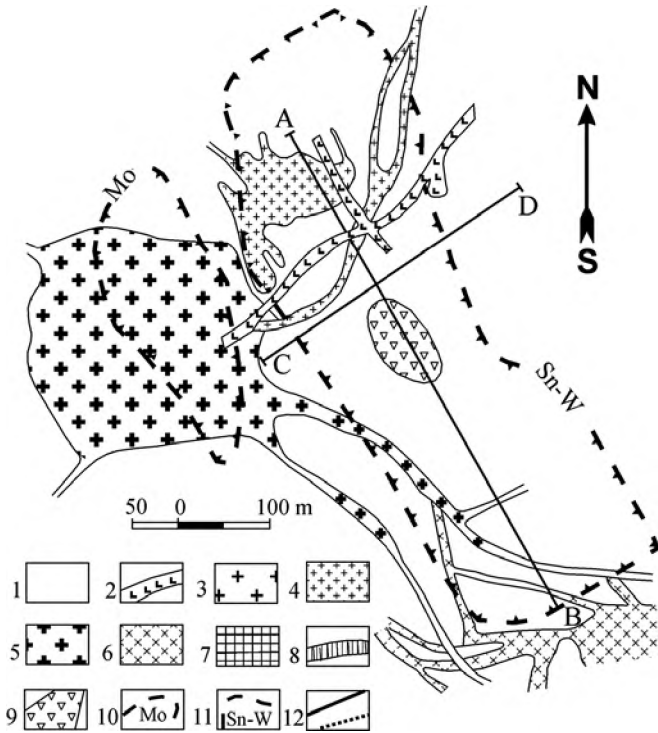


Fig. 5.7. Schematic geological map of the Tigrinoye deposit, after Orlovsky et al. (1994).

(1) country rocks of the Zhuravlevka Terrane (siltstone and sandstone); (2) Neogene basaltic dikes; Late Cretaceous granites of the Lesser stock: (3) porphyritic leucogranite with pisolitic quartz and zinnwaldite; (4) porphyritic granite with protolithionite and zinnwaldite; Intrusive rocks of the Greater stock: (5) Late Cretaceous granite porphyry and rhyolite porphyry, (6) Early (?) monzodiorite and diorite porphyry; (7) Tigrenok greisen body; (8) stocksheider; (9) hydrothermal breccia; (10) contour of molybdenite mineralization; (11) contour of the Tigrinoye wolframite-cassiterite stockwork; (12) geological boundary, proved and inferred. Some rock units are shown only on cross sections, see Fig. 5.8

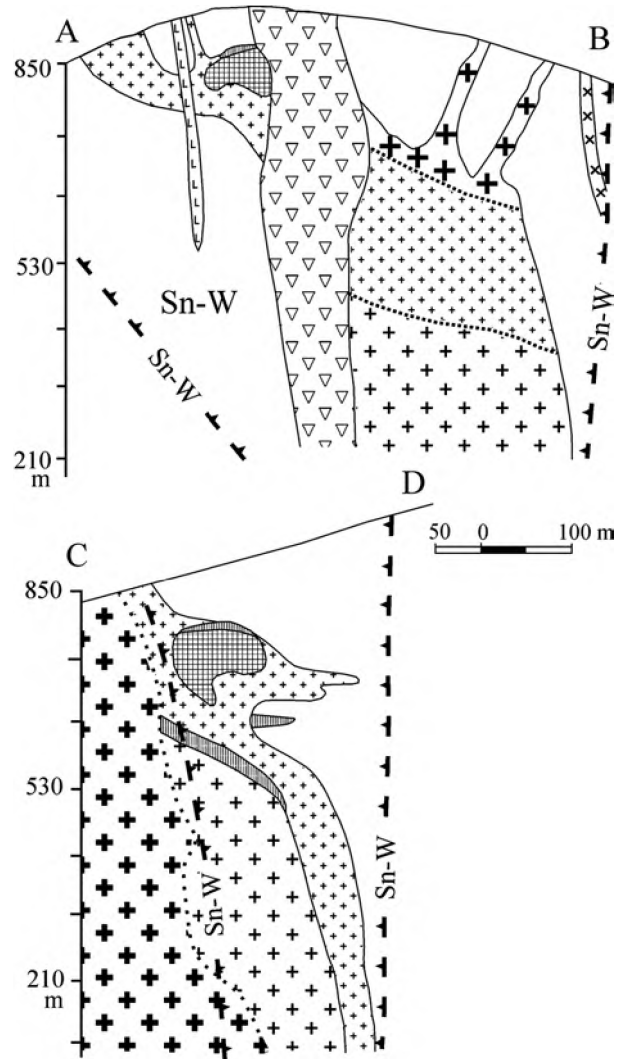


Fig. 5.8. Geological sections across the Tigrinoye deposit along lines A-B and C-D.

See Fig. 5.7 for section line location and symbols

crystals and clots are incorporated into the microgranite groundmass. Rare flakes of fluorbiotite and protolithionite are noticed. The granite porphyry is affected by a slight greisenization and cut by quartz veinlets with finely dispersed molybdenite that imparts a dark color to the veinlets. The contact between the granite porphyry and Li-F granite of the Lesser stock was crossed by boreholes. The character of intersection indicates that the former rock is older. Two subphases are recognized in the younger granite of the Lesser stock: protolithionite (zinnwaldite) granite and zinnwaldite granite with pisolitic quartz (Gonevchuk et al., 1991). The Rb-Sr age of the protolithionite granite yielded 73.2 ± 0.2 Ma with $I_{Sr} = 0.7112 \pm 0.0012$. The zinnwaldite granite was dated at 67 ± 2 Ma, $I_s = 0.7294 \pm 0.0052$ (Rub et al., 1998). The mineralogy and geochemical signature of both granites correspond to Li-F rare-metal granite (Table 5.2). All

granitic rocks are enriched in Sc (20-30 ppm) and Y (up to 357 ppm in protolithionite granite). The Sc content in micas attains 150-250 ppm.

The highest partial water pressure, as well as Li and F activities are characteristic of the final intrusive phase. As deduced from the study of melt inclusions in quartz, the Li-F granite crystallized at a temperature of about 700°C (Pakhomova, personal communication).

Ore mineralization. The Mo and W-Sn granite-related ores are known at the Tigrinoye deposit (Ruchkin et al., 1986; Korostelev et al., 1990). The molybdenite mineralization is hosted in the older granite porphyry of the Greater stock. Thin quartz and quartz-adularia veinlets with zinnwaldite selvages contain molybdenite, bismuth minerals, and gold. The veinlets gently dip to the east and northeast making up a stockwork, so far contoured only tentatively (Figs. 5.7 and 5.8). The specific stockwork parameters and its

Average oxide (wt %) and trace elements (ppm) contents in granitoids from the Tigrinoe deposit, after Gonevchuk et al. (1998)

Oxide	Granite porphyry of the Greater stock (<i>n</i> = 10)		Medium-grained granite of the Lesser stock (<i>n</i> = 16)		Granite with pisolitic quartz (<i>n</i> = 7)	
	X	V	X	V	X	V
SiO ₂	75.74	1.0	75.73	0.9	71.72	1.0
TiO ₂	0.06	31.1	0.03	28.4	0.01	72.6
Al ₂ O ₃	13.34	2.9	13.18	3.8	16.18	4.5
Fe ₂ O ₃	0.20	48.7	0.17	2.4	0.23	49.4
FeO	0.55	43.7	0.60	39.9	0.55	58.4
MnO	0.01	52.6	0.03	61.8	0.09	33.1
MgO	0.13	95.3	0.10	84.5	0.12	123.6
CaO	0.48	37.7	0.45	60.3	0.36	30.7
Na ₂ O	4.00	10.7	4.13	14.3	5.87	9.8
K ₂ O	4.98	14.1	4.52	8.4	3.56	16.7
Li ₂ O	0.01	43.2	0.08	42.3	0.11	67.1
Rb ₂ O	0.05	25.7	0.13	35.5	0.12	20.4
F	0.53	33.2	0.55	36.0	0.80	25.3
Ni	6.9	45.5	3.6	82.0	2.9	99.8
Co	2.6	81.1	0.17	49.8	-	-
Cr	7.2	35.3	1.93	66.3	10.1	40.1
V	9.2	89.3	8.6	169.3	3.3	80.0
Cu	45.3	124.8	21.7	96.2	25.6	81.6
Sn	20.5	106.5	27.9	78.6	38.3	75.2
Pb	78.5	138.9	75.5	39.6	55.8	11.6
Zn	102.3	98.2	162.0	99.7	243.7	82.9
B	29.0	97.7	14.9	108.2	18.1	7.1
Mo	12.21	101.4	4.28	173.1	11.34	91.6
Ag	113	162.1	1.25	168.9	1.10	67.5
W	32.0	73.4	53.0	156.1	302.1	90.5
Be	5.9	52.7	6.8	48.6	5.0	13.4
Nb	50.4	20.3	55.3	51.8	86.0	22.0
Y	125.0	49.3	357.3	55.6	27.4	138.6
Sc	87.5	35.4	166.3	90.6	125.8	41.5
Ba	16		30		16	
Sr	22		40		18	
Na ₂ O/K ₂ O	0.80		0.91		1.65	
K/Rb	83		32		27	

Note: X is the average; V is the variation coefficient. Ba and Sr contents are averages of 5 analyses.

economic significance remain undetermined. The main W-Sn ore zone is a linear stockwork (at least, 150×600 m) hosted in granites of the Lesser stock and nearby hornfels extends in a northwestern (315-340°) direction (Fig. 5.7). A body of massive quartz-topaz-mica greisen and stockscheiders are localized at the southern contact of the Lesser stock, which is considered to be an intrusion equant in plan (120×150 m) with longitudinal and latitudinal offsets (Figs. 5.7 and 5.8). The central part of the stock is occupied by a vertical pipe of hydrothermal explosion breccia from the greisenized granite into hornfels and reaches the surface (Fig. 5.8).

Formation conditions. Six progressively formed postmagmatic mineral assemblages are recognized: (1) quartz (2) quartz-molybdenite and quartz-adularia with molybdenite, bismuth minerals, and gold; (3) quartz-topaz-mica greisen with disseminated cassiterite, wolframite, arsenopyrite, sphalerite, and stannite; (4) quartz-cassiterite-wolframite with sporadic potassium feldspar; (5) quartz-sulfide (arsenopyrite, sphalerite, stannite, and bismuth minerals), occasionally with wolframite and cassiterite; (6) quartz-carbonate-sulfide with sporadic pyrrhotite and pyrite, fluorite, and triplite. The economic assemblages of the greisen and quartz veins were formed at a temperature

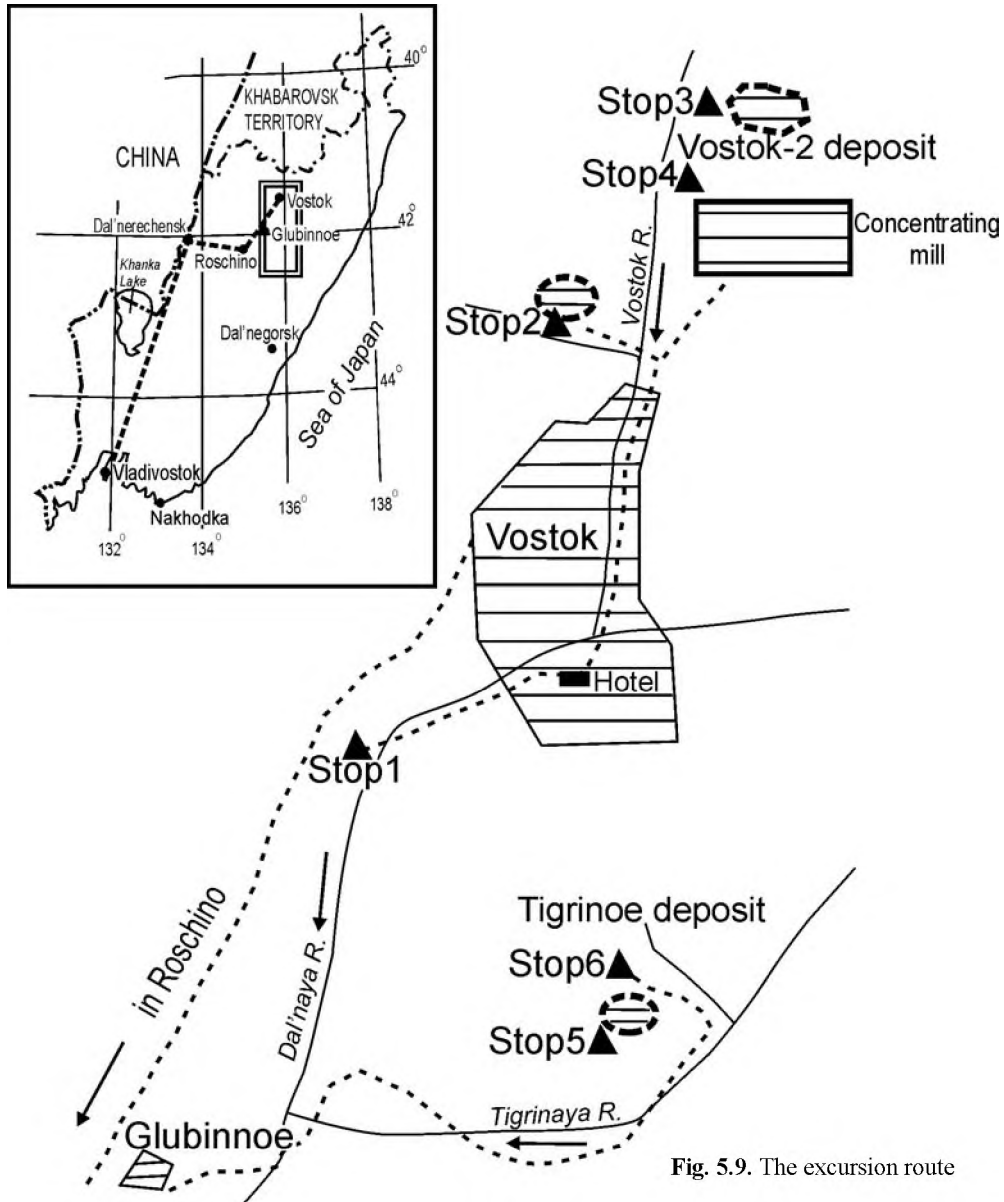


Fig. 5.9. The excursion route

of 400--200°C. The quartz-wolframite, quartz-topaz, and quartz-cassiterite assemblages crystallized at a higher temperature than the quartz-sulfide. Enrichment in sulfides including high-indium sphalerite and stannite (25% of Sn in ore) is a specific feature of the deposit. Granites and ore minerals (wolframite, cassiterite) are enriched in rare elements (Nb, Ta, Sc). The occurrence of molybdenite, bismuth minerals, and gold at the Sn-W deposit is also notable.

EXCURSION POINTS (Fig. 5.9)

The Vostok-2 deposit

Stop 1. The outcrop on the left bank of the Dal'naya River south of the Vostok Settlement. Granodiorite and monzodiorite of the Dalnensky pluton, (128 Ma).

Stop 2. Right bank of the Vostok stream, 5 km upstream the settlement. Open pit No. 1. Marble olivoliths metamorphosed at the contact with the Late Cretaceous Biserny granitoid pluton (98 Ma). Paleogene basalt with lherzolite nodules (Paleogene).

Stop 3. Dump of the open pit at the Vostok-2 deposit, the level of 720 m. Granodiorite of Central stock (111 Ma), skarn, and scheelite-sulphide ore types.

Stop 4. Mine at the level of 520-480 m. Granodiorite of the Central stock, skarn, and various ore types.

The Tigrinoye deposit

Stop 5. The upper cutting. The Li-F granite of the Lesser stock and ore stockwork.

Stop 6. Dumps of Adit no. 5. Granite of the Lesser stock, stockscheider, greisen, and quartz-cassiterite ore.

REFERENCES

- Gonevchuk, V.G. and Gonevchuk, G.A., Magmatic factors of juxtaposed Sn-W and Mo mineralization at the Tigrinoe deposit, in: *Sootnoshenie raznykh tipov orudneniya vulkano-plutonicheskikh pojasov Aziatsko-Tikhookeanskoj zony sochleneniya* (Relationships between various types of ore mineralization in volcanic-plutonic belts of the Asian-Pacific Junction zone), Vladivostok: Far East Branch, Russian Academy of Sciences, 1991, pp. 111-120.*
- Gonevchuk, V.G., Gonevchuk, G.A., Ignat'ev, A.V., and Korostelev, P.G., New data on the age of rare-metal granites in the central Sikhote-Alin, *Tikhookean Geol.*, 1987, no. 4, pp. 125-126.*
- Gonevchuk, V.G., Gonevchuk, G.A., Kokorin, A.M., Korostelev, P.G., and Semenyak, B.I., Rare-metal (Li-F) granites and related mineralization in the Arminsky ore district (Primorye, Russia), in *Anatomy and textures of ore-bearing granitoids of Sikhote-Alin (Primorye Region, Russia) and related mineralization*, Potsdam, 1998, pp. 20-24.
- Gvozdev, V.I., Geology, mineralogy, and genesis of the Agylinsky copper-tungsten deposit in Yakutia, in: *Rudnye mestorozhdeniya kontinental'nykh okrain* (Ore deposits of continental margins), 2001, vol. 2, no. 2, Vladivostok: Dalnauka, pp. 367-397.*
- Gvozdev, V.I., Ignat'ev, A.V., et al., $\delta^{18}\text{O}$ and $\delta^{13}\text{C}$ of carbonates at the Vostok-2 deposit, Primorye, *Tikhookean Geol.*, 1999, vol. 18, no. 1, pp. 50-58.**
- Gvozdev, V.I., Ignat'ev, A.I., Ukhaneva, N.G., and Velivetskaya, T.A., Oxygen and carbon isotopic compositions of carbonates from the skarn scheelite-sulfide deposits in Primorye, *Dokl. Ross. Akad. Nauk*, 1999, vol. 367, no. 5, pp. 671-673.**
- Ishihara, S., Gonevchuk, V.G., Gonevchuk, G.A., Korostelev, P.G., Sayadyan, G.R., and Semenyak, B.I., Mineralization age of granitoid-related ore deposits in the southern Russian Far east, *Resource Geol.*, 1997, vol. 47, no. 5, pp. 255-261.
- Ivanova, V.L., Petrology of granitoids at the Vostok-2 deposit, *PhD Thesis*, Vladivostok: Far East geological Institute, 1975.*
- Khanchuk, A.I., Ore formation in the Russian Far East: a paleogeodynamic interpretation, in *Rudnye mestorozhdeniya kontinental'nykh okrain* (Ore deposits of continental margins), 2000, vol. 1, pp. 5-33.*
- Khanchuk, A.I., Ratkin, V.V., Ryazantseva, M.D., Golozubov, V.V., and Gonokhova, N.G., *Geologiya i poleznye iskopaemye Primorskogo kraya* (Geology and mineral resources of the Primorye region), Vladivostok: Dalnauka, 1996, 66 p.*
- Khetchikov, L.N., Pakhomova, V.A., Gvozdev, V.I., and Rub, A.K., Fluid regime of some granitoid systems, *Preprint of the Far East Geological Institute*, Vladivostok, 1991, 40 p.
- Khetchikov, L.N., Pakhomova, V.A., Gvozdev, V.I., and Zhuravlev, D.Z., The age of ore mineralization and some genetic characteristics of the Vostok-2 skarn scheelite-sulfide deposits in the central Sikhote-Alin, *Rudy Metally*, 1999, no. 2, pp. 30-36.*
- Korostelev, P.G., Gonevchuk, V.G., Gonevchuk, G.A., Gorbach, G.I., Zalevskaya, V.N., Kokorin, A.M., Kokorina, D.K., Levchuk, L.S., and Nedashkovsky, A.P., Mineral assemblages of a greisen tungsten-tin deposit, Primorye, in *Mineralnye assotsiatsii na Dalnem Vostoke* (Mineral assemblages in the Far East, Vladivostok: Far East Branch, Academy of Sciences of the USSR, 1990, pp. 17-61.*
- Krymsky, R. Sh., Belyatsky, B.V., Levsky, L.K., and Rub, M.G., Age and genesis of scheelite ore deposit Vostok-2 (Primorye) with references to the Rb-Sr and Sm-Nd isotopic data, in: *Mineral deposits: Research and exploration where do they meet?*, Papunen, H., Ed., Proc. the 4th Biennial SGA Meeting, Turku, 11-13 August 1997, Rotterdam: Balkema, 1997, pp. 651-653.
- Krymsky, R. Sh., Pavlov, V.A., Rub, M.G., et al., Rb-Sr and Sm-Nd isotopic characteristics of granitoids and ores at the Vostok-2 scheelite deposit, Primorye, *Petrologiya*, 1998, vol. 6, no. 1, pp. 3-15.**
- Levashov, G.B., *Geokhimiya pagennykh magmatitov aktivnykh zon kontinental'nykh okrain* (Geochemistry of igneous rock associations at active continental margins), Vladivostok: Far East Branch, Academy of Sciences of the USSR, 1991, 380 p.*
- Olovorudnye mestorozhdeniya SSSR* (Tin deposits of the USSR), vol. 2, book 1: *Geologiya olovorudnykh mestorozhdenii* (Geology of tin deposits), Moscow: Nedra, 1986, 429 p.*
- Pakhomova, V.A., Khetchikov, L.N., and Gvozdev, V.I., The fluid phase composition of rare-metal granites in Primorye: evidence from cryometric study of fluid inclusions in quartz, *Tikhookean Geol.*, 1991, no. 2, pp. 99-102.*
- Pakhomova, V.A., Rub, A.K., Khetchikov, L.N., and Rub, M.G., The fluid phase in melts of rare-metal granites in the central Sikhote-Alin, *Izv. Akad. Nauk SSSR, Ser. Geol.*, 1992, no. 3, pp. 147-151.*
- Rodionov, S.M., Shapenko, V.V., and Rodionova, L.N., Structures of localization and genesis of tin-tungsten deposits of the central Sikhote-Alin, *Geol. Rudn. Mestorozhd.*, 1984, no. 1, pp. 2-30.*
- Rub, A.K., Rub, M.G., and Sandomirova, G.P., Results of Rb-Sr dating and specific compositional features of rare-metal granites from the Tigrinoe ore deposit (Central Sikhote-Alin), *Dokl. Ross. Akad. Nauk*, 1998, vol. 319, no. 4, pp. 952-956.**
- Rub, M.G., Rub, A.K., and Akimov, V.M., Rare-metal granites of the central Sikhote-Alin, *Izvl. Akad. Nauk SSSR, Ser. Gepl.*, 1986, no. 7, pp. 33-56.*
- Rub, M.G., Pavlov, V.A., Gladkov, N.G., et al., *Olovonosnye i volframnosnye granity nekotorykh raionov SSSR* (Tin- and tungsten-bearing granites in some regions of the USSR), Moscow: Nauka, 1982, 261 p.*
- Rub, M.G., Rub, A.K., Krivoshchekov, N.N., and Ashikhmin, N.A., Rare-metal granites at the Tigrinoe deposit, central Sikhote-Alin, *Petrologiya*, 1998, vol. 6, no. 1, pp. 16-29.**
- Ruchkin, G.V., Schnaider, M.S., Schnaider, A.A., Ivakin, A.N., Levshuk, A.E., Orlovsky, V.V., Larioshkin, A.K., and Akimov, V.M., A model of Sn-W deposit formation, *Geol. Rudn. Mestorozhd.*, 1987, no. 2, pp. 85-88.*
- Stepanov, G.N., *Mineralogiya, petrografiya, i genesis skarnovo-sheelite-sulfidnykh mestorozhdenii Dal'nego Vostoka* (Mineralogy, petrography, and genesis of skarn scheelite-sulfide deposits in the Far East), Moscow: Nauka, 1977, 178 p.*
- Tomson, I.N., Tananaeva, G.A., Polokhov, V.P., The relationships between different types of tin mineralization in the southern Sikhote-Alin, *Geol. Rudn. Mestorozhd.*, 1996, vol. 38, no. 4, pp. 357-372.**

* In Russian.

** English translation is available.



THE DALNEGORSK ORE DISTRICT

G.P. Vasilenko

Far East Geological Institute (FEGI), Far East Branch, Russian Academy of Sciences, Vladivostok

HISTORY OF DEVELOPMENT

The Dalnegorsk ore district (DOD) with its mining and chemical industries plays a most important role in economics of the Russian Far East (Fig. 6.1). The first mine was developed in 1912 on the basis of the Verkhnee deposit. The SIKHALI Mining and Metallurgical Integrated Works (presently the DAL'POLIMETALL Joint-Stock Company) started to operate in 1927 as a successor of the AGOT Company. A small metallurgical works for lead concentrate processing and a coastal terminal have been built up in the Rudnaya Pristan Settlement. A narrow-gauge railway, 35 km long, connected Dalnegorsk with the metallurgical works and the moorage. The DAL'POLIMETALL Company currently owns the deposits with 10% of total Pb reserves and 7% of total Zn reserves in Russia.

Prospecting for boron mineralization in skarn started in 1945 following the recommendation given by Academician S.S. Smirnov. As a result, the world largest Dalnegorsk borosilicate skarn deposit was discovered. A modern complex for mining and processing chemical raw materials (presently belongs to the BOR Joint-Stock Company) was developed on the basis of this deposit.

In the 1970–1980s, a number of new gold and silver-gold primary deposits including the Nikolaevsky and Mayminovsky deposits were found; the latter will be visited during the excursion.

GEOLOGICAL SUMMARY

General outlines. According to the present-day view (Yushmanov et al., 1989; Golozubov and Khanchuk, 1995), DOD is a fragment of a Late Jurassic–Early Cretaceous accretionary wedge, or the Taukhe River Terrane (Fig. 6.2). Two tectonically juxtaposed subterrane are recognized in the accretionary wedge section: Silinka River and Gorbusha River (Fig. 6.3). A sequence of Berriasian–Valanginian intercalating siltstone and sandstone, 3500 m thick, occurs at the base of the Silinka River Subterrane. This sequence is overlain by an olistostrome unit; the siltstone and sandstone matrix contains Valanginian fossils and entrains olistoliths of Carboniferous–Permian and Middle–Upper Triassic limestones with chert, basalt, and sandstone interlayers. The olistostrome nappes reach 5 km in extent and 790 m in thickness. They commonly pinch out at a depth of 1–3 km. The size of limestone

blocks varies from a few centimeters to few kilometers; the largest blocks crop out in anticline cores.

Olistostrome nappes of the Silinka River Subterrane are overthrust by the Gorbusha River Subterrane composed of intercalating siltstone, sandstone, and glassy chert of the flyschoid sequence at its base. Microfossils and plant remains indicate a Triassic–Lower Cretaceous age. The overlying olistostrome, more than 1000 m thick, contains blocks and small sheets of underlying Gorbusha River sandstone, interlayers of siliceous breccia with Triassic conodonts and Middle–Late Jurassic radiolaria. The imbricated structure of the Gorbusha River Subterrane provides four- or fivefold recurrence of sedimentary rhythms and formation of a peculiar tectonic package, up to 2500 m in total thickness. The section is topped by flyschoid rocks of the Taukhe River Formation (~ 1000 m), which are related to the Ustinovka Subterrane.

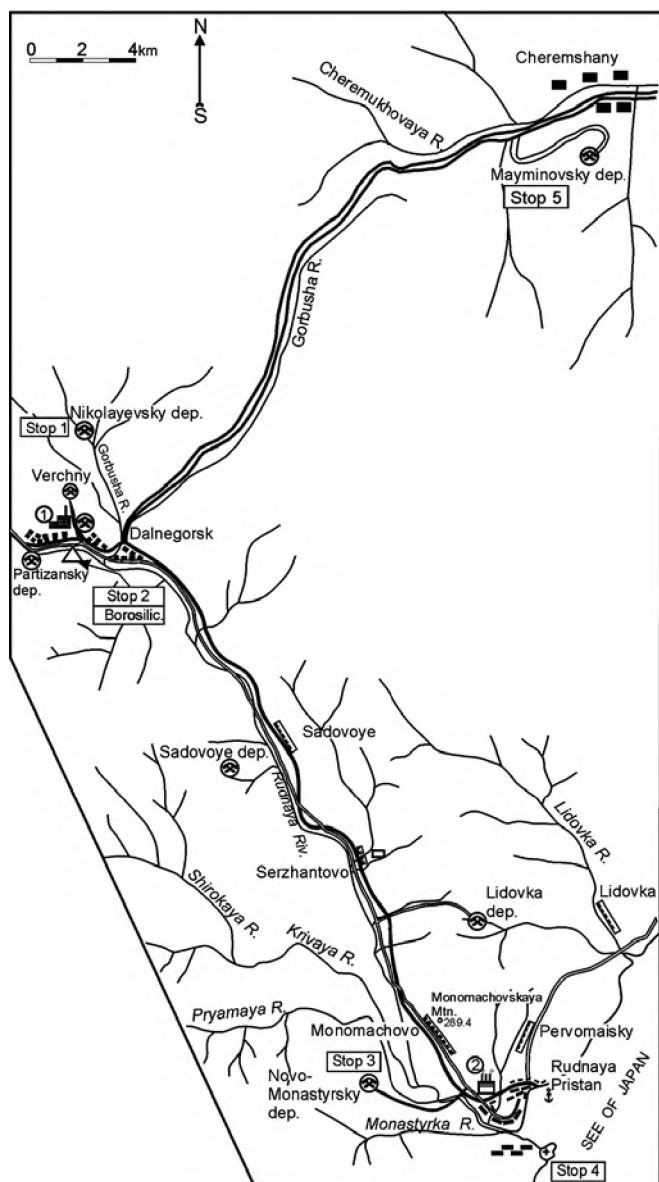


Fig. 6.1. Index map of field excursion in the Dal'negorsk district.

(1) concentrating mill; (2) metallurgical works

The accretionary wedge formation was completed in the Hauterivian; in the late Albian the system of anticlines and synclines of a northeastern direction was formed. Reverse and thrust faults at the fold limbs dip southeastward.

In the Cenomanian, the Taukhe River Terrane was involved in the subduction-related interaction between continental and oceanic plates. This process resulted in the formation of a volcanic belt unconformably covering the accretionary wedge.

Igneous rocks. Six volcanic-plutonic complexes are recognized in DOD.

The first, Sinancha Complex (Cenomanian–Turonian) comprises tuffaceous conglomerate, tuffite, basaltic andesite and basalt lavas and tuffs of the *Si-*

nancha Formation (800 m). Extrusions and dikes of pyroxene-amphibole andesite are spatially associated with volcanic flows. Small comagmatic intrusions are composed of gabbrodiorite and diorite. These rocks belong to the calc-alkaline series slightly enriched in alkali metals and LREE.

The second, Primorsky Complex (Turonian–Campanian) consists of rhyolitic and rhyodacitic ignimbrite and lava of the *Primorsky Formation* (up to 2150 m thick) and comagmatic hypabyssal intrusions of dioritic-granitic composition. The silicic rocks are distinguished by their elevated Fe/Mg ratio and alkali metal contents; they are also enriched in Pb (20–70 ppm), Zn (50–200 ppm), and Mo (2–7 ppm) (Mikhailov, 1989).

The third, Dalnegorsk Complex (late Senonian–Maestrichtian) is composed of andesitic-dacitic lavas and pyroclastic rocks and less abundant rhyolitic and basaltic andesitic volcanics of the *Siyanovo Formation*, up to 1000 m in total thickness. The rocks belong to the high-alumina calc-alkaline series. The comagmatic gabbro-granodiorite-granite series is enriched in Pb (up to 300 ppm), Zn (up to 486 ppm), and Ag (up to 1–2 ppm). Four intrusive phases are recognized: (1) gabbrodiorite, (2) granodiorite, adamellite, and tonalite, (3) granite and granite porphyry, and (4) leucogranite and aplite. The final phases of the fractionated series are enriched in minor elements (pluton of the 27th Creek). The K-Ar age is estimated as 69–55 Ma. Relationships between rocks of the second and third phases can be observed in coastal cliffs (Fig. 6.4).

At Briner Cape occurs the contact between granodiorite of the second phase and rhyodacite of the *Siyanovo Formation*.

The fourth, Bogopol Complex (Danian) is composed of rhyolitic lavas including glassy varieties and ignimbrites of the *Bogopol Formation*, about 1000 m in total thickness. Hypabyssal intrusions of granite, leucogranite and granite porphyry are spatially associated with volcanic rocks. The igneous rocks are high-silicic and high-aluminous; potassium prevails over sodium; high Pb (10–57 ppm) Zn (24–120 ppm), and Sn (2–8 ppm) are typical.

The fifth, Kuznetsovo Complex (Early Paleogene) occurs only in the northeastern DOD where it consists of basalt and basaltic andesite flows of the *Kuznetsovo Formation*, 550–710 m in thickness. Comagmatic dikes and small stocks of diabase and lamprophyre are noticed.

The sequence of volcanic-plutonic complexes is completed by emplacement of the *Sikhali Complex* of appinitic minor intrusions (isite,¹ essexite-diabase,

¹ Isite (after the Is River in the Urals) is a fine-grained rock consisting of amphibole (predominant mineral) and small amounts of clinopyroxene, plagioclase and magnetite.

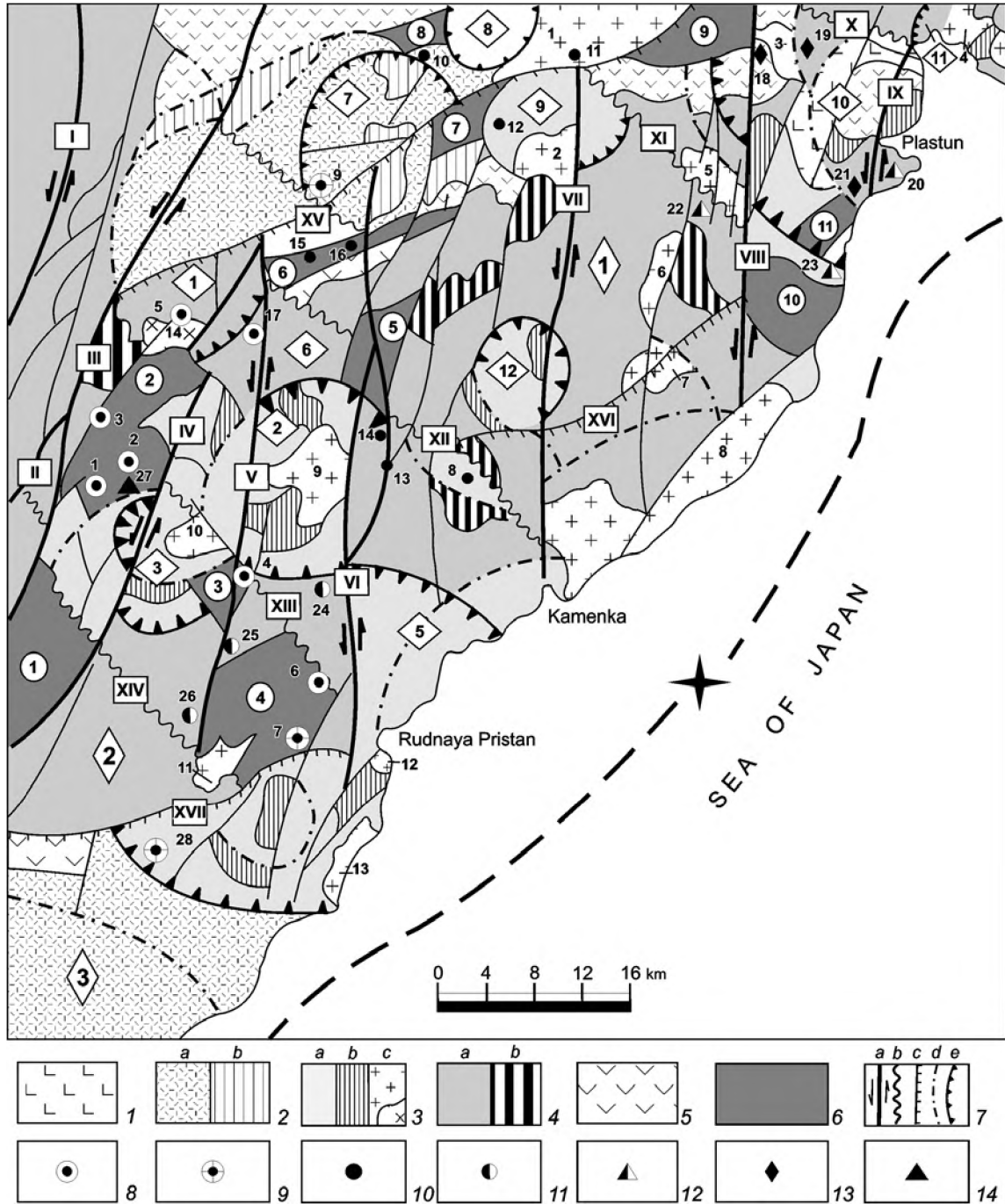


Fig. 6.2. Geostructural map of the Dalnegorsk ore district, modified after R.V. Korol, V.V. Vetrennikov, B.V. Kuznetsov, and V.A. Mikhailov.

Volcanic-intrusive complexes: (1) Kuznetsovo basalt-liparite; (2) Bogopolie trachyliparite with cover (a) and extrusive facies (b); (3) Dalnegorsk rhyodacite with cover (a), extrusive (b) and intrusive (c) facies [massifs (numerals on the map): (1) Evlampievsky, (2) Sarafanny, (3) Utesny, (4) Egorovsky, (5) Beresovy, (6) Oleniy, (7) Kedrovsky, (8) Oprichninsky, (9) Araratsky, (10) 27th Kluch, (11) Prymaya Mt., (12) Brinner, (13) Pribrezhny, and (14) Nikolaevsky]; (4) Primorsky rhyolite with cover (a) and extrusive (b) facies; (5) Sinancha andesite with volcanogenic molasse of the Petrozuevsky suite. (6) outcrops of the pre-Upper Cretaceous basement (Taukhe terrane fragments) [blocks (numeral in circle): (1) Vysokogorsky, (2) Dalnegorsk, (3) Sadovy, (4) Monomakhovo, (5) Lidovka, (6) Alikovsky, (7) Cheremukhovy, (8) Kamenka, (9) Dzhigitovsky, (10) Kedrovsky, and (11) Dukhovskiy]; (7) faults: (a) deep sinistral faults [(I) Vostochny, (II) Nezhdankovsky, (III) Dalnegorsk, (IV) Gorbushinsky, (V) Monastyrsky, (VI) Monomakhovo, (VII) Sheptunsky, (VIII) Plastun, and (IX) Astashevsky], (b) tension zones [(X) Dzhigitovsky, (XI) Kedrovsky, (XII) Smyslovsky, (XIII) Sadovy, and (XIV) Tigrovy], (c) upthrust-thrusts [(XV) Cheremshansky, (XVI) Oprichninsky, and (XVII) Zerkalny], (d) ring faults, (e) boundaries of the volcanotectonic structures. *Ore formations and deposit types:* (8) skarn-base-metal; (9) cassiterite-sulfide; (10) silver-base-metal polymetallic of vein type; (11) gold; (12) copper-molybdenum; (13) copper-porphyry, (14) borosilicate.

Volcanotectonic structures (numeral in "reclining" rhomb): (1) Nikolaevsky, (2) Trikluchevsky, (3) Solontsovy, (4) Monastyrsky, (5) Brinner, (6) Dovgalevsky-Gorbushinsky, (7) Kedrovsky, (8) Ozerkovy, (9) Sarafanny, (10) Plastun, and (11) Egorovsky. *Gross ignimbrite fields* (numeral in "vertical" rhomb): (1) Sheptunsky, (2) Kisinsky, and (3) Zerkalnensky.

Deposits: (1) Partizansky, (2) Pervy Sovetsky, (3) Verhkny, (4) Sadovy, (5) Nikolaevsky, (6) Lidovka, (7) Novo-Monastyrsky, (8) Krasnogorsky, (9) Cheremukhov (Bolshaya Sinancha), (10) Kamenny, (11) Krasnoskalny, (12) Sarafanny, (13) Zavetny, (14) Artsevsky, (15) Kirillovsky, (16) Maiminovskiy, (17) Dovgalevsky, (18) Bezymyanny, (19) Elizavetinsky, (20) Yakubovsky, (21) Plastun, (22) Oleny, (23) Ozerkovsky, (24) Maysky, (25) Berezoby, (26) Pasechy, (27) Dalnegorsk, and (28) Kisinsky. Dotted line shows position of the Beregovoy fault with magmatic center

trachyandesite, leucite trachyte) exposed in the open pit of the borosilicate deposit (Govorov, 1977). These rocks are enriched in Mg and Ca and depleted in Na and Fe. They are also depleted in Cu, Zn, Pb, Ag, and Sn in comparison with dikes of the Dalnegorsk Complex.

Thus, the principal characteristic feature of DOD that controls the metallogeny of its particular units is a combination of accretionary wedges with volcanotectonic structures of the central type. The Dalnegorsk, Lidovka, Sadovy, and Monomakhovsky blocks are large basement inliers. The Dalnegorsk, Solontsovy Hill, Briner Cape, Kedrovyy Creek, and Plastun volcanotectonic structures of the first order are surrounded by smaller volcanic calderas.

Northeastern strike-slip faults and conjugated northwestern normal faults are most important struc-

tural elements in DOD. The Dalnegorsk Shear Zone, 1.5–2.0 km in width, hosts the large Verkhnee and Nikolaevskoe deposits (Utkin, 1989). As follows from displacement of limestone and chert layers, the total magnitude of sinistral slip reaches 7.6 km. In the west, this zone is conjugated with the Nezhdanka River Thrust Fault. Turbidite of the Zhuravlevka River Terrane is overthrust here by the Taukhe River accretionary wedge. Northwestern grabens filled with volcanic rocks are regarded as pull-apart structures.

Ore mineralization. The localization of ore deposits in the central DOD is controlled by the Dalnegorsk intrusive dome-shaped structure (IDS) bounded in the west and east by sinistral strike-slip faults of northeasterly direction (Korsunov, 1991; Yushmanov, 1997). Normal faults and pull-apart structures striking

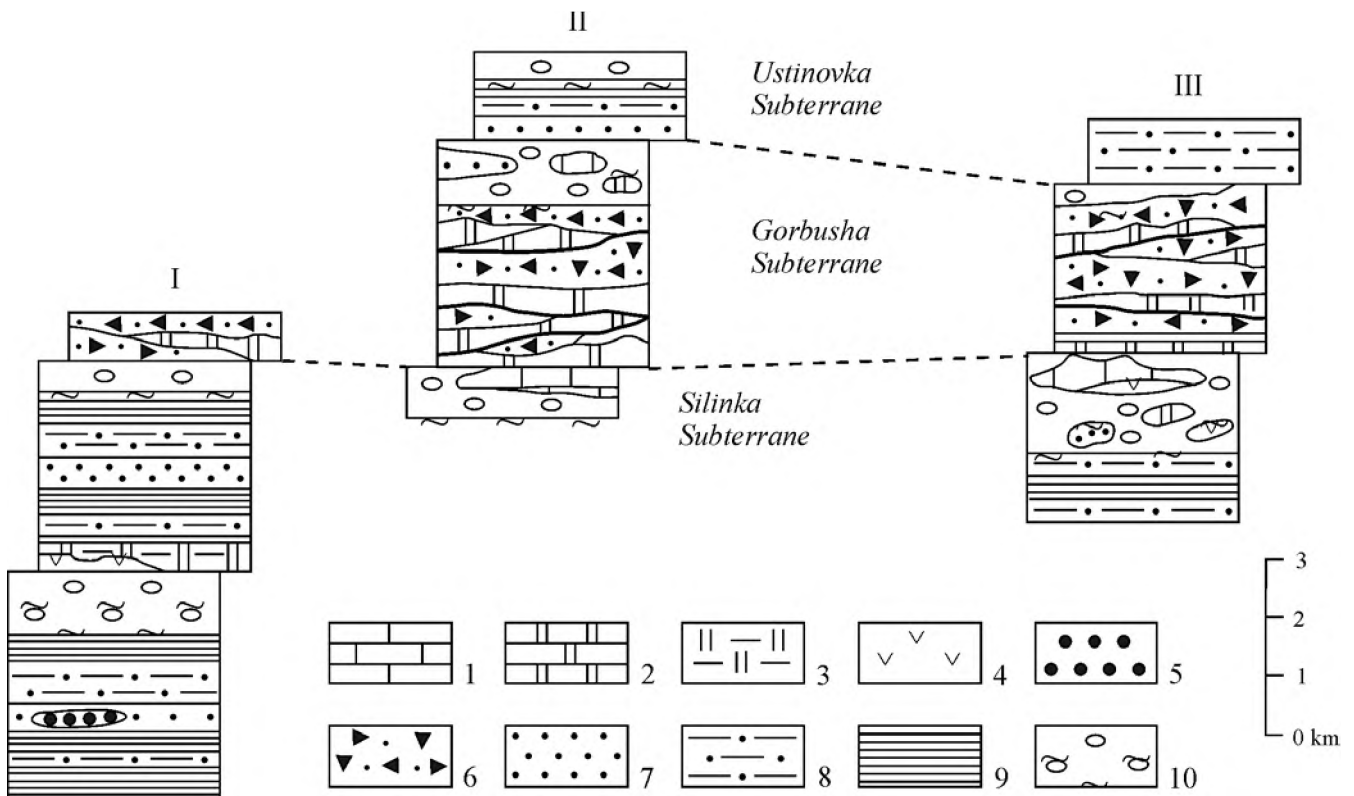


Fig. 6.3. Tectonostratigraphic columns of the northern Taukhe River Terrane, after Golozubov and Khanchuk (1995).

(I, II) Kavalerovo and (III) Dal'negorsk districts.

(1) Middle-Upper Triassic limestone; (2) Lower Triassic – Upper Jurassic chert; Middle-Upper Jurassic chert and siliceous tuffite; (4) Triassic-Jurassic basalt; Berriasian-Valanginian rocks: (5) conglomerate and coarse-grained sandstone, (6) inequigranular quartz-feldspar sandstone with chert and siltstone inclusions, (7) fine- and medium-grained sandstone, (8) flysch, (9) siltstone with sandstone interlayers; (10) Valanginian mixtite

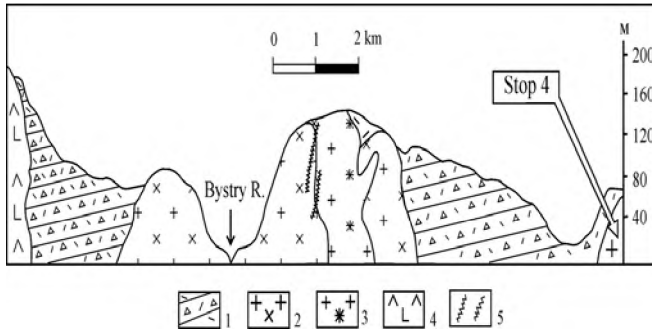


Fig. 6.4. Geological sketch of coastal cliffs, after I.N. Gorovov.

(1) rhyodacite tuff of the Siyanovo Formation; *Dalnégorsk Complex*: (2) diorite and quartz diorite of the second intrusive phase; (3) tourmalinized granite of the third intrusive phase; (4) neck of basaltic andesite, the first intrusive phase; (5) mineralized zones with quartz, arsenopyrite, wolframite, native bismuth, and molybdenite

in a northwestern direction serve as IDS boundaries in the north and south (Fig. 6.5). The near-latitudinal Trikluchevsky volcanotectonic depression (VTD) is localized in the central IDS. Its root is represented by the Mount Ararat granodioritic pluton. Small VTD filled with andesite are situated in marginal parts of IDS. A semicircle of basement inliers surrounds IDS in the west. The basement rocks crop out in erosional and tectonic windows from beneath the Maestrichtian-Danian volcanics.

The vertical magnitude of the IDS uplift is about one kilometer. The central, most eroded part of the dome is absolutely barren and is rimmed by an outer zone with economic ore. Ore deposition was controlled by lithological factors. Large base-metal skarn orebodies are confined to olistostrome units of the Silinka River Complex, whereas vein, stockwork, and disseminated mineralization is hosted in terrigenous rocks. Ag and Ag-Au mineralization is traced along the IDS margin.

The geology and metallogeny of other central-type structure is exemplified hereafter by the Kedrovyy volcanotectonic structure. Here, a general metallogenic zoning of DOD is located where the base-metal skarn and Ag-Pb-Zn vein deposits give way to quartz-wolframite and cassiterite-sulfide ores toward the Sea of Japan shelf and eventually to a Cu-Mo stockwork mineralization at the coastal cliffs.

The orebodies have a diverse morphology including (1) steeply and gently dipping pipelike and vein-shaped bodies within fault zones at contacts between carbonate and aluminosilicate rocks; (2) pipelike and lenticular bodies in limestone; (3) gently dipping stratiform lodes at contacts between carbonate and aluminosilicate rocks; (4) gently dipping len-

ticular bodies in limestone of the Gorbusha River Complex; (5) bodies with a complicated morphology at contacts between limestone blocks and volcanic rocks, and (6) quartz-carbonate-sulfide veins in aluminosilicate rocks.

Efficient prospecting guides for ore localization were worked out during exploration. They include: (1) olistostrome units of the Silinka River Complex (Fig. 6.6); (2) northeastern and northwestern faults and their junctions; (3) abrupt bends of fold limbs; (4) dome-shaped basement inliers covered by volcanics that serve as traps for ascending fluid flows; (5) contacts between carbonate and terrigenous rocks in the close proximity to faults; (6) limestone blocks incorporated into a volcanic matrix within large fault zones; (7) localization of ore deposits in the marginal parts of volcanotectonic depressions; (8) close spatial relations between the ore mineralization and intrusions of the Dalnegorsk Complex; (9) disseminated mineralization and haloes of albite-epidote propylitic, phyllic, and argillic alterations above the blind orebodies; (10) zoned geochemical haloes (Garbuzov et al., 1987).

Many of these prospecting guides are characteristic of the Nikolaevsky deposit, the largest in the district.

THE NIKOLAEVSKY BASE-METAL SKARN DEPOSIT [STOP 1]

Geological summary. The deposit is situated in the marginal part of the Nikolaevsky Creek Depression close to its boundary with the Dalnegorsk Horst (Fig. 6.6). A sedimentary sequence of Middle Jurassic age (Silinka River Complex) and Upper Cretaceous rhyolite and rhyodacite (Primorsky and Dalnegorsk complexes) serve as host rocks. Intrusive rocks comprise dikes of various compositions, subvolcanic granite porphyry, and the Nikolaevsky Creek gabbrodiorite intrusion. Country rocks are severely altered. The limestone is replaced by extended lenses of pyroxene and garnet-pyroxene skarn. Acid volcanics, especially those above the skarn lodes underwent propylitic and phyllic alteration. Pb, Zn, Ag, and other geochemical haloes reside in the upper volcanics (Fig. 6.7).

The Nikolaevsky Creek gabbrodiorite intrusion, about 1.2 km² in area, is cut by granite porphyry plugs. It is a part of an intrusive dome at the intersection of the Pribrezhny I Fault and a system of second-order faults. A negative gravity anomaly is related to the central part of this structure and surrounded by a

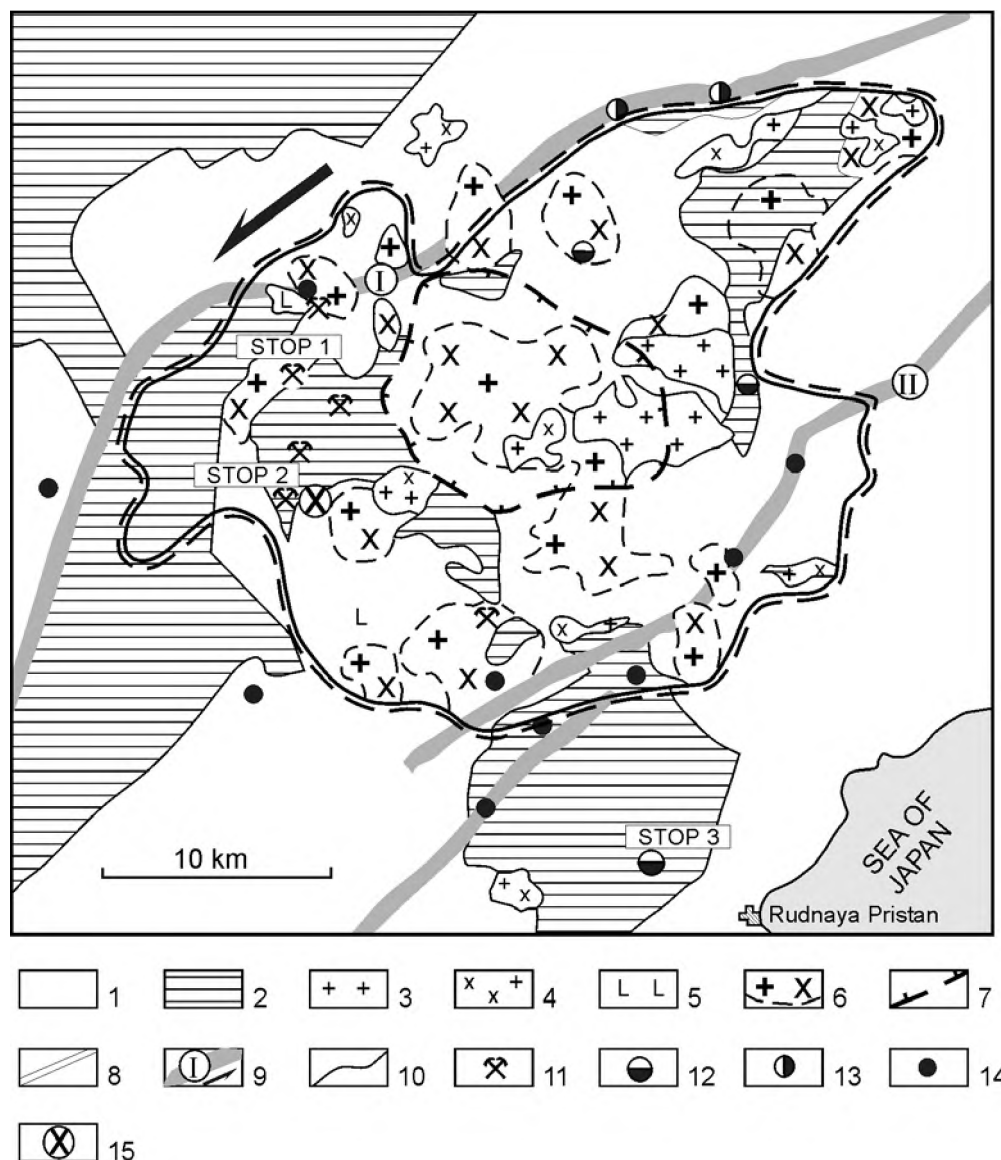


Fig. 6.5. Deep geological structure and localization of ore mineralization in the central Dal'negorsk ore district, after Yu.P. Yushmanov.

(1) Upper Cretaceous volcanics; (2) Lower Cretaceous terrigenous complexes; *Late Cretaceous intrusions*: (3) granite, (4) gabbrodiorite, (5) gabbrodiorite, (6) pluton contours at the depth from gravimetric data; (7) volcanic depression; (8) projection of intrusive dome; (9) large strike-slip faults: Pribrezhny I and Pribrezhny II; (10) geological boundaries. **Ore deposits**: (11) base-metal skarn (in operation), *veined ore deposits and occurrences*: (12) tin and base-metal, (13) silver and base-metal, (14) gold and silver; (15) Dal'negorsk borosilicate deposit

positive anomaly of the outer zone. The contour of a hidden pluton is delineated by arcuate fields of rocks with a high resistance (2000 Ω m) and by positive magnetic anomalies. The ethmolith-shaped intrusion has a cupola-like apex with local projections at a depth of 1600–1800 m. The initial depth of emplacement is estimated as 2.0–2.5 km. Massive equigranular gabbroic rocks occur at deep levels of the intrusion (horizons of –220 and –420 m at the Nikolaevsky deposit), whereas fine-grained porphyritic rocks are typical of its upper part. The Nikolaevsky Creek intru-

sion is suggested to be a root zone of a basaltic andesite volcano. The K-Ar age of gabbrodiorite of the first phase is close to 83 Ma.

Igneous rocks. The coarse- and medium-grained diorite and quartz diorite (Table 6.1) are the main igneous rock varieties; gabbrodiorite and gabbro are of subordinate importance. Fine-grained porphyritic rocks occur near the contact. The gabbrodiorite crystallized in the following succession: (1) intergrowths of large plagioclase (An₆₀₋₇₀) and pyroxene crystals, (2) medium-grained aggregate of plagioclase An₄₆₋₂₆,

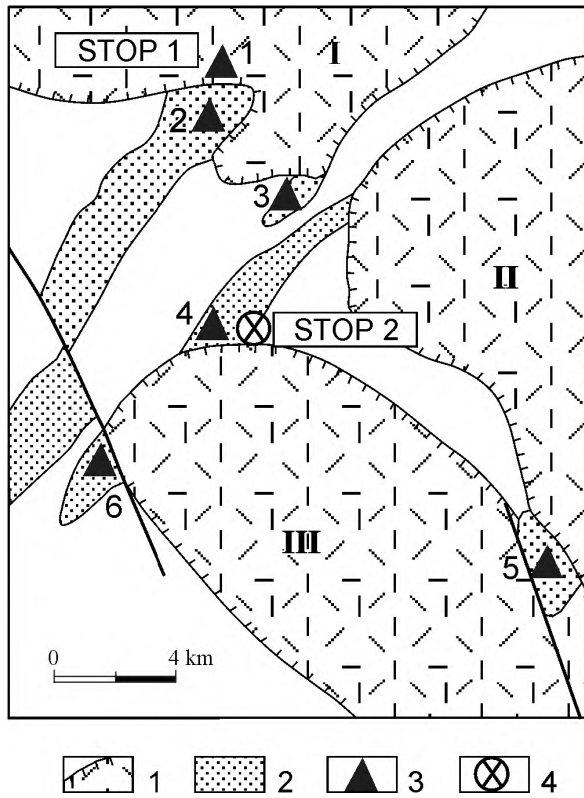


Fig. 6.6. Structural and lithological factors controlling the localization of base-metal skarn deposits in the Dal'negorsk district, after V.V. Ratkin. (1) Late Cretaceous volcanotectonic depressions (*numerals in the figure*: (I) Nicolaevsky Creek, (II) Trilyuchevskaya, (III) Solontsovskaya); (2) Lower Cretaceous olistostromic units (*numerals in the figure*: (1) Nikolaevskoc, (2) Verkhnee, (3) Pervoe Sovetskoe, (4) Partizanskoe, (5) Sadovoe, (6) Svetly Otvod); (4) Dal'negorsk borosilicate deposit

augite, quartz, and opaque minerals, and (3) quartz-feldspar granophyric aggregates with hornblende, biotite, and apatite (Table 6.1). The chemical compositions of feldspars are given in Table 6.2 and of dark-colored minerals, in Table 6.3.

Opaque minerals are composed of magnetite associated with granophyre intergrowths, ilmenite incorporated into augite, as well as of pyrrhotite and pyrite replacing magnetite and ilmenite.

The granite porphyry cuts the gabbrodiorite and consists of large (up to 0.5 cm) glomerophyric plagioclase (An₂₅₋₃₀), quartz, K-Na feldspar, and amphibole phenocrysts incorporated into a fine-grained granophyric groundmass. Quartz-feldspar granophyric aggregates often makes up coronas around the glomerophyric plagioclase.

The large gabbrodiorite pluton and minor granite porphyry intrusions are contrasting in composition (Table 6.4). They are spatially separated and thus are not members of a common fractionation series.

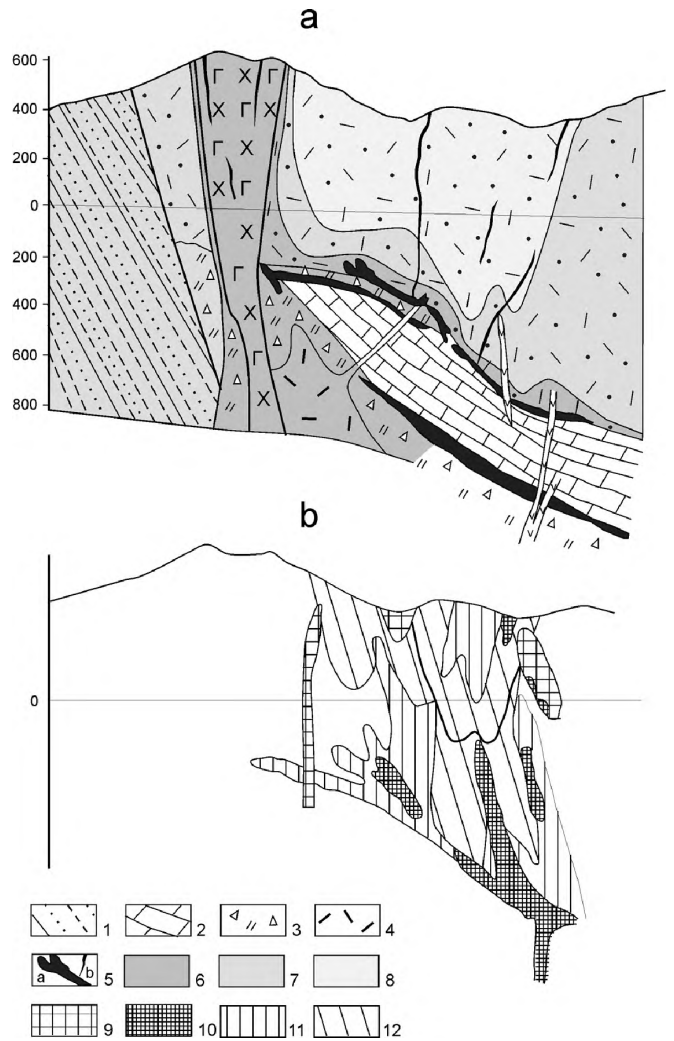


Fig. 6.7. Hydrothermal alteration (a) and geochemical (b) zoning of the Nikolaevsky deposit, a cross-section. The horizontal scale is arbitrary.

(1) terrigenous rocks in the basement; (2) limestone olistolith; (3) siliceous breccia; (4) rhyolite of vent facies; (5) contact-related base-metal skarn (a) and cross-cutting veined (b) orebodies; *altered rocks*: (6) actinolite-chlorite-epidote, (7) epidote-chlorite-sericite, and (8) quartz-chlorite-hydromica; *element assemblages in geochemical haloes*: (9) W-Mo-Sn-Ag, (10) Pb-Zn-Cu, (11) Pb-Zn-Ag, and (12) Pb-Ag-Sn

Ore mineralization. Contact-related and cross-cutting orebodies are distinguished by their morphology and structure.

The contact-related blanketlike lodes and lenses of infiltration skarn are localized at contacts between the limestone unit and both overlying volcanic rocks (the Vostok lode) and underlying sedimentary breccia (Nizhnee, Podizvestkovoe, and Rezervnoe orebodies). The morphologically complex orebodies are confined to limestone blocks torn away from the main unit (Glybovooe orebody).

Modal mineral compositions (vol %) of the Nikolaevsky Creek intrusion

Sample number	Rock	Pl	Px	Amph	Opaque	Qtz	Kfs	Ap	Secondary minerals
A-422	Gabbrodiorite	66.5	24.1	-	3.0	1.5	2.2	1.5	1.2
G-137	Gabbrodiorite	68.0	18.4	-	5.8	2.9	3.2	0.7	1.0
A-424	Gabbrodiorite	70.1	21.9	-	1.7	-	5.1	1.0	0.2
A-423/7	Gabbrodiorite	67.2	21.2	-	2.4	-	3.4	0.6	5.2
A-423/4	Diorite	61.0	12.3	3.5	4.1	7.2	6.3	0.5	5.1
G-153	Diorite	59.4	17.8	6.2	2.4	6.0	7.0	0.3	0.9
A-422/5	Diorite	61.7	16.9	0.9	4.2	6.9	5.0	0.6	3.8
A-423/5	Diorite	64.9	10.1	2.3	2.9	6.3	8.4	1.1	4.0
G-199	Quartz diorite	49.2	3.2	12.3	2.0	13.1	7.3	0.8	12.1

Cross-cutting extended veins and stockwork zones, 0.3–5.0 m in width, reside in the upper volcanics at a depth of 500–800 m (Serebryanaya, North-eastern, and Northwestern zones). Veins and veinlets cross-cut the massive sulfide skarn ore at a depth of 500–800 m (Fig. 6.7). Hedenbergite is markedly bleached at the contact with veins (Fig. 6.8).

A specific morphology is typical of orebodies hosted in the rhyolitic neck and its surroundings. The sulfide disseminations, thin quartz-sericite-sulfide

veinlets, small pockets and lenses occur close to the neck contacts and vanish away from the neck.

Ore mineralogy and geochemistry. More than 60 minerals were reported from the deposit.

Hedenbergite is the major mineral (up to 90% of total skarn volume) that consists of hedenbergite, johannsenite, and diopside end members and forms radiate, short columnar, and cryptocrystalline aggregates. The downward depletion in Si, Fe, Na, the concomitant enrichment in Al and Ca, and the growth of

Table 6.2

Chemical compositions and crystallochemical coefficients of feldspars from gabbrodiorite, the Nikolaevsky Creek intrusion

Component	A-422			A-422/5		A-423		
	1	2	3	4	5	6	7	8
SiO ₂ , wt %	54.43	65.31	51.20	65.82	53.69	54.34	63.28	65.97
TiO ₂	0.01	0.01	0.01	0.01	0.01	0.01	0.01	0.01
Al ₂ O ₃	28.64	21.38	29.92	18.63	28.92	28.91	22.53	18.97
FeO	0.37	0.14	0.55	0.06	0.69	0.71	0.22	0.31
MgO	0.03	-	0.04	-	0.19	0.02	-	0.04
CaO	9.46	1.95	14.04	0.31	11.56	11.90	4.38	0.06
Na ₂ O	5.68	10.07	3.44	2.79	4.64	4.30	6.59	1.58
K ₂ O	0.53	0.14	0.24	13.00	0.45	0.40	0.45	14.80
Total	99.15	99.01	99.42	100.62	100.15	100.60	97.46	101.75
Si	2.490	2.895	2.350	2.992	2.433	2.448	2.845	2.984
Al	1.544	1.117	1.618	0.998	1.544	1.534	1.193	1.011
Fe	0.014	0.005	0.021	0.002	0.026	0.027	0.008	0.012
Mg	0.002	-	0.003	-	0.013	0.001	-	0.003
Ca	0.463	0.092	0.690	0.015	0.561	0.574	0.211	0.003
Na	0.506	0.865	0.306	0.246	0.407	0.375	0.574	0.139
K	0.031	0.008	0.014	0.754	0.026	0.023	0.026	0.854
An	46.3	9.5	68.3	1.5	56.5	59.0	26.0	0.3
Ab	50.6	89.7	30.3	24.2	40.9	38.6	70.8	14.0
Or	3.1	0.8	1.4	74.3	2.6	2.4	3.2	85.7

Note: (1–3, 5–7) plagioclase; (4, 8) K-feldspar. See Table 6.1 for sample numbers.

Table 6.3

Chemical compositions and crystallochemical coefficients of clinopyroxenes (1, 2) and amphiboles (3, 4) from gabbrodiorite, the Nikolaevsky Creek intrusion

Component	1	2	3	4
	A-422	A-422/5	A-422/5	A-423
SiO ₂ , wt %	50.96	50.36	53.27	49.24
TiO ₂	0.01	0.01	0.01	0.44
Al ₂ O ₃	2.37	0.56	1.40	3.90
FeO	18.75	20.08	18.26	22.12
MgO	11.54	7.95	12.12	9.25
MnO	0.15	0.13	0.22	0.29
CaO	12.26	19.58	11.44	11.28
Na ₂ O	0.31	0.27	0.25	0.85
K ₂ O	0.11	0.03	0.10	1.11
Total	96.46	98.97	97.07	98.48
Si	2.004	1.992	7.900	7.443
Al _T	-	0.008	0.100	0.557
Al _{VI}	0.110	0.018	0.145	0.137
Ti	-	-	0.001	0.050
Fe ²⁺	0.616	0.664	2.264	2.795
Mg	0.676	0.468	2.677	2.082
Mn	0.005	0.004	0.027	0.037
Ca	0.516	0.829	1.817	1.827
Na	0.024	0.021	0.072	0.249
K	0.005	0.002	0.019	0.213

Note: See Table 6.1 for sample numbers.

iron oxidation degree are noticed. Trace element contents in hedenbergite are (ppm): In (1.82), Se (8.5), Te (1.8), Tl (1.3), Ga (4.1), and Ge (10.7).

Abundant calcite of several generations fills interstitial spaces between hedenbergite crystals, occurs in quartz-carbonate-sulfide orebodies, and forms euhedral crystals in cavities. The CaO: MnO: FeO: MgO ratio is equal to (1) 46:2:1:0.7; (2) 39:1.5:1:0, and (3) 26:2:0.8:1. The association of calcite with quartz (10-60% of the vein volume) is typical.

Ilvaite, garnet, fluorite, wollastonite, diopside, danburite, and datolite are less abundant. Albite, chlorite, epidote, prehnite, and muscovite are and in altered rocks.

Sphalerite (Cd-bearing Fe-rich marmatite) with Se, Te, Tl, Ge, and Sn admixtures prevails over other ore minerals. Galena of two generations is the second (up to 4% of orebody volume). Galena I contains (wt %): Bi (0.024), Ag (0.040), and Sb (0.037); in the Nizhnyaya lode: Bi (0.63) and Ag (0.14). Galena II contains (wt %): Bi (0.773), Ag (0.309), and Sb (0.01). In addition, the galena of both generations

contains (ppm): Se (12.5), Te (11.4), In (1.4), Ge (1.73), Tl (1.03).

Pyrrhotite, chalcopyrite, arsenopyrite, pyrite, stannite, and stibnite are less abundant. Pyrargyrite, miargyrite, freibergite, andorite, diaphorite, and owyheeite were found in near-surface segments of veins in association with jamsonite and boulangerite.

Three ore types are recognized: (1) skarn-sulfide, (2) quartz-calcite-sulfide, and (3) quartz-carbonate-sulfide with sulfosalts.

Ores (1) and (2) commonly are massive, irregularly disseminated, or banded; the Pb and Zn grade decreases with depth. Granoblastic, cataclastic, emulsion, idiomorphic, and interstitial textures are typical.

Two ore varieties are distinguished in type (3): (i) Ag-Bi ore with impregnated, pocket-impregnated, and less developed massive, brecciated, occasionally drusy textures occurring at deep levels of veins, where quartz, calcite, ankerite, sphalerite, galena, pyrrhotite, and arsenopyrite are abundant and (ii) Sb-As ore at the upper levels of veins. The amount of sulfides diminishes at the expense of Ag-bearing sulfosalts, quartz, sericite, chlorite, and hydromica.

Formation conditions. The deposit was formed in the Late Cretaceous-Paleogene at the end of the evolution of the Dalnegorsk volcanic-plutonic complex. The ore was deposited during two stages: (1) skarn-sulfide and (2) quartz-carbonate-sulfide. Mineral assemblages of the first stage were deposited at a temperature of 440-250°C with a vertical temperature gradient of about 10°C/100 m. The early quartz-sulfide and the late quartz-calcite-sulfosalts mineral assemblages in the cross-cutting veins were formed at a temperature of 400-100°C. The vein mineralization was developed at a shallower depth in comparison with the earlier skarn-sulfide ore. This mineralization distinguishes the Nikolaevsky deposit from other deposits of the Dalnegorsk ore district.

THE DALNEGORSK BOROSILICATE DEPOSIT [STOP 2]

Geological summary. The Dalnegorsk borosilicate deposit is situated in the central part of the ore district (Fig. 6.6) on the right-hand bank of the Rudnaya River. Host rocks are represented by olistostromes of the Silinka River Complex with limestone olistoliths of the Middle-Upper Triassic. Limestone lenses vary in size from 150-300 m to 3.5 km. They extend northeastward and plunge at angles of 70-80° to a depth of 1700 m. In the southeast, the Silinka River Complex is overthrust by the Gorbusha Com-

Major and trace element compositions of rocks from the Nikolaevsky Creek intrusion

Component	1	2	3	4	5	6	7	8	9
	A-422	A-424	A-423/7	A-423/4	A-423/5	A-422/5	A-422/3	V-1558	G-952
SiO ₂ , wt%	48.69	50.70	52.04	54.90	54.90	55.79	66.50	68.85	74.69
TiO ₂	1.34	0.70	0.86	1.14	0.94	0.82	0.60	0.33	0.12
Al ₂ O ₃	20.45	21.40	20.33	17.77	17.70	18.00	15.11	14.85	13.45
Fe ₂ O ₃	2.37	0.29	0.58	4.19	0.75	1.76	1.37	0.06	1.45
FeO	6.14	6.14	6.28	2.89	6.53	5.06	2.23	2.89	0.69
MnO	0.14	0.13	0.19	0.06	0.14	0.14	0.06	0.01	0.11
MgO	3.12	3.90	2.68	2.55	3.43	3.41	2.15	0.65	0.59
CaO	9.83	9.28	7.88	8.11	6.32	7.19	3.40	2.02	1.10
Na ₂ O	3.23	3.24	3.65	2.79	2.99	2.93	3.14	3.89	1.52
K ₂ O	0.799	1.21	2.40	1.66	2.27	2.04	3.04	3.09	4.09
P ₂ O ₅	0.60	0.41	0.30	0.23	0.45	0.25	0.09	0.38	0.07
H ₂ O ⁻	-	0.35	0.29	-	-	-	0.11	0.33	-
LOI	3.25	2.41	2.71	3.70	3.14	2.32	2.55	2.24	2.17
Total	99.95	100.16	100.19	99.99	99.56	99.69	100.35	99.59	100.05
Rb, ppm	43	40	60	41	76	86	115	n.d.	138
Sr	521	545	523	400	443	448	323	n.d.	68
Ba	201	260	66	375	629	403	698	n.d.	800
Zr	71	66	119	144	208	172	348	n.d.	126
Nb	10	17	7	13	11	12	20	n.d.	14
La	16	13	29	29	48	39	59	n.d.	26
Ce	24	29	22	35	60	46	71	n.d.	63
Nd	4	14	13	9	30	23	39	n.d.	20
Y	31	20	35	35	43	32	50	n.d.	41
Ni	16	41	37	23	39	25	10	8	15
Co	25	21	28	26	27	18	11	10	8
Cr	20	64	16	19	24	48	19	9	26
V	300	250	150	190	180	200	110	63	59
Cu	96	76	86	80	84	73	72	17	12
Zn	99	140	130	86	160	93	46	63	64
Ag	0.07	0.08	0.04	0.05	0.05	0.07	0.05	0.04	0.12
Pb	12	14	27	14	45	25	25	30	45
Sn	2	2	1	3	2	3	4	4	3
Mo	1.5	1.9	1.3	1.9	1.6	1.8	2.6	4	1.3
B	33	19	19	21	25	26	22	19	34
F	400	400	60	400	430	480	230	n.d.	n.d.

Notes: (1-6) gabbro-diorite; (7) cm-wide vein of granophyric granite in diorite; (8, 9) granite porphyry. See Table 6.1 for sample numbers.

plex composed of siltstone, sandstone, and chert with shale and basalt interlayers.

N-S faults divide the borosilicate skarn zone into six blocks (Fig. 6.9). The blocks, up to 1 km in cross section, are traced to a depth of 1.0–1.5 km. Vertical displacements along such faults reach a few hundred meters. The Central and Dolinny blocks show most uplift, and the rocks in these blocks are

completely skarnified. Marginal blocks are relatively subsided.

Igneous rocks. Igneous rocks comprise basic sills and dikes of the Gorbusha olistostrome complex, which are not related to the ore mineralization, and the Dalnegorsk and Sikhali volcanic-plutonic complexes.

The Dalnegorsk Complex is represented by a hidden granitic pluton beneath the borosilicate de-

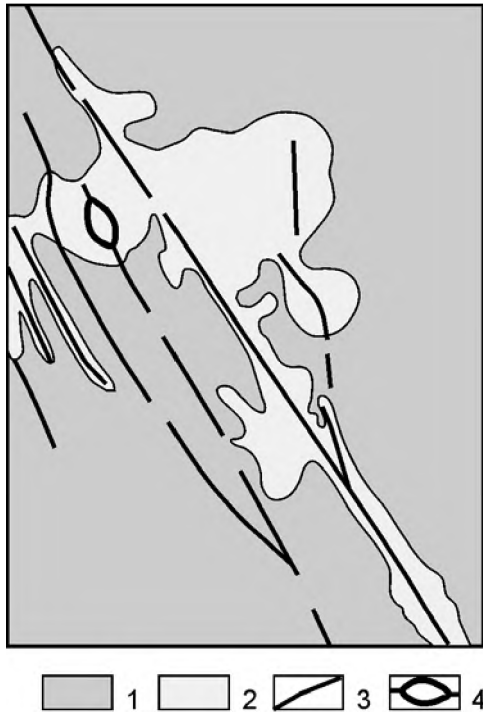


Fig. 6.8. Cross-cutting relationships between the Vostok skarn lode and veined orebodies.
 (1) hedenbergite skarn; (2) bleached skarn; (3) quartz-carbonate-sulphide veinlets; (4) miarolitic cavity

posit. Four boreholes penetrated the granitic rocks. The horizontal distance between the deepest of these boreholes attains 700 m. Three types of granitic rocks were identified: (1) biotite-amphibole porphyritic adamellite at the deepest levels; (2) aplite-like and granophyric granites of the apical zone and offsets; (3) a granite porphyry dike, 12 m thick. The mineral compositions of igneous rocks are presented in Table 6.5 and their chemical compositions, in Table 6.6.

Yu.K. Pustov (IGEM RAS, Moscow) determined the K-Ar age of adamellite at 59–64 Ma, and the granite was dated at 50 Ma.

Adamellite is a pinkish gray porphyritic rock of hypidiomorphic texture with plagioclase (22–26 vol %), quartz (15–20 vol %), and less abundant K-Na feldspar ($Or_{53}Ab_{47}$, $2V = 54-60^\circ$), amphibole (Table 6.7), and biotite (Table 6.8) phenocrysts occupying ca. 6 vol % (Table 6.5).

The plagioclase from adamellite forms large zoned tabular crystals and intergrowths of 4-5 and more grains, up to 6–10 mm in size. A crystal core consisting of ordered labrador is surrounded by outer zones composed of low-ordered andesine and oligoclase. The plagioclase from the groundmass is distinguished from the intergrowths by its composition ($An_{30-26-24}$), high ordering, the lack of pronounced zoning, and by a lesser crystal size.

Accessory apatite, zircon, and ilmenite occur as inclusions in plagioclase and dark-colored minerals. Ortite forms large (up to 0.5 mm) crystals.

Aplite-like and granophyric granites are penetrated by boreholes at a depth of 1170–1190 m where they occur as near-contact facies and separate intrusive bodies. The contact with adamellite was not cut by boreholes. The thickness of granitic bodies is 50–60 m.

This is a light-colored fine-grained porphyritic rock with aplitic, granophyric, granitic, and locally pegmatoid textures. The granite contains 35–40 vol % of quartz and up to 40 vol % of K-Na feldspar ($Or_{60}Ab_{40}$). This composition occupies the central part of the granite field on the Streckeisen triangle; the SiO_2 content is within the range of 72–74 wt % (Table 6.6).

The plagioclase from the granite is more sodic (An_{35-18}) than that from the adamellite; the zoning is less pronounced. Glomeroporphyritic intergrowths with zoned crystals (An_{60-44}) are encountered only occasionally. Dark-colored minerals are composed of the brown-green hornblende (Table 6.7) and biotite (Table 6.8). Rare grains of Fe-rich salite (Table 6.7) were noticed.

The granite porphyry was penetrated by one borehole at depths of 1160–1164 m and 1170–1175 m. This is a light gray very fine-grained porphyritic rock. Phenocrysts vary from 2 to 4 mm in size against 0.05–0.10 mm of the grains in aplitic groundmass. The granite porphyry consists of the same major and accessory minerals as those of the above-mentioned adamellite and granite, but is enriched by 10–15 vol % in K-Na feldspar ($Or_{60}Ab_{40}$) (Table 6.5). The ordered plagioclase fits An_{26-18} in composition; more calcic plagioclase (An_{45-30}) was reported from the central parts of the glomeroporphyritic intergrowths. The chemical composition of the granite porphyry is given in Table 6.6.

Sikhali Volcanoplutonic Complex distinguished by Govorov (1977) is represented by a number of dikes and small rock stocks belonging to an alkaline-potassium series with the following succession of rocks: isite, hornblende shonkinite, essexite-diabase, epileucitic trachyte, and trachyaandesite. All rock types in this complex show a stable predominance of K in respect to Na and a deficit of microelements of siderophile, chalcophile, lithophylic groups. According to Govorov, these rocks are the products of fault-related rather than zoned melting of the upper mantle metasomatic substrate represented by an eclogitized gabbroid asthenolith with juvenile entry of H_2O , K, and B volatile compounds. The rocks are dated as 72 to 35.6 Ma.

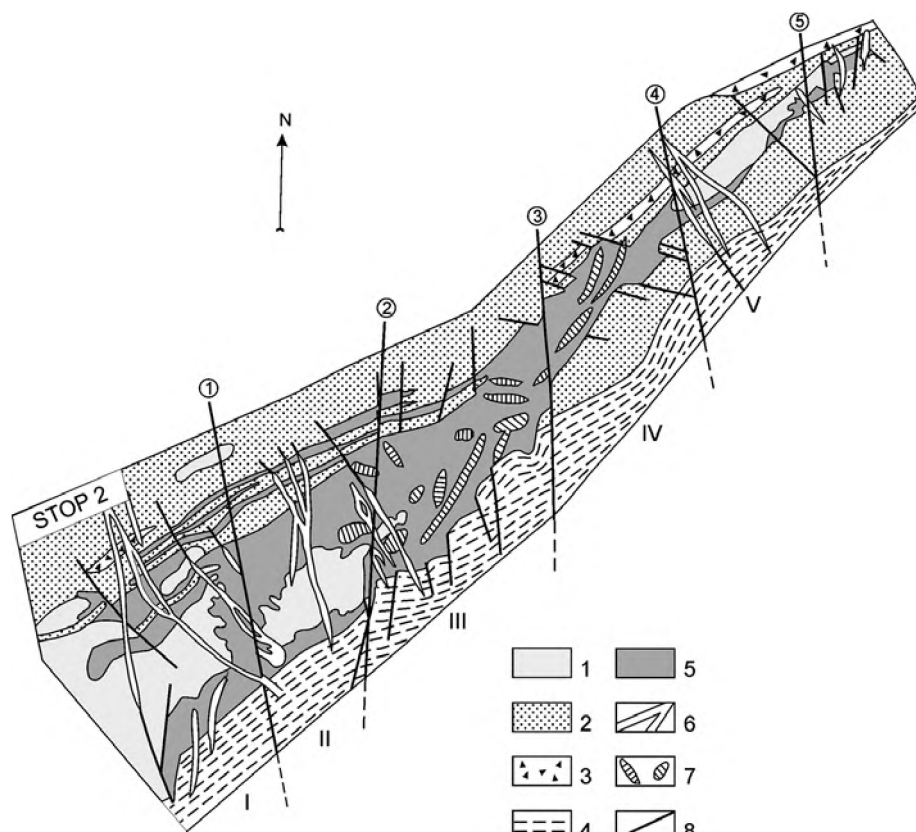


Fig. 6.9. Geological sketch map of the Dal'negorsk borosilicate deposit. Compiled by V.V. Ratkin using the data reported by N.A. Nosenko (1996).

(1) Triassic limestone; (2) Lower Cretaceous sandstone; (3) sedimentary breccia with small limestone and chert fragments; (4) Triassic-Jurassic siliceous rocks and Lower Cretaceous siltstone; (5) skarn zone; (6) Paleogene and (7) Early Cretaceous basic dikes; (8) faults (*numerals in the figure*): (1) Zapadny, (2) Khrustal'ny, (3) Kremnisty, (4) Sentabr'sky, (5) Flangovy; *blocks*: (I) Partizansky, (II) Zapadny, (III) Tsentralny, (IV) Dolinny, (V) Levoberezhny, (VI) Zapareval'ny

Skarn. The Dalnegorsk borosilicate deposit is a concordant stratiform skarn body extending for 3.5 km. The skarn mainly replaces the limestone and, to a lesser extent, the terrigenous rocks. The skarnified rocks reach 540 m in thickness and extend for 1728 m down dip. The thickness of altered terrigenous rocks is less than 15m. Nearly N-E and northeastern faults and limestone/granite contact control the localization of skarn alteration.

The main skarn body is largely composed of wollastonite, garnet, pyroxene, quartz, calcite, datolite, danburite, and axinite; epidote, chlorite, sericite, albite, actinolite, fluorite, apophyllite, stilpnomelane, siderite, manganocalcite, ilvaite, hematite, hisingerite, Fe, Pb, Zn, Cu, Co, and As sulfides are present in lesser amounts; native Bi and Sb also occur.

Wollastonite forms two generations. The white or cream-colored pink columnar-radiating wollastonite of the first generation mainly occurs at deep levels. Wollastonite of the second generation was reported both from the lower and the upper parts of skarn body. At the bottom, the mineral is white,

whereas at the top it is pinkish-brown. The chemical composition of wollastonite differs from the theoretical formula by a depletion in SiO_2 (1.85-2.15 wt %), CaO (4.82-10.78 wt %) and by an enrichment in FeO (4.61 wt %) and MnO (6.26 wt %). The ferro-manganous wollastonite (1) with >3 wt % of the total $\text{Fe}_2\text{O}_3 + \text{FeO} + \text{MnO}$ sum, (2) manganous wollastonite with 1.5-3.0 wt % of this sum, and (3) the wollastonite proper with < 1.5 wt % of the above sum are recognized. Variety (1) occurs at the upper levels of central blocks, variety (2) is related to the middle and lower levels, and variety (3) is confined to the deep part of the deposit. Ni, Cr, V, and Sn contents in wollastonite increase from white (deep-seated) to brown (shallow-seated) varieties; the reverse tendency is revealed for B, Pb, Zn, and Ag.

Pyroxene of two generations occurs in all skarn types. *The first generation* is a light green to greenish gray mineral. Fine-grained and columnar-radiating aggregates of this mineral are known from the near-contact zone and sporadically at a distance from the contact in association with garnet and wollastonite.

Modal mineral compositions (vol %) of granitic rocks from the Dalnegorsk pluton

NN	Borehole	Sample	Depth, m	Phenocrysts				Groundmass						Secondary minerals
				Qtz	Pl	Fsp	Bt+Amph	Qtz	Pl	Fsp	Bt	Amph	Accessory	
1	753	A-474-b	1158	16.6	9.8	-	-	22.8	13.5	34.2	-	0.9	0.2	2.0
2	//	A-474-c	1160	6.1	8.9	6.1	0.5	30.6	10.4	35.8	-	-	-	1.6
3	//	A-474-e	1164	3.4	26.7	2.1	0.8	26.0	10.2	30.2	-	-	0.2	0.4
4	//	A-474-f	1174	17.8	21.8	-	6.3	21.8	12.9	19.0	-	0.3	0.1	-
5	//	A-474-g	1177	14.4	27.3	-	5.5	22.0	6.5	20.2	2.5	1.1	0.2	0.3
6	//	A-474-i	1189	12.4	26.3	-	-	18.6	8.2	25.5	0.1	8.2	0.1	0.6
7	//	A-474-o	1201	21.3	25.0	-	3.5	20.9	6.5	19.1	1.5	1.1	0.1	1.0
8	//	A-474-p	1217	8.5	29.0	-	-	27.2	6.7	20.1	6.3	1.5	0.1	0.8
9	753A	753-a ₁	1103	-	-	-	-	39.4	27.7	32.3	-	0.5	0.1	-
10	//	753-a ₂	1106	2.5	5.0	-	-	32.6	17.8	40.5	1.3	-	0.3	-
11	//	753-a ₄	1112	-	11.3	-	-	31.7	17.2	34.9	4.6	-	0.3	-
12	//	753-a ₉	1126	-	16.7	-	-	35.7	15.1	28.5	-	3.0	0.6	0.4
13	//	753-a ₁₄	1140	14.3	14.9	-	-	24.9	11.7	28.7	-	5.0	0.5	-
14	972	(6)	1211	14.3	14.9	-	-	38.0	28.9	31.6	0.2	0.2	0.1	1.0
15	875	(5)	1204	-	-	-	-	24.3	43.3	30.4	1.1	0.5	0.2	0.2
16	//	(6)	1205	-	-	-	-	36.6	23.1	37.1	1.6	1.5	0.1	-

Notes: (1, 9-16) granite; (2, 3) granite porphyry; (4-8) adamellite.

The pyroxene of the second generation is green or dark green and occurs as coarse- and medium-grained aggregates. The radiating aggregates are predominant in the hedenbergite-datolite facies of the skarn body. Diopside, Fe- and Al-hedenbergite are most common.

Diopside is a major mineral in the endoskarn replacing the granite, while hedenbergite is typical of exoskarn replacing the limestone. High Zn (up to 650 ppm), Ni (up to 62.5 ppm), V (up to 49 ppm), Cu (up to 56 ppm), Sn (up to 13.7 ppm), Ag (up to 0.15 ppm) and B (up to 500 ppm) contents are typical of pyroxene.

Garnet mainly occurs in marginal parts of the skarn body. Dark green fine-grained garnet is noticed both in the endo- and exocontact zones of the granitic pluton, where it replaces the wollastonite and pyroxene. Greenish yellow, pink and orange garnet grains form massive pockets and lenses within the orebody. Light green translucent garnet occurs in cavities in association with quartz and calcite. The garnet is related to the andradite-grossular series. $Andr_{66.4}Gros_{21.8}$ is typical for skarn replacing limestone; $Andr_5Gros_{86}$ and $Andr_{24}Gros_{62.2}$ are characteristic of skarn replacing terrigenous rocks and granite, respectively. All garnet varieties are enriched in Sn (up to 52 ppm), B (95.4 ppm), Cu (up to 80.1 ppm), Ag (0.16 ppm), Cr (110 ppm), and Ni (up to 60.2 ppm).

Axinite was found in skarn at the limestone/sandstone contact. Along with other borosilicates, it forms the Aksinitovaya and Vodorazdel'naya lodes.

Danburite – the major borosilicate of the deposit – occurs in the upper levels, where it makes up the monomineral lenses and pockets. At lower levels (from 700 to 1,100 m), this mineral occurs in thin-banded aggregates intercalating with pale green datolite, pyroxene, and less abundant wollastonite.

Two types of alteration with their specific zoning are recognized:

- *contact-related bimetasomatic skarn alteration* with the following downward succession of zones: (1) wollastonite, (2) pyroxene and wollastonite, (3) garnet-pyroxene, (4) garnet (grossular) replacing granite, and (5) pyroxene-garnet replacing granite;
- *infiltration skarn alteration* extending along steeply dipping fractures with zones (from top to the bottom): (1) garnet, (2) pyroxene garnet, (3) pyroxene and along the lode axis with zones (from bottom to the top): (1) wollastonite, (2) datolite-wollastonite, (3) datolite-pyroxene, and (4) garnet-datolite.

The longitudinal zoning of the skarn lens is expressed by various degrees of alteration: at the south-

Major and trace element compositions of granitic rocks from the Dalnegorsk pluton

Component	Samples from borehole 753 (see Table 5)							
	A-474b	B-14971	A-474c	A-474e	A-474f	A-474g	A-474p	B-1498a
	Depth, m							
	1150	1158	1160	1164	1174	1177	1217	1326
	Granite		Granite porphyry		Adamellite			
SiO ₂ , wt%	74.30	72.73	72.93	72.46	70.69	71.35	72.35	69.32
TiO ₂	0.25	0.020	0.27	0.23	0.27	0.31	0.26	0.42
Al ₂ O ₃	13.30	13.08	13.92	13.76	14.55	13.84	13.37	14.36
Fe ₂ O ₃	0.35	1.24	0.64	0.89	1.03	0.50	0.89	1.38
FeO	1.19	0.95	0.51	0.74	1.38	2.44	1.92	2.26
MnO	0.04	0.07	0.06	0.05	0.01	0.01	0.01	0.07
MgO	0.37	0.06	0.66	0.40	0.82	0.90	0.85	0.72
CaO	2.73	3.64	2.47	3.90	2.88	2.65	2.21	3.31
Na ₂ O	2.78	2.45	2.83	3.40	3.90	3.62	3.74	3.74
K ₂ O	3.70	4.67	4.39	4.12	3.04	3.10	3.14	3.09
P ₂ O ₅	0.05	0.12	0.10	0.06	0.08	0.10	0.10	0.19
H ₂ O [*]	0.30	-	0.31	-	-	-	0.39	0.23
LOI	0.59	0.42	0.64	0.03	0.87	0.99	0.51	0.61
Total	99.59	99.63	99.73	100.04	99.54	99.80	99.73	99.70
Rb, ppm	110	n.d.	134	92	99	75	97	n.d.
Sr	135	n.d.	131	198	226	208	251	n.d.
Ba	729	n.d.	916	761	816	694	671	n.d.
Zr	125	n.d.	125	158	170	186	159	n.d.
Nb	11	n.d.	8	11	9	11	9	n.d.
La	53	n.d.	35	46	28	40	22	n.d.
Ce	70	n.d.	56	60	51	68	49	n.d.
Nd	43	n.d.	30	34	23	43	28	n.d.
Y	14	n.d.	14	16	21	14	19	n.d.
Ni	9	n.d.	10	14	16	15	17	n.d.
Co	4	n.d.	3	5	7	6	7	n.d.
Cr	26	n.d.	9	17	17	14	11	n.d.
V	43	n.d.	34	38	56	75	61	n.d.
Cu	12	n.d.	10	13	12	16	14	n.d.
Zn	38	n.d.	38	37	40	53	42	n.d.
Ag	0.19	n.d.	0.23	0.16	0.16	0.12	0.09	n.d.
Pb	50	n.d.	50	48	53	49	37	n.d.
Sn	9	n.d.	6	12	7	16	12	n.d.
Mo	3.4	n.d.	4.0	5.2	4.5	3.2	1.6	n.d.
B	33	n.d.	64	22	41	47	31	n.d.
F	280	n.d.	260	340	n.d.	630	n.d.	n.d.

western and northeastern flanks the skarn occurs sporadically, whereas complete replacement of limestone is established in the central part.

- The borosilicate mineralization is expressed as stratiform lodes, lenses, pockets and disseminations. Limits of the mineralized zone are con-

trolled by upper and lower limestone contacts. Pipelike Aksinitovaya and Vodorazdel'naya lodes, and the vein-shaped Levoberezhnaya lode are controlled by faults and fractures.

Three types of boron ore are recognized: datolite (Glavnaya and Malaya lodes);

Chemical compositions and crystallochemical coefficients of amphiboles (1-8), and clinopyroxene (9) from granitic rocks of the Dalnegorsk pluton

Component	1	2	3	4	5	6	7	8	9
	A-474b	A-474c	A-474e	A-474k	A-474p	B-1498o	B-1497d	CB-753	A-474e
SiO ₂ , wt%	44.31	44.38	44.29	45.35	45.32	45.52	45.32	42.60	51.49
TiO ₂	1.38	1.66	1.56	1.29	1.45	0.33	1.94	1.65	0.00
Al ₂ O ₃	8.23	8.42	8.19	7.70	7.37	8.51	7.88	8.48	0.20
FeO _{total}	20.68	19.83	20.60	23.34	19.94	23.34	20.11	19.45	18.38
MnO	0.44	0.25	0.35	0.56	0.40	0.69	0.26	0.46	0.55
MgO	8.86	9.90	9.14	8.29	9.65	7.02	9.83	6.23	6.62
CaO	10.34	10.66	10.53	10.5	10.34	11.30	10.73	11.81	22.51
Na ₂ O	2.01	1.85	2.18	2.13	1.83	1.32	1.84	1.20	0.28
K ₂ O	0.95	0.89	0.95	0.77	0.67	1.08	0.90	0.53	-
P ₂ O ₅	-	-	-	-	-	-	-	0.64	-
F	-	-	-	-	-	-	-	0.33	-
Total	97.24	97.84	97.78	99.98	97.08	96.12	98.81	99.96	100.09
Si	6.805	6.738	6.766	6.841	6.931	6.735	6.812	6.715	2.013
Al _{IV}	1.195	1.262	1.234	1.159	1.069	1.265	1.188	1.285	0.009
Al _{VI}	0.295	0.245	0.241	0.210	0.256	0.324	0.207	0.290	-
Ti	0.159	0.190	0.179	0.146	0.166	0.039	0.219	0.196	-
Fe ²⁺	2.656	2.518	2.632	2.945	2.545	3.090	2.527	2.564	0.600
Mg	2.029	2.241	2.082	1.864	2.195	1.657	2.202	1.464	0.386
Mn	0.057	0.032	0.045	0.072	0.052	0.091	0.033	0.061	0.018
Ca	1.701	1.734	1.724	1.705	1.690	1.916	1.727	1.995	0.947
Na	0.599	0.545	0.646	0.623	0.541	0.405	0.535	0.367	0.020
K	0.186	0.172	0.185	0.148	0.130	0.219	0.173	0.107	-
f	56.7	52.9	55.8	61.2	53.7	65.1	53.4	67.1	60.87
L	11.5	11.6	11.4	10.5	10.5	12.2	10.8	12.8	-

Notes: (1, 4, 7) granite; (2, 3, 9) granite porphyry; (5, 6, 8) adamellite; dash denotes "not determined".

- danburite-datolite (Levoberezhnaya lode and the Skrytoe orebody);
- axinite-datolite (Aksinitovaya and Vodorazdel'naya lodes).

The amount of ore decreases with depth giving way to barren skarn and unaltered rocks.

Medium- and coarse-grained borosilicate ore is characterized by massive, banded, or brecciated structures. Large concentrically zoned spherical aggregates with rhythmically alternating bands of wollastonite, pyroxene, garnet, datolite, and other minerals are especially interesting. Khetchikov, Ratkin and other researchers suggest that these aggregates were formed in open cavities.

Formation conditions of the Dalnegorsk borosilicate deposit are discussed in terms of three competing genetic concepts. According to the concept developed by Nosenko and Ratkin, the boron minerali-

zation of the first stage was related to the Cenomanian-Turonian stage of magmatic activity and predated the deposition of the base-metal ore in the Dalnegorsk district (Nosenko et al., 1990). In the Maestrichtian and Danian, the B-bearing skarn was modified by hydrothermal solutions derived from an intermediate magmatic melt crystallized as intrusive rocks belonging to the second phase of the Dalnegorsk volcanic-plutonic complex (Fig. 6.10). Ratkin suggests that sequential isotopic fractionation of boron during the hydrothermal process resulted in the isotopic homogeneity of this element (Table 6.9).

An alternative concept (Govorov, 1977) assumes that all base-metal skarn deposits of the district were related to the second phase of the Dalnegorsk Complex, whereas the B-bearing assemblages accompanied emplacement of the appinitic rocks of the Sikhali volcanic-plutonic complex. Primary melts of the ap-

Chemical compositions and crystallochemical coefficients of biotites from granitic rocks of the Dalnegorsk pluton

Component	1	2	3	4	5	6	7	8
	B-1498o	A-474p	B-1497d	A-4741	A-474m	A-474n	A-474s	H-1481
SiO ₂ , wt%	38.06	34.05	34.23	34.56	34.95	34.77	35.33	35.72
TiO ₂	1.64	3.51	4.31	4.11	4.54	4.14	4.36	4.33
Al ₂ O ₃	12.75	14.18	12.50	14.28	13.47	14.17	4.16	12.37
FeO _{total}	22.16	28.06	26.72	24.87	26.49	24.02	23.48	24.15
MnO	0.36	0.19	0.28	0.38	0.27	0.42	0.28	0.32
MgO	11.40	6.94	7.46	8.0	6.44	7.35	7.66	7.98
CaO	0.03	0.04	-	0.05	0.01	-	-	-
Na ₂ O	0.12	0.12	0.29	0.18	0.20	0.31	0.30	0.32
K ₂ O	9.79	8.78	9.14	7.84	9.20	8.81	9.10	9.17
Total	96.30	95.86	94.94	94.78	95.58	94.00	94.78	94.35
Si	2.921	2.711	2.789	2.725	2.774	2.769	2.782	2.910
Al _{IV}	1.079	1.289	1.201	1.275	1.226	1.231	1.218	1.09
Al _{VI}	0.074	0.042	-	0.051	0.034	0.093	0.096	0.098
Ti	0.095	0.210	0.264	0.244	0.271	0.248	0.258	0.265
Fe ²⁺	1.422	1.868	0.821	1.639	1.758	1.599	1.545	1.645
Mg	1.303	0.823	0.906	0.998	0.762	0.872	0.899	0.969
Mn	0.023	0.013	0.019	0.025	0.018	0.028	0.025	0.022
Ca	0.003	0.003	-	0.004	-	-	-	-
Na	0.017	0.018	0.046	0.028	0.031	0.048	0.046	0.050
K	0.958	0.0892	0.950	0.788	0.932	0.895	0.913	0.953
f	51.1	69.4	66.8	62.1	69.7	64.7	63.2	62.9
L	17.0	19.8	17.9	19.8	19.2	20.2	20.1	17.7

Notes: (1, 2) adamellite; (3-8) granite.

pinitic series were generated by melting of an eclogitized basic asthenolith affected by ascending deep fluid that provided a supply of water and volatile K- and B-bearing compounds. The major types of igneous rocks were produced in sequence: isite-shonkinite-leucite trachyte, which reflects the falling temperature and enrichment in volatiles. The borosilicate metasomatism is considered to develop much later than the formation of base-metal skarn deposits. Thus, the Sikhali volcanic-plutonic complex was formed in the final stage of evolution of the East Sikhote Alin volcanic belt and marks the onset of general tectonomagmatic reactivation of orogenic structures in Sikhote Alin initiated by the opening of deep-water basins of the Sea of Japan and Sea of Okhotsk.

In the recent years, E.L. Shkol'nik, V.I. Gvozdev, T.A. Punina, S.V. Malinko, and other researchers worked out a hypothesis of initial sedimentary accumulation of boron in a rift-related lagoon. This concept is based on the structural similarity of skarn with stromatolite colonies in limestone and on the specific

character of isotopic fractionation of boron in sequential mineral assemblages. Further, boron was involved in retrograde migration of ascending fluid and deposited in skarn assemblages varying in composition in compliance with the thermogradient field near the cooling intrusion. This idea has important practical implications inferring that the B-bearing basins could exist in adjacent areas with similar paleogeographic environment.

THE NOVO-MONASTYRSKY TIN AND BASE-METAL DEPOSIT [STOP 3]

Geological summary. The deposit is situated 40 km southeast of Dalnegorsk on the right-hand bank of the Pryamaya River, a right tributary of the Rudnaya River near the Monomakhovo Village (Fig. 6.1). The deposit is related to the Monomakhovo Horst, an inlier of Jurassic-Early Cretaceous basement overlain by Late Cretaceous volcanics. The Monastyrka River and Monomakhovo strike-slip fault zones bound the

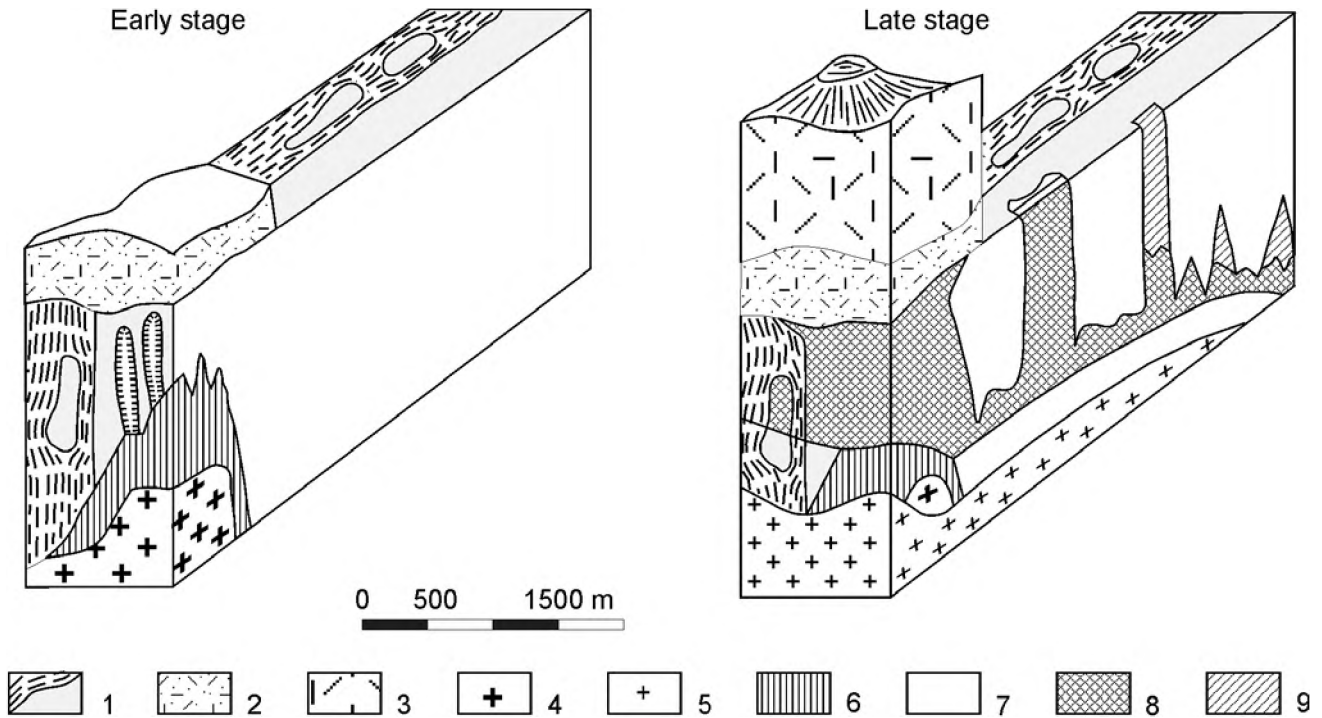


Fig. 6.10. Two-stage formation of the Dal'negorsk borosilicate deposit – a basic diagram, after Ratkin.

(1) limestone blocks and terrigenous host rocks; (2) Cenomanian-Turonian ignimbrite; (3) Maestrichtian-Danian andesite and dacite; (4) Cenomanian-Turonian granite; (5) Maestrichtian-Danian granodiorite; (6) early grossular-wollastonite skarn; (7) cavities filled with datolite-hedenbergite-wollastonite balls and danburite druses; (8) late ilvaite-garnet-hedenbergite skarn with low-grade base-metal mineralization; (9) late Pb-Zn sulphide ore

horst in the east and west. The northern and southern boundaries can be traced along the Tigrovyy Creek and Lidovka normal faults. On the southeast, the Zerkal'naya River Fault separates the horst from the Monastyrka River Caldera (Fig. 6.11). The Monomakhovo Anticline is the main structural element of the basement inlier. Basement rocks are fragments of

Table 6.9

The boron isotopic compositions in borosilicates from skarn deposits of the Dalnegorsk ore district

Sample number	Mineral	¹⁰ B/ ¹¹ B	δ ¹¹ B, %	Deposit
621-2-1	Datolite	4.0048	-9.62	Dalnegorsk
621-2-2	//	3.9825	-15.13	//
641-1	//	3.9841	-14.74	//
641-12	//	3.9809	-15.53	//
607-3	//	3.9968	-11.60	//
PH-20	//	3.9277	-28.69	//
641-7	Axinite	3.9683	-18.65	//
599-13	Danburite	4.1152	+17.68	//
570-2	Axinite	4.0535	+2.42	Partizanskoe

Notes: NIST SRM (951) Standard – a boric acid with ¹⁰B/¹¹B = 0.2473 – was used by an analysis and computation. Analyses were performed with ICP-MS at the West Coast Analytical Service, USA.

the Ustinovka Subterrane (Fig. 6.3). The section, about 1250 m thick, consists of intercalated siltstone and sandstone; synsedimentation breccia and basal conglomerate occupy a significant part of the section. The basement is unconformably overlain by a volcanogenic sedimentary unit of the East Sikhote Alin Volcanic Belt. Conglomerate, siltstone, and coarse-grained sandstone with a total thickness of 1270 m occur at the base of the section. The Cenomanian-Turonian age of this unit is supported by presence of *Inoceramus concenyricus* Park.

Igneous rocks. The sedimentary unit underlies a light gray crystalloclastic and lithocrystalloclastic rhyolitic tuff, 2400 m thick with plant remains of Santonian-Campanian age. Close to the orebodies, the rhyolitic tuff is transformed into epidote-carbonate-sericite altered rocks.

The basement and volcanic cover are cut by minor intrusions of granite porphyry, comagmatic to the acid volcanics; quartz diorite and basic intrusive rocks occur on the northern flank of the deposit (Fig. 6.12).

The granite porphyry is exposed forms as plugs and sheetlike bodies, 5-130 m thick and 60-700 m long, in basins of the Eleninsky and Mukhlyninsky creeks. The granite porphyry is a white or pinkish white rock with massive or flow-banded structure.

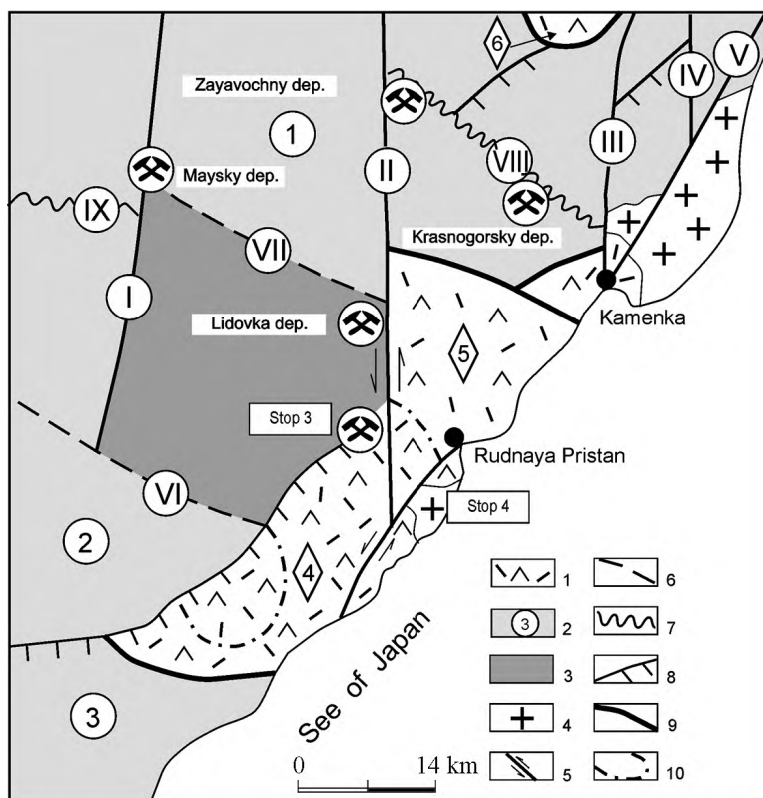


Fig. 6.11. Tectonic sketch of the southeastern Dal'negorsk ore district, after V.V. Korol, V.A. Mikhailov et al.

(1) andesidacitic and rhyolitic flows of the Dal'negorsk Volcanoplutonic Complex; (2) fields of ignimbrites of the Primorskaya Formation; (3) basement rocks in the Monomakhovo horst; (4) granodiorite, granite, and leucogranite of the Dal'negorsk Volcanoplutonic Complex; (5) large wrench fault zones; (6) large normal faults; (7) extension zones; (8) Zerkal'naya River thrust-fault zone; (9) caldera boundaries; (10) ring faults.

Numerals in the figure: *Ignimbrite fields:* (1) Sheptun, (2) Kisinskoe, (3) Zerkal'naya River; *caldera boundaries:* (4) Monasteryka River, (5) Briner, (6) Verkhnesheptun; *wrench fault zones:* (I) Monomakhovo, (II) Monasteryka River, (III) Sheptun, (IV) Plastun, (V) Astashevo; *normal faults:* (VI) Tigrovyy Creek, (VII) Lidovka; *extension zones:* Smyslovo, (IX) Sadovoe

Phenocrysts largely consist of quartz and plagioclase (An_{25}); the latter almost completely replaced by finely squamous sericite. Rare biotite and hornblende crystals occur. The groundmass consists of K-Na feldspar, quartz, albite, and carbonate. At the Mukhlyninsky prospect, a granite porphyry hosts ore mineralization. The granite porphyry is close in composition to the average aplite-like granite from the Coastal Zone: 71.5 wt % SiO_2 , 15 wt % Al_2O_3 , and 7 wt % $Na_2O + K_2O$. MgO, CaO, and FeO contents are low; K_2O slightly prevails over Na_2O . The granite porphyry is enriched in Pb (70 ppm), Zn (80–120 ppm), Sn (up to 7 ppm), and Ag (0.1–0.3 ppm). The enrichment is especially pronounced near orebodies and faults.

A quartz diorite forms a small (220 × 60 m) plug on the right-hand bank of Zabyty Creek. The plug contacts are steep (80–85°) and uneven; a short offset propagates into the silicified country rocks. This is a dark gray fine-grained massive rock with clearly expressed globular jointing. The texture varies from hy-

pidiomorphic to porphyritic. The rock consists (vol %) of plagioclase (75–80), hornblende (10), biotite, pyroxene, quartz, and K-Na feldspar; accessory apatite, zircon, and rare titanite are present. Light gray microgranitic spots are observed within the quartz diorite plug. Elongated amygdules filled with calcite (core) and bipyramidal quartz (outer rim) are confined to the near-contact zone. Radiating-fibrous aggregates of green chlorite and small (0.2 mm) cassiterite grains occasionally occur in amygdules.

Numerous dikes of intermediate and basic porphyritic rocks have been mapped within the ore field. They extend in a submeridional direction and dip steeply east- and westward. The dikes are 200–700 m long; their thickness varies from 0.2–5.0 m to 15–20 m. In dioritic dikes, the phenocrysts occupy 10–15% of the rock volume and are composed of plagioclase An_{43-45} , more or less replaced by sericite, as well as by clinopyroxene, hornblende, and magnetite. The groundmass is almost completely replaced by chlorite and carbonate. In basic dikes,

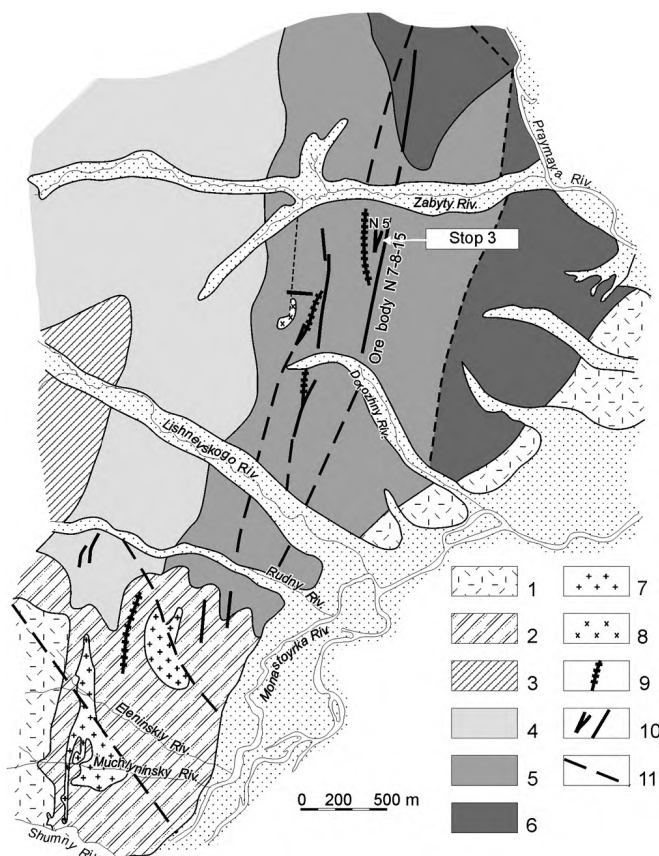


Fig. 6.12. Geological map of the Novo-Monastyrsky deposit.

Upper Cretaceous volcanics of the East Sikhote-Alin Volcanic Belt: (1) tuff of the Primorsky Formation and volcanogenic molasses of the Petrozuevo Formation, *terrigenous rocks of the Valanginian matrix:* (2) sandstone unite with siltstone interlayers, (3) flyschoid unit: sandstone and siltstone, (4) siltstone unit with rare sandstone interlayers, (5) unit of monotonous gray silty shale, (6) arkose sandstone and gritstone; (7) granite porphyry intrusion of the Primorsky Volcanoplutonic Complex; *the Dal'negorsk Volcanoplutonic Complex:* (8) diorite plug and (9) porphyritic dikes; (10) oreveins and alteration zones; (11) faults

plagioclase phenocrysts occupy up to 60 vol %; in addition, orthopyroxene, olivine, and augite occur. The groundmass is replaced by chlorite, actinolite, and sericite. High Pb, Zn, Ag, and Mo contents (298, 486, 0.1–1.0, and up to 20 ppm, respectively) are typical.

Intermediate and basic dikes belong to the second phase of the Dalnegorsk Complex. Tin and base-metal mineralization is closely related to the Dalnegorsk volcanic-plutonic complex supported by relationships between porphyritic dikes and ore veins. Some orebodies cross-cut and displace these dikes; at the same time, a basic dike cuts the ore zone with pyrrhotite, sphalerite, and galena. This dike, in turn, is cut by numerous quartz-calcite-pyrite veinlets, which complete the hydrothermal mineralization in the de-

posit. Similar relationships were observed at other deposits (Verkhnee, Smirnovskoe, and Lidovka).

The main orebodies and porphyritic dikes are localized along extended (up to 800–1200 m) shear fractures striking 20–30° NE parallel to the fold axes in the basement and dipping northwestward at angles of 65–75°.

Postmineral tectonics gave rise to numerous gliding planes and gouges along faults with a displacement ranging from 0.2–0.4 to 4–6 m.

Morphology and composition of orebodies.

The ore field covers about 5 km² and encompasses 15 orebodies of two morphological types. The first comprises mineralized shear zones and veins in extended shear fractures of a northeastern direction (orebodies nos. 7-8-15, 9, 14-16, 10, Parallelnaya vein). Their thickness reaches 1–2 m; some segments are up to 2200 m long. The second type is expressed as lenticular bodies related to fracture junctions; their thickness locally reaches 30 m (orebodies nos. 5 and 12). About 85% of total reserves are contained in orebodies nos. 7-8-15 and 5.

Ore zone no. 7-8-15 is traced for 2200 m along strike and for 500 m down dip. The zone strikes 10–20° NE and dips northwestward at angles of 60–75°. The thickness of the zone varies from 0.2–0.3 m to 17 m, 0.5–2.0 m on average. This is a linear shear zone that transects deformed siltstone and sandstone passing at some intervals into a filled vein. The oxidation zone extends down to 40 m (Fig. 6.13) and is composed of limonite, scorodite, cerussite, and smithsonite. The Pb grade in the oxidation zone is variable (0.02–16.78%); the average grade is 2.73% for a thickness of 2.14 m. The Zn content is below 1 % and Sn, below 0.13%.

Massive primary ore is confined to filled veins; stringer-disseminated ore is hosted in shear zones. Pyrrhotite, galena, sphalerite and less abundant chalcocopyrite, arsenopyrite, cassiterite in association with chlorite, quartz, muscovite, and carbonate are major minerals. A stannite and vallerite emulsion in sphalerite was detected under a microscope.

The ore-bearing zone is divided into northern, central, and southern segments.

Orebodies of the northern segment contain almost half of total reserves. Pb and Zn grades are 4.12 and 4.38%, respectively for a thickness of 1.3 m. The economic ore extends to a depth of 500m.

In the central segment, the Pb and Zn grades diminish to 2.22 and 3.76% for a thickness of 1.56 m, respectively. The economic ore extends to a depth of 230 m.

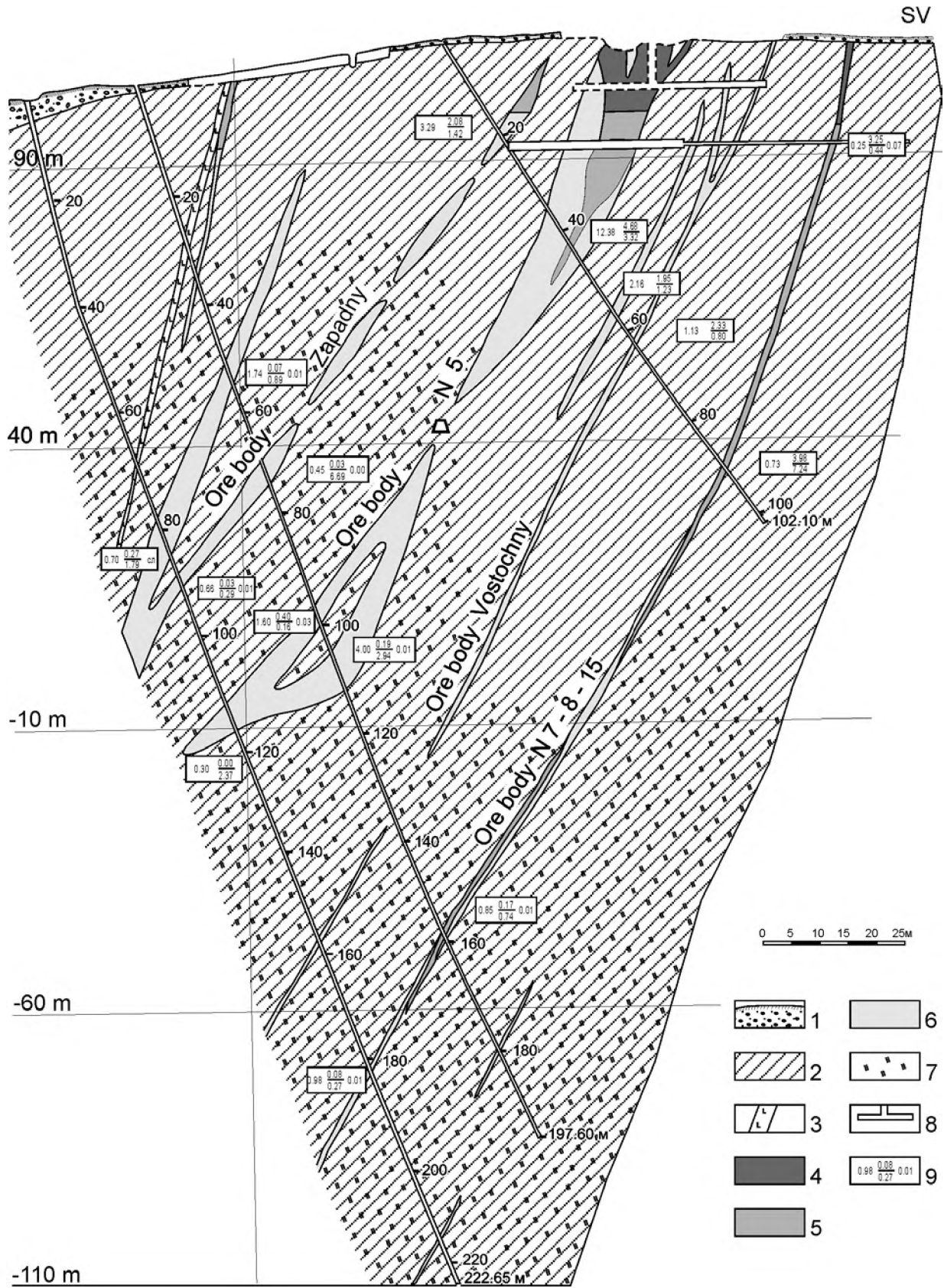


Fig. 6.13. Typical geological section across the Novo-Monastyrsky deposit.
 (1) talus; (2) light gray silty shale; (3) diorite porphyry and dolerite dikes; (4) oxidized sulphide ore; (5) massive primary ore; (6) linear and lenticular zones of stringer-dissiminated mineralization; (7) intensely biotitized country rocks; (8) workings; (9) sampling data

In the southern segment, the Pb and Zn grades are 3.10 and 3.77% for a thickness of 2.23 m, the Sn content increases to 0.16–0.22%. The depth of economic ore is 180 m.

Ore zone no. 7-8-15 is partly exhausted; 24 thou. ton of ore with 3.19% Pb and 3.45% Zn have been mined out.

Ore zone no. 5 is a lenticular body, 3-30 m thick, which is traced for 130 m along strike and 185 m down dip. The lower limit of economic ore is delineated at a depth of 160 m. The ore zone has been mined out for a depth of 50 m. The upper 12 m are in the oxidation zone. Limonite, pyromorphite, malachite, azurite, scorodite, smithsonite are the secondary minerals of the oxidation zone; grains and pockets of primary galena, sphalerite, and pyrrhotite are sporadically retained. The Pb and Zn grades in the oxidation zone are 4.94 and 0.28% for a thickness of 7.04 m, respectively. The tin grade reaches 0.20–0.35%.

The primary ore is commonly massive or closely impregnated (at the lower levels). Galena, pyrrhotite, and sphalerite are major ore minerals; sphalerite increases with depth. A lens of disseminated quartz-pyrrhotite ore with sparse arsenopyrite and chalcopyrite pockets is localized between -40 and -10 m levels. Galena and sphalerite are virtually lacking here. Pb and Zn grades in the economic ore are 2.13 and 4.16%, respectively, for a thickness of 10.23 m. About 123 thou. ton of ore with 4.41% Pb and 4.48% Zn have been mined out from the open pit.

Ore composition, typification, and zoning. Pb, Zn, and Sn are major ore components. In addition, In, Cd, Ag, and Bi were recovered in the course of metallurgical processing. Sb, As, Fe, Mg, Mn, Ga, Be, Cu, and S admixtures were detected in the ore.

Galena is the major Pb mineral of the primary ore; cerussite is predominant in the oxidized ore. In ore zone no. 5, the Pb content decreases with depth; in ore zone no. 7-8-15, the lead is uniformly distributed up-dip, and the northern flank is highly enriched in Pb. Two galena generations are recognized. Galena I in association with sphalerite and pyrrhotite is most abundant; galena II occurs as small grains in late veinlets of pink ankerite. Galena I bears signs of dynamometamorphism: thin bands of this mineral flow around quartz, sphalerite, and pyrrhotite grains imparting a rhythmically banded appearance of the ore. Thin intergrowths of galena I with chalcopyrite, stannite, native silver, pyrargyrite, and fault ore can be seen under the microscope. Galena I contains 6–240 ppm Ag and 50–120 ppm Bi.

Sphalerite is also subdivided into two generations. Early sphalerite is the most abundant; it forms

large pockets and monomineral lenses in the banded ore. The mineral is Fe-rich (up to 16.4 wt % Fe) and contains emulsion impregnations of pyrrhotite, chalcopyrite, stannite, and cubanite.

Like galena II, the late sphalerite is related to the cross-cutting veinlets and is associated with pink ankerite. The Zn grade in the economic ore is 3.40–4.73%; the oxidation zone is depleted in Zn.

Sphalerite is a carrier of In and Cd; the In content in the ore ranges from 10 to 1150 ppm (62 ppm, on the average) and the average Cd content is 249 ppm.

The low Sn content in the ore is provided by small pockets and grains (up to 0.2 mm) of cassiterite in association with pyrite, chlorite, quartz, muscovite, and arsenopyrite. Cassiterite crystals are of dipyrnidal and pyramidal-prismatic habit with bent twins. An outer stannite rim replaces cassiterite, and thin sulfide veinlets cut this mineral. The tin mineralization has no economic importance.

The following types of ore are recognized.

1. Massive galena-sphalerite-pyrrhotite ore occurs in almost all orebodies. The size of mineral grains varies from 3 to 6 mm in the coarse-grained ore and from 0.5 to 2.0 mm in the fine-grained ore. The ore texture is allotriomorphic; sparse pockets of colloform pyrite and marcasite occur.

2. Disseminated mineralization as pockets and dispersed sulfide grains in altered rocks is confined to the middle and lower levels of economic ore. Corrosion, network, replacement, and skeletal textures are typical.

3. Stockwork ore is distinguished from the above types by closely spaced ore veinlets and characteristic network texture (northern flank of the ore zone no. 7-8-15).

4. Ocellar sulfide ore as equant sulfide accumulations in altered rocks resulted from selective replacement of host rocks, especially the limestone fragments in conglomerate and breccia; the cherty clasts remain unaltered.

5. Oxidized ore with cellular, porous, colloform, and spongy textures (upper level of the zone no. 5).

Formation conditions. Four stages of mineral deposition are recognized at the deposit:

- (1) quartz-arsenopyrite with pyrite and cassiterite;

- (2) galena-sphalerite, the most important in economic respect;

- (3) carbonate-sphalerite as an association of pink ankerite with chalcopyrite, late galena, and sphalerite;

- (4) quartz-pyrite-calcite network of thin branching veinlets, widespread throughout the deposit.

The mineral assemblages related to the different stages were often deposited in same places with sequential replacement producing the above-mentioned textures.

Hydrothermal ore formation resulted in filling of open cavities and metasomatic replacement of wall-rock. A study of fluid inclusions in quartz has shown that a hydrothermal solution of Ca-Na bicarbonate-sulfide type was circulating at the first quartz-arsenopyrite stage; the temperature is estimated as 465-325°C and the fluid pressure, as 18.5-19.0 MPa. The economic assemblages were deposited from a Mg-Na sulfide-bicarbonate solution at 380-240°C and under 7.2 MPa. The filtration of high-temperature and gas-saturated solution of the first stage gave rise to the formation of a broad halo of phyllic and silicified rocks. Deposition of galena-sphalerite ore was accompanied by epidote-chlorite-ankerite alteration.

Formation of the Novo-Monastyrsky deposit was related to the emplacement of granodiorite as the second phase of the Dalnegorsk Complex. The magmatic activity resulted in the pervasive biotitization of country rocks, which is extensively developed in the middle and lower levels of the deposit. Long-term ore formation was interrupted by emplacement of premineral dikes of quartz diorite porphyry and intramineral basic dikes.

THE MAIMINOVSKY SILVER-LEAD-ZINC DEPOSIT [STOP 5]

Geology of the Kedrovyy volcanotectonic structure. The Maiminovskiy deposit is situated on the right-hand bank of the Cheremukhovaya (Sinancha) River 30 km northeast of Dalnegorsk within the Cheremshany (Sinancha) ore cluster at the southern flank of the East Sikhote Alin volcanic belt. The Kedrovyy volcanotectonic structure, which is a pivot of tectonomagmatic activity, is surrounded by marginal volcanic calderas: Perevalny, Bazovaya River, Ozerkovy Creek, and Mount Sarafan (Fig. 6.14). In the south, the Kedrovyy volcanotectonic structure borders on the Artsevskiy volcanotectonic structure and is bounded by the Sheptun ignimbrite field in the south-east (beyond limits of the map).

The polychronous Kedrovyy volcanotectonic structure developed from the Senomanian-Turonian to the Danian and Paleogene. About 80% of its territory is occupied by Upper Cretaceous stratified volcanics and extrusions; Lower Cretaceous sedimentary rocks crop out in erosional windows. Thus, two structural stages are recognized. The lower structural

stage is composed of Berriasian-Valanginian terrigenous rocks of the Taukhe Formation. The Kirillovskiy Inlier (10 x 1.2 km) consists of siltstone with sporadic sandstone interlayers. The Kamenny Inlier (7 x 1 km) is mainly composed of sandstone, conglomerate, and gritstone with siltstone interlayers. The Kirillovskiy Inlier on the right-hand bank of the Cheremukhovaya River is a large horst-like uplift elongated in a NE direction. The terrigenous rocks are folded into a large anticline with small complicated folds on limbs. A graben-syncline filled with volcanogenic molasse of the Petrozuevo Formation is superimposed on the central part of inlier. The molasse is intruded by granite porphyry of the Alikovskiy intrusion. The Kamenny Inlier on the left-hand bank of the Cheremukhovaya River extends in the NE direction and is cut off by the Mount Kabanchik intrusion.

Upper Cretaceous stratified volcanics unconformably overlap the terrigenous rocks. All five volcanic-plutonic complexes described in the introductory section are known from the Kedrovyy volcanotectonic structure. The first, Sinancha Complex comprises the molassoid rocks of the Petrozuevo Formation (400-600 m) and andesitic lavas and tuffs of the Sinancha Formation (80-400 m). The next, Primorskiy Complex is composed of rhyolitic lavas, ignimbrites and tuffs of the Primorskiy Formation in association with comagmatic extrusions and subvolcanic intrusions of quartz porphyry and granite porphyry. These rocks are unconformably overlain by rhyodacitic ignimbrites and tuffs of the Siyanovo Formation (860-930 m). Together with a comagmatic gabbro-diorite-granodiorite association, they make up the Dalnegorsk Complex. The fourth, Bogopol Complex consists of rhyolitic lavas, ignimbrites, and tuffs of the Bogopol Formation (flows and vent facies, 1280-2800 m in total thickness) along with comagmatic extrusions, dikes, and subvolcanic intrusions of granite porphyry. The fifth, Kuznetsovo Complex comprises flows of basaltic andesite belonging to the Kuznetsovo Formation (550-710 m) and basic dikes including lamprophyres, especially abundant at the Cheremukhovyy, Maiminovskiy, and Kamenny deposits where they are commonly localized in the same NW and NE faults as orebodies.

In addition, the Kedrovyy volcanotectonic structure is divided into several sectors by arcuate and radiating fault. Most of the deposits are related to junctions of large faults. The ore is characterized by a high Ag content varying from 154 ppm in tin-base-metal assemblages at the Cheremukhovyy deposit to 12,384 ppm in the galena-sphalerite assemblage of the Kamenny deposit.

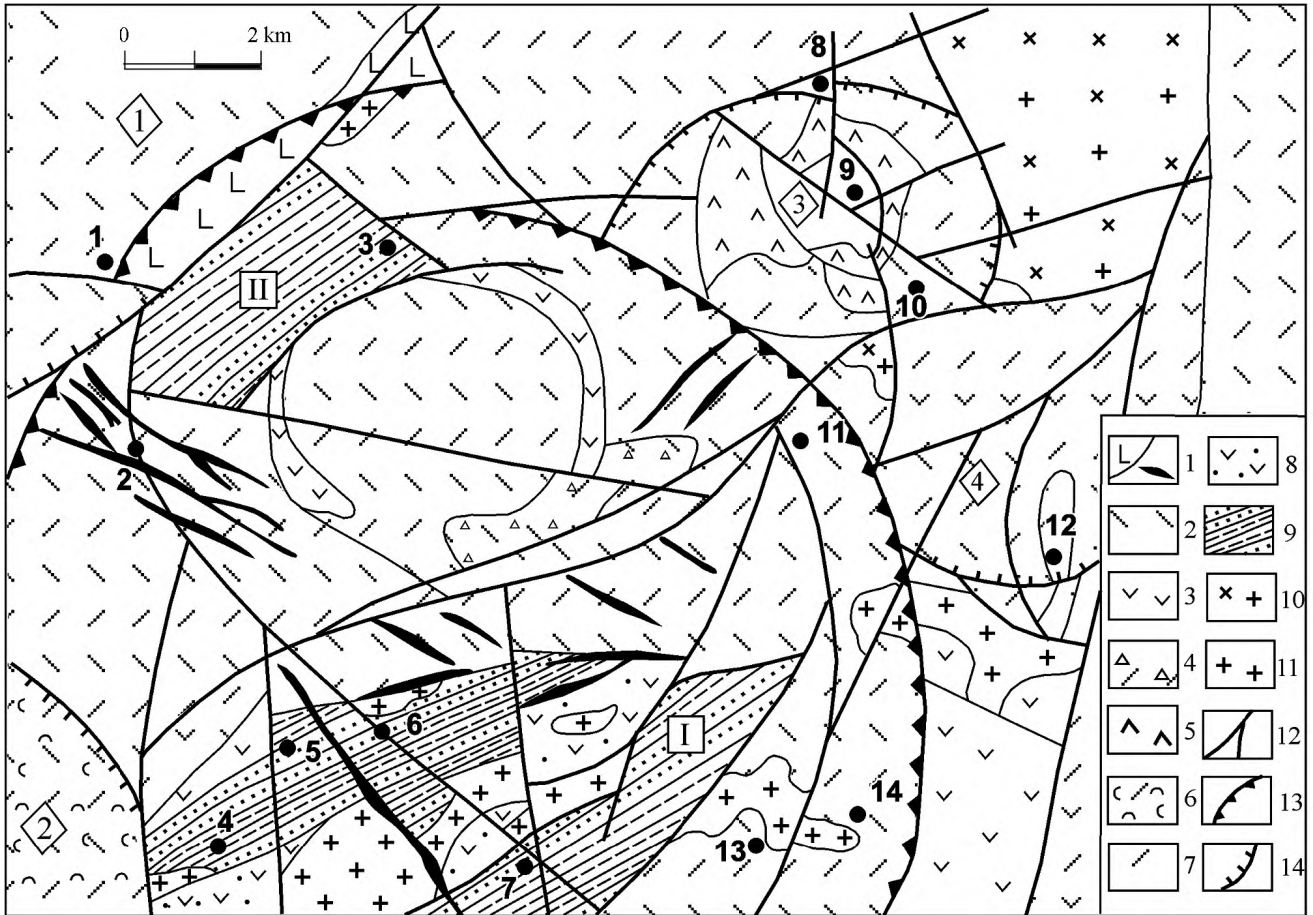


Fig. 6.14. The Kedrovyy volcanotectonic structure as a central part of the Cheremshany ore cluster, after V.V. Vetrennikov and V.A. Mikhailov.

(1) volcanic flows and dikes of the Kuznetsovo Complex: basalt, basaltic andesite, and lamprophyre; (2) rhyolite, (3) rhyodacite, and (4) pyroclastic vent facies of the Bogopol Complex; (5) rhyodacitic lava and ignimbrite of the Dal'negorsk Complex (Siyano-novo Formation); (6) rhyolitic tuff and ignimbrite of the Primorsky Complex; (7) andesitic and dacitic lavas and tuffs of the Sinancha Complex; (8) tuffaceous siltstone, sandstone, gritstone, and basaltic andesite flows of the Petrozuevo Formation; (9) Berriasian-Valanginian siltstone with sandstone interlayers (Taukhe Formation); (10) granodiorite of the Dal'negorsk Complex; (11) granite porphyry of the Primorsky Complex; (12) faults; (13) boundary of the Kedrovyy volcanotectonic structure; (14) boundaries of volcanic calderas (numerals in rhombs): 1 – Bazovy, 2 – Pereval'ny, 3 – Ozerkovy, 4 – Mount Sarafan.

Basement inliers (numerals in squares): I – Kirillovsky, II – Kamensky.

Ore deposits and prospects (filled circles in the map): 1 – Magnetitovoe, 2 – Cheremshany, 3 – Kamenny, 4 – Kirillovsky, 5 – Piloramny, 6 – Maiminovskiy, 7 – Verkhne-Alikovskiy, 8 – Yevlampievskiy; 9 – Ozerkovy, 10 – Krasnoskal'ny, 11 – Vodopadny, 12 – Mount Sarafan, 13 – Verkhne-Polyanskyy, (14) Vysokogorskyy

Geology of the Maiminovskiy deposit. The major orebodies are hosted in Berriasian-Valanginian terrigenous rocks of the Taukhe Formation (Fig. 6.15), which is subdivided into two members. The lower member (860–1360 m) consists of 80% of arkose sandstone with siltstone interlayers and is the host for the main reserves of the silver–base-metal ore. The upper member (650 m) is largely composed of siltstone with sparse sandstone interlayers and is overlain by Upper Cretaceous volcanics with a sharp unconformity (Fig. 6.16).

Three younger volcanic-plutonic complexes are recognized in the area of deposit. The first, Sinancha Complex consists of a volcanogenic molasse of the

Petrozuevo Formation, flows and extrusion of basaltic andesite belonging to the Sinancha Formation (wt %): SiO₂ (52.46), Al₂O₃ (16.91), K₂O (4.26), Na₂O (2.18), MgO (2.62), FeO + Fe₂O₃ (4.00). The Bogopol Complex is composed of rhyolitic flows, extrusion, dikes, and subvolcanic granite porphyry. The granite porphyry of the largest Alikovskiy intrusion is a light gray massive rock with quartz, albite, oligoclase, and potassium feldspar phenocrysts occupying up to 60% of the rock volume. The hornfels aureole around this intrusion extends for 200 m in width. The average chemical composition of the granite porphyry (wt %): SiO₂ (73.58), TiO₂ (0.23), Al₂O₃ (12.20), FeO (0.94), Fe₂O₃ (2.17), MnO (0.06), MgO (0.46), CaO (1.30),

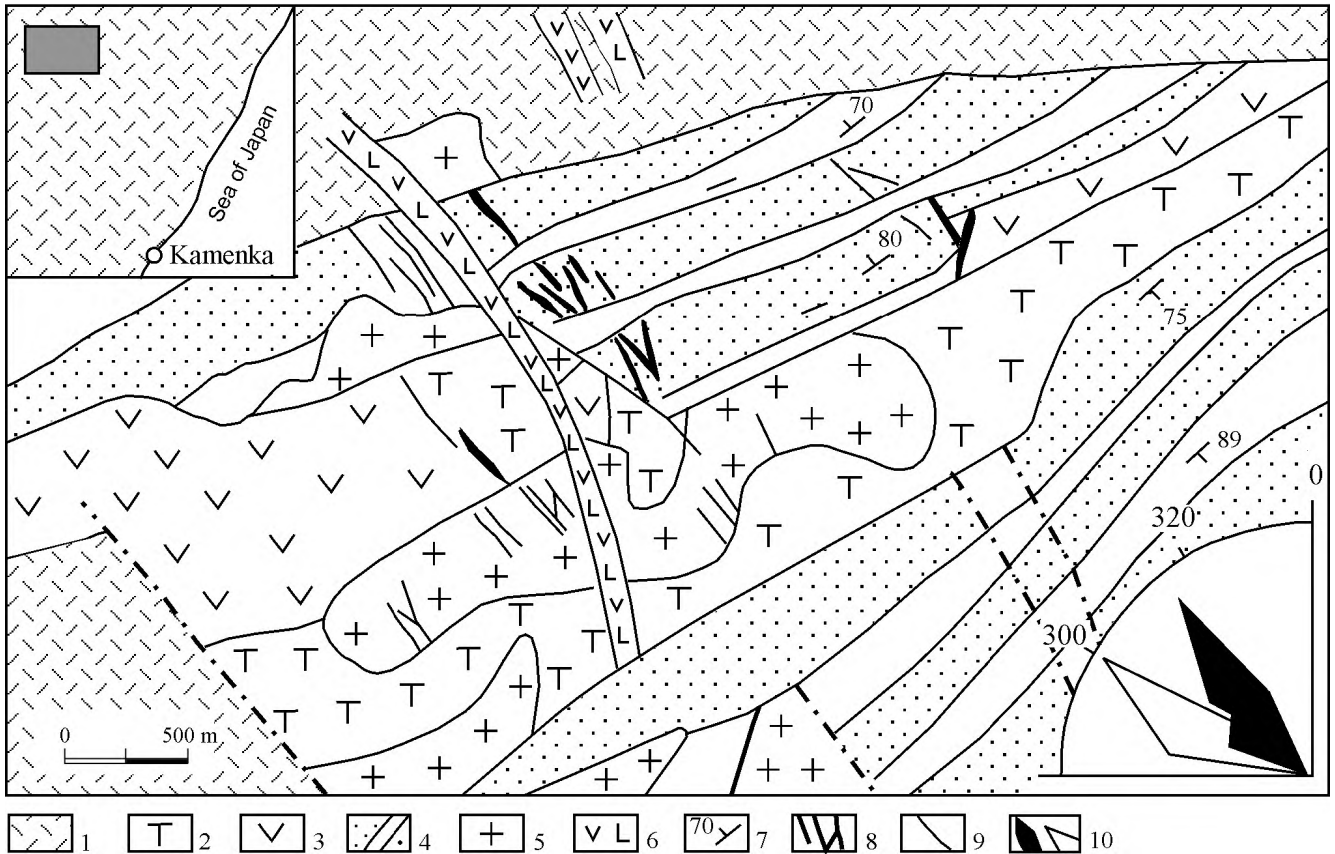


Fig. 6.15. Schematic geological map of the Maiminovskiy deposit, after Yu.P. Yushmanov.

(1) rhyolitic tuff and ignimbrite; (2) rhyolitic and rhyodacitic tuffs; (3) andesite; (4) intercalating sandstones and siltstones; (5) granite porphyry; (6) basaltic andesite; (7) strike and dip symbol; (8) ore-bearing ladder fractures; (9) major faults; (10) rose diagram of barren (open symbol) and ore-bearing (filled symbol) fractures

Na₂O (2.41), K₂O (4.05). The rock contains 11–298 ppm Pb, 64–468 ppm Zn, and 0.1–1.0 ppm Ag revealing a distinct correlation between Pb, Zn, and Ag.

Separate dikes of basaltic andesite belonging to the Kuznetsovo Complex (Paleogene) extend for 2.5 km in a NW direction; their thickness varies from 0.5 to 20–30 m.

Altered rocks. The host rocks underwent contact metamorphism, phyllic alteration, and propylitization. A hornfels aureole around the Alikovskiy granite porphyry intrusion, 50–300 m wide, is superimposed on the country sandstone, siltstone, and rhyolite. The mineral composition of the hornfels is as follows (vol %): quartz (12), biotite (3–7), sericite (5–30), chlorite (3–7), muscovite (1–7), and albite (1–3). Phyllic zones, 1.5 x 6 km, are localized on the northwestern flank of deposit where they reveal a zoning (from inner to the outer zones): quartz + muscovite → quartz + muscovite + tourmaline → quartz + sericite + chlorite → quartz + sericite + adularia. Pockets of cassiterite, sphalerite, pyrite, and arsenopyrite occur in quartz-adularia veinlets. About 2/3 of the deposit area

is occupied by propylites of epidote-chlorite, quartz-chlorite-albite, and chlorite-sericite facies that replace sandstone, rhyolite, and basaltic andesite.

Structure of deposit. The economic mineralization is localized in the northwestern limb of an anticline composed of arkose sandstone with siltstone interlayers. The sandstone-siltstone contacts are commonly complicated by tectonic detachments extending in a NE direction. The ore is hosted in NW shears arranged en echelon that cut the sandstone layers from one contact to another. Ore veins dip at angles 75–85° NE. Ore shoots are confined to junctions of longitudinal detachments and transverse shears. Some orebodies are localized under a low-angle thrust fault extending in a latitudinal direction.

Orebodies. 32 orebodies are known at the deposit. They are concentrated in the Central and Southeastern areas as mineralized shear fractures. Zones of metasomatic replacement occur between closely spaced fractures. The ore is distributed nonuniformly in particular ore shoots. Orebodies are grouped into a number of vein suites.

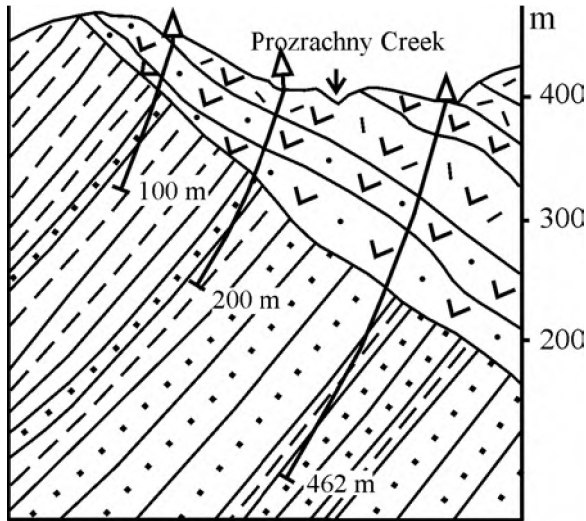


Fig. 6.16. Relationship between volcanic flows and base-metamorphic rocks.
See Fig. 6.15 for legend

The vein suite of orebodies nos. 1–3 is localized at the headwater of the Maiminovskiy Creek. Fracture zones with quartz-sulfide veinlets vary in thickness from 0.2–0.4 to 15 m at the surface and pass with depth into veins, 20–40 m thick. Bulges, up to 80 m thick, are noticed at sandstone-siltstone contacts. Zone no. 1 (Fig. 6.17) is the main orebody containing 38%

of the total reserves. This zone was traced for 1900 m along strike and for 490 down dip. The high-grade ore contains 2.69% Pb (up to 14% in particular sections), 16.44% Zn, and 195–504 g/t Ag.

The vein suite of orebodies nos. 4–12 comprises eight closely spaced orebodies localized in sandstones as fracture zones with lenticular veins and chaotically oriented veinlets. Some zones are 0.4–0.6 m thick, widening up to 20 m in bulges. The zones were traced for 600 m along the strike and for 240 m down the dip. The grade of ore is as follows: 1.68–11.02% Pb, 14.70–18.96% Zn, and 213–1416 g/t Ag.

Mineral composition of ore. Galena and sphalerite are major ore minerals (about 80 wt %). Arsenopyrite, chalcopyrite, pyrite, and freibergite are second in abundance (1–10 wt %). The content of pyrrhotite, polybasite, stephanite, acanthite, native silver, and pyrrhotite is below 1 wt %. Quartz, carbonate, fluorite, and heulandite are gangue minerals.

Typomorphism of minerals. Two generations of sphalerite are distinguished. Sphalerite I (marmatite) is a dark brown medium- and coarse-crystalline mineral that occurs in the massive ore, pockets, and separate impregnations in association with early arsenopyrite, chalcopyrite, and pyrite. Abundant emulsion disseminations of chalcopyrite with formation of lat-

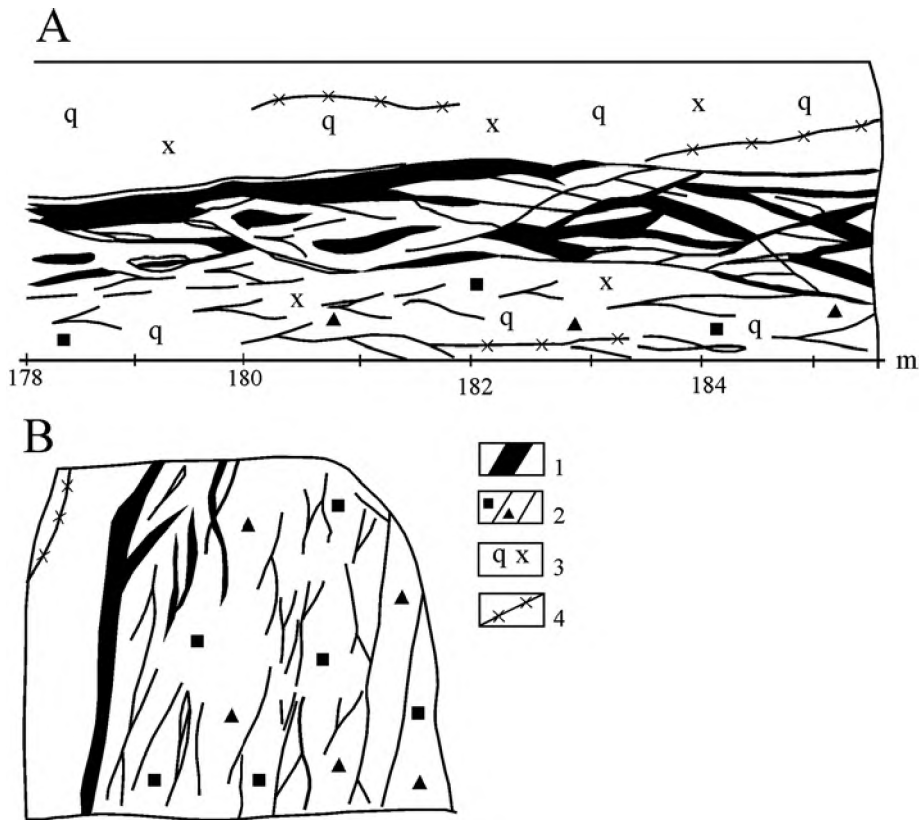


Fig. 6.17. Ore zone no. 1, adit no. 2. (A) adit wall, (B) adit face.
(1) massive ore; (2) stringer-disseminated ore; (3) quartz-chlorite altered rock; (4) quartz veinlets

ticed exsolution structure are typical. The average chemical composition of marmatite is as follows (wt %): Zn (53.15), Fe (12.75), Mn (0.54), and S (34.15); $a_0 = 5.56 \text{ \AA}$; microhardness is 182 kg-force/mm².

Sphalerite II (cleiophane) is a light brown or honey yellow mineral, commonly color zoned with a light outer zone and a dark core. It is devoid of chalcopyrite emulsion, associated with late arsenopyrite, and replaced by freibergite. The Fe content does not exceed 0.9–1.5 wt %; sphalerite II contains up to 1.50–1.86% Cd and 0.03–0.068% Ag; $a_0 = 5.40 \text{ \AA}$; microhardness is 202 kg-force/mm².

Galena occurs as medium- and coarse-crystalline aggregates in the massive ore. Grains often underwent cataclasis and were transformed into bleischweif. Galena contains 0.06–0.44% Ag and 0.09–0.42% Sb, apparently, as a PbS–AgSbS₂ solid solution. The amount of silver as an admixture does not exceed 2% of the total Ag content in this mineral. Most Ag is contained in the sulfosalt inclusions: freibergite, polybasite, stephanite, pyrargyrite, and acanthite. These inclusions are submicroscopic in size; however, 72.7% Ag fall precisely on these inclusions; 20% is related to the inclusion of native silver. The Bi content in galena is below 0.01–0.046%.

Arsenopyrite is observed as rhombic grains in sandstone and as thin rims along selvages of quartz-sulfide veins. The mineral contains up to 0.0n% Co, Ni, Ag, Cu, and Sb, and 0.0004% Au.

Chalcopyrite is present in two generations. *Chalcopyrite I* occurs as separate grains, pockets, and thin veinlets in association with the early sphalerite, arsenopyrite, and pyrite. *Chalcopyrite II* is typical of the late sulfosalt-sulfide assemblage. The average chemical composition of the mineral (wt %): Cu (33.61), Fe (29.47), S (35.87), Ag (0.15–0.40), Sb (up to 0.040), Zn (up to 0.40), and Sn (up to 0.379). Enrichment in Ag is caused by inclusions of acanthite and native silver.

Freibergite is the most abundant Ag-bearing mineral of the hypogene ore (up to 10 wt % of ore). The mineral occurs as visible inclusions in pockets and veinlets in association with arsenopyrite II and galena II. Freibergite contains (wt %): As (up to 1), Ag (23.35–35.53), Cu (12.87–22.99), Fe (4.45–5.24), Zn (0.45–2.33), Sb (24.61–26.40), and S (20.05–22.75).

Polybasite, pyrargyrite, and acanthite make up separate pockets and cross-cutting veinlets in association with galena II, freibergite, and chalcopyrite II. Grains of these minerals vary from 0.02–0.06 to 0.15 mm in size.

Native silver is associated with pyrrhotite and late chalcopyrite as separate equant grains, 0.01–0.1 mm in diameter and as less abundant cross-cutting veinlets. Admixtures (wt %) of Sb (3.72), As (0.76), Au (0.869), Hg (1.18), Cu (0.81), Te (0.24), and Fe (0.52) have been detected.

Secondary silver minerals: cerargyrite and argentojarosite occur in a zone of sulfide ore oxidation as ochres within the quartz-hydromica mass. At the total Ag content of 900 g/t in the primary ore, 200–250 g/t Ag in the oxidation zone is of cerargyrite.

Cd, Bi, S, Cu, and Au are accompanying components in the ore. According to emission spectroscopy results, the sulfide sulfur content varies from 3.16 to 4.87% of the total ore mass. The presence of As (0.08–0.70%) is related to arsenopyrite and fahlore. The Sb content in sulfide assemblages attains 25.6%. If the average Cu grade in the ore is 0.24%; however, the lead concentrate contains 2–3% Cu, and the Zn concentrate, 1.0–1.5% Cu. The average Cd grade in ore is 0.02%; 10% of this value is from the lead concentrate and up to 70%, from the zinc concentrate. The In content in the concentrate is below 0.01%.

The Au content in oxidation zone is within a range of 0.2–1.7 g/t and occasionally reaches 3.5 g/t. The grade of primary ore is 0.2–0.8 g/t Au (0.37 g/t, on the average). The Au content of 0.8 g/t for 0.8 m was established in one section crossing zone no. 11. The average content in composite samples is 0.01–0.13 g/t Au; 10–20% of this value turn into the lead concentrate and 20–40%, into the zinc concentrate.

Ore structures and textures. Brecciated, replacement, stringer-disseminated, massive, and banded ore structures are most abundant. Loop, cockade, emulsion, and subgraphic textures are also common. Four paragenetic mineral assemblages were outlined based on structural and textural patterns of ore:

- (1) quartz–arsenopyrite with pyrite;
- (2) sphalerite–chalcopyrite–pyrite;
- (3) arsenopyrite II–galena–freibergite;
- (4) Ag sulfosalt–native silver.

Filling of open cavities and metasomatic replacement are the main mechanisms of ore deposition.

Conclusions. The Maiminovskiy deposit of Ag-bearing Pb–Zn ore is medium-size in resources and hydrothermal vein-type in origin. The uneven distribution of ore mineralization with ore shoots is typical. Recovery reaches 91% for Pb, 82.2% for Zn, and 73% for Ag. Profitable underground mining requires an annual mine capacity of ≥ 100 thou. tons of ore. The deposit has reserves for 15.7 years. Reserve growth is related to the western and southeastern flanks of the

deposit where the Pb and Zn haloes were established in the basement rocks. Numerous vein ore occurrences (Vysokogorsky, Verkhne-Polyansky, Magnitny, Osenny, etc) are known in a radius of 3–5 km beyond the ore field.

REFERENCES

- Novoe v geologii Dalnegorskogo raiona* (News in geology of the Dalnegorsk district), Vladivostok, 1984. (In Russian.)
- Polimetallicheskie mestorozhdeniya Dal'nego Vostoka* (Base-metal deposits in the Far East), Vladivostok, 1981.*
- Golozubov, V.V., Khanchuk, A.I., Kemkin, I.V., et al., *Taukhinskii i Zhuravlevskii terreiny (Yuzhnyi Sikhote-Alin)* (The Taukhe and Zhuravlevka terranes in the southern Sikhote Alin), Vladivostok: Far East Division, Russian Academy of Sciences, 1992, 83 p.*
- Baskina, V.A., *Magmatizm Tetyukhinskogo raiona (Yuzhnoe Primorye) i zakonomernosti razvitiya nekotorykh vulkano-plutonicheskikh assotsiatsii* (Magmatism of the Tetyukhe district in the southern Primorye and evolution of some volcanic-plutonic associations), Moscow: Nauka, 1965.*
- Efimova, M.I., Blagodareva N.S., Vasilenko, G.P., et al., Temperature parameters of endogenic ore formation in the Far East, in: *Termobarogeokhimiya i rudogenez* (Thermobarogeochemistry and ore formation), Vladivostok, 1980.*
- Dobrovolskaya, M.G., Baskina, V.A., Balashova, S.P., et al., The sequence of ore formation and basic dikes at the Nikolaevskoe deposit in the southern Primorye, *Geol. Rudn. Mestorozhd.*, 1990, no. 1, pp. 85–97.
- Kokorin, A.M. and Kokorina, D.K., Formation conditions of ore deposits in the Dalnegorsk district: results of fluid inclusion study in minerals, in: *Novye dannye po mineralogii Dal'nego Vostoka* (New data on mineralogy in the Far East), Vladivostok: Far East Division, Academy of Sciences of the USSR, 1987, pp. 102–117.*
- Malakhov, V.V., Ignat'ev, A.V., and Nosenko, I.A., Formation conditions of boric mineralization at the Dalnegorsk deposit: evidence from chemical and isotopic compositions of carbonates, in: *Novye dannye po mineralogii Dal'nego Vostoka* (New data on mineralogy in the Far East), Vladivostok: Far East Division, Academy of Sciences of the USSR, 1987, pp. 68–76.*
- Mikhailov, V.A., *Magmatizm vulkano-tektonicheskikh struktur yuzhnoi chasti Vostochno-Sikhote-Alin'skogo vulkanicheskogo poyasa* (Magmatism in volcanotectonic structures of the southern East Sikhote Alin volcanic belt), Vladivostok: Far East Division, Academy of Sciences of the USSR, 1989, 170 p.*
- Nosenko, I.A., Ratkin, V.V., Logvenchev, P.I., Polokhov, V.P., and Pustov, Yu.K., The Dalnegorsk borosilicate deposit as a product of polychronous skarnification, *Dokl. Akad. Nauk SSSR*, 1990, vol. 231, no. 1, pp. 178–182.*
- Parnyakov, V.P. and Markevich, V.S., Age of olistostrome sequences in the Dalnegorsk district, *Tikhookean. Geol.*, 1989, no. 1, pp. 47–52.*
- Radkevich, E.A., Ratkin, V.V., Babich, O.N., et al., *Tikhookenskaya okraina Azii. Metallogeniya* (Pacific margin of Asia. Metallogeny), Vladivostok: Far East Division, Russian Academy of Sciences, 1991, 204 p.*
- Yushmanov, Yu.P., Growth tectonic nappes in the Coastal Zone of the eastern Sikhote Alin: a case of the Dalnegorsk ore district, *Tikhookean. Geol.*, 1986, no. 3, pp. 99–107.*



SOUTHWEST PRIMORYE (THE VOZNESENKA ORE DISTRICT)

M. D. Ryazantseva

Primorsky Prospecting and Mapping Expedition – Federal State Unitary Geological, Vladivostok

INTRODUCTION

The Voznesenka ore district is situated in southwestern Primorye (Fig. 7.1). Preobrazhensky first found fluorite in the vicinity of Voznesenka Village in 1924. In 1948, Materikov discovered the first fluorite ore in situ. Exploration carried out in 1947–1950 established the unique extension of the Voznesenka fluorite deposit and representing a previously unknown mica-fluorite type of ore mineralization (Materikov, 1961). Subsequently, a number of other fluorite prospects have been found. The almost all fluorite, tin, and rare-metal deposits and ore occurrences known to date in the Voznesenka ore district were found during 5–7 years from the onset of prospecting and geological exploration. Thus, a new ore district in the western Primorye previously considered to be barren was discovered in the late 1940s and early 1950s and became a subject of thorough studies. Not only a new ore district but also complex mineral resources new for the territory of Primorye have been investigated. Fluorite in the ore is associated with Be, Rb, Li, Cs; the zinc ore is enriched in Mo, In, Au, and Ag; tin is associated with W, Be, and U. The discovery of the Voznesenka ore district initiated the development of a new large mining center in Primorye.

GEOLOGICAL OUTLINES

The Voznesenka ore district is a fragment of Paleozoic passive continental margin and a part of the Khanka Lake median mass, or composite terrane with extensively developed Lower Cambrian near-shore marine terrigenous and carbonate rocks. Their age is supported by findings of archaeocyathids and blue-green algae. The western boundary of the district extends along the contact of a large batholith composed of Silurian collision-related metagranites (Grodekovo Complex). A meridional fault along the Ilistaya River valley serves as the eastern boundary. The southern and northern boundaries are buried beneath thick coal-bearing sequences filling Mesozoic and Cenozoic basins. The ore-bearing area is clearly delineated by a gravity maximum against the gravity lows related to the sedimentary basins.

The stratigraphic section of the Voznesenka ore district is characterized by alternating terrigenous and carbonate units that grade into one another as a complex set of facies. The sedimentary rocks are de-

formed into a system of tight anticlines and synclines striking northwest and overturned to the northeast. Three groups of faults are recognized. The first group of synorogenic faults comprises longitudinal thrust and reverse faults extending in a NW direction. Paleozoic postorogenic strike-slip and reverse faults of the second group extend in northeastern, meridional, and latitudinal directions. They are oblique and transverse with respect to the folds. The Western and Eastern faults belonging to this group bound the ore district in the west and east, respectively. The Main (Voznesenka) Fault in the center of the district controls a belt of gabbro, diorite, syenite, and granosyenite porphyry intrusions of Silurian age (Fig. 7.1). Mesozoic and Cenozoic faults of the third group are regarded as rejuvenated Paleozoic tectonic lines. The posterior displacements were particularly remarkable along latitudinal faults that border the deep superimposed basins. In addition to clearly expressed faults, the fracture zones are traced as guides for hidden faults in the basement that played a pivotal role in localization of igneous rocks and ore mineralization (Ryazantsev, 1973).

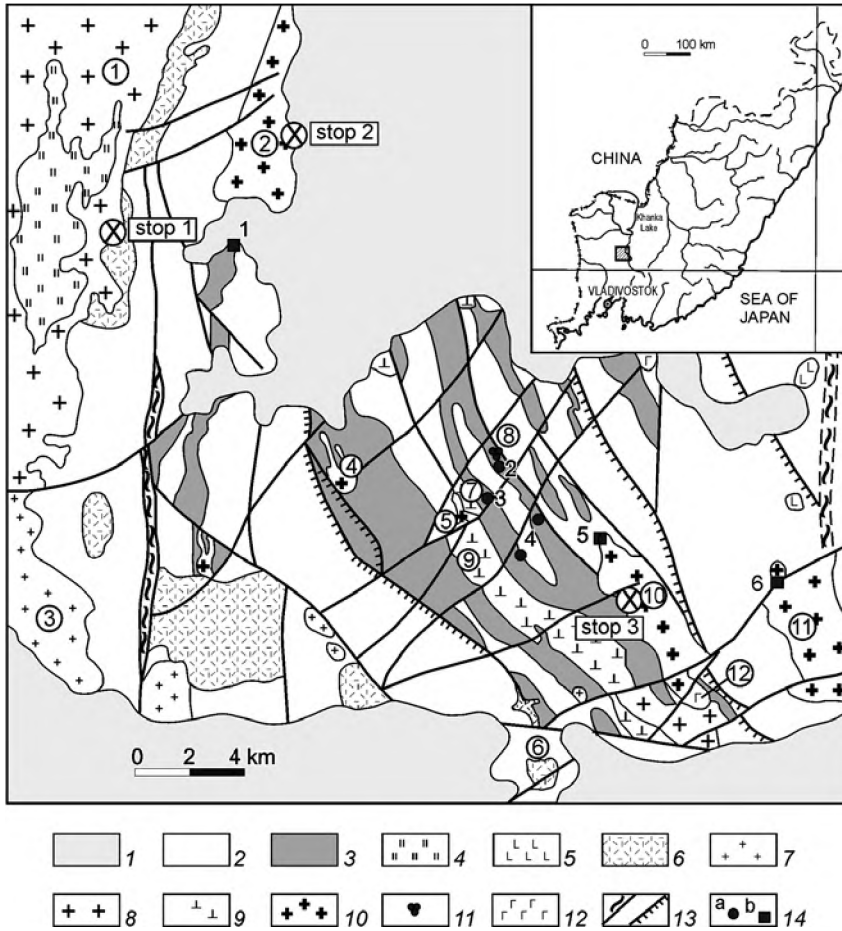


Fig. 7.1. Geological map of the Voznesenka ore district.

(1) Cenozoic basins; Lower Cambrian (2) terrigenous and (3) carbonate rocks; (4) Precambrian and Cambrian metamorphic rocks in the roof of Silurian (Grodekovo) granite; (5) Neogene basalt; (6) Devonian volcanic rocks; (7) Devonian (Grigor'evka) granite; (8) Silurian (Grodekovo) granite; (9) Silurian gabbro, diorite, and monzodiorite; (10) Ordovician (Yaroslavsky) granite; (11) Ordovician (Voznesenka) biotite-protolithionite granite; (12) Cambrian gabbro; (13) fault; (14) fluorite (a) and tin (b) deposits (numerals in the figure): 1 – Pervomaisky, 2 – Pogranichny, 3 – Voznesenka, 4 – Lagerny, 5 – Yaroslavsky, 6 – Chapaevsky. Plutons (numerals in circles): (1) Grodekovo, (2) Pervomaisky, (3) Grigor'evka, (4) Pology, (5) Savchenkov, (6) Boikovskiy, (7) Voznesenka, (8) Pogranichny, (9) Moskalenkovskiy, (10) Yaroslavskiy, (11) Chikheza, (12) Chapaevskiy

PLUTONIC ROCKS

The following plutonic rock complexes are known in the ore district: Cambrian–Ordovician (?) gabbro and pyroxenite, Ordovician Voznesenka Complex of rare-metal granites and leucogranites, Silurian gabbro-monzonite-syenite and Grodekovo granite complexes, and Late Paleozoic Grigor'evka granite complex. Representative chemical analyses of plutonic rocks are given in Table 7.1.

Early Paleozoic gabbro-pyroxenite complex embraces small intrusions in the southern part of the ore district (Fig. 7.1). They were emplaced into Lower Cambrian sedimentary rocks and are, in turn, cut by Silurian granites of the Grodekovo Complex. Gabbroic rocks belong to the normal calc-alkaline series. Pyroxenites occur as small bodies grading into gabbro and are not known as separate intrusions.

Silurian gabbro and monzodiorite intrusions of unspecified geodynamic setting are controlled by the northwestern fault that divides the Voznesenka ore district into two blocks with different stratigraphic sections (Fig. 7.1). The alkalinity of intrusive rocks

increases northwestward, so that monzodiorite is known only at the northern termination of the intrusive belt near the Moskalenkov Village.

Silurian collision-related granites of the Grodekovo batholith crop out in the western part of the ore district. Numerous relict blocks of gneisses and metamorphic schists are embedded in the granites. Migmatites and granitic gneisses occur in transitional zones between granite and remnants of country rocks. The granite itself is also gneissose in appearance. Three petrographic granite varieties are distinguished: (1) medium- and coarse-grained biotite granite, (2) fine-grained, commonly porphyritic aplite-like leucogranite, and (3) amphibole-biotite granite. The first variety is the most widespread. Fine-grained porphyritic aplite-like granite is observed as local bodies of various shape and size within the batholith. Biotite granite has a standard mineral composition. Latticed microcline with a narrow outer rim of albite is typical. Zircon, monazite, apatite, ilmenite, titanite, and garnet are identified as accessory minerals. The silica content varies within a range of 69–75 wt % (74 wt %, on the average). The Na₂O + K₂O sum is 7.5–10.6 wt %

Table 7.1

Representative chemical compositions (wt %) of granitic rocks from the Voznesenka ore district

	1	2	3	4	5	6
SiO ₂	74.39	71.69	72.02	73.82	70.79	74.68
TiO ₂	0.11	0.25	0.21	0.16	0.03	0.19
Al ₂ O ₃	13.29	14.49	14.88	13.54	16.30	14.24
Fe ₂ O ₃	0.81	0.71	0.65	0.65	0.58	0.00
FeO	0.64	0.72	0.64	0.64	0.54	0.97
MnO	0.00	0.06	0.05	0.04	0.02	0.02
MgO	0.32	0.52	0.31	0.20	0.49	0.10
CaO	0.89	0.72	1.30	0.42	0.56	0.14
Na ₂ O	2.99	2.98	3.24	3.89	5.43	4.67
K ₂ O	4.83	5.26	4.47	4.56	2.72	4.25
P ₂ O ₅	0.13	0.18	0.17	0.08	0.04	0.02
LOI					0.92	
H ₂ O ⁺	1.22	1.76	1.50	1.82	-	0.43
H ₂ O ⁻	0.10	0.00	0.00	0.00	-	0.06
F	0.01	0.64	0.23	0.08	1.45	0.30
Total	99.73	99.98	99.67	99.90	99.87	100.07
O=F ₂		0.27	0.10	0.03	0.61	0.13
Total	99.73	99.71	99.57	99.87	99.26	99.94

Note: (1) Silurian (Grodokovo) collision-related granite (Stop 1); (2) Ordovician intraplate biotite granite; (3) Ordovician intraplate biotite granite (Yaroslavsky pluton, Stop 2); (4) Ordovician intraplate biotite granite (Chikheza pluton); (5) Ordovician intraplate protolithionite granite (Voznesenka pluton, Stop 3); (6) Ordovician intraplate protolithionite granite (Pogranichy pluton, depth of 1200 m).

(8.5 wt %, on the average); K/Na ratio is close to 1.5. A representative chemical composition of the Grodekovo Granite is shown in Table 7.1. All granites are peraluminous and corundum-normative with an alumina index ($al' = Al_2O_3 / (FeO + Fe_2O_3 + MgO)$) of 10–11. Thus, the Silurian granites are typical autochthonous paligenetic granitoids (Ryazantseva, 1976). Their Rb–Sr age was estimated as 403–411 Ma (Ryazantseva et al., 1994).

Ordovician Voznesenka Complex of intraplate setting is composed of biotite and protolithionite granites regarded as separate intrusive phases (Govorov, 1977) or facies (M.G. Rub and A.K. Rub, 1986).

The biotite granite is a medium-grained, often porphyritic tourmaline-bearing rock that crops out as small (8–12 km²) sheetlike intrusions and stocks with steep contacts. Lower Cambrian terrigenous and carbonate rocks are metamorphosed at contacts with these granites. The limestone is marmorized, skarnified, and impregnated with fluorite. Terrigenous rocks are converted into hornfels and contain tourmaline.

No direct relationships of the intraplate Voznesenka Granite with the Silurian collision-related granite are known. The biotite granite makes up three large plutons: Yaroslavsky, Chikheza, and Pervomaisky and several smaller intrusions (Fig. 7.1). The Yaroslavsky pluton is situated in the central part of the ore district where it extends for 7 km in a NW direction having a width of 1.0–1.5 km. Its SW and NE contacts steeply (50–70°) dip to the southwest. The northern contact gently plunges to the northwest and is complicated by numerous offsets. The Chikheza pluton is localized east of the Yaroslavsky pluton and occupies an area of 5 km². The Pervomaisky pluton, >4 km² in area and >7 km long, is exposed in the western part of Voznesenka district being controlled by a meridional fault and overlapped by Cenozoic sediments in the north and south.

The biotite granite consists of potassium feldspar (45%), often with microcline lattice, quartz (30%), oligoclase and albite-oligoclase (25%), and biotite (2–5%). Tourmaline (schorl) is known from the Yaroslavsky and Pervomaisky plutons. This mineral also occurs in pegmatoid segregations as intergrowths with quartz and potassium feldspar. Tourmaline in association with fluorite and sericite develops as a product of postmagmatic alteration. Zircon, apatite, rutile, allanite, monazite, cassiterite, fluorite, tourmaline, and magnetite are typical accessory minerals. The average silica content is 73.5 wt %; Na₂O + K₂O sum is 8.3–9.0 wt %; K/Na = 1.6 (see Table 7.1 for representative chemical compositions). The granite is peraluminous and contains 820–2600 ppm F and 200–300 ppm Li. Rb–Sr and Sm–Nd timing yielded ~450 Ma (Late Ordovician).

The biotite-protolithionite leucogranite also crop out at the surface as small intrusions with severely greisenized apical portions. According to the geophysical data partly supported by drilling down to a depth of 700–800 m, the Voznesenka and Pogranichny intrusions are salients of the larger pluton composed of Li-F granites with protolithionite, lepidolite, and topaz.

The leucogranite of the Pogranichny intrusion has been studied in detail. This intrusion is exposed at the surface as a narrow northwestern ridge extending for 0.8 km and having a width of 50–300 m. At a depth of 100 m in the east and 300 m in the west, the intrusion abruptly widens and its contacts become gently dipping. Numerous offsets extend from the granite roof. Three facies of granitic rocks replace one another from top to the bottom: leucogranite of the

near-contact zone, main leucogranite, and deep-seated protolithionite granite.

The protolithionite granite is a light gray or greenish gray medium-grained inequigranular rock consisting of microcline, albite, and quartz in approximately equal amounts. The protolithionite content attains 4–5 vol %; topaz occurs in appreciable quantities. According to Rub et al. (1971), protolithionite is a primary magmatic mineral. The mica composition systematically varies from protolithionite at depth to Fe-rich lepidolite in the apical portion of the intrusion (Rub, 1980). Zircon, its variety "cyrtolite", apatite, xenotime, fluorite, topaz, columbite, strüverite, and cassiterite are accessory minerals.

The Li-F granites are peraluminous and contain 8.7–9.3 wt % Na₂O + K₂O with Na/K ≥ 1. The agpaite index is 0.62–0.65. The prevalence of sodium over potassium is largely provided by albitization, which is notable even at a depth of 1200 m. The CaO, MgO, and FeO contents are commonly no higher than 0.1–0.2 wt %. The fluorine content reaches 3.7 wt %. This element was also detected in water extracts from fluid inclusions in quartz (0.50–0.54 wt %). Topaz was identified in these inclusions as a daughter solid phase. High Li (400 ppm), Rb (1500 ppm), Sn (80 ppm), Nb (50 ppm), Ta (7 ppm) along with low Sr (<100) are typical. The Rb-Sr and Sm-Nd ages of the granite were estimated as 440–450 Ma (Belyatsky et al., 1999).

The results of a Rb-Sr isotopic study led to the suggestion that Precambrian metamorphic rocks and the Cambrian terrigenous-carbonate sequence were affected by deep fluids and served as a source of granitic magma (Ryazantseva et al., 1994). The high initial ⁸⁷Sr/⁸⁶Sr ratio (0.736) indicates that the generation of granites was presumably related to a diapir of kimberlite-like mantle-derived magma that provided heat and fluid supply to the crustal sources.

The early stage of autometamorphic alteration gave rise to albitization, formation of topaz greisen, and to the deposition of tantalite-columbite-strüverite and the early cassiterite mineralization. The late stage resulted in the formation of fine-grained topaz-quartz, muscovite-quartz, and fluorite-topaz-quartz greisen varieties that replaced the granites and were locally enriched in the late cassiterite and wolframite. The late greisen crosses the previously altered granite and is localized as linear fault-controlled zones, pockets, and vein-shaped bodies. The country terrigenous rocks also underwent greisenization; carbonate beds were transformed into peculiar mica-fluorite metasomatic rocks.

ORE MINERALIZATION RELATED TO THE ORDOVICIAN GRANITES

The wolframite-bearing cassiterite-quartz and cassiterite-silicate-sulfide vein deposits are related to the Ordovician *biotite granite*. The ore mineralization is accompanied by intense tourmalinization and deposition of sparse beryllium minerals and fluorite. Tin mineralization hosted in carbonate rocks has some specific features (Materikov, 1961).

The Chapaevsky W-Sn deposit is spatially related to the Chikheza pluton. Quartz veins with cassiterite, wolframite, and acicular beryl as well as greisen-hosted cassiterite mineralization are known at this deposit.

The Yaroslavsky Sn deposit discovered by Materikov in 1948 is related to the pluton composed of tourmalinized biotite granite. The deposit is localized in the axial zone of an anticline made up of Lower Cambrian limestone and slate with sandstone interlayers. The fold is cut by longitudinal (NW), transverse (N–S), and diagonal (NNE) faults controlling the spatial distribution of orebodies, as well as granite, microdiorite, and dolerite dikes. Limestone serves as the main host rock for ore mineralization.

Four orebody types are recognized: (1) steeply dipping thick quartz veins rimmed with Sn-bearing quartz-tourmaline altered rocks and transected by late tourmaline-fluorite, sulfide-poor tourmaline-cassiterite-quartz, and quartz-sulfide veins; (2) gently dipping metasomatic lodes of quartz-tourmaline and fluorite ores hosted in limestone and skarn at the anticline crest; (3) steeply dipping vein-shaped bodies related to oblique fractures and composed of silicified and quartz-tourmaline metasomatic rocks replacing limestone, slate, and sandstone; sulfide-poor tourmaline-cassiterite-quartz veins cut the altered rocks; (4) oxidized quartz-sulfide-cassiterite veins associated with subordinate tourmaline-cassiterite-quartz ore. The intense tourmalinization of aluminosilicate rocks, skarnification of carbonate rocks, and their replacement by fluorite predated the ore deposition.

The Pervomaisky Sn deposit is situated in the western part of the Voznesenka ore district and resides in Lower Cambrian carbonate rocks intruded by Ordovician biotite granite. The stockwork ore zones and ore-bearing veins are recognized. Two spatially separated types of ore mineralization – cassiterite-tourmaline-fluorite and cassiterite-sulfide – are distinguished within the ore zone that extends for 7–8 km.

The Ta-(Nb) deposits are related to the *rare-metal Voznesenka Granite*. The Ta mineralization was

formed at an early autometamorphic stage and is associated with early topaz greisen. The rare-metal-fluorite mineralization is related to late linear greisen zones in granites and to the specific apocarbonate greisen replacing limestone (Govorov, 1960). The apocarbonate mica-fluorite ore bears Be mineralization and is enriched in Rb, Li, and Cs concentrated in mica. Deposits of this type can be compared with the Ermakovka fluorite-berillium deposit in the Transbaikalian region.

Dikes of aplite, fine-grained granite, granite porphyry and microdiorite, dolerite, and picrodolerite are abundant in the Voznesenka ore district. They are grouped into extended suites mainly striking in a NW direction. Pre-, intra-, and postmineral dikes are distinguished.

The Ta-(Nb) mineralization of strüverite-tantalite-columbite type is related to the Pogranichny and Voznesenka plutons composed of rare-metal topaz-lithionite-albite granite. Fine (0.03–0.05 mm) disseminations of tantalite-columbite, strüverite, and less abundant microlite are dispersed through the greisenized leucogranite together with cassiterite. The greatest amount of strüverite and the highest Ta/Nb ratio in tantalite-columbite varying from 1:3 to 1:1 are reached in the uppermost zone. The character of tantaloniobate distribution, their systematic spatial relations to the crystalline topaz, development of aggregates and discontinuous veinlets of these minerals indicates the metasomatic origin of the Ta-Nb mineralization and its formation at the stage of the early topaz greisen (Rub, 1980).

The fluorite mineralization in the Voznesenka ore district can be defined as rare-metal-fluorite ore type (Ryazantseva et al., 1992) hosted in carbonate rocks (only occasionally in granite) with formation of metasomatic lodes and stockworks of complex morphology above the granite apex or near lateral contacts. The host rocks were affected by skarnification, greisenization, feldspathization, and tourmalinization. Be mineralization is associated with fluorite.

The Voznesenka ore field comprises the Voznesenka, Pogranichny, and Lagerny rare-metal-fluorite deposits, Nagorny and Ovrzhny prospects (Fig. 7.2). The ore field is localized in an asymmetric syncline elongated in a NW direction (320–350°), which attains 1.5–2.0 km in width (at the surface) and is traced for 10 km. The syncline is composed of Lower Cambrian limestone and slate. The northeastern limb of the syncline dips at angles 45–70° SW; the opposite limb dips steeply at angles 65–85° NE. The Voznesenka deposit is localized in the western steep limb while the

Pogranichny deposit occupies the relatively gentle eastern limb. The area of the Lagerny deposit covers both limbs. Faults transect the syncline in longitudinal, transverse, and oblique directions cutting it into wedge-shaped blocks displaced relatively to one another. The Voznesenka Thrust Fault and Pogranichny Reverse Fault bound the ore field in W and E, respectively. The rare-metal granite crops out as narrow intrusions elongated in a NW direction concordant to the fold structure. The granite bodies at the Voznesenka and Pogranichny deposits abruptly widen at a depth of 800–1200 m merging into a single pluton.

The rare-metal-fluorite deposits and prospects of the Voznesenka ore field belong to the mica-fluorite type, except a topaz-fluorite lode at the Pogranichny deposit (Ryazantseva et al., 1992). The mica-fluorite ore is a product of metasomatic replacement of limestone or skarn and considered to be a desilicified greisen (Govorov, 1960). All orebodies are similar in composition and make up a spatial system related to the common source of ore-bearing solutions that were circulating contemporaneously in different parts of the ore field along contacts of premineral dikes and granitic intrusions. The typomorphic features of fluorite, the ore structure, and variation of fluorite grade have shown that the ore lodes were formed under low-permeable screens of slates and thrust faults at a temperature gradually falling from 360 to 130°C. Variable alkalinity of the solution and a high fluorine activity are suggested (Kupriyanova and Shpanov, 1997).

THE VOZNESENKA DEPOSIT

Geological summary. The deposit as a part of the Voznesenka ore field (Fig. 7.2) is hosted in Lower Cambrian bituminiferous limestone (Volkusha Formation) in the southwestern limb of the Voznesenka Syncline complicated with a second-order anticline striking 325–335° NW (Fig. 7.3). Dip angles vary from 30 to 80°. In the east, the deposit is bounded by the contact of limestone with slate of the Kovalenkov Formation. The western boundary extends along the Voznesenka Thrust Fault dipping 35–65° SW. A gently dipping tectonic zone is conjugated with this fault. The mica-fluorite mineralization was formed beneath the tectonic zone as under a screen.

Igneous rocks. Rare-metal porphyritic granite crops out in the northern flank of the deposit as a narrow dike-shaped intrusion (Fig. 7.3). In the central part, the granite occurs at a depth of 500 m and gradually rises to a depth of 100 m toward the southern flank. Numerous granitic offsets converted into fluo-

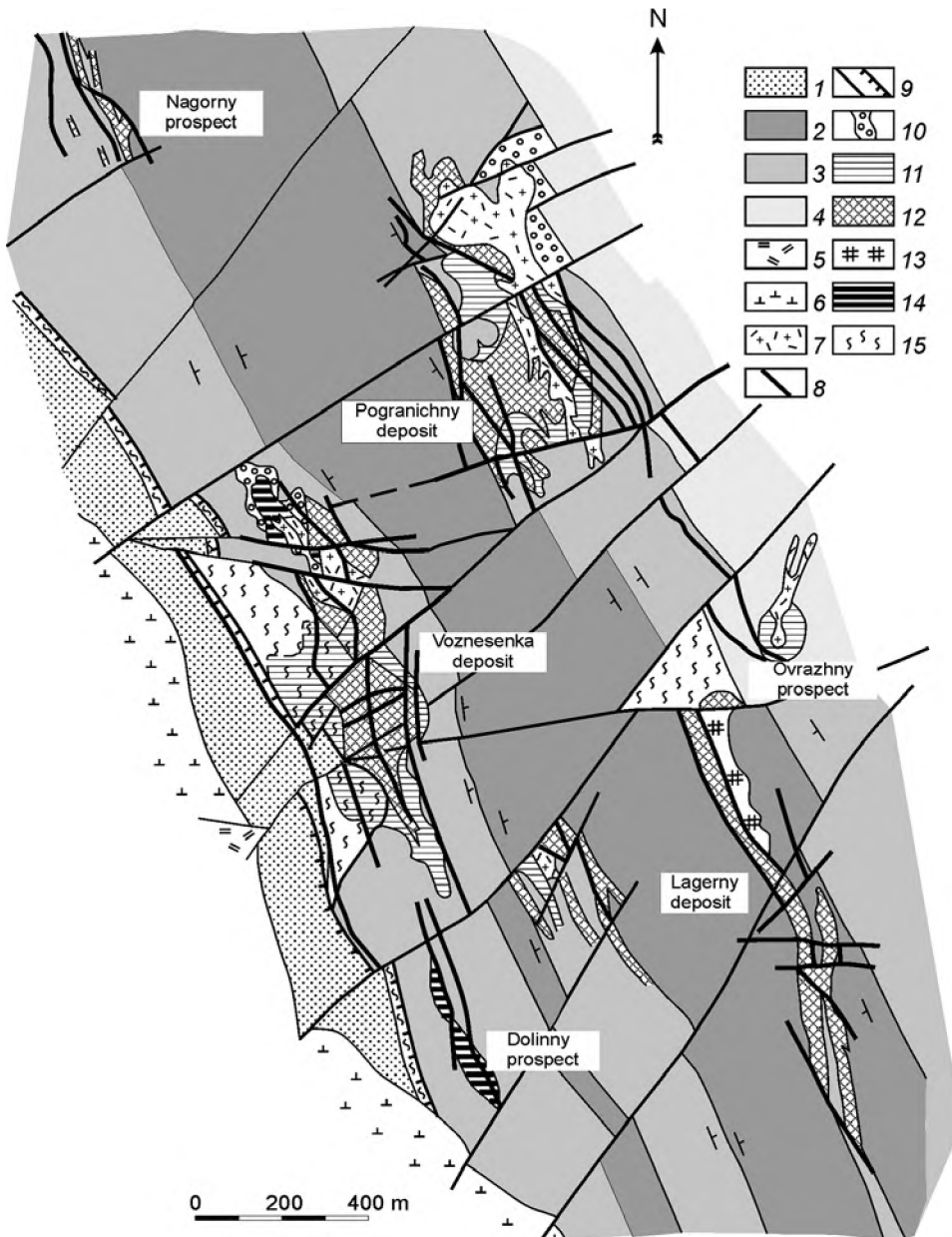


Fig. 7.2. Schematic geological map of the Voznesenka ore field.

(1) siltstone; (2) quartz-sericite slate; (3) limestone; (4) graphite schist; (5) granite porphyry; (6) Silurian diorite and monzodiorite; (7) Ordovician greisenized granite; (8) basic and intermediate dikes; (9) faults; (10) skarn; (11) fluoritized limestone; (12) fluorite ore; (13) zone of quartz-topaz veinlets with wolframite and cassiterite; (14) base-metal ore; (15) tectonite

rite-bearing quartz-mica and quartz-topaz greisen are localized within orebodies. The apical portion of the pluton is also greisenized while the granite at deeper levels underwent albitization. Abundant intermediate and basic dikes form a ramified system (Androsov and Ryzantseva, 1992).

Ore mineralization. The ore zone extends for 1.5 km in a nearly N-S direction concordant to the host limestone. The zone attains 500 m in width as a combination of vertical columnar and gently dipping stratified bodies occurring above the granitic pluton. Transverse premineral faults of northeastern and latitudinal directions divide the deposit into three large blocks (Fig. 7.4).

The central block hosts the Main orebody – a vertical ore column, ellipsoidal in plan and pipe-like in

the vertical section, slightly widening upward (Fig. 7.5).

The Eastern and Western stratified orebodies are localized in the northern block near the contact with granite. Sphalerite- and magnetite-bearing skarn separates the fluorite orebodies from granite.

The southern block hosts the Southern Offset, a vertical metasomatic lode with roughly parallel contacts and a small arcuate bend at lower levels. Its morphology is complicated at the upper levels due to low-angle offsets abruptly pinching out down the dip. The metasomatic orebodies have no definite boundaries and are countered by a cutoff of 20 wt % CaF_2 . The internal orebody structure is heterogeneous. Fluorite ore alternates with limestone impregnated to some

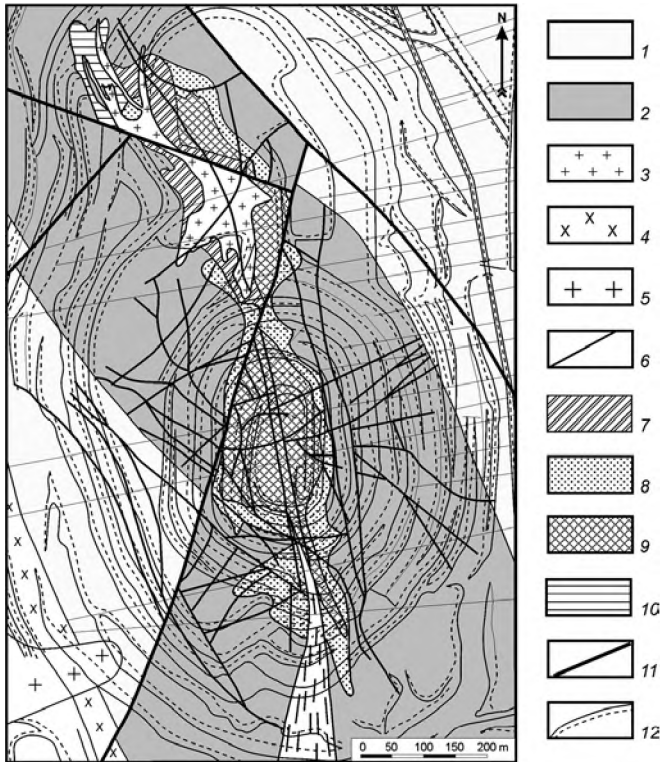


Fig. 7.3. The Voznesenka deposit (plan of open pit). (1) slate; (2) limestone; (3) greisenized granite; (4) diorite; (5) rhyolite; (6) basic and intermediate dikes; (7) skarn; (8) fluoritized limestone; (9) fluorite ore; (10) base-metal ore; (11) fault; (12) open pit bench

extent with fluorite and is cut by numerous basic-intermediate dikes and granitic offsets.

Several compositional and textural ore types are recognized (Kupriyanova and Shpanov, 1997).

The dark gray to black *apocarbonate* (alteration carbonate) massive and alveolar ore is predominant at the deposit. Fluorite is separated from mica as rounded, somewhat oblong grains, varying from fractions of millimeter to 1–3 cm in size. The fluorite grade ranges from 20 to 60%. Interstitial space be-

tween fluorite grains is filled with a fine-grained aggregate of Li-variety muscovite and muscovite; albite and tourmaline are rather abundant. Anhedral grains, small prismatic crystals, and radiate sheaflike intergrowths of phenakite occur in the interstitial space (Kupriyanova and Shpanov, 1997). Ephesite (margarite), calcite, dolomite, and sellaite appear at the northern and southern terminations of the Main orebody.

The *aposkarn* ore is localized at the northern flank and at lower levels close to the granitic pluton. The sulfide-bearing fine-grained mica-fluorite ore occurs as light gray, greenish, or lilac rocks of hornfels appearance. Irregular spots are noticed. Average fluorite grade is about 35%. The fluorite grain size is 0.01 mm and smaller and mica-fluorite intergrowths are typical. Sulfides are contained as fine disseminations of pyrite, arsenopyrite, and sphalerite (Kupriyanova and Shpanov, 1997).

The *breccia-type ore* with albite-quartz-mica cement is known from the central part of the deposit. Fragments are composed of apocarbonate and aposkarn ores. The relative amount of clastic material varies from a few fragments to 45 vol %. The fragment dimensions are variable, from fractions to tens of centimeters. The chaotically oriented fragments are angular and elongated along bedding (Kupriyanova and Shpanov, 1997).

Typical chemical compositions of different fluorite ore types are presented in Table 7.2.

Three principal mineral assemblages are recognized: (1) fluorite-albite with fluorite veinlets and pockets, (2) muscovite-albite-fluorite, and (3) muscovite-fluorite. Assemblages (2) and (3) are abundant in the breccia-type and apocarbonate ores. Muscovite often gives way to ephesite and lepidolite. Tourmaline, topaz, sellaite, calcite, phenakite, and chrysoberyl are also noticed in the ore.

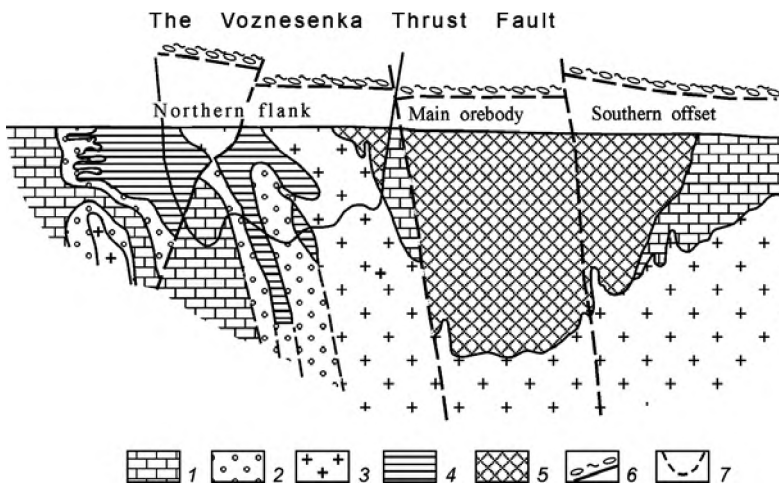


Fig. 7.4. The Voznesenka deposit: schematic longitudinal section including the eroded upper part. (1) limestone; (2) skarn; (3) granite; (4) base-metal ore; (5) fluorite ore; (6) fault

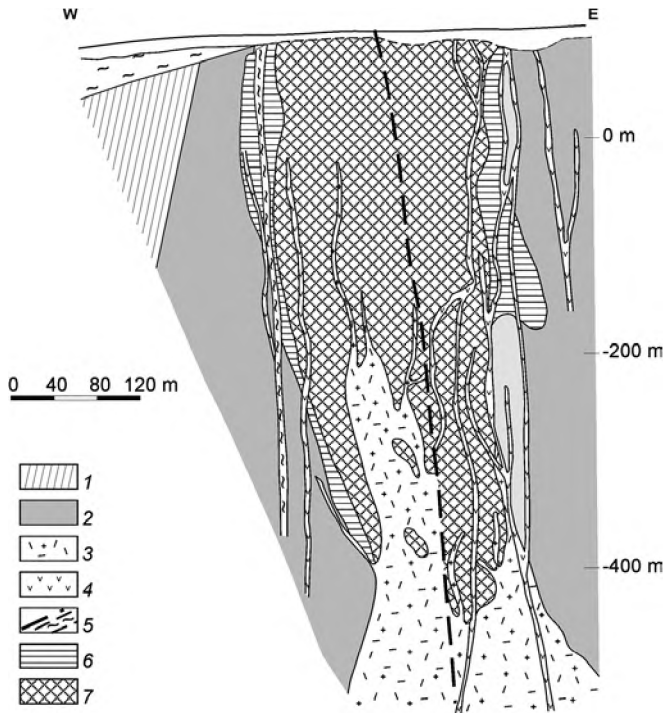


Fig. 7.5. Geological section across the Main orebody of the Voznesenka deposit.

(1) slate; (2) limestone; (3) greisenized granite; (4) basic and intermediate dikes; (5) fault and fault zone; (6) fluoritized limestone; (7) fluorite ore

Formation conditions. Ore deposition proceeded at a gradually falling temperature under a pressure of 480–1330 bar. Fluorite precipitated from magnesium-sodium chloride solutions occasionally containing potassium and iron chlorides. Salt concentration decreased with falling temperature. Carbon dioxide is a typical component the solution responsible for the apocarbonate fluorite ore formation (Bredikhina, 1990).

THE POGRANICHNY DEPOSIT

Geological summary. The Pogranichny deposit is situated 1 km northeast of the Voznesenka deposit in the eastern limb of the Voznesenka Syncline and localized in the same Lower Cambrian limestone conformably overlain by slate of the Kovalenkov Formation (Fig. 7.2). The sedimentary rocks are intruded by the rare-metal Voznesenka Granite. The localization of the Pogranichny deposit is controlled by a system of northeastern normal and strike-slip faults that intersect the syncline limb. The geological boundaries of the deposit are delineated by the contact of limestone (Volkusha Formation) and slate (Kovalenkov Formation) in the west, by the termination of granitic pluton in the north, by the Pogranichny Reverse Fault in the

Chemical composition (wt %) of mica-fluorite ore from the Voznesenka deposit

Component	Apocarbonate ore	Breccia-type ore	Aposkarn ore
CaF ₂	32.19	47.16	36.04
CaCO ₃	21.34	4.43	1.37
SiO ₂	19.19	22.23	30.76
Fe ₂ O ₃	0.78	0.95	0.89
Al ₂ O ₃	8.98	12.45	8.75
MgO	8.80	7.52	5.49
BeO	0.15	0.13	0.069
Li ₂ O	0.243	0.496	0.723
Rb ₂ O	0.233	0.364	0.430
Cs ₂ O	0.019	0.025	0.021
K ₂ O	1.94	2.97	3.95
Na ₂ O	0.62	0.65	1.51
S _{sulfide}	0.080	0.041	0.058
S _{total}	0.098	0.16	0.09

east, and the Southern Strike-Slip Fault in the south. The leucogranite pluton is only slightly eroded and crops out as a narrow ridge extending for 800 m in a northwestern direction. The ridge varies in width from 30–50 m in the south to 150–300 m in the northern part of deposit. In cross section, this is a steep salient, somewhat overturned to the northeast. The western intrusive contact becomes low-angle (30–40°) with depth, whereas the eastern contact, on the contrary, is traced as approximately vertical below a level of 100 m. The intrusion gradually plunges to the northwest, where it was penetrated by boreholes at a depth of 750–800 m. The granite is transformed into greisen down to a depth of 100–150 m. Greisenized granite was traced to a depth of 200–250 m. An albitized variety occupies a depth interval from 200–250 to 400–450 m giving way to unaltered biotite-protolithionite granite at greater depth. Quartz-mica, quartz-topaz, topaz-fluorite, and transitional greisen varieties are known. Diorite porphyry and dolerite dikes are abundant as three swarms of a NW direction controlled by fracture zones (Fig. 7.6).

Mica-fluorite and topaz-fluorite ores are distinguished at the Pogranichny deposit (Rub, 1980). The localization of the mica-fluorite ore is controlled not only by faults but also by the contact of granite with limestone and by the low-angle contact of the limestone with overlying slate. Some small orebodies are controlled by intraformational detachments. Mica-fluorite ore forms complex metasomatic lodes of ir-

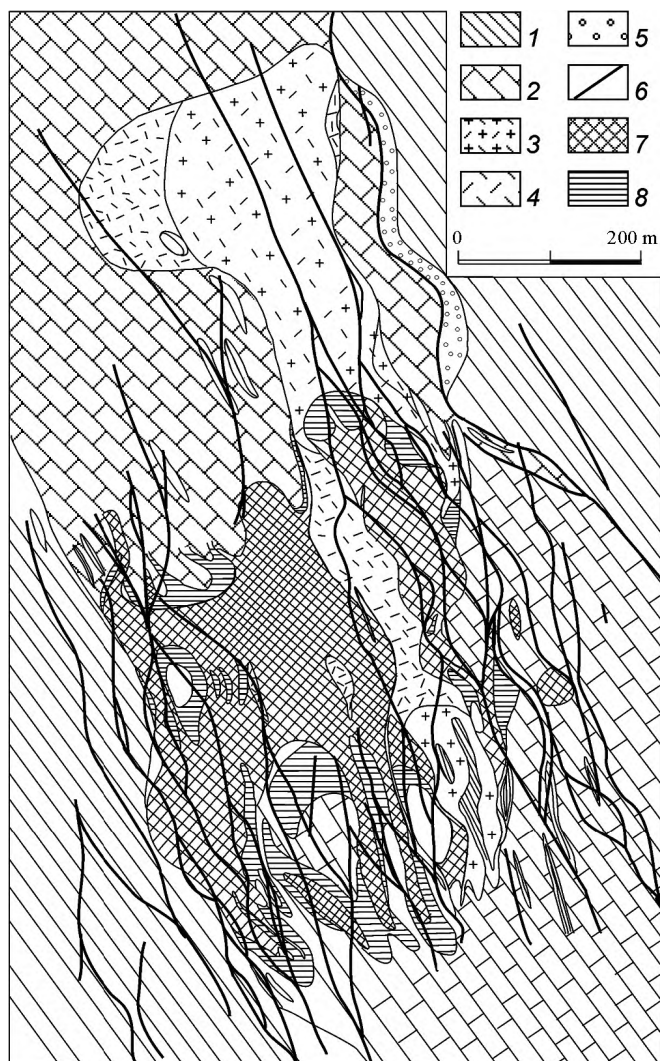


Fig. 7.6. Schematic geological map of the Pogranichny deposit.

(1) slate; (2) limestone; (3) greisenized granite; (4) greisen; (5) skarn; (6) dikes of intermediate composition; (7) fluorite ore; (8) fluoritized limestone

regular morphology. They surround the granitic intrusion and pinch out along strike and down dip (Fig. 7.7).

Moving away from the intrusive contact, the ore lodes become stratiform and concordant with bedding in the limestone. Their internal structure is complex and characterized by alternation of the fluorite ore, limestone impregnated by fluorite, and barren limestone. The thin Eastern and thick Western lodes were contoured. The morphology of the Eastern lode is entirely determined by the shape of the contact with granite that underlies the lode. At a depth below 100 m, the intrusive contact becomes vertical, and the ore pinches out. The Western metasomatic lode extends for 2 km and consists of several ribbons extending parallel to the limestone bedding and composed of

fluorite ore intercalated with fluoritized and barren limestones. The so-called Near-contact and Subslate orebodies are separate in cross section. The Near-contact orebody is localized immediately at the contact of limestone with granite and mimics the contact surface in outline. The bulges of this orebody were established only close to the surface. The orebody thickness is markedly reduced with depth where it locally pinches out totally. At the northern flank of deposit, the Near-contact orebody is traced for a considerable distance and plunges in a NW direction to a depth of 1000 m toward the Nagomy prospect. At the southern flank, the Near-contact orebody merges with the Subslate body at a depth of 120–150 m making up a common lode gradually pinching out along the strike. The Subslate orebody is related to the contact between limestone and slate being localized within limestone. The slate is impregnated with fluorite near the contact. The orebody is a complex alternation of thin interlayers of fluorite ore and fluoritized limestone.

Massive, banded, small-augen, festooned banded, pseudobrecciated structures and subgraphic texture are typical of the mica-fluorite ore at the Pogranichny deposit. Apocarbonate, aposilicate (apogranite), and breccia-type ores are recognized (Kupriyanova and Shpanov, 1997).

Apocarbonate ore is similar in many respects to the same ore known from the Voznesenka deposit. Some varieties differ from the latter by a rhythmically banded structure and a very fine-grained texture. Banding is determined by intercalation of violet-gray mica-fluorite laminae with a fine alveolar structure (from 0.5–1.5 to 20 cm thick) and white opaque laminae of chrysoberyl-mica composition, 0.1–2.0 mm in thickness (Kupriyanova and Shpanov, 1997). Laminae are wavy-festooned in shape. Micas are composed of muscovite and ephesite. Tourmaline and calcite are abundant; sulfides are also noticed.

Breccia-type ore is typical of this deposit. Angular, commonly oblong fragments, 0.5–10 cm in size, are composed of alveolar and rhythmically banded mica-fluorite ore and white apogranite greisen. The fragments are cemented by fine-grained (0.01–0.001 mm) mica-fluorite material, black-colored due to impregnation with carbonaceous matter. The proportion of clastic material and cement varies from clast- to matrix-supported breccia (Kupriyanova and Shpanov, 1997). Euclase occurs in ore of this type.

Apogranite topaz-fluorite greisen ore is closely related in space and origin to the mica-fluorite ore.

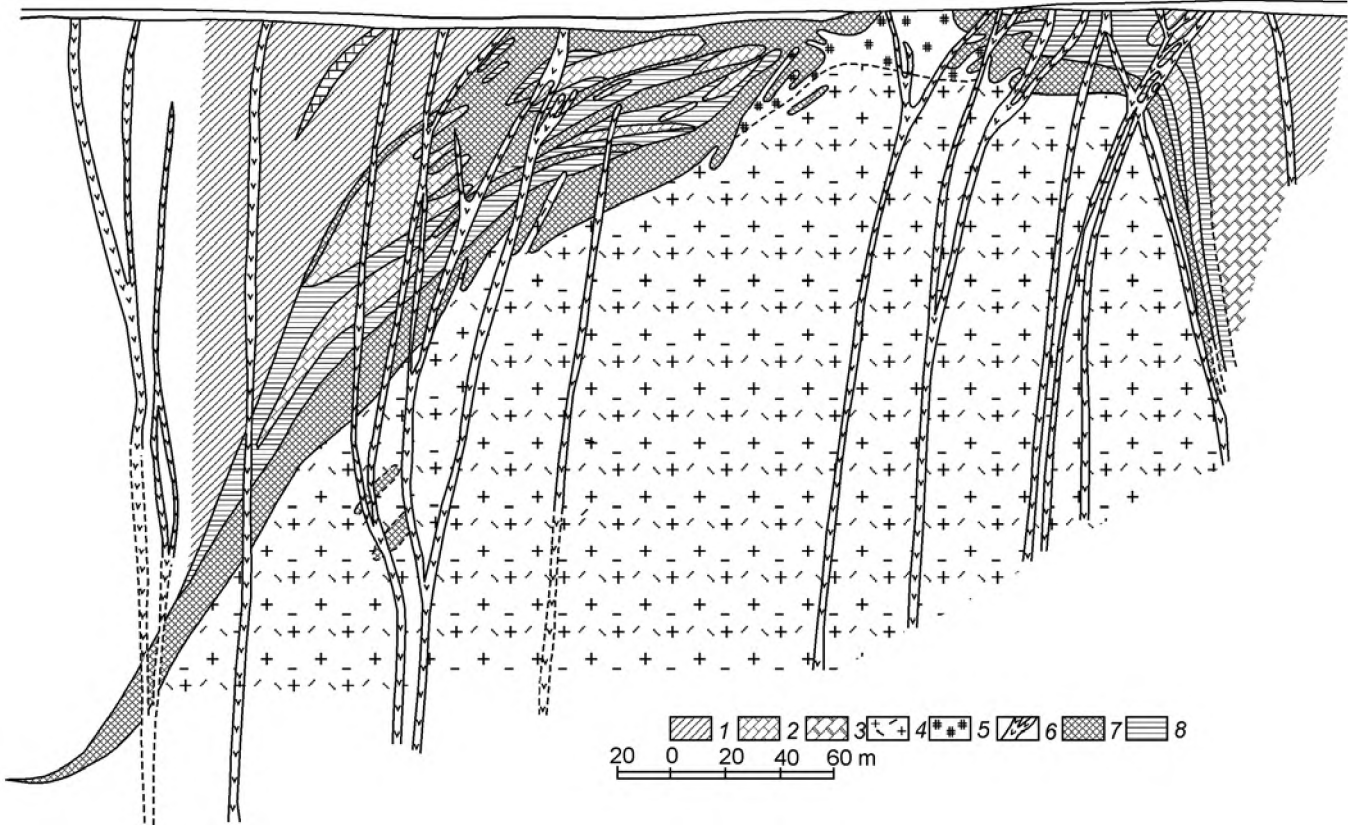


Fig. 7.7. Geological section across the Pogranichny deposit.

(1) slate; (2) limestone; (3) skarn; (4) granite; (5) quartz-topaz greisen with fluorite; (6) basic and intermediate dikes; (7) fluorite ore; (8) fluoritized limestone

Greisenization was accompanied by intense fluorine metasomatism both in granites and country rocks. The ore forms a metasomatic lode compact and irregular in shape at the crest of granitic ridge (Fig. 7.6). The lode is slightly elongated in a NW direction and not exposed at the surface. It is surrounded by quartz-mica greisen. The topaz-fluorite greisen is gradually replaced by low-grade quartz-topaz greisen both south and northward and also beneath the orebody. The upper and lower boundaries of the ore zone are approximately horizontal and coincide with boundaries of the quartz-microcline zone, which was formed in the granitic protolith as a result of feldspathization. The topaz-fluorite ore is white in color with a violet hue. The fine-grained texture in combination with massive, banded, festooned, and block structures are typical. Fluorite, topaz, and quartz are the major minerals; diasporite and pyrophyllite are also common. Mica is extremely rare. Cassiterite, wolframite, and columbite are sporadically noticed. Fluorite occurs as irregular pockets, disseminations, and veinlets. Various tints of violet color are typical; white translucent and light brown varieties are also known. Fluorite is closely associated with topaz. Thin needles of this

mineral are incorporated into fluorite grains. Fluorite also rims the aggregates of fibrous and acicular topaz as cockade selvages. The fluorite grade drops from the center of the metasomatic lode to its periphery.

THE LAGERNY DEPOSIT

The Lagerny deposit is situated south of the Voznesenka and Pogranichny deposits. The ore zone extends for 1.5 km in a NW direction in both limbs of the Voznesenka Syncline along the contact between limestone and slate. The stratiform orebodies dip to meet each other in the syncline core and are bound by transverse faults pinching out in the south. The thickness of stockwork-type orebodies increases down dip. Metasomatic mica-fluorite veinlets of the ore stockworks are cut by pegmatoid quartz-plagioclase veins, topaz veinlets with wolframite and cassiterite, quartz veinlets with beryl, tourmaline-quartz veinlets with wolframite and cassiterite, quartz veinlets with beryl, tourmaline-quartz veinlets with wolframite and cassiterite, quartz-fluorite-tourmaline, sulfide-bearing quartz veinlets, calcite-fluorite, and calcite veinlets. Premineral transverse strike-slip and reverse faults

divide the ore-bearing area into several blocks. A granitic intrusion with a roof as a ridge complicated by a "palisade" of steeply dipping offsets occurs at a depth of 300–400 m (Fig. 7.8).

The granite is greisenized as also at the Pogranichny and Voznesenka deposits.

In addition to the deposits described above, the *Nagorny*, *Ovrazhny*, and *Severny* prospects are localized in the Voznesenka ore field.

The fluorite mineralization is also known beyond this field at the Yaroslavsky tin deposit where fluorite is a constituent of the cassiterite-tourmaline-fluorite and sulfide-quartz-fluorite assemblages. The special mica-fluorite type is developed only locally. Separate fluorite prospects are situated beyond the tin ore field at the contact of the Voznesenka Granite and limestone.

Thin fluorite veinlets are known from the Pervomaisky ore zone (Fig. 7.1), where they occur in limestone and dolomite of the Pervomaisky Formation. The stockwork of the Blue zone at the Pervomaisky tin deposit consists of quartz-feldspar, mica-fluorite, sulfide-bearing cassiterite-fluorite, carbonate-fluorite, and sulfide-fluorite veinlets.

The Lower Cambrian limestone of the Volkusha Formation is the main host rock for the fluorite mineralization in the Voznesenka ore district. The organogenic limestone of this formation stands out against other sedimentary rocks of the district with a high fluorine content of about 800 ppm. Based on this, some researchers refer the fluorite mineralization to the stratiform fluorite-base metal type and regard the carbonate rocks as a source of the ore matter. It cannot also be ruled out that the pre-orogenic fluorite

ore of hydrothermal sedimentary origin was subsequently modified by the later skarnification and greisenization.

EXCURSION POINTS

Stop 1. *The Grodekovo batholith*

The batholith occupies a vast area west of the Voznesenka ore field.

Quarry at the 33 km of the Mikhailovka–Khotol Highway.

Silurian Grodekovo Plutonic Complex: The Rb–Sr age is 408–411 Ma.

The collision-related geodynamic type.

Granitic rocks intrude Lower Cambrian sedimentary rocks and contain numerous relict blocks of Precambrian metamorphic rocks.

Main granite varieties:

- (1) biotite microcline medium-grained granite;
- (2) aplite-like fine-grained leucogranite;
- (3) biotite-amphibole granite.

Mineral composition of granites (vol %): quartz (30), microcline (40), plagioclase (25), biotite (3–5), and amphibole (2).

Accessory minerals: monazite, apatite, ilmenite, zircon, titanite, and garnet.

Petrochemical affinity: peraluminous corundum-normative high-K granite ($K/Na = 1.4–1.5$).

Small iron and base-metal occurrences are related to the Grodekovo Granite.

Stop 2. *The Yaroslavsky pluton*

The pluton is exposed at the southern outskirts of the Yaroslavsky Settlement.

Ordovician Yaroslavsky Plutonic Complex: The U–Pb age is 455 Ma.

The intraplate geodynamic type.

Granitic rocks intrude Lower Cambrian carbonate and terrigenous rocks.

The tourmaline-bearing biotite medium-grained porphyritic leucogranite with potassium feldspar and quartz phenocrysts; leucogranite was locally affected by greisenization.

Mineral composition of granites (vol %): quartz (25–30), potassium feldspar (40), plagioclase (20–25), and biotite (0.5–4.0).

Accessory minerals: zircon, apatite, magnetite, cassiterite, fluorite, and rutile.

Petrochemical affinity: peraluminous high-K leucogranite ($K/Na = 1.6$) enriched in F and B.

Stop 3. *The Voznesenka pluton*

The southern outskirts of the Voznesenka Village. The Voznesenka fluorite open pit.

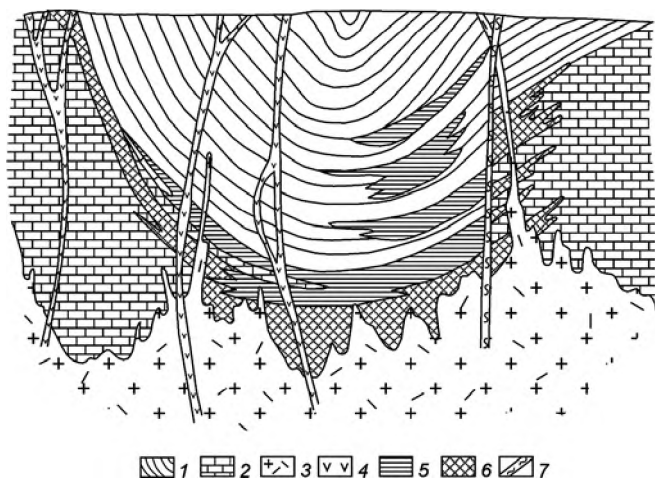


Fig. 7.8. Geological section across the Lagerny deposit. (1) slate; (2) limestone; (3) greisenized granite; (4) basic and intermediate dikes; (5) fluoritized limestone; (6) fluorite ore; (7) fault zone

Ordovician Voznesenka Plutonic Complex: Rb-Sr and Sm-Nd age is 450 Ma.

The intraplate geodynamic type.

Granitic rocks intrude Lower Cambrian carbonate, terrigenous rocks and Silurian diorite.

The severely albitized and greisenized biotite-protolithionite granite.

Mineral composition (vol %): quartz (30), potassium feldspar (30), albite (30), biotite (5), protolithionite (5).

Accessory minerals: zircon, cassiterite, apatite, tourmaline, topaz, fluorite, magnetite, strüverite, columbite, and xenotime.

Petrochemical affinity: Li-F peraluminous K-Na-granite (K/Na = 0.8).

Granitic rocks contain Ta-Nb mineralization; unique rare-metal-fluorite mineralization is hosted in country limestone.

Stop 4. The Lipovy Hill intrusion

The intrusion extends in a NW direction and is controlled by a fault that divides two subzones of the Voznesenka Zone with different types of stratigraphic section. Quarry on the northern slope of the Lipovy Hill.

Silurian complex of gabbro, diorite, and monzodiorite.

Plutonic rocks intrude Lower Cambrian terrigenous sequence.

Sm-Nd and Rb-Sr age is 406–415 Ma.

Stop 5. A general view on the Voznesenka rare-metal-fluorite deposit

Highest point at the northern steep wall of the open pit. Contours of the Main orebody, faults, diorite exposed at the western wall, and granite porphyry at the southern wall can be observed.

Stop 6. Protolithionite-biotite granite

Light gray fine- and medium-grained greisenized granite at the western wall of the open pit at the level of +20 m (see STOP 3 in the above section for the rock characteristics).

Stop 7. Garnet-pyroxene-vesuvianite skarn with sphalerite and magnetite

Western wall of the open pit at the level of +20 m.

Stop 8. Main orebody

Dark violet massive fine-to-medium-grained mica-fluorite ore with a grade of 30–35% CaF₂ on the open pit bottom at the level of –150 m. A microdiorite dike composed of greenish gray fine-grained rock is impregnated with fluorite near contacts.

Stop 9. Open pit at the Pogranichny deposit

Topaz-fluorite ore in the central part of open pit and mica-fluorite ore at the western wall.

REFERENCES

Androsov, D.V. and Ratkin, V.V., The pre-orogenic massive sulfide zinc ore at the Voznesenka greisen deposit, Primorye, *Geol. Rudn. Mestorozhd.*, 1990, no. 5, pp. 46–58.*

Androsov, D.V. and Ryazantseva M.D., Relationships between dikes and base-metal-fluorite ore at the Voznesenka deposit, Primorsky region, *Proc. Dalnedra Assoc.*, vol. 2, Khabarovsk: Dalnedra, 1992, pp. 50–60.*

Belyatsky, B.V., Krymsky, R.S., Rub, M.G., Pavlov, V.A., and Rub, A.K., Age and genetic relationships of rare-metal ore-bearing granites of Voznesenka ore Field, Primorye: Rb-Sr and Sm-Nd isotopic data, in: *Mineral deposits: Processes to processing*, Rotterdam: Balkema, 1999, pp.313-317.

Bredikhina, S.A., Physicochemical conditions of fluorite formation at deposits of the Voznesenka ore field, Primorye, *Geol. Geofyz.*, 1990, no. 12, pp. 78–86.*

Govorov, I.N., Greisenization of limestone and intruding granite, in *Magmatizm i svyaz s nim poleznykh iskopaemykh* (Magmatism and related mineral resources), Moscow: Gosgeoltekhizdat, 1960, pp. 522–530.*

Govorov, I.N., *Geokhimiya rudnykh raionov Primor'ya* (Geochemistry of ore districts in Primorye), Moscow: Nauka, 1977, 250 s.*

Kupriyanova, I.I. and Shpanov, E.P., Beryllium-fluorite deposits of the Voznesenka ore district, *Geol. Rudn. Mestorozhd.*, 1996, vol. 38, no. 1, pp. 3–14.**

Kupriyanova, I.I. and Shpanov, E.P., Beryllium-fluorite ores in the Voznesenka ore district, Primorye, Russia, *Geol. Rudn. Mestorozhd.*, 1997, vol. 39, no. 5, pp. 442–455.

Materikov, M.P., A new genetic type of economic fluorite deposits, *Miner. syr'e*, vol. 2, Moscow: VIMS, 1961, pp. 37–46.*

Materikov, M.P., Specific features of the tin deposits hosted in carbonate rocks, *Sov. Geol.*, 1961, no. 9, pp.96-107.*

Ratkin, V.V., Lead and zinc metallogeny at the Pacific margin of Asia, *DSc Thesis (Geol.-Mineral.)*, Moscow, 1995.

Rub, A.K., *Tipomorfnye osobennosti mineralov-sputnikov tantalovogo i olovyannogo orudneniya* (Typical features of minerals associated with Ta and Sn ores), Moscow: Nedra, 1980, 152p.*

Rub, M.G. and Rub, A.K., New geological and geochemical data on igneous rocks of the Khanka Lake district, *Tikhookean. Geol.*, 1986, no. 5, pp. 57–67.

Rub, M.G., Rub, A.K., and Loseva, T.I., Micas as indicators of granite ore potential, *Izv. Akad. Nauk SSSR, Ser. Geol.*, 1971, no. 10, pp. 73–85.*

Ryazantsev, A.A., Structural, magmatic, and lithological controls of ore mineralization in the Voznesenka ore district, Primorye, *PhD Thesis (Geol.-Mineral.)*, Vladivostok: FEGI, 1973.

Ryazantseva, M.D., Comparative characteristics of the Voznesenka and Grodekovo granites in the southern Khanka Lake Massif, in: *Izverzhennyye porody Vostoka Azii* (Igneous rocks of the eastern Asia), Vladivostok: Far East Sci. Center, 1976, pp. 69–73.*

Ryazantseva, M.D. and Shkurko, E.I., *Flyuorite Primor'ya* (Fluorite in Primorye), Moscow: Nedra, 1992, 158 p.*

Ryazantseva, M.D., Gerasimov, N.S., and Govorov, I.N., Rb-Sr isochrons and petrogenesis of igneous rocks of the Voznesenka ore district, *Tikhookean. Geol.*, 1994, vol. 13, no. 4, pp. 60–73.**

Ryazantseva, M.D., Golozubov, V.V., Ratkin, V.V., and Sokarev, A.N., Geodynamic typification of granitoids in Primorye, *Tikhookean. Geol.*, 1998, vol. 17, no. 5, pp. 11–26.**

* In Russian.

** English translation is available.



GEOLOGY, MAGMATISM, AND GOLD MINERALIZATION OF SOUTH PRIMORYE (THE ASKOLD STRIKE-SLIP FAULT ZONE, SERGEEVKA TERRANE)

G. R. Sayadyan

Far East Geological Institute (FEGI), Far East Branch, Russian Academy of Sciences

OUTLINES OF REGIONAL GEOLOGY

The territory that will be visited during the excursion is situated in southern Primorye and covers the coastal zone (town of Fokino and Strelok Bay) and nearby Askold Island.

The objects of the excursion are localized in the Sergeevka Terrane (Khanchuk, 2000), a fragment of Mesozoic passive continental margin (Fig. 8.1). The terrane is composed of the Sergeevka gabbroids including large plutons of metagabbro (523 ± 3 Ma) and metadiorite (504 ± 3 Ma) with blocks of metaterigenous rocks and granitic gneiss therein. The gabbroic rocks were metamorphosed under conditions of epidote-amphibolite facies and reveal a distinct banding. Sinitsa and Khanchuk (1991) provided evidence for the synkinematic nature of the Sergeevka gabbroids. The gabbroic rocks are intruded by the Early Ordovician Taudemi biotite granite (493 ± 12 Ma) and the Tafuin muscovite granite (492 ± 12 Ma) (Khanchuk, 1993). Normal granite, leucogranite, and hybrid intrusive rocks varying from plagiogranite to diorite in composition are typical of the Taudemi Complex; the rocks are often gneissic in appearance. The Tafuin Granite is more leucocratic.

Stratified Middle and Upper Paleozoic rocks that unconformably overlie the Cambrian-Ordovician terrane are Devonian and Permian volcanosedimentary and terrigenous sequences. Upper Devonian tuffs overlie eroded gabbroic rocks of the Sergeevka Terrane (Sinitsa, 1998). Granitic rocks are overlapped by Permian volcanosedimentary sequences of the Dunai, Abrek, and Chandalaz formations. According to geochemical signatures, they are defined as subduction-related (island-arc) and riftogenic (backarc) rock asso-

ciations (Levashev et al., 1989; Levashev, 1991). The section is overlain by Triassic, Jurassic, and Lower Cretaceous sequences (Fig. 8.2). Volcanic and terrigenous rocks of the Chandalaz Formation are overlain by a basal unit of a Triassic megarhythm consisting of sandstone and conglomerate. Rhythmically bedded siltstone and sandstone of the lower subformation of the Simeuza Formation lie above this with an erosional surface at the base. The Triassic section is completed by an upper subformation of rhythmically intercalated sandstone, siltstone, and limestone. A Jurassic megarhythm comprises conglomerate, sandstone, siltstone with fluidal structures, and limestone of the Shitukha Formation; overlying sandstone with fluidal structures, gritstone lenses, and nodular siltstone belong to the Chigan Formation. The Cretaceous section is composed of rhythmically alternating conglomerate, gritstone, sandstone, siltstone, and mudstone with coal and limestone interlayers (Fig. 8.2).

A hierarchical series of genetically related linear structures of strike-slip nature controls the localization of ore districts, deposits, and particular orebodies in the southern Far East of Russia (Utkin, 1989, 1990). Gold deposits, ore occurrences, and showings of the Sergeevka Terrane are grouped into the Askold, Partizansk, and West Partizansk linear metallogenic zones striking in a NNE direction (Fig. 8.3). The first of these zones with the Askold Island gold deposit and the Mount Krinichny ore field therein has been studied most thoroughly (Khomich and Sayadyan, 1995; Sayadyan et al., 1995, 1996, 1998, 1999). The Askold Strike-Slip Fault Zone crosses the Dunai-Okrainka Horst (Utkin, 1996), or the Dunai Subzone of the South Primorye lithotectonic zone (Vasil'ev, 1965; Nazarenko and Bazhanov, 1987) where metagabbroids

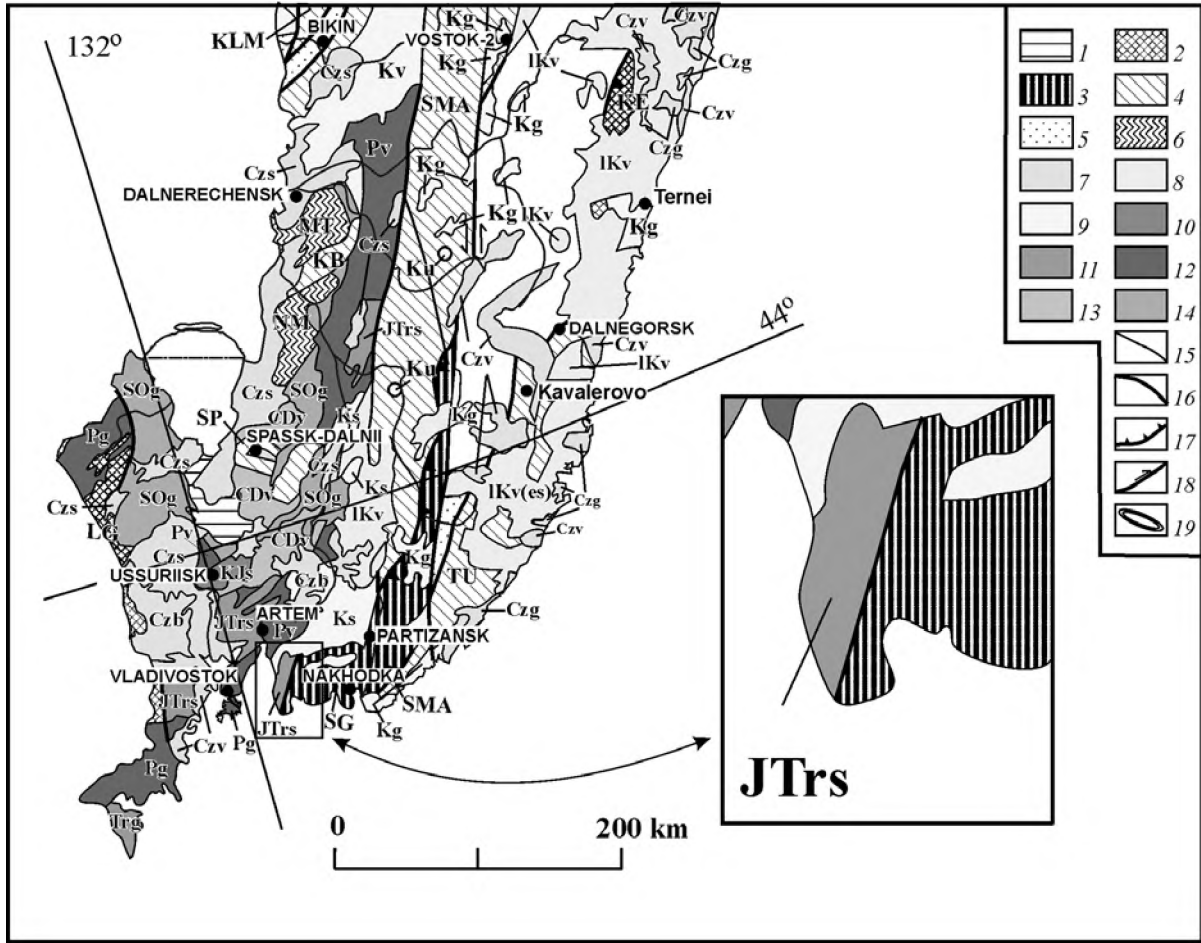


Fig. 8.1. Paleodynamic complexes of the Russian Far East, a fragment of the map compiled by Khanchuk (2000).

Terranes: (1) passive continental margin, (2) island arc, (3) active continental margin, (4) accretion prism, (5) turbidite basin, (6) metamorphic; *age of overlying sequences and postaccretionary complexes:* (7) Cenozoic, (8) Late Cretaceous, (9) Early and Late Cretaceous, (10) Late Jurassic and Early Cretaceous, (11) Late Triassic and Middle Jurassic, (12) Middle Carboniferous and Early Triassic, (13) Devonian and Early Carboniferous, (14) Ordovician and Silurian; (15) stratigraphic and intrusive contacts; (16) postaccretionary faults; (17) postaccretionary thrust faults and direction of their hanging wall displacement; (18) postaccretionary strike-slip faults; direction of relative slip is shown by arrow; (19) complexes of metamorphic cores.

Overlying sedimentary rocks: (Czs) Cenozoic, (Iks) Upper Cretaceous, (Ks) Lower Cretaceous, (KJs) Jurassic and Cretaceous, (Jtrs) Triassic and Jurassic; *volcanosedimentary rocks:* (Czb) Cenozoic basalts of transform margin, (Czv) Cenozoic bimodal series of transform margin, (IKv) Upper Cretaceous rocks of active margin, (Kv) Lower Cretaceous rocks of transform margin, (Jv) Jurassic rocks of active margin, (Pv) Permian riftogenic rocks, (CD) Devonian and Carboniferous riftogenic rocks.

Plutonic rocks. (Ku) Early Cretaceous alkaline ultramafic and mafic rocks of transform margin; *granitoids:* (Czg) Early Cenozoic (transform margin of Californian type), (lkg) Late Cretaceous (active margin), (Kg) Early Cretaceous (transform margin), (Jg) Jurassic and Cretaceous (transform) margin, (Trg) Triassic (collision-related), (Pg) Permian (active margin), (Sog) Ordovician and Silurian.

Terranes (type and age): (NSC) North Asian (craton), (BU) Bureya (metamorphic), (AMG) Amgu, or Ul'ban (continental margin, turbidite type, Jurassic), (BD) Badzhal (accretionary prism, Jurassic), (BL) Baladek (craton), (GL) Galam (accretionary prism, Paleozoic), (KB) Kabarga (accretionary prism, Early Paleozoic), (KE) Kem (island arc, Early Cretaceous), (KLM) Kisilevka-Manoma (accretionary prism, Early Cretaceous), (KR) Khor (island arc, Late Paleozoic), (LG) Laoelin-Grodekovo (island arc, Permian), (MK) Lesser Khingan (accretionary prism, Early Paleozoic), (ML) Mel'gin (accretionary prism, Early Paleozoic), (MT) Matveevka (island arc, Early Paleozoic), (NM) Nakhimovo (metamorphic, Early Paleozoic), (SMA) Samarka (accretionary prism, Jurassic), (SG) Sergeevka (passive continental margin, Mesozoic), (SP) Spassk (accretionary prism, Early Paleozoic), (TU) Taukhi (accretionary prism, Early Cretaceous), (TD) Tukuringra-Dzhagdy (accretionary prism, Late Paleozoic), (UB) Un'ya-Bom (marginal continental turbidite basin, Jurassic), (UR) Urmi (passive continental margin, Late Paleozoic) (VS) Voznesenka (passive continental margin, Early Paleozoic), (ZRA) Zhuravlev-Amur (marginal continental turbidite basin, Early Cretaceous).

Sedimentary basins: (az) Amur-Zeya (Late Jurassic-Quaternary), (bg) Blagoveshchensk (Late Cretaceous-Quaternary), (bu) Bureya (Early Jurassic-Early Cretaceous).

Volcanic-plutonic belts: (es) East Sikhote-Alin (Late Cretaceous), (ko) Khingan-Okhotsk (Cretaceous), (oc) Okhotsk-Chukotka (early Albian-Late Cretaceous), (uo) Umlekan-Ogodzha (Cretaceous)

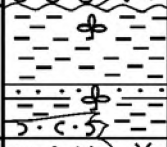
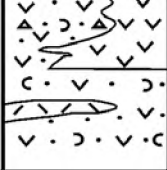
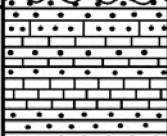
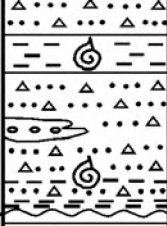
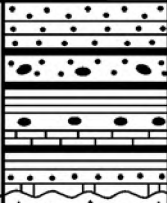
Erathem	System	Series	Stage	Units of regional stratigraphic scale	Age index	Column	Thickness, m	Formation, sequence			
									MESOZOIC		
PALEOZOIC	Permian	Upper	Tatarian	Chandalaz	P ₂ čn		235	Chandalaz Fm. Siltstone, sandstone, conglomerate, and tuffaceous conglomerate. Plant remains: <i>Prynadaeropteris karpovii</i> (Radcz.) Radcz., <i>Cordaites</i> , etc.			
			Ufimian	Abrek	P ₁₋₂ ab		200	Abrek Fm. Siltstone, sandstone, and tuffaceous siltstone. Plant remains: <i>Cordaites primorskiensis</i> Zim., <i>C. ex. gr. lotifolius</i> , <i>Rfloria ex. gr. derzavini</i> (Neub) S. Meyen, etc.			
		Lower	Kungurian		Dunai	P ₁ dn		>250	Dunai Fm. Psammitic and psephitic lithic tuffs of andesitic composition, andesite, and rhyolite		
			Asselian, Sakmarian, and Artinskian								
		MESOZOIC	Triassic	Lower	Olenekian		T ₁₋₂ šm ₁		260	Lower subformation Siltstone with sandstone interlayers. Fossils: <i>Felebenites tscherhyshewiensis</i>	
					Shimeuz Fm.						
				Middle	Anisian		T ₁₋₂ sm ₂		220	Upper subformation Intercalating sandstone and siltstone, interlayers of calcareous sandstone	
					Shimeuz Fm.						
				Jurassic	Lower	Hettangian		I ₁ st		220	Shetukha Fm. Sandstone, siltstone with roiling structures, and conglomerate
Upper	Volgian					I ₃ čq		350	Chiganovo Fm. Sandstone with roiling structure, nodular siltstone, and conglomerate lenses. Fossils: <i>Partechicearas schetuchaense</i> Chud., <i>Buchia</i> sp. Ident., <i>Virgatoshincies spadel</i> .		
Cretaceous	Lower	Aptian		K ₁ sč		300	Suchan Fm. Conglomerate, gritstone, sandstone, siltstone, coal, mudstone, and limestone interlayers				

Fig. 8.2. A fragment of stratigraphic column of the Dunai Subzone in the southern Sergeevska Terrane, after Vasil'ev (1965)

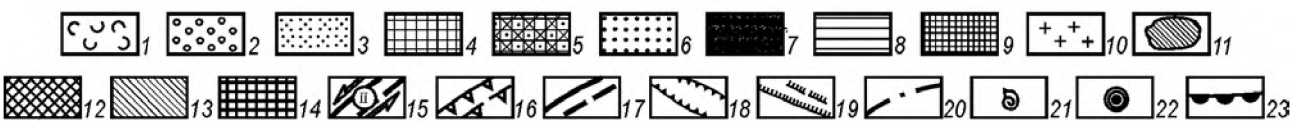
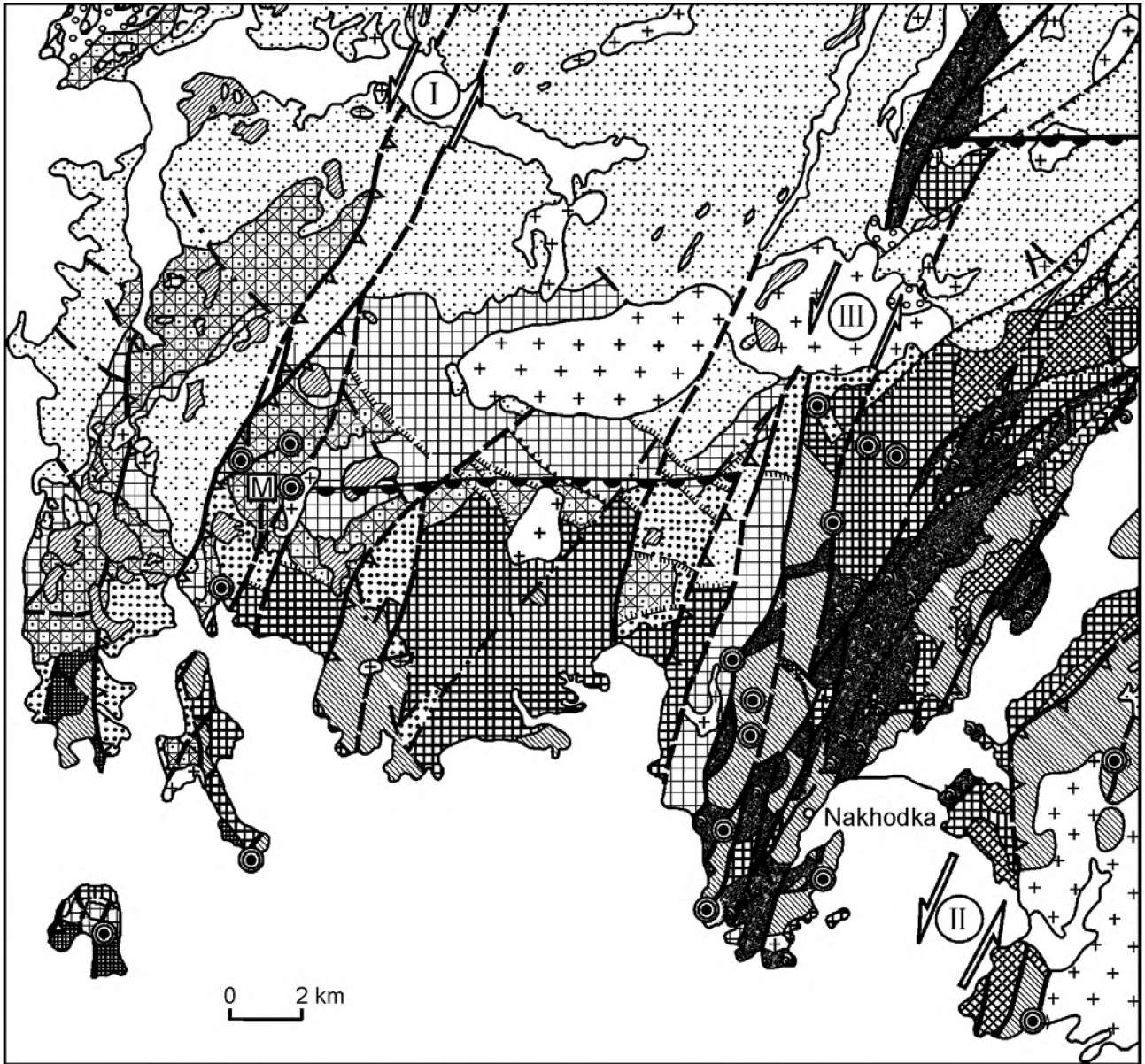


Fig. 8.3. Geological map of part of southern Primorye, after Utkin (1978).

(1) Neogene basalt and basaltic andesite; (2) Eocene and Oligocene sandstone, siltstone, lava breccia, and tuffs; (3) Cretaceous sandstone, siltstone, mudstone, coal, intermediate and acid lavas and tuffs; (4) Jurassic arkose, polymictic, and tuffaceous sandstones, siltstones, and conglomerates; (5) Lower and Middle Triassic sandstone, siltstone, and conglomerate; (6) Permian sandstone, siltstone, and mudstone with plant remains; carbonaceous shale, conglomerate, tuffaceous conglomerate and sandstone, intermediate and acid lavas and tuffs (Dunai, Pospelovo, Vladivostok, and Chandalaz formations); (7) Upper Permian tuffaceous conglomerate and sandstone, limestone with fossils (Chandalaz Formation); (8) Silurian and Devonian siltstone, sandstone shale, chert, and tuffite (Vangou Group); (9) Archean (?) and Riphean (?) gneisses, crystalline schists, metaterrigenous rocks, and marble lenses (Putyanin Formation); (10) Late Cretaceous and Paleogene granitic plutons; (11) Late Cretaceous minor intrusions of diorite and andesite porphyries and gabbrodiabase; (12) Late Permian granite and granodiorite; (13) Early Paleozoic basic and intermediate intrusions; (14) Early Paleozoic plagiogranite, granodiorite, and diorite; (15) strike-slip and thrust fault zones: (I) Askold, (II) Partizansk, (III) West Partizansk; (16) major thrust faults; (17) other major faults, mainly sinistral strike-slip faults; (18) auxiliary thrust faults; (19) normal faults; (20) other faults; (21) findings of Upper Permian fossils; (22) ore deposits (M – Krinichny ore field) and occurrences; (23) generalized northern boundary of the latitudinal pull-apart structure compensated by Early Paleozoic granitoids

and granitoids of the Sergeevka Terrane crop out. The northern flank of the shear zone controls the Mount Krinichny ore field including the gold deposit of the same name and a number of gold occurrences at Soldatsky, Bol'shoi, Krasny Tolsty, Podsobny, Pashkeev streams, and Mount Sakhmaya Golova. The Domashlino and Putyanin Island ore occurrences are hosted in the middle segment of the Askold Strike-Slip Fault Zone while the gold mineralization of Askold Island is localized at its southern flank.

IGNEOUS ROCKS OF THE KRINICHNY ORE FIELD

Late Paleozoic and Mesozoic igneous rocks that intrude Permian, Triassic, and Jurassic terrigenous rocks occupy about 30% of the ore field area (Fig. 8.4).

Late Permian diabase and quartz diabase are exposed as thin (commonly less than 1–2 m) dikes and sills residing in Permian country rocks in the southwestern ore field at the divides that separate the Tolsty Stream from the Podsobny and Masyatsakhe Stream. Porphyritic, occasionally amygdaloidal rocks are colored in brown, brownish green tints. The Late Permian age was accepted taking into account that they cut Permian country rocks and are not known from younger stratified units (Suturin, 1992). Thus, they are the oldest igneous rocks exposed within the ore field (Fig. 8.5).

Three Cretaceous multiphase intrusive complexes and a complex of postmineral dikes are recognized. The older gabbro-monzonite-granodiorite complex is widespread in the coastal part of the Sergeevka Terrane. Small gabbroic stocks and dikes (1st phase), monzonitoids (2nd phase), and granodiorite (3rd phase) are exposed in the Krinichny ore field, where they intrude Permian, Triassic, and Jurassic country rocks. Cross-cutting relations between sequential intrusive phases were observed. The rocks reveal a slight enrichment in K₂O in comparison with younger intrusions (Table; Fig. 8.6).

Proxene-amphibole and pyroxene gabbroids of the first phase crop out at the headwaters of Tolsty Stream, on the right bank of the Tserkovny Stream, at headwaters of the left effluent of the Podsobny Creek, and on the right bank of the Pashkeev Creek. These are phaneritic coarse-grained, occasionally medium- and fine-grained meso- and melanocratic rocks. Coarse-grained light gray gabbro is commonly taxitic and banded whereas the medium- and fine-grained varieties are darker and massive. Gabbro of the first

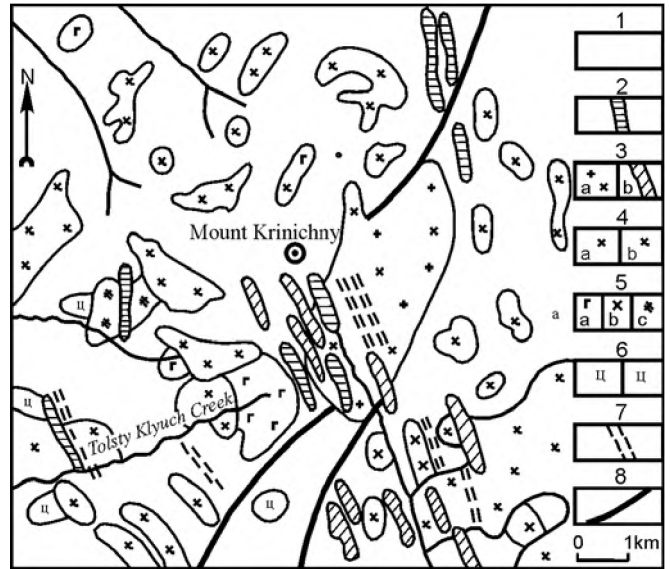


Fig. 8.4. Localization of igneous rock complexes and gold mineralization in the Krinichny ore field – a generalized scheme. Modified after Shlykov et al. (1981) and Suturin et al. (1992).

(1) Permian, Triassic, and Jurassic terrigenous rocks; igneous rock complexes: (2) basalt-andesite, (3) granodiorite-granite: (a) 1st phase, (b) 2nd phase; (4) diorite and diorite porphyry: (a) 1st phase, (b) 2nd phase; (5) gabbro-monzonite-granodiorite: (a) 1st phase, (b) 2nd phase, (3) 3rd phase; (6) diabase; (7) mineralized quartz veins and stockwork ore zones; (8) faults. Minor intrusions are shown out of scale

phase is characterized by a lowered alumina index [$Al^* = Al_2O_3 / (Fe_2O_3 + FeO + MgO)$] and is normal in alkalinity.

Isolated outcrops of medium- and fine-grained, gray and dark gray massive amphibole monzodiorite and biotite-amphibole monzonite belonging to the second phase are known only from the upper reaches of the Rudnevka River. They are distinguished by a high alumina index (Al^*) and elevated alkalinity. These rocks are cut by younger diorite porphyry.

The biotite-amphibole granodiorite of the third phase makes up small intrusions at the headwaters of Podsobny Stream, as well as stocks and dikes cutting gabbroic rocks of the first phase on the right bank of the Tolsty Stream. These are coarse-grained leucocratic and less abundant mesocratic rocks with a banded (gneissic) structure. They are characterized by the high alumina index and normal alkalinity. The early Cretaceous age of the gabbro-monzonite-granodiorite complex is supported by geologic relationships.

The next Mesozoic complex of diorite and diorite porphyry (two intrusive phases) is widespread in the ore field (40% of all igneous rocks). Stocks, dikes, and other minor intrusions of irregular shape were emplaced into Permian, Triassic, and Jurassic country

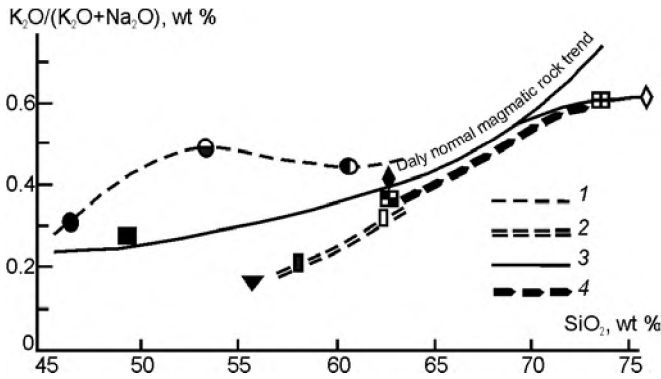


Fig. 8.6. Variation of $K_2O/(K_2O + Na_2O)$ ratio in igneous rocks from the Askold Strike-Slip Fault Zone. The Mount Krinichny ore field: (1) gabbro-monzonite-granodiorite complex, (2) diorite-diorite porphyry complex; (3) granodiorite-granite complex; (4) the Askold Island deposit, granodiorite-granite complex

rocks (Fig. 8.4). The rocks are characterized by a normal total alkalinity and distinguished by a marked prevalence of sodium over potassium (Table). The alumina index (Al^*) of the pyroxene-amphibole diorite and the quartz diorite of the first phase is high; in biotite-amphibole diorite (andesite) porphyry of the second phase this parameter is even more high (Table).

The Early Cretaceous age of diorite and diorite porphyry is determined from relationships with stratified fossiliferous units and with igneous rocks dated by isotopic methods (Fig. 8.5)

The younger granodiorite-granite complex of the Krinichny ore field consists of two intrusive phases. The first phase is represented by the zoned pluton of Krinichny (Kislovsky, 1934; Epshtein, 1968). Marginal zones of this pluton are composed of coarse- and medium-grained leucocratic and medium-grained meso- and melanocratic quartz diorite and tonalite while the core consists of quartz monzodiorite and granodiorite (Fig. 8.7). Leucocratic coarse-grained massive adamellite was penetrated by Borehole 20 at a depth of 225 m. Different rock varieties grade into one another. The zoned structure of the pluton is a result of magma fractionation during crystallization. Granitoids contain xenoliths of country rock sediments and older diorite and diorite porphyry. Rare quartz diorite and granodiorite dikes are noticed.

Thin dikes of biotite granite, granite porphyry, aplite, phyrlic and aphyric rhyolites, and rhyodacite that cut the Krinichny pluton are regarded as the second intrusive phase. Granitoids of the first phase intrude Permian, Triassic, and Jurassic strata and cut

Table

Average chemical compositions (wt %) of igneous rocks from the Krinichny ore field and Askold Island deposit

Oxide	Krinichny ore field								Askold Island deposit			
	Gabbro-monzonite-granodiorite complex			Diorite-diorite porphyry complex		Granodiorite-granite complex		Basalt-andesite complex	Granodiorite-granite complex		Basalt-andesite complex	
	I	II	III	I	II	I	II		I	II		
SiO ₂	46.56	53.11	61.42	58.04	62.03	62.81	75.75	56.38	62.79	73.32	49.63	
TiO	0.99	1.40	0.41	0.44	0.74	0.65	0.13	0.96	0.63	0.25	1.88	
Al ₂ O ₃	14.49	18.19	17.79	17.62	17.27	16.57	12.99	17.73	17.56	14.25	17.71	
Fe ₂ O ₃	3.82	3.18	2.88	3.42	2.03	3.12	0.45	3.09	2.31	1.09	5.64	
FeO	6.93	4.19	2.07	3.91	2.62	1.90	1.01	3.20	2.02	0.88	4.20	
MnO	0.22	0.14	0.11	0.19	0.13	0.10	0.04	0.08	0.09	0.05	0.15	
MgO	10.75	2.61	2.22	3.39	2.56	3.73	0.31	4.35	2.71	0.89	4.08	
CaO	11.20	5.09	3.93	6.56	2.63	4.61	0.76	6.35	4.99	1.58	5.71	
Na ₂ O	1.70	4.06	3.29	3.54	5.08	3.75	2.89	3.84	3.94	2.13	3.96	
K ₂ O	0.81	4.00	2.66	0.92	1.93	2.17	4.64	0.84	2.89	3.51	1.56	
LOI	1.73	2.52	2.62	1.48	2.03	1.18	0.65	2.76	0.37	0.91	0.62	
<i>n</i>	4	2	6	4	9	12	7	3	19	24	4	
<i>K</i> ₁	0.32	0.50	0.45	0.21	0.28	0.37	0.61	0.18	0.34	0.62	0.28	
<i>K</i> ₂	2.10	1.01	1.24	3.85	2.63	1.73	0.64	4.57	1.93	0.61	3.54	
<i>K</i> ₃	2.51	8.06	5.95	4.46	7.01	5.92	7.63	4.68	5.98	5.64	5.52	
<i>al</i> [*]	0.67	1.82	2.51	1.64	2.40	1.89	7.34	1.67	2.49	5.01	1.27	
Symbol	●	◐	◑	■	□	◆	◇	▼	▣	▤	■	

Note: I, II, III are intrusive phases (from older to the younger). Petrochemical parameters (wt %): $K_1 = K_2O/(K_2O + Na_2O)$; $K_2 = Na_2O/K_2O$; $K_3 = K_2O + Na_2O$; $al^* = Al_2O_3/(Fe_2O_3 + FeO + MgO)$; *n* is number of samples. Symbols correspond to Fig. 8.6.

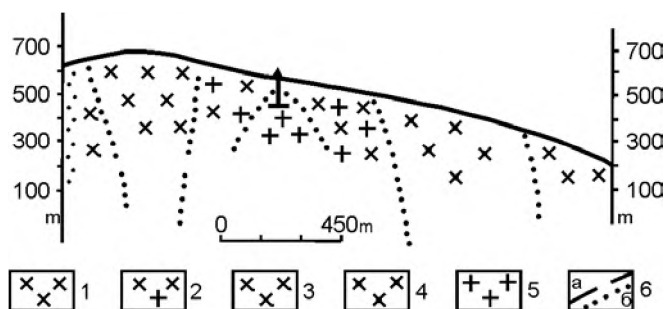


Fig. 8.7. Section across the Krinichny zonal pluton. (1) quartz diorite; (2) granodiorite; (3) tonalite; (4) quartz monzodiorite; (5) adamellite; (6) facies boundary; Borehole 20 is shown

Late Permian and Early Cretaceous intrusions. The Rb-Sr isochron age of the Krinichny pluton is 104 ± 1 Ma; K-Ar timing yielded 97.4 and 97.9 Ma. These estimates correspond to the late Albian (Sayadyan, 1996; Sayadyan et al., 1996; Sayadyan and Ishihara, 1997; Ishihara et al., 1997).

Cross-cutting relationships of the dikes belonging to the second phase with older igneous rocks together with K-Ar age of biotite and feldspar (86.6 ± 2.2 Ma) indicate that these rocks were emplaced in the late Coniacian or early Santonian (Fig. 8.5).

The magmatic evolution of the Krinichny ore field was completed with small dikes of basalt, basaltic andesite, and less abundant spessartite, diorite porphyry, and odinite. These rocks are characterized by the prevalence of sodium over potassium and a high alumina index (Table; Fig. 8.6). The K-Ar age of amphibole and plagioclase from a basaltic andesite dike yielded 76.2 ± 2.6 Ma (middle Campanian).

The sequence of intrusive rocks at Askold Island deposit is the same as that in the Krinichny ore field (Fig. 8.5).

GOLD MINERALIZATION IN THE ASKOLD STRIKE-SLIP FAULT ZONE

Stockwork and vein gold mineralization of so-called gold-rare-metal type (*Osnovnye tipy...*, 1984) is known from the Askold Strike-Slip Fault Zone (Gorbatyuk, 1975; Gorbatyuk and Molchanov, 1986). The main primary deposits are hosted in granitoids belonging to the first phase of the granodiorite-granite complex in plutons of the Mount Krinichny and Askold Island. The ore zones, up to few hundred meters in length, are linear stockworks with closely spaced veins and veinlets extending for tens of meters without mutual intersections. Spacing between veinlets is measured in a few centimeters (occasionally, by

decimeters) and is commonly commensurable with veinlet thickness. In outer zones of plutons and in country rocks, the ore mineralization is concentrated in groups of closely spaced veins or in isolated branching veins varying in thickness from 1–2 cm to 1–2 m or even more (Gudkov, 1921; Annert, 1928; Epshtein, 1968; Sayadyan, 1996; Sayadyan and Mitrokhin, 1997, 1999).

Three stages of gold mineralization are recognized (Epshtein, 1978; Gorbatyuk, 1975; Efimova, 1980; Gorbatyuk and Molchanov, 1986). Thin quartz-pyrite veinlets with gold and small amounts of tourmaline and arsenopyrite were formed in the first stage. Most of the gold related to this stage occurs as equant and irregular clots in interstitial spaces of the fine-grained quartz. Some gold grains reveal crystal faces and look like small bars. Occasionally, gold is associated with pyrite. The homogenization temperature of primary fluid inclusions in veinlets of milky white quartz is $280\text{--}320^\circ\text{C}$. Gold of the early mineral assemblage is characterized by a high fineness (898–912); Te, Bi, Cu, Fe, Pt, and Se were detected as impurities. The wallrock underwent a slight silicification.

The major mass of Au-bearing quartz veinlets was formed during the second, sulfide-quartz stage. Sulfides and sulfosalts (sphalerite, galena, chalcopyrite, fahlore, (grey copper ore) molybdenite, stannite, bismuthinite, and tellurobismuthite) are hosted in combed quartz. The homogenization temperature of fluid inclusions in quartz is $210\text{--}220^\circ\text{C}$. Gold of the second generation is closely associated with chalcopyrite, galena, and sphalerite. Commonly occurring at quartz-sulfide boundaries, gold forms hooked, thin tabular and nodular aggregates and rims around sulfides; the fineness of gold is 780–856. Extensively developed quartz-sericite altered rocks with fine sulfide and gold disseminations are typical of the second stage.

Veins and veinlets of finely combed translucent quartz with sporadic pyrite, sericite, and carbonate, as well as calcite veinlets were formed in the final barren stage. The homogenization temperature of fluid inclusions in the barren quartz is $120\text{--}140^\circ\text{C}$.

The K-Ar age of altered rocks closely related to the gold mineralization in the Krinichny ore field is 76.2 ± 1.9 Ma (muscovite) and 84.2 ± 1.9 Ma (feldspar). The K-Ar age of muscovite from altered rocks on Askold Island was estimated as 83.8 ± 1.9 Ma (Sayadyan, 1986; Sayadyan and Ishihara, 1997; Ishihara et al., 1997). Virtually the same Ar-Ar age of whole rock samples from the Askold Island deposit (82.3 ± 0.3 Ma) was reported by Ivanov and Leier (1997).

The ore mineralization is superimposed on intrusive rocks of the granodiorite-granite complex. Dikes of the basalt-andesite complex cross the quartz veinlets; they contain xenoliths of quartz veins, and thus are postmineral.

Ore-bearing stockworks, quartz veins and veinlets strike $290\text{--}295^\circ$ and $325\text{--}350^\circ$ NW and occasionally are oriented in a meridional direction being concordant in orientation with pre- and postmineral dikes (Figs. 8.4 and 8.8).

The Krinichny pluton can be regarded as a sinistral duplex, about 1.5 km wide, bounded by Krinichny I (K-I) and Krinichny II (K-II) strike-slip faults extending $25\text{--}30^\circ$ NNE. The duplex was formed under regional transpression oriented at $340\text{--}345^\circ$ NNW (Fig. 8.8). The shape of the pluton in plan is close to a parallelogram with NNE sides elongated parallel to the boundary strike-slip faults. The intrusive chamber of the Krinichny pluton (first phase of the granodiorite-granite complex) is considered to be a deep-seated pull-apart structure filled with magmatic melt about 100 Ma ago. The dikes of the second intrusive phase were emplaced 86–87 Ma ago along NNW tensile fractures initiated by recurrent slip along the boundary faults (Fig. 8.8). The same deformation pattern was retained during stockwork and vein ore formation ~84 Ma ago. Swarms of postmineral dikes were intruded about 76 Ma ago using the previously formed NNW fracture zones for their ascent (Sayadyan and Mitrokhin, 1999).

EXCURSION POINTS

The Krinichny ore field

Stop 1. The Mount Krinichny, a general view from the towering top.

Stop 2. The southern slope of the Mount Krinichny, the Krinichny primary gold deposit, Borehole 20. Relationships between ore-bearing quartz veins and host rocks of granodiorite-granite complex; structural studies.

Stop 3. The headwater of the Rudnevka River. Cross-cutting relationships between dikes of granite (2nd phase) and diorite (1st phase); structural studies.

Stop 4. The headwater of the Rudnevka River. Cross-cutting relationships between postmineral dike of basaltic andesite and quartz diorite belonging to the first phase of granodiorite-granite complex; structural studies.

Stop 5. The open pit on the right bank of the Tolsty Stream (1) Cross-cutting and conformable relationships of andesite porphyry dikes and sills (2nd phase of diorite-diorite porphyry complex) with Permian volcanosedimentary rocks. (2) Relationships

between gold-quartz mineralization and postmineral dikes of basalt-andesite complex; structural studies.

Askold Island deposit

Stop 6. Central part of the Naezdnik (Horseman) Bay. (1) Cross-cutting relationships between postmineral basic and intermediate dikes and granitoids of the granodiorite-granite complex; structural studies. (2) Study of coastal sediments and search for pebbles of ore-bearing quartz.

Stop 7. The left coast of the Naezdnik Bay. (1) Cross-cutting relationships between granodiorite (1st phase) and granite (2nd phase) of the granodiorite-

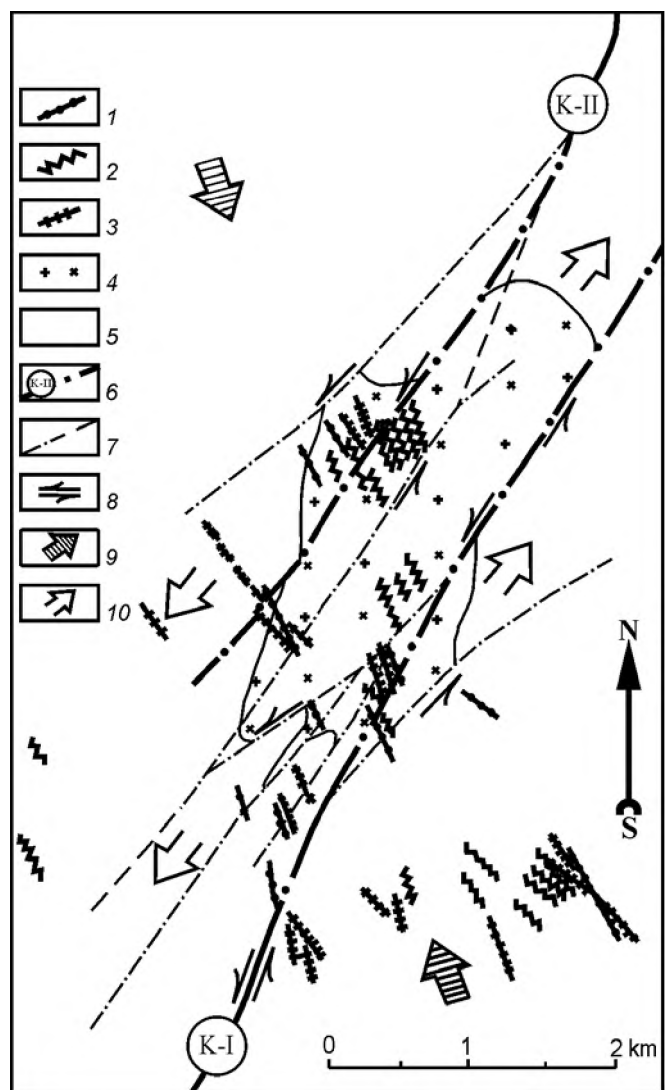


Fig. 8.8. Structural scheme of the Krinichny ore field.

(1) postmineral basic and intermediate dikes; (2) Au-bearing linear stockworks and quartz veins; (3) premineral dikes; (4) granodiorite of the second phase of granodiorite-granite complex; (5) country rocks; (6) sinistral faults K-I and K-II controlling the localization of the Krinichny pluton; (7) auxiliary faults; (8) slip direction; (9) direction of regional compression; (10) pull-apart direction

granite complex. (2) Quartz veinlets hosted in granitoids of the 1st and 2nd phases; structural studies.

Stop 8. The left coast of the Næzdnik Bay. Cross-cutting relationships between premineral porphyry dikes (2nd phase of granodiorite-granite complex) and postmineral basic and intermediate dikes.

REFERENCES

- Anert, E.E., *Bogatsyva nedr Dal'nego Vostoka* (Riches of subsurface of the Far East), Khabarovsk-Vladovostok: Knizhnoe delo, 1928, 932 p.*
- Efimova, M.I., Solyanik, V.A., Naumkin, P.A., and Yakovets, V.A., Physicochemical formation conditions of altered rocks at gold deposits in Primorye, Abstracts of papers, *Vsesoyuznoe soveshchanie po termobarogeokhimi* (All-Union Conference on Thermobarogeochimistry), Vladivostok, 1980, pp. 130–134.*
- Gorbatyuk, O.I., Native gold and formation conditions of deposits in the southern Primorye, *PhD Thesis (Geol.-Mineral.)*, Vladivostok: Far East Geological Institute, 1975.*
- Gorbatyuk, O.I. and Molchanov, V.P., Formation of gold mineralization in Primorye, in: *Termobarogeokhimiya endogennykh protsessov* (Thermobarogeochimistry of endogenic processes), Vladivostok, 1986, pp. 84–88.*
- Gudkov, P.P., The Askold Mine and other gold deposits on the Askold Island, in: *Materialy po geoligii i poleznym iskopaym Dal'nego Vostoka* (Geology and mineral resources of the Far East), Vladivostok: State Far East Univ., 1921, vol. 20, pp. 1–25.*
- Ishihara, S., Gonevchuk, V., Gonevchuk, G., Korostelev, G., Sayadyan, G., Semenyak, B. and Ratkin V., Mineralization age of granitoid-related ore deposits in the Southern Primorye, *Russian Far East, Resource Geology*, 1997, vol. 45, no. 5, pp. 255–261.
- Ivanov, V.V. and Leier, P., Age and types of gold and gold-silver mineralization in granitoids of the southern Primorye, Abstracts of papers, *Vserossiiskoe soveshchanie "Zolotoe orudnenie i granitoidnyi magmatizm Severnoi Patsifiki"* (All-Russia Conference "Gold mineralization and granitoid magmatism in the northern Pacific"), Magadan, 1997, pp. 104–106.*
- Khanchuk, A.I., Geological structure and evolution of continental framework of the northwestern Pacific, *DSc Thesis (Geol.-Mineral.)*, Moscow: Geological Institute, 1993.*
- Khanchuk, A.I., Ore formation in the Russian Far East: a paleogeodynamic interpretation, in *Rudnye mestorozhdeniya kontinental'nykh okrain* (Ore deposits of continental margins), 2000, vol. 1, pp. 5–33.*
- Khomich, V.G. and Sayadyan, G.R., Structure of the Krinichny gold ore field and localization of ore mineralization therein, *Proc. Far East State Technical University*, 1995, vol. 115, Ser. 4, pp. 43–49.*
- Levashov, G.B., *Geokhimiya pagemnykh magmatitov aktivnykh zon kontinental'nykh okrain* (Geochemistry of igneous rock associations at active continental margins), Vladivostok: Far East Division, Academy of Sciences of the USSR, 1991, 380 p.*
- Levashev, G.B., Rybalko, V.I., Izosov, L.A., Soroka, V.P., Kovalenko, S.V., Fedchin, F.G., Martynov, Yu.A., Sokarev, A.N., Volosov, A.G., Kulichenko, A.G., Prishchepa T.K., and Semenyak, L.E., *Tectono-magmaticheskie sistemy akkretionnoi kory* (Tectono-magmatic systems of accretionary crust), Vladivostok: Far East Division, Academy of Sciences of the USSR, 1989, 340 p.*
- Mitrokhin, A.N. and Sayadyan, G.R., The Krinichny strike-slip ore-magmatic transtension duplex (southern Primorye), Abstract of papers, *XXXII Vserossiiskoe tektonicheskoe soveshchanie "Tektonika, geodinamika, protsessy magmatizma i metamorfizma"* (XXXII All-Russia Tectonic Conference "Tectonics, Geodynamics, Magmatic and Metamorphic Processes"), Moscow: 1999, vol. 2, pp. 6–9.*
- Mitrokhin, A.N., Sorokin, B.K., and Sayadyan, G.R., Strike-slip duplexes and their ore potential, Abstract of papers, *XXX Vserossiiskoe tektonicheskoe soveshchanie "Tektonika Azii"* (XXX All-Russia Tectonic Conference "Tectonics of Asia"), Moscow: 1997, pp. 112–114.*
- Nazarenko, L.F. and Bazhanov, V.A., Geology of Primorye, part I, Stratigraphy, *Preprint of Geological Far East Institute*, Vladivostok, 1986, 68 p.*
- Osnovnye tipy rudnykh formatsii* (Main types of ore deposits), Kosygin, Yu.A. and Kulesh, E.A., Eds, Moscow: Nauka, 1984, 316 p.*
- Sayadyan, G.R., Gonevchuk, V.G., Gerasimov, N.S., and Khomich, V.G., Age and formation sequence of igneous rocks in the Krinichny ore field: geological and isotopic-geochemical evidence, in: *Mineralogo-geokhimicheskie indikatory rudonosnosti i petrogenezisa* (Mineralogical and geochemical indicators of ore potential and petrogenesis), Vladivostok: Dalnauka, 1996, pp. 93–105.*
- Sayadyan, G.R., Relationships between igneous rocks and ore mineralization in the Krinichny ore field, Abstracts of papers, *III Mezhdunarodnyi nauchnyi simpozium "Zakonomernosti stroeniya i evolyutsii geosfer"* (III International Scientific Symposium "Structure and evolution of geospheres"), Vladivostok, 1996, part II, pp. 66–68.*
- Sayadyan, G.R., Absolute and relative age of igneous rocks in the Krinichny ore field, southern Primorye, Abstracts of papers, *III Mezhdunarodnyi nauchnyi simpozium "Zakonomernosti stroeniya i evolyutsii geosfer"* (III International Scientific Symposium "Structure and evolution of geospheres"), Vladivostok, 1996, part II, pp. 68–71.*
- Sayadyan, G.R. and Mitrokhin, A.N., Structural geodynamic correlation of granitoid magmatism and gold mineralization in the Krinichny ore field (southern Primorye), Abstracts of papers, *Vserossiiskoe soveshchanie "Zolotoe orudnenie i granitoidnyi magmatizm Severnoi Patsifiki"* (All-Russia Conference "Gold mineralization and granitoid magmatism in the northern Pacific"), Magadan, 1997, pp. 196–198.*
- Sayadyan, G.R. and Mitrokhin A.M. Strike-slip fault extensional duplex and ore-magmatic dinamozonality (Krinichny gold deposit, Southern Primorye), Abstracts of papers, *Mezhdunarodnyi seminar i respublikanskaya shkola molodykh uchennykh "Strukturnyi analiz v geologicheskikh issledovaniyakh"* (International Seminar and Regional School of Young Scientists "Structural analysis in geological studies"), Tomsk: Tomsk State University, 1999, pp. 168–170.
- Sayadyan, G.R., Pakhomova, V.A., and Zalishchak, B.L., Geological age marks of quartz-gold mineralization on the Askold Island, southern Primorye, *IV Mezhdunarodnyi nauchnyi simpozium "Zakonomernosti stroeniya i evolyutsii geosfer"* (IV International Scientific Symposium "Structure and evolution of geospheres"), Khabarovsk, 1998, pp. 250–251.*
- Sinitsa, S.M. and Khanchuk, A.I., Primary gneissic facies of gabbroic rocks, the southern Primorye, *Dokl. Akad. Nauk SSSR*, 1991, vol. 317, no. 6, pp. 1446–1449.*
- Sinitsa, S.M., Paradox of cleavage, *Tikhookean. Geol.*, 1998, vol. 17, no. 1, pp. 3–12.*
- Utkin, V.P., *Sdvigovye dislokatsii i metodika ikh izucheniya* (Strike-slip dislocations and methods of their study), Moscow: Nauka, 1980, 144 pp.*
- Utkin, V.P., Sayadyan, G.R., and Khomich, V.P., The strike-slip geodynamic regime as a crucial factor in localization of Cretaceous gold-bearing ore-magmatic systems, *IV Mezhdunarodnyi nauchnyi simpozium "Zakonomernosti stroeniya i evolyutsii geosfer"* (IV International Scientific Symposium "Structure and evolution of geospheres"), Khabarovsk, 1998, pp. 266–269.*

* In Russian.



MIOCENE-TO-QUATERNARY CENTER OF VOLCANIC, HYDROTHERMAL, AND ORE-FORMING ACTIVITY IN THE SOUTHERN KAMCHATKA

V.M. Okrugin, M.E. Zelensky

Institute of Volcanology, Far East Branch, Russian Academy of Sciences, Petropavlovsk-Kamchatsky

THE KAMCHATKA REGION: AN OVERVIEW

The Kamchatka Region is situated in the extreme northeast of the Russian Federation and occupies the Kamchatka Peninsula, Komandorsky Islands, and Koryakia on the mainland. The northern boundary of the region, approximately along 65° N, is close to the Northern Polar Circle and corresponds to the latitude of Belomorsk, Reykjavik, Trondheim, and Fairbanks. The southernmost point (Lopatka Cape) has a similar latitude to Brussels, Krakow, Semei (Semipalatinsk), and Kiev (50°57' N). The extent of the region from north to south is more than 1600 km. The northeastern mainland part reaches 640 km in width; the widest portion of the peninsula is 470 km across. The peninsula is connected to the continent by a neck of land, up to 100 km wide (Parapolsky Dol). The Sea of Okhotsk in the west, Bering Sea in the east, and Pacific Ocean in the southeast surround Kamchatka (Fig. 9.1). The total area of the region (472300 km²) amounts to 2.8% of the Russian territory. Mountain ranges, volcano peaks, volcanic plateaus, vast lowlands, and tundra impart a unique appearance to Kamchatka. Kamchatka and the Kuril Islands make up a large segment of the Circum-Pacific volcanic belt and represent the only province of active volcanism in Russia.

Volcanic activity in Kamchatka has a long and complex history that started in the Cretaceous 140–130 Ma ago and continues now. Four extended and nearly parallel volcanic belts of different ages replace one another from the northwest to the southeast (Fig. 1) exhibiting a progressive shift of the ocean–continent transition zone in the same direction (Okrugin, 1995; Petrenko, 1999). The oldest Okhotsk-Chukotka belt was formed in the Cretaceous and Paleogene. The Koryak–Western Kamchatka belt evolved during the Eo-

cene and Oligocene. The axial Central Kamchatka belt was active in the Oligocene–Quaternary. The youngest and the most active Eastern Kamchatka belt extends along the eastern coast of the peninsula (Fig. 9.2).

Quaternary volcanic activity concentrated in two eastern belts. No less than 220 large composite volcanic edifices (shield volcanoes, stratovolcanoes, and calderas) and more than 2100 small cinder cones, lava domes, and extrusions formed here over the last million years (Kozhemyaka, 1991). 29 of 31 active volcanoes, including the highest (4750 m) and most active Klyuchevsky volcano, are localized in the East Kamchatka belt. The Ichinsky and Khangar volcanoes in the Central Kamchatka belt reveal a weak fumarolic activity.

One of the most active seismic zones extends along the Pacific coast from Ust'-Kamchatsk (settlement at the mouth of Kamchatka River) to Tokyo. Strong earthquakes with a magnitude of ≥ 7 have a cycle of 140 ± 60 years. Four earthquakes with $M = 7$ and two earthquakes with $M = 8$ were recorded in the vicinity of Petropavlovsk-Kamchatsky in the 20th century (Fedotov, 1991).

The mineral resources known in Kamchatka include, gas, coal, building materials, agrochemical raw materials, copper, nickel, cobalt, tin, mercury, lead, zinc, platinum, gold, silver and gems. Resources of only four economic deposits (Ametistovy, Aginsky, Rodnikovoy, and Asachinsky) amount to 150 t Au and 600 t Ag. Resources of 20 poorly studied prospects from 6 gold ore districts are estimated a no less than 1,000 t Au and 5,000–10,000 t Ag (Patoka, 1998; Petrenko, 1999). However, none of the known primary Au-Ag deposits are mined as yet. According to various sources, 10–17 t of gold have been mined from placers.

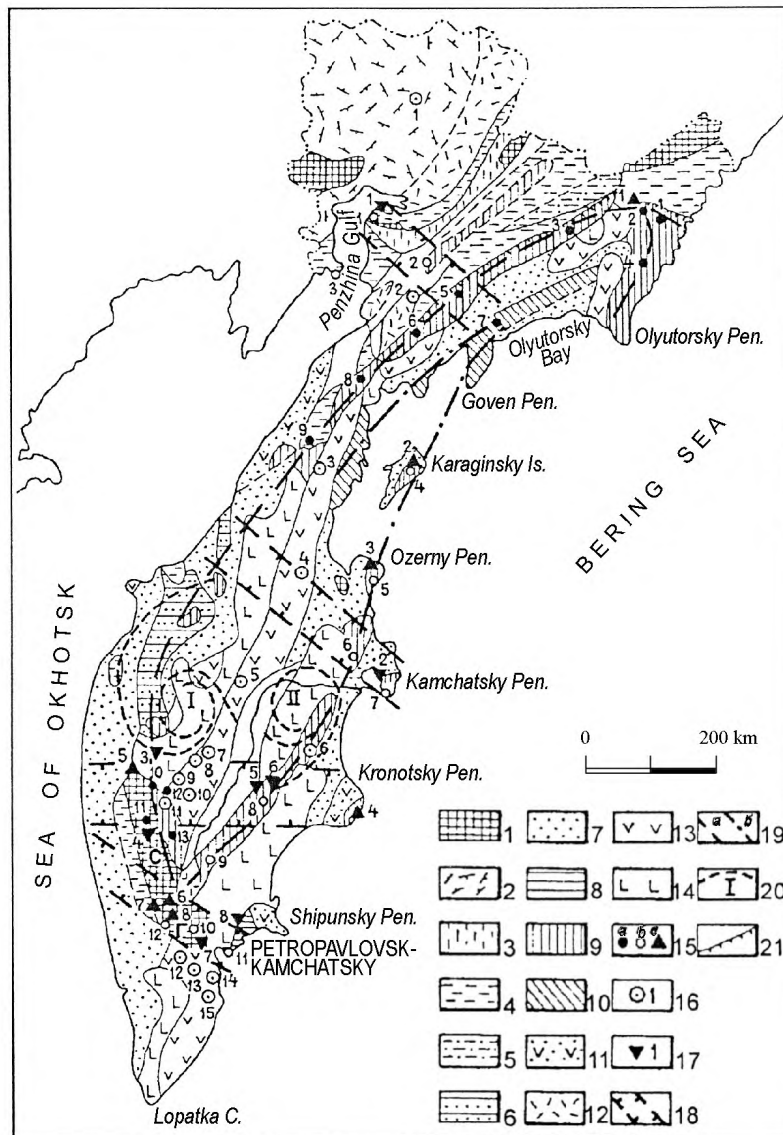


Fig. 9.1. Map of base-metal and noble-metal ore occurrences in Kamchatka (by Baikov, 2002).

(1) basement inliers composed of Precambrian, Paleozoic, and Mesozoic metamorphic rocks: (S) Sredinny and (G) Ganalsky; (2) Cretaceous volcanic rocks of the Okhotsk Belt; *terrigenous rocks*: (3) Lower Cretaceous, (4) Upper Cretaceous, (5) Upper Cretaceous-to-Paleogene, (6) Paleogene, (7) Paleogene-to-Neogene; *submarine volcanosedimentary rocks*: (8) Lower Cretaceous, (9) Upper Cretaceous-to-Paleogene, (10) Paleogene, (11) Paleogene-to-Neogene (Miocene); *subaerial volcanics*: (12) Paleogene-to-Neogene, (13) Neogene, (14) Quaternary; (15) PGE occurrences related to (a) dunite-pyroxenite-gabbro massifs, (b) dunite-peridotite massifs, (c) Cu-Ni sulfide mineralization; (16) gold deposits and occurrences; (17) diamond occurrences; (18) deep zones of latitudinal and northwestern transverse dislocations; (19) axes of PGE ore zones: (a) Koryak–West Kamchatka, (b) Olyutor–East Kamchatka; (20) inferred contours of vortical tectonomagmatic structures: (a) West Kamchatka (Uksichan), (II) East Kamchatka (Klyuchevsky); (21) reverse and thrust faults.

Ore occurrences and deposits (numbers on map): *PGE occurrences related to dunite-pyroxenite-gabbro massifs*: Itchayvayam River (1), Epil'chik (2), Pakhachi River (3), Tamanvayam River (4), Vyvenka River (Seynab and Gal'moenan massifs) (5), Vetrovayamskoe (6), Gytyralya River (7), Pustoy River (8), Shamanka River (9), Khim River (10), and Filippa River (11); *Au- and PGE-bearing porphyry copper occurrences*: Kirganikskoe (12) and Sharomskoe (13); *PGE occurrences related to dunite-peridotite massifs*: Valinzhegen Peninsula (1), Kuyul'skoe (2), Elistratov Peninsula (3) Karaginsky Island (4), Ozerny Peninsula (5), Kumroch Ridge (Krotonskoe) (6), Kamchatsky Peninsula (7), Poputnaya Mountain (8), Zhupanovskoe (9), Sumnoy Creek (10), Pakovaya Bay (11), and Blizhnyaya Gol'tsovka River (12); *PGE occurrences related to Cu-Ni sulfide mineralization*: Epil'chik (1), Karaginsky Island (2), Ozerny Peninsula (3), Kronotsky Peninsula (4), Shanuch (5), Dukuk (6), Kvinum (7), and Kuvalorog (8); *gold deposits and occurrences*: Sergeevskoe (1), Ametistivoe (2), Eruvayamskoe (3), Ozernovskoe (4), Apapel'skoe (5), Kumroch (6), Sukharikovskoe (7), Aginskoe (8), Baranievskoe (9), Zolotoe (10), Oganchinskoe (11), Banno-Karymshinskoe (12), Rodnikovoe (13), Mutnovskoe (14), and Asachinskoe (15); *diamond occurrences*: Velinzhegensky Peninsula (1), Kamchatsky Peninsula (2), Ichinskoe (3), Filippa River (4), Ozerny Creek (5), Uzkiy Creek (6), and Avachinskoe (7)

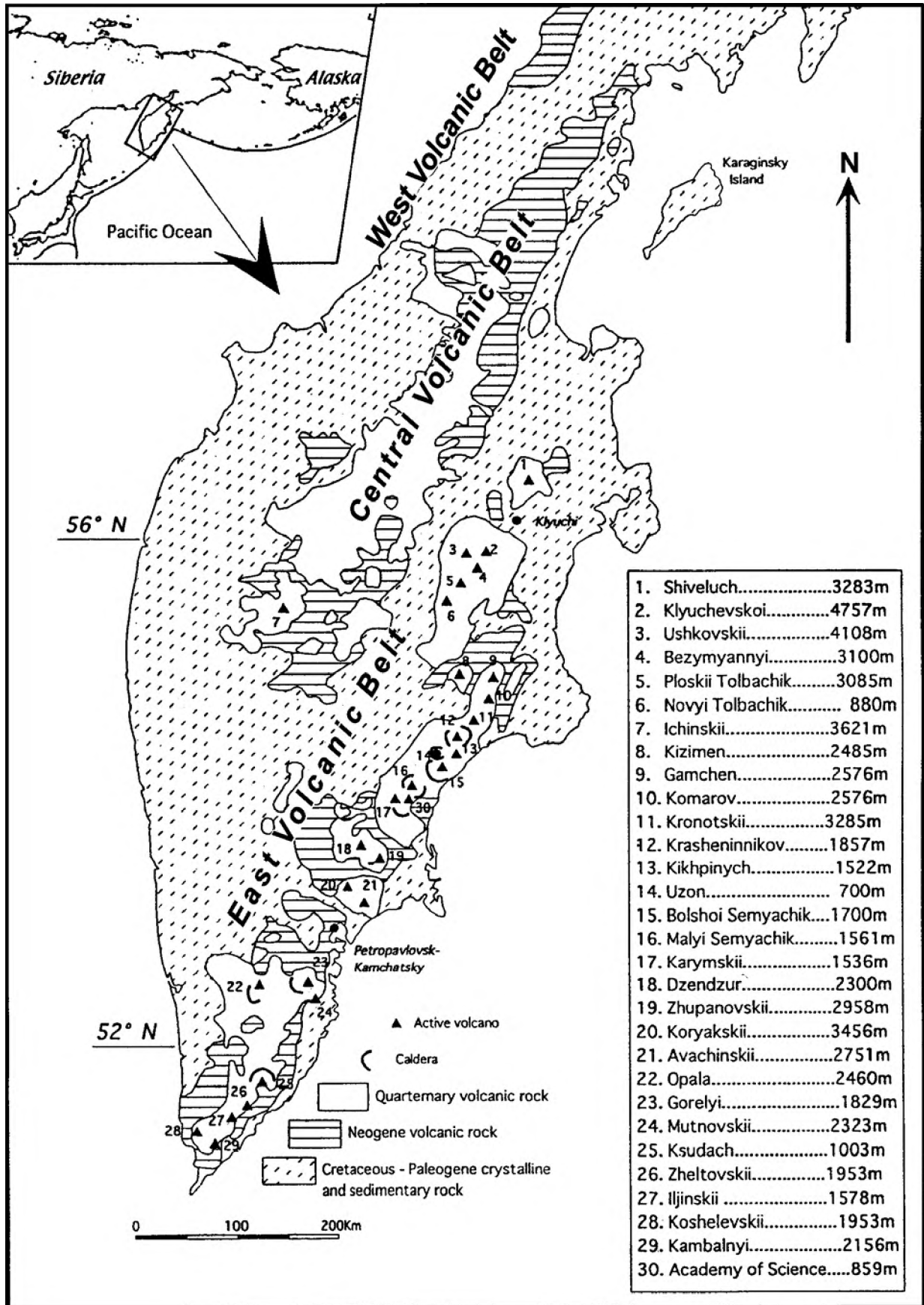


Fig. 9.2. Active volcanoes of Kamchatka Peninsula

Kamchatka, or more precisely, the northern Koryak region is one of the main PGE producers in Russia (Vil'danova, 2002). The Levtyrynvayam and Ledyanaya placer deposits localized in the Vatyn-Vyven zone of the Koryak-Kamchatka platinum belt yielded about 35 t of platinum.

The sulfide Cu–Ni deposits (Shanuch, Dukuk-Kuvalorog and Kvinum groups) are the subject of mining activity. The nickel resources of the Shanuch deposit are estimated as 70,000 t. The massive and disseminated Cu–Ni ores contain no less than 4% Ni, about 1.6% Cu, tenths of percent Co, as well as Pt and Au (Baikov, 2001).

Kamchatka possesses resources for fuel and power supply that could solve all the problems of the region in this respect. The volume of developed gas reserves in the Kolpakovo Trough of the western Kamchatka is estimated as >16 billion m³. Detailed study of prospective structure might further increase reserves by 20–25 billion m³. The ultimate coal and lignite reserves exceed 10 Mt. A further possible addition in reserves is estimated at 300 Mt while the annual demand is about 400 kt.

Up to 70–75% of thermal water resources of Russia are concentrated in Kamchatka. Most of them are related to thermal springs. More than 160 groups of thermal springs are localized in four geothermal provinces. 16 spring groups in northern Kamchatka and 26 groups in central Kamchatka are spatially related to the Central Kamchatka volcanic belt. East Kamchatka and South Kamchatka provinces, mainly controlled by the East Kamchatka volcanic belt, comprise 52 and 55 groups, respectively. Geothermal activity in southern Kamchatka is the most intensive and diverse. Four high-temperature hydrothermal systems (Bolshe-Banny, Mutnovsky, Pauzhetsky, and Koshelevsky) are localized therein. The localization of these provinces is mainly controlled by the East Kamchatka volcanic belt (Sugrobov, 1991). Geothermal resources of the most accessible thermal occurrences yield up to 10 thousand Gcal/hr of heat. The Verkhne-Mutnovsky geothermal power station (12MWt in power) and the first stage of the Mutnovsky station (50 MWt in power) are in operation.

THE GENERAL GEOLOGY OF SOUTHERN KAMCHATKA

Southern Kamchatka is a vast territory that is situated south of Petropavlovsk-Kamchatsky and extends to the southernmost Lopatka Cape. The maximum width of this area at the latitude of the regional

center is 210 km; the distance from the latter to the Lopatka Cape is about 300 km. The Malka-Petropavlovsk zone of transverse dislocations that markedly deforms the Central and East Kamchatka volcanic belts is considered to be the northeastern geological boundary of this province. Mesozoic sedimentary rocks and Paleozoic metamorphic complexes of the Ganalsky Range Inlier are situated in the north and northwest. The relatively stable Golygino Trough filled with recent molasse trends along the western coast.

The eastern coastal zone is occupied by the Coastal Horst composed of the oldest rocks including Oligocene and Miocene volcanic and volcanosedimentary rocks intruded by granitoid plutons of Neogene age, e.g., Akhomten and Saranny (Fig. 9.3). The largest Akhomten pluton is situated 80–90 km south of Petropavlovsk-Kamchatsky. The exposed portion of this pluton, oval in plan, covers an area of about 150 km² and consists of rocks varying in composition from gabbro to granite, granite-pegmatite, and aplite. Their age was estimated as 11.4–14.7 Ma.

The Kambalny-Gorelovsky Graben is the next large regional structure filled with a thick sequence of Neogene-Quaternary rocks.

In general, more than 70% of the territory is occupied by Tertiary volcanic and volcanic-plutonic associations. The Central Kamchatka and East Kamchatka (Kuril-Kronotsky) deep faults control the localization of volcanic edifices within Oligocene-to-Quaternary and Pliocene-to-Quaternary volcanic belts, respectively (Petrenko, 1999). These regional faults in combination with other tectonic lines extending in four directions determine the block structure of this region. Igneous rocks and ore deposits are largely controlled by nearly N-S faults (Petrenko, 1999).

Oligocene and Miocene volcanic rocks are variable in composition with a prevalence of andesites. They correspond to the island-arc stage of the Central Kamchatka volcanic belt evolution in the Sredinny Range and make up the positive structures of the Coastal Horst.

A Late Miocene and Pliocene bimodal basalt-andesite-rhyolite association was formed under subaerial conditions. Volcanic edifices of this age are grouped into Eastern and Western linear zones that merge in the south with the formation of the Pauzhetka domal volcanic structure. Volcanoes are deeply eroded, and their feeding systems (dikes) and hypabyssal magma chambers (basic and intermediate subvolcanic intrusions) crop out at the present-day surface. In structural terms, they are defined as the

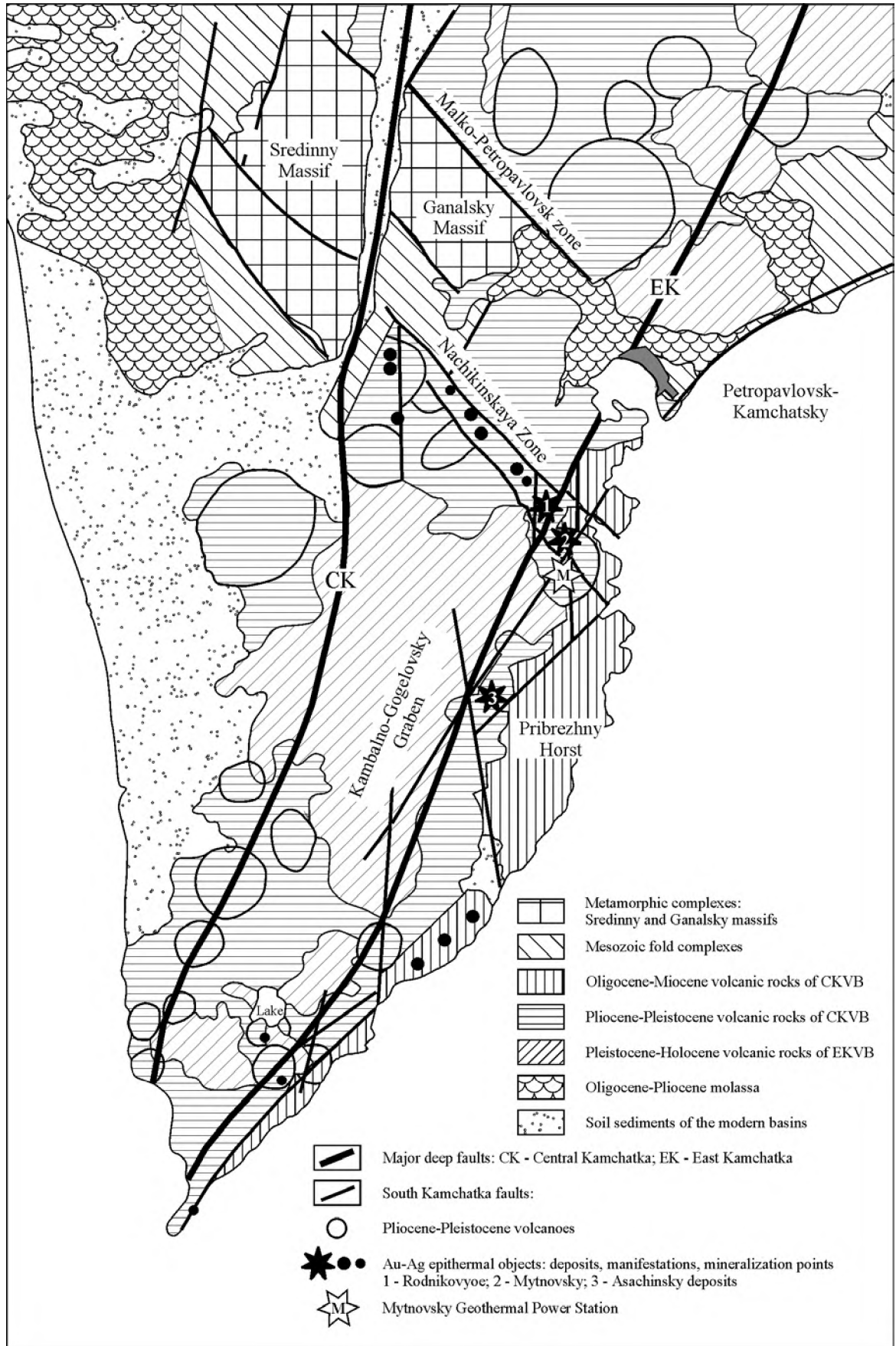


Fig. 9.3. Tectonic map of southern Kamchatka

Western Horst. The Malka-Petropavlovsk zone of transverse dislocations was formed at that time as a final episode in the evolution of the Central Kamchatka volcanic belt (trench-arc system).

The intensive Quaternary volcanic activity is related to the East Kamchatka volcanic belt pertaining to the younger trench-arc system. More than 60 polygenetic volcanoes mainly composed of basalts, basaltic andesites, and andesites developed at that time contemporaneously with vast fields of acid ignimbrites and pumices. The total volume of erupted material is estimated as 2300–2500 km³ (Kozhemyaka, 1991). Eight active volcanoes and five geothermal systems including the largest Mutnovsky and Koshelevsky systems are known. The territory is rich in various mineral deposits: four epithermal Au-Ag deposits (Rodnikov, Mutnovsky, Asachinsky, and Porozisty), more than 30 ore occurrences and numerous showings are localized therein (Fig. 9.4). Building material deposits are developed, and three geothermal power stations (Pauzhetsky, North Mutnovsky, and Mutnovsky) are in operation. Numerous resorts were developed at thermal springs.

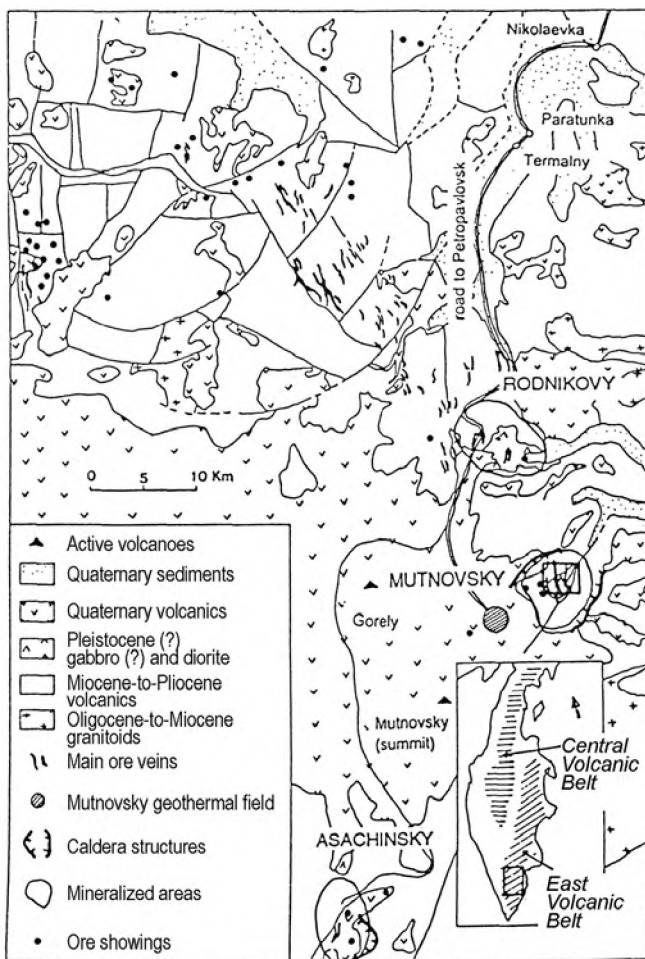


Fig. 9.4. Geological scheme of the Mutnovsky district

Several large centers of endogenic activity are localized in this region (Vasilevsky, 1977; Okrugin, 1995). The objects of our excursion are localized within the Mutnovsky-Asachinsky center.

The Mutnovsky volcano: fumarole activity, gas transport of elements, and mineral formation in a zone of high-temperature fumarole discharge

The Mutnovsky volcano with the main peak (2323 m) at 52°21' N and 158°16' E is situated 75 km south of Petropavlovsk-Kamchatsky and 20 km from the Pacific coast. This is the most active volcano of the East Kamchatka belt. Geologic setting and structure of the volcano were described in detail by Martynov et al. (1995), Selyangin (1993), and Sharapov et al. (1979).

Volcano activity is related to the late Pleistocene and Holocene (Melekestsev et al., 1987, 1990). According to Selyangin (1993), "the volcanic edifice consists of four consecutively formed double stratovolcanoes resulting from similar sequences of events: growth of cone – formation of the summit caldera (crater) – growth of the intracaldera edifice – extinction of volcano. After that the conduit has been shifted, and the cycle repeated in a new place". High-alumina basalt and basaltic andesite are most typical volcanic rocks. Lavas with olivine, plagioclase, and clinopyroxene phenocrysts are most abundant. Small extrusions of rhyodacites are localized on the north-western slope of the volcano (Martynov, et al., 1995; Selyangin, 1993).

The volcano morphology is shown in Fig. 9.5. Two craters, 1.5×2.0 km² and 1.3×1.3 km², partly overlapping each other, are situated northwest and west of the summit. The craters are partly filled with ice. The Vulkannaya River that drains a glacier flows out from the northeastern crater and descends along a deep gorge. A small active crater, the so-called Active Funnel is situated between both craters. This is a bowl-shape closed crater, 350×450 m² at the upper edge with a flat bottom ~150 m in diameter and steep (35–90°) walls 70–200 m high (Fig. 9.5).

The Active Funnel was formed as a result of explosive eruption during the last outburst of volcanic activity, probably 1200–1300 years ago (Selyangin, 1993). Melekestsev (1987) suggested that the crater could arise in the course of eruption in 1848–1854.

Recent activity is characterized by weak phreatomagmatic eruptions. All of them except the 2002 eruption, were related to the Active Funnel crater. Several historical eruptions are known, the last two have been described in detail. The eruption 1960–1961 consisted of ejection of resurgent ash through the fissures opened at the bottom of the Active Funnel

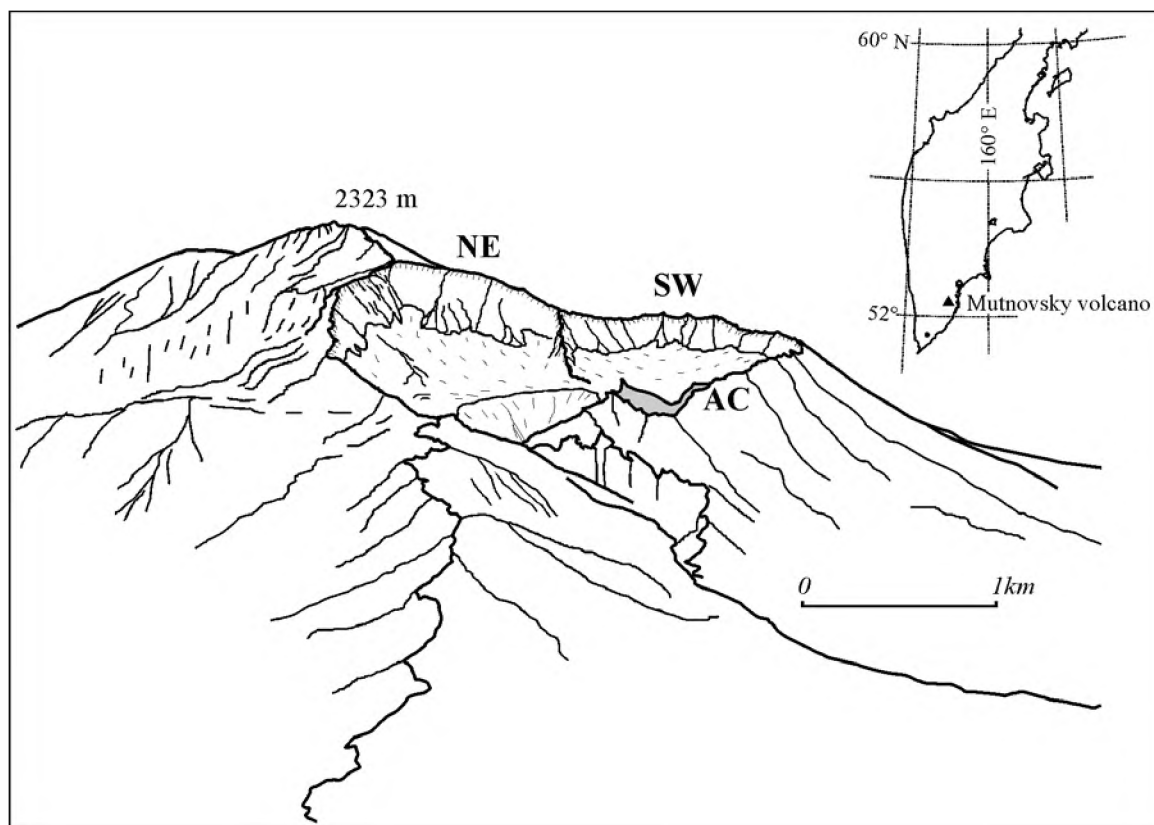


Fig. 9.5. The Mutnovsky volcano as viewed from the northwest. (NE) Northeastern Crater; (SW) Southwestern Crater; (AF) Active Funnel

fissures opened at the bottom of the Active Funnel (Vakin et al., 1966). A purely freatic eruption took place on March 17, 2000 (Okrugin et al., 2000; Zelen-sky et al., 2002). The warm lake that was formed in the old crater, about 300 m along the long axis, cooled during a few months. One more explosion crater, approximately 60 m in diameter, was simultaneously formed inside the active crater (Fig. 9.6).

Intense fumarolic activity is typical for the volcano between eruptions. Most of the volcanic rocks bear traces of this activity and are deeply altered as a result of gas and hydrothermal metamorphism. Two present-day fumarolic fields are situated in the lowest part of the northeastern crater. The thermal manifestations differ in morphology (fumaroles, steaming areas, boiling cauldrons), temperature, and gas composition. Several sites with steam jets heated to 100°C occur at the foot of the northern slope of the volcano. The most powerful gas emissions at a temperature reaching 520°C (2002) are confined to the Active Funnel.

The Upper fumarole field of the Northeastern Crater is localized above the right bank of the Vulkannaya River at a hypsometric level of 1470–1490 m (Fig. 9.6). Most of gases are discharged at site 20×70 m. The highest temperature was 281°C in 1981 and 262°C

in 2002. Formerly, the temperature reached 320°C (Polyak, 1966; Taran et al., 1991). The amount of fumarolic incrustations is not great and they consist of ammonium sulfate and chloride rims (sal ammoniac, mascagnite, letovicite) and altered zones 5–10 cm thick at the immediate contact with gas emissions. Small quantities of sulfur occur at the steamy sites with a temperature of gas emissions as 90–160°C along with sassolite, hallo-trichite–pickeringite and alunogen. As has previously been estimated (Vakin et al., 1966; Murav'ev et al., 1983; Polyak, 1966), approximately 100 kg/s of vapor are discharged in the Upper fumarole field.

The Bottom fumarole field is situated on the left bank of the Vulkannaya River, at an almost flat area, 90×250 m² with elevations of 1480–1490 m (Fig. 9.6). The site is largely composed of bottom sediments of the lake that existed here before 1961 (Vakin et al., 1966; Marenina, 1956). This fact is impressed in the field name. The hydrothermal manifestations of the bottom field are diverse and include classic fumaroles with sulfur incrustations of variable thickness, boiling (mud) cauldrons, acid lakes, and steamy areas. The temperature of gas emissions was 98–1260°C in 2002. The fumarole incrustations consist of sulfur, gypsum,

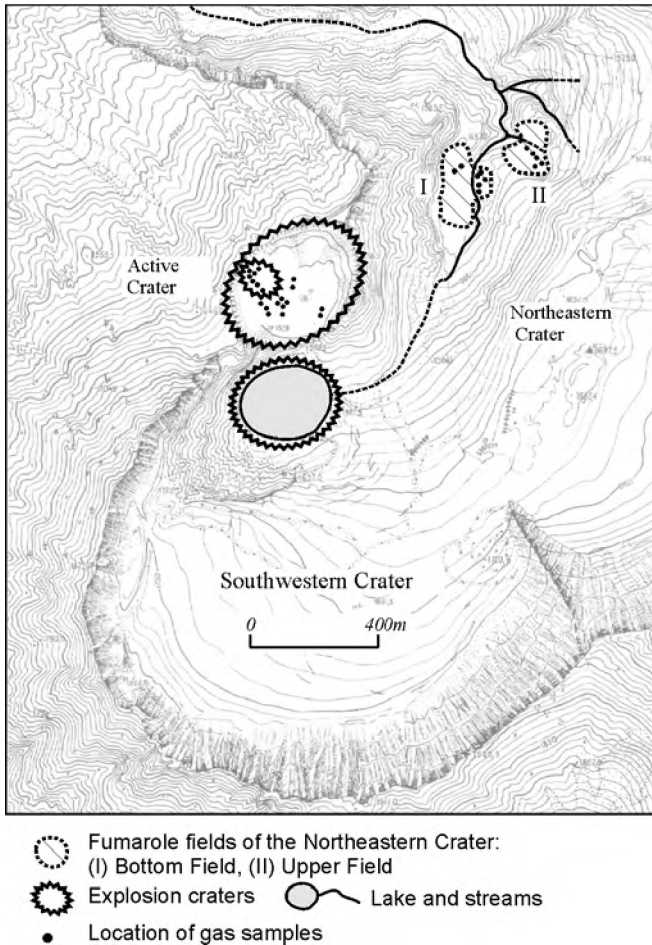


Fig. 9.6. Fumarolic fields of the Mutnovsky volcano

halotrichite–pickeringite, and alunogen (Serafimova, 1966; Okrugin, 1995). After displacement of the glacier in 1996–1998 (Gavrilenko et al., 2001), a new site of fumarole gas discharge, 20×50 m² in size, appeared on the right bank of the Vulkannaya River; with the highest temperature 247°C in 2002.

Up to 80% of the total gas discharge at the volcano occurs within the Active Funnel. The fumarole temperature was probably high (700–800°C) immediately after eruption in 1961, and slowly decreased over several years. A red glow was still observed in many fissures in 1963, and the measured temperature was above 750°C (Vakin et al., 1966). The maximum temperature in 1984 was 540°C (Taran et al., 1991). The present-day gas emissions from the Active Funnel are localized at the bottom, southern and southwestern walls of the crater at an absolute height of 1530–1600 m (Figs. 9.6 and 9.7). Small variations of the maximum temperature within 510–524°C were recorded in 1997–2002. The March 2000 phreatic explosion destroyed a part of the field with the highest-temperature fumaroles. However, the fumaroles that escaped de-



Fig. 9.7. Appearance of high-temperature fumaroles; quartz tubes for sublimate sampling are seen

struction retained their temperature and composition. The fumarole fields with temperatures from 300 to 510°C arose around a new explosive crater inside the previously existing Active Funnel. The high-temperature fumaroles of the Active Funnel appreciably differ from the fumaroles of the Northeastern Crater both in appearance (Fig. 9.7) and gas composition (Table 9.1). The most diverse mineral assemblages of incrustations are related to the highest-temperature gas discharges.

The fumarole gases largely consist of water vapor (91.5–98.0 wt %); SO₂ and CO₂ prevail among magmatic gases (Table 9.1).

The isotopic compositions (δD – $\delta^{18}O$) of the water vapor from fumaroles of the Mutnovsky volcano lie along the mixing line of magmatic and local meteoric waters (Fig. 9.8). The relative amount of the magmatic component attains 31–58% for the highest-temperature fumaroles of the Active Funnel. The strong correlation between $\delta^{18}O$ and concentrations of acid gases (HCl, HF, HBr, SO₂ + H₂S) clearly indicates their magmatic origin (Fig. 9.9).

Table 9.1

The chemical composition of fumarolic gases, mg/kg (samples taken in 2001)

Sample	T, °C	H ₂ O	CO ₂	H ₂ S	SO ₂	HCl	HF	HBr	CO	CH ₄	H ₂	He
A1	507	928000	32800	5800	28500	3400	660	3,7	3,60	0,092	33	0,017
A5	410	923000	34500	5700	31400	3850	820	4,1	0,19	0,064	5,2	0,018
A6	450	914000	24800	8800	46300	4600	870	6,1	0,34	0,040	13	0,014
A8	153	971000	12300	5100	3100	4800	28	1,8	0,12	2,5	0,93	0,019
A9	281	983000	13700	1100	1500	80	8		0,0098	28,3	0,55	0,0025

Note: Samples A1, A5, and A6 are from the Active Funnel, A8, from the Bottom Field, and A9, from the Upper Field.

The following trace elements are typical of the high-temperature gases (mg/kg of gas): B (18–27), As (6–8), Se (0.1–0.5), Te (0.15–0.35), Br (3.5–6.0), I (1.1–1.7), Cd (0.007–0.025), Tl (0.03–0.10), Pb (0.025–0.12), and Bi (0.03–0.06). A peculiar mineralization is formed in the discharge zone due to cooling gases. The source of trace elements remains ambiguous.

The highest-temperature (400–520°C) gases are discharged within an area of approximately 10×25 m

in the lower part of the southwestern wall of Active Funnel. The fumarole site is an oblique outcrop composed of fractured rocks (Fig. 9.7). The gas jets through holes and fissures, up to 10–15 cm wide, with a velocity varying from a few meters to a few tens of meters per second. The rock is readily split into fragments, 10–20 cm in size. As a rule, the core of such fragments consists of altered basalt surrounded by a rather loose outer zone, 5–20 mm wide, which is a product of gas–rock interaction. Sublimates, mainly

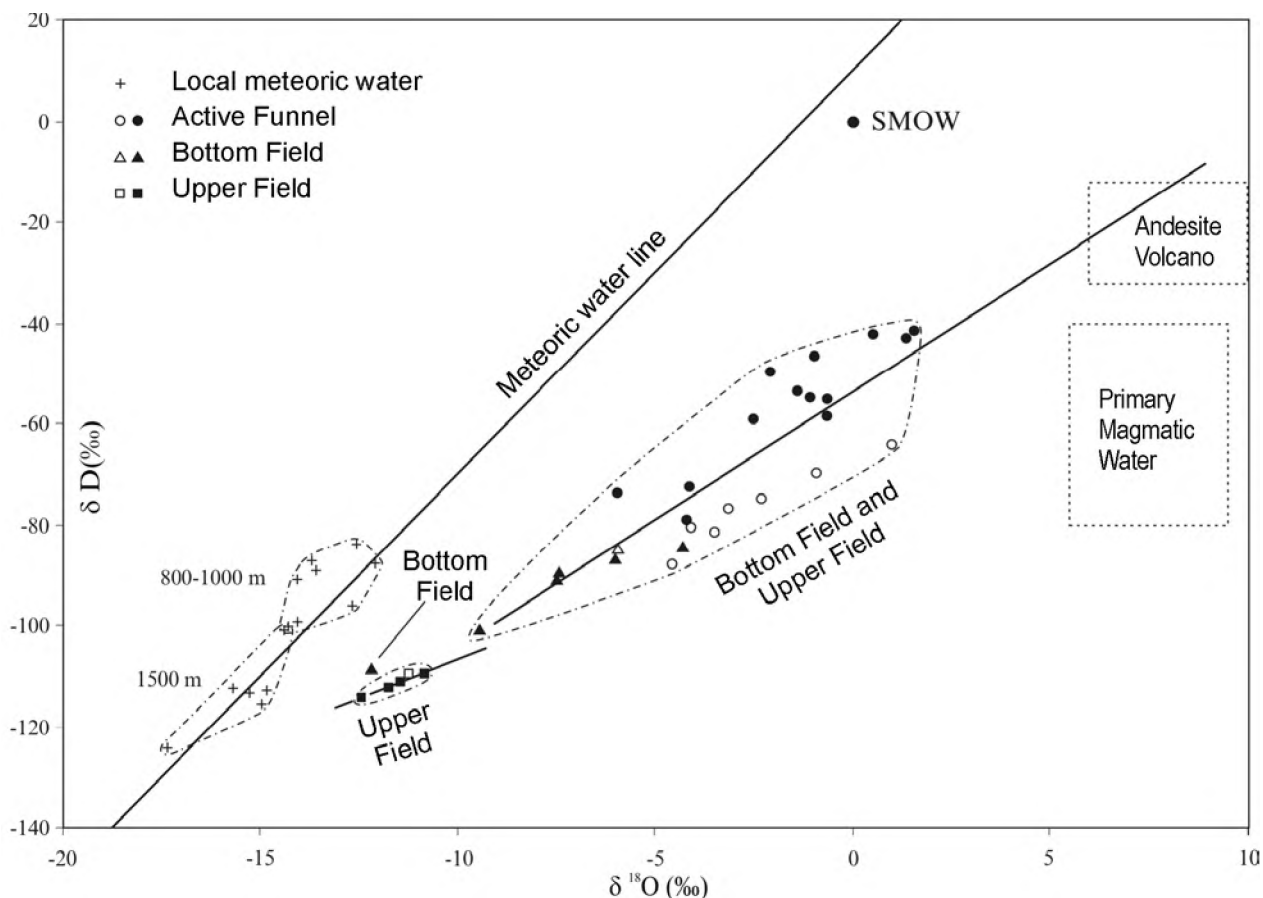


Fig. 9.8. δD vs. δ¹⁸O of fumarolic water vapor and meteoric water at the Mutnovsky volcano. Samples taken in 2001 are denoted by open symbols, in 2002, by solid symbols

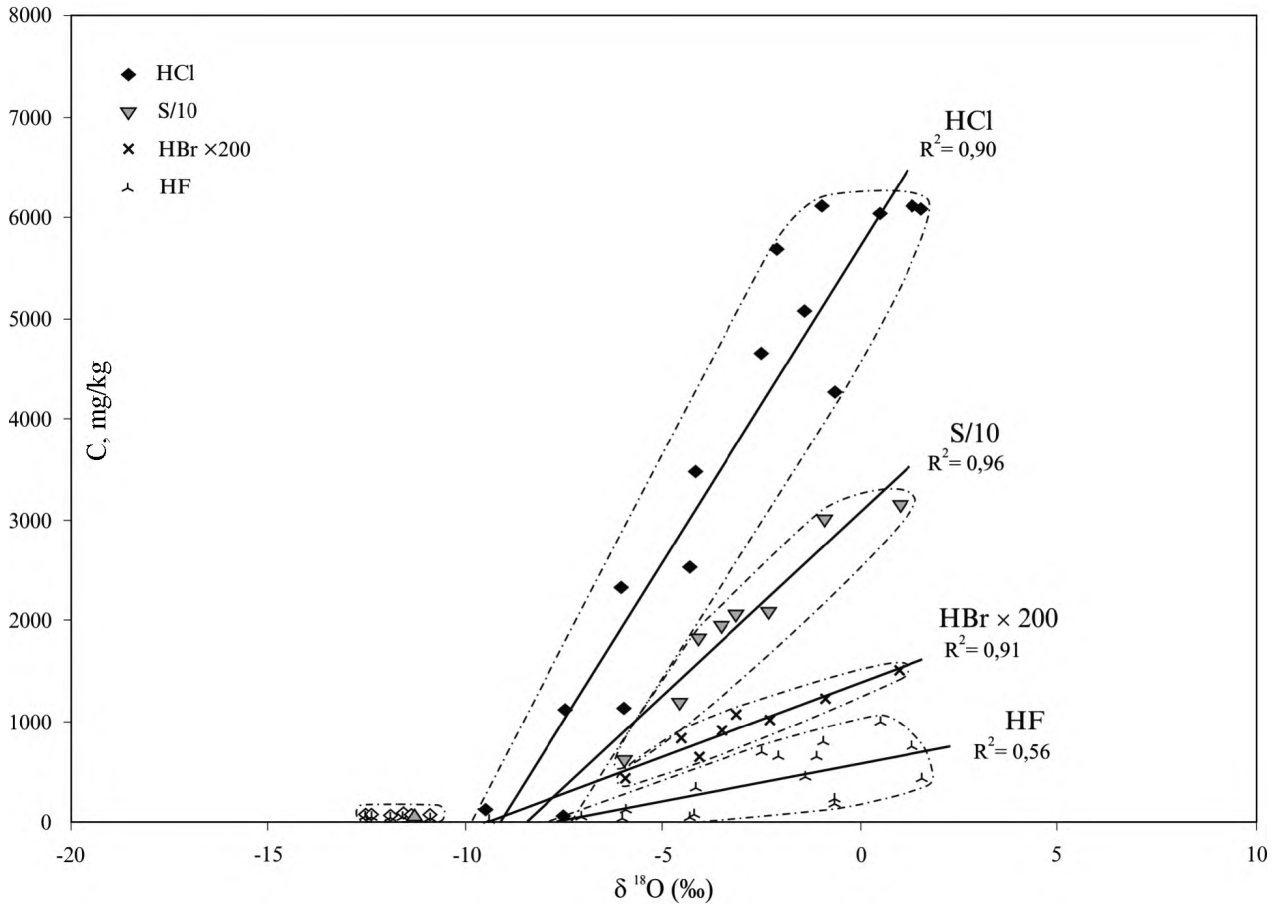


Fig. 9.9. HF, HCl, HBr, and S vs. $\delta^{18}\text{O}$ of fumarolic water vapor

Table 9.2

Minerals of sublimates from high-temperature fumaroles of the Active Funnel

Mineral	Formula	Occurrence depth, cm	Temperature range, °C	Abundance
Sulfur	S	0–10	150–50	*****
Pyrrhotite	FeS	20–50	500–480	**
Pyrite	FeS ₂	1–20	480–300	*****
Greenockite	CdS	2–10	470–440	***
Bismuthinite	Bi ₂ S ₃	0–5	~250–100	**
Sulfosalt1	Cd ₃ (Pb _{0,75} Fe _{0,25})Bi ₁₀ S ₁₈ Se	5–15	450–320	*****
Sulfosalt2	Cd ₂ Pb ₈ Bi ₁₁ S ₂₄ Se ₃	2–10	430–320	***
Sulfosalt3	As ₃ Pb ₃ Bi ₂ S ₁₀ Cl ₂	1–5	400–270	**
Sulfosalt4	As ₅ Pb ₁₀ S ₁₅ Cl ₂ BrI ₂	1–5	350–270	*
Arsenian sulfur	As _{2-x} S ₅	0–5	240–50	*****
Halite	NaCl	0–20	470–250	*****
Thallium–leadhalogenides	PbTl ₃ Cl ₂ I ₃	1–5	320–180	*
Bismoclite	BiOCl	2–10	~250–200	**
Sodiumsulfate	Na _{1,86} (Ca,Fe,Mg) _{0,07} SO ₄	0–5	~450–300	*****
Anglesite	PbSO ₄	0–5	~250–50	***
Bismuthoxy sulfate	Bi ₂ O(SO ₄) ₂	2–10	~250–200	*

Note. Estimated temperatures. Abundance: *single crystals, ** rare phases, *** phases of medium abundance, **** abundant phases, ***** major minerals. The phases identified under natural conditions for the first time are given in *italics*; formulae of these minerals should be regarded as preliminary.

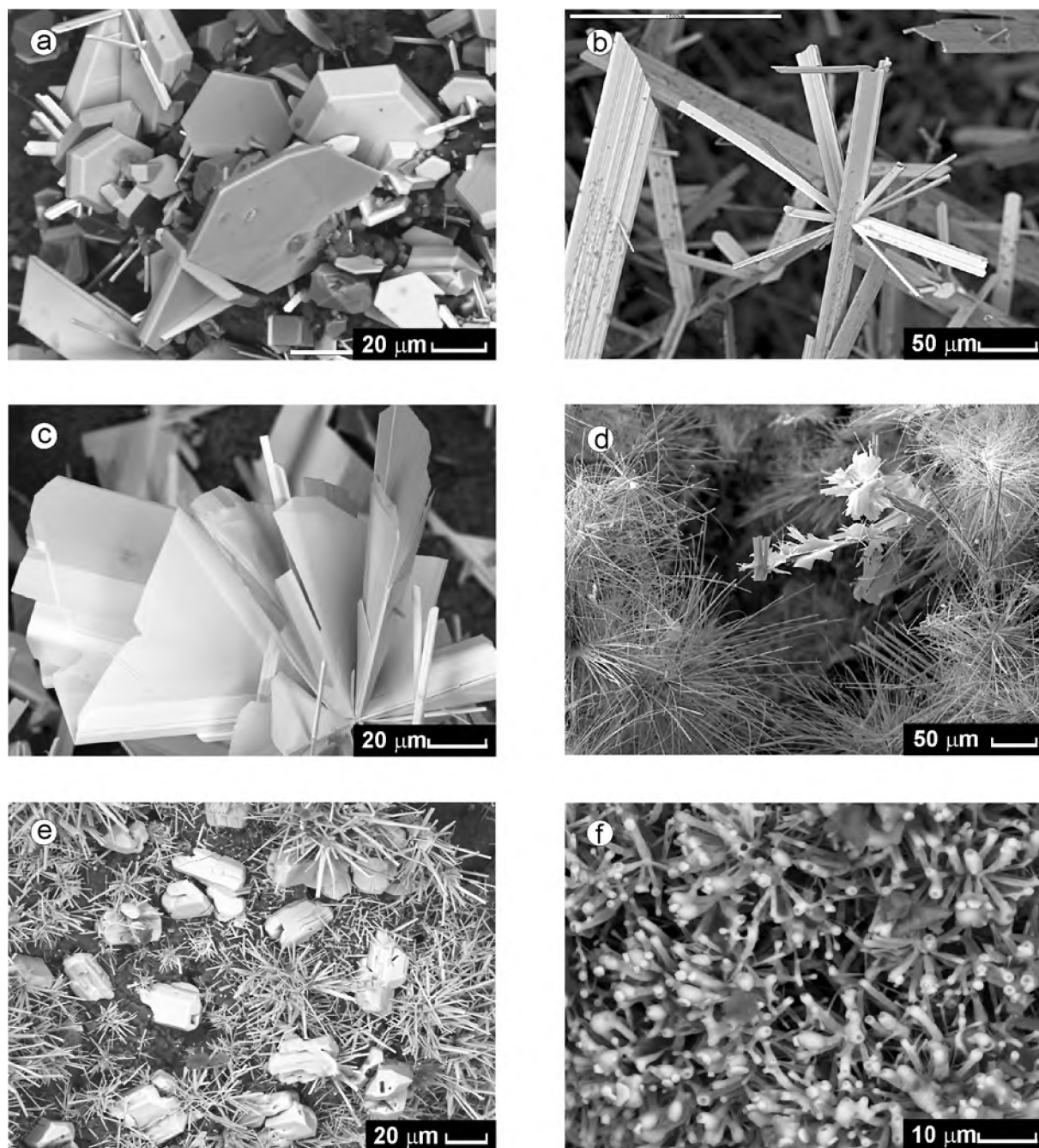


Fig. 9.10. Mode of occurrence of some sublimates.

(a) hexagonal greenockite (CdS) crystals; (b) sulfosalt $\text{Cd}_3\text{PbBi}_{10}(\text{S,Se})_{19}$; (c) sulfosalt $\text{Cd}_4\text{PbBi}_6(\text{S,Se})_{14}$; (d) halogen-bearing sulfosalt $\text{Pb}_9(\text{As,Bi})_9\text{S}_{20}\text{Cl}_5$ (thin needles) + sulfosalt $\text{Cd}_4\text{PbBi}_6(\text{S,Se})_{14}$ (leaves); (e) sulfosalt $\text{AsPb}_2\text{S}_3(\text{Cl,Br,I})$ (isometric crystals) + sulfosalt $\text{Cd}_4\text{PbBi}_6(\text{S,Se})_{14}$ (needles); (f) X-ray-amorphous arsenous sulfur

sulfides, sulfosalts, and halogenides precipitate on this substrate in some fissures and vugs. The surface of relatively cold parts of the fumarolic field is covered with a thin layer of bright orange arsenous sulfur.

All fumarole minerals of the Active Funnel are either sublimates or products of gas–rock interaction. Sixteen minerals were identified among sublimates (Table 9.2). They belong to the native elements, sulfides, sulfosalts (Fig. 9.10), halogenides and oxyha-

logenides, sulfates and oxysulfates. An X-ray-amorphous compound of S and As was conventionally referred to as a sulfide. The products of gas–rock reactions comprise 35 minerals including sulfides, halogenides, oxides and hydroxides, sulfates and silicates. Most of the compounds identified among the sublimates were previously unknown for Kamchatka volcanoes (Vergasova and Nadezhnaya, 1992; Serafimova, 1979, 1992; Okrugin, 1995, 2001a).

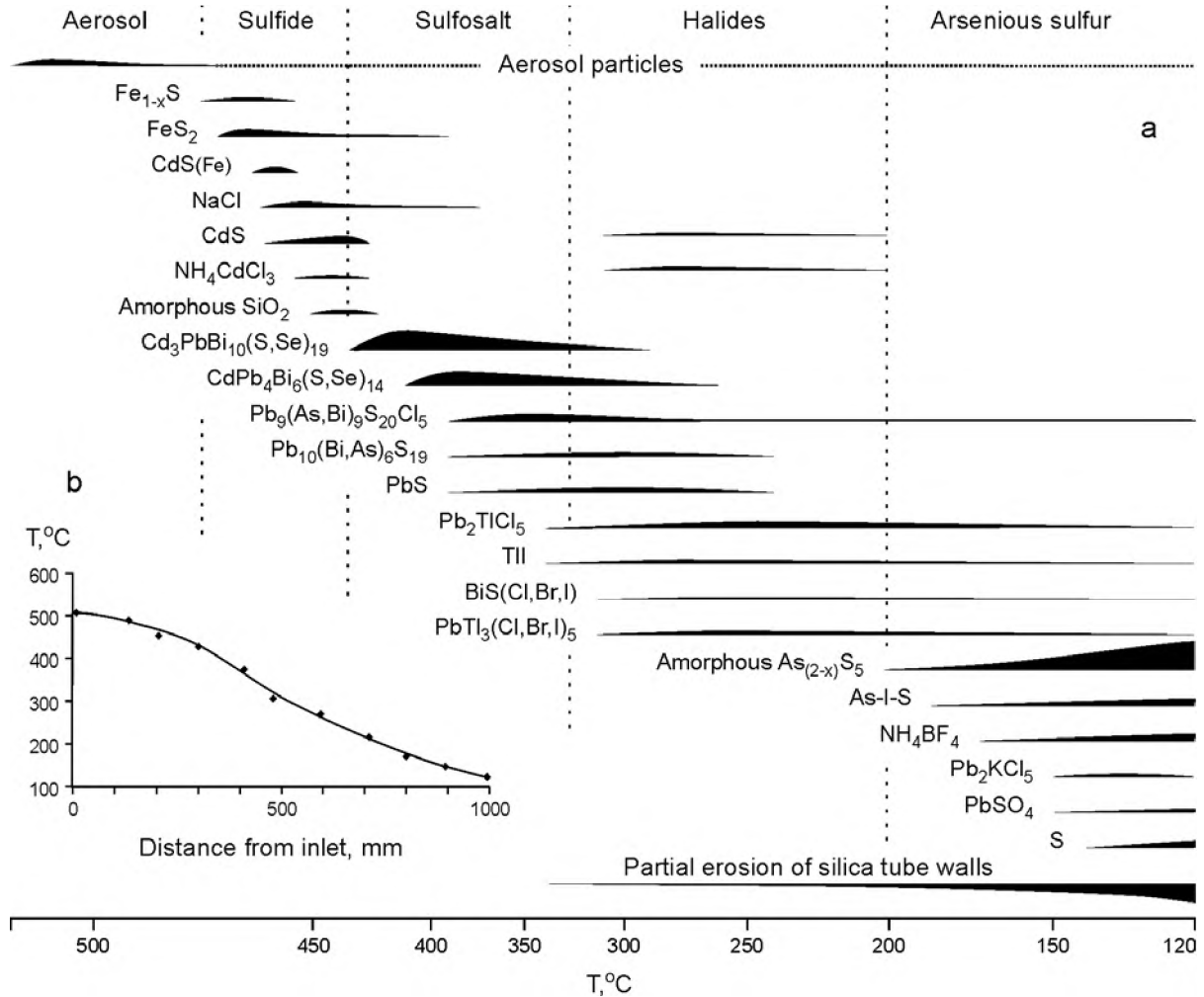


Fig. 9.11. The consecutive sublimate precipitation along silica tubes vs. temperature (a) and temperature vs. distance from tube inlet (b)

Some of the sulfosalts are close in properties and compositions to the rare sulfosalts from the La Fossa crater at the Vulcano Island in Italy (Borodaev et al., 1998; Fulignati and Sbrana, 1998; Garavelli et al., 1997; Mozgova et al., 1995).

The trace element composition of high-temperature gases and mineral formation conditions at their discharge was studied with quartz tubes inserted in fumarolic vents at a temperature of 470–507°C (Fig. 9.7). Gas moves through the tubes gradually cooling, and the solid phases precipitate on their walls as sublimates (Le Guern, 1982). This method is especially efficient in combination with thermodynamic modelling of the process.

Twenty-one phases were identified among sublimates with SEM-EDS; 12 of them were confirmed with XRD. The succession of precipitation strictly depends on the temperature. Each phase precipitates within a temperature range determined by element concentration in gas and the thermodynamic proper-

ties of individual species. Simple sulfides are replaced with temperature decrease by complex sulfosalts, sulfohalogenides, and halogenides; As–S compounds precipitate at the lowest temperature (Fig. 9.11). Sublimates are enriched in Cd, Tl, and I. Two new Cd-bearing sulfosalts: $\text{Cd}_3\text{PbBi}_{10}(\text{S,Se})_{19}$ and $\text{CdPb}_4\text{Bi}_6(\text{S,Se})_{14}$ containing 9 and 4 at. % Cd have been identified. Thallium was detected as three different halogenides. Seven phases contain iodine as a major or minor component; four phases contain bromine.

The X-ray-amorphous arsenous sulfur is the most unusual compound among the sublimates of the Mutnovsky volcano. This compound precipitates at a temperature below 220°C as thin hollow fibers containing 24–30 at. % As, 0.9–1.9% Se, 0.3–0.6% Te; the rest is sulfur. This compound most likely is nonstoichiometric $\text{As}_2\text{S}_3\text{--S}$ solid solution, which is formed by the joint precipitation of both components from the gas phase. The distribution of the major cation-

forming elements (Na, Fe, Cd, Tl, Pb, Bi, and As) in sublimates is controlled by their own phases. Some minor elements enrich the highest-temperature sublimates (Fig. 9.12). Elevated Sn concentrations (up to 0.5%), as well as In (up to 0.25%), Cu, Zn, Mo (up to 0.1%) were detected with ICP-MS and ICP-AES; Ag, Au (50–75 ppm), Re (6–17 ppm), and Pt (1 ppm) were also determined. The coherent Mo and Re distribution along the tube suggests that these elements precipitate as a single phase, which was not determined because of the small quantity. Other minor elements may also form poorly detectable tiny crystals or isomorphous admixtures in major phases.

Thermodynamic modeling of element transport and precipitation during gas–sublimate and gas–rock interaction was carried out. The aim of this study was to explain the observed and experimentally obtained mineral assemblages in the zone of fumarolic gas discharge and to determine probable speciation of the elements in the gas phase and their concentrations under the given conditions. According to the modeling results (Fig. 9.13), metals are mainly transported as halogenides, although other compounds, e.g., AlF_2O , $\text{Fe}(\text{OH})_2$, PbS , BiS , or native substances (Cd) may be significant at high temperatures. It is known that bromides and iodides of many metals have a high volatility, but chlorides dominate because of low HBr and HI concentrations in gas. The calculated forms of transport are generally consistent with previously obtained results (Symonds and Reed, 1993; Churakov et al., 2000). Cd, Pb, and Bi mainly precipitate as sulfides at a high temperature and as halogenides at a lower temperature. At the same time, Fe occurs in sublimates only as sulfides and Tl as halogenides. Cd, Tl, Pb and Bi reveal a tendency to form complex compounds instead of simple sulfides and halogenides in the calculated models. Bi, Pb, and especially Tl form diverse iodides in sublimates.

The total emission of different substances from the volcano was estimated from the fumarolic gas composition and the bulk discharge of fumarole fields. Measurements of the thermal power and discharge of fumarole fields in the northeastern crater of the Mutnovsky volcano in 1963 and 1981 yielded results of about 120 kg (Murav'ev et al., 1983; Polyak, 1966). The discharge of fumarole fields of the Active Funnel was estimated as 485–500 kg (Polyak, 1966) from the suggestion that the specific intensity of fumarolic activity was higher than in the northeastern crater. The estimated emission of main components and microelements is given in Table 9.3 from two alternative

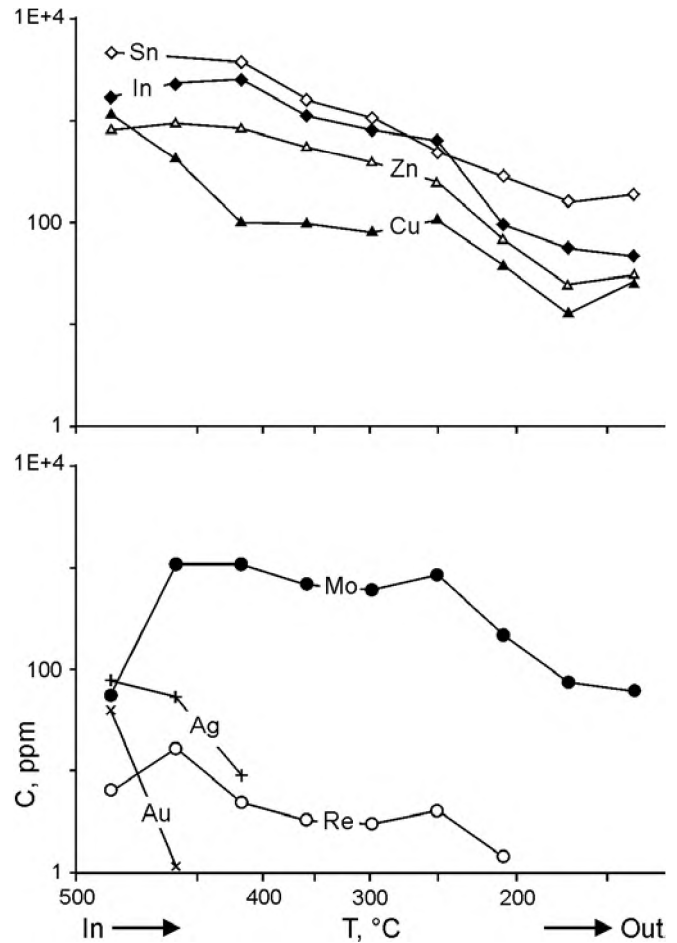


Fig. 9.12. Variation of minor element contents vs. temperature along the silica tube

assessments of bulk discharge of the Mutnovsky volcano. The estimation is for the three most hot and intense fumarolic fields taking into account the weight coefficients. According to the results obtained, the emission of elements is very low. The sum of Cd + Tl + Pb + Bi is only 1.0–7.5 kg a day. The discharge of B, As, and Na is somewhat higher (a few hundred kilograms a day). The lowest and highest discharge values for the same elements from the La Fossa crater are given for comparative purposes (Cheynet, 2000). An approximate estimate of the bulk ore elements precipitated during the existence of a high-temperature fumarole field (over 40 years), including mineral forms and enrichment of rocks in these elements yields several hundred kilograms for As and the Cd + Tl + Pb + Bi sum. Hence, the gain of heavy elements in the discharge zone amounts to tenths of percent and to hundredths of percent for As. The discharge conditions are not favorable for local concentration and the elements emitted by the volcano mostly disperse in the atmosphere.

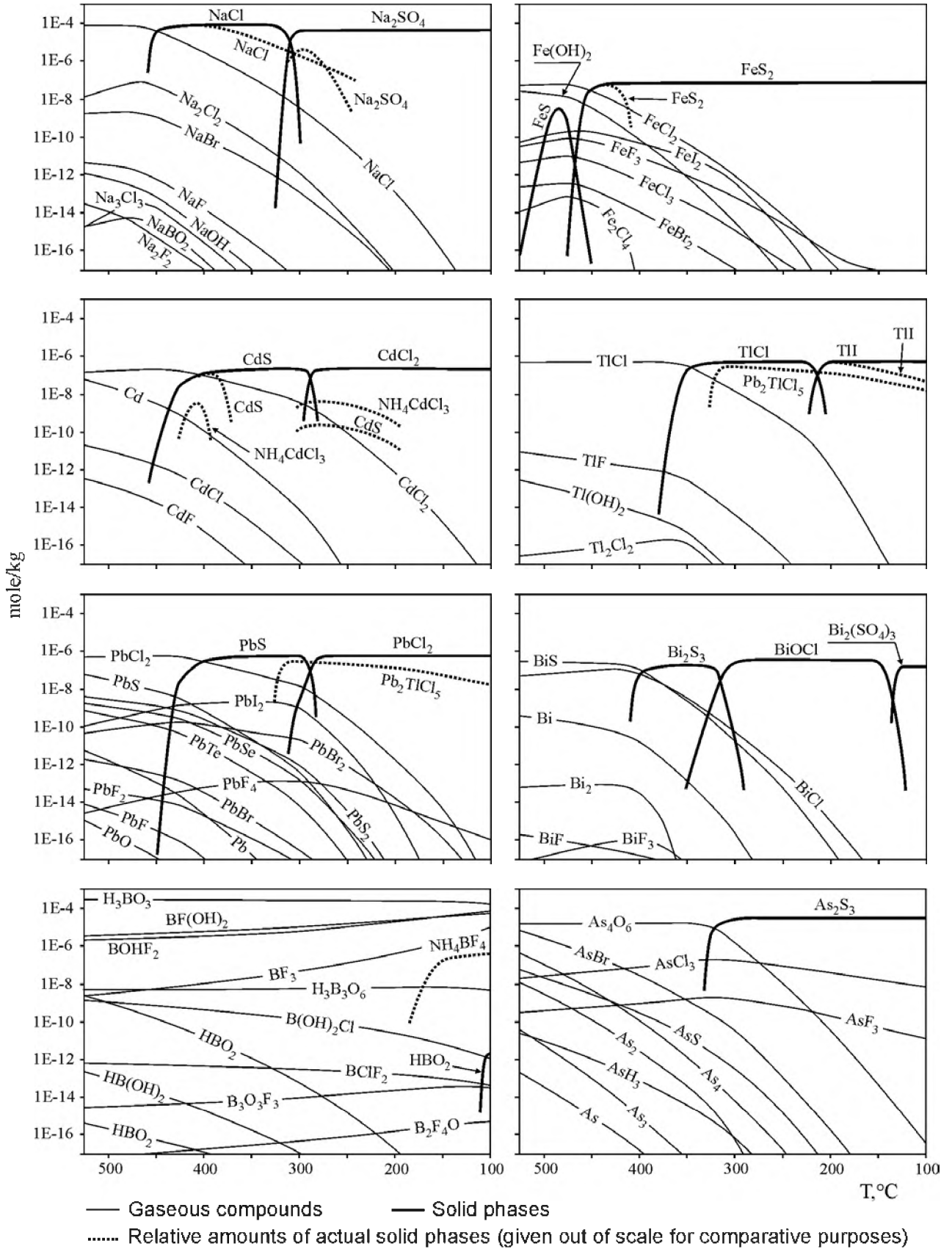


Fig. 9.13. Calculated concentrations of gaseous compounds and stability fields of solid phases during fumarolic gas cooling within a temperature range of 507-100°C and at a pressure of 1 bar

Table 9.3

 Estimated emissions from the Mutnovsky volcano
and La Fossa crater, kg/day

Component	Mutnovsky		La Fossa	
	1	2	3	4
H ₂ O	5.3·10 ⁶	39·10 ⁶	5.7·10 ⁶	1.2·10 ⁶
CO ₂	180·10 ³	1300·10 ³	1700	350·10 ³
H ₂ S	38·10 ³	280·10 ³	70·10 ³	15·10 ³
SO ₂	200·10 ³	1500·10 ³	76·10 ³	16·10 ³
HCl	22·10 ³	170·10 ³	21·10 ³	4.4·10 ³
HF	4.5·10 ³	34·10 ³	6.4·10 ³	1.4·10 ³
Br	25	180		
I	7	53		
Se	1.8	14		
Te	1.4	10		
B	130	970		
Na	25	180		
As	39	290	14	2.5
Cd	0.07	0.6	0.26	0.048
Pb	0.34	2.6	13	2.5
Bi	0.3	2.2	2.5	0.44
Tl	0.3	2.2	0.26	0.048

THE MUTNOVSKY GEOTHERMAL DEPOSIT

Geothermal energy is a highly promising area of economic development of Kamchatka. The first geothermal power station in Russia Puzhetka with an initial output of 5 MWt was put in operation in 1966; its power increased up to 11 MWt in 1979. Three geothermal power stations successfully function in Kamchatka at the present time. In addition to the Puzhetka station, the Verkhne-Mutnovsky pilot station (12 MWt) started in December 2000 and the Mutnovsky 1 station (50 MWt), in September 2002. The new stations have been built at the Mutnovsky geothermal deposit of the North Mutnovsky high-temperature geothermal system, a largest geothermal system of Kamchatka. The energy resources are estimated as $71.28 \cdot 10^{18}$ J.

The Mutnovsky geothermal field is situated 70–75 km southwest of Petropavlovsk-Kamchatsky on a volcanic plateau at elevations of 700–900 m and localized in the central part of this system. The Mutnovsky geothermal system (Mutnovsky geothermal dis-

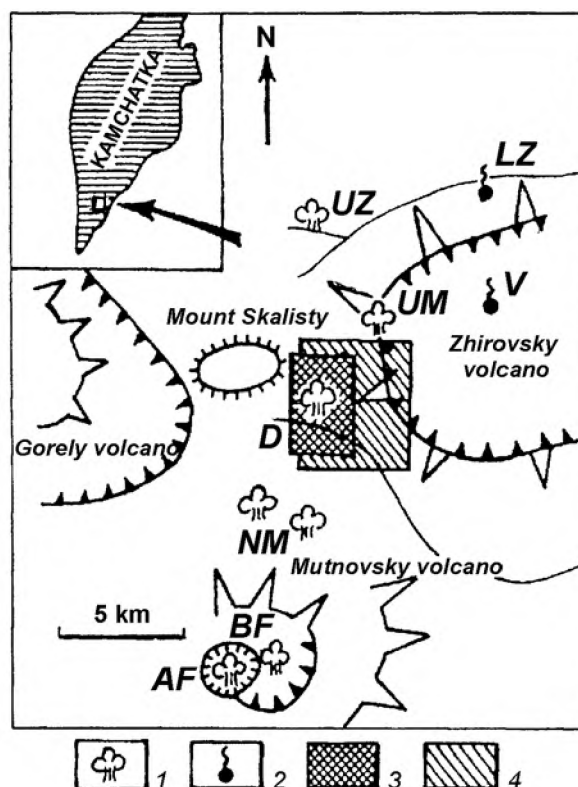


Fig. 9.14. The Mutnovsky hydrothermal deposit (Dachny prospect).

(1) natural vapor jets: (AF) Active Funnel, (BF) Bottom Field, (NM) North Mutnovsky (western and eastern), (D) Dachny, (UM) Upper Mutnovsky, (UZ) Upper Zhirovsky; (2) hot springs: (V) Voinovsky, (LZ) Lower Zhirovsky; contours of modeling areas: (3) 1993, (4) 1996 (by Kiryukhin, 2002)

trict, after Okrugin, 1995) is extremely diverse as concerns present-day volcanic and postvolcanic activity. Three field groups are recognized: (1) fumarolic fields of the active Mutnovsky and Gorely volcanoes, (2) thermal fields and water-vapor springs of the North Mutnovsky volcanotectonic zone, and (3) thermal fields and ascending hot springs in river valleys (Vakin, 1976, 1986; Okrugin, 1995; Kiryukhin, 1998). The largest heat occurrences: Dachny, North Mutnovsky, and Perevalny contain the main heat carrier resources and are localized within the North Mutnovsky volcanotectonic zone. This zone is a graben-like basin controlled by a large N-S fault (Lonshakov, 1979; Leonov, 1989; Kiryukhin, 2002). A combination of its N-S zone of tectonic dislocations with NW and NE faults and E-W faults along with lithological traps provide favorable conditions for hot water and vapor accumulation (Fig. 9.14).

The deformed Oligocene and lower Pliocene volcanosedimentary rocks (conglomerates, tuffaceous sandstones, tuffs, and silicic lavas) crop out in can-

yon-like river valleys; their apparent thickness attains 1500 m. The upper Pliocene and lower Pleistocene basalts and basaltic andesites of the Zhirovsky paleo-volcano are about 650 m thick. Pleistocene and Holocene volcanics comprise from bottom to top: (a) ignimbrite of the first phase of the Gorely volcano, (b) transitional lava and pyroclastic unit, (c) volcanics and pyroclastics of the Skalisty, Dvugorby, and Pal'chik volcanoes, (d) pumice tuffs of the Dachny hydrotherms, (e) ignimbrite of the second phase of the Gorely volcano, (f) lavas and pyroclastics of the Mutnovsky and Plosky volcanoes, and (g) pumice tuffs at passes (mountain ridges) and (h) downfall deposits and talus. The total thickness reaches 2000 m.

The Dachny springs appear to be a series of gas and steam jets on steep slopes and talwegs of canyon-like ravines. Interacting with groundwater in depressions, the gas and steam jets form various boiling potholes, springs gathered into five groups (Utiny, Medvezhy, Utrenny, and Aktivny groups are the largest), thermal lakes, and swamps, as large as one square kilometer in total area (Vakin, 1976, 1986). All of them are related to the pumice tuff capped by ignimbrite flows. The Aktivny group is deemed to be the largest and the most pictorial. It is situated within the funnel of a phreatic explosion, 250 m in diameter, in the foothills of a large silicic extrusion. The North Mutnovsky group of hydrotherms is localized on the northern slope of the Mutnovsky volcano and consists of Western and Eastern thermal fields. The Perevalny springs are situated in the northwestern district in

close proximity to the vein zones of the Mutnovsky epithermal gold and base-metal deposit.

The fumarole fields of the Mutnovsky and Gorely crater zones are major heat energy sources. The compositions of fumarolic gases are given in Table 9.1. The condensates of vapor-gas jets in thermal fields of the North Mutnovsky tectonic zone are poorly-mineralized solutions ($\text{HCO}_3\text{-NH}_4$) having pH close to the neutral value. The gas phase contains CO_2 , H_2S , N_2 , H_2 , and CH_4 . The acid sulfate water in the boiling mud potholes is enriched in Pb, Zn, As, Sb, and Mn. The thermal springs in the river and creek valleys are close to the nitric-carbonated overheated pressure water.

Kiryukhin (2002) distinguishes the Main and Northeastern ascending heat-carrier flows fixed by temperature anomalies as high as 300°C. The Main flow is related to the southeastern contact of a diorite intrusion penetrated by boreholes at a depth of 1.5–2.0 km. This intrusion provides permeability and feeds the geothermal reservoir with heat. It is thought that the thawing glacier in the Mutnovsky volcano crater, 8 km away, may be a water source as indicated by isotopic geochemistry.

THE RODNIKOVY EPITHERMAL GOLD-SILVER DEPOSIT

The Rodnikovoy orefield is situated in the Yelizovo District of the Kamchatka Region and occupies an area of 22 km² with coordinates of the central part (52°39'08" N and 158°12'45" E, Figs. 9.15 and 9.16). The orefield contains the Rodnikovoy deposit (southeastern part), Carbonate (northeastern part) and Vilyucha (western flank) ore occurrences. There is another Mutnovsky epithermal deposit in close proximity (10 km to the south) to Rodnikovoy.

The ore field is localized within a semiring structure of volcanic origin, about 8 km in diameter, known as the Vilyucha volcanotectonic structure (Lonshakov, 1979; Petrenko, 1999), which is controlled by the South Kamchatka submeridional normal fault system, the northeastern faults of the extreme NW flank of the Mutnovsky regional fault, and E-W Karymchinsky permeable zone, which coincide here (Figs. 9.3, 9.4, and 9.16).

The Rodnikovoy deposit was discovered in 1977 during geological mapping at a scale of 1:50,000. The central part of the deposit (7 km²) has been explored by boreholes and two adits. The estimated reserves are 40 t Au and 340 t Ag. Ore zones were not contoured either along strike or down dip. Relations to the Viluy-

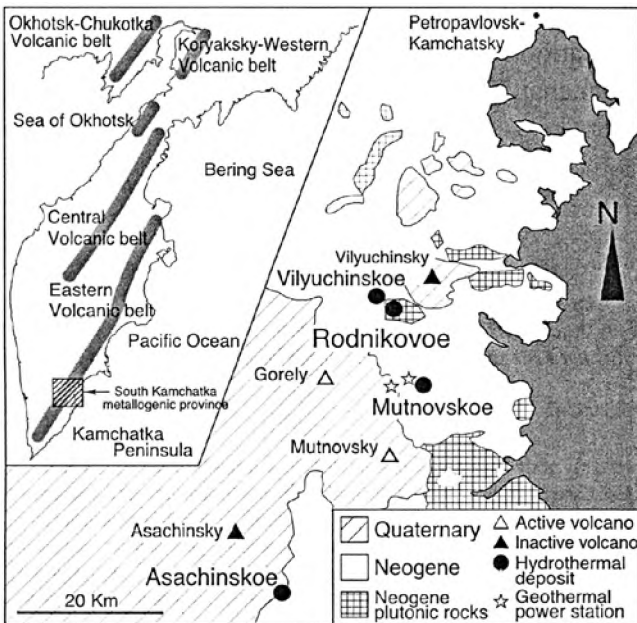


Fig. 9.15. Simplified geological map of the southern Kamchatka metallogenic province

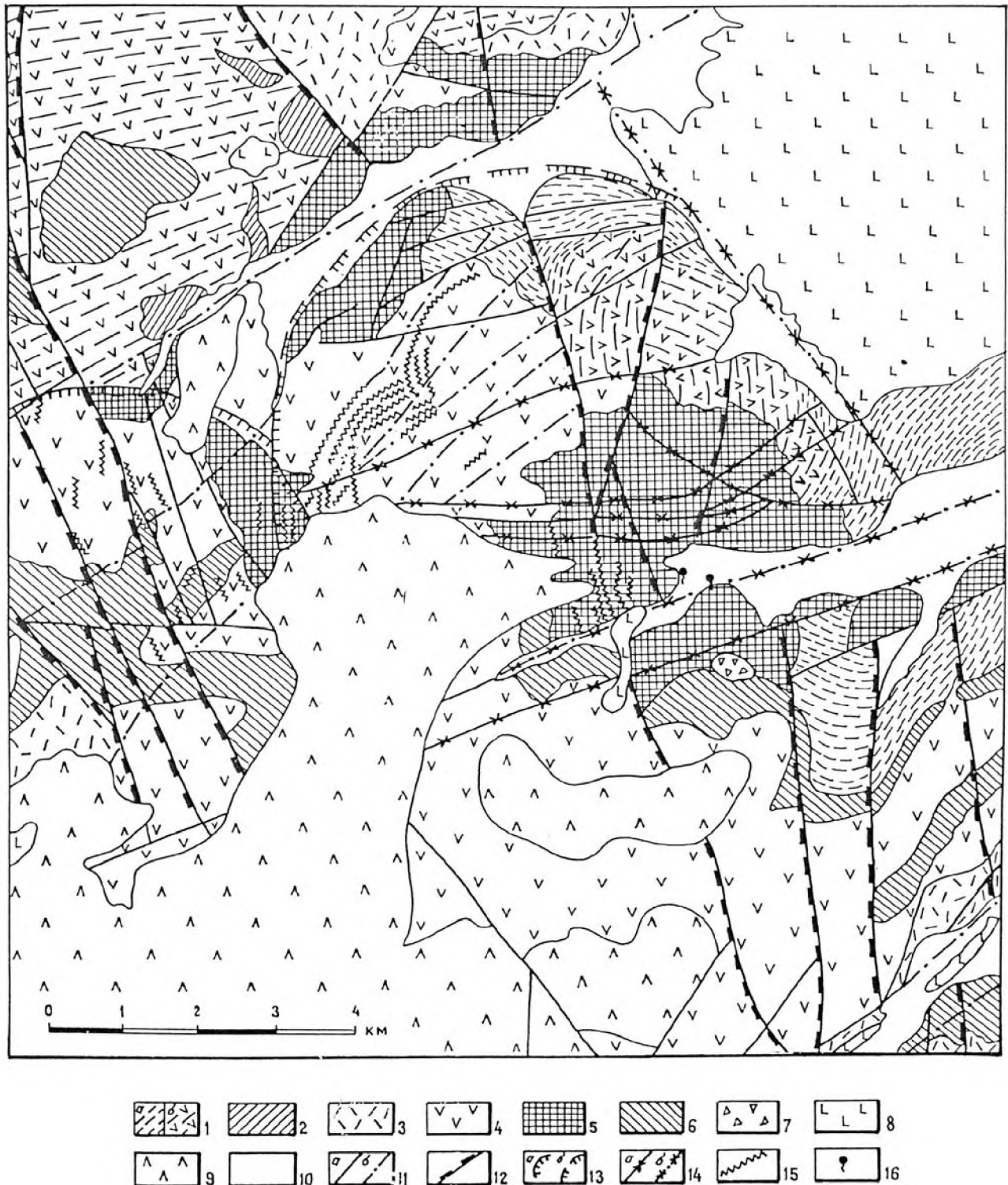


Fig. 9.16. Geostrucural scheme of the Rodnikovy ore field.

Pre-ore assemblage: (1) Oligocene-to-Miocene volcanicogenic-sedimentary island arc formations, (2) Oligocene-to-Miocene intrusive and subvolcanic bodies, (3) Miocene-to-Pliocene dacite, rhyodacite, and tuff; *Pliocene ore-hosting assemblage:* (4) effusive and pyroclastics, (5) gabbro and gabbrodiorite, (6) subvolcanic rhyolite-to-andesite, (7) explosive breccia; *Pleistocene-to-Holocene post-ore volcanic assemblage:* (8) basalt and andesite, (9) andesitic dacite, dacite, and rhyolite; (10) Quarternary loose sediments; (11) long-lived normal faults of the Mutnovsky deep fault system; (12) southern Kamchatka ore-controlling normal fault system; (13) faults bounding the Rodnikovy and Bystrinsky volcano-tectonic structures; (14) post-ore noetectonic faults; (15) quartz veins; (16) contemporary thermal springs

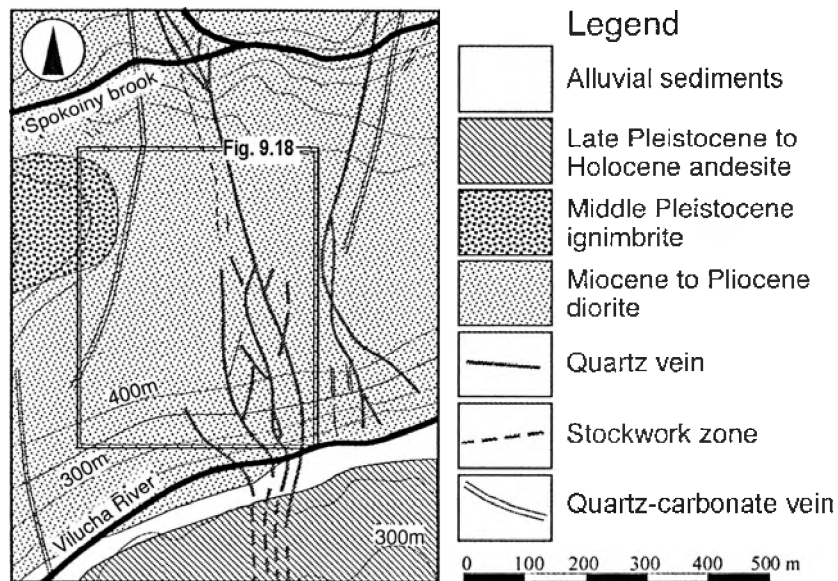


Fig. 9.17. Geological map of the Rodnikov deposit

cha occurrence (2.0–2.5 km to the northwest), Carbonate occurrence (1.2 km to the north), Skazka vein zone (5 km downstream the Vilyucha River), and Mutnovsky deposit remain unknown.

The deposit is localized at the junction of southern segments of the Central Kamchatka and East Kamchatka volcanic belts with the Malka-Petropavlovsk zone of transverse dislocations (Fig. 9.15). The meridional normal fault system of southern Kamchatka is especially important as an ore-controlling structure. Relicts of the volcanic structure that hosts the orebodies are localized at the intersection of this fault system with the Karymchinsky permeable zone (Petrenko, 1999).

The oldest rocks are exposed in cliffs of the Vilyucha and Zhirovsky bays and in the middle and lower reaches of the Vilyucha River. The strongly deformed Oligocene and Miocene volcanic and volcanosedimentary rocks are related to the island-arc stage in the evolution of the Central Kamchatka volcanic belt. In the northeast, these rocks are intruded by granosyenite of the Sarany intrusive complex.

The ore-bearing rocks are composed of Pliocene subvolcanic intrusions, diverse in shape and dimensions, varying from andesite to rhyolite in composition. Almost all orebodies are hosted in gabbro and diorite making up a relatively large intrusion (Fig. 9.17). The lava and pyroclastic facies occur at the headwaters of the Vilyucha and Paratunka rivers. These rocks are interpreted as remnants of an eroded Rodnikov paleovolcano and its exposed magma chamber (Okrugin, 1995; Petrenko, 1999).

The Quaternary volcanics of the East Kamchatka volcanic belt are post-ore. They comprise middle Pleistocene ignimbrite flows of the Gorely volcano (100 m thick at the southwestern flank of the deposit), upper Pleistocene and Holocene basaltic andesite of the Vilyuchinsky volcano (northeastern part of the deposit), and rhyolites and tuffs at the southern flank.

The host gabbro and diorite vary from fine-grained varieties near the contacts to fully phaneritic rocks in the central part of the intrusion. Numerous xenoliths of country rocks, segregations of silicic derivatives, and brecciated rocks are typical of the contact zone. The intrusive rocks are affected by regional propylitic alteration with formation of epidote-chlorite-actinolite and chlorite-carbonate-epidote mineral assemblages.

The hydrothermal alteration resulted in the formation of four mineral assemblages: hydromica-"sericite"-kaolinite, quartz-hydromica-"sericite" with adularia, quartz, and quartz-adularia. Adularia from veins and metasomatic rocks reveals zoning and is enriched in barium (up to 2.5–3.6 wt % Ba). K_2O , Li_2O , S, SiO_2 , Hg contents increase in proximity to orebodies, while Al_2O_3 , Na_2O , and CaO contents drop.

Orebodies include a series of quartz-carbonate veins grouped into the Rodnikov ore zone (Figs. 9.16–9.18) controlled by a vertical, nearly N-S fault with components of normal and strike-slip displacements. The vertical separation attains 350 m (Petrenko, 1999). A combination of N-S, NW and NE faults determines a complex en echelon arranged

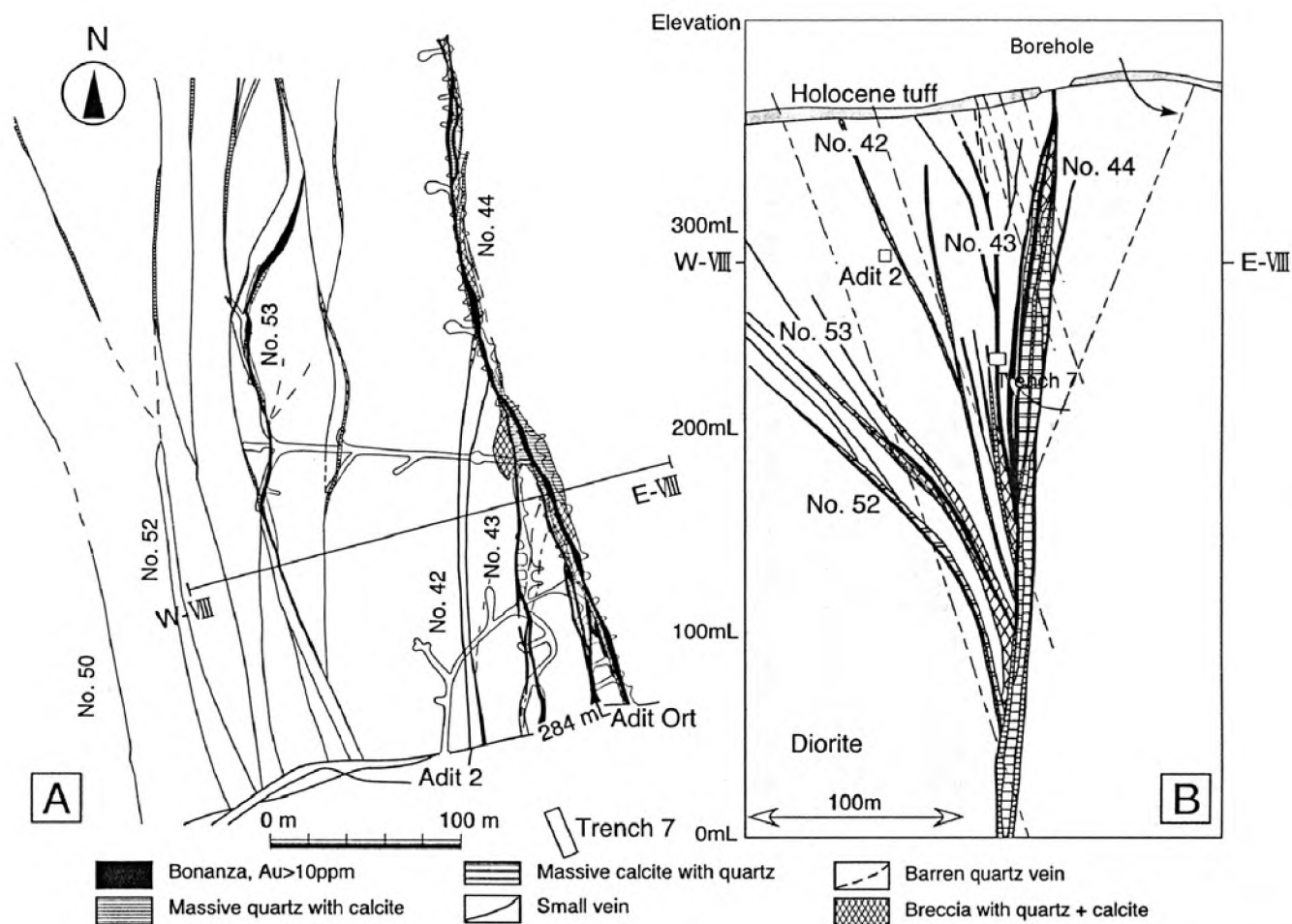


Fig. 9.18. (A) horizontal and (B) vertical sections across the Rodnikovoy deposit. The virtual position of Adit 2, Adit ort and Trench 7 are projected on the section

structure of the ore zone bending along the strike and down the dip. The steeply dipping ($80\text{--}90^\circ$ W) stem Vein 44 is combined with small auxiliary veins (nos. 42, 43, 52, and 53) dipping at angles $45\text{--}80^\circ$ E. Vein 44 is exposed on the left bank of the Vilyucha River near Adit 2. The vein zone reaches 100 m in thickness and extends for more than two kilometers. The vertical range of ore mineralization is 300 m. The ore zone structure simplifies with depth, where all veins merge into one vertical stem vein. The thickness of orebodies varies from 0.4 to 8.4 m; they extend for 70–1430 m along strike and for 230 m down dip. The ore zone is overlapped by Quaternary loose sediments, pyroclastic rocks, and rhyolites on the right bank of the Vilyucha River. Here, boreholes cut thin veins and veinlets.

The ores are of low sulfidation quartz-adularia vein type (White, 1995; Hedenquist, 1996). The amount of ore minerals in quartz-carbonate-adularia veins commonly does not exceed 3–5% (Okrugin, 1995; Takahashi, 2002a, 2002b); sulfide and sulfosalt

content increases to 10–25% only in small pockets and lenses. Gold and silver are distributed through veins extremely nonuniformly. The Au grade varies from 0.1 to 130–140 g/t (300–1200 g/t in isolated ore shoots). The average grade is 2.5–30.5 g/t Au, and the mean Au/Ag ratio is 1/10. The Ag grade varies from 1–2 to 300–700 g/t (150–200 g/t, on the average). Ores are banded, colloform, crustified, massive, and brecciated.

The mineral composition of the ore is fairly simple (Table 9.4). Quartz, calcite, and to some extent adularia are major minerals. Ore minerals occur as fine segregations, lenses, and microbands consisting of native gold, argentite, minerals of the stibiopearceite–arsenopolybasite series, aguilarite, naumannite, fahlore with variable Ag content, very rare lenaite, and Pb–Zn–Cu sulfides. The small (from 5–10 to 50–150 μm) native gold (electrum) grains are variable in composition and microstructure. The Ag content within a grain changes from 27.5 to 65.5 wt %. Dendritic aggregates with elements of mosaic and sub-

The mineral composition of ore at the Rodnikov deposit

Ore minerals		Gangue minerals	
Pyrite	FeS ₂ (As = 0-6.8%)	Quartz	SiO ₂
Sphalerite	ZnS (Cd = 0-0.5%)	Calcite	CaSO ₃
Galena	PbS	Opal	SiO ₂ ·nH ₂ O
Chalcopyrite	CuFeS ₂	Adularia	KAlSi ₃ O ₈ (Ba = 0-3.7%)
Stibiopearceite–arsenopolybasite	(AgCu) ₁₆ (AsSb) ₂ S ₁₁ (Se = 0-5.2%)	Albite	NaAlSi ₃ O ₈
Argentite	Ag ₂ S (Se = 0-5.9%)	Sericite	KAl ₂ (Si ₃ Al)O ₁₀ (OH,F) ₂
Acanthite	Ag ₂ S	Beidellite	Na _{0.5} Al ₂ (Si _{3.5} Al _{0.5})O ₁₀ (OH) ₂ ·n(H ₂ O)
Tetrahedrite	(CuFe) ₁₂ (AsSb) ₄ S ₁₃ (Zn, Ag = 7-8%)	Montmorillonite	(Na,Ca) _{0.3} (Al,Mg) ₂ Si ₄ O ₁₀ (OH) ₂ ·n(H ₂ O)
Lenaite	AgFeS ₂	Illite	KAl ₂ Si ₃ AlO ₁₀ (OH) ₂
Stembergite	AgFe ₂ S ₃	Kaolinite	Al ₂ Si ₂ O ₅ (OH) ₄
Jalpaite	Ag ₃ CuS ₂	Chlorite	(Mg,Fe,Al) ₁₂ (SiAl) ₈ O ₂₀ (OH) ₁₀
Stephanite	Ag ₅ SbS ₄	Anhydrite	CaSO ₄
Hessite	Ag ₂ Te	Apatite	Ca ₃ (PO ₄) ₂
Clausthalite	PbSe	Fluorite	CaF ₂
Aquilarite	Ag ₂ S		
Hodrushite	Cu ₈ Bi ₁₂ S ₂₂		
Bismuthinite	Bi ₂ S ₃		
Arsenopyrite	FeAsS		
Tetradymite	Bi ₂ Te ₂ S		
Chalcocite	Cu ₂ S		
Covellite	CuS		
Electrum	Au-Ag (Au = 34.5-72.5%)		
Native silver	Ag		
Cinnabar	HgS		

Note: (As – 0-6.8%) – limits of variations, wt %

block structure are typical. Some stibiopearceite–arsenopolybasite and argentite domains are enriched in Se. A few ore shoots at the southwestern and eastern flanks contain sphalerite, galena, pyrite, and chalcopyrite in amounts attaining 30–40%. The pyrite disseminations are most typical of outer contact zones rather than of ores where the pyrite content abruptly falls. Zoning of pyrite is emphasized by a variable As content. The heterogeneous and zoned structure of ore minerals is a characteristic feature of Au–Ag deposits from southern Kamchatka.

The ore formation was multistage (no less than six stages), and the process cannot be regarded as completely ended (Fig. 9.19). The economic mineral assemblages precipitated from true and colloidal solutions at 150–250°C. Ore deposition proceeded at a depth of about 170 m below the groundwater table and was accompanied by boiling, hydrothermal explosion, brecciation, metasomatic replacement, oscillation and rejuvenation (Figs. 9.20 and 9.21). The S, C,

and Sr isotope compositions of rocks and minerals from the ore zones suggests a mantle source. According to the geological data and results of K–Ar timing (veins 42–44), the age of ore formation is 0.9–1.1 Ma and thus corresponds to the late Pliocene–early Pleistocene (Takahashi, 2002a, 2002b; Okrugin, 2003b). The host gabbro and diorite are much older: isotopic dates vary from 12.1 to 3.76 Ma (Okrugin, 2001b; Chashchin, 2001; Okrugin, 2003b).

The hydrothermal activity in the vicinity of the deposit still goes on in connection with the evolution of the Vilyucha hydrothermal ore-forming system (Tazaki, 2003). Numerous thermal springs emit a sodic chloride-carbonate water with elevated B, Mn, Fe, Sr, and As contents (Table 9.5). The springs are divided into three groups:

The largest Vilyucha Springs are situated 750 m east of the Rodnikov camp on the right bank of the Vilyucha River. This is a series of travertine domes,

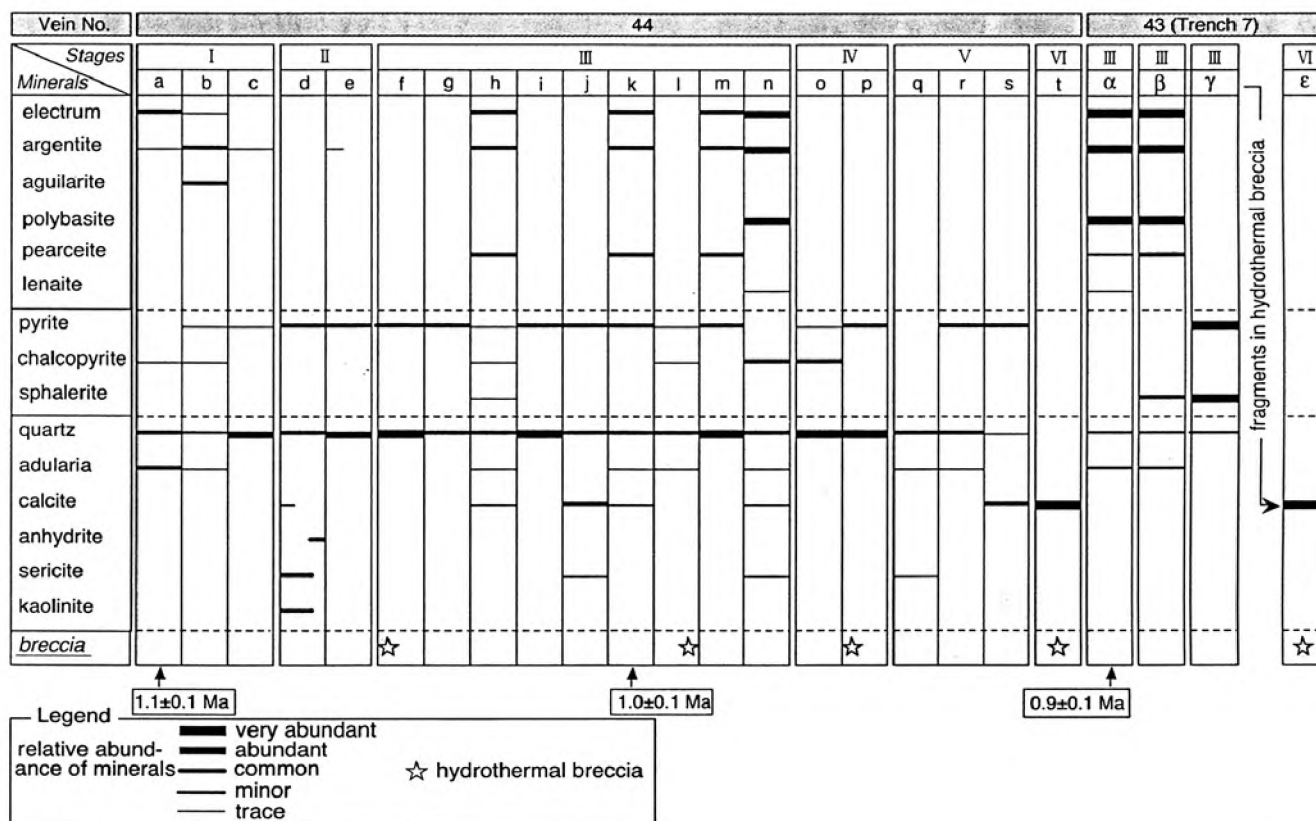


Fig. 9.19. Mineralization stages and paragenetic sequence of ore and gangue minerals from Vein No. 44 (280 mL) and Vein No. 43 (220 mL) at the Rodnikovoy deposit. K-Ar ages are given for adularia sampled from veins

terraces, and swamp sites with thermal water discharges (1–2 l/s, $T = 40–55^{\circ}\text{C}$) traced along the flood-plain terrace for 1.3 km. The second group of springs is directly confined to the camp. A large travertine field (40×60 m) with domes and springs existed here formerly. Only two springs with a temperature of 39–46°C are now active. Two hydrogeological boreholes penetrated a hydrothermal reservoir heated to 55.5–78.5°C.

The third group of hydrothermal springs was found in the course of driving Adit 1. It is situated 800 m upstream of the camp. Adit 1 here crosses (180–560 m) the fractured zones with a thermal water discharge. A cavern heated to 110–125°C was opened within an interval of 271–275 m. The hot water (91.5°C) flows out from this cavern at a rate of 2.4 l/s. The discharge drastically falls in winter, when the supply of meteoric water along the fracture zone ceases and heating of the rocks markedly increases.

Diverse sulfates, phosphates, carbonates, as well as quartz, pyrite, and adularia (Table 9.6) precipitate on the adit walls during this drying stage. In summer, when the amount of percolating water becomes much greater, some newly formed minerals are dissolved.

The primary mineral assemblages of orebodies, under the influence of such hot zones due to the effect of modern hydrothermal solutions, are modified with formation of new phases. For example, the thin (up to

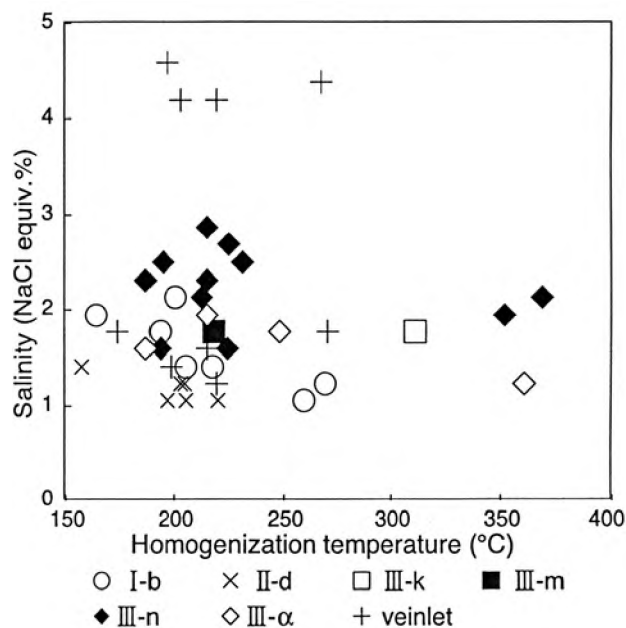


Fig. 9.20. Salinity vs. homogenization temperature of fluid inclusions

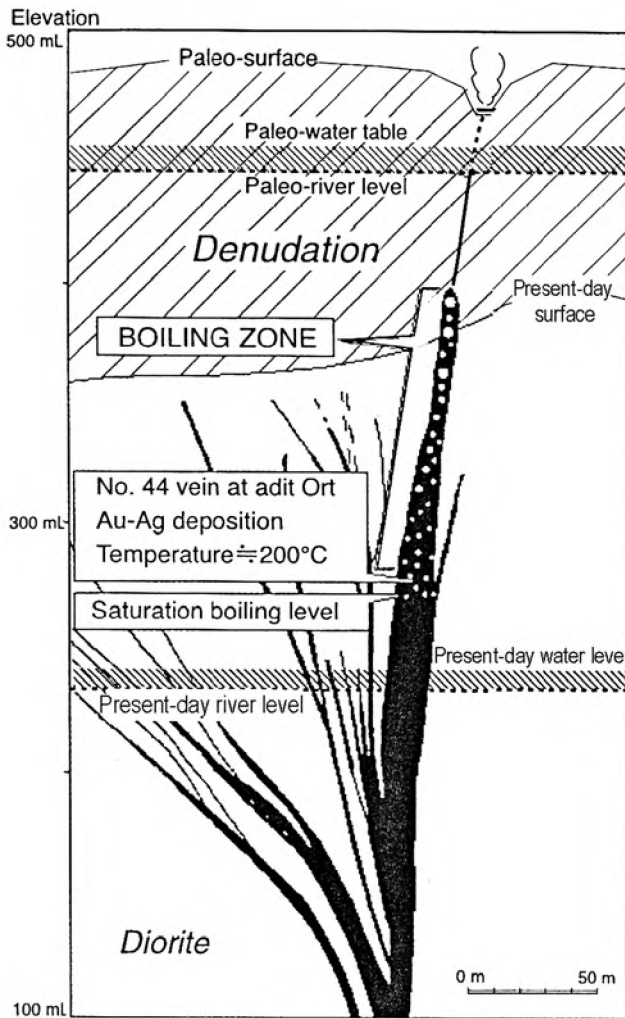


Fig. 9.21. A schematic model of gold deposition in Vein 44 at the Rodnikovy deposit

2–3 mm) crusts of proustite, xanthoconite, pyrite, quartz, and adularia crystals grow over stibiopearceite–arsenopolybasite aggregates with native gold inclusions. Sulfosalt matrices are broken down with the release of myrmekite-like native gold and altaite and complex intergrowths containing Tl, Bi, Sb, As, Se, O, and S. Hot zones are distinguished by drastic enrichment of both minerals and altered rocks in Hg. The proustite-pyrargyrite aggregates precipitated on samples of sulfide ores from the Mutnovsky and Kumroch deposits placed in the hot zone for 14 months.

The travertine terraces and domes precipitated at the present surface from the sodic chloride-carbonate water heated to 54–78°C. The travertine consists of calcite, aragonite, opal, Fe and Mn oxides and hydroxides, Fe, Cu, Zn, and Hg sulfides, and native gold with a complex micromorphology. Although the thermal water has a high temperature, mineralization,

and anomalous heavy metal concentrations, an algal and microbial biomat community with extreme bacterial diversity formed here. Such bacterial communities are typical for hydrothermal systems. However, the biomats of the Vilyucha system reveal an especially wide variety including green and diatomic algae, cyanobacteria, baculiform and cocco-like bacterial cells. The microorganisms that form a considerable biomass of this ecosystem occur as separate cells, 0.5–2.0 μm in diameter, and large colonies or aggregates including mineral particles. Microorganisms thereby actively participate in mineral formation. The biomineralization proceeds not only as active sorption and accumulation on the cell wall surface as indicated by bacterial cells with dense multilayer envelopes-capsules and the cells having a cover of fine mineral particles, as large as 200 nm (Fig. 9.22). Findings of cells with intracellular mineral inclusions suggest an active transport or passive diffusion of metallic ions inside the bacterial cell (Tazaki, 2003).

The Rodnikovy deposit is comparable in geology, mineralogy, and age (1.1–0.9 Ma) with the Hishikari (1.25–0.66 Ma) and Koruyu (1.2–0.8 Ma) epithermal deposits in Japan. This analogy makes the Rodnikovy deposit still more prospective (Izawa, 1993; Rodionov, 1997; Okrugin, 2003b).

THE MUTNOVSKY GOLD AND BASE-METAL DEPOSIT

The deposit is situated in the middle reaches in the Mutnovsky and Gorelovsky rivers, originating on the northern slope of the Mutnovsky volcano. The deposit is localized between the Rodnikovy Au-Ag deposit and the North Mutnovsky geothermal deposit. The geological exploration was carried out in 1975–1981. About 20 boreholes have been drilled and many workings at the surface were driven and sunk. The deposit is controversially discussed with respect to its classification as typical epithermal deposit (White, 1995; Hedenquist, 1996), with evidence mostly of the high sulfidation quartz-adularia vein types but also some evidence of low sulphidation. The orebodies here are composed of both mineral assemblages: low-sulfide (gold-quartz with carbonates) and base-metal sulfide (Cu, Pb, Zn sulfides and Sb, As, Ag, Te sulfides together with silver and gold tellurides). The ultimate reserves are as follows: 28 t Au, 1600 t Ag, as much as 300 kt Pb + Cu + Zn with average grades of 2–12 g/t Au and Ag/Au = 50–300 (Patoka, 1998; Petrenko, 1999; Okrugin, 2001b).

Minerals found in zones of anomalous heat flow (adits 1 and 2) and in the Vilyucha zone of hydrothermal activity

Ore minerals		Gangue minerals	
Proustite	Ag ₃ AsS ₃	Quartz	SiO ₂
Xanthoconite	Ag ₃ AsS ₃	Opal	SiO ₂ ·nH ₂ O
Pyrite	FeS ₂ As = 0.0-3.4%	Hydrogoethite	FeO·nH ₂ O
Chalcopyrite	CuFeS ₂	Epsomite	MgSO ₄ ·7H ₂ O
Chalcocite	Cu ₂ S	Hexahydrate	MgSO ₄ ·6H ₂ O
Altaite	PbTe	Starkeyite	MgSO ₄ ·4H ₂ O
Native gold	Au Ag = 40.6-80.5%	Pickeringite	MgAl ₂ (SO ₄) ₄ ·22H ₂ O
Complex, poorly identified phases, containing	Te, Se, Pb, Cu, Sb, Tl, As, Bi, O, and S.	Habotrichite	FeAl(SO ₄) ₄ ·22H ₂ O
		Alunite	KAl ₃ (OH) ₆ (SO ₄) ₂
		Alunogen	Al ₂ (SO ₄) ₃ ·17H ₂ O
		Apjohnite	MnAl ₂ (SO ₄) ₄ ·22H ₂ O
		Bloedite	NaMg(SO ₄) ₂ ·H ₂ O
		Brushite	CaPO ₃ OH ₂ ·H ₂ O
		Thenardite	Na ₂ SO ₄
		Arcanite	K ₂ SO ₄
		Gypsum	CaSO ₄ ·2H ₂ O
		Anhydrite	CaSO ₄
		Minamiite	(NaCa) ₁₋₄ Al ₃ (SO ₄) ₂ (OH) ₆
		Wattevilleite	Na ₂ Ca(SO ₄) ₂ ·H ₂ O
		Halite	NaCl
		Sulphur	S (S,Se)
		Calcite	CaCO ₃
		Aragonite	CaCO ₃
		Glauberite	Na ₂ Ca(SO ₄) ₂
		Caledonite	Cu ₂ Pb ₅ (SO ₄) ₃ CO ₃ (OH) ₆
		Kaolinite	KAl(SO ₄) ₂ ·11H ₂ O
		Sassolite	B(OH) ₃
		Adularia	KAlSi ₃ O ₈
		<u>Mascagnite</u>	(NH ₄) ₂ SO ₄
		Alum:	
		Tschermigite	(NH ₄)Al(SO ₄) ₂ 12H ₂ O
		Sodium-Alum	NaAl(SO ₄) ₂ 12H ₂ O
		Potassium-Alum	KAl(SO ₄) ₂ 12H ₂ O

This deposit is very similar in many geological, mineralogical, and geochemical respects to the Toyoha complex Ag- and In-bearing Pb-Zn vein deposit, the largest of this type in Japan (Hamada, 2000). The Toyoha deposit was formed 3.1–0.49 Ma ago and thus is virtually coeval with the Mutnovsky deposit (3.3–0.25 Ma).

The Mutnovsky deposit also reveals many features resembling the Rodnikov deposit: (1) localization within the same volcanic belt; (2) control by the same submeridional normal fault system; (3) similar structural patterns; (4) close spatial relations to the

Pliocene-Quaternary igneous rocks and the presence of older gabbro and diorite intrusions as hosts for ore-bodies (Figs. 9.23 and 9.24); (5) inhomogeneity and zoning of ore minerals; (6) ore precipitation from true and colloidal solutions having similar *PTX* parameters and a deep-seated source of sulfur (Fig. 9.25), strontium, and carbon; boiling, brecciation, rejuvenation, and oscillation during ore deposition; (7) presence of active hydrothermal springs and hot rocks at a depth; (8) extremely nonuniform Au and Ag distribution in ore veins, and (9) considerable vertical range of ore mineralization. At the same time, there are some dif-

The chemical composition of water in the Vilyucha hydrothermal system

Parameters (components in mg/l)	Sample number				
	VM2	VM3	VM4	VM5	VM6
Temperature of water, °C	37.5	46	56.5	71.8	55.1
Temperature of air, °C	2	9	2	2	2
Date	05.05.03	05.05.03	05.05.03	05.05.03	05.05.03
Time	8:00	12:00	8:15	8:30	11:00
Sample location	Outflow from Adit 1	Radon spring	Well 1	Well 2 (heating)	Travertine dome
pH	7.94	7.1	6.6	6.68	6.66
NH ₄ ⁺	0.1	<0.1	<0.1	<0.1	<0.1
Na ⁺	86	126	188	190	189
K ⁺	4.9	5.8	8.0	8.7	8.1
Ca ²⁺	52	74	112	101	118
Mg ²⁺	9.7	2.4	8.5	8.5	6.1
Cations	152.7	208.3	316.6	309.3	321.1
HCO ₃ ⁻	150	250	370	350	390
Cl ⁻	94	110	180	190	170
SO ₄ ²⁻	77	130	200	210	160
F ⁻	0.5	1.0	1.3	1.3	1.3
Anions	321.5	491.0	761.3	751.3	721.3
H ₃ BO ₃	15.5	14.8	26.0	19.8	14.8
H ₄ SiO _{4b}	77	190	240	250	230
H ₄ SiO _{4k}	41	4.7	30	29	41
Mineralization	474.2	699.3	1077.9.	1060.6	1042.4
Li	0.33	0.53	0.74	0.75	0.63
Al	0.005	0.004	0.010	0.004	0.010
Mn	0.002	0.030	0.37	0.36	0.64
Fe	0.01	-	7.2	0.37	0.22
<i>Cu</i>	1.7	1.8	2.3	2.7	2.0
<i>Zn</i>	2.3	3.1	3.5	4.3	16
<i>Ge</i>	4.2	6.6	10	10	9.1
As	0.22	0.27	0.44	0.42	0.37
Br	0.26	0.39	0.46	0.49	0.43
Rb	0.04	0.040	0.060	0.070	0.060
Sr	0.30	0.54	0.94	0.95	0.84
Mo	1.5	1.3	3.1	2.0	1.8
<i>Cd</i>		-	0.04	0.04	0.5
<i>Sb</i>	2.0	4.1	0.032	6.4	3.7
Cs	0.03	0.04	0.06	0.06	0.05
Ba	0.03	0.03	0.06	0.06	0.06
<i>W</i>	4.1	1.7	6.6	7.3	4.6
<i>Pb</i>	0.59	0.085	0.1	0.17	0.41

Note: Cd, Sb, Cu, Zn, Ge, Mo, W, and Pb concentrations are given in µg/l (highlighted in *italics*).

ferences, largely caused by scale, age, and duration of one or other factors.

The deformed Oligocene and Miocene volcanosedimentary rocks are related to the island-arc

stage in the evolution of this territory. They were broken at pre-Pliocene times into blocks that are exposed as cuestas gently dipping to the northwest, east, and southeast. The apparent thickness reaches 1000 m

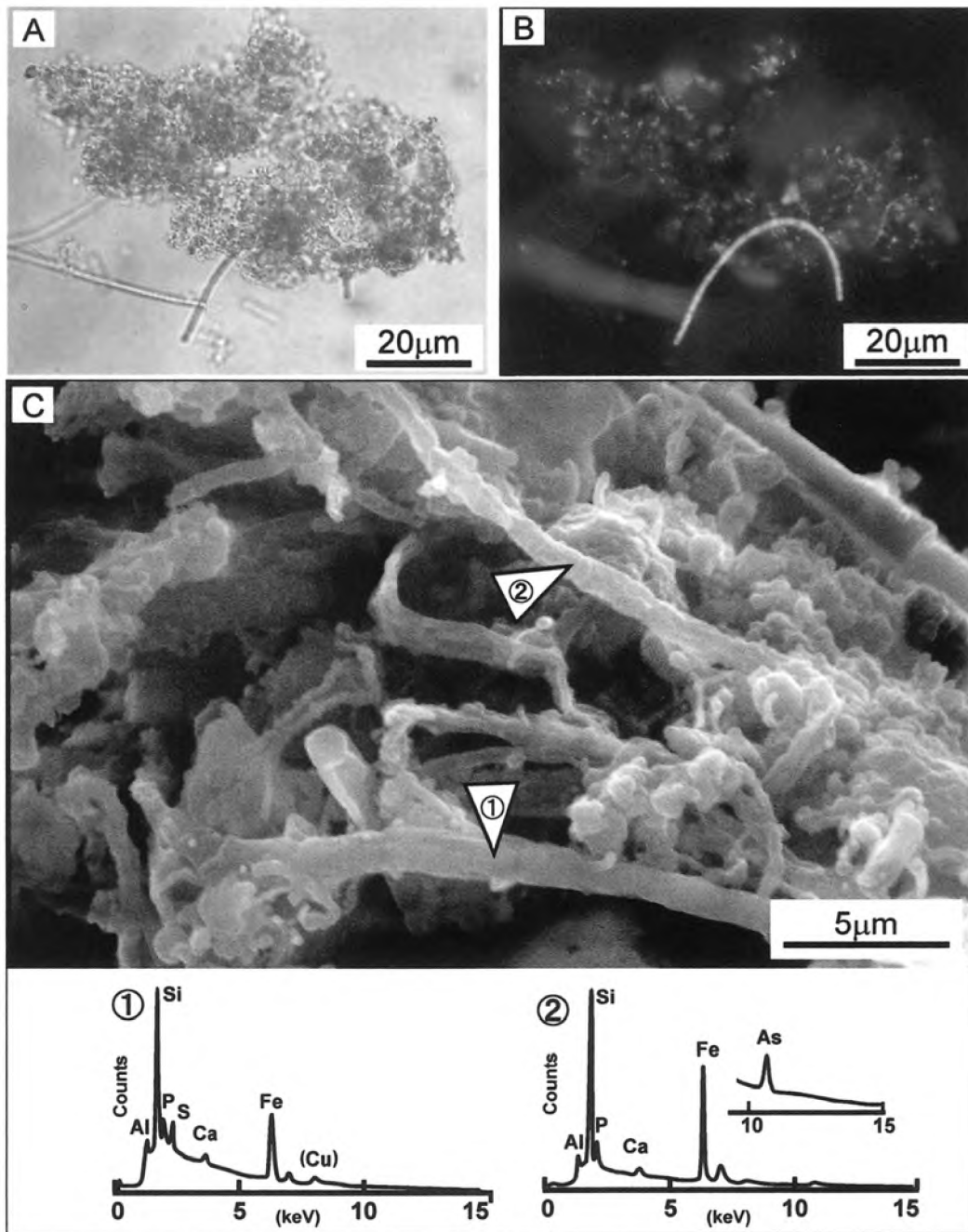


Fig. 9.22. Micrographs of reddish microbial mats collected from natural springs on the travertine dome (V 5-5) of the Vilyuchinskies hot springs. Optical light and epifluorescence micrographs (A, B) show mineral particles and diversity of bacteria and filamentous cyanobacteria attached to mineral aggregates. SEM image and EDX spectra (C) of filamentous bacteria showing the presence of Si and Fe associated with As in filamentous bacteria, covered with mineral capsule. Analytical points are marked by arrows

(Fig. 9.24). These rocks host the vein zones in the extreme north, east, and southeast of the deposit. The bedded tuffite with Pliocene plant remains overlaps the older eroded rocks with a sharp unconformity and, in turn, underlies volcanic rocks of the Zhirovsky paleovolcano (Petrenko, 1991, 1995). This volcano was a complex, polygenetic, and long-lived asymmetric edifice. The thickness of lava and pyroclastic facies in

its uplifted eastern part was 0.5–0.6 km and increased to 1.2–1.5 km in the western sector. Volcanic activity was mainly explosive and gave rise to the deposition of thick sequences consisting of agglomerates and coarse tuffs (Aprel'kov, 1964). Basic and intermediate lavas were erupted during quiet periods. A high degree of magma fractionation indicates specific conditions characterizing the feeding magmatic reservoirs

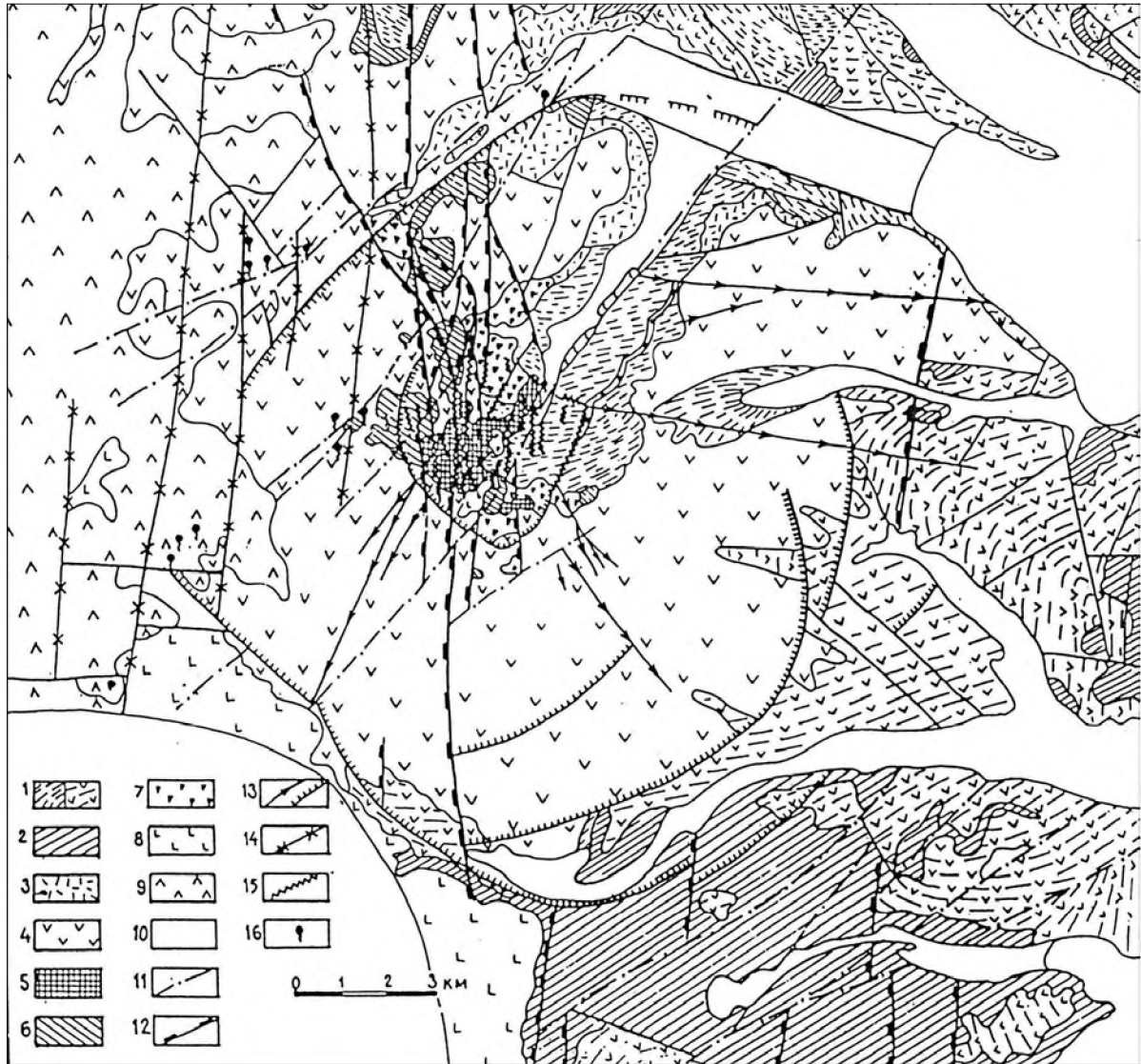


Fig. 9.23. The structural scheme of the Mutnovsky ore field (by Petrenko, 1999).

Premineal rock complex: (1) Oligocene-to-Miocene volcanosedimentary and volcanic island-arc rocks, (2) Oligocene-to-Miocene intrusive rocks (subvolcanic intrusions), (3) Pliocene dacitic and rhyodacitic tuffs; *Pliocene-Pleistocene ore-bearing complex of the Zhirovsky paleovolcano:* (4) lavas and pyroclastic rocks, (5) Pliocene gabbro and diorite intrusions, (6) subvolcanic intrusions, (7) explosion breccia of vent facies; *Pleistocene-to-Holocene postmineral volcanic complex:* (8) basalt and basaltic andesite, (9) andesite, dacite, and rhyolite; (10) Quaternary loose sediments; (11) long-living normal faults of the Mutnovsky deep fault zone; (12) South Kamchatka normal fault system (ore-controlling); (13) radial and concentric fractures of the Zhirovsky volcanotectonic structure; (14) faults of the Paratunsky-Asachinsky pull-apart zone; (15) quartz and quartz-sulfide veins; (16) active thermal springs

and conduit systems (Sheimovich, 1989). Quaternary basic, intermediate, and acid volcanics are the youngest igneous rocks (Sandimirov, 1993).

The central part of the deposit is the best studied. The orebodies make up a stockwork-vein zone, 3×4 km in size that comprises the nearly vertical thick stem vein (Determining Vein), a few smaller secondary auxiliary veins, and numerous variously oriented veinlets. About 80% of the reserves are confined to the Determining Vein, which reveals a complex internal structure with an echelon arrangement, vergence,

bulges, up to 20–30 m thick, and pinches. The vein is traced for 2650 m along the strike; vertical range of ore mineralization reaches 400 m. The northern segment of the vein zone, 1100 m long, is composed of low-sulfide ore and contains the main Au reserves. The southern segment (1600 m) consists of base-metal sulfide ore and is distinguished by a deeper erosion level. The host rocks exposed in river canyons are represented by intrusions varying in size and morphology and composed of gabbro, gabbrodiorite, and dolerite. Most of these intrusions may be regarded as feeding

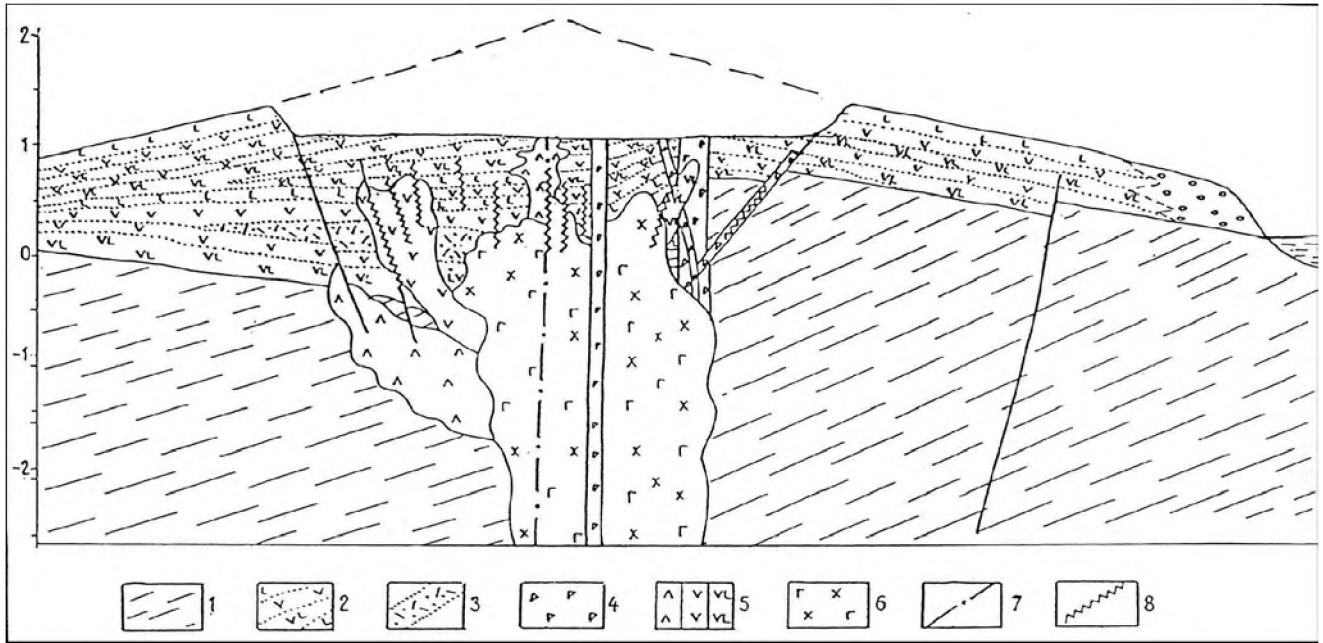


Fig. 9.24. Section across the Zhirovsky paleovolcano: a reconstruction for the time of ore deposition (by Petrenko, 1999). (1) Oligocene-to-Miocene volcanosedimentary rocks of the basement; *rock complex of the Zhirovsky paleovolcano*: (2) basic and intermediate lavas and pyroclastic rocks, (3) dacitic and rhyolitic tuffs filling caldera, (4) explosion breccia of vent facies, (5) subvolcanic intrusions (dacite, andesite, and basaltic andesite), (6) gabbro and diorite intrusions; (7) major faults; (8) quartz and quartz-sulfide veins.

systems and shallow-seated magma chamber of the Zhirovsky paleovolcano. It should be noted that these rocks were not penetrated by numerous boreholes drilled on the northern flank, as well as by Borehole 13c on the southern flank. Basic and intermediate tuffs, silicic lithic and crystal tuffs, and subordinate thin lava flows, from basalt to rhyolite in composition, serve here as host rocks.

The ore is characterized by combined banded and colloform-banded, crustified-banded, cockade massive, and stringer-disseminated structures; brecciated ore is typical. The mineral composition of the ore is diverse (Table 9.7); ore minerals are commonly zonal and reveal a nonuniform impurity distribution. Two sphalerite varieties, one containing up to 10–12 wt % Fe and another up to 10.5 wt % Mn, may be seen in the same specimen (central part of the deposit). Sphalerite with zoned Fe and Mn distribution occurs together with this mineral revealing zoned patterns of Cd (up to 6.5%) and In (up to 9.7%) contents. Zoned fahlore with variable As, Sb, and Ag contents associates with freibergite (small inclusions in galena) and goldfieldite (inclusions in sphalerite) that contains as much as 26.5% Ag and up to 2.3% Se. Zoned As-bearing pyrite is typical. The As content in some zones of this mineral may be as high as 10.0–10.5 wt %. Native gold of complex dendritic morphology is very fine (10–150 μm). The largest grain, 1.2 mm in size, was found in base-metal sulfide

size, was found in base-metal sulfide ore. The Ag content in this grain varies from 29.5 to 41.5%. Local domains are practically devoid of Ag, but contain up to 2.5–3.0 wt % Hg. The inhomogeneous structure of the ore was probably caused by its formation under

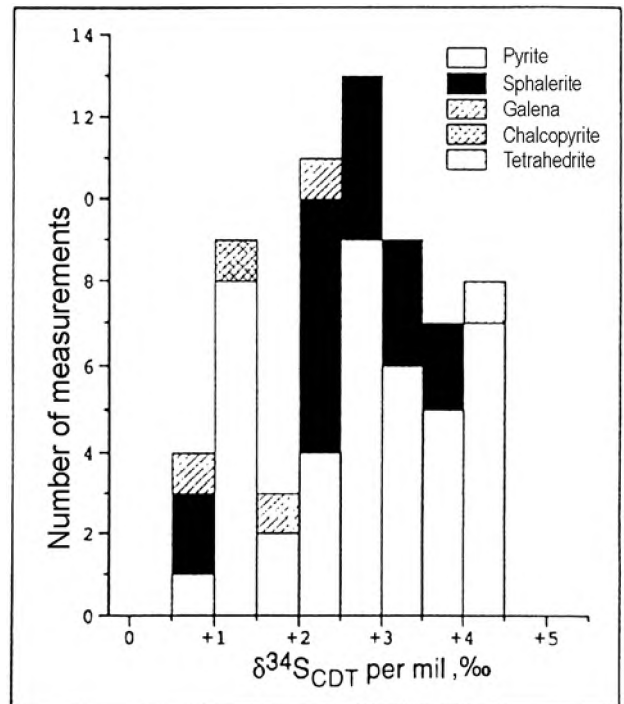


Fig. 9.25. Sulfur isotopic composition of sulfides from the Mutnovsky ore veins

Table 9.7

Mineral composition of primary gold and base-metal ore at the Mutnovsky deposit

Ore minerals	Gangue minerals
Pyrite	Quartz
Sphalerite	Chalcedony
Chalcopyrite	Opal
Galena	Calcite
Alabandite	Rhodochrosite
Marcasite	Manganocalcite
Tennantite-tetrahedrite	Sericite
Argentite	Adularia
Stembergite	Albite
Proustite	Kaolinite
Pyrrargyrite	Montmorillonite
Stibiopearceite-arsenopolybasite	Prehnite
Luzonite	Chlorite
Arsenopyrite	Epidote
Pyrrhotite	Fluorite
Molybdenite	Smectite
Bourmonite	Alunite
Colusite	Zircon
Mawsonite	Gypsum
Stannoidite	Apatite
Canfieldite	Jarosite
Cinnabar	Brushite
Hessite	Zeolites
Sylvanite	Dolomite
Altaite	Magnesite
Tellurobismuthite	Siderite
Tetradymite	Barite
Native gold	Anhydrite
Native silver	
Native aluminium	
Native iron	
Covellite	
Chalcocite	
Stibnite	
Rutile	
Magnetite	
Pyrolusite	
Jacobsite	
Manganite	

hypabyassal conditions and a wide variation of *PTX* parameters serves as additional evidence for its young age. The ore retained its pristine appearance without undergoing subsequent modification and alteration.

The specific features of the Mutnovsky deposit are as follows: (1) diverse composition and facies ap-

pearance of Quaternary volcanics related to the East Kamchatka volcanic belt; (2) relatively good preservation of the Pliocene-to-Pleistocene volcanic edifice due to a shallower erosion level; (3) wide variation of mineral and structural features of ore and a wide range of trace element contents in pyrite, sphalerite, fahlore, alabandite, and carbonates; (4) enrichment of ore in Mn and various modes of manganese occurrence from its own mineral phases to incorporation into sulfides and even sulfosalts; (5) elevated contents of As, Sb, Hg, and especially Cd (as much as 125 ppm in the bulk vein and 6–7 wt % in sphalerite), In (90–130 ppm in the bulk orebodies and up to 9–11% in sphalerite), and Ag (freibergite-type fahlore, hessite, Au and Ag tellurides); (6) abundant argillic and sericitic alteration along with a deficiency in adularia; sericite is the main potassium concentrator (as much as 6–8 wt %), whereas adularia is distributed unevenly varying from single grains to fine aggregative disseminations; (7) enrichment of ore and altered wall-rock in Hg (up to 50–2000 ppb); (8) long-term and large-scale ore formation with the appreciable contribution of the recently formed hydrothermal minerals (Lattanzi, 1995; Lonshakov, 1977; Okrugin, 2001b).

The distance from the major Determining Vein to the North Mutnovsky vapor-hydrothermal deposit does not exceed 1.5–2.5 km. Boreholes penetrated the reservoirs of the vapor-water mixture heated to 260–270°C beneath the North Mutnovsky deposit. The Voinovsky thermal springs on the northern flank of the deposit emit only 600 m downstream from the base-metal gold ore zone. In total, five groups of active hydrothermal springs are known at the deposit. They are accompanied by intense deposition of As- and Au-bearing pyrite, cinnabar, adularia, gypsum, and other minerals. Pyrite, arsenopyrite, cinnabar, sphalerite, galena, chalcopyrite, native gold, alunite, kaolinite, sericite, manganocalcite, quartz, and less abundant adularia were established in the feeding zone of the Voinovsky springs exposed on both banks of the V-shaped Mutnovsky River valley. The zoned As-bearing pyrite locally contains up to 0.5–0.6 wt % Au. Hydrothermal activity at the deposit occurred is going on in the oscillatory-rejuvenation regime during the last 3.5 Ma (Okrugin, 2001b, 2003b; Takahashi, 2002a, 2002b), and this process still remains unfinished.

The idea of long-living ore and volcanic centers was developed by Vasilevsky et al. (1977). In particular, the Mutnovsky-Asachinsky center of this kind comprising the Rodnikovoy, Mutnovsky, and Asachinsky epithermal deposits, Mutnovsky high-temperature

hydrothermal system, and Mutnovsky and Gorely active volcanoes was distinguished by these authors. The center boundaries may be a matter of debate, but the fact that this center actually exists casts no doubt. Magmatic, hydrothermal, and ore-forming activity evolved here since the Miocene. New types of mineral deposit, particularly related to the Akhomten granitoids may be found here, e.g., porphyry copper deposits similar to those known from Papua New Guinea and Indonesia.

REFERENCES

- Aprelkov, S.E. and Sheimovich, V.S., An ancient volcano in the southeastern Kamchatka with active hydrothermal occurrences, *Bull. Vulkanol. Stantsii.*, 1964, no. 36, pp. 48–60.*
- Baikov, A.I., The problems of non-linear metallogeny of Kamchatka, in: *Petrologiya i metallogeniya bazit-giperbazitovykh kompleksov Kamchatki* (Petrology and metallogeny of mafic-ultramafic complexes of Kamchatka), Moscow: Nauchny Mir, 2001, pp. 267–284.*
- Borodaev, Y.S., Garavelli, A., Kuzmina, O.V., Mozgova, N.N., Organova, N.I., Trubkin N.V., and Vurro, F., Rare sulfosalts from Vulcano, Aeolian Islands, Italy. I. Se-bearing kirkiite, $Pb_{10}(Bi,As)_6(S,Se)_{19}$, *Can. Mineral.*, 1998, vol. 36, pp. 1105–1114.
- Chashchin, A.A., Khetchikov, L.N., Ivanov, V.V., et al., The fluid regime of igneous rock formation and Au-Ag mineralization of the Vilyucha volcanotectonic structure (Southern Kamchatka), in: *Rudnye mestorozhdeniya kontinental'nykh okrain (Ore deposits of continental margins)*, vol. 2, pt. 2, Vladivostok, 2001, pp. 341–366.*
- Cheyne, B., Dall'Aglio, M., Garavelli, A., Grasso, M.F., and Vurro, F., Trace elements from fumaroles at Vulcano Island (Italy): rates of transport and a thermochemical model, *J. Volcanol. Geoth. Res.*, 2000, vol. 95, pp. 273–283.
- Churakov, S.V., Tkachenko, S.I., Korzhinsky, M.A., et al., Thermodynamic modelling of compositional evolution of high-temperature fumarolic gases at the Kudryavy volcano, Iturup Island, Kuril Islands, *Geokhimiya*, 2000, no. 5, pp. 485–501.*
- Fedotov, S.A., Mechanism of volcanic activity in Kamchatka, *Kuril-Kamchatka arc, and the similar structures*, in: *Deistvuyushchie vulkany Kamchatki* (Active volcanoes of Kamchatka), vol. 1, Moscow: Nauka, 1991, pp. 18–35.*
- Fulignati, P. and Sbrana, A., Presence of native gold and tellurium in the active high-sulfidation hydrothermal system of the La Fossa volcano Vulcano, Italy, *J. Volcanol. Geoth. Res.*, 1998, vol. 86, pp. 187–198.
- Garavelli, A., Laviano, R., and Vurro, F., Sublimate deposition from hydrothermal fluids at the Fossa crater – Vulcano, Italy, *Eur. J. Mineral.*, 1997, vol. 9, pp. 423–432.
- Hamada, M. and Imai, A., Sulfur isotopic study of the Toyoha deposit, Hokkaido, Japan – comparison between the earlier-stage and the later-stage veins, *Resource Geology*, 2000, vol. 50, no. 2, 113–122.
- Hedenquist, J.W., Isawa, E., Arribas, A.Jr., and White, N.C., *15 color plates: epithermal gold deposits: styles, characteristics, and exploration*, Society of Resource Geology, 1996.
- Izawa, E., Kurihara, M., and Itaya, T., K-Ar ages and the initial Ar isotopic ratio of adularia-quartz veins from the Hishikari gold deposit, Japan, *Resource Geology*, 1993, Spec. Issue, vol. 14, pp. 63–69.
- Kiryukhin, A.V., Slotsov, I.V., Delemen, I.F., Lesnykh, M.D., Polyakov, A.Y., Kalacheva, E.G., and Rychka, I.A., The Mutnovsky geothermal field through three-dimensional hydrogeological model, in: *Mineralization in arc volcanic-hydrothermal systems (Kamchatka, Kuril and Japanese Isles)*, Petropavlovsk-Kamchatsky, 1998, 203–205.
- Kiryukhin, A.V., *Modelirovanie ekspluatatsii geotermal'nykh mestorozhdenii* (Modeling of geothermal deposit exploitation), Vladivostok: Dalnauka, 2002, 114 p.*
- Kozhemyaka, N.N., Tectonic setting and overview of volcanoes in southern Kamchatka, in: *Deistvuyushchie vulkany Kamchatki* (Active volcanoes of Kamchatka), Vladivostok: Dalnauka, pp. 276–281.*
- Lattanzi, P., Okrugin, V., Corsini, F., Ignatjev, A., Okrugina, A., and Chubarov, V., Geology, mineralogy and geochemistry of base and precious metal mineralization in the Mutnovskaya area, Kamchatka, Russia, *SEG Newsletter*, 1995, vol. 20, pp. 6–9.
- Le Guern, F. and Bernard, A.A., New method for sampling and analyzing volcanic sublimates. Application to Merapi volcano, *J. Volcanol. Geotherm. Res.*, 1982, vol. 12, pp. 133–146.
- Leonov, V.L., *Strukturnye usloviya lokalizatsii vysokotemperaturnykh gidroterm* (Structural conditions of high-temperature hydrotherms localization), Moscow: Nauka, 1989, 104 p.*
- Lonshakov, E.A., Vakin, V.A., Bocharova, G.I., and Okrugin, V.M., Volcanogenic ore veins in the southeastern Kamchatka, *Geol. Rudn. Mestorozhd.*, 1977, no. 4, pp. 121–124.*
- Lonshakov, E.A., Series of volcanotectonic structures and structure-rock parageneses in the southern Kamchatka district, *Bull. Vulkanol. Stantsii*, 1979, no. 57, pp. 79–91.
- Marenina, T.Yu., Geology and petrography of the Mutnovsky volcano, *Trudy Lab. Vulkanol.*, 1956, no. 12.*
- Martynov, Yu.A., Perepelov, A.B., and Chashchin, A.A., Geochemical typification of basaltoids in the Mutnovsky volcanic field (Southern Kamchatka), *Tikhookean. Geol.*, 1995, vol. 14, no. 5, pp. 72–83.*
- Melekestsev, I.V., Braitseva, O.A., and Ponomareva, A.A., Dynamics of the Mutnovsky and Gorely volcanoes in Holocene and volcanic hazard for the adjacent districts, *Vulkanol. Seismol.*, 1987, no. 3, pp. 3–18.*
- Melekestsev, I.V., Braitseva, O.A., Ponomareva, A.A., and Sulerzhitsky, L.D., Age and formation dynamics of active volcanoes in the Kuril–Kamchatka region, *Izv. Akad. Nauk SSSR, Ser. Geol.*, 1990, no. 4, pp. 17–31.*
- Mozgova, N.N., Kuzmina, O.V., Organova, N.I., and Laputina, I.P., New data on sulphosalt assemblages at Vulcano (Italy), *Rend. Soc. Ital. Mineral. Petrol.*, 1985, vol. 40, pp. 277–283.
- Murav'ev, A.V., Polyak, B.G., Turkov, V.P., and Kozlovseva, S.V., A reappraisal of heat power of fumarole activity at the Mutnovsky volcano, *Vulkanol. Seismol.*, 1983, no. 5, pp. 51–63.*
- Okrugin, V., WRI-8 post-session field trip to Kamchatka, part 1: Mutnovskoe geothermal field, *The 8th Intern. Symp. on water-rock interaction*, Vladivostok, 1995, pp. 1–28.
- Okrugin, V., Zelensky, M., Marynova, V., Okrugina, A., Senyukov, S., and Sergeeva, S. Last news about volcanic activity in Kamchatka Peninsula: Mutnovskii and Gorelyi volcanoes especially, *Bull. Res. Centre for North Eurasia and North Pacific Regions, Hokkaido University*, 2001a, vol. 1, pp. 146–163.
- Okrugin, V., Okrugina, A., Mataueda, H., and Ono, S., Mutnovskoe epithermal Au-polymetallic deposit of the Southern Kamchatka, Russia // *Abstracts with programs, Society of Resource Geology, June 13–15, 2001*, Tokyo, 2001b, p. 30.

* In Russian.

- Okrugin, V., Tazaki, K., and Belkova, N., Hydrothermal mineral formation systems of Kamchatka and the biomineralization, *Proc. Intern. Symposium of the Kanazawa University, 21st-Century COE Program, March 17-18, 2003*, Kanazawa, Japan, 2003a, vol.1. pp.235-238.
- Okrugin, V.M., New data on age and genesis of epithermal deposits in the continent-ocean transitional zone, Northwestern Pacific, in: *Proc. All-Russia Conference, XII Annual Meeting of the Northeastern Division, 2003b*.
- Patoka, M.G., Litvinov, A.F., and Petrenko, I.D., Kamchatka – a new gold-bearing province of Russia, in: *Mineralization in arc volcanic-hydrothermal systems (Kamchatka, Kuril and Japanese isles)*, Petropavlovsk-Kamchatsky, 1998, 72-75.
- Petrenko, I.D. and Bol'shakov, N.M., Structural setting and age of the gold-silver ore mineralization in the southern Kamchatka as exemplified by the Mutnovsky deposit, *Tikhookean. Geol.*, 1991, no. 5, pp. 100-111.*
- Petrenko, I.D., *Zoloto-serebryannaya formatsiya Kamchatki (Silver-gold deposits of Kamchatka)*, 1999, pp. 5-115.*
- Polyak, B.G., *Geotermicheskie osobennosti oblasti sovremennogo vulkanizma (na primere Kamchatki) (Geothermics of active volcanism: a case of Kamchatka)*, Moscow: Nauka, 1966, 180 p.*
- Rodionov, S.M. and Khanchuk, A.I., Hishikari-type ore deposits and prospects of their discovery at the eastern margin of Russia, *Tikhookean. Geol.*, 1997, vol. 16, no. 5, pp. 34-45.*
- Sandimirov, I.V., Pampura, V.D., Sandimirova, G.P., and Gudkova, V.N. The age of base-metal and gold ore mineralization of the Zhirovsky volcanic ore center, the southern Kamchatka, *Dokl. Akad. Nauk*, 1993, vol. 329, no. 5, pp. 637-639.*
- Selyangin, O.B., News on the Mutnovsky volcano: structure, evolution, and forecast, *Vulkanol. Seismol.*, 1993, no. 1, pp. 17-35.*
- Serafimova, E.K., Chemical composition of fumarolic gases at the Mutnovsky volcano, *Byull. Vulkanol. Stantsii*, 1966, no. 42, pp. 56-65.*
- Serafimova, E.K., *Mineralogiya vozgonov vulkanov Kamchatki (Mineralogy of sublimates at volcanoes of Kamchatka)*, Moscow: Nauka, 1979, 167 p.*
- Serafimova, E.K., Mineral assemblages of volcanic sublimates, in: *Posteruptivnoe mineraloobrazovanie na aktivnykh vulkanakh Kamchatki (Posteruptive mineral formation at the active volcanoes in Kamchatka)*, Pt. 1, Vladivostok: Izd-vo Far East Branch, Academy of Sciences of the USSR, 1992, pp. 31-52.*
- Sharapov, V.N., Simbirev, I.B., Tret'yakov, G.A., et al., *Magmatizm i gidrotermal'nye sistemy Mutnovskogo bloka Yuzhnoy Kamchatki (Magmatism and hydrothermal systems of the Mutnovsky block in the southern Kamchatka)*, Novosibirsk: Nauka, 1979, 152 p.*
- Sheimovich, V.S. and Patoka, M.G., *Geologicheskoe stroenie zon aktivnogo kainozoiskogo vulkanizma (Geology of zones of active Cenozoic volcanism)*, Moscow: Nauka, 1989.*
- Symonds, R.B. and Reed, M.H., Calculation of multicomponent chemical equilibria in gas-solid-liquid systems: calculation methods, thermochemical data and applications to studies of high-temperature volcanic gases with examples from Mount St. Helens, *Am. J. Sci.*, 1993, vol. 293, pp. 758-864.
- Takahashi, R., Matsueda, H., and Okrugin, V., Hydrothermal gold mineralization at the Rodnikovoy deposit in South Kamchatka, *Resource Geology*, 2002a, vol. 47, no. 4, pp. 359-370.
- Takahashi, R., Matsueda, H., Okrugin, V., Okrugina, A., and Ono, S., Outline of hydrothermal activity and related mineralization in Kamchatka, Russia, *Abstracts with programs the Society of Resource Geology, June 19-21, 2002*, Tokyo, 2002b, p.4.
- Taran, Yu.A., Vakin, E.A., Pilipenko, V.N., and Rozhkov, A.M., Geochemical studies in the crater of Mutnovsky volcano, *Vulkanol. Seismol.*, 1991, no. 5, pp. 37-55.
- Tazaki, K., Okrugin, V., Masayuki, O., Belkova, N., Islam, R., Chaerun, S.K., Wakimoto, R., Sato, K., and Moriichi, S., Heavy metallic concentration in microbial mats found at hydrothermal systems, Kamchatka, Russia, *Sci. Rept. Kanazawa Univ.*, 2003, vol. 47, no. 1-2, pp. 12-45.
- Vakin, E.A., Kirsanov, I.T., and Pronin, A.A., Active funnel of the Mutnovsky volcano, *Bull. Vulkanol. Stantsii.*, 1966, no. 40, pp. 25-36.*
- Vakin, E.A., Kirsanov, I.T., and Kirsanova, T.P., Thermal fields and hot springs of the Mutnovsky volcanic district, in: *Gidrotermal'nye sistemy i termal'nye polya Kamchatki (Hydrothermal systems and thermal fields in Kamchatka)*, Moscow: Nauka, 1976, pp. 85-115.*
- Vakin, E.A., Pilipenko, G.F., and Sugrobov, V.M., The general characteristics of the Mutnovsky deposit and resource forecasting, in: *Geotermicheskie i geokhimicheskie issledovaniya vysokotemperaturnykh geoterm (Geothermal and geochemical investigations of high-temperature geotherms)*, Moscow, Nauka, 1986, pp. 6-40.*
- Vasilevsky, M.M., Zimin, V.M., and Okrugin, V.M., Volcanic ore centers in the southeastern Kamchatka, in: *Prognoznaya otsenka rudonosnosti vulkanogennykh formatsii (Forecasting of ore potential of volcanic rock associations)*, Moscow: Nauka, 1977, pp. 122-128.*
- Vergasova, L.P. and Nadezhnaya, T.B., New minerals found at the volcanoes in Kamchatka: a review, in: *Posteruptivnoe mineraloobrazovanie na aktivnykh vulkanakh Kamchatki (Posteruptive mineral formation at the active volcanoes in Kamchatka)*, Pt. 2, Vladivostok: Izd-vo Far East Branch, Academy of Sciences of the USSR, 1992, pp. 3-21.*
- Vil'danova, E. Yu., Zaitsev, V.P., Kravchenko, L.I. et al., *Koryaksko-Kamchatskii region – novaya platinonosnaya provintsiya Rossii (The Koryak-Kamchatka region – a new platinumiferous province in Russia)*, St. Petersburg: Cartograph. Printing House VSEGEI, 2002, 383 p.*
- White, N.C. and Hedenquist, J.W., Epithermal gold deposits: styles, characteristics, and exploration, *Soc. Econ. Geol.*, 1995, vol. 23, pp. 9-13.
- Zelensky, M.E., Ovsyannikov, A.A., Gavrilenko, G.M., and Senyukov, S.L., The March 2002 Mutnovsky volcano eruption (Kamchatka), *Vulkanol. Seismol.*, 2002, no. 6, pp. 25-28.*